UNIVERSIDAD DE LA RIOJA

TESIS DOCTORAL

Título
Conformationally restricted Tn antigen mimics: synthesis, structural analysis and biological properties
Autor/es
Claudio D. Navo Nájera
Director/es
Jesús Manuel Peregrina García y Gonzalo Jiménez Osés
Facultad
Facultad de Ciencia y Tecnología
Titulación
Departamento
Química
Curso Académico

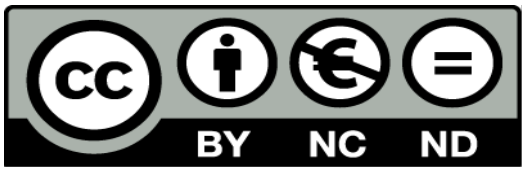

Conformationally Restricted Tn Antigen Mimics: Synthesis, Structural Analysis and Biological Properties

Claudio D. Navo Nájera
Universidad de La Rioja
2018

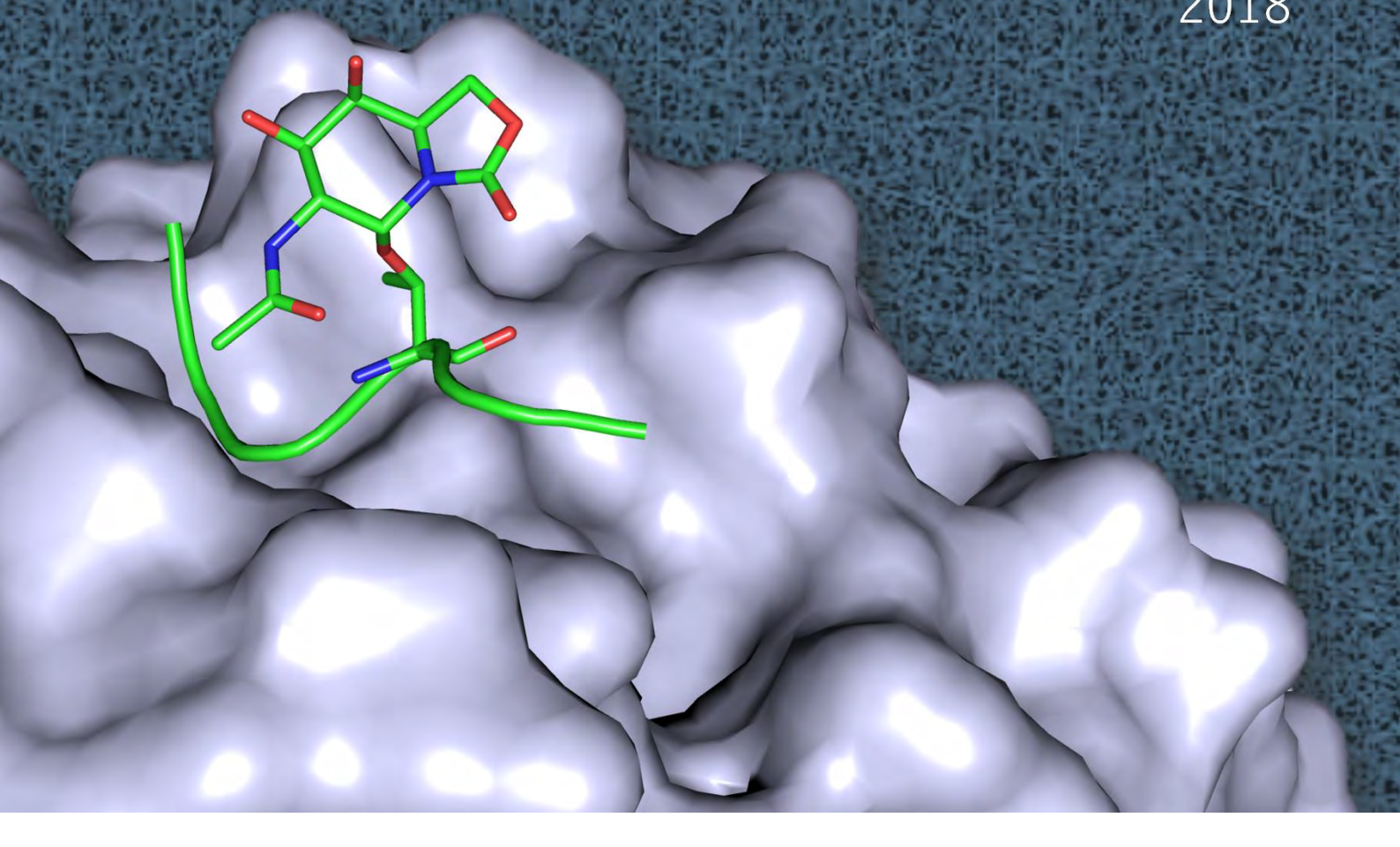

FACULTAD DE CIENCIA Y TECNOLOGÍA

DEPARTAMENTO DE QUÍMICA
ÁREA DE QUÍMICA ORGÁNICA

TESIS DOCTORAL

CONFORMATIONALLY RESTRICTED TN ANTIGEN MIMICS: SYNTHESIS, STRUCTURAL ANALYSIS AND BIOLOGICAL PROPERTIES

Memoria presentada en la Universidad de La Rioja
para optar al grado de Doctor en Química por

Claudio D. Navo Nájera

Junio 2018

JESÚS MANUEL PEREGRINA GARCÍA, Catedrático de Química Orgánica del Departamento de Química de la Universidad de la Rioja y

GONZALO JIMÉNEZ OSÉS, Investigador Ramón y Cajal del Departamento de Química de la Universidad de la Rioja

CERTIFICAN:

Que la memoria ***"Conformationally restricted Tn antigen mimics: synthesis, structural analysis and biological properties"*** *ha sido realizada por el Licenciado* ***Claudio D. Navo Nájera*** *en el Departamento de Química de la Universidad de La Rioja bajo su inmediata dirección y reúne las condiciones exigidas para optar al grado de Doctor en Química.*

Logroño, junio 2018

Los directores,

Jesús M. Peregrina	Gonzalo Jiménez-Osés

A mis padres, mi hermana, a Nuria y a toda mi familia.

Cuando las cosas salen mal, puedes jurar, llorar o reír.
Por qué no elegir reír.

Agradecimientos

Ha llovido ya mucho desde que empecé mis peripecias químicas en este grupo y, aun así, parece que fuera ayer. Este periodo de tiempo me ha servido para aprender muchas cosas, tanto en el ámbito profesional como en el personal. Y esto no hubiera sido posible sin vosotros.

En primer lugar, me gustaría agradecer a mis directores de Tesis. A ***Pere*** por haberme dado la oportunidad de formar parte de este grupo de investigación y por haberme guiado y dirigido durante todos años. Y a ***Gonzalo***, por toda la ayuda prestada tanto dentro del laboratorio como fuera de éste, y por su paciencia, haciendo ver que la química no es tan difícil después de todo. Por supuesto, también al resto de "seniors" del grupo, ***Alberto***, ***Paco***, ***Héctor*** y ***Marimar,*** por todo lo que me han ido enseñando y ayudando a lo largo de todos estos años, ya desde el día en que empecé la carrera.

Por supuesto, a todos mis compañeros de laboratorio, de cada uno de ellos me llevo un trocito de sabiduría. A ***Nuria***, gracias por estar a mi lado desde el primer día y por acompañarme en este viaje tanto en los buenos, como en los malos momentos. A ***Iris***, por ese carácter tan peculiar y por haberme ensañado a cómo sobrevivir a un posible ataque zombi catastrófico. A ***Xhenti***, mi italoalbanoriojana favorita, por esos "cafecinhos" a cualquier hora del día que espabilan a cualquiera. A ***Pablo***, un grande en todos los sentidos, por esos buenos ratos en el laboratorio y en el frontón. A ***Guille***, el científico, por su humor tan característico. A ***Ismael***, por esas largas discusiones científicas. A ***Emilio***, la experiencia personificada, por todos esos consejos que hacen que la vida parezca un poquito menos difícil. Y a las recién llegadas,

Paula y ***Alicia***, por vuestro entusiasmo e ilusión contagioso. Que no se acabe nunca. A las *viejas glorias* del grupo, en especial a ***Charlie***, mi mentor, por haberme ido enseñando los entresijos del laboratorio con tanta paciencia y dedicación, a ***Fer***, ***Eva***, ***Lara***, ***Nuria***, ***Víctor S.***, ***Víctor R.***, ***Mada, Iván*** y ***Marta I.*** por llenar el laboratorio de buen rollo y optimismo. Y también a todos mis "tutelados" de TFG y TFM, ***Marcos***, ***Javi***, ***Alicia***, ***Juan*** y ***Marina***. Gracias a todos ellos he aprendido mucho de lo que uno esperaría, además de los buenos ratos, tanto dentro como fuera del laboratorio.

A los demás becarios y miembros de otros grupos de investigación de la UR, especialmente a los ***fotos***, los vecinos de al lado, y los ***aurones*** y ***platineros***. Y también a los encargados de que los laboratorios funcionen como deben, ***Nines***, ***Ernesto***, ***Jorge***, ***Montse***, ***Amaya*** y demás equipo del Servicio de Laboratorios.

A toda mi familia, especialmente a mis padres y a mi hermana. A mis tías, tíos, primas y primos, por su apoyo y cariño incondicional en todo momento, y a todos mis amigos, por hacerme desconectar de vez en cuando.

Por último, me gustaría agradecer al Ministerio de Economía y Competitividad (MINECO), por la beca F.P.I. (BES-I-2013-064139) y la ayuda para realizar estancias breves en centros de investigación internacionales (EEBB-I-16-11434), así como por los distintos proyectos (CTQ2012-36365, CTQ2015-67727-R, UNLR13-4E-1931, CTQ2015-70524-R y RYC-2013-14706) y a la Universidad de La Rioja, por las ayudas a tesis doctorales (ATUR), así como por conformar el marco humano y científico idóneo para el desarrollo de este trabajo.

Abstract

In this Doctoral Thesis, novel unnatural and conformationally restricted glyco-amino-acids are presented. The restrictions aim to fix a bioactive three-dimensional structure in order to increase the interactions with target biomolecules, such as enzymes, lectins or antibodies, given the energetic penalty associated to conformational changes from the free-state to the bound-state. In this way, higher inhibition ratios, stronger recognition, or even higher immune responses are expected.

The synthesis of a new family of conformationally-locked *C*-glyco-amino-acids is exposed throughout chapter 2. These compounds were obtained through a double diastereoselective Michael addition between a chiral bicyclic serine equivalent and a nitrogalactal derivative. These unnatural glycosides adopt quite rigid structures and show affinities for lectins similar to those found for natural compounds, like the Tn antigen. This antigen is one of the most specific human tumor-associated structures, which has been related to carcinoma aggressiveness and is considered an important cancer biomarker.

Following the same methodology, a set of potential glycosidase inhibitors is presented in chapter **3**. Glycosidases hydrolyze glycosidic bonds and are involved in several biological processes, being the design of more potent and selective glycosidase inhibitors therefore essential. *In vitro* screening of such compounds showed highly selective inhibition of bovine liver β-galactosidase and specific inhibition of human β-glucocerebrosidase among lysosomal glycosidases for derivatives bearing long alkyl chains. The best

lead was found to behave as pharmacological chaperone in Gaucher fibroblast with homozygous N370S and F213I mutations, with enzyme activity enhancements similar to those encountered for the reference compound Ambroxol®.

The synthesis of serine and threonine glycomimetics α-*O*-linked to sp^2-iminosugars is addressed in chapter **4**. The key step in our synthesis is the completely diastereoselective α-*O*-glycosylation, which is mainly due to strong anomeric effects and reduced torsional strains imposed by the bicyclic system. These amino acids were incorporated into mucin-type peptides, particularly MUC1, which is overexpressed and aberrantly glycosylated in cancer cells, and their ability to be recognized by anti-MUC1 antibodies was then evaluated. Owing to the high affinity showed by one of the candidates, being even higher to that found for the natural Tn antigen, a complete conformational study was performed, combining crystallographic techniques and computational modelling, with the aim of designing and synthesizing a carbohydrate-based cancer vaccine, which is currently being evaluated.

Finally, the most relevant results obtained during two international short-term research stays are briefly discussed in chapter **5**. At M. Brimble's research group (University of Auckland, New Zealand), the bacteriocin glycocin F was fully synthesized, as well as an analog incorporating an unnatural amino acid. On the other hand, at W. van der Donk's lab (University of Illinois, US), the formation of lantipeptide duramycin catalyzed by the enzyme DurN was studied from a computational point of view.

Resumen

En esta Tesis Doctoral se presentan nuevos aminoácidos glicosilados no naturales conformacionalmente restringidos, con el objetivo de fijar una estructura tridimensional bioactiva. Así, la interacción de estos compuestos con biomoléculas diana, tales como enzimas, lectinas o anticuerpos, se incrementaría, debido al gasto energético asociado a los cambios conformacionales que tienen lugar entre la molécula en estado libre y cuando está interaccionando con la proteína. De esta forma, se espera producir una inhibición más potente, un reconocimiento más fuerte o, incluso, una respuesta inmune mayor.

A lo largo del capítulo **2**, se expone la síntesis de distintas familias de *C*-glico-aminoácidos conformacionalmente restringidos, que fueron obtenidos a partir de una reacción de Michael doblemente diastereoselectiva entre un equivalente bicíclico de serina quiral y un derivado de nitrogalactal. Estos glicósidos no naturales adoptan estructuras rígidas y muestran afinidades por lectinas similares a las obtenidas para compuestos bioactivos naturales, tales como el antígeno Tn, que es una de las estructuras asociadas a tumores humanos más específicas, relacionada además con la agresividad del carcinoma y considerado un importante biomarcador del cáncer.

Siguiendo la misma metodología, en el capitulo **3** se presenta la síntesis de una librería de potenciales inhibidores de glicosidasas. Éstas son enzimas que hidrolizan enlaces glicosídicos y están involucradas en multitud de procesos biológicos, de ahí la importancia de obtener nuevos inhibidores más potentes y selectivos. Los inhibidores que contienen cadenas alifáticas largas

mostraron una inhibición selectiva de β-galactosidasa bovina y una inhibición específica de la enzima lisosomal humana β-glucocerebrosidasa. El mejor de los candidatos mostró, además, aumentos en la actividad de dicha enzima similares al compuesto de referencia Ambroxol®, actuando como chaperona farmacológica en fibroblastos de Gaucher con las mutaciones N370S y F213I.

En el capítulo **4** se discute la síntesis de glicomiméticos de serina y treonina unidos a sp^2-iminoazúcares mediante un enlace α-*O*-glicosídico. La etapa clave en la síntesis es la α-*O*-glicosilación completamente diastereoselectiva, debida a fuertes efectos anoméricos y al reducido estrés torsional impuesto por el sistema bicíclico. Estos aminoácidos se incorporaron en péptidos de tipo mucina, en concreto MUC1, que está sobreexpresada y aberrantemente glicosilada en células cancerosas, y se estudió su capacidad de ser reconocidos por anticuerpos anti-MUC1. Dada la alta afinidad mostrada por uno de los derivados sintetizados, siendo superior a la encontrada para el antígeno Tn natural, se realizó un estudio conformacional completo, combinando técnicas cristalográficas y modelos teóricos, con el fin de diseñar una vacuna terapéutica contra el cáncer, la cual está siendo actualmente evaluada.

Por último, en el capítulo **5** se comentan brevemente los resultados más notorios obtenidos durante dos estancias pre-doctorales. Por un lado, en el grupo de investigación de M. Brimble (Universidad de Auckland, Nueva Zelanda), se sintetizó el glicopéptido bactericida glycocin F así como un análogo que incorpora un aminoácido no natural. Por otra parte, en el laboratorio de W. van der Donk (Universidad de Illinois, EEUU), se estudió la reacción de formación de lisinoalaninas en el lantipéptido duramycin catalizada por la enzima DurN desde un punto de vista teórico.

CONTENTS

Abbreviations

$[\alpha]_D^{25}$	specific rotation
δ	chemical shift
ΔE	relative electronic energy
ΔG	relative Gibbs free energy
ΔH	relative enthalpy
ε	dielectric permitivity
°C	celsius degree
^{1}H NMR	proton nuclear magnetic resonance
^{13}C NMR	carbon-13 nuclear magnetic resonance
9-BBN	9-borabicyclo[3.3.1]nonane
Å	angstrom
Abu	2-aminobutyric acid
ABX	ambroxol
Ac	acetyl
Ac_2O	acetic anhydride
AIBN	azobisisobutyronitrile
APP	3-amino-6,7-dihydroxy-3,5-bis(hydroxymethyl)hexa-hydropyrano[3,2-*b*]pyrrol-2(1*H*)-one
aq.	aqueous
Ar	aryl
Arom	aromatic
BLI	bio-layer interferometry
Bn	benzyl
Boc	tert-butoxycarbonyl
Boc_2O	di-*tert*-butyl dicarbonate
Bu	butyl
^{t}Bu	*tert*-butyl
^{t}BuOH	*tert*-butanol
c	concentration (g/100 mL)
ca.	circa
CAN	cerium ammonium nitrate
cat.	catalyst or catalytic
cc.	concentrated

COSY	^{1}H-^{1}H correlation NMR spectroscopy
Cp	cyclopentyl
CS	castanospermine
d	doublet
DCM	dichloromethane
dd	doublet of doublets
DFT	density functional theory
Dha	dehydroalanine
Dhb	dehydrobutyrine
DIC	*N*,*N*'-diisopropylcarbodiimide
DIPEA	*N*,*N*-diisopropylethylamine
DMAP	4-(dimethylamino)pyridine
DMF	dimethylformamide
DNJ	1-deoxynojirimycin
dppf	1,1′-bis(diphenylphosphino)ferrocene
dq	doublet of quartets
dt	doublet of triplets
E	electronic energy
E^2	second-order perturbation energy
Ed.	editorial
EDT	1,2-ethanodithiol
EDTA	ethylenediaminetetraacetic acid
ELLA	enzyme-linked lectin assay
eq	equation
equiv.	equivalents
Et	ethyl
Et_2O	diethyl ether
EtOAc	ethyl acetate
EtOH	ethanol
eV	electronvolt
Fmoc	9-fluorenylmethyloxycarbonyl
freq.	frequency
G	Gibbs free energy
Gal	galactose
GalNAc	*N*-acetylgalactosamine
GCase	β-glucocerebrosidase

GccF	glycocin F
Glc	glucose
GlcNAc	*N*-acetylglucosamine
H	enthalpy
HBTU	*N*,*N*,*N*′,*N*′-tetramethyl-O-(1*H*-benzotriazol-1-yl)uronium hexafluorophosphate
HMBC	heteronuclear multiple bond correlation
HMPA	hexamethylphosphoramide
HPA	*Helix pomatia* agglutinin
HPLC	high performance liquid chromatography
HRMS	high resolution mass spectrometry
HRP	horseradish peroxidase
HSQC	heteronuclear single quantum correlation
Hya	β-hydroxyaspartic acid
Hz	hertz
IC_{50}	half-maximal inhibitory concentration
IEF-PCM	integral equation formalism version of the polarizable continuum model
IRC	intrinsic reaction coordinate
J	coupling constant
K	kelvin degree
K_D	dissociation constant
K_i	inhibition constant
λ	wavelength
Lan	lanthionine
LHMDS	lithium bis(trimethylsilyl)amide
m	multiplet
mAb	monoclonal antibody
MBHA	4-methylbenzhydrylamine
MD	molecular dynamics
MD-tar	molecular dynamics with weighted time-averaged re-straints
Me	methyl
MeCN	acetonitrile
MeLan	methyllanthionine
MeOH	methanol
MeSer	α-methylserine

MHz	megahertz
MS	mass spectrometry
MW-SPPS	microwave-assisted solid-phase peptide synthesis
NBO	natural bond orbital
NCL	native chemical ligation
NMR	nuclear magnetic resonance
NOE	nuclear Overhauser effect
NOESY	nuclear Overhauser effect spectroscopy
OMN	5*N*,6*O*-(oxomethylidene)nojirimycin
p	*para* position
Pam, Palm	palmitoyl
PDB	protein data bank
PG	protecting group
Ph	phenyl
Phth	phthalamidyl
ppm	parts per million
PSO	pyranose–sulfanyloxazoline
***p*-TsOH**	*para*-toluenesulfonic acid
Py	pyridine
q	quartet
QM	quantum mechanics
R	substituent
R.T.	room temperature
RiPP	ribosomally synthesized and post-translationally modified peptide
RMSD	root-mean-square deviation
RP-HPLC	reversed-phase HPLC
s	singlet
S	entropy
sat.	saturated
SBA	soybean agglutinin
SBL	soybean lectin
scFv	single-chain variable fragment
SPPS	solid-phase peptide synthesis
SPR	surface plasmon resonance
TACA	tumor-associated carbohydrate antigen

TBS	tert-butyldimethylsilyl
TEA	triethylamine
TFA	trifluoroacetic acid
THF	tetrahydrofuran
Thz	thiazolidine
TIPS	triisopropylsilyl
TIS	triisopropylsilane
TLC	thin layer chromatography
TMB	2,2,3,3-tetramethoxybutane, 3,3,5,5-tetramethylbenzidine
TMS	tetramethylsilane
TMSOTf	trimethylsilyl trifluoromethanesulfonate
Ts	tosyl
VVA	*Vicia villosa* agglutinin
z	charge
ZPE	zero-point energy

Amino acid	**3-letter code**	**1-letter code**
Alanine	Ala	A
Arginine	Arg	R
Asparagine	Asn	N
Aspartic acid	Asp	D
Cysteine	Cys	C
Glutamic acid	Glu	E
Glutamine	Gln	Q
Glycine	Gly	G
Histidine	His	H
Isoleucine	Ile	I
Leucine	Leu	L
Lysine	Lys	K
Methionine	Met	M
Phenylalanine	Phe	F
Proline	Pro	P
Serine	Ser	S
Threonine	Thr	T
Tryptophan	Trp	W
Tyrosine	Tyr	Y
Valine	Val	V

Chapter 1.
Introduction and main goals

Carbohydrates are the most abundant biomolecules on Earth and represent one of the main macronutrients in the diet of human beings. They were solely considered as a source of energy for a long time, although during the second half of the 20th century it was demonstrated that, additionally, they were able to interact with certain proteins, named lectins nowadays. Since then, the significance of glycobiology has enormously increased, proving the participation of carbohydrates in several biological processes,[1–6] such as intercellular recognition and interactions between cells and external agents. In fact, cell membranes are covered by glycolipids and glycoproteins, conforming the glycocalyx (figure **1.1**),[7] that are responsible for these interactions, leading to beneficial biological events including fertilization and immune response, as well as adverse disease processes, such as inflammation, viral and bacterial infections, and cancer metastasis.

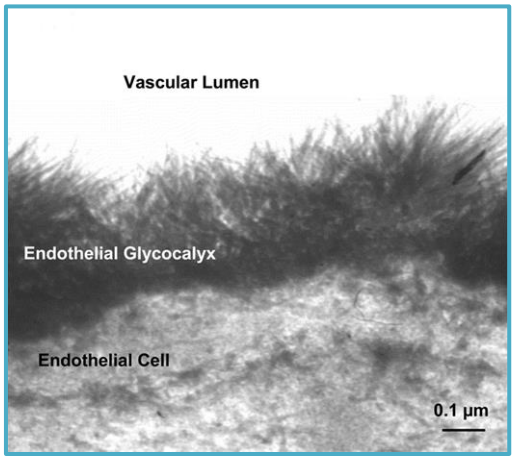

Figure 1.1. Electron microscopic view of the endothelial glycocalyx.[7]

1.1. The Tn antigen

The Tn antigen is a specific human tumor-associated carbohydrate antigen (TACA) formed by *N*-acetylgalactosamine (GalNAc) α-*O*-linked to either serine (Ser) or threonine (Thr) residues.[8] Despite being quite small and having a simple structure, the Tn antigen has attracted a great deal of interest since its identification in 1957 by Moreau.[9] However, its structure was not defined until 1975 by Dahl, using co-elution in gas-liquid chromatography.[10] The Tn antigen is found in glycoproteins of human cells as a cryptic GalNAc-containing antigen and is a precursor for many types of *O*-glycans (figure **1.2**).[11]

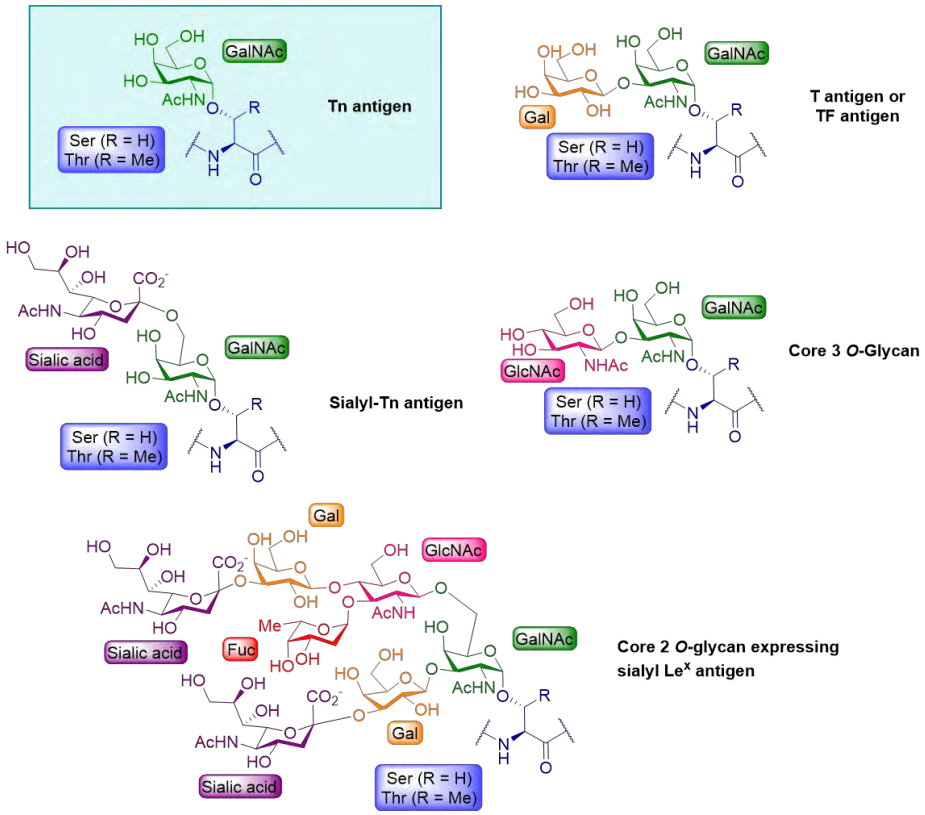

Figure 1.2. Structures of the Tn antigen (top-left) and some *O*-glycan derivatives of the Tn antigen.

Springer proved in 1974 that the Tn antigen was correlated with breast carcinoma, where it is highly expressed in over 90% of cases.[12] It has also been reported in ovarian,[13] bladder,[14] cervical,[15,16] colon,[17,18] lung,[19] stomach,[20] pancreatic,[21] and prostate tumors,[22] and it has been linked with metastatic behavior and tumor expansion.[8,23] It has therefore been attracting a great deal of interest for the development of new vaccines for cancer treatment.[24–26] It is in addition implicated in HIV infection.[27]

Several methodologies have been developed in order to effectively synthesize the Tn antigen (scheme **1.1**). The first strategy was reported by Kaifu and Osawa[28] in 1977 and subsequently several other groups described different synthetic approaches. Paulsen and Hölck envisioned a Koenigs-Knorr type of reaction between azidosugar halogen donors and protected Ser or Thr residues in the presence of silver salts as promoters to obtain the α anomer selectively.[29] Later, Schmidt reported an alternative method involving a *O*-Michael type reaction between a protected Ser or Thr residue and a 2-nitroglycan as Michael acceptor, which allows controlling the anomeric selection depending on the base used.[30] More recently, Brimble and co-workers described the use of boron trifluoride-diethylether complex ($BF_3 \cdot Et_2O$) as a promoter and tetra-*O*-acetate-2-azido-2-deoxygalactose as a donor to achieve α-selection.[31] Despite the large amount of synthetic approaches to the Tn antigen, many groups are still investigating on new and more effective methodologies. For instance, Andreana and co-workers used *N*-phthalamide-protected amino acids acceptors and thiophenyl glycosyl donors to enhance glycosylation yields.[32] Peregrina and co-workers have just reported a more unusual strategy, using nucleophilic carbohydrates with cyclic sulfamidates.[33]

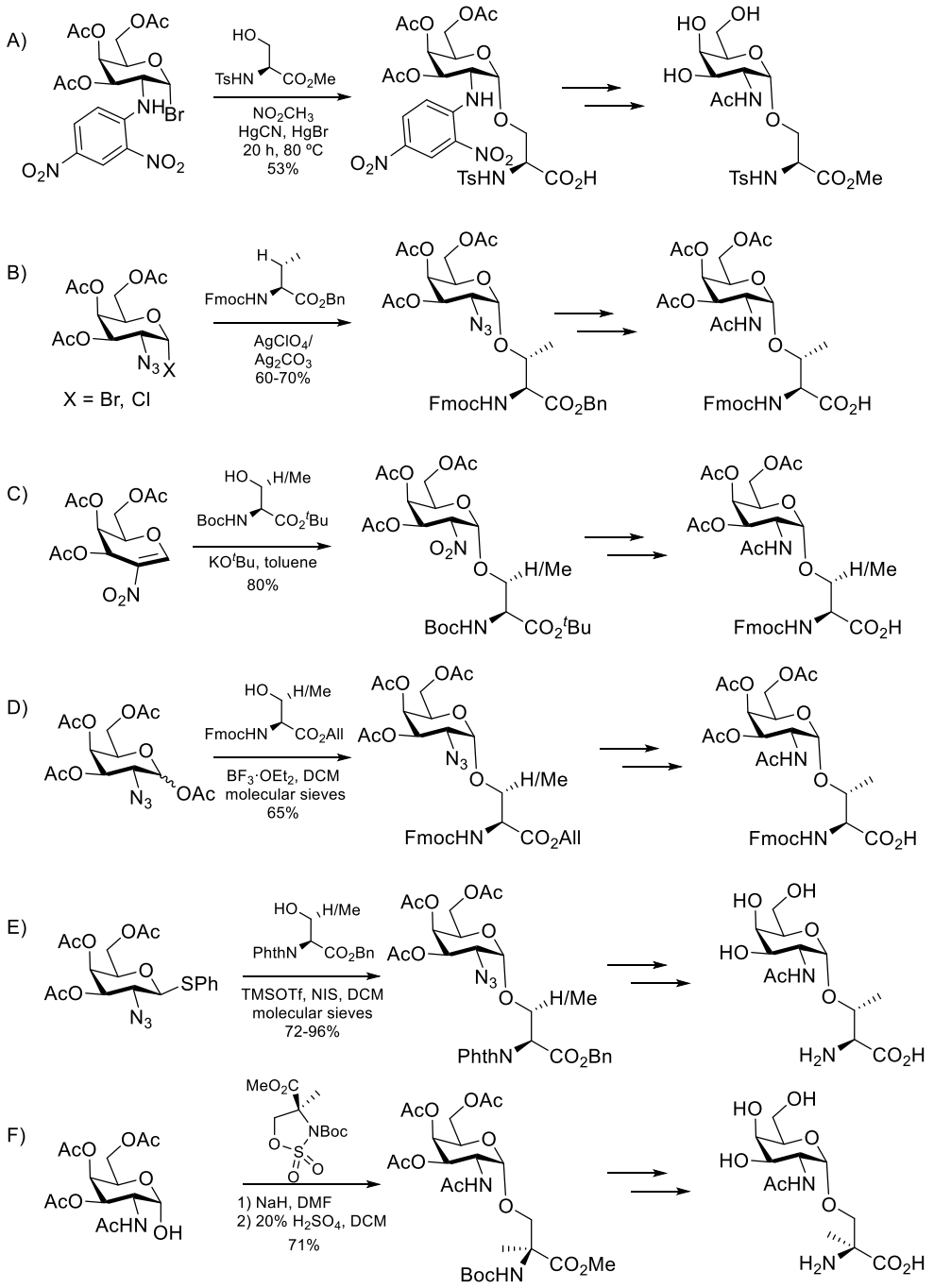

Scheme 1.1. Chemical synthesis of the Tn antigen by glycosylation of Ser or Thr building blocks. A) Kaifu-Osawa's strategy. B) Koenigs-Knorr's strategy. C) Schmidt's strategy. D) Brimble's strategy. E) Andreana's strategy. F) Peregrina's strategy.

Since its discovery, no distinction has been traditionally made between serine or threonine Tn antigens. However, more and more studies show that this is not entirely true. For instance, the presence of GalNAc-Thr residue instead of GalNAc-Ser is crucial for the activity of antifreeze glycoproteins.[34] Along these lines, our research group has been studying these behavior differences during the last years from a structural point of view. It was observed that both derivatives presented extended conformation for the peptide backbone[35,36] and that the carbohydrate moiety of GalNAc-Ser presents a parallel orientation with respect to the peptide backbone, whereas the sugar moiety of GalNAc-Thr is disposed almost perpendicularly to the underlying amino acid, forced by the presence of the β-methyl group. This conformational difference supports the fact that each Tn antigen derivative presents a completely different first hydration shell, including bridging water molecules that are trapped persistently in different pockets arising from such arrangements.[35–37] This characteristic feature, though confirmed by theoretical calculations (figure **1.3**), is currently being investigated by gas-phase IR spectroscopy.

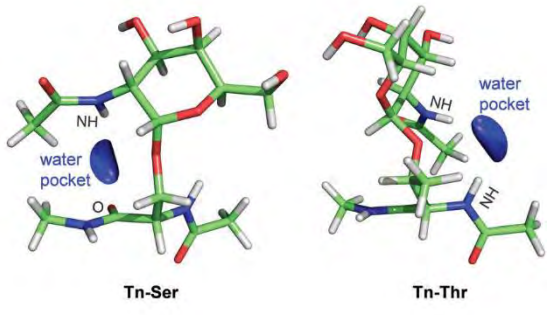

Figure 1.3. Theoretical geometries obtained for GalNAc-Ser (left) and GalNAc-Thr (right) diamides, highlighting the water pocket between the carbohydrate moiety and the peptide backbone.

GalNAc substructure is known to effectively bind to lectins from plants and animals. This feature has been exploited to determine the expression of the Tn antigen in cancer cells.[38] *Vicia villosa* agglutinin (VVA),[39] soybean agglutinin (SBA)[40] or the snail-derived *Helix pomatia* agglutinin (HPA)[41] are a few examples of lectins used for studying expression of the Tn antigen. It has recently been discovered that lectins are able to differentiate between serine- and threonine-Tn antigens.[42] In this way, SBA and VVA prefer the Thr-Tn antigen, whereas HPA prefers the Ser-Tn antigen. This observation is in agreement with the previously mentioned conformational differentiation between both antigens.

1.2. Mucins

Mucins[43–45] are the most abundant glycoproteins in mucus which play a key role in several biological processes,[46–48] such as tissue inflammation, immune response or intercellular recognition. To date, 21 different mucins (MUC1 to MUC21) have been discovered, all of them having a variable number of tandem repeat domains rich in proline (P), serine (S) and threonine (T) residues. The most studied mucin is the so-called MUC1,[49–52] which is constituted by 20 to 125 tandem-type repeats of a core sequence of 20 amino acids: HGV**TS**APD**T**RPAPG**ST**APPA (figure **1.4**). This sequence has five potential *O*-glycosylation sites, two Ser residues and three Thr residues[53] (bold and underlined letters) to which large amounts of *O*-glycans are linked, and three important regions: GVTSA-region is the starting point for GalNAc transferases enzymes;[54] PDTR-region is recognized by anti-MUC1 antibodies;[55,56] and GSTAP-region is recognized by anti-Tn antigen antibodies.[57]

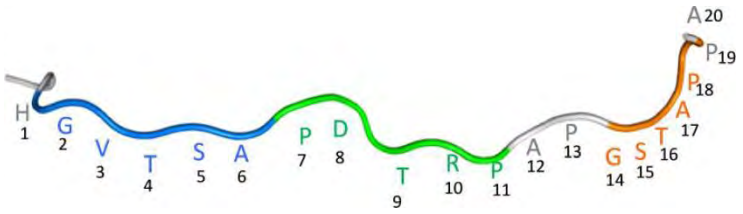

Figure 1.4. Tandem-repeated sequence of MUC1 showing the different regions: GVTSA (blue), PDTR (green) and GSTAP (orange).

The highly dense thicket of *O*-glycans in healthy cell membranes is always initiated by α-GalNAc, forming the Tn antigen (figure **1.1**). However, tumor MUC1 usually presents low glycosylation and abnormal sugar chain extensions as result of the malfunction of some glycosyltransferases (figure **1.5**). This fact results in an exposure of antigens on the surface of cancer cells.[58–61] Consequently, immune system would be able to recognize those antigens and trigger an immune response.

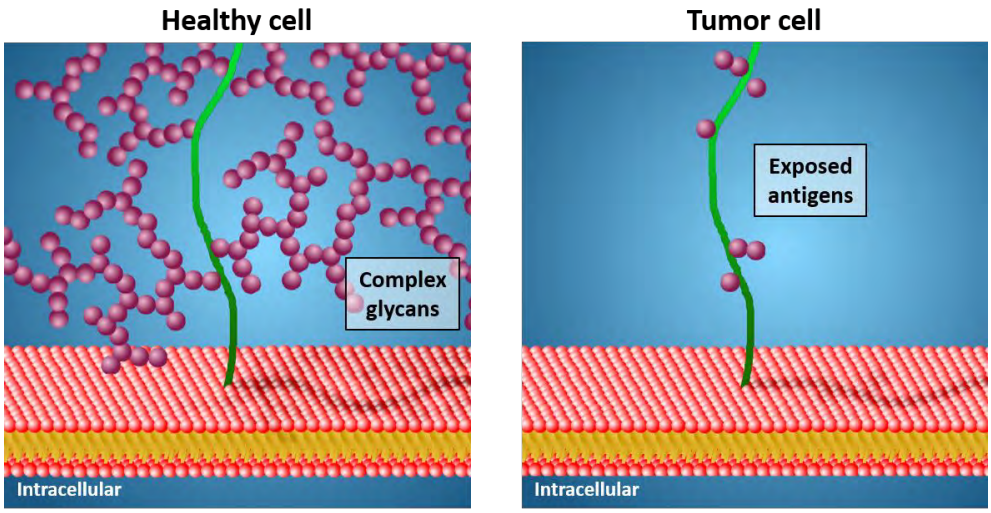

Figure 1.5. Different glycosylation patterns in healthy and tumor cells.

Several monoclonal antibodies (mAbs) are able to recognize these exposed antigens, binding specifically to cancer cells. For instance, the sequence PDTR of MUC1 is a well-known immunogenic epitope recognized by anti-MUC1 antibodies[62,63] like mAb SM3, which has great potential for use in the early diagnosis and treatment of breast cancer.[64] X-ray structures of naked and glycosylated MUC1 fragments in complex with scFv-SM3 antibody have recently been reported by Corzana and co-workers (figure **1.6**).[65] Again, it was demonstrated that threonine and serine Tn antigens are not equivalent in either their binding affinities and conformational preferences.

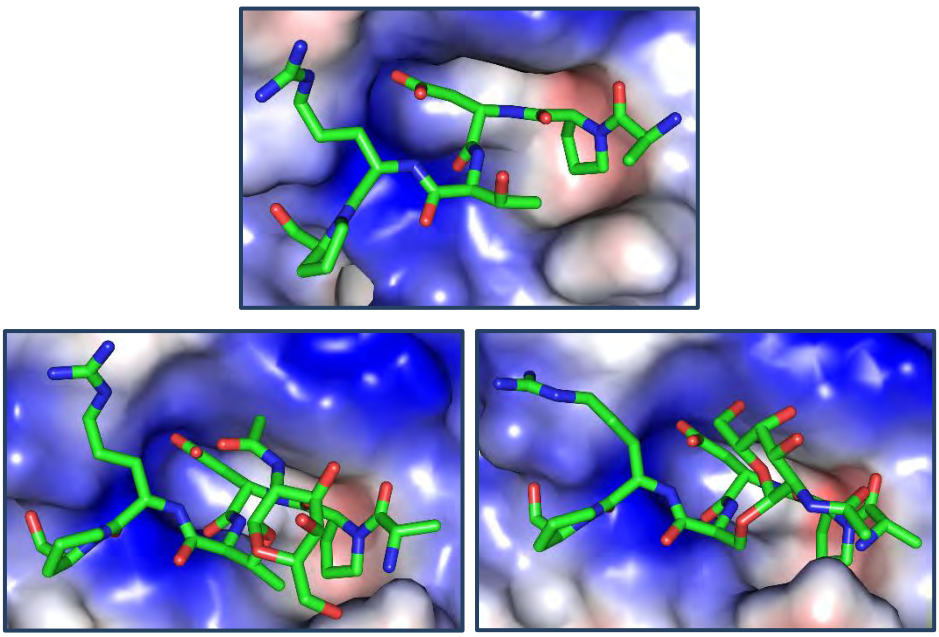

Figure 1.6. X-ray structures obtained for scFv-SM3 antibody in complex with the naked APDTRP sequence (top), the threonine-glycosylated APDT*RP sequence (bottom-left), and the serine-glycosylated APDS*RP sequence (bottom-right).

It has been recently reported that interactions between TACAs and lectins present in cells of the immune system play a key role in the metastatic cascade of some carcinoma cells.[18,66,67] Thus, MUC1 mucin is considered a

promising target for the development of cancer immunotherapy (carbohydrate-based vaccines).[68–72] In this sense, Kunz and co-workers[73] reported in 2001 the first synthesis and immunological evaluation of a fully synthetic two-component cancer therapeutic vaccine (Figure **1.7**). It consisted of a glycododecapeptide from tumor-associated MUC1 (GVT*SAPDTR-PAP, T* = Sialyl-Tn) and a T-cell epitope peptide (YSYFPSV) from tetanus toxoid as immunostimulant, both connected by a flexible spacer. Unfortunately, the overall immune response produced by this vaccine was weak.

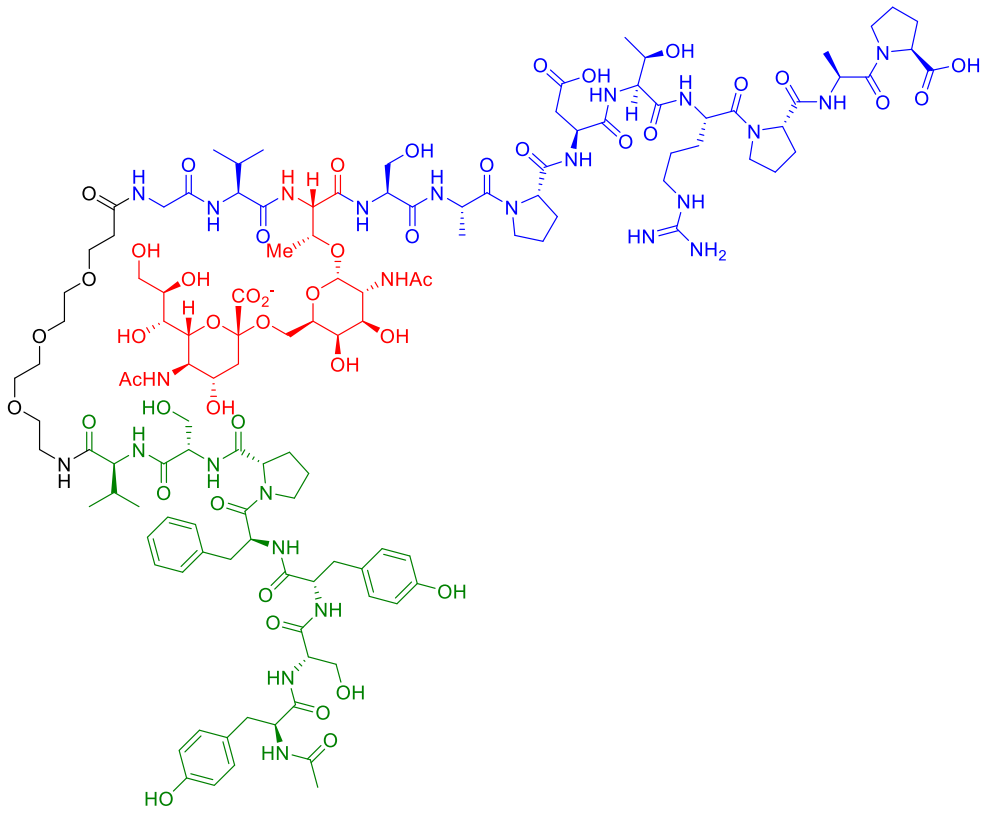

Figure 1.7. Chemical structure of the two-component vaccine. Ac-YSYFPSV-spacer-GVT*SAPDTRPAP-OH, T* = Sialyl-Tn.

Since then, several research groups[74–87] have been seeking to develop "multicomponent" approaches, looking for enhancements in immune

response. As an example, Boons and co-workers[24] developed a three-component vaccine combining a glycodecapeptide from tumor-associated MUC1 (TSAPDT*RPAP, T* = Tn antigen), a T-cell epitope peptide from Poliovirus (KLFAVWKITYKDT) and an immunoadjuvant lipopeptide (Pam_3CysSK_4) which showed strong induction in immune responses in mice and the elicited antibodies were able to reduce the tumor growth (figure **1.8**).

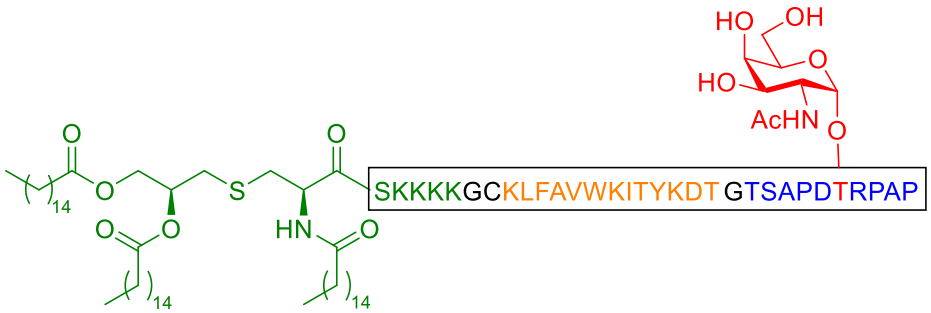

Figure 1.8. Chemical structure of the three-component vaccine. $Pam_3CysSKKKK$-GCKLFAVWKITYKDTGTSAPDT*RPAP, T* = Tn antigen.

Unluckily, most of the carbohydrate-based vaccines have failed in clinical trials despite the massive efforts. One reason to which this lack of success has been attributed is the immunotolerance or resistance to carbohydrate antibody efficacy.[88] Although anti-Tn, anti-sTn or anti-TF antibodies have been detected in many individuals, the immune response was certainly insufficient. This is usually connected to the short biological half-life carbohydrates have due to chemical or enzymatic liability of the glycosidic bond. This feature has created a great deal of interest in synthesizing non-natural glycopeptides analogs, which would be more resistant to degradation and would therefore provide stronger and longer lasting immunogenicity and protective efficacy.

1.3. Mimicking the Tn antigen

Synthesizing analogs of natural carbohydrates and glycopeptides[89–91] allows us to better understand different biochemical processes, and offers a collection of new candidates for biological targets. In this regard, carbohydrate mimics have been recently introduced into carbohydrate-based cancer vaccines aiming to improve their immunogenicity.[92–95] There are three main types of glycopeptide modifications:

a) Carbohydrate modification

Some of the most common alterations in carbohydrate chemistry are azasugars,[96] carbasugars[97] or thiosugars,[98] where the endocyclic oxygen is replaced by a nitrogen, a carbon or a sulfur atom respectively, enhancing the stability towards degradation (figure **1.9**).

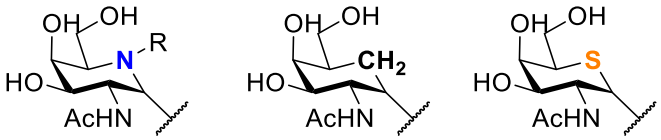

Figure 1.9. Structural comparison of aza-, carba- and thiosugars.

Another approach would be the incorporation of fluorine atoms into carbohydrate moieties of antigens, which has shown to be a promising approach to improve immunogenicity (figure **1.10**).[99–105]

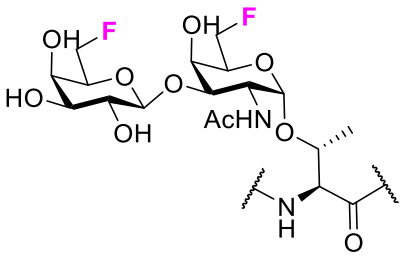

Figure 1.10. Difluoro-T-antigen incorporated in a carbohydrate-based vaccine.[100]

b) Glycosidic linkage modification

Substitution of the exocyclic oxygen of glycosyl-amino-acids by a carbon[106] or sulfur[107] atom is an alternative methodology to improve their stability towards degradation (figure **1.11**).

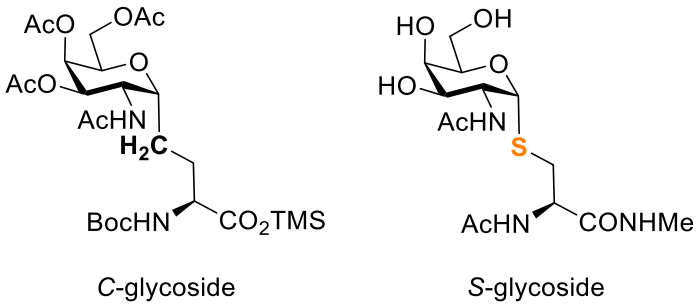

Figure 1.11. Chemical structure of a *C*-glycoside[108] and an *S*-glycoside,[109] analogs of the Tn antigen.

Increasing the distance between the carbohydrate moiety and the underlying amino acid has also been proposed, incorporating homoserine,[110] or *O*-(mercaptopropyl)serine/threonine[111] in mucin-like glycopeptide antigen analogues (figure **1.12**).

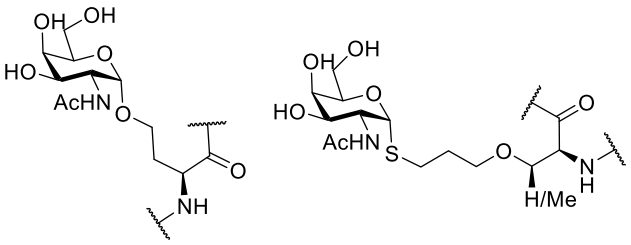

Homoserine Tn antigen analogue

O-(mercaptopropyl)serine/threonine Tn antigen analogue

Figure 1.12. Chemical structure of elongated Tn antigen analogs.

c) Amino acid modification

Introduction of unnatural amino acids in carbohydrate-based vaccines has shown to be a promising approach. As demonstrated by Corzana and co-workers,[112] incorporation of a glycosylated α-methylserine residue in a MUC1-based vaccine produced antibodies able to recognize native MUC1 present on cancer cells in mice (figure **1.13**).

Figure 1.13. Three-component carbohydrate-based vaccine incorporating glycosylated α-methylserine as aTn antigen analog.

Similarly, substitution of a natural proline residue by fluoro- or difluoroproline at a certain position enhanced the affinity towards anti-MUC1 antibodies, making these derivatives promising candidates for early detection of tumors (figure **1.14**).[113]

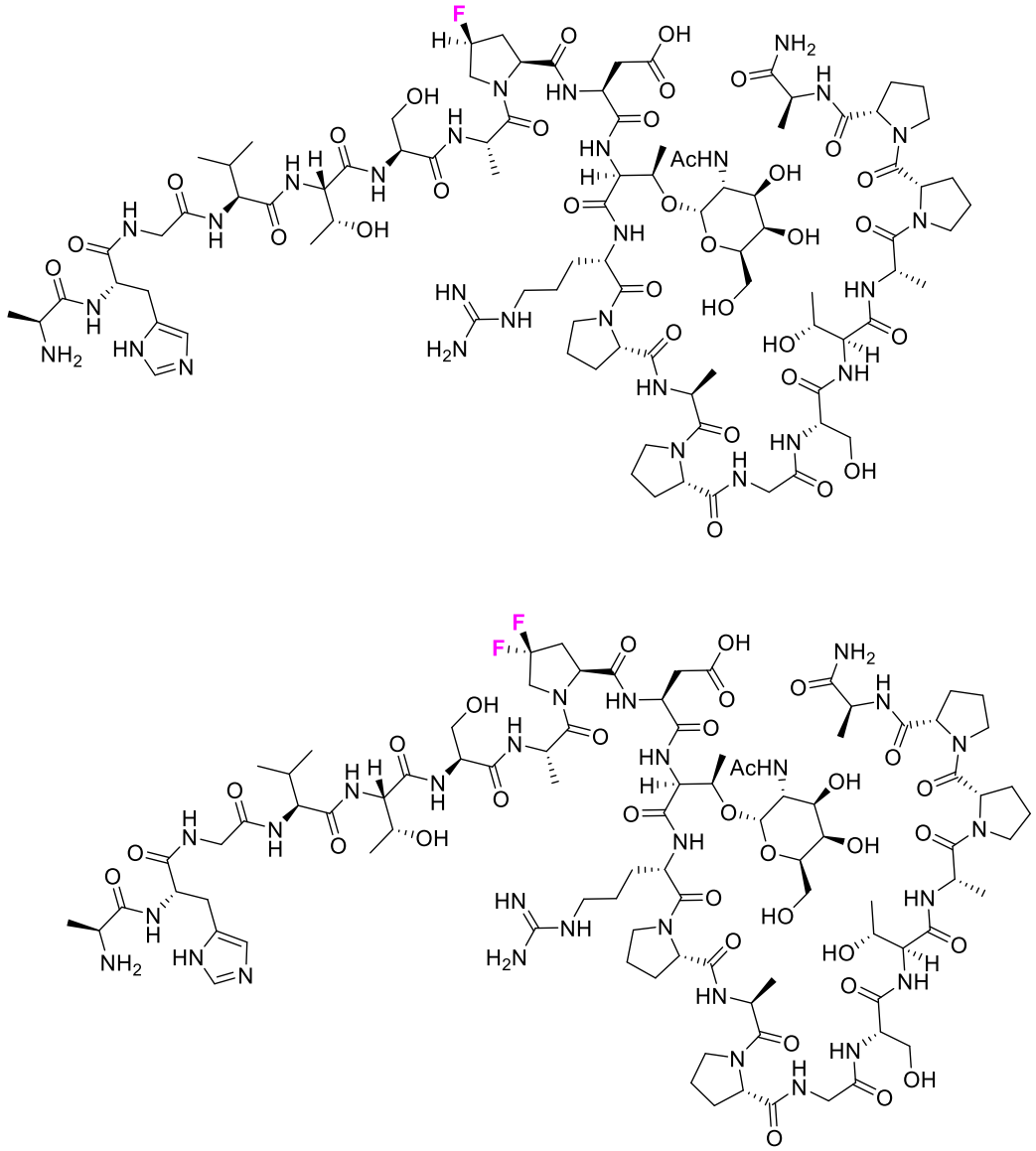

Figure 1.14. Rational-designed fluorinated (top) and difluorinated (bottom) MUC1. AHGVTSAfPDT*RPAPGSTAPPA. T* = Tn antigen.

1.4. Glycosidases

Glycosidases, or glycoside hydrolases, are enzymes that catalyze the hydrolysis of glycosidic bonds (figure **1.15**). They are involved in a large number of biological processes, such as degradation of polysaccharides or the deglycosylation-reglycosylation sequence in the maturation and functionalization of glycoproteins and are, therefore, essential for all living organisms that rely on carbohydrates processing. Any malfunction of these enzymes usually leads to meaningful biological and pathological consequences. This has hence boosted research in compounds that interfere with their activity as potential drug candidates.[114–117]

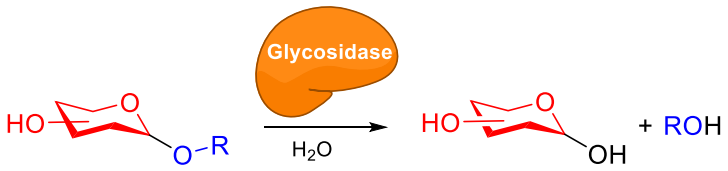

Figure 1.15. Glycoside hydrolysis catalyzed by a glycosidase.

Polyhydroxylated piperidines (azasugars), such as 1-deoxynojirimicin (DNJ) or the bicyclic analog castanospermine (CS), are natural products that have been investigated as glycosidase inhibitors[114–123] due to their structural analogy to monosaccharides (figure **1.16**). This similarity allows them to compete with the natural substrate for the active site of glycosidases, acting as inhibitors. However, the low stability of aminoacetal functional groups does not allow the structure of the putative carbohydrate substrates to be completely reproduced, which is usually translated into low selectivities. Additionally, the lack of a defined anomeric configuration often results in simultaneous inhibition of glycosidases that act on anomeric substrates, i.e.

α- and β-glucosidases, which is a severe disadvantage for clinical applications.[124]

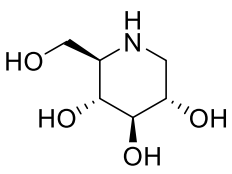

1-deoxynojirimycin (DNJ)

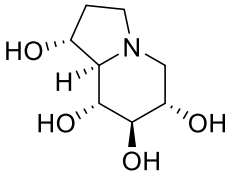

castanospermine (CS)

Figure 1.16. Structures of DNJ and CS.

This lack of specificity in glycosidase inhibition has led to the design of analogs of naturally occurring molecules targeting medically relevant enzymes.[125–136] Molecular models that mirror both the glycon- and aglycon-like parts of carbohydrates and that possess a well-defined anomeric or pseudo-anomeric configuration are more suitable for this purpose.[137] In this context, sp^2-iminosugars,[138–142] in which a nitrogen atom is endocyclic and forming part of an oxazolidinone ring, facilitate the incorporation of pseudo-anomeric substituents via *O*-, *S*-, or *N*-glycosidic binding (figure **1.17**). This family of compounds shows total discrimination between α- and β-glycosidase enzymes and has been used for designing specific α-glucosidase inhibitors which showed anticancer and antileishmanial properties.[143–148]

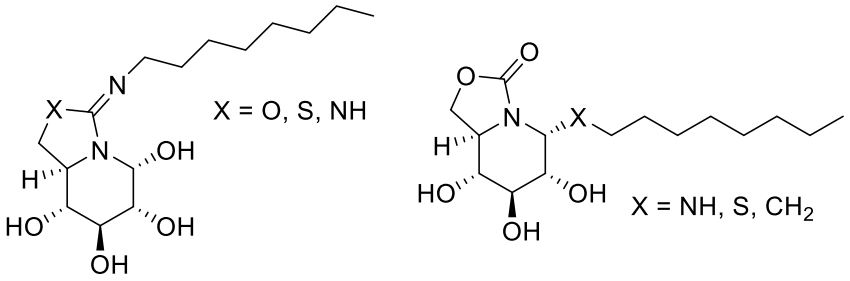

Figure 1.17. sp^2-iminosugars.

On the other hand, *N*-alkylated bicyclic isoureas and guanidines derived from aminocyclitol scaffolds showed a very selective inhibition ratios against human lysosomal β-glucosidase, behaving as strong pharmacological chaperones with potential for the treatment of Gaucher disease (figure **1.18**).[149]

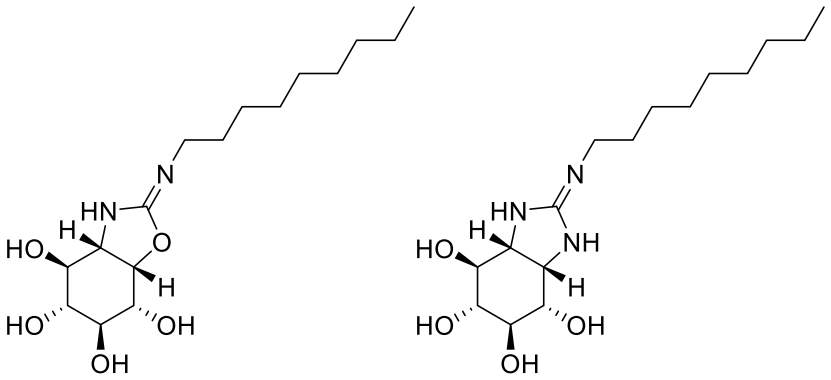

Figure 1.18. Bicyclic isoureas and guadinines

Interestingly, non-iminosugar-type *N*-alkylated bicyclic scaffolds maintaining the pyranose ring have also shown very selective inhibitory activities with strong pharmacological chaperone potential. In this way, Thiamet-G, a fused pyranose-thiazoline derivative, acts as a potent inhibitor of β-*N*-acetylglucosaminidase and is currently being investigated as a potential

therapeutic target for the treatment of Alzheimer's disease.[150–155] Along these lines, derivatives of the pyranose-sulfanyl-1,3-oxazoline family (PSO) have been recently reported as β-glucosidase inhibitors, whose activity is highly dependent on the nature of the *S*-substituent (figure **1.19**). Some of these derivatives have been identified as new pharmacological chaperones for Gaucher disease.[156]

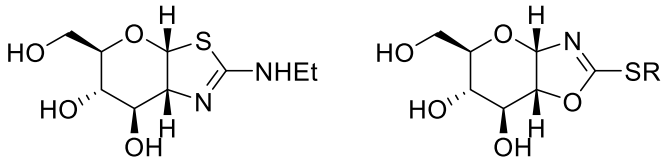

Figure 1.19. Structure of Thiamet-G and PSO derivatives.

In contrast, pyrano[3,2-*b*]pyrrole scaffolds, which have also been proposed as a possibility for synthesizing glycosidase inhibitors,[157,158] have attracted less interest, probably due to the lack of effective synthetic methods (figure **1.20**). Only a few molecules combining a pyrrole segment to a 2-amino-*C*-glycoside backbone, which act as glycosidase inhibitors have been reported. In addition, they show moderate inhibition of galactosidases without differentiating between α- and β-anomers. This seems to have slowed down optimization of the affinity and selectivity towards biomedically relevant enzyme targets.[159–162]

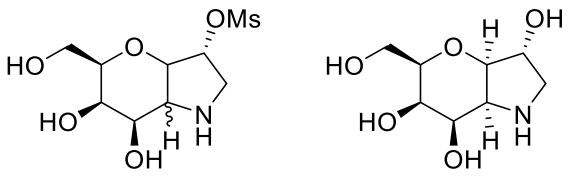

Figure 1.20. Pyrano[3,2-*b*]pyrrole derivatives.

The development of efficient synthetic routes affording this kind of molecules with structurally diversity-oriented strategy is therefore of great interest. The access to conformationally locked structures able to bear different substituents is particularly attractive[163–166] since many medically relevant glycosidases act on substrates with branched aglycone segments.[167]

1.5. Main goals

Considering the importance of designing new TACAs able to mimic the behavior of natural antigens (Tn) and glycoproteins (MUC1) along with the need for new selective glycosidase inhibitors, we propose in this Doctoral Thesis the synthesis of conformationally locked glyco-amino-acids as structural analogs of the Tn antigen, and their subsequent incorporation into MUC1-like glycopeptides. The conformational space of these new analogs will be analyzed combining experimental data (NMR, X-ray diffraction) with computational methods (MD, QM).

Hence, *Chapter 2* is focused on the synthesis of new *C*-glyco-amino-acids derived from serine analogs of the Tn antigen, which showed certain conformational restraints due to covalent bonds existing between the carbohydrate and amino acid moieties.

Due to the structural similarities of these new *C*-glyco-amino-acids with several glycosidase inhibitors and pharmacological chaperones, the behavior of some of these derivatives as glycosidase inhibitors and pharmacological chaperones is addressed throughout *Chapter 3*.

On the other hand, the glycosylation reaction between hydroxylated amino acids Ser and Thr, and non-natural sp^2-iminosugars (Gal-, Glc-, GalNAc- and GlcNAc-like) is discussed in *Chapter 4*, as well as the incorporation of this new non-natural *O*-glycosyl-amino-acids into MUC1-like glycopeptides and, finally, into a sp^2-iminosugar-based vaccine.

The most relevant results obtained at each international short-term research stay (Brimble's and van der Donk's groups, respectively), comprising the total synthesis of the diglycosylated bacteriocin Glycocin F and an analog incorporating an unnatural glycosylated amino acid, and the computational study of the lysinoalanine formation mechanism in duramycin catalyzed by DurN, will be briefly mentioned in *Chapter 5*.

1.6. References

(1) Lis, H.; Sharon, N. *Chem. Rev.* **1998**, *98*, 637–674.
(2) Koeller, K. M.; Wong, C.-H. *Nat. Biotechnol.* **2000**, *18*, 835–841.
(3) Maeder, T. *Sci. Am.* **2002**, *287*, 40–47.
(4) Rojo, J.; Morales, J. C.; Penades, S. *Top. Curr. Chem.* **2002**, *218*, 45–92.
(5) Bertozzi, C. R.; Kiessling, L. L. *Science* **2001**, *291*, 2357–2364.
(6) Fukuda, M. *Bioorg. Med. Chem.* **1995**, *3*, 207–215.
(7) Chappell, D.; Jacob, M.; Hofmann-Kiefer, K.; Conzen, P.; Rehm, M. *Anesthesiology* **2008**, *109*, 723–740.
(8) Ju, T.; Otto, V. I.; Cummings, R. D. *Angew. Chem. Int. Ed.* **2011**, *50*, 1770–1791.
(9) Moreau, R.; Dausset, J.; Bernard, J.; Moullec, J. *Bull. Mem. Soc. Med. Hop. Paris* **1957**, *73*, 569–587.
(10) Dahr, W.; Uhlenbruck, G.; Gunson, H. H.; Hart, M. *Vox Sang.* **1975**, *29*, 36–50.
(11) Dahr, W.; Uhlenbruck, G.; Bird, G. W. G. *Vox Sang.* **1974**, *27*, 29–42.
(12) Springer, G. F.; Desai, P. R.; Banatwala, I. *Naturwissenschaften* **1974**, *61*, 457–458.
(13) Davidson, B.; Berner, A.; Nesland, J. M.; Risberg, B.; Kristensen, G. B.; Tropé, C. G.; Bryne, M. *Hum. Pathol.* **2000**, *31*, 1081–1087.

(14) Costa, C.; Pereira, S.; Lima, L.; Peixoto, A.; Fernandes, E.; Neves, D.; Neves, M.; Gaiteiro, C.; Tavares, A.; Da Costa, R. M. G.; Cruz, R.; Amaro, T.; Oliveira, P. A.; Ferreira, J. A.; Santos, L. L. *PLoS One* **2015**, *10,* e0141253.
(15) Hirao, T.; Sakamoto, Y.; Kamada, M.; Hamada, S.-I.; Aono, T. *Cancer* **1993**, *72*, 154–159.
(16) Terasawa, K.; Furumoto, H.; Kamada, M.; Aono, T. *Cancer Res.* **1996**, *56*, 2229–2232.
(17) Itzkowitz, S. H.; Yuan, M.; Montgomery, C. K.; Kjeldsen, T.; Takahashi, H. K.; Bigbee, W. L.; Kim, Y. S. *Cancer Res.* **1989**, *49*, 197–204.
(18) Byrd, J. C.; Bresalier, R. S. *Cancer Metastasis Rev.* **2004**, *23*, 77–99.
(19) Lopez-Ferrer, A.; Barranco, C.; De Bolos, C. *Am. J. Clin. Pathol.* **2002**, *118*, 749–755.
(20) Ohshio, G.; Imamura, T.; Imamura, M.; Yamabe, H.; Sakahara, H.; Nakada, H.; Yamashina, I. *J. Cancer Res. Clin. Oncol.* **1995**, *121*, 247–252.
(21) Remmers, N.; Anderson, J. M.; Linde, E. M.; DiMaio, D. J.; Lazenby, A. J.; Wandall, H. H.; Mandel, U.; Clausen, H.; Yu, F.; Hollingsworth, M. A. *Clin. Cancer Res.* **2013**, *19*, 1981–1993.
(22) Zhang, S.; Zhang, H. S.; Reuter, V. E.; Slovin, S. F.; Scher, H. I.; Livingston, P. O. *Clin. Cancer Res.* **1998**, *4*, 295–302.
(23) Fu, C.; Zhao, H.; Wang, Y.; Cai, H.; Xiao, Y.; Zeng, Y.; Chen, H. *HLA* **2016**, *88*, 275–286.
(24) Lakshminarayanan, V.; Thompson, P.; Wolfert, M. A.; Buskas, T.; Bradley, J. M.; Pathangey, L. B.; Madsen, C. S.; Cohen, P. A.; Gendler, S. J.; Boons, G.-J. *Proc. Natl. Acad. Sci.* **2012**, *109*, 261–266.
(25) Heimburg-Molinaro, J.; Lum, M.; Vijay, G.; Jain, M.; Almogren, A.; Rittenhouse-Olson, K. *Vaccine* **2011**, *29*, 8802–8826.
(26) Westerlind, U.; Schröder, H.; Hobel, A.; Gaidzik, N.; Kaiser, A.; Niemeyer, C. M.; Schmitt, E.; Waldmann, H.; Kunz, H. *Angew. Chem. Int. Ed.* **2009**, *48*, 8263–8267.
(27) Hansen, J. E.; Nielsen, C.; Arendrup, M.; Olofsson, S.; Mathiesen, L.; Nielsen, J. O.; Clausen, H. *J. Virol.* **1991**, *65*, 6461–6467.
(28) Kaifu, R.; Osawa, T. *Carbohydr. Res.* **1977**, *58*, 235–239.
(29) Paulsen, H.; Hölck, J.-P. *Carbohydr. Res.* **1982**, *109*, 89–107.
(30) Winterfeld, G. A.; Ito, Y.; Ogawa, T.; Schmidt, R. R. *Eur. J. Org. Chem.* **1999**, 1167–1171.
(31) Lee, D. J.; Harris, P. W. R.; Kowalczyk, R.; Dunbar, P. R.; Brimble, M. A. *Synthesis* **2010**, 763–769.
(32) Shaik, A. A.; Nishat, S.; Andreana, P. R. *Org. Lett.* **2015**, *17*, 2582–2585.
(33) Tovillas, P.; García-González, I.; Oroz, P.; Mazo, N.; Avenoza, A.; Corzana, F.; Jiménez-Osés, G.; Busto, J. H.; Peregrina, J. M. *J. Org. Chem.* **2018**, *83*, 4973–4980.
(34) Tachibana, Y.; Fletcher, G. L.; Fujitani, N.; Tsuda, S.; Monde, K.; Nishimura, S. I. *Angew. Chem. Int. Ed.* **2004**, *43*, 856–870.
(35) Corzana, F.; Busto, J. H.; Jiménez-Osés, G.; Asensio, J. L.; Jiménez-Barbero, J.; Peregrina, J. M.; Avenoza, A. *J. Am. Chem. Soc.* **2006**, *128*, 14640–14648.

(36) Corzana, F.; Busto, J. H.; Jiménez-Osés, G.; De Luis, M. G.; Asensio, J. L.; Jiménez-Barbero, J.; Peregrina, J. M.; Avenoza, A. *J. Am. Chem. Soc.* **2007**, *129*, 9458–9467.
(37) Corzana, F.; Busto, J. H.; De Luis, M. G.; Jiménez-Barbero, J.; Avenoza, A.; Peregrina, J. M. *Chem. Eur. J.* **2009**, *15*, 3863–3874.
(38) Konska, G.; Guerry, M.; Caldefie-Chezet, F.; De Latour, M.; Guillot, J. *Oncol. Rep.* **2006**, *15*, 305–310.
(39) Tollefsen, S. E.; Kornfeld, R. *J. Biol. Chem.* **1983**, *258*, 5172–5176.
(40) Dam, T. K.; Gerken, T. A.; Cavada, B. S.; Nascimento, K. S.; Moura, T. R.; Brewer, C. F. *J. Biol. Chem.* **2007**, *282*, 28256–28263.
(41) Hammarström, S.; Murphy, L. A.; Goldstein, I. J.; Etzler, M. E. *Biochemistry* **1977**, *16*, 2750–2755.
(42) Madariaga, D.; Martínez-Sáez, N.; Somovilla, V. J.; García-García, L.; Berbis, M. Á.; Valero-Gónzalez, J.; Martín-Santamaría, S.; Hurtado-Guerrero, R.; Asensio, J. L.; Jiménez-Barbero, J.; Avenoza, A.; Busto, J. H.; Corzana, F.; Peregrina, J. M. *Chem. Eur. J.* **2014**, *20*, 12616–12627.
(43) Strous, G. J.; Dekker, J. *Crit. Rev. Biochem. Mol. Biol.* **1992**, *27*, 57–92.
(44) Hang, H. C.; Bertozzi, C. R. *Bioorg. Med. Chem.* **2005**, *13*, 5021–5034.
(45) Fumoto, M.; Hinou, H.; Ohta, T.; Ito, T.; Yamada, K.; Takimoto, A.; Kondo, H.; Shimizu, H.; Inazu, T.; Nakahara, Y.; Nishimura, S. I. *J. Am. Chem. Soc.* **2005**, *127*, 11804–11818.
(46) Dwek, R. A. *Chem. Rev.* **1996**, *96*, 683–720.
(47) Sears, P.; Wong, C. H. *Cell. Mol. Life Sci.* **1998**, *54*, 223–252.
(48) Gaidzik, N.; Westerlind, U.; Kunz, H. *Chem. Soc. Rev.* **2013**, *42*, 4421.
(49) Taylor-Papadimitriou, J.; Burchell, J.; Miles, D. W.; Dalziel, M. *Biochim. Biophys. Acta - Mol. Basis Dis.* **1999**, *1455*, 301–313.
(50) Taylor-Papadimitriou, J.; Burchell, J. M.; Plunkett, T.; Graham, R.; Correa, I.; Miles, D.; Smith, M. *J. Mammary Gland Biol. Neoplasia* **2002**, *7*, 209–221.
(51) Parry, A. L.; Clemson, N. A.; Ellis, J.; Bernhard, S. S. R.; Davis, B. G.; Cameron, N. R. *J. Am. Chem. Soc.* **2013**, *135*, 9362–9365.
(52) Martínez-Sáez, N.; Peregrina, J. M.; Corzana, F. *Chem. Soc. Rev.* **2017**, *7154*, 7154–7175.
(53) Müller, S.; Goletz, S.; Packer, N.; Gooley, A.; Lawson, A. M.; Hanisch, F.-G. *J. Biol. Chem.* **1997**, *272*, 24780–24793.
(54) Dziadek, S.; Griesinger, C.; Kunz, H.; Reinscheid, U. M. *Chem. Eur. J.* **2006**, *12*, 4981–4993.
(55) Takeuchi, H.; Kato, K.; Denda-Nagai, K.; Hanisch, F.-G.; Clausen, H.; Irimura, T. *J. Immunol. Methods* **2002**, *270*, 199–209.
(56) Burchell, J.; Gendler, S.; Taylor-Papadimitriou, J.; Girling, A.; Lewis, A.; Millis, R.; Lamport, D. *Cancer Res.* **1987**, *47*, 5476–5482.
(57) Huang, Z. H.; Shi, L.; Ma, J. W.; Sun, Z. Y.; Cai, H.; Chen, Y. X.; Zhao, Y. F.; Li, Y. M. *J. Am. Chem. Soc.* **2012**, *134*, 8730–8733.
(58) Sell, S. *Hum. Pathol.* **1990**, *21*, 1003–1019.
(59) Hakomori, S. I.; Zhang, Y. *Chem. Biol.* **1997**, *4*, 97–104.
(60) Taylor-Papadimitriou, J.; Epenetos, A. A. *Trends Biotechnol.* **1994**, *12*, 227–

233.
(61) Gabius, H. J. *Eur. J. Biochem.* **1997**, *243*, 543–576.
(62) Gendler, S.; Taylor-Papadimitriou, J.; Duhig, T.; Rothbard, J.; Burchel, J. *J. Biol. Chem.* **1988**, *263*, 12820–12823.
(63) Karsten, U.; Serttas, N.; Paulsen, H.; Danielczyk, A.; Goletz, S. *Glycobiology* **2004**, *14*, 681–692.
(64) Dokurno, P.; Bates, P. A.; Band, H. A.; Stewart, L. M. D.; Lally, J. M.; Burchell, J. M.; Taylor-Papadimitriou, J.; Snary, D.; Sternberg, M. J. E.; Freemont, P. S. *J. Mol. Biol.* **1998**, *284*, 713–728.
(65) Martínez-Sáez, N.; Castro-López, J.; Valero-González, J.; Madariaga, D.; Compañón, I.; Somovilla, V. J.; Salvadó, M.; Asensio, J. L.; Jiménez-Barbero, J.; Avenoza, A.; Busto, J. H.; Bernardes, G. J. L.; Peregrina, J. M.; Hurtado-Guerrero, R.; Corzana, F. *Angew. Chem. Int. Ed.* **2015**, *54*, 9830–9834.
(66) Zhao, Q.; Guo, X.; Nash, G. B.; Stone, P. C.; Hilkens, J.; Rhodes, J. M.; Yu, L. G. *Cancer Res.* **2009**, *69*, 6799–6806.
(67) Inamdar, S. R.; Savanur, M. A.; Eligar, S. M.; Chachadi, V. B.; Nagre, N. N.; Chen, C.; Barclays, M.; Ingle, A.; Mahajan, P.; Borges, A.; Shastry, P.; Kalraiya, R. D.; Swamy, B. M.; Rhodes, J. M.; Yu, L. G. *Glycobiology* **2012**, *22*, 1227–1235.
(68) Buskas, T.; Thompson, P.; Boons, G.-J. *Chem. Commun.* **2009**, *0*, 5335.
(69) Gaidzik, N.; Westerlind, U.; Kunz, H. *Chem. Soc. Rev.* **2013**, *42*, 4421.
(70) Wolfert, M. A.; Boons, G.-J. *Nat. Chem. Biol.* **2013**, *9*, 776–784.
(71) Wilson, R. M.; Danishefsky, S. J. *J. Am. Chem. Soc.* **2013**, *135*, 14462–14472.
(72) Cai, H.; Sun, Z. Y.; Chen, M. S.; Zhao, Y. F.; Kunz, H.; Li, Y. M. *Angew. Chem. Int. Ed.* **2014**, *53*, 1699–1703.
(73) Keil, S.; Claus, C.; Dippold, W.; Kunz, H. *Angew. Chem. Int. Ed.* **2001**, *40*, 366–369.
(74) Brocke, C.; Kunz, H. *Bioorg. Med. Chem.* **2002**, *10*, 3085–3112.
(75) Dziadek, S.; Kunz, H. *Chem. Rec.* **2004**, *3*, 308–321.
(76) Lai, Z.; Schreiber, J. R. *Vaccine* **2009**, *27*, 3137–3144.
(77) Costantino, P.; Rappuoli, R.; Berti, F. *Expert Opin. Drug Discov.* **2011**, *6*, 1045–1066.
(78) Tarp, M. A.; Clausen, H. *Biochim. Biophys. Acta - Gen. Subj.* **2008**, *1780*, 546–563.
(79) Hanisch, F.-G.; Ninkovic, T. *Curr. Protein Pept. Sci.* **2006**, *7*, 307–315.
(80) Jaracz, S.; Chen, J.; Kuznetsova, L. V; Ojima, I. *Bioorg. Med. Chem.* **2005**, *13*, 5043–5054.
(81) Danishefsky, S.; Allen, J. *Angew. Chem. Int. Ed.* **2000**, *39*, 836–863.
(82) Slovin, S. F.; Ragupathi, G.; Musselli, C.; Olkiewicz, K.; Verbel, D.; Kuduk, S. D.; Schwarz, J. B.; Sames, D.; Danishefsky, S.; Livingston, P. O.; Scher, H. I. *J. Clin. Oncol.* **2003**, *21*, 4292–4298.
(83) Galonić, D. P.; Gin, D. Y. *Nature* **2007**, *446*, 1000–1007.
(84) Hang, H. C.; Bertozzi, C. R. *Bioorg. Med. Chem.* **2005**, *13*, 5021–5034.
(85) Dube, D. H.; Bertozzi, C. R. *Nat. Rev. Drug Discov.* **2005**, *4*, 477–488.
(86) Ragupathi, G.; Coltart, D. M.; Williams, L. J.; Koide, F.; Kagan, E.; Allen, J.;

Harris, C.; Glunz, P. W.; Livingston, P. O.; Danishefsky, S. J. *Proc. Natl. Acad. Sci.* **2002**, *99*, 13699–13704.
(87) Buskas, T.; Ingale, S.; Boons, G. J. *Angew. Chem. Int. Ed.* **2005**, *44*, 5985–5988.
(88) Beatty, G. L.; Gladney, W. L. *Clin. Cancer Res.* **2015**, *21*, 687–692.
(89) Westerlind, U. *Beilstein J. Org. Chem.* **2012**, *8*, 804–818.
(90) Jiménez-Barbero, J.; Dragoni, E.; Venturis, C.; Nannucci, F.; Ardá, A.; Fontanella, M.; André, S.; Cañada, F. J.; Gabius, H. J.; Nativi, C. *Chem. Eur. J.* **2009**, *15*, 10423–10431.
(91) Koester, D. C.; Holkenbrink, A.; Werz, D. B. *Synthesis* **2010**, 3217–3242.
(92) Guo, Z.; Wang, Q. *Curr. Opin. Chem. Biol.* **2009**, *13*, 608–617.
(93) Wang, Q.; Ekanayaka, S. A.; Wu, J.; Zhang, J.; Guo, Z. *Bioconjug. Chem.* **2008**, *19*, 2060–2067.
(94) Wang, Q.; Guo, Z. *ACS Med. Chem. Lett.* **2011**, *2*, 373–378.
(95) Liu, C. C.; Ye, X. S. *Glycoconj. J.* **2012**, *29*, 259–271.
(96) Asano, N. In *Glycoscience*; Springer Berlin Heidelberg: Berlin, Heidelberg, 2008; pp 1887–1911.
(97) Kobayashi, Y. In *Glycoscience*; 2008; pp 1915–1997.
(98) Steiner, A.; Stütz, A.; Wrodnigg, T. In *Glycoscience*; Springer Berlin Heidelberg: Berlin, Heidelberg, 2008; pp 1999–2020.
(99) Mersch, C.; Wagner, S.; Hoffmann-Röder, A. *Synlett* **2009**, 2167–2171.
(100) Hoffmann-Röder, A.; Kaiser, A.; Wagner, S.; Gaidzik, N.; Kowalczyk, D.; Westerlind, U.; Gerlitzki, B.; Schmitt, E.; Kunz, H. *Angew. Chem. Int. Ed.* **2010**, *49*, 8498–8503.
(101) Wang, J. S.; Li, H. G.; Zou, G. Z.; Wang, L. X. *Org. Biomol. Chem.* **2007**, *5*, 1529–1540.
(102) Yang, F.; Zheng, X. J.; Huo, C. X.; Wang, Y.; Zhang, Y.; Ye, X. S. *ACS Chem. Biol.* **2011**, *6*, 252–259.
(103) Hoffmann-Röder, A.; Johannes, M. *Chem. Commun.* **2011**, *47*, 9903.
(104) Oberbillig, T.; Mersch, C.; Wagner, S.; Hoffmann-Röder, A. *Chem. Commun.* **2012**, *48*, 1487–1489.
(105) Yan, J.; Chen, X.; Wang, F.; Cao, H. *Org. Biomol. Chem.* **2013**, *11*, 842–848.
(106) Sadraei, S. I.; Reynolds, M. R.; Trant, J. F. *Adv. Carbohydr. Chem. Biochem.* **2017**, *74*, 137–237.
(107) Pachamuthu, K.; Schmidt, R. R. *Chem. Rev.* **2006**, *106*, 160–187.
(108) Röhrig, C. H.; Takhi, M.; Schmidt, R. R. *Synlett* **2001**, 1170–1172.
(109) Aydillo, C.; Compañón, I.; Avenoza, A.; Busto, J. H.; Corzana, F.; Peregrina, J. M.; Zurbano, M. M. *J. Am. Chem. Soc.* **2014**, *136*, 789–800.
(110) Vichier-Guerre, S.; Lo-Man, R.; Huteau, V.; Dériaud, E.; Leclerc, C.; Bay, S. *Bioorg. Med. Chem. Lett.* **2004**, *14*, 3567–3570.
(111) Rojas-Ocáriz, V.; Compañón, I.; Aydillo, C.; Castro-Lopez, J.; Jiménez-Barbero, J.; Hurtado-Guerrero, R.; Avenoza, A.; Zurbano, M. M.; Peregrina, J. M.; Busto, J. H.; Corzana, F. *J. Org. Chem.* **2016**, *81*, 5929–5941.
(112) Martínez-Sáez, N.; Supekar, N. T.; Wolfert, M. A.; Bermejo, I. A.; Hurtado-Guerrero, R.; Asensio, J. L.; Jiménez-Barbero, J.; Busto, J. H.; Avenoza, A.;

Boons, G.-J.; Peregrina, J. M.; Corzana, F. *Chem. Sci.* **2016**, *7*, 2294–2301.
(113) Somovilla, V. J.; Bermejo, I. A.; Albuquerque, I. S.; Martínez-Sáez, N.; Castro-López, J.; García-Martín, F.; Compañón, I.; Hinou, H.; Nishimura, S. I.; Jiménez-Barbero, J.; Asensio, J. L.; Avenoza, A.; Busto, J. H.; Hurtado-Guerrero, R.; Peregrina, J. M.; Bernardes, G. J. L.; Corzana, F. *J. Am. Chem. Soc.* **2017**, *139*, 18255–18261.
(114) Gloster, T. M.; Vocadlo, D. J. *Nat. Chem. Biol.* **2012**, *8*, 683–694.
(115) Stütz, A. E. *Iminosugars as Glycosidase Inhibitors : Nojirimycin and Beyond*; Wiley-VCH, 1999.
(116) Compain, P.; Martin, O. R. *Iminosugars : From Synthesis to Therapeutic Applications*; Wiley-VCH, 2007.
(117) Stütz, A. E.; Wrodnigg, T. M. *Adv. Carbohydr. Chem. Biochem.* **2011**, *66*, 187–298.
(118) Wrodnigg, T. M.; Steiner, A. J.; Ueberbacher, B. J. *Anticancer. Agents Med. Chem.* **2008**, *8*, 77–85.
(119) Durantel, D.; Alotte, C.; Zoulim, F. *Curr. Opin. Investig. Drugs* **2007**, *8*, 125–129.
(120) Greimel, P.; Spreitz, J.; Stütz, a E.; Wrodnigg, T. M. *Curr. Top. Med. Chem.* **2003**, *3*, 513–523.
(121) Wrodnigg, T. M.; Sprenger, F. K. F.; T.M., W.; F.K., S. *Mini-Rev. Med. Chem.* **2004**, *4*, 437–459.
(122) Scott, L.; Spencer, C. *Drugs* **2000**, *59*, 521–549.
(123) Butters, T. D.; Dwek, R. A.; Platt, F. M. *Chem. Rev.* **2000**, *100*, 4683–4696.
(124) Horne, G.; Wilson, F. X.; Tinsley, J.; Williams, D. H.; Storer, R. *Drug Discov. Today* **2011**, *16*, 107–118.
(125) Bhat, C.; Tilve, S. G. *RSC Adv.* **2014**, *4*, 5405.
(126) Compain, P. *Synlett* **2014**, 1215–1240.
(127) Jiang, J.; Kallemeijn, W. W.; Wright, D. W.; van den Nieuwendijk, A. M. C. H.; Rohde, V. C.; Folch, E. C.; van den Elst, H.; Florea, B. I.; Scheij, S.; Donker-Koopman, W. E.; Verhoek, M.; Li, N.; Schürmann, M.; Mink, D.; Boot, R. G.; Codée, J. D. C.; van der Marel, G. A.; Davies, G. J.; Aerts, J. M. F. G.; Overkleeft, H. S. *Chem. Sci.* **2015**, *6*, 2782–2789.
(128) Parmeggiani, C.; Catarzi, S.; Matassini, C.; D'Adamio, G.; Morrone, A.; Goti, A.; Paoli, P.; Cardona, F. *ChemBioChem* **2015**, *16*, 2054–2064.
(129) Lahiri, R.; Ansari, A. A.; Vankar, Y. D. *Chem. Soc. Rev.* **2013**, *42*, 5102–5118.
(130) Dragutan, I.; Dragutan, V.; Demonceau, A. *RSC Adv.* **2012**, *2*, 719–736.
(131) Stocker, B. L.; Dangerfield, E. M.; Win-Mason, A. L.; Haslett, G. W.; Timmer, M. S. M. *Eur. J. Org. Chem.* **2010**, 1615–1637.
(132) Boisson, J.; Thomasset, A.; Racine, E.; Cividino, P.; Sainte-Luce, T. B.; Poisson, J.-F. O.; Behr, J.-B.; Py, S. *Org. Lett.* **2015**, *17*, 3662–3665.
(133) Kato, A.; Zhang, Z. L.; Wang, H. Y.; Jia, Y. M.; Yu, C. Y.; Kinami, K.; Hirokami, Y.; Tsuji, Y.; Adachi, I.; Nash, R. J.; Fleet, G. W. J.; Koseki, J.; Nakagome, I.; Hirono, S. *J. Org. Chem.* **2015**, *80*, 4501–4515.
(134) Parihar, V. S.; Pawar, N. J.; Ghosh, S.; Chopade, B.; Kumbhar, N.; Dhavale,

D. D. *RSC Adv.* **2015**, *5*, 52907–52915.
(135) de la Fuente, A.; Mena-Barragán, T.; Farrar-Tobar, R. A.; Verdaguer, X.; García Fernández, J. M.; Ortiz Mellet, C.; Riera, A. *Org. Biomol. Chem.* **2015**, *13*, 6500–6510.
(136) Tran, A. T.; Luo, B.; Jagadeesh, Y.; Auberger, N.; Désiré, J.; Nakagawa, S.; Kato, A.; Zhang, Y.; Blériot, Y.; Sollogoub, M. *Carbohydr. Res.* **2015**, *409*, 56–62.
(137) Biela-Banaš, A.; Oulaïdi, F.; Front, S.; Gallienne, E.; Ikeda-Obatake, K.; Asano, N.; Wenger, D. A.; Martin, O. R. *ChemMedChem* **2014**, *9*, 2647–2652.
(138) Mena-Barragán, T.; Narita, A.; Matias, D.; Tiscornia, G.; Nanba, E.; Ohno, K.; Suzuki, Y.; Higaki, K.; Garcia Fernández, J. M.; Ortiz Mellet, C. *Angew. Chem. Int. Ed.* **2015**, *54*, 11696–11700.
(139) Yu, Y.; Mena-Barragán, T.; Higaki, K.; Johnson, J. L.; Drury, J. E.; Lieberman, R. L.; Nakasone, N.; Ninomiya, H.; Tsukimura, T.; Sakuraba, H.; Suzuki, Y.; Nanba, E.; Ortiz Mellet, C.; García Fernández, J. M.; Ohno, K. *ACS Chem. Biol.* **2014**, *9*, 1460–1469.
(140) Tiscornia, G.; Lorenzo Vivas, E.; Matalonga, L.; Berniakovich, I.; Barragán Monasterio, M.; Eguizábal, C.; Gort, L.; González, F.; Ortiz mellet, C.; García Fernández, J. M.; Ribes, A.; Veiga, A.; Izpisua Belmonte, J. C. *Hum. Mol. Genet.* **2013**, *22*, 633–645.
(141) Kooij, R.; Branderhorst, H. M.; Bonte, S.; Wieclawska, S.; Martin, N. I.; Pieters, R. J. *Med. Chem. Commun.* **2013**, *4*, 387–393.
(142) Luan, Z.; Higaki, K.; Aguilar-Moncayo, M.; Li, L.; Ninomiya, H.; Nanba, E.; Ohno, K.; García-Moreno, M. I.; Ortiz Mellet, C.; García Fernández, J. M.; Suzuki, Y. *ChemBioChem* **2010**, *11*, 2453–2464.
(143) Sánchez-Fernández, E. M.; Gómez-Pérez, V.; García-Hernández, R.; García Fernández, J. M.; Plata, G. B.; Padrón, J. M.; Ortiz Mellet, C.; Castanys, S.; Gamarro, F. *RSC Adv.* **2015**, *5*, 21812–21822.
(144) Allan, G.; Ouadid-Ahidouch, H.; Sanchez-Fernandez, E. M.; Risquez-Cuadro, R.; Garcia Fernandez, J. M.; Ortiz-Mellet, C.; Ahidouch, A. *PLoS One* **2013**, *8*, e76411.
(145) Rísquez-Cuadro, R.; García Fernández, J. M.; Nierengarten, J. F.; Ortiz Mellet, C. *Chem. Eur. J.* **2013**, *19*, 16791–16803.
(146) Sánchez-Fernández, E. M.; Rísquez-Cuadro, R.; Ortiz Mellet, C.; García Fernández, J. M.; Nieto, P. M.; Angulo, J. *Chem. Eur. J.* **2012**, *18*, 8527–8539.
(147) Sánchez-Fernández, E. M.; Rísquez-Cuadro, R.; Chasseraud, M.; Ahidouch, A.; Ortiz Mellet, C.; Ouadid-Ahidouch, H.; García Fernández, J. M. *Chem. Commun.* **2010**, *46*, 5328.
(148) Sánchez-Fernández, E. M.; Rísquez-Cuadro, R.; Aguilar-Moncayo, M.; García-Moreno, M. I.; Ortiz Mellet, C.; García Fernández, J. M. *Org. Lett.* **2009**, *11*, 3306–3309.
(149) Trapero, A.; Alfonso, I.; Butters, T. D.; Llebaria, A. *J. Am. Chem. Soc* **2011**, *133*, 5474–5484.
(150) Wani, W. Y.; Ouyang, X.; Benavides, G. A.; Redmann, M.; Cofield, S. S.; Shacka, J. J.; Chatham, J. C.; Darley-Usmar, V.; Zhang, J. *Mol. Brain* **2017**,

10.
(151) Hastings, N. B.; Wang, X.; Song, L.; Butts, B. D.; Grotz, D.; Hargreaves, R.; Fred Hess, J.; Hong, K. L. K.; Huang, C. R. R.; Hyde, L.; Laverty, M.; Lee, J.; Levitan, D.; Lu, S. X.; Maguire, M.; Mahadomrongkul, V.; McEachern, E. J.; Ouyang, X.; Rosahl, T. W.; Selnick, H.; Stanton, M.; Terracina, G.; Vocadlo, D. J.; Wang, G.; Duffy, J. L.; Parker, E. M.; Zhang, L. *Mol. Neurodegener.* **2017**, *12*, 1–16.
(152) Grima, J. C.; Daigle, J. G.; Arbez, N.; Cunningham, K. C.; Zhang, K.; Ochaba, J.; Geater, C.; Morozko, E.; Stocksdale, J.; Glatzer, J. C.; Pham, J. T.; Ahmed, I.; Peng, Q.; Wadhwa, H.; Pletnikova, O.; Troncoso, J. C.; Duan, W.; Snyder, S. H.; Ranum, L. P. W.; Thompson, L. M.; Lloyd, T. E.; Ross, C. A.; Rothstein, J. D. *Neuron* **2017**, *94*, 93–107.e6.
(153) Yuzwa, S. A.; Macauley, M. S.; Heinonen, J. E.; Shan, X.; Dennis, R. J.; He, Y.; Whitworth, G. E.; Stubbs, K. A.; McEachern, E. J.; Davies, G. J.; Vocadlo, D. J. *Nat. Chem. Biol.* **2008**, *4*, 483–490.
(154) Yu, Y.; Zhang, L.; Li, X.; Run, X.; Liang, Z.; Li, Y.; Liu, Y.; Lee, M. H.; Grundke-Iqbal, I.; Iqbal, K.; Vocadlo, D. J.; Liu, F.; Gong, C. X. *PLoS One* **2012**, *7*, e35277.
(155) Yuzwa, S. A.; Shan, X.; Macauley, M. S.; Clark, T.; Skorobogatko, Y.; Vosseller, K.; Vocadlo, D. J. *Nat. Chem. Biol.* **2012**, *8*, 393–399.
(156) Castilla, J.; Rísquez, R.; Higaki, K.; Nanba, E.; Ohno, K.; Suzuki, Y.; Díaz, Y.; Ortiz Mellet, C.; García Fernández, J. M.; Castillón, S. *Eur. J. Med. Chem.* **2015**, *90*, 258–266.
(157) Jayakanthan, K.; Vankar, Y. D. *Tetrahedron Lett.* **2006**, *47*, 8667–8671.
(158) Doddi, V. R.; Kokatla, H. P.; Pal, A. P. J.; Basak, R. K.; Vankar, Y. D. *Eur. J. Org. Chem.* **2008**, 5731–5739.
(159) Ma, X.; Tang, Q.; Ke, J.; Wang, H.; Zou, W.; Shao, H. *Carbohydr. Res.* **2013**, *366*, 55–62.
(160) Ella-Menye, J. R.; Nie, X.; Wang, G. *Carbohydr. Res.* **2008**, *343*, 1743–1753.
(161) Pachamuthu, K.; Gupta, A.; Das, J.; Schmidt, R. R.; Vankar, Y. D. *Eur. J. Org. Chem.* **2002**, 1479–1483.
(162) Francisco, C. G.; Herrera, A. J.; Martín, Á.; Pérez-Martín, I.; Suárez, E. *Tetrahedron Lett.* **2007**, *48*, 6384–6388.
(163) Sánchez-Fernández, E. M.; Álvarez, E.; Ortiz Mellet, C.; García Fernández, J. M. *J. Org. Chem.* **2014**, *79*, 11722–11728.
(164) Senthilkumar, S.; Prasad, S. S.; Kumar, P. S.; Baskaran, S. *Chem. Commun.* **2014**, *50*, 1549.
(165) Santana, A. G.; Paz, N. R.; Francisco, C. G.; Suárez, E.; González, C. C. *J. Org. Chem.* **2013**, *78*, 7527–7543.
(166) Wennekes, T.; Van Den Berg, R. J. B. H. N.; Boltje, T. J.; Donker-Koopman, W. E.; Kuijper, B.; Van Der Marel, G. A.; Strijland, A.; Verhagen, C. P.; Aerts, J. M. F. G.; Overkleeft, H. S. *Eur. J. Org. Chem.* **2010**, 1258–1283.
(167) Wennekes, T.; Van Den Berg, R. J. B. H. N.; Boot, R. G.; Van Der Marel, G. A.; Overkleeft, H. S.; Aerts, J. M. F. G. *Angew. Chem. Int. Ed.* **2009**, *48*, 8848–8869.

Chapter 2. Conformationally restricted Tn antigen mimics

2.1. Introduction

As discussed in *Chapter 1*, the Tn antigen is closely related to several types of cancer, as well as to metastatic processes and tumor growth. It is a highly specific human TACA and is regarded as a convenient cancer biomarker. On the other hand, synthesizing analogs of natural TACAs allows us to better understand different biochemical processes and offers a collection of new candidates for biological targets. In this sense, *C*-glycosides,[1–4] which lack the labile carbohydrate-characteristic acetal group, have been investigated as more resistant to enzymatic or hydrolytic degradation carbohydrate analogs. Stereoselective *C*-glycosylation has been extensively studied using natural carbohydrates as chiral starting compounds.

One of the most used methodology to obtain *C*-glycoside TACA analogues is the cross-coupling reaction catalyzed by palladium or other transition metals. Tan and co-workers reported a Suzuki-Miyaura cross coupling approach using halogenated glycans and olefins in the presence of 9-borabicyclo[3.3.1]nonane (9-BBN) and a palladium catalyst. This mild coupling is suitable for using Fmoc protection and represents a powerful methodology for obtaining new TACA derivatives (scheme **2.1**).[5]

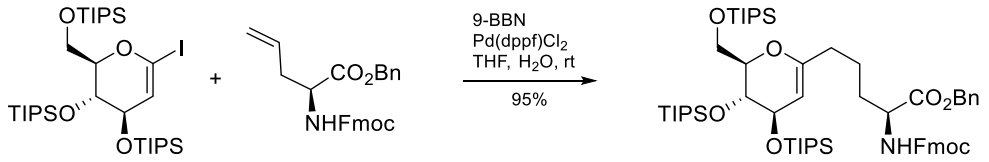

Scheme 2.1. Suzuki-Miyaura cross-coupling leading to TACA derivatives.

Although the use of an anomeric anion is limited due to instability, there are a few cases already reported.[6] For instance, glycosyl ylide has been proposed for obtaining *C*-glycosylated TACA analogs. As reported by Lieberknecht and co-workers,[7] Garner's aldehyde reacted with the ylide generated *in situ* from a galactose derivative. The corresponding *C*-glycoside could be afforded after two additional reaction steps (scheme **2.2**).

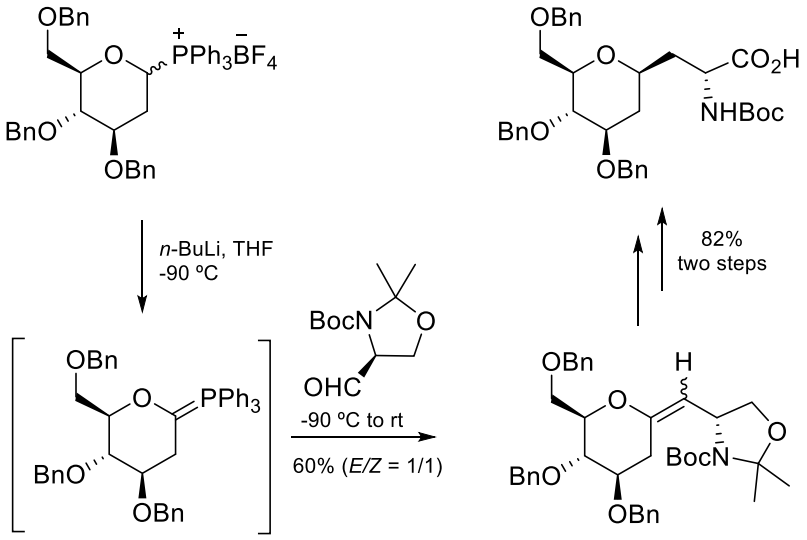

Scheme 2.2. Use of glycosyl ylides in *C*-glycosylation.

Samarium diiodide (SmI_2) can be used in a similar way for stabilizing anomeric anions in *N*-(acetyl)galactosamine derivatives. Remarkably, this methodology provides α-anomer selectively, presumably due to a strong coordination between the samarium atom and the *N*-acetyl group. This chemistry can be employed for synthesizing *C*-glycosylated Tn antigen analogs (scheme **2.3**).[8]

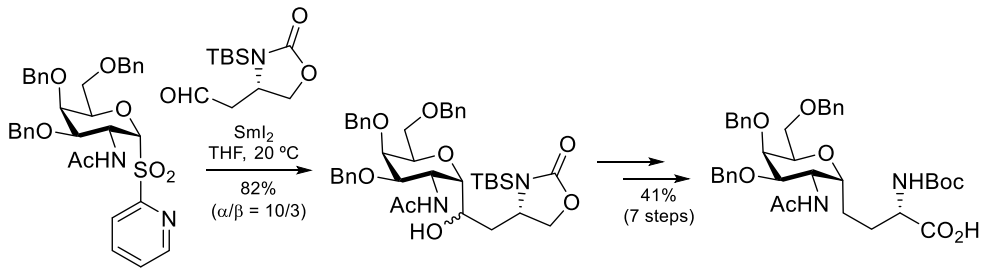

Scheme 2.3. Samarium-mediated *C*-glycosylation.

A more efficient method to obtain the last mentioned *C*-glycoside was developed by Schmidt and co-workers.[9] *C*-glycosylation was performed by means of a radical reaction under neutral conditions, compatible with most common functional and protecting groups used for glyco-amino-acids. In this case, the *C*-glycosylated Tn antigen mimic was afforded after four additional reaction steps (scheme **2.4**).

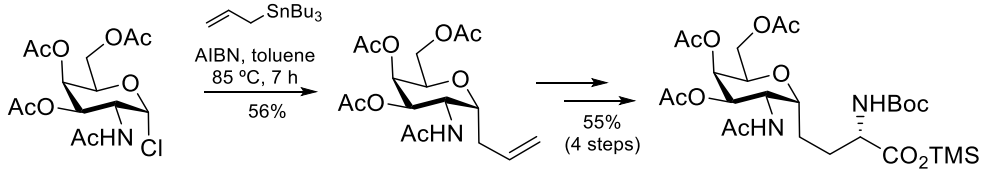

Scheme 2.4. Radical mediated allylation.

Our research group has a wide experience in synthesizing non-natural amino acids, more specifically β-hydroxy-α,α-disubstituted amino acids,[10–19] incorporating them into biologically relevant glycopeptides and studying the conformational space of these molecules in aqueous solution,[20–28] either in the free-state or in complex with target molecules (binding). One of the most recent and efficient methodology to prepare these amino acids was developed by our research group and consists of the α-alkylation of a bicyclic *N*,*O*-acetal derived from serine (**1a**).[29–32] This reac-

tion takes place diastereoselectively and with retention of the original configuration, leading to enantiomerically pure α-alkylserines. This bicyclic scaffold reacts similarly with methyl acrylates in domino Michael-Dieckmann processes,[33] always with retention of the configuration and high diastereoselectivities (scheme **2.5**).

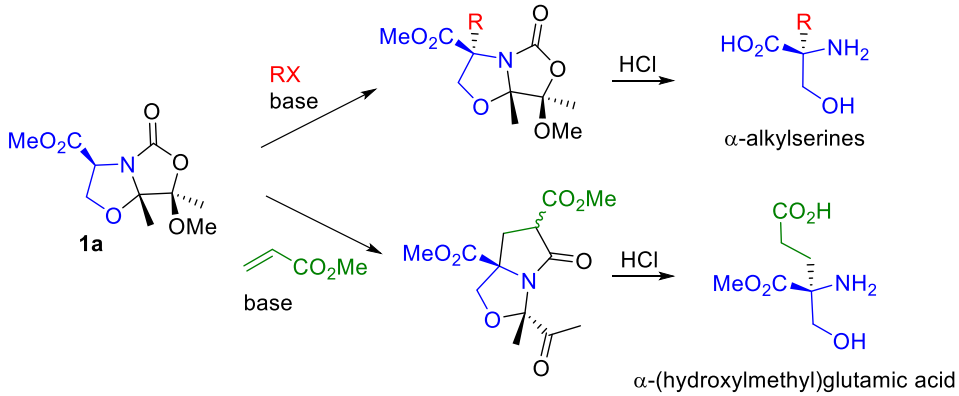

Scheme 2.5. Bicyclic *N*,*O*-acetal α-alkylation and Michael-type addition.

2.2. Goals

Bearing all these concepts in mind and inspired by the excellent results that bicyclic compound **1a** showed in Michael-type additions towards acrylates, we have developed a modification of Schmidt's glycosylation methodology,[34–39] which involves an *O*-Michael-type addition of the hydroxyl groups of serine or threonine to 2-nitroglycals, using bicyclic *N*,*O*-acetal **1a** (scheme **2.6**).

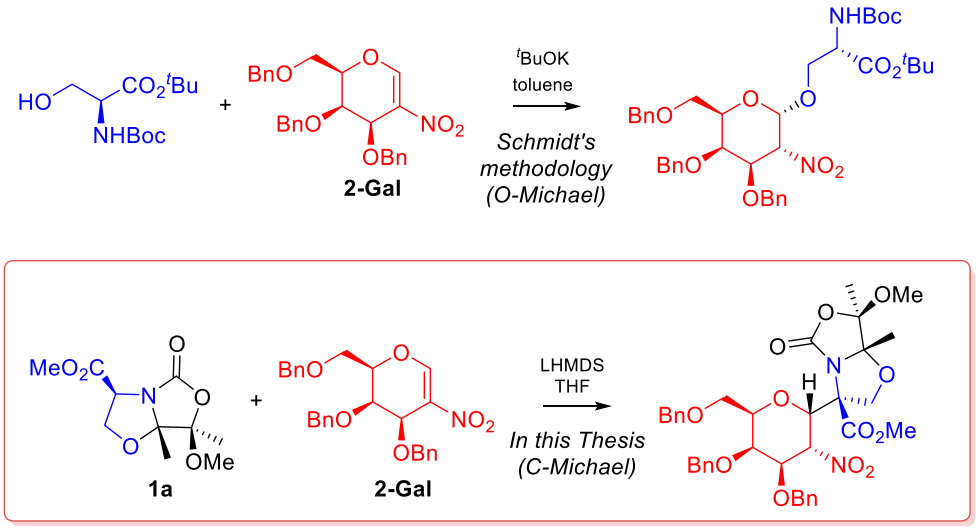

Scheme 2.6. Comparison between Schmidt's methodology and the one studied in this Thesis.

Based on this methodology, we designed new conformationally restricted *C*-glycoside Tn antigen mimics by exploring several structural modifications. The first two families of analogs involve *C*-glycoside bicyclic systems in which the acetamido group of the carbohydrate moiety is covalently bound either to the carboxylic group of the amino acid, forming a pyrrolidinone, or to the amino group of the amino acid, forming a cyclic urea. The last family comprises α-(α-GalNAc)-serine derivatives (figure **2.1**).

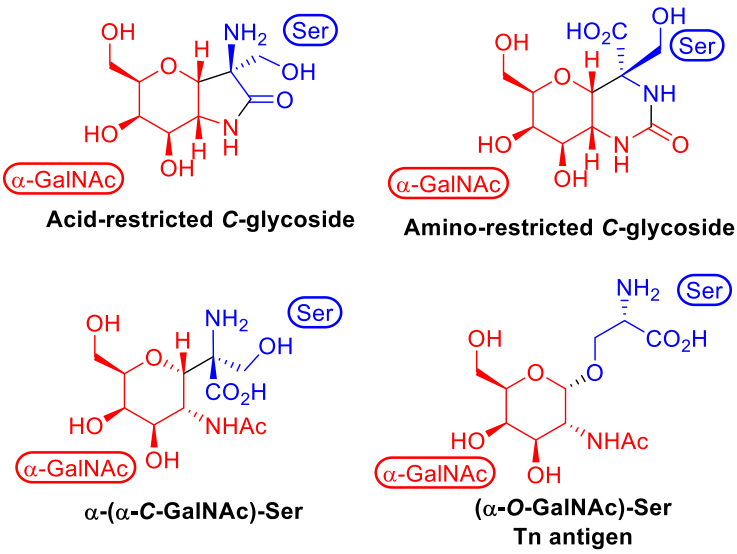

Figure 2.1. Structure of *C*-glycosides analogs and the Tn antigen.

2.3. Double diastereoselective Michael-type addition

The synthesis of the *N*,*O*-bicyclic acetal **1a** was achieved following the methodology previously reported by our group.[29] Commercially available (*S*)-*N*-Boc-serine methyl ester was reacted with 2,2,3,3-tetramethoxybutane (TMB) and *p*-toluensulfonic acid (*p*-TsOH) in toluene under reflux for 4 hours, affording compound **1a** in 75% yield (scheme **2.7**).

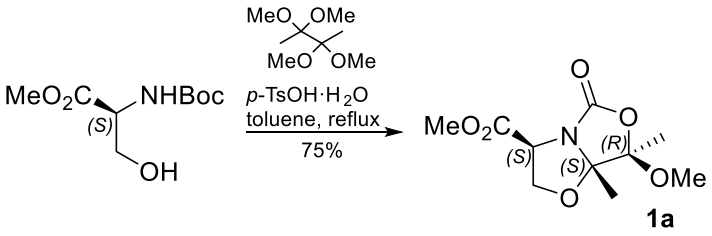

Scheme 2.7. Synthesis of bicyclic serine equivalent **1a**.

As glycan donors, 2-nitro-tri-*O*-benzyl-D-galactal **2-Gal** and 2-nitro-tri-*O*-benzyl-D-glucal **2-Glc** were synthesized following the methodology described by Schmidt and co-workers.[34,40] Acetyl nitrate was *in-situ* prepared by addition of 65% HNO_3 to ice-cooled acetic anhydride (Ac_2O). Temperature is then lowered to -50 ºC and Ac_2O solutions of commercially available tri-*O*-benzyl-D-galactal and tri-*O*-benzyl-D-glucal were slowly added. After stirring for 30 min, the reaction was quenched and the crude mixture was dissolved in DCM. Triethylamine (TEA) was then added and the mixture was stirred for 30 min at room temperature, obtaining compounds **2-Gal** (81%) and **2-Glc** (72%) after column chromatography (scheme **2.8**).

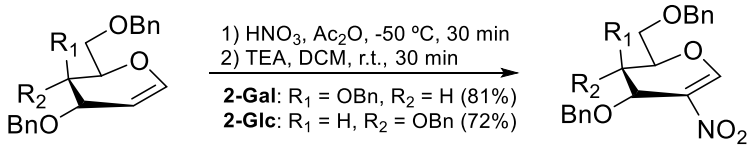

Scheme 2.8. Synthesis of nitroglycans **2-Gal** and **2-Glc**.

Initially, a double diastereoselective Michael-type addition[41–45] of the bicyclic serine equivalent **1a** to the nitrogalactal derivative **2-Gal** was optimized, analyzing the influence of additives such as hexamethylphosphoramide (HMPA), the amount of electrophile and base equivalents, and the reaction times. Tetrahydrofuran (THF) was used as a solvent, the temperature was set to -78 ºC, and lithium bis(trimethylsilyl)amide (LHMDS) was used as a base due to the excellent results obtained in previously reported Michael additions of compound **1a** to acrylates[33] (scheme **2.9**).

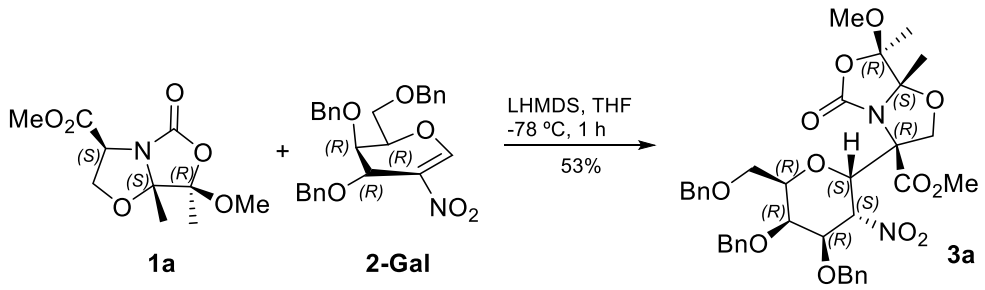

Scheme 2.9. Double asymmetric *C*-Michael reaction.

Table 2.1. Effect of HMPA, excess of **2-Gal** and LHMDS and reaction time on the yield of Michael addition.

Entry	2-Gal (equiv.)	HMPA (equiv.)	LHMDS (equiv.)	Time (min)	Yield (%)[a]
1	1	4	2	60	40
2	1	0	2	60	44
3	1.4	0	2	60	43
4	1	0	2.6	60	49
5	1	0	2.6	90	53
6	1	0	2.6	120	48

[a]Obtained after column chromatography (hexane/EtOAc, 9:1).

In agreement with previous reports from our group, a unique diastereoisomer **3a** was obtained among the eight possible ones in all cases (Scheme **2.9**). As shown in table **2.1**, the presence of additives (HMPA) did not affect significantly the yield (entries **1** and **2**), nor did addition of a slight excess of nitrogalactal **2-Gal** (entry **3**). However, the addition of 2.6 equivalents of base and longer reaction times led to small yield increase (entries **4-6**).

Appropriate monocrystals of adduct **3a** were obtained and analyzed by X-ray diffraction, which allowed us to confirm the absolute configuration

of all stereocenters (figure **2.2**). In this case, three new stereocenters were created and controlled, two of them coming from the nitroglycal unit. In this sense, Schmidt and co-workers had previously observed the same diastereoinduction exploring Michael additions to 2-nitrogalactals.[34–39] However, Schmidt's reaction seems to involve a quite complex mechanism, since changing the base and/or the type of nucleophile afforded different stereoselectivities.[36,37]

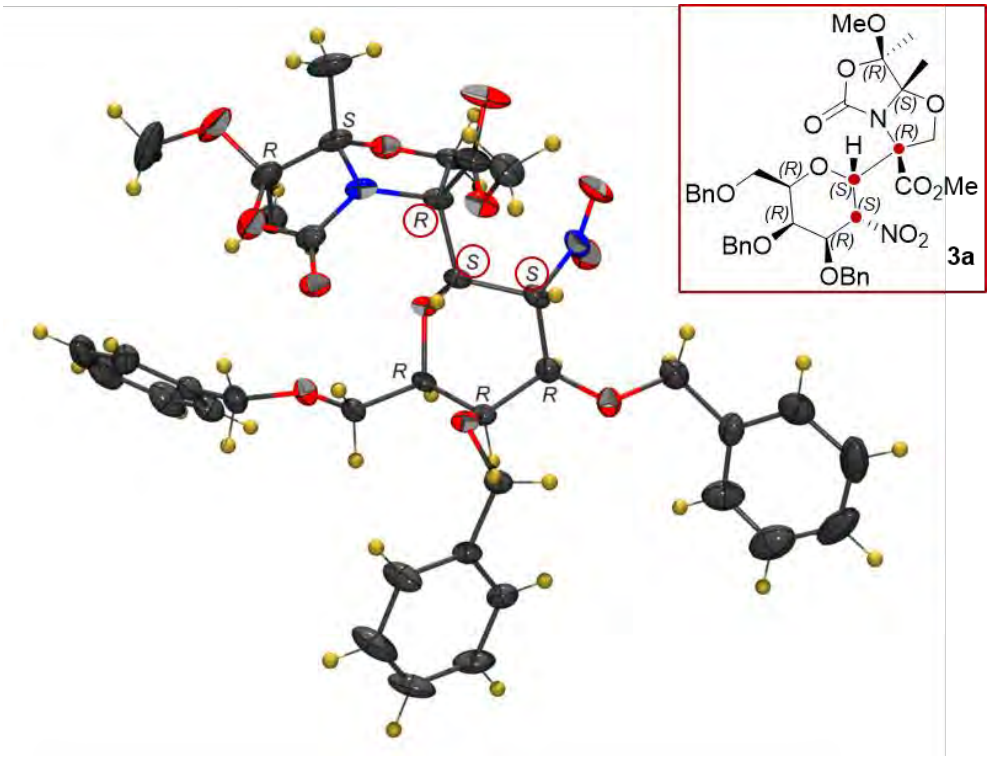

Figure 2.2. ORTEP3 diagram obtained by X-ray diffraction of compound **3a**, highlighting in red the new stereocenters.

On the other hand, the third stereocenter comes from the bicyclic serine derivative **1a**, which is a chiral *C*-nucleophile. Although the corresponding enolate is expected to be planar and the Cα carbon would there-

fore lose its chirality, we have observed total control of its configuration, maintaining the same configuration as in the starting material **1a**. It is now labeled as *R* due to the change in the priority of the attached groups. This relevant behavior had already been observed in previously published asymmetric reactions,[29–31,33] in which a highly pyramidalized ester enolate is proposed to be the source of this stereoselection.

Using this methodology, the α anomer is obtained, although this terminology cannot be used because the carbohydrate does not have a chair-like conformation, at least in solid state. Instead, it adopts a boat-like conformation, which is energetically disfavored compared to the typical chair-like conformation in *O*-glycosides (figure **2.3**).

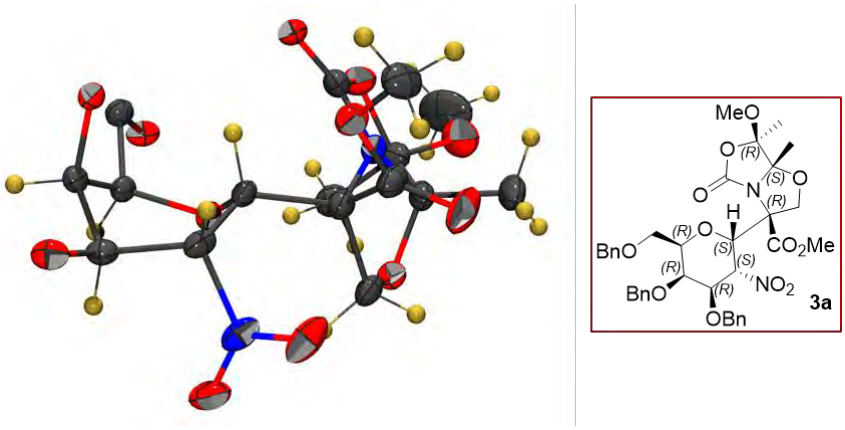

Figure 2.3. Carbohydrate boat-like conformation of compound **3a**. Benzyl groups have been omitted for clarity.

In order to evaluate the influence of bulkier esters, the same doubly diastereoselective Michael addition was performed using bicyclic derivatives **1b** (benzyl ester) and **1c** (*tert*-butyl ester). The synthesis of bicyclic compound **1b** was achieved following the same procedure as described for

compound **1a** but using (*S*)-*N*-Boc-L-serine benzyl ester. The bicyclic derivative **1c** could not be obtained by this methodology, due to hydrolysis of the *tert*-butyl ester, and was obtained starting from bicyclic compound **1a** instead. Methyl ester group was hydrolyzed using 5 equivalents of $LiOH \cdot H_2O$ in THF/H_2O at 0 ºC for 30 min. pH was then lowered to 2-3 with an aqueous 2 M HCl solution and the corresponding carboxylic acid was esterified using a mixture of *tert*-butanol (^{t}BuOH), di-*tert*-butyl dicarbonate (Boc_2O) and 4-(dimethylamino)pyridine (DMAP) at room temperature for 3 hours (scheme **2.10**).

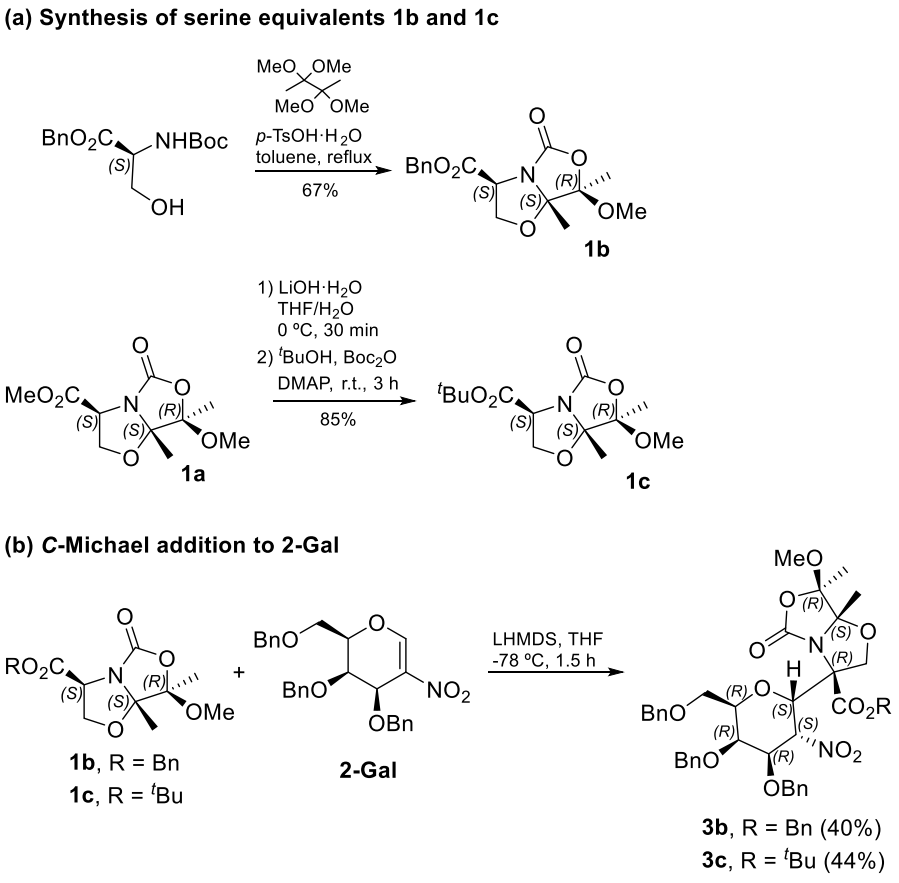

Scheme 2.10. (a) Synthesis of serine equivalents **1b** and **1c**. (b) Double asymmetric *C*-Michael reaction.

The Michael addition reactions of bicyclic compounds **1b** and **1c** were completely diastereoselective, affording in both cases unique compounds **3b** and **3c**, respectively, whose absolute configurations matches those observed in adduct **3a**.

Finally, we explored the reactivity of chiral bicycle **1a** towards nitroglucal derivative **2-Glc**. Previously optimized conditions were assayed (Table **2.2**, entry **1**), affording a complex mixture of compounds. After purification by column chromatography, only a small amount of the Michael adduct was isolated. Addition of 4 equivalents of HMPA to the reaction mixture slightly improved the yield (34%, entry **2**). Using 2 equivalents of nitroglucal **2-Glc**, 2 equivalents of LHMDS and 4 equivalents of HMPA for 2 hours at -78 ºC afforded the best yield (entry **3**), although not as good as the one obtained using nitrogalactal **2-Gal** as electrophile (53%).

Table 2.2. Effect of HMPA, excess of **2-Glc** and LHMDS and reaction time on the yield of Michael addition.

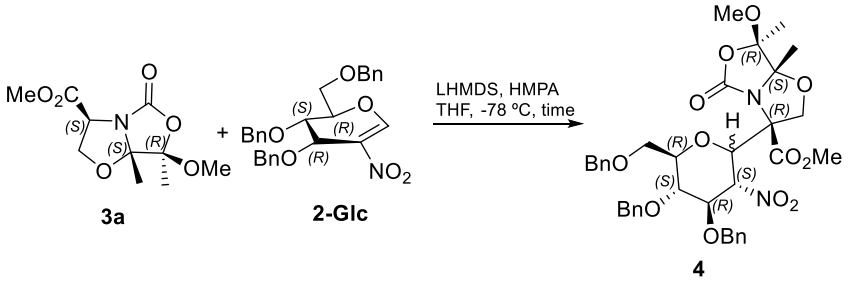

Entry	2-Glc (equiv.)	HMPA (equiv.)	LHMDS (equiv.)	Time (min)	Yield (%)[a]
1	1	0	2.6	90	14
2	1	4	2.6	90	20
3	2	4	2	120	34

[a]Obtained after column chromatography (hexane/EtOAc, 9:1).

The isolated compound turned out to be a 9:1 mixture of two diastereoisomers, as judged by ^{1}H NMR experiments. Unfortunately, their absolute configurations could not be confirmed, due to the lack of appropriate monocrystals. Schmidt and co-workers[46] already reported that the nitro group tends to prefer the equatorial position after Michael-type additions to 2-nitroglucal or 2-nitrogalactal derivatives. Additionally, it has been well stablished and proven that the absolute configuration of the Cα of the serine derivative **1a** does not change due to pyramidalization of the enolate. Therefore, the two compound mixture likely corresponds to the α- and β-anomers (scheme **2.11**).

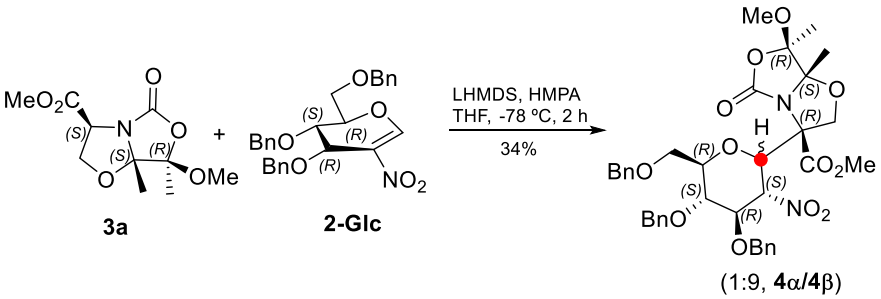

Scheme 2.11. Double asymmetric C-Michael reaction on nitroglucal **2-Glc**.

The anomeric protons inherit two different characteristics due to their local environment: chemical shift due to shielding from the external magnetic field and *J*-coupling (J_{HH}) from hydrogens on the adjacent carbon (C2). The equatorial (α) anomeric proton resonates further downfield from the axial (β). The second characteristic is the spin-spin coupling ($^{3}J_{HH}$), which depends on the dihedral angle between vicinal protons, as demonstrated by Nobel-prized Martin Karplus[47,48] in the 1960s. For instance, α-D-glucose anomeric proton resonates at 5.23 ppm and has a coupling constant

of 3.7 Hz in D_2O. However, β-D-glucose anomeric proton resonates at 4.64 ppm and has a coupling constant of 7.9 Hz (figure **2.4**).

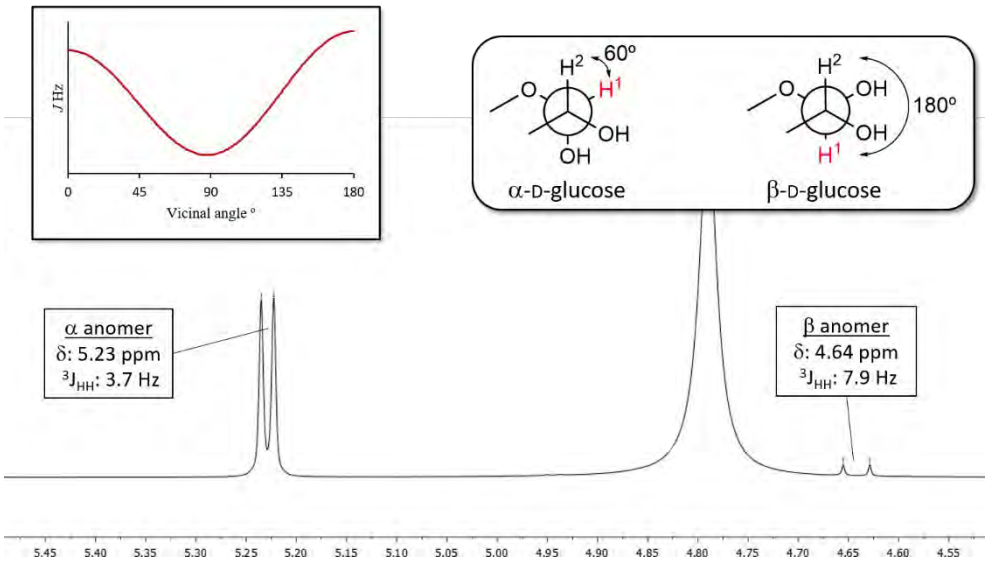

Figure 2.4. ^{1}H NMR (300 MHz, D_2O) for glucose and typical Karplus equation graph.

Applying these observations to the isolated mixture of **4α** and **4β**, we were able to determine that the main compound corresponds to **4β** (δ = 5.79 ppm, $^3J_{HH}$ = 9.1 Hz) and the minor compound corresponds to **4α** (δ = 5.84 ppm, $^3J_{HH}$ = 4.3 Hz) (figure **2.5**). Notably, the opposite configuration of C4 in Glc induced an inversion in stereoselectivity with respect to Gal, likely due to less steric hindrance occurring at the top (β) face.

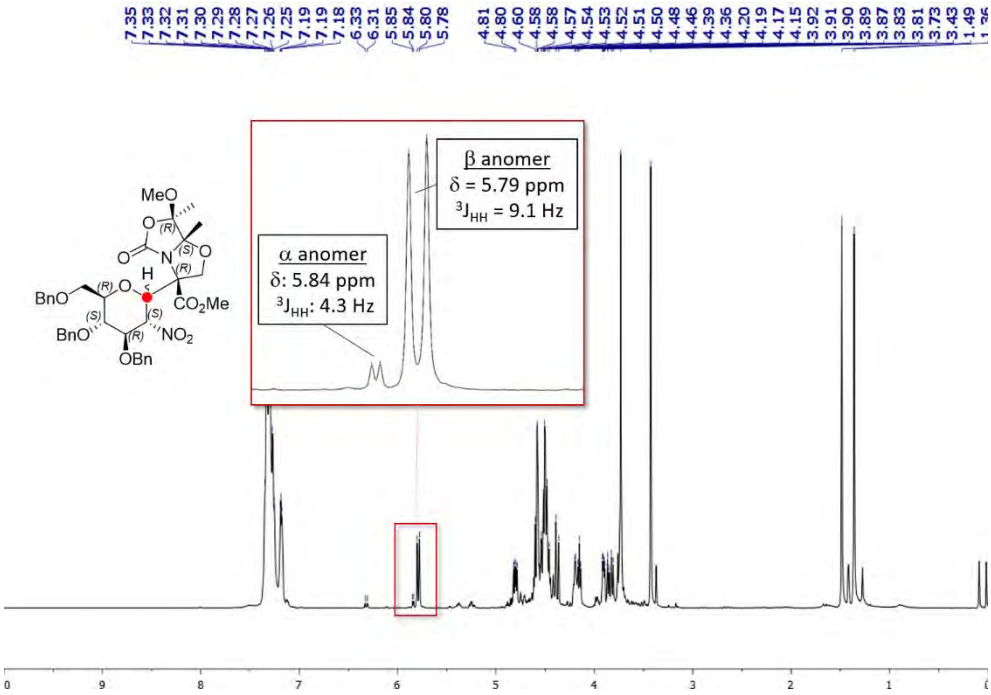

Figure 2.5. ^{1}H NMR (400 MHz, $CDCl_3$) for the mixture of compounds **4α** and **4β**.

This family of Michael adducts can be regarded as protected serine *C*-glycosides and were used as starting materials for synthesizing Tn antigen mimics, particularly nitrogalactose derivatives.

2.4. *C*-glycosides analogs of the Tn antigen

Once the Michael reaction between serine bicyclic derivatives **1a-c** and nitroglycans was optimized, we focused on performing different functional group transformations on the Michael adducts **3a-c** that allowed us to obtain the desired *C*-glycoside analogs of Tn antingen. Depending on the sequence of transformations and the protecting groups of the starting material (methyl, benzyl or *tert*-butyl esters), we would be able to obtain con-

formationally extended or restricted serine *C*-glycosides with different groups attached to the amino, hydroxyl, or acid groups (scheme **2.12**).

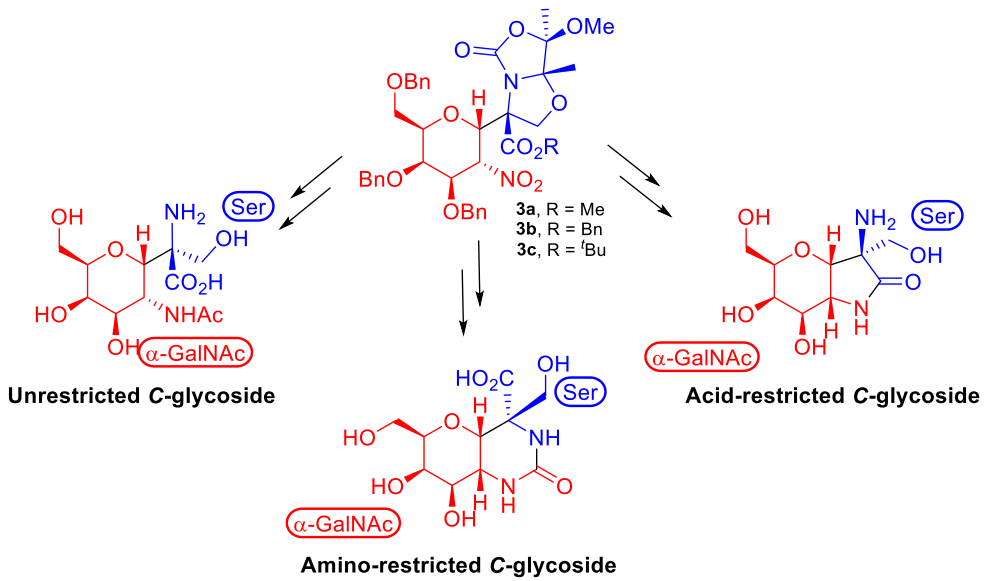

Scheme 2.12. Transformation of Michael adducts **3a-c** into final *C*-glycosides.

2.4.1. Acid-restricted *C*-glycosides

This family of compounds are bicyclic *C*-glycosides, in which the 2-acetamido group of the carbohydrate moiety has lost its methyl group. The amide group is instead attached to Cα of the underlying amino acid and presents a *cis* disposition of the amide and the anomeric substituent. This motif aims to restrict the conformational flexibility of the most relevant torsions. One of the Tn antigen mimics obtained through this approach (**9**) exhibits a hydroxymethyl group attached to the Cα of the amino acid (figure **2.6**).

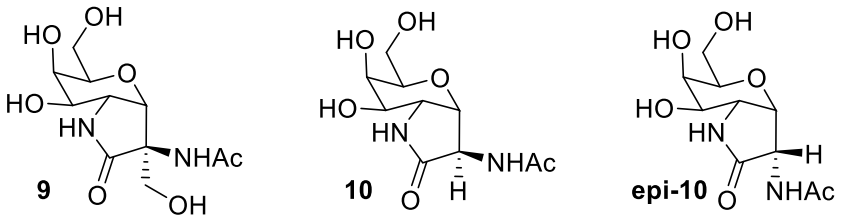

Figure 2.6. Structure of acid-restricted Tn antigen analogs.

The first step to obtain the acid-restricted serine *C*-glycosides involved the use of platinized Raney® nickel[49] as a catalyst under hydrogen atmosphere. It provided a selective method for reducing the nitro group of compound **3a** to the corresponding amine, which immediately reacted with the methyl ester group, forming the corresponding γ-lactam derivative **5** in 57% yield (scheme **2.13**).

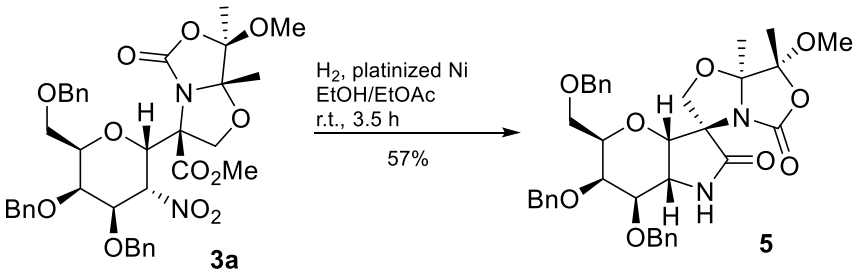

Scheme 2.13. Synthesis of compound **5**.

Concomitant hydrolysis of the oxazolidine and oxazolidinone rings of compound **5** by treatment with 4 M HCl in THF at 40 ºC for 16 hours, followed by acetylation of the amino and hydroxyl groups using Ac_2O in pyridine afforded compound **6** in a good yield (87%) (scheme **2.14**).

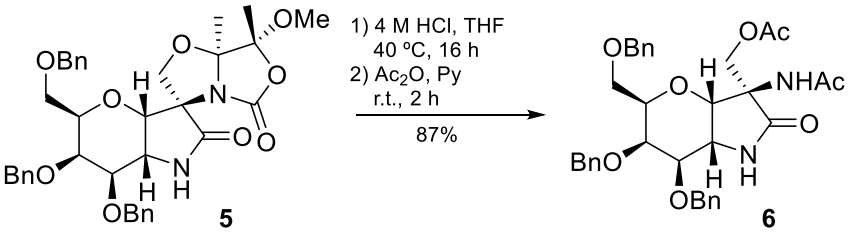

Scheme 2.14. Synthesis of compound **6**.

Alcohol **7** was obtained in an excellent yield (95%) by reacting compound **6** with a saturated solution of sodium methoxide (NaOMe) in methanol (MeOH) at pH 9 for 1.5 hours followed by a treatment with activated Dowex® 50WX8 resin (scheme **2.15**).

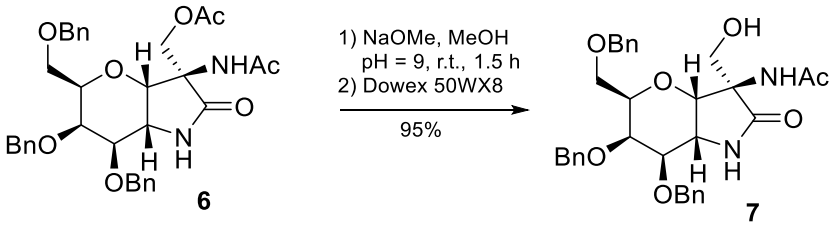

Scheme 2.15. Synthesis of compound **7**.

Direct oxidation of the primary alcohol to the carboxylic acid was attempted using different methodologies: Jones reagent (CrO_3),[50,51] O_2 and Pd/C[52] or RuO_4.[53] However, none of them afforded the desired compound. Starting material or decomposition products were observed instead. Compound **7** was therefore oxidized to the corresponding aldehyde using the Dess-Martin reagent.[54,55] The reaction crude was then treated with freshly-prepared Tollens reagent ($[Ag(NH_3)_2]^+$)[56] to give the carboxylic acid, which quickly suffered a decarboxylation reaction during the acidic workup, to afford a mixture of compounds **8a** and **8b** (scheme **2.16**). Both compounds

could be separated by column chromatography and the corresponding structures were elucidated by NMR experiments, particularly by 2D NOESY experiments.

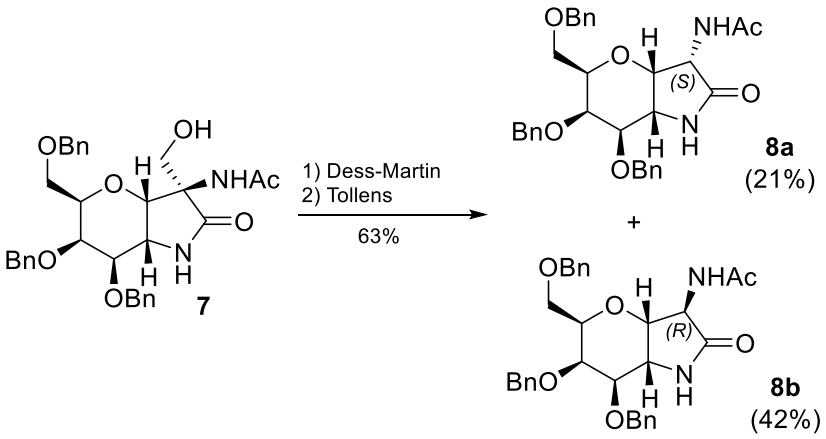

Scheme 2.16. Oxidation of alcohol **7** to obtain **8a** and **8b**.

As shown in figure **2.7**, the H3-H3a and H3-H7a cross-peaks in the NOESY spectrum of compound **8a** confirmed the *S*-configuration of C3. On the other hand, no H3-H3a cross-peak was detected in the NOESY spectrum of compound **8b**. Instead, H3-H5 and H3-H7 cross-peaks revealed the *R*-configuration of C3 for compound **8b**.

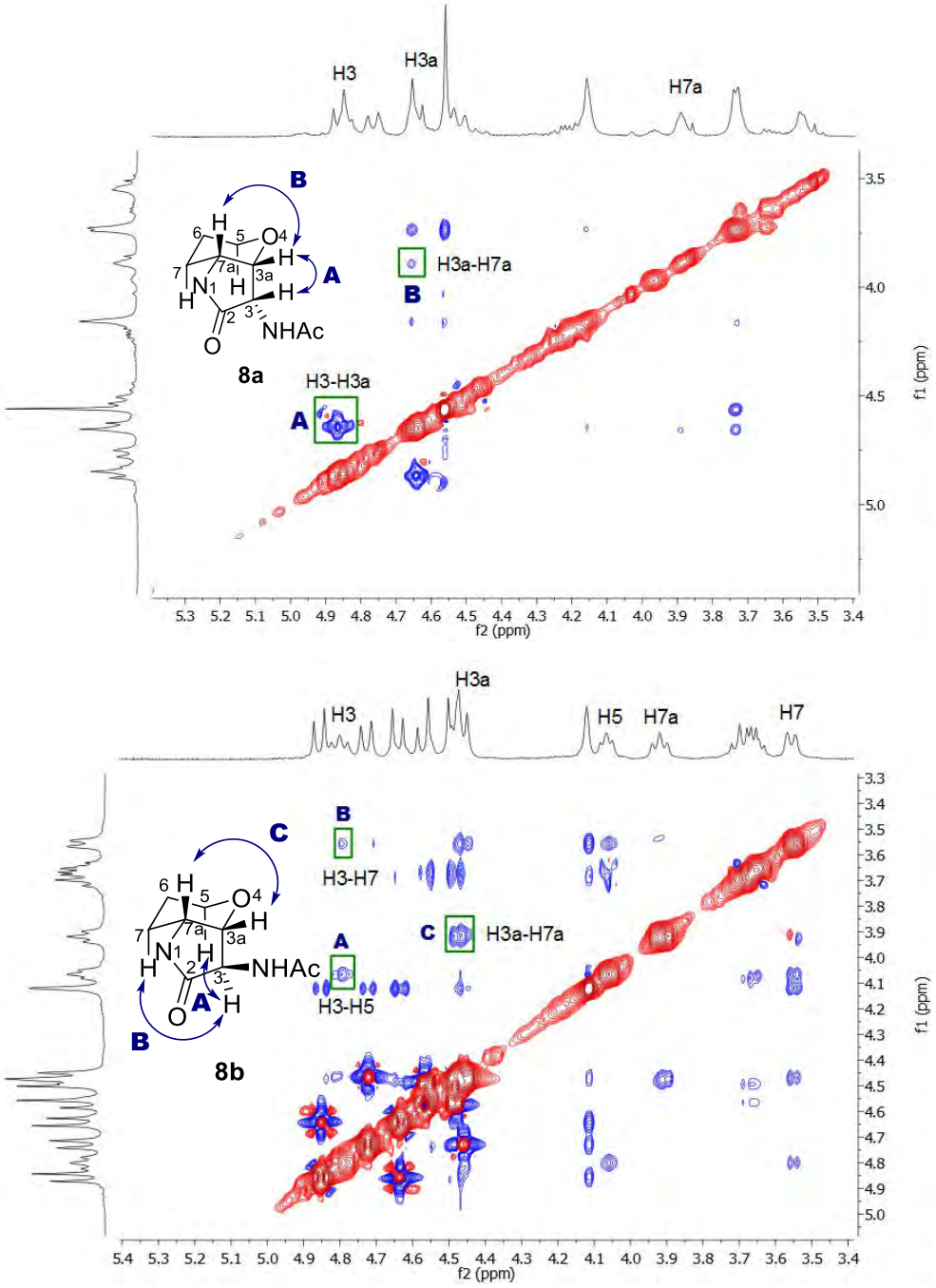

Figure 2.7. Elucidation of structures of **8a** and **8b** from NOESY experiments. *O*-benzyl groups of the carbohydrate moieties have been omitted for clarity.

Finally, the *O*-benzyl groups of compounds **7**, **8a** and **8b** were finally removed by hydrogenolysis using palladium on carbon as a catalyst, and a few drops of concentrated aqueous HCl in MeOH for 16 hours. Final compounds **9**, **epi-10** and **10** were obtained in good yields after purification by extractions with water and EtOAc (scheme **2.17**).

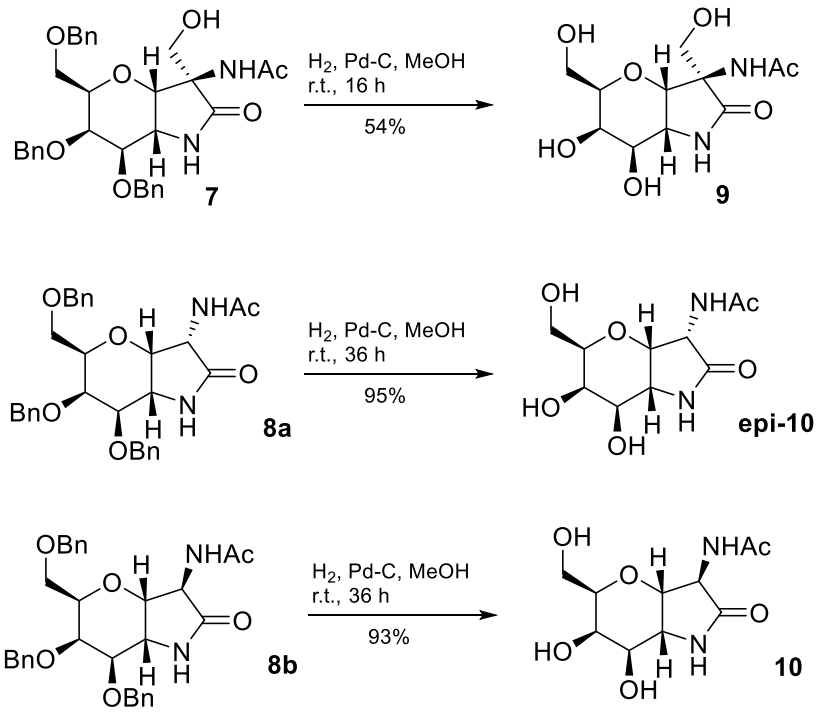

Scheme 2.17. Hydrogenolysis to obtain the Tn antigen mimics **9**, **epi-10** and **10**.

Conformational analysis

It is crucial to know the conformational preferences and the dynamics of glyco-amino-acid analogs to understand their bioactivity. The presentation mode of the carbohydrate moiety usually plays a key role on the interactions established between biomolecules. In this sense, Nuclear Overhauser Effect SpectroscopY (NOESY) in combination with Molecular Dynamics (MD) simulations is a very powerful technique to obtain conformational information from biomolecules. Cross-peaks from NOESY experiments correlate hydrogens through space, which are at distances usually shorter than 5 Å. The interatomic distance between proton *a* and *b* (r_{ab}) can be calculated based on the measured volume of the cross-peak (V_{ab}) and a scaling constant that can be determined based on known fixes distances (equation **2.1**).

$$r_{ab} = \left(\frac{c}{V_{ab}}\right)^{-6}$$

Equation 2.1. Determining distances between hydrogens from NOESY experiments.

These experimental time-averaged distances can be used as restrains in Molecular Dynamic simulations (MD-tar) to build a dynamic three-dimensional model of biomolecules. MD-tar were performed for mimics **9**, **epi-10** and **10** following the protocol described by our research group.[21] The results obtained from the simulations for all of the compounds showed a close agreement, between the distances obtained in the computational models and the experimental NMR data. The peptide backbone of all of the compounds, including the natural Tn antigen with serine, showed

mainly an extended conformation, being the non-natural derivatives generally more rigid than the natural one. Another remarkable difference is the relative orientation of the carbohydrate moiety and the peptide backbone, which shows a clearly parallel alignment in the case of the natural Tn antigen with serine. In fact, the conformations showed by these mimics are different from those observed in other reported mucin-like glycopeptides[57,58] (figure **2.8**).

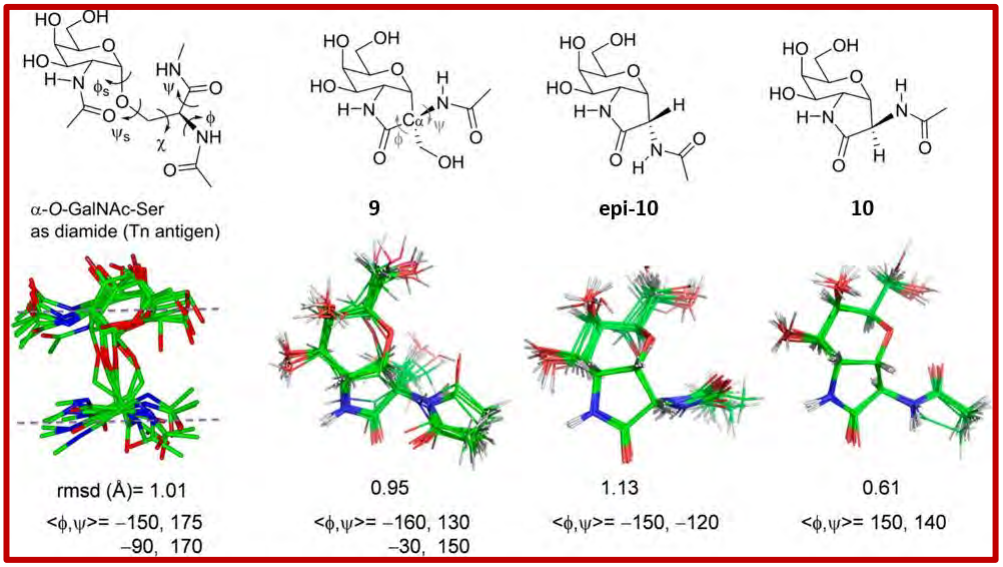

Figure 2.8. Ensembles for the Tn antigen (α-*O*-GalNAc-Ser), **9**, **epi-10** and **10** obtained from the 80 ns MD-tar simulations, showing the root-mean-square deviations (RMSD, Å) for heavy atom superimposition.

On the other hand, compound **10** displayed only the $^4C_1$ conformation for the carbohydrate moiety, while mimics **9** and **epi-10** showed about a 20% of a "twist-boat" conformation in solution. This conformation was also observed in the solid state for Michael-adduct **3a**.

Molecular recognition

In order for new compounds to be considered as glycomimics, they must retain bioactivity, meaning they must serve as ligands for specific receptors. We studied the affinities of these non-natural glyco-amino-acids towards two lectins: soybean agglutinin lectin (SBL) and *vicia villosa*-B-4 agglutinin lectin (VVL). SBL has been previously used to develop a model for lectin binding to MUC-1 mucins, showing a quite high affinity for GalNAc and for the Tn antigen.[59] Besides, this lectin is readily available and stable, and the 3D structure in complex with GalNAc is already known (figure **2.9**).[60] VVL also shows a high specificity for GalNAc,[61,62] the glycan moiety of the Tn antigen.

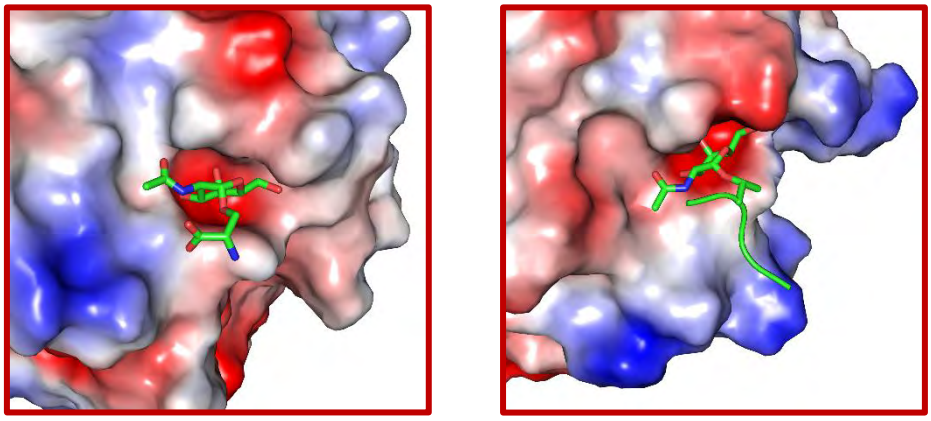

Figure 2.9. X-ray structures for SBL (left) and VVL (right) lectins in complex with the Tn antigen.

As a positive control for the molecular recognition assay, diamide of the natural Tn antigen with serine was also synthesized by reacting **Ac-Ser-NHMe** with **2-Gal** following Schmidt's procedure.[22,34] Reduction of the

nitro group and acetylation of the corresponding amine, followed by hydrogenolysis to cleave the *O*-benzyl groups afforded natural Tn as diamide (scheme **2.18**).

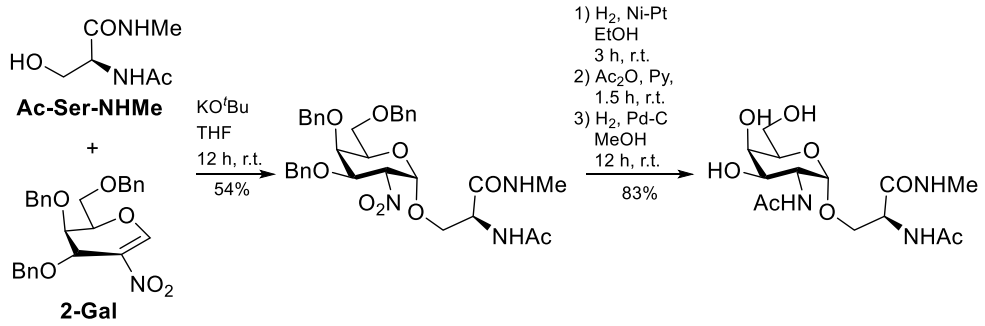

Scheme 2.18. Synthesis of the serine Tn antigen as a diamide.

In order to estimate these affinities, competition-tailored enzyme-linked lectin assays (ELLA) were performed. This technique is not quantitative, but allows comparing relative affinities to lectins. The experiment can be performed in a standard 96-well plate and usually requires the immobilization of glycoconjugates on the surface of the well that are used as the competition reference. After blocking of the unreacted positions of the well, the antigen and a biotinylated lectin are added. After allowing the lectin to bind to the antigen or to the glycopeptidic reference, the well is washed, so the lectin-antigen complexes are removed. The lectin-glycoconjugate complexes are still attached to the plate and can be detected by treatment with horseradish peroxidase (HRP) conjugated to streptavidin followed by oxidation with 3,3,5,5-tetramethylbenzidine (TMB) and sulfuric acid. This turns the solution from blue to yellow and the absorbance at 450 nm can be measured and plotted against the antigen concentration. A decay of the absorbance is thus expected as the concentration of antigen increases.

In our case, the glycopeptide Ala-Pro-Asp-Thr(GalNAc)-Arg-Pro was selected as competition reference. It can be inferred from these experiments that SBL has a preference for the natural Ser-Tn antigen, being compound **9** the best non-natural candidate. Glycomimics **9** and **10** showed inhibition at a concentration over 500 μM and quite adequate at a concentration of 1000 μM. This behavior was also found for compound **9** with VVL (figure **2.10**).

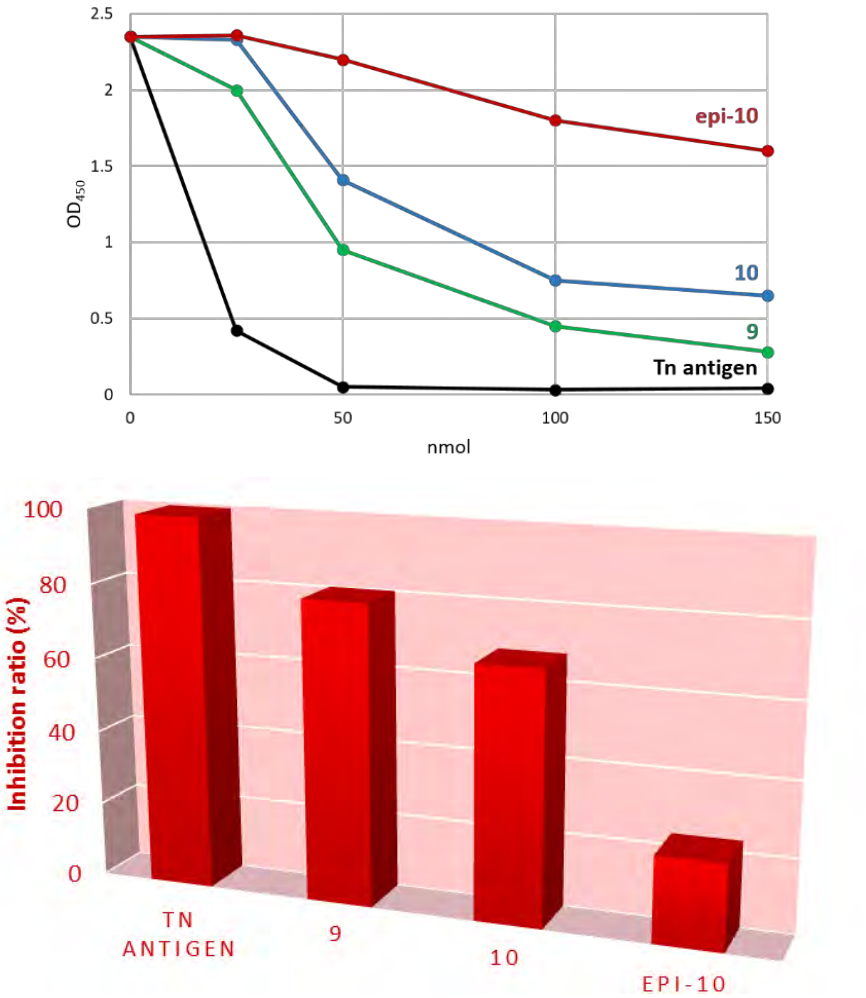

Figure 2.10. Binding curves (top) and inhibition ratio at 1000 μM (bottom) obtained for the Tn antigen and mimics **9**, **10** and **epi-10** in the competition ELLA assay towards SBL.

Of note, even though compounds **9** and **10** are not structurally similar analogues of the Tn antigen, as the conformational analysis illustrated, they are indeed recognized by SBL and VVL and can therefore be regarded as Tn antigen mimics. Hence, a close structural similarity between the natural compound and the mimic is not needed in this case.

Apparently, the configuration of the Cα considerably affects to the carbohydrate-lectin interaction. **Epi-10** showed a much lower affinity that compounds **9** and **10**. A putative 3D model of the three complexes with SBL was derived from MD simulations to shed light on these experimental observations. Generally, the interactions between the protein and the glyco-amino-acid are quite similar to those found in the modeled 3D structure of the Tn antigen in complex with SBL.[60] The difference between **10** and **epi-10** affinities could be attributed to the fact that Hα is involved in a hydrophobic interaction with the aromatic ring of Phe128 of SBL. This stabilizing interaction becomes destabilizing in the case of **epi-10**, in which the acetamido group is pointing to the aromatic ring (figure **2.11**).

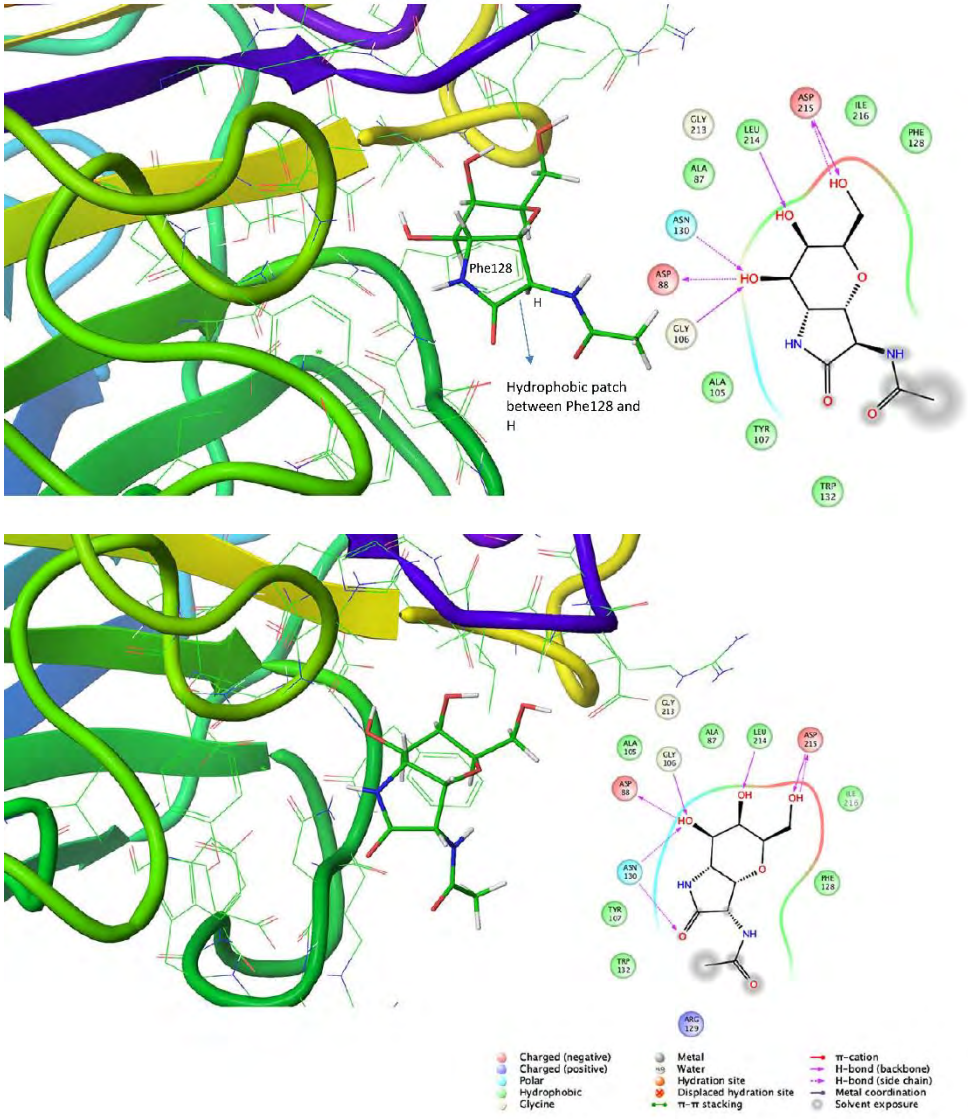

Figure 2.11. Snapshot taken from the unrestrained 20 ns MD simulation for SBL:**10** (top) and SBL:**epi-10** (bottom), together with the ligand interaction diagram obtained with Maestro 9.3.5 software.

The higher affinity observed for compound **9** may be explained by a highly populated hydrogen bond between the CH_2OH group of the ligand and Arg129 of SBL, which cannot take place in **10** and **epi-10** mimics (figure **2.12**).

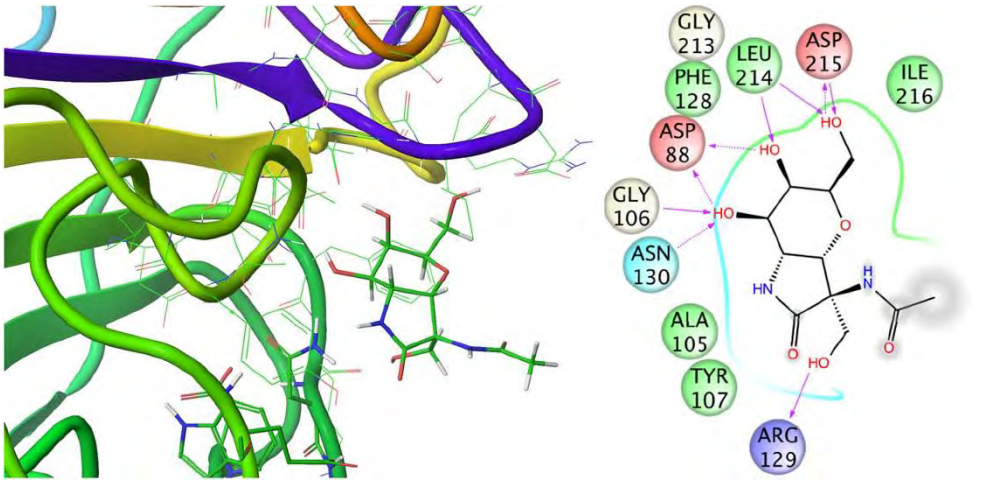

Figure 2.12. Snapshot taken from the unrestrained 20 ns MD simulation for SBL:**9** together with the ligand interaction diagram obtained with Maestro 9.3.5 software.

2.4.2. Amino-restricted *C*-glycosides free amino acids

In this case, compound **12** is a bicyclic *C*-glycoside as well, but the amide group of the carbohydrate moiety is attached to the nitrogen of the underlying amino acid forming a cyclic urea. It exhibits a hydroxymethyl group attached to the Cα of the amino acid and a free carboxylic acid (figure **2.13**).

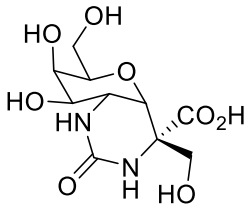

Figure 2.13. Structure of amino-restricted C-glycoside amino acid **12**.

To synthesize this bicyclic system, compounds **3b** or **3c** can be used as starting materials. Selective nitro group reduction using platinized

Nickel Raney® can be used to obtain tricyclic derivatives **11b-c**, although obtained yields are quite low (< 20%) due to formation of lactam **5** (scheme **2.19**).

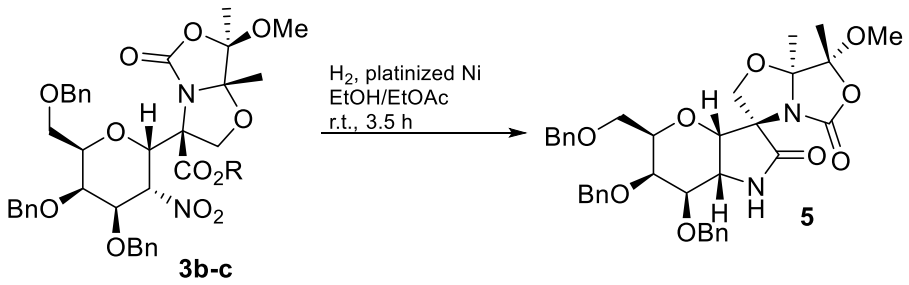

Scheme 2.19. The use of platinized Ni favors formation of lactam **5**.

A variation of the previously mentioned procedure to selectively reduce the nitro group was hence developed. The use of Zn under acidic conditions provides a mild method for reducing nitro groups to amines in the presence of other reducible groups. Treatment of compounds **3b-c** with Zn dust in THF-HCl-HOAc at 0 ºC for 1 h afforded the amine, which immediately reacted with the oxazolidinone forming the urea moiety. Carbonyl recovery led to formation of a pendant methylketone group with concomintant methanol loss. Filtration and purification by column chromatography afforded compounds **11b** and **11c** in moderate yields (45-56%, scheme **2.20**). Small amounts of compound **5** were isolated as well (<15% yield).

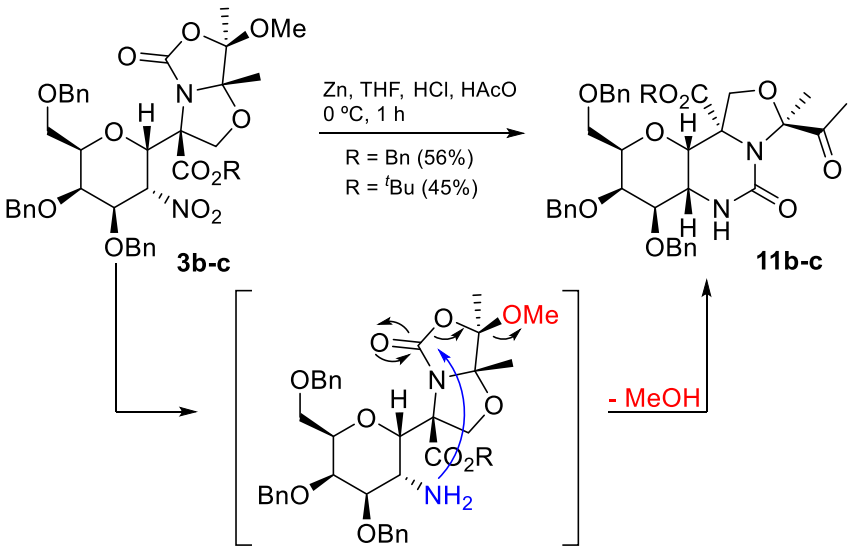

Scheme 2.20. Formation of tricyclic compounds **11b-c**.

Acidic hydrolysis using an aqueous 6 M HCl solution under reflux for 16 hours led to the deprotection of all protecting groups: *N*,*O*-acetal was hydrolyzed to give the free ureidoalcohol; benzyl or *tert*-butyl esters gave the corresponding carboxylic acid; and the *O*-benzyl ethers afforded the corresponding alcohols. Purification by RP-HPLC afforded the amino-restricted *C*-glycoside **12** in moderate yield (40% scheme **2.21**).

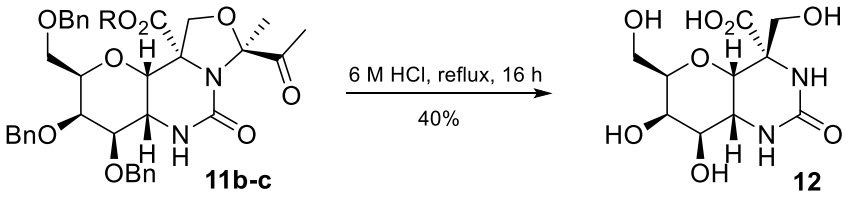

Scheme 2.21. Synthesis of amino-restricted serine *C*-glycoside.

The conformational study and the corresponding bioactivity assays (surface plasmon resonance, SPR) of this compound are currently being performed.

2.4.3. Unrestricted *C*-glycoside free amino acid

In this final case, there is no conformational restriction other than the *C*-glycosidic bond between the GalNAc moiety and the Cα of serine. The first step to obtain the unrestricted serine *C*-glycoside was a selective reduction of the nitro group of compounds **3a-c** and concomitant acetylation of the formed amine. The use of Zn under acidic conditions allow simultaneous nitro reduction and amine acetylation. Thus, compounds **3a-c** were treated with Zn dust and sat. aq. $CuSO_4$ in THF-HOAc-Ac_2O (3:2:1) at room temperature for 4 hours. This is a quite common methodology to reduce and *N*-acylate azides,[63–65] which have proven to work also for nitro groups. The corresponding *N*-acetamides **13a-c** were obtained in moderate yields (scheme **2.22**).

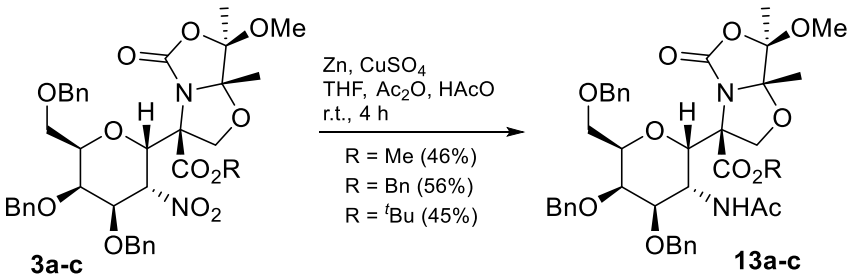

Scheme 2.22. Simultaneous reduction and *N*-acetylation of compounds **13a-c**.

The shortest pathway to obtain the unprotected glyco-amino-acid was to perform an acidic hydrolysis of compound **13b** (benzyl ester), to deprotect the amino and hydroxyl groups of serine, followed by hydrogenation to deprotect the carboxylic acid and the hydroxyl groups of the carbohydrate moiety. Compound **13b** was hence reacted with an aqueous 4 M HCl solution in THF at 40 ºC for 16 h to afford the corresponding aminoal-

cohol hydrocholoride, which was directly subjected to hydrogenation, using Pd-C as a catalyst in methanol (MeOH) at room temperature for 16 h. Three drops of cc. HCl were required to achieve complete deprotection. Purification by RP-HPLC afforded *C*-glyco-amino-acid **14** (scheme **2.23**).

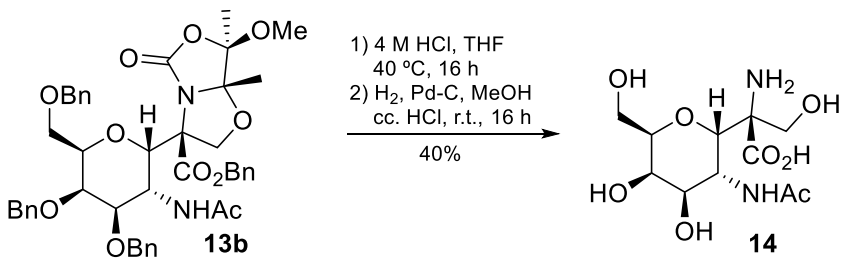

Scheme 2.23. Synthesis of free *C*-glyco-amino-acid **14**.

The conformational study and the corresponding bioactivity assays (surface plasmon resonance, SPR) of this compound are currently being performed.

2.5. Conclusions

Throughout this chapter, we have developed and optimized a completely diastereoselective double asymmetric *C*-Michael-type addition of three different bicyclic serine equivalents as an entry to new *C*-glycosides Tn antigen mimics. This was, to the best of our knowledge, the first example of obtaining C-glycosides through Michael addition on 2-nitroglycal derivatives. Depending on the nature of the ester group and the conditions used for reducing the nitro group to amine, we were able to obtain three different families of conformationally locked *C*-glycosides. The conformational analyses of these scaffolds were performed combining NMR spectroscopy and molecular modelling, showing in all cases a high rigidity due to the *C*-glycosidic bond and to the bicyclic structure. Bicyclic compounds **9**

and **10** retained bioactivity for SBA and VVA lectins, as proven by competition-tailored ELLA experiments, and can therefore be regarded as Tn antigen analogs. These results shed light into conformational aspects relevant for molecular recognition processes between carbohydrates and lectins.

This work has been published as an article entitled "A Double Diastereoselective Michael-type Addition as an Entry to Conformationally Restricted Tn Antigen Mimics" in the *Journal of Organic Chemistry*, **2013**, *78*, 10968-10977.

Additionally, other restricted Tn antigen mimics (**12** and **14**) have been developed and are currently under investigation.

2.6. References

(1) Kuberan, B.; Sikkander, S. A.; Tomiyama, H.; Linhardt, R. J. *Angew. Chem. Int. Ed.* **2003**, *42*, 2073–2075.
(2) Cipolla, L.; Rescigno, M.; Leone, A.; Peri, F.; La Ferla, B.; Nicotra, F. *Bioorg. Med. Chem.* **2002**, *10*, 1639–1646.
(3) Awad, L.; Madani, R.; Gillig, A.; Kolympadi, M.; Philgren, M.; Muhs, A.; Gérard, C.; Vogel, P. *Chem. Eur. J.* **2012**, *18*, 8578–8582.
(4) Dondoni, A.; Marra, A. *Chem. Rev.* **2000**, *100*, 4395–4421.
(5) Potuzak, J. S.; Tan, D. S. *Tetrahedron Lett.* **2004**, *45*, 1797–1801.
(6) Somsák, L. *Chem. Rev.* **2001**, *101*, 81–135.
(7) Lieberknecht, A.; Griesser, H.; Krämer, B.; Bravo, R. D.; Colinas, P. A.; Grigera, R. J. *Tetrahedron* **1999**, *55*, 6475–6482.
(8) Urban, D.; Skrydstrup, T.; Beau, J.-M. *Chem. Commun.* **1998**, *9*, 955–956.
(9) Röhrig, C. H.; Takhi, M.; Schmidt, R. R. *Synlett* **2001**, 1170–1172.
(10) Avenoza, A.; Cativiela, C.; Corzana, F.; Peregrina, J. M.; Zurbano, M. M. *Tetrahedron: Asymmetry* **2000**, *11*, 2195–2204.
(11) Avenoza, A.; Cativiela, C.; Corzana, F.; Peregrina, J. M.; Sucunza, D.; Zurbano, M. M. *Tetrahedron: Asymmetry* **2001**, *12*, 949–957.
(12) Avenoza, A.; Barriobero, J. I.; Cativiela, C.; Fernández-Recio, M. A.; Peregrina, J. M.; Rodríguez, F. *Tetrahedron* **2001**, *57*, 2745–2755.
(13) Avenoza, A.; Barriobero, J. I.; Busto, J. H.; Cativiela, C.; Peregrina, J. M. *Tetrahedron: Asymmetry* **2002**, *13*, 625–632.

(14) Avenoza, A.; Busto, J. H.; Cativiela, C.; Peregrina, J. M.; Sucunza, D.; Zurbano, M. M. *Tetrahedron: Asymmetry* **2003**, *14*, 399–405.
(15) Avenoza, A.; Busto, J. H.; Canal, N.; Peregrina, J. M. *Chem. Commun.* **2003**, *12*, 1376–1377.
(16) Avenoza, A.; Busto, J. H.; Corzana, F.; Jiménez-Osés, G.; París, M.; Peregrina, J. M.; Sucunza, D.; Zurbano, M. M. *Tetrahedron: Asymmetry* **2004**, *15*, 131–137.
(17) Avenoza, A.; Busto, J. H.; Corzana, F.; Peregrina, J. M.; Sucunza, D.; Zurbano, M. M. *Synthesis* **2005**, 575–578.
(18) Avenoza, A.; Busto, J. H.; Canal, N.; Peregrina, J. M. *J. Org. Chem.* **2005**, *70*, 330–333.
(19) Avenoza, A.; Busto, J. H.; Canal, N.; Peregrina, J. M.; Pérez-Fernández, M. *Org. Lett.* **2005**, *7*, 3597–3600.
(20) Avenoza, A.; Peregrina, J. M.; San Martín, E. *Tetrahedron Lett.* **2003**, *44*, 6413–6416.
(21) Corzana, F.; Busto, J. H.; Engelsen, S. B.; Jiménez-Barberó, J.; Asensio, J. L.; Peregrina, J. M.; Avenoza, A. *Chem. Eur. J.* **2006**, *12*, 7864–7871.
(22) Corzana, F.; Busto, J. H.; Jiménez-Osés, G.; Asensio, J. L.; Jiménez-Barbero, J.; Peregrina, J. M.; Avenoza, A. *J. Am. Chem. Soc.* **2006**, *128*, 14640–14648.
(23) Corzana, F.; Busto, J. H.; Jiménez-Osés, G.; García De Luis, M.; Asensio, J. L.; Jiménez-Barbero, J.; Peregrina, J. M.; Avenoza, A. *J. Am. Chem. Soc.* **2007**, *129*, 9458–9467.
(24) Fernández-Tejada, A.; Corzana, F.; Busto, J. H.; Jiménez-Osés, G.; Peregrina, J. M.; Avenoza, A. *Chem. Eur. J.* **2008**, *14*, 7042–7058.
(25) Fernández-Tejada, A.; Corzana, F.; Busto, J. H.; Avenoza, A.; Peregrina, J. M. *J. Org. Chem.* **2009**, *74*, 9305–9313.
(26) Fernández-Tejada, A.; Corzana, F.; Busto, J. H.; Avenoza, A.; Peregrina, J. M. *Org. Biomol. Chem.* **2009**, *7*, 2885–2893.
(27) Fernández-Tejada, A.; Corzana, F.; Busto, J. H.; Jiménez-Osés, G.; Jiménez-Barbero, J.; Avenoza, A.; Peregrina, J. M. *Chem. Eur. J.* **2009**, *15*, 7297–7301.
(28) Corzana, F.; Busto, J. H.; García De Luis, M.; Fernández-Tejada, A.; Rodríguez, F.; Jiménez-Barbero, J.; Avenoza, A.; Peregrina, J. M. *Eur. J. Org. Chem.* **2010**, 3525–3542.
(29) Aydillo, C.; Jiménez-Osés, G.; Busto, J. H.; Peregrina, J. M.; Zurbano, M. M.; Avenoza, A. *Chem. Eur. J.* **2007**, *13*, 4840–4848.
(30) Jiménez-Osés, G.; Aydillo, C.; Busto, J. H.; Zurbano, M. M.; Peregrina, J. M.; Avenoza, A. *J. Org. Chem.* **2007**, *72*, 5399–5402.
(31) Aydillo, C.; Avenoza, A.; Busto, J. H.; Jiménez-Osés, G.; Peregrina, J. M.; Zurbano, M. M. *Tetrahedron: Asymmetry* **2008**, *19*, 2829–2834.
(32) Jiménez-Osés, G.; Aydillo, C.; Busto, J. H.; Zurbano, M. M.; Peregrina, J. M.; Avenoza, A. *J. Org. Chem.* **2014**, *79*, 2556–2563.
(33) Aydillo, C.; Jiménez-Osés, G.; Avenoza, A.; Busto, J. H.; Peregrina, J. M.; Zurbano, M. M. *J. Org. Chem.* **2011**, *76*, 6990–6996.
(34) Winterfeld, G. A.; Ito, Y.; Ogawa, T.; Schmidt, R. R. *Eur. J. Org. Chem.*

1999, 1167–1171.
(35) Zhu, X.; Schmidt, R. R. *Angew. Chem. Int. Ed.* **2009**, *48*, 1900–1934.
(36) Das, J.; Schmidt, R. R. *Eur. J. Org. Chem.* **1998**, 1609–1613.
(37) Pachamuthu, K.; Gupta, A.; Das, J.; Schmidt, R. R.; Vankar, Y. D. *Eur. J. Org. Chem.* **2002**, 1479–1483.
(38) Vedachalam, S.; Tan, S. M.; Teo, H. P.; Cai, S.; Liu, X. W. *Org. Lett.* **2012**, *14*, 174–177.
(39) Xue, W.; Sun, J.; Yu, B. *J. Org. Chem.* **2009**, *74*, 5079–5082.
(40) Winterfeld, G. A.; Schmidt, R. R. *Angew. Chem. Int. Ed.* **2001**, *40*, 2654–2657.
(41) Masamune, S.; Choy, W.; Petersen, J. S.; Sita, L. R. *Angew. Chem. Int. Ed.* **1985**, *24*, 1–30.
(42) Kolodiazhnyi, O. I. *Tetrahedron* **2003**, *59*, 5953–6018.
(43) Davies, S. G.; Lee, J. A.; Roberts, P. M.; Thomson, J. E.; Yin, J. *Tetrahedron* **2011**, *67*, 6382–6403.
(44) Kunz, H.; Weiβmüller, J.; Müller, B. *Tetrahedron Lett.* **1984**, *25*, 3571–3574.
(45) Kunz, H.; Müller, B.; Weissmüller, J. *Carbohydr. Res.* **1987**, *171*, 25–34.
(46) Schmidt, R. R.; Vankar, Y. D. *Acc. Chem. Res.* **2008**, *41*, 1059–1073.
(47) Karplus, M. *J. Am. Chem. Soc.* **1963**, *85*, 2870–2871.
(48) Karplus, M. *J. Chem. Phys.* **1959**, *30*, 11–15.
(49) Nishimura, S. *Bull. Chem. Soc. Jpn.* **1959**, *32*, 61–64.
(50) Heilbron, I.; Jones, E. R. H.; Sondheimer, F. *J. Chem. Soc.* **1947**, 1586–1590.
(51) Heilbron, I.; Jones, E. R. H.; Sondheimer, F. *J. Chem. Soc.* **1949**, 604–607.
(52) An, G.; Ahn, H.; De Castro, K. A.; Rhee, H. *Synthesis* **2010**, 477–485.
(53) Carlsen, P. H. J.; Katsuki, T.; Martin, V. S.; Sharpless, K. B. *J. Org. Chem.* **1981**, *46*, 3936–3938.
(54) Dess, D. B.; Martin, J. C. *J. Org. Chem.* **1983**, *48*, 4155–4156.
(55) Dess, D. B.; Martin, J. C. *J. Am. Chem. Soc.* **1991**, *113*, 7277–7287.
(56) Tollens, B. *Berichte der Dtsch. Chem. Gesellschaft* **1882**, *15*, 1635–1639.
(57) Braun, P.; Davies, G. M.; Price, M. R.; Williams, P. M.; Tendler, S. J. B.; Kunz, H. *Bioorg. Med. Chem.* **1998**, *6*, 1531–1545.
(58) Kuhn, A.; Kunz, H. *Angew. Chem. Int. Ed.* **2007**, *46*, 454–458.
(59) Dam, T. K.; Gerken, T. A.; Cavada, B. S.; Nascimento, K. S.; Moura, T. R.; Brewer, C. F. *J. Biol. Chem.* **2007**, *282*, 28256–28263.
(60) Rao, V. S. R.; Lam, K.; Qasba, P. K. *J. Biomol. Struct. Dyn.* **1998**, *15*, 853–860.
(61) Godula, K.; Bertozzi, C. R. *J. Am. Chem. Soc.* **2012**, *134*, 15732–15742.
(62) Tollefsen, S. E.; Kornfeld, R. *J. Biol. Chem.* **1983**, *258*, 5165–5171.
(63) Lee, D. J.; Harris, P. W. R.; Brimble, M. A. *Org. Biomol. Chem* **2011**, *9*, 1621–1626.
(64) Meinjohanns, E.; Meldal, M.; Schleyer, A.; Paulsen, H.; Bock, K. *J. Chem. Soc., Perkin Trans. 1* **1996**, 985–993.
(65) Bourgault, J. P.; Trabbic, K. R.; Shi, M.; Andreana, P. R.; Edu, P. A. *Org. Biomol. Chem* **2014**, *12*, 1699–1702.

Chapter 3. Glycosidase inhibitors and pharmacological chaperones based on *C*-glycosides

3.1. Introduction

During the last decades, enzymes have been, and still are, a primary target for the development and design of new drug candidates, since slight alterations in the behavior and bioactivity of enzymes lead to immediate and defined effects.[1] In fact, they represent around the half (47%) of the marketed small-molecule drug launched targets, despite the increasingly use of drugs that target extracellular receptors (figure **3.1**).[2]

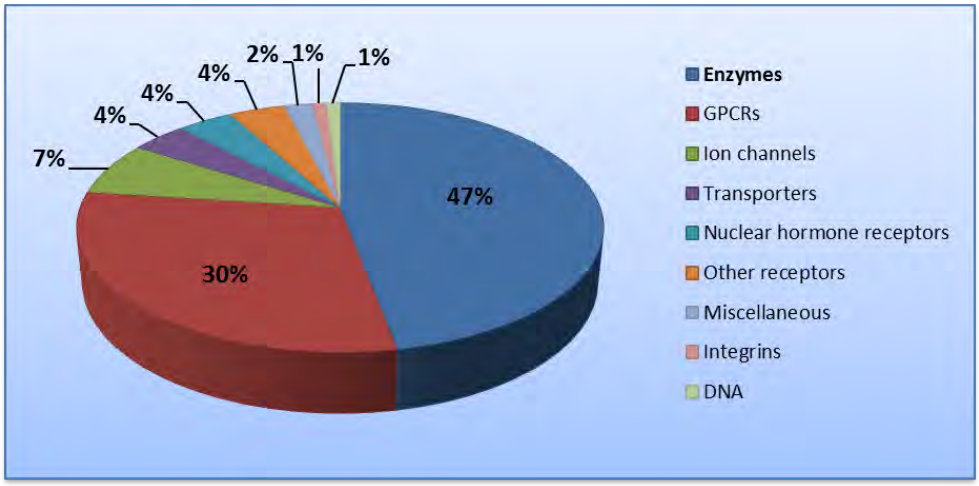

Figure 3.1. Marketed small-molecule drug targets by biochemical class. GPCR: G-protein-coupled receptor. *Source*: redrawn from Hopkins and Groom (2002).[2]

Enzyme catalysis is essential for living organisms and consequently the selective inhibition of certain enzymes can be very effective for the chemical treatment of infectious diseases produced by viruses or bacteria, or for the regulation and refurbishment of malfunctioning enzymes. A selection of enzyme inhibitors that are in clinical use or trial is shown in table **3.1**.

Table 3.1. Selected enzyme inhibitors in clinical use or trial.[3]

Compound	Target enzyme	Clinical use
Acetazolamide	Carbonic anhydrase	Glaucoma
Acyclovir	Viral DNA polymerase	Herpes
Amprenavir, indinavir, nelfinavir, ritonavir, saquinavir	HIV protease	AIDS
Allopurinol	Xanthine oxidase	Gout
Argatroban	Thrombin	Heart disease
Aspirin	Cyclooxygenases	Inflammation, pain, fever
Amoxicillin	Penicillin binding proteins	Bacterial infection
Captopril, enalapril	Angiotensin converting enzyme	Hypertension
Carbidopa	Dopa decarboxylase	Parkinson's disease
Celebrex, Vioxx	Cyclooxygenase-2	Inflammation
CI-1040, PD0325901	MAP kinase	Cancer
Clavulanate	β-Lactamase	Bacterial resistance
Digoxin	Na^+, K^+ ATPase	Heart disease
Efavirenz, nevirapine	HIV reverse transcriptase	AIDS
Epristeride, finasteride, dutasteride	Steroid 5α-reductase	Bening prostate hyperplasia, male pattern baldness
Fluorouracil	Thymidylate synthase	Cancer
Leflunomide	Dihydroorotate dehydrogenase	Inflammation
Lovastatin	HMG-CoA reductase	Cholesterol lowering
Methotrexate	Dihydrofolate reductase	Cancer, immunosuppresion
Nitecapone	Catechol-*O*-methyltransferase	Parkinson's disease
Norfloxacin	DNA gyrase	Urinary tract infection
Omeprazol	H^+, K^+ ATPase	Peptic ulcers
PALA	Aspartate transcarbamoylase	Cancer
Sorbinol	Aldose reductase	Diabetic retinopathy
Trimethoprim	Bacterial dihydrofolate reductase	Bacterial infections
Viagra, Levitra	Phosphodiesterase	Erectile dysfunction

Inhibitor binding can be either reversible or irreversible. Irreversible inhibitors usually bind covalently to the enzyme, changing it chemically. On the other hand, reversible inhibitors interact non-covalently with the enzyme, producing three different types of mechanisms (figure **3.2**):

- Competitive: the inhibitor binds exclusively to the enzyme. Binding of the inhibitor and the substrate to the enzyme are mutually exclusive.
- Uncompetitive: the inhibitor binds exclusively to the enzyme-substrate complex or a subsequent species, with little or no affinity for the free enzyme.
- Noncompetitive: the inhibitor binds to both, the free enzyme and the enzyme-substrate complex or subsequent species.

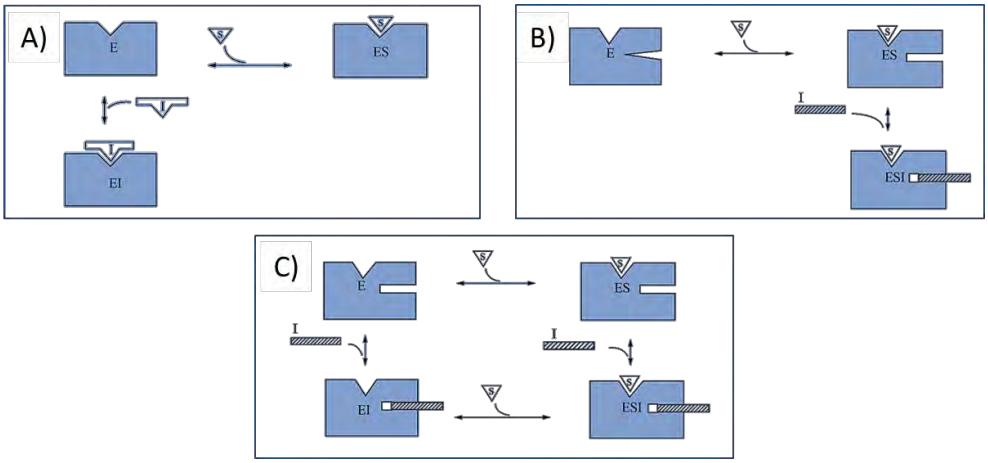

Figure 3.2. Cartoon representations of the three reversible enzyme inhibition mechanisms: A) competitive, B) uncompetitive, C) noncompetitive. *Source*: redrawn from Copeland (2013).[3]

As previously addressed, glycosidase enzymes hydrolyze glycosidic bonds and are involved in several biological processes, which makes them a great target for the development of new drug candidates.[4–7] The number of glycosidase inhibitors increases continuously, and the development and design of new potent and selective inhibitors is an extremely active field of research.[8–10]

3.2. Goals

With this background in mind, we conceived 3-**a**mino-6,7-dihydroxy-3,5-bis(hydroxymethyl)hexahydro**p**yrano[3,2-*b*]**p**yrrol-2(1*H*)-one (APP) derivatives (compound **9**) as a new family of glycosidase inhibitors. The amino and hydroxymethyl groups simultaneously attached to the quaternary anomeric carbon warrant chemical and enzymatic stability, may also provide selectivity, and enable the incorporation of aglycone moieties. In this sense, palmitoyl and acetyl groups were selected as long and short alkyl chains, respectively, to obtain a library of mono- and disubstituted APP derivatives (figure **3.3**). The affinity and selectivity of these candidates were evaluated against several commercially available glycosidase enzymes.

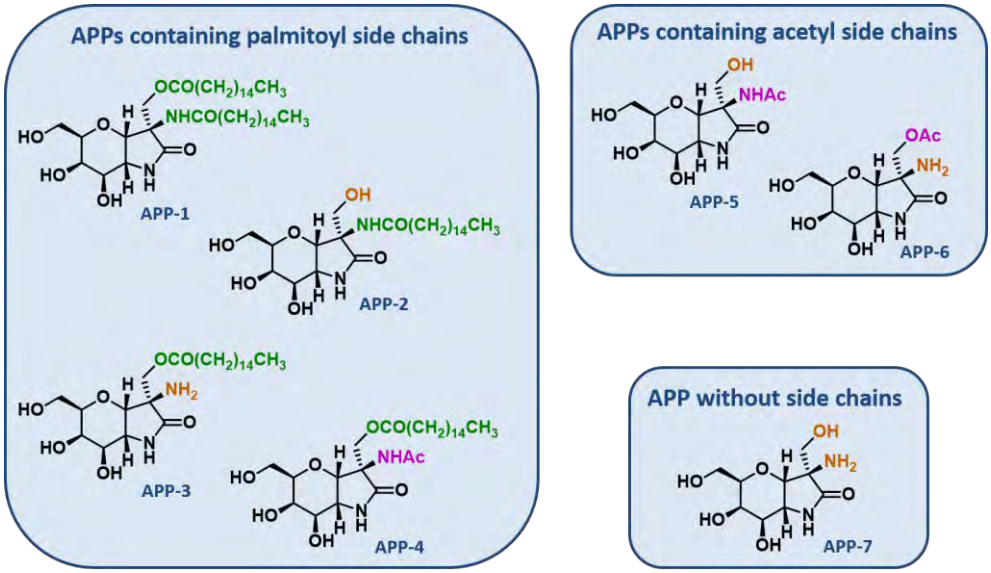

Figure 3.3. New APP derivatives as glycosidase inhibitors candidates.

3.3. Synthesis

Previously described compound **5** was used as starting material to obtain all of the APP derivatives. First, a simultaneous hydrolysis of the oxazolidine and oxazolidinone rings was performed by treatment with 4 M HCl in THF (1:4) at 40 ºC for 16 h. This was followed by reaction of the hydrochloride salt with propylene oxide in EtOH at reflux for 2 h to obtain amino alcohol derivative **15** in a good yield (71%) (scheme **3.1**).

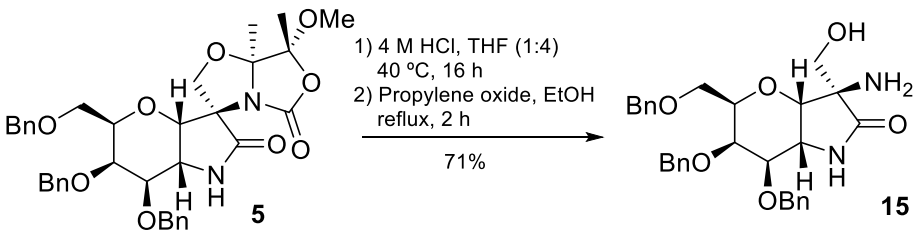

Scheme 3.1. Synthesis of aminoalcohol **15**.

Simultaneous acylation of amino and alcohol groups of derivative **15** using palmitoyl chloride (PalmCl) and TEA in DCM at room temperature for 12 h afforded dipalmitoylated compound **16** in a good yield (70%). Subsequent hydrogenolysis in MeOH using Pd-C as a catalyst at room temperature for 16 h afforded unprotected **APP-1** in an excellent yield (93%) (scheme **3.2**).

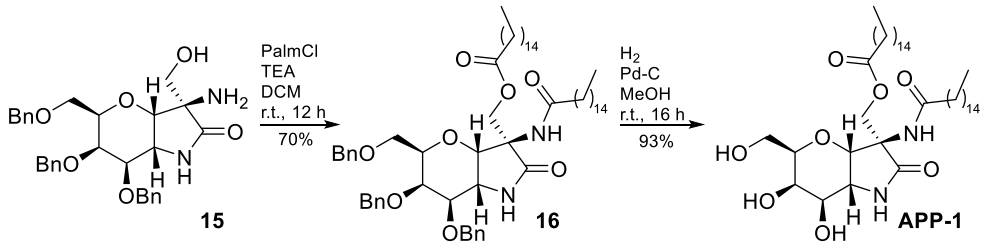

Scheme 3.2. Synthesis of derivative **16** and **APP-1**.

Selective de-*O*-acylation was performed on derivative **16** by treatment with sodium methoxide in MeOH for 90 min, affording alcohol **17**. Deprotection of *O*-benzyl ethers was achieved by hydrogenolysis following the previously described procedure. **APP-2**, which bears a single-chain *N*-palmitoyl aglycone moiety, was therefore obtained in 72% global yield (scheme **3.3**).

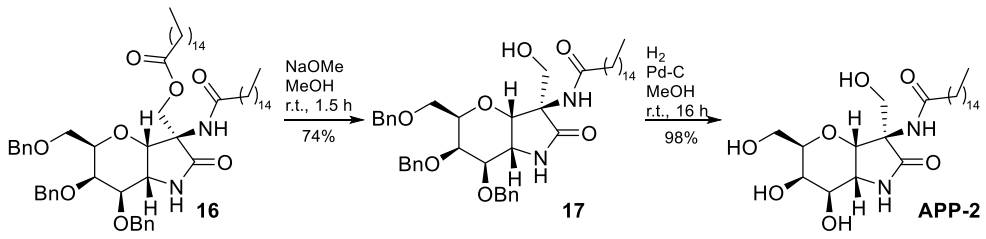

Scheme 3.3. Synthesis of derivative **17** and **APP-2**.

Analogous mono-*O*-palmitoylated **APP-3**, which has an unprotected amino group in the aglycone, was obtained from spirocyclic precursor **5** in four steps. First, an acidic hydrolysis with 4 M HCl in THF (1:4) at 40 ºC for 16 h, followed by a regioselective *O*-palmitoylation[11] by treatment with palmitoyl chloride in 100% TFA at room temperature for 15 minutes was performed. Neutralization with propylene oxide to obtain adduct **18** and, finally, hydrogenolysis of the *O*-benzyl groups afforded **APP-3** in 62% overall yield (scheme **3.4**).

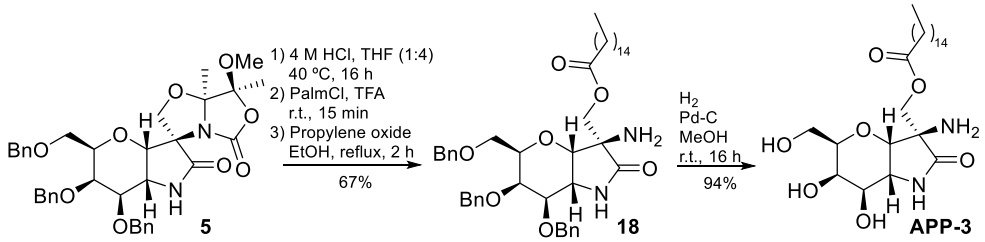

Scheme 3.4. Synthesis of adduct **18** and **APP-3.**

Palmitoylation of *N*-acetyl alcohol derivative **7**, presented in *Chapter 2.4.1*, with palmitoyl chloride and TEA in DCM, followed by hydrogenolysis of the corresponding amidoester **19**, led to *N*-acetyl-*O*-palmitoyl **APP-4** (scheme **3.5**).

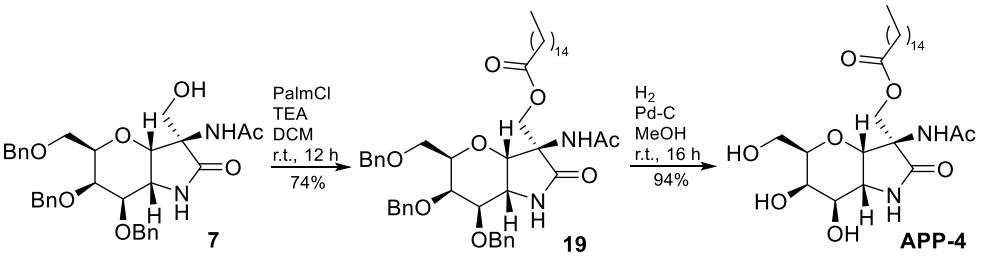

Scheme 3.5. Synthesis of compound **19** and **APP-4**.

To synthesize mono-acetylated **APP-5** and **APP-6**, similar procedures to those previously described were applied. In the case of **APP-5**, it was synthesized as described in *Chapter 2.4.1* (compound **9**), and **APP-6** was obtained by acidic hydrolysis of precursor **5**, followed by regioselective *O*-acetylation using AcCl in 100% TFA at room temperature for 15 min, neutralization with propylene oxide to obtain adduct **20** and, finally, hydrogenolysis of the *O*-benzyl groups (40% overall yield) (scheme **3.6**).

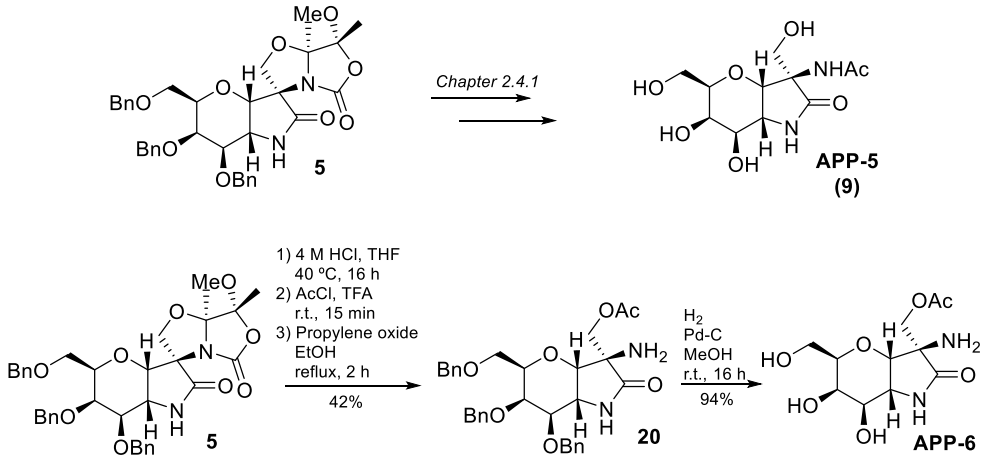

Scheme 3.6. Synthesis of **APP-5** and **APP-6**.

Finally, unprotected aminoalcohol derivative **APP-7** was efficiently obtained by hydrogenolysis of compound **15** (scheme **3.7**).

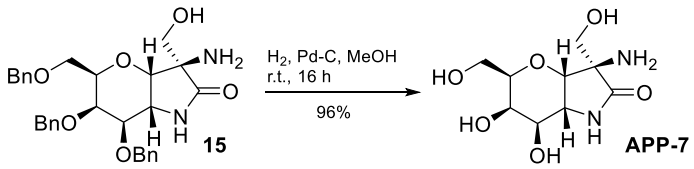

Scheme 3.7. Synthesis of **APP-7**.

3.4. Glycosidase inhibitory activity

In order to determine their ability to act as glycosidase inhibitors and in collaboration with Carmen Ortíz-Mellet's (University of Seville) and José Manuel García-Fernández's (IIQ-CSIC, Uiversity of Seville) groups, **APPs 1-7** were evaluated against several commercially available glycosidase enzymes. These enzymes included α-glucosidase (baker yeast), β-glucosidase (bovine liver and almonds), α-galactosidase (green coffee), β-galactosidase (bovine liver and *E. coli*), isomaltase (baker yeast), amyloglucosidase (*A. niger*), α-mannosidase (Jack bean), β-mannosidase (*H. pomatia*) and β-*N*-acetylglucosaminidase (human placenta, bovine liver and Jack bean). The corresponding inhibition constants (K_i, μM) were determined from the slope of Lineweaver-Burk plots (see figure **3.4** for a representative example) and are collected in Table **3.2**. No inhibition was detected for any of the compounds at concentrations up to 2 mM against amyloglucosidase (*A. niger*) (pH 5.5), β-glucosidase (almonds) (pH 7.3), β-galactosidase (*E. coli*) (pH 5.5) α-mannosidase (Jack bean) (pH 5.5), β-mannosidase (*H. pomatia*) (pH 5.5) and β-*N*-acetylglucosaminidase (human placenta, bovine liver and Jack bean) (pH 5.5). However, when inhibition was detected, it was competitive in all cases.

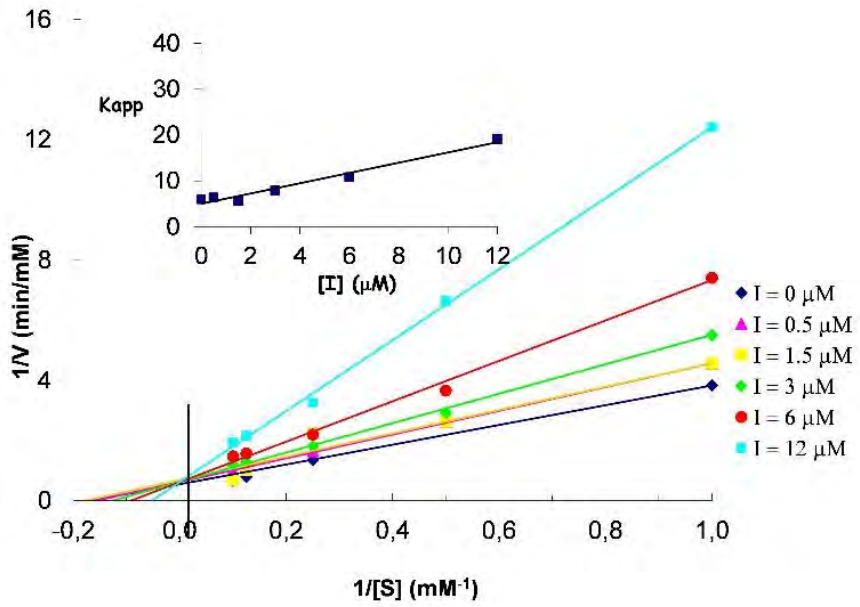

Figure 3.4. Lineweaver-Burk plot for K_i determination (5.8 μM) of **APP-2** against β-galactosidase (bovine liver) (pH 7.3). Two replicas were done for each experiment.

Table 3.2. Glycosidase inhibitory activities (K_i, μM) for APPs.

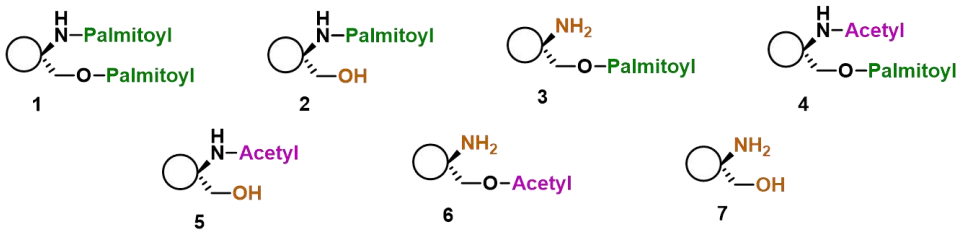

Enzymes	APP-1	APP-2	APP-3	APP-4	APP-5	APP-6	APP-7
Isomaltase (baker's yeast)	80 ± 9	34 ± 4	13 ± 1	19 ± 2	n.i.	97 ± 11	283 ± 31
α-glucosidase (baker's yeast)	255 ± 25	124 ± 13	27 ± 3	244 ± 28	n.i.	n.i.	532 ± 58
β-galactosidase (baker's yeast)	**10 ± 1**	**5.8 ± 0.6**	86 ± 9	**9.3 ± 8**	n.i.	n.i.	n.i.
α-galactosidase (green coffee)	657 ± 72	515 ± 56	67 ± 7	n.i.	n.i.	n.i.	n.i.

Bold numbers represent full K_i determined from the slope of Lineweaver-Burk plots and double reciprocal analysis. n.i. not inhibition.

The first conclusion that can be extracted from the data is the necessity of hydrophobic moieties on the aglycone (**APPs 1-4**) to obtain significant activity at a micromolar level. Isomaltase (K_i, 13-80) and β-galactosidase (K_i, 5.8-86) showed to be the most sensitive enzymes to APP inhibition. The presence of a large alkyl chain at the oxygen atom (**APP-3** and **APP-4**) clearly favors the inhibition against isomaltase and α-glucosidase. This behavior is quite the opposite of the observed in the case of mammalian β-galactosidase. **APPs 1-3** are highly selective, discriminating α- from β-galactosidase. This is perplexing since APPs are locked in a putative α configuration of the glycosidic linkage.

3.5. Pharmacological chaperone for Gaucher disease

Gaucher disease is a genetic disorder caused by a hereditary deficiency of the enzyme glucocerebrosidase (GCase). This enzyme acts within lysosomes and hydrolyzes the glycosphingolipid glucosylceramide, also known as glucocerebroside (figure **3.5**). Absence or malfunction of this enzyme, because of a mutation, leads to accumulation of glucocerebroside within the cell, eventually killing it and causing the disease.

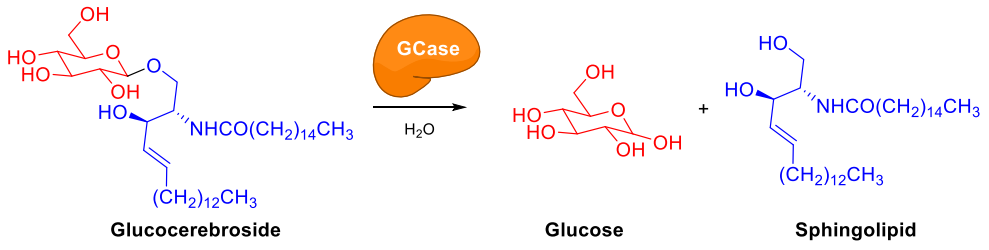

Figure 3.5. Glucosylceramide hydrolysis catalyzed by GCase.

Some inhibitors of GCase are able to bind to its active site at low concentrations and stabilize the appropriate folding, acting as pharmacological chaperones that make it easier for the enzyme to get into the lysosomes. Development of new inhibitors able to act as pharmacological chaperones for mutant forms of human β-glucocerebrosidase is therefore attracting a great deal of interest in the field of biochemistry. A preliminary parameter to select candidates as pharmacological chaperones for Gaucher disease is commonly the inhibition strength towards bovine liver β-glucosidase/β-galactosidase,[12] although the predictive character of the data must be taken with care.[13] In this sense and in collaboration with the Research Center for Bioscience and Technology (University of Tottori, Japan), the inhibitory potency of **APPs 1-4** was evaluated against GCase (Table **3.3**) as well as the IC_{50} values (Table **3.4**), namely the concentration of inhibitor that achieves 50% inhibition. The corresponding data for the non-glycomimetic type pharmacological chaperone Ambroxol® (ABX, figure **3.6**), which is a mucolytic drug currently in preclinical studies for the treatment of Gaucher disease,[14–17] are included as comparison. The influence of pH was also evaluated since it is another relevant parameter for selecting chaperone candidates.[18]

Table 3.3. Glycosidase inhibitory activities *in vitro* (K_i, μM) for **APPs 1-4** against human GCase at different pH values.

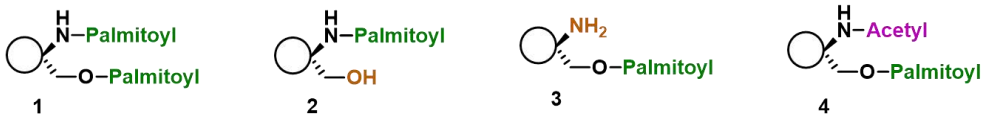

Enzymes	APP-1	APP-2	APP-3	APP-4
GCase (pH 7.0)	33 ± 4	20 ± 1	37 ± 2	52 ± 2
GCase (pH 5.0)	334 ± 12	204 ± 7	410 ± 14	537 ± 10

Table 3.4. IC_{50} values (μM) against human GCase for **APPs 1-4** at different pH values.

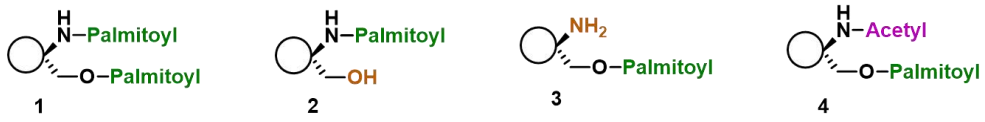

Enzymes	APP-1	APP-2	APP-3	APP-4	ABX
GCase (pH 7.0)	41 ± 1	23 ± 1	49 ± 2	67 ± 5	7.6 ± 0.5
GCase (pH 5.0)	470 ± 20	272 ± 10	606 ± 10	707 ± 20	67 ± 5

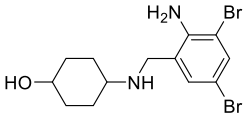

ABX

Figure 3.6. Structure of pharmacological chaperone Ambroxol® (ABX)

In this case, the presence of a long alkyl chain at the oxygen atom of APP derivatives seems to be detrimental for the human GCase inhibition. Although **APP-2** (IC_{50} 23 μM at pH 7.0) is a 1.8- to 2.9-fold stronger inhibitor than the other candidates assayed (IC_{50} 41-67 μM at pH 7.0), it is slightly weaker than the reference compound ABX (IC_{50} 7.6 μM at pH 7.0). A remarkable observation is that no inhibition was detected against other lysosomal enzymes, such as α-glucosidase, α-galactosidase, β-galactosidase, and β-hexosaminidase. Most interesting, an about one order of magnitude decrease in GCase inhibition strength was observed at pH 5, which is a highly favorable feature for chaperone candidates. Due to the promising results obtained for **APP-2** as GCase inhibitor, we decided to gain further structural information by performing 200 ns MD simulations on **APP-2** in complex with the human GCase (PDB code: 5LVX) (figures **3.7** and **3.8**).

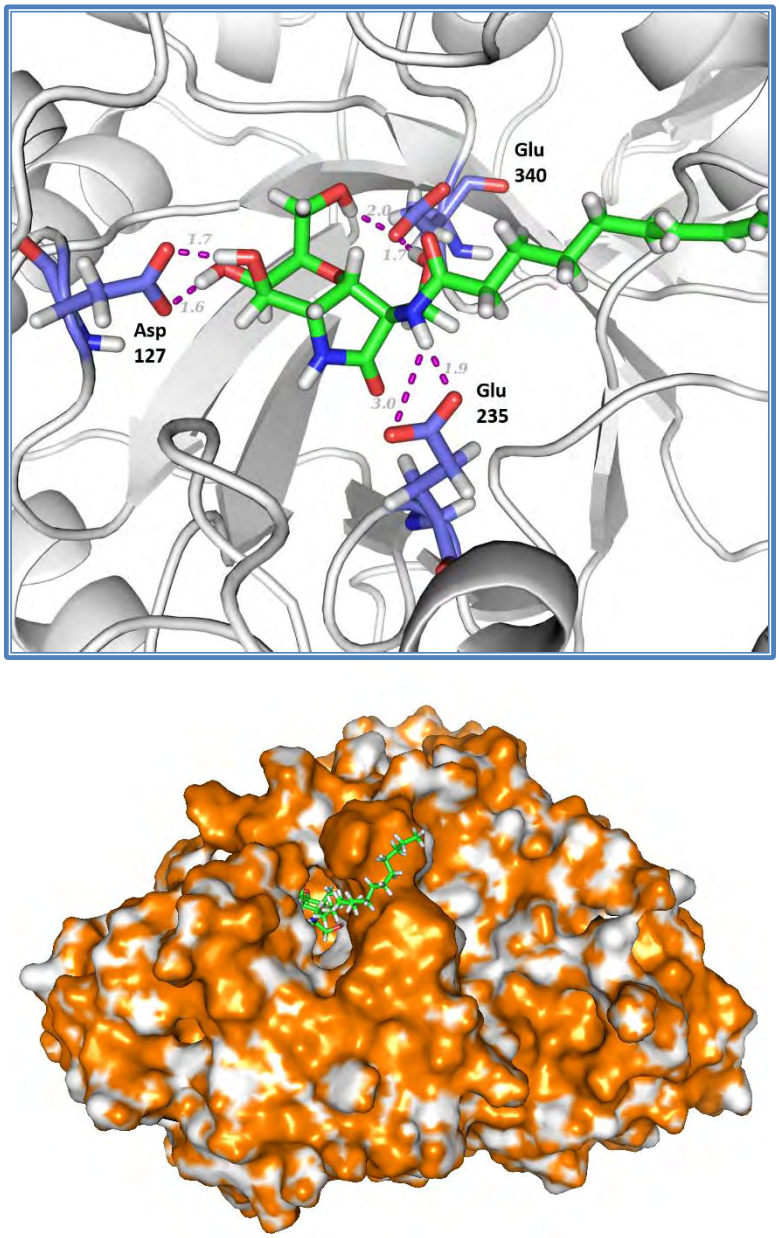

Figure 3.7. Representative frame obtained from the 200 ns MD simulation showing the hydrogen bonds between the glycone unit of **APP-2** and the residues in the binding site (top). The side chain of compound **APP-2** is engaged in hydrophobic contacts with the surface of the enzyme (bottom). The hydrophobic residues of the enzyme are shown in orange.

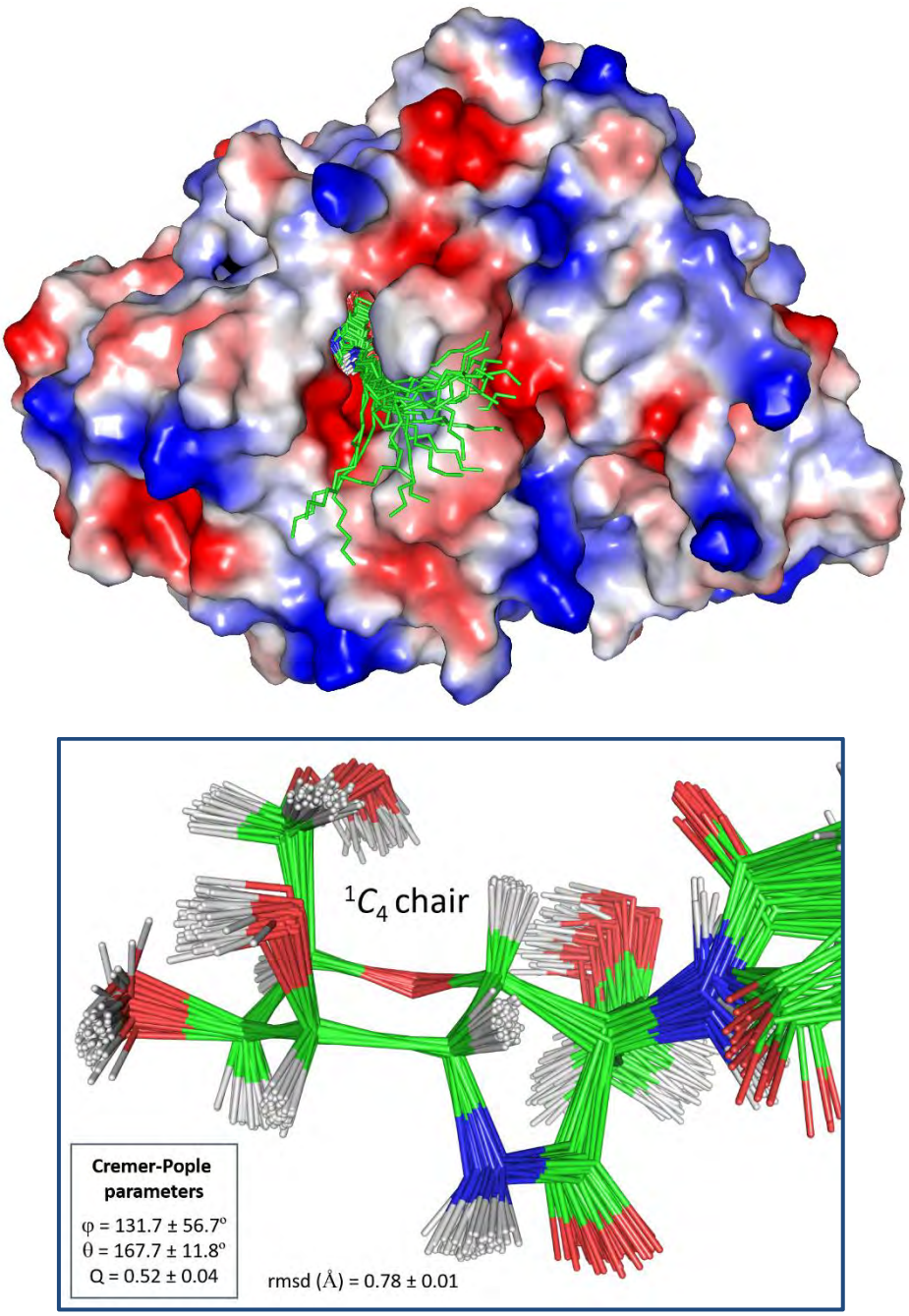

Figure 3.8. Ensemble obtained from an unrestrained 200 ns MD simulation performed on **APP-2**:GCase complex. The electrostatic potential surface of the protein is also represented. Red represents a net negative surface potential, and blue denotes a net positive surface potential. **APP-2** is shown as a stick model colored according to atom type.

Although the natural substrate of GCase is D-glucosylceramide, D-galacto configured glycomimetics have also shown to fit well in the catalytic site.[19] In the case of **APP-2**, the bicyclic scaffold is involved in a hydrogen bond network similarly to other glycomimetic-type competitive inhibitors.[20] Throughout the whole simulation, the hydroxyl groups at C3 and C4 interact with the carboxylate of Asp127, forcing the sugar moiety to adopt an unusual $^{1}C_{4}$ conformation according to the Cremer-Pople puckering parameters[21] for the average conformation (figure **3.8**). On the other hand, the exocyclic amide is engaged in a hydrogen bond with the catalytic nucleophile Glu235. The large difference in the inhibitory constants of APPs at neutral and acidic pH may be due to protonation of these residues. These interactions consequently force the alkylic chain to be oriented towards the hydrophobic region at the entrance of the active site, increasing the stability of the complex.

Even though **APP-2** showed the best inhibition properties, the four amphiphilic APPs were further assayed using healthy and Gaucher fibroblasts from patients with N370S, F213I or L444P GCase mutations, which are associated to the non-neuropathic (type 1) and neuropathic (type 2 and 3) Gaucher disease, respectively.[22] N370S is the most common mutation and is located at the catalytic domain of GCase. It is sensitive to the enzyme replacement or substrate reduction therapies currently available. F213I mutation is also located at the catalytic domain, whereas L444P mutation is located at a noncatalytic domain, making pharmacological chaperones less effective to it.[23,24] Cells were cultured for 5 days with and without APPs (2 and 20 μM) and lysed. The activity of GCase was then determined using 3-methylumbelliferyl-β-D-glucopyranoside as a substrate. Fold change in en-

zyme activity was monitored relative to the control in the absence of any inhibitor (figure **3.9**).

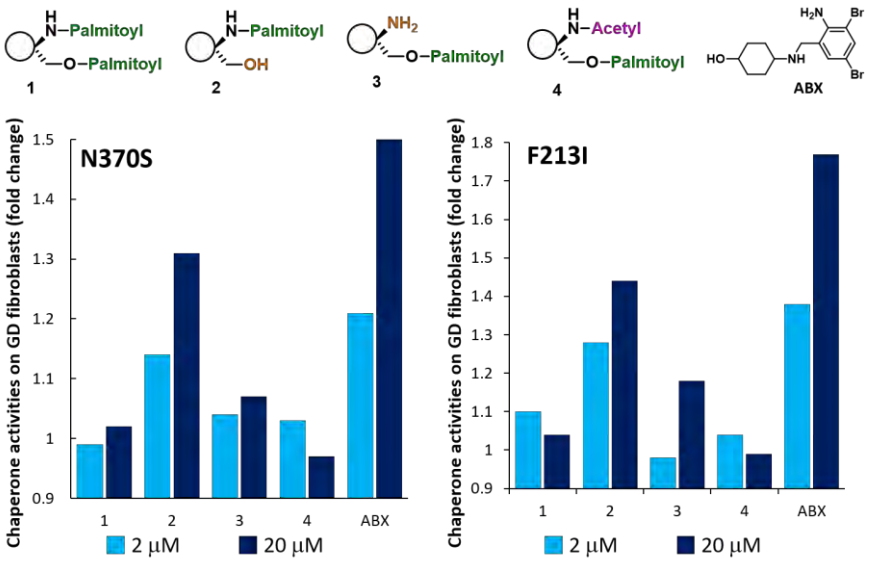

Figure 3.9. Comparative effect of **APPs 1-4** and ABX at 2 and 20 µM concentrations on the activity enhancements for N370S (left panel) and F213I (right panel).

APP-2 showed to significantly enhance the activity of N370S and F213I GCase mutants with relative increases of 1.3- and 1.5-folds, relatively, which are similar to those found for reference ABX (1.5 and 1.8-folds respectively) at 20 µM. In addition, none of the APPs exhibited toxicity on either the healthy or the mutant cell lines assayed after incubating for 5 days.

3.6. Conclusions

A library of conformationally locked *C*-glycosides based on 3-amino-6,7-dihydroxy-3,5-bis(hydroxymethyl)hexahydropyrano[3,2-*b*]pyrrol-2(1*H*)-one (APP) scaffolds have been synthesized using a totally stere-

ocontrolled Michael *C*-type addition of *C*-serine equivalent **1a** to nitrogalactal **2-Gal** and subsequential reduction of the nitro group as key steps. APP derivatives bearing long hydrophobic substituents (APPs **1-4**) showed μM competitive inhibition activity against bovine liver β-galactosidase and, most interestingly, against human lysosomal β-glucocerebrosidase (GCase) at neutral pH. The decrease of activity at lower pH values (pH 5.0) makes these compounds good candidates as pharmacological chaperones for Gaucher disease. In fact, **APP-2** was able to enhance the activity of N370S and F213I GCase mutants in fibroblasts of Gaucher patients similarly to the reference compound Ambroxol®. The interactions that stabilize the complex **APP-2** and GCase were explained by MD simulations, showing that the Glu235 residue orients the alkyl chain towards a hydrophobic pocket in the enzyme. Protonation of this residue may be responsible of the decrease of activity, which is interesting for further pH-dependent chaperone design.

This work has been published as an article entitled "Conformationally-locked *C*-glycosides: tuning aglycone interactions for optimal chaperone behaviour in Gaucher fibroblasts" in the journal *Organic and Biomolecular Chemistry*, **2016**, *14*, 1473-1484.

3.7. References

(1) Ramsay, R.; Tipton, K. *Molecules* **2017**, *22*, 1192.
(2) Hopkins, A. L.; Groom, C. R. *Nat. Rev. Drug Discov.* **2002**, *1*, 727–730.
(3) Copeland, R. A. *Evaluation of Enzyme Inhibitors in Drug Discovery : A Guide for Medicinal Chemists and Pharmacologists*, 2nd ed.; Wiley-VCH, 2013.
(4) Gloster, T. M.; Vocadlo, D. J. *Nat. Chem. Biol.* **2012**, *8*, 683–694.
(5) Stütz, A. E. *Iminosugars as Glycosidase Inhibitors : Nojirimycin and Beyond*; Wiley-VCH, 1999.
(6) Compain, P.; Martin, O. R. *Iminosugars : From Synthesis to Therapeutic Applications*; Wiley-VCH, 2007.

(7) Stütz, A. E.; Wrodnigg, T. M. *Adv. Carbohydr. Chem. Biochem.* **2011**, *66*, 187–298.
(8) Gloster, T. M.; Davies, G. J. *Org. Biomol. Chem.* **2010**, *8*, 305–320.
(9) Asano, N. *Cell. Mol. Life Sci.* **2009**, *66*, 1479–1492.
(10) Lillelund, V. H.; Jensen, H. H.; Liang, X.; Bols, M. *Chem. Rev.* **2002**, *102*, 515–553.
(11) Yousefi-Salakdeh, E.; Johansson, J.; Strömberg, R. *Biochem. J.* **1999**, *343*, 557–562.
(12) Castilla, J.; Rísquez, R.; Cruz, D.; Higaki, K.; Nanba, E.; Ohno, K.; Suzuki, Y.; Díaz, Y.; Ortiz Mellet, C.; García Fernández, J. M.; Castillón, S. *J. Med. Chem.* **2012**, *55*, 6857–6865.
(13) Mena-Barragán, T.; García-Moreno, M. I.; Nanba, E.; Higaki, K.; Concia, A. L.; Clapés, P.; García Fernández, J. M.; Ortiz Mellet, C. *Eur. J. Med. Chem.* **2016**, *121*, 880–891.
(14) Zimran, A.; Altarescu, G.; Elstein, D. *Blood Cells, Mol. Dis.* **2013**, *50*, 134–137.
(15) McNeill, A.; Magalhaes, J.; Shen, C.; Chau, K. Y.; Hughes, D.; Mehta, A.; Foltynie, T.; Cooper, J. M.; Abramov, A. Y.; Gegg, M.; Schapira, A. H. V. *Brain* **2014**, *137*, 1481–1495.
(16) Migdalska-Richards, A.; Ko, W. K. D.; Li, Q.; Bezard, E.; Schapira, A. H. V. *Synapse* **2017**, *71*, e21967.
(17) Ishay, Y.; Zimran, A.; Szer, J.; Dinur, T.; Ilan, Y.; Arkadir, D. *Blood Cells, Mol. Dis.* **2018**, *68*, 117–120.
(18) Lieberman, R. L.; D'Aquino, J. A.; Ringe, D.; Petsko, G. A. *Biochemistry* **2009**, *48*, 4816–4827.
(19) Aguilar-Moncayo, M.; Gloster, T. M.; Turkenburg, J. P.; García-Moreno, M. I.; Ortiz Mellet, C.; Davies, G. J.; García Fernández, J. M. *Org. Biomol. Chem.* **2009**, *7*, 2738–2747.
(20) Aguilar-Moncayo, M.; García-Moreno, M. I.; Trapero, A.; Egido-Gabás, M.; Llebaria, A.; García Fernández, J. M.; Ortiz-Mellet, C. *Org. Biomol. Chem.* **2011**, *9*, 3698–3713.
(21) Cremer, D.; Pople, J. A. *J. Am. Chem. Soc.* **1975**, *97*, 1354–1358.
(22) Hruska, K. S.; LaMarca, M. E.; Scott, C. R.; Sidransky, E. *Hum. Mutat.* **2008**, *29*, 567–583.
(23) De La Mata, M.; Cotán, D.; Oropesa-Ávila, M.; Garrido-Maraver, J.; Cordero, M. D.; Villanueva Paz, M.; Pavón, A. D.; Alcocer-Gómez, E.; De Lavera, I.; Ybot-González, P.; Zaderenko, A. P.; Ortiz Mellet, C.; García Fernández, J. M.; Sánchez-Alcázar, J. A. *Sci. Rep.* **2015**, *5*, 10903.
(24) Alfonso, P.; Andreu, V.; Pino-Angeles, A.; Moya-García, A. A.; García-Moreno, M. I.; Rodríguez-Rey, J. C.; Sánchez-Jiménez, F.; Pocoví, M.; Ortiz Mellet, C.; García Fernández, J. M.; Giraldo, P. *ChemBioChem* **2013**, *14*, 943–949.

Chapter 4.
MUC1 epitopes incorporating sp^2-iminosugars

4.1. Introduction

Historically, iminosugar-type glycomimetic derivatives such as castanospermine or swainsonine (Figure **4.1**) have been shown to exert a broad range of biological activities by acting as inhibitors or effectors of carbohydrate processing enzymes, with strong potential in therapies targeted at cancer, viral or bacterial infections, diabetes and glycosphingolipid storage disorders, among others.[1–6]

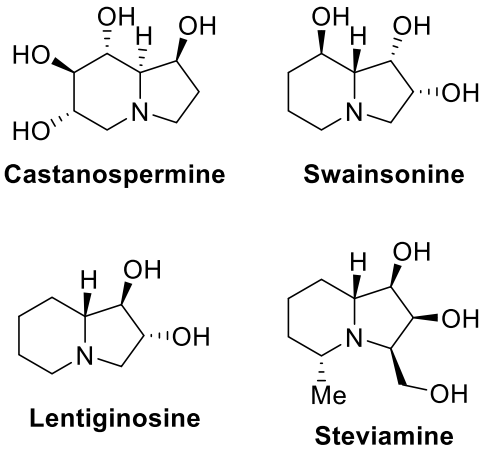

Figure 4.1. Naturally occurring iminosugar-type glycomimetics.

Although the possibility of addressing other carbohydrate binding biochemical targets (lectins or antibodies) has been pointed out, this aspect remains essentially unexplored. A main problem is the difficulty to mimick the natural glycosidic bond in the iminosugar series. Indeed, the lability of the hemiaminal functional group prevents accessing iminosugar *O*-glycosides and the same applies for the analogous *S*- or *N*-linked conjugates. Recently, this strong restriction was overcome in the closely related *sp*²-iminosugar series,[7,8] where the endocyclic nitrogen is part of a pseudoamide functionality. For instance, it was found that α-linked pseudoglycoside derivatives of 5*N*,6*O*-(oxomethylidene)nojirimycin (OMN), incorporating a

castanospermine-related bicyclic carbamate moiety, exhibited total configurational and conformational stability in aqueous solution, superseding acyclic iminosugar derivatives[9–11] (figure **4.2**).

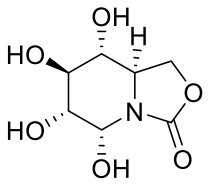

5*N*,6*O*-(oxomethylidine)nojirimycin (OMN)

Figure 4.2. Structure of sp^2-iminosugar OMN.

Noteworthy, some of the conjugates of OMN were found to act simultaneously as glycosidase inhibitors and as lectin ligands.[12] This unique multimodal glycomimetic behaviour expands the potential of sp^2-iminosugar glycosides beyond glycosidase inhibitor design, paving the way for their further engineering towards general carbohydrate recognition.

4.2. Goals

Given the observed preference of sp^2-iminosugar conjugates for axially oriented aglycone substituents, we envisioned that they would be promising scaffolds for the design of α-*O*-linked glycopeptide analogues, among which the Tn antigen is a paradigmatic example. The first goal was the synthesis of eight α-*O*-linked pseudoglycosylamino acids incorporating sp^2-iminosugar frameworks with hydroxylation patterns analogous to those of D-galactose (α-sp^2Gal), D-glucose (α-sp^2Glc), *N*-acetyl-D-galactosamine (α-sp^2GalNAc) and *N*-acetyl-D-glucosamine (α-sp^2GlcNAc), and Ser or Thr

(compounds **21-28**) in adequately protected forms as building blocks for solid phase peptide chain extension (figure **4.3**). This work was done in collaboration with Carmen Ortíz-Mellet's (University of Seville) and José Manuel García-Fernández's (IIQ-CSIC, University of Seville) groups.

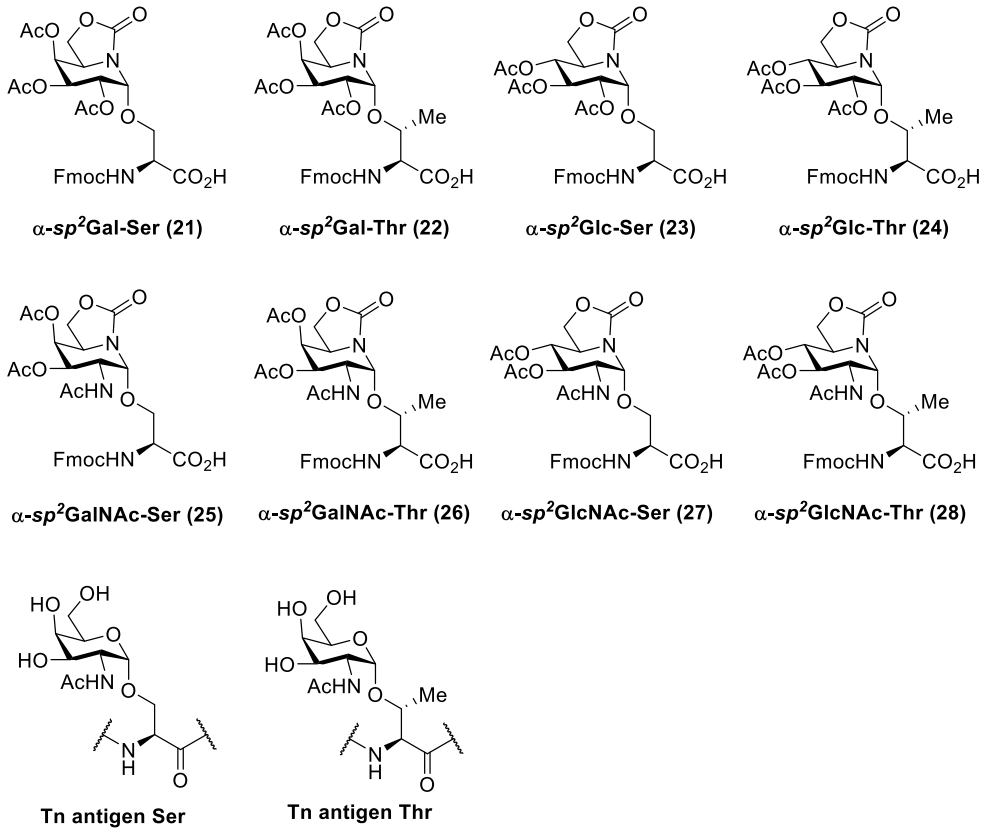

Figure 4.3. Structure of the synthesized sp^2-iminosugars Tn antigen analogs and the natural Tn antigens as building blocks for solid phase peptide synthesis (**21-28**).

For the latter purpose, we focused our attention on MUC1 mucin, which usually displays the Tn antigen in cancerous cells, and particularly in its most immunogenic domain (Ala-Pro-Asp-Thr-Arg-Pro).[13] Consequently, we have carried out the synthesis of the eight *O*-glycohexapeptides Ala-Pro-Asp-Ser/Thr(α-sp^2Gal/Glc/GalNAc/GlcNAc)-Arg-Pro (**29-36**). In all cases,

the carbohydrate moiety is conformationally restricted by a five-membered carbamate fused to the piperidine ring through the O6 oxygen atom (table **4.1**).

Table 4.1. Glycopeptides **29-36** incorporating sp^2-iminosugar Tn antigen mimics.

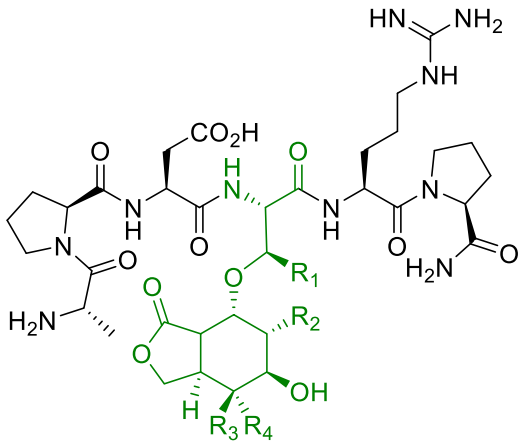

	R_1	R_2	R_3	R_4	Sequence
29	H	OH	OH	H	Ala-Pro-Asp-Ser(α-sp^2Gal)-Arg-Pro-NH_2
30	Me	OH	OH	H	Ala-Pro-Asp-Thr(α-sp^2Gal)-Arg-Pro-NH_2
31	H	OH	H	OH	Ala-Pro-Asp-Ser(α-sp^2Glc)-Arg-Pro-NH_2
32	Me	OH	H	OH	Ala-Pro-Asp-Thr(α-sp^2Glc)-Arg-Pro-NH_2
33	H	NHAc	OH	H	Ala-Pro-Asp-Ser(α-sp^2GalNAc)-Arg-Pro-NH_2
34	Me	NHAc	OH	H	Ala-Pro-Asp-Thr(α-sp^2GalNAc)-Arg-Pro-NH_2
35	H	NHAc	H	OH	Ala-Pro-Asp-Ser(α-sp^2GlcNAc)-Arg-Pro-NH_2
36	Me	NHAc	H	OH	Ala-Pro-Asp-Thr(α-sp^2GlcNAc)-Arg-Pro-NH_2

4.3. Galactose and glucose *sp²*-iminosugar mimics

In order to obtain galactosyl derivatives **21** and **22**, tetraacetate **37-Gal**[14] was firstly reacted with pyridinium poly(hydrogen fluoride) (HF/Py)[15] to obtain the pseudoglycosyl fluoride **38-Gal** in 84% yield as a stable solid. Compound **38-Gal** was selected as a suitable donor for the key α-glycosylation step, which reacted smoothly with *N*-Fmoc-serine *tert*-butyl ester (Fmoc-Ser-O^{t}Bu)[16] or *N*-Fmoc-threonine *tert*-butyl ester (Fmoc-Thr-O^{t}Bu)[16] in the presence of boron trifluoride-diethyl ether ($BF_3 \cdot Et_2O$) as a glycosylation promoter. Concomitant cleavage of the *tert*-butyl ester was also observed, to give the corresponding *N*-protected pseudoglycosylamino acids **21** and **22** in 73% and 91% yield, respectively. Removal of the Fmoc group in **21** and **22** with piperidine and final deacetylation under standard sodium methoxide-catalyzed conditions provided the fully unprotected Tn antigen mimics **39** and **40.** *N*-protected compounds **23** and **24**, as well as free amino acids **41** and **42**, were likewise synthesized starting from tetraacetate **37-Glc**[14] (scheme **4.1**). The complete synthesis of the protected (**21-24**) and unprotected amino acids (**39-42**) was performed at the University of Seville.

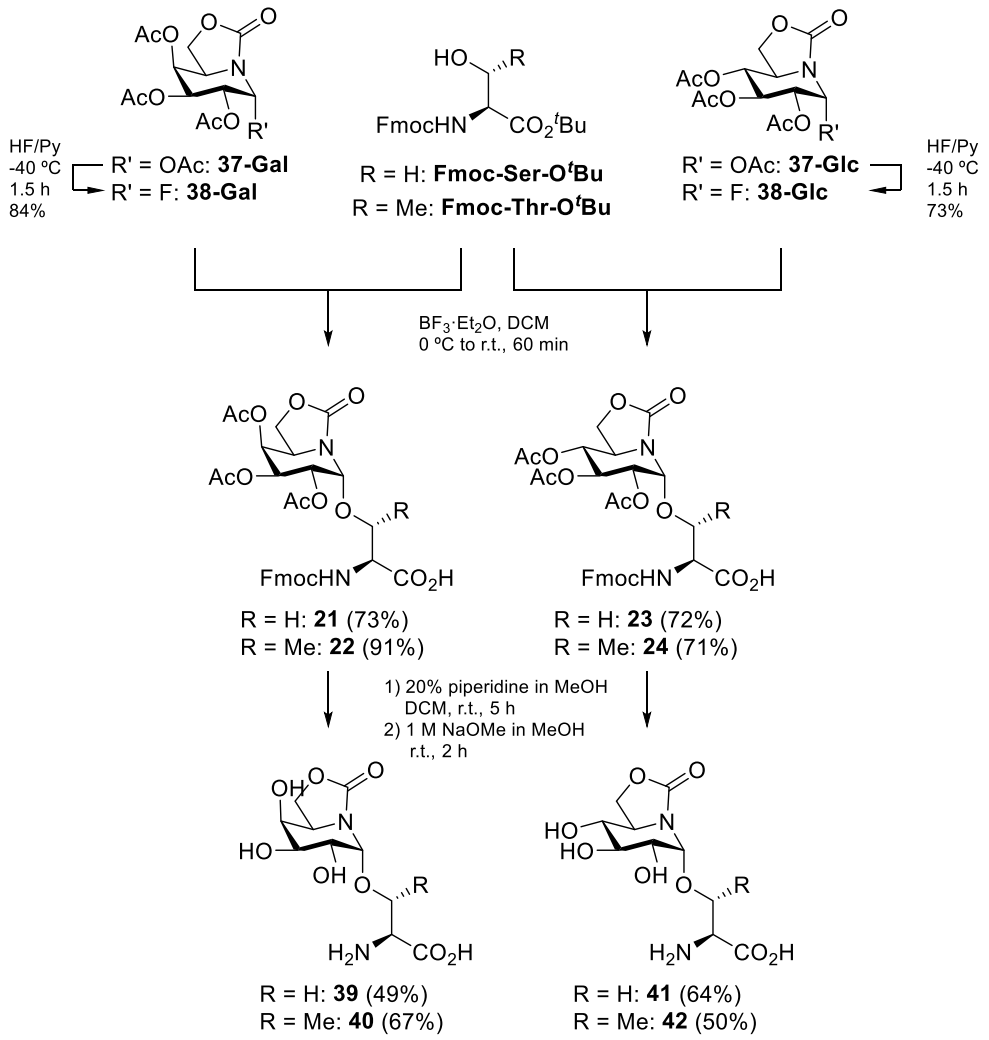

Scheme 4.1. Synthesis of building blocks **21-24** and unprotected amino acids **39-42**.

Despite the acetyl-protecting group at O2 usually participates in glycosylation reactions favoring the β-orientation of the glycosyl acceptor, only the α-anomer was obtained using pseudoglycosyl fluorides **38-Gal** and **38-Glc** as glycosyl donors. To get a deeper insight into the rationales governing this pathways reactivity, the reaction profiles for both α- and β-glycosylation from the presumed iminium cation intermediate **I** (Figure **4.4**)

using methanol as model glycosyl acceptor were calculated using quantum mechanics.

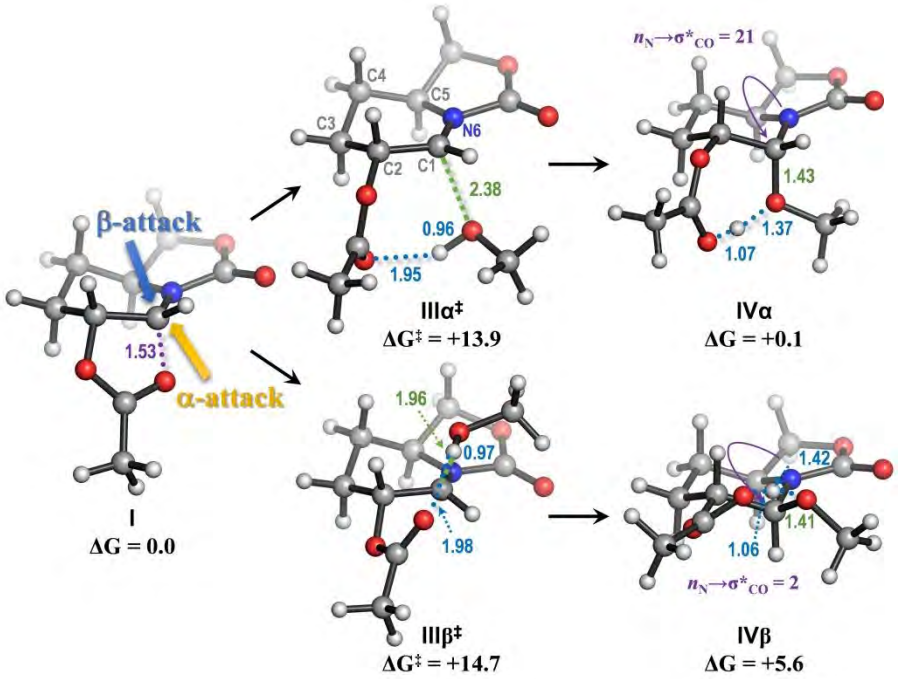

Figure 4.4. Model glycosylation reactions calculated with PCM_{H2O}/M06-2X/def2-TZVPP. Free energies (ΔG) and hyperconjugative interactions ($n_N \rightarrow \sigma^*_{CO}$) are given in kcal mol^{-1}, and distances in Angstrom (Å).

The approach toward the *Re* face of the iminium double bond (α-attack) was found to be kinetically favoured by *ca.* 1 kcal mol^{-1} due to the less torsional strain developed around the C1–C2 bond[17] in the earlier transition state (TS) **IIIα**‡ (figure **4.5**).

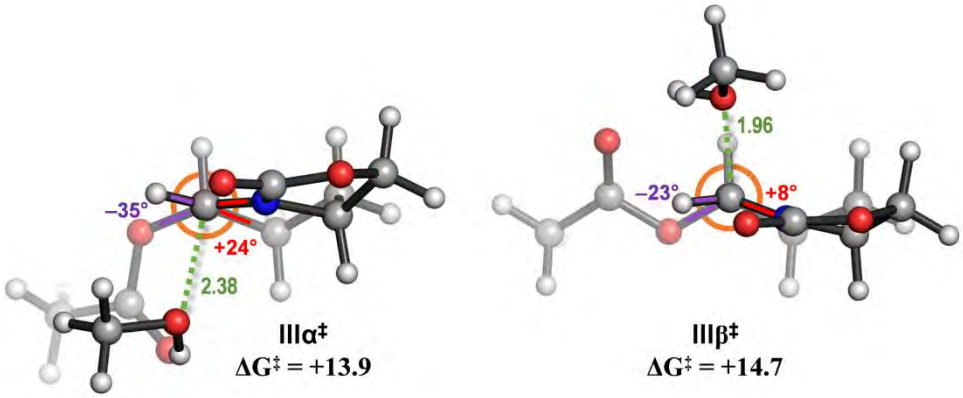

Figure 4.5. Newman projections around the C1-C2 bond for the lowest transition structures. The more favored **IIIα**‡ shows a more staggered arrangement than the disfavored **IIIβ**‡ due to the upward pyramidalization of C1.

Also, the much stronger anomeric effect hypothesized for the post-TS cationic product **IVα** (chair conformation, OMe in axial position) with respect to **IVβ** (chair conformation, OMe in equatorial position), was verified by Natural Bond Orbitals (NBO) calculations of the $n_N \rightarrow \sigma^*_{CO}$ hyperconjugative interactions[18] (table **4.2**). This lack of stabilization makes the β-addition pathway endergonic and reversible, while the α-addition is nearly thermoneutral. Of note, the neutral β-anomer was calculated to preferentially adopt a twist-boat conformation, in agreement with previous observations for sp^2-imino-β-thioglycosides by NMR spectroscopy.[9]

Table 4.2. NBO second order perturbation energies (E^2, kcal mol^{-1}) calculated with PCM_{H2O}/M06-2X/def2-TZVPP.

Structure	$n_N \rightarrow \sigma^*_{CO}$ (endo-anomeric)	$\sigma_{NC} \rightarrow \sigma^*_{CO}$ (endo-anomeric)	Total
IVa	20.5		**20.5**
IVb	1.7	3.1	**4.8**

These results demonstrate the privileged architecture of sp^2-iminosugars to deploy strong conformational bias for the complete stereocontrol of glycosylation reactions, avoiding the need for chromatographic separation of α- and β-anomers inherent to most glycosylation methods, particularly in α-*O*-glycopeptide synthesis.

The four protected Tn antigen mimics **21-24** were next engaged in solid phase peptide synthesis (SPPS) to obtain the target α-*O*-pseudoglycohexapeptides **29-32**. Protected natural amino acids were automatically coupled to Rink Amide MBHA resin using HBTU/DIPEA as coupling agents and a 20% piperidine solution in DMF for Fmoc removal. Coupling of the pseudoglycosyl amino acid building block to the peptide sequence was performed manually to maximize the yield. After completion of the sequences, the α-*O*-glycopeptide mimics were cleaved from the resin using trifluoroacetic acid (TFA), with simultaneous removal of all the acid-labile side-chain protecting groups. Purification by preparative HPLC and subsequent lyophilization gave **29-32** in good overall yields (figure **4.6**).

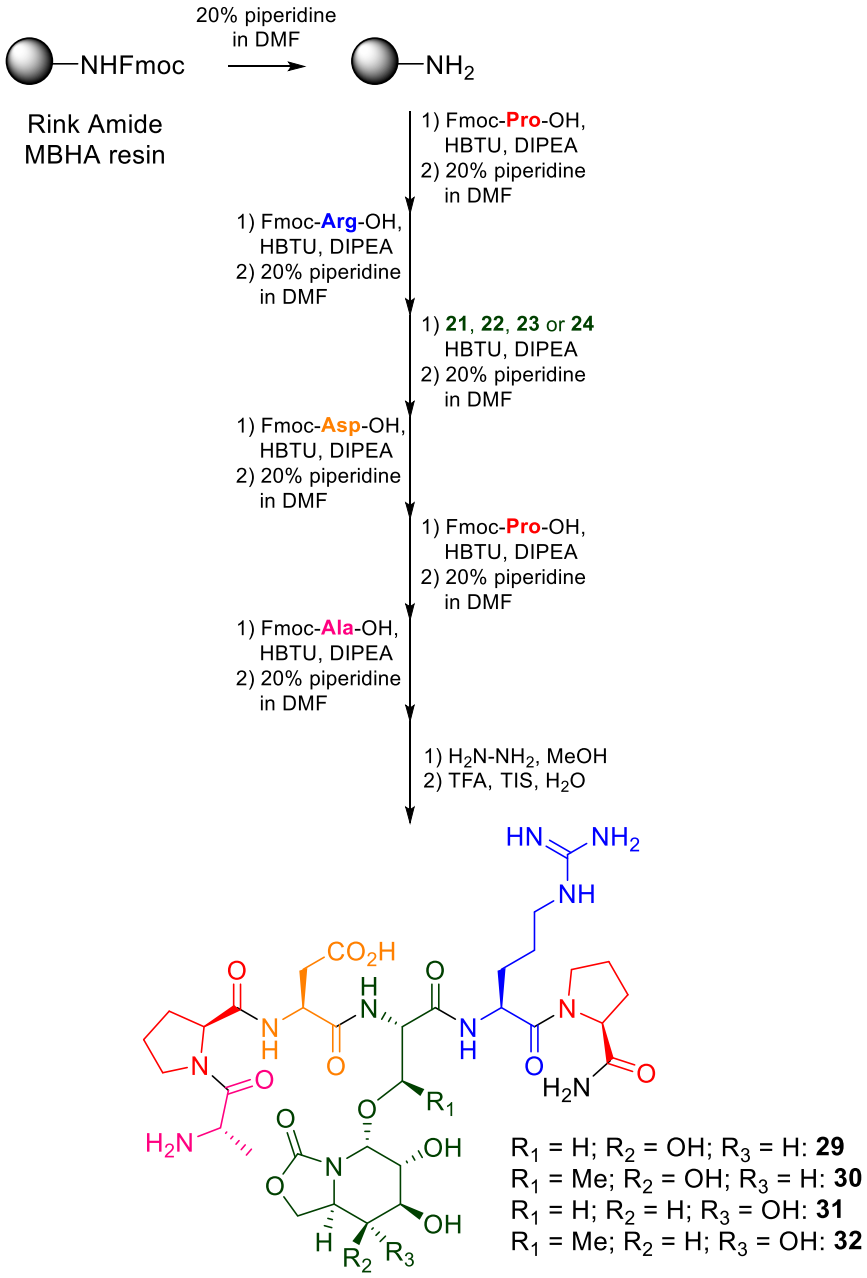

Figure 4.6. Synthetic strategy for obtaining glycopeptides **29-32** by SPPS.

To test the capabilities of the new sp^2-iminosugar derived α-*O*-glycopeptide mimics **29-32** to reproduce the biorecognition properties of the natural MUC1 immunogenic domains, their binding affinities towards biotinylated soybean agglutinin (SBA) were preliminary evaluated. The parent natural antigen Ala-Pro-Asp-Thr(α-*O*-GalNAc)-Arg-Pro **43**, previously synthesized in the same way as glycopeptides **29-32** using **Fmoc-Thr(α-*O*-GalNAc)-OH** building block,[19] was used as a positive control in an enzyme-linked lectin assay (ELLA) (figure **4.7**).

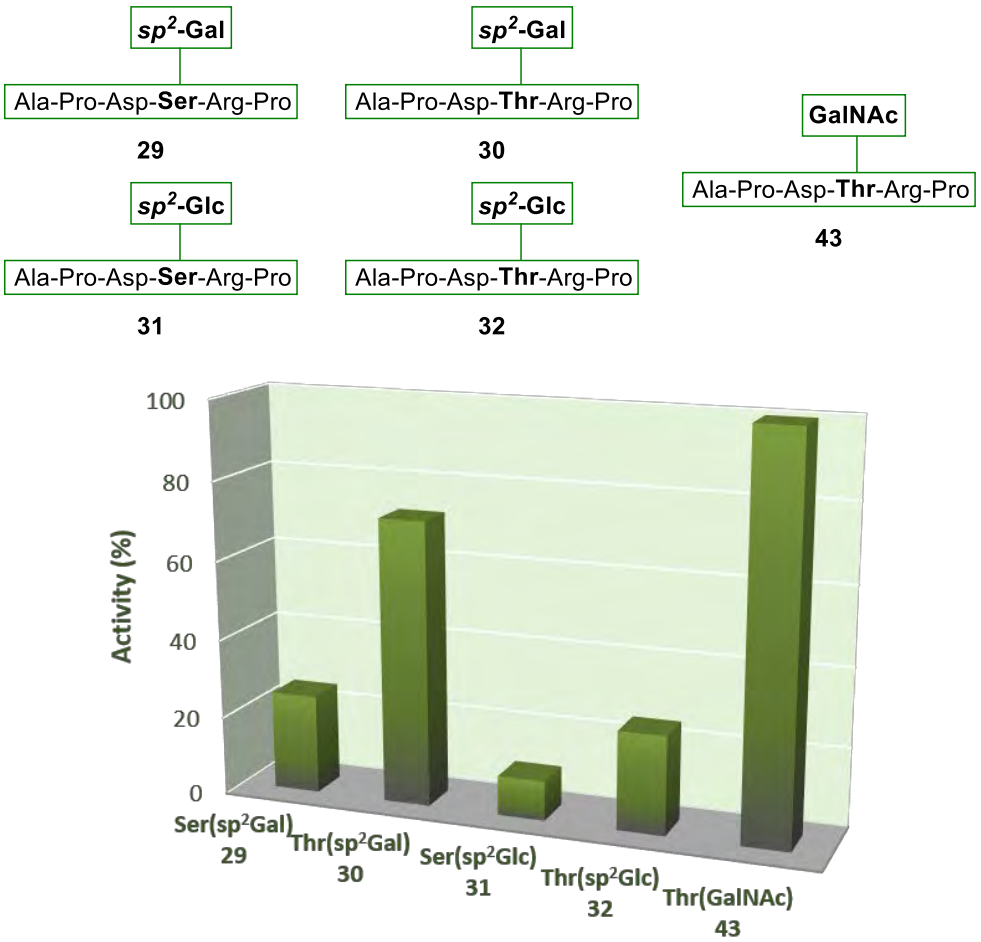

Figure 4.7. Activity expressed in percentage respect to **43** of sp^2-iminosugar α-*O*-glycopeptides **29-32** (250 nmol) bound to SBA.

The data indicated that, at the same pseudoglycopeptide concentration, Thr-linked derivatives (**30**, **32**) are better ligands than Ser-linked conjugates (**29**, **31**), which is in agreement with previous observations in the classical glycopeptide series.[19–21] The α- sp^2Gal conjugates (**29**, **30**), matching the configurational pattern of the natural Tn antigen, are better recognized than the sp^2Glc C4-epimers with identical amino acid sequence (**31**, **32**). In fact, compound **30** behaves as a rather good mimic of the Tn antigen in this assay (above 70% affinity relative to **43**), being one of the very few non-carbohydrate ligands recognized by SBA.[22] It should be noted that the sp^2-iminosugar fragment in the new conjugates lacks the *N*-acetyl moiety, considered key for recognition of carbohydrate ligands by SBA.

Additional information at the atomic level was obtained by running unrestrained 100 ns MD simulations of compound **30** bound to SBA (PDB code: 4D69; figure **4.8**). Although the pose calculated for derivative **30** differs from the one observed for the parent glycopeptide **43** in the crystal structure,[23] several contacts were conserved. Those include the CH-π patch observed between the α-face of the glycone moiety and Phe128 in the protein and the hydrogen bonds formed between hydroxyl groups OH4 and OH3 with the side chain of Asp88. The carbonyl group of the sp^2-iminosugar moiety additionally engages in hydrogen bonds with the NH groups of Leu214 and Asp215. The peptide backbone, in particular Asp and Arg residues, is also recognized through hydrogen bonds with multiple amino acids of the lectin.

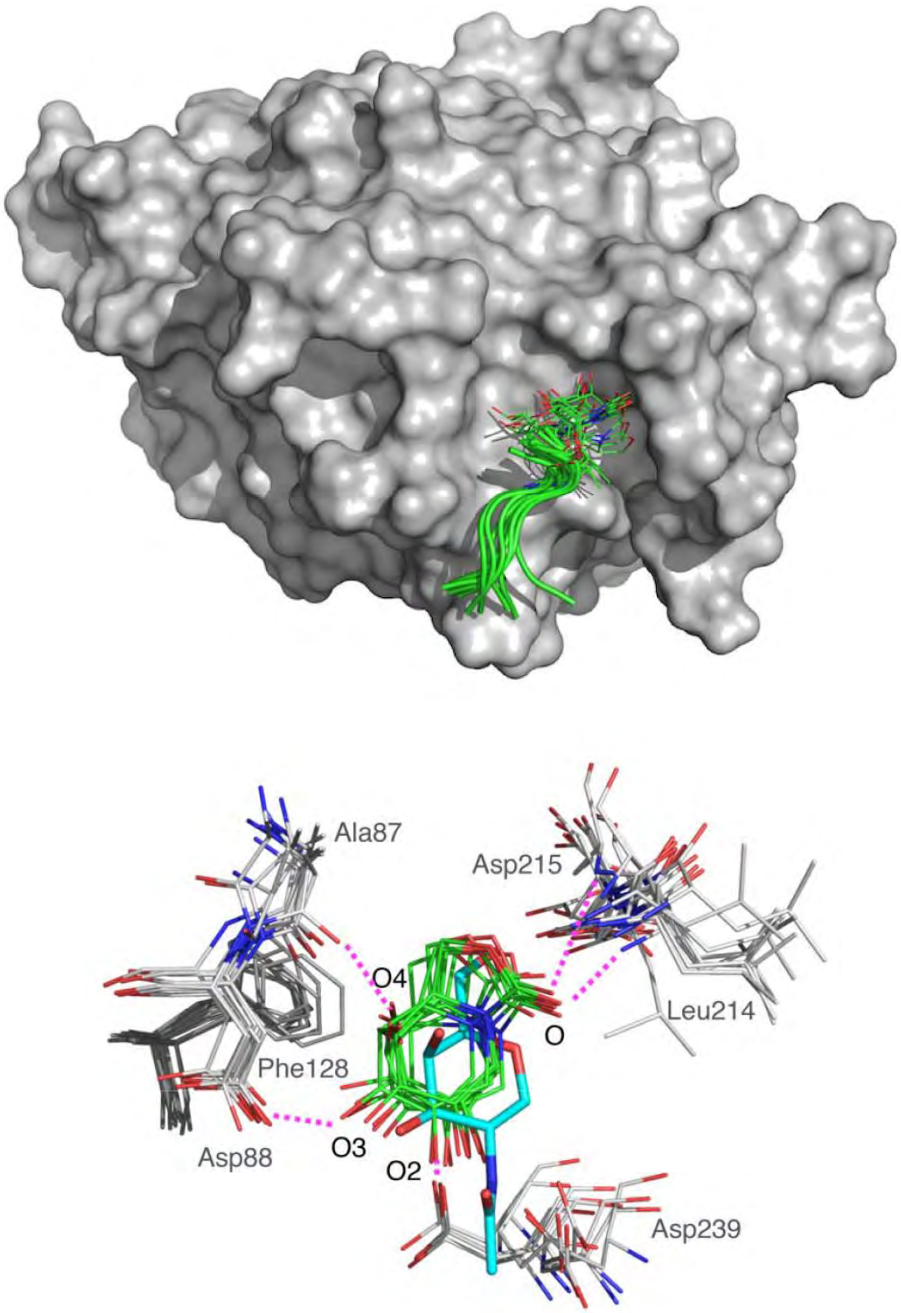

Figure 4.8. Different views of 100 ns MD simulation of the complex SBA:**30** (top) and overlay of representative frames from the 100 ns MD simulation of the complex SBA:**30** and the GalNAc residue (cyan) of the crystal structure of SBA:**43** complex (bottom).

Bearing in mind the existing background on sp^2-iminosugar as glycosidase inhibitors, we next tested the impact of the peptide chain in conjugates **29-32** and **39-42** on the inhibitory properties towards four selected enzymes with glucosidase and galactosidase activities (table **4.3**).

Table 4.3. Inhibition constants (K_i [μM]) for glycocojugates **29-32** and **39-42**.

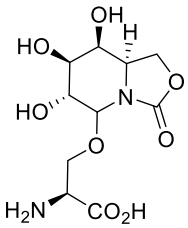

39

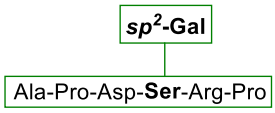

29

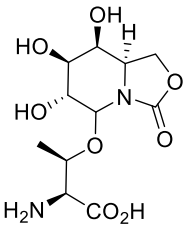

40

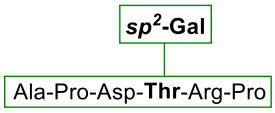

30

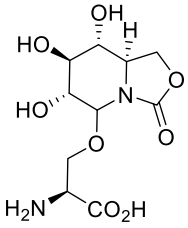

41

31

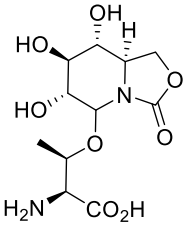

42

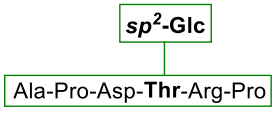

32

Enzyme	39	29	40	30	41	31	42	32
β-galactosidase (bovine liver)	284	48	n.i.	72	n.i.	n.i.	n.i.	n.i.
β-galactosidase (E. Coli)	n.i.	134	n.i.	17	n.i.	n.i.	n.i.	n.i.
Isomaltase (baker's yeast)	n.i.	110	n.i.	43	n.i.	287	n.i.	91
α-glucosidase (baker's yeast)	n.i.	110	n.i.	191	129	330	n.i.	266

The corresponding inhibition constants (K_i) were indeed strongly dependent on the chemical nature of the compound. Thus, *sp*²-iminosugar glycosylamino acids (**39-42**) exhibited no or very low inhibition, whereas the MUC1-related pseudoglycopeptides (**29-32**) behaved as moderate to potent inhibitors of some of the enzymes tested. When comparing threonine-linked and serine-linked derivatives, the former generally showed stronger inhibitory activities. The effect of the aglycone in the inhibitory properties is particularly significant in the α- *sp*²Gal series, going from no inhibition in the case of the amino acid conjugates **39** and **40** to a respectable K_i value of 17 μM against *E. coli* β-galactosidase for pseudoglycohexapeptide **30**.

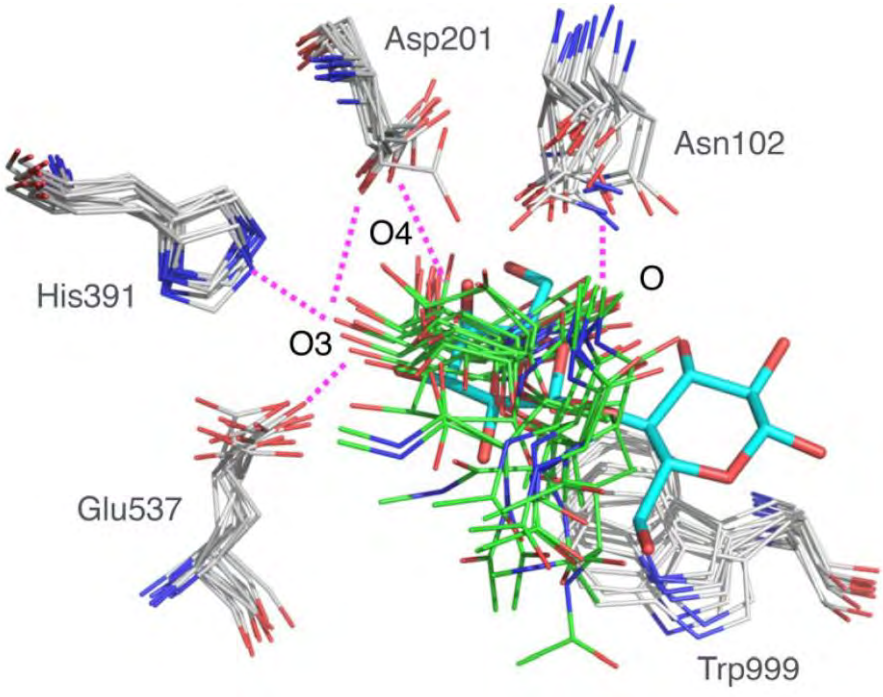

Figure 4.9. Overlay of representative frames from the 100 ns MD simulation of the complex β-galactosidase (PDB code: 1JYN):**30*** and the lactose residue (cyan) of the crystal structure with this galactosidase.

100 ns MD simulations (figure **4.9**) on the complex between this enzyme and a simplified version of **30** (namely the α- *sp*^{2}Gal-*N*-acetylthreonine methylamide glycoside) indicated that the pose calculated for the *sp*^{2}-iminosugar residue differs slightly from that found in the crystal structure for the galactose moiety in lactose.[24] However, several contacts were conserved, such as hydrogen bonds of OH4 with Asp201 and OH3 with His391, Glu537 and Asp201. Additionally, the carbonyl group of this iminosugar engages in a hydrogen bond with the side chain of Asn102 and the methyl group of the threonine residue in a hydrophobic contact with Trp999. This latter interaction may be responsible for the best affinity of the threonine versus serine derivatives. In addition, the peptide backbone is involved in some stabilizing contacts with the enzyme, which could explain the enhancement in the affinity of compound **30** in comparison to pseudoglycosylamino acid **40**. Altogether, these observations corroborate the potential of peptide chain modifications in the new *sp*^{2}-iminosugar-based glycopeptide mimics for tuning the binding properties towards catalytic and non-catalytic protein partners.

4.4. GalNAc and GlcNAc *sp*^{2}-iminosugar mimics

In order to obtain *N*-acetylgalactosaminyl derivatives **25** and **26**, a slightly longer synthetic approach was performed. Initially, tetraacetate **37-Gal**[14] was converted into the pseudogalactal derivative **44-Gal** by reaction with HBr/AcOH and further *in situ* elimination by treatment with Cp_2TiCl_2 and Mn dust. Azidonitration of compound **44-Gal** with NaN_3 in the presence of cerium ammonium nitrate (CAN) gave the 2-azido-2-deoxy sugar

mimic **45-Gal**, which was acetylated and reacted with HF/Py to afford compound **46-Gal**. Analogously to galactosyl derivatives **21** and **22**, compound **46-Gal** was reacted with conveniently protected Ser and Thr in the presence of boron trifluoride-diethyl ether ($BF_3 \cdot Et_2O$) as a glycosylation promoter, with concomitant cleavage of the *tert*-butyl ester, providing the α-*O*-linked pseudoglycosides **47** and **48**, respectively. Reduction of the azido group and concomitant acetylation of the formed amine afforded the target 2-acetamido-2-deoxysugar glycosylamino acid derivatives **25** and **26**, respectively. *N*-acetylglucosamine derivatives **27** and **28** were likewise synthesized starting from tetraacetate **37-Glc**[14] (scheme **4.2**). The complete synthesis of the protected (**25-28**) was performed at the University of Seville.

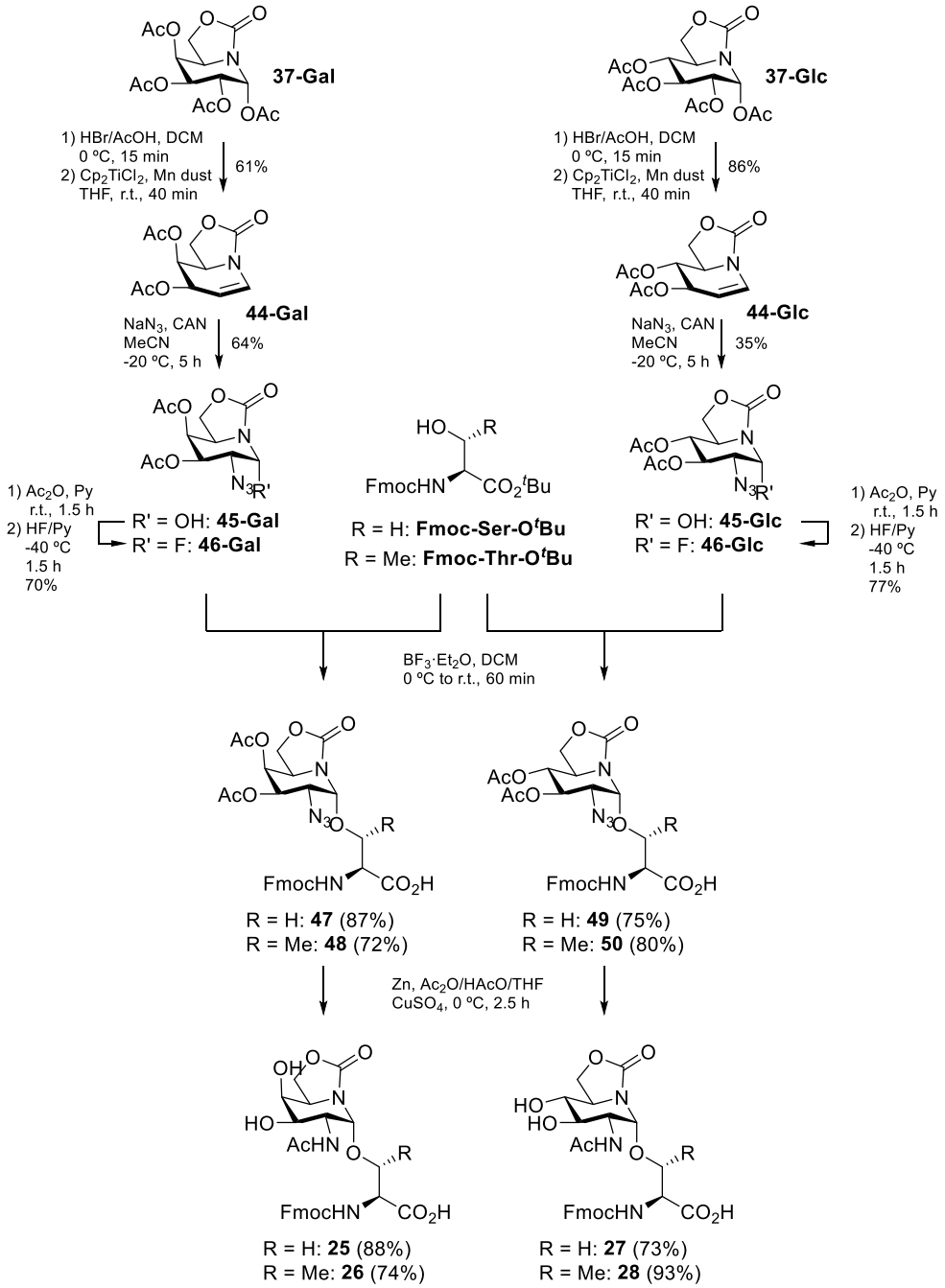

Scheme 4.2. Synthesis of building blocks **25-28**.

Again, the glycosylation reaction took place with complete α-selectivity, as occurred with galacto and gluco derivatives. To get a deeper insight into the rationales governing this pathways reactivity, the reaction profiles for both α- and β-glycosylation from the presumed C2-azide iminium cation intermediate **Ib** (figure **4.10**) using methanol as model glycosyl acceptor were calculated.

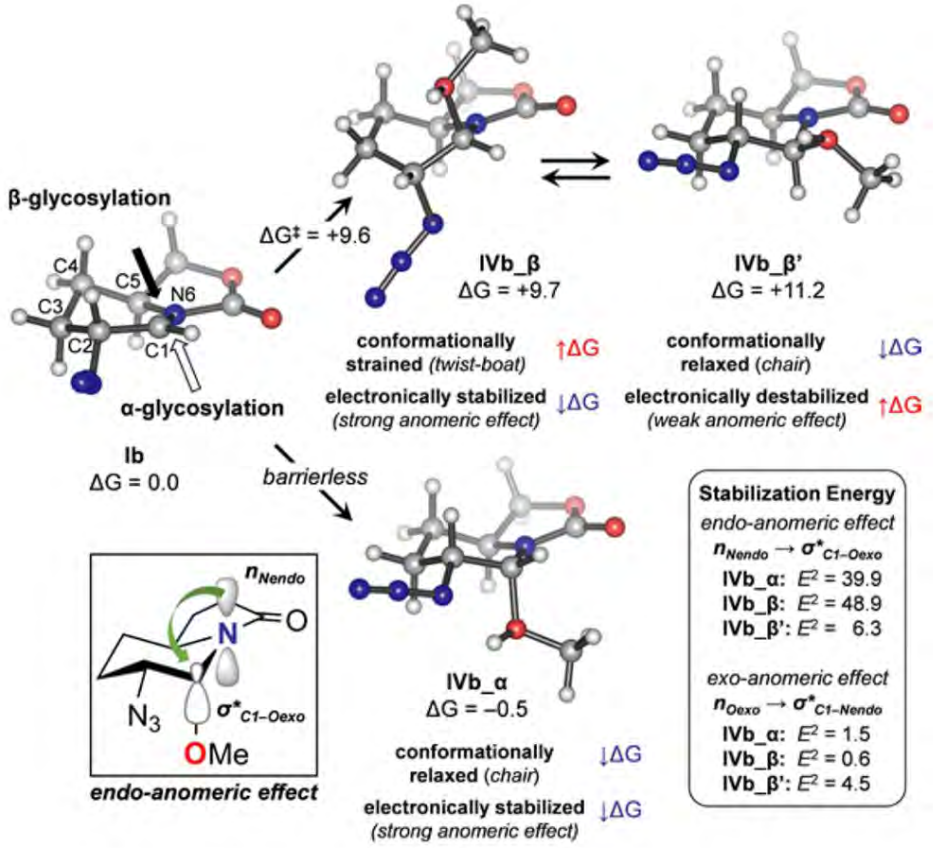

Figure 4.10. Model glycosylation reactions calculated with PCM_{H2O}/M06-2X/def-TZVPP. Free energies (ΔG) and conjugative interactions (E^2) are given in kcal mol^{-1}. The NBO orbitals involved in the endo-anomeric hyperconjugation are shown in the inset.

No transition state could be located for the α-approximation due to the minimal rearrangement needed to adopt the chairlike conformation in intermediate **IVb_α**. This approximation was therefore found enthalpically barrierless, as opposed to the β-approximation, whose calculated activation barrier was around 10 kcal mol^{-1} due to a greater distortion of the cation structure required to adopt the transition structure **IIIb_β**‡ leading to intermediate **IVb_β**. As occurred for the C2-acetyl substituted **I**, the much stronger anomeric effect hypothesized for the post-TS cationic product **IVb_α** with respect to **IVb_β** was verified by NBO calculations (figure **4.10**) and the neutral β-anomer was also calculated to preferentially adopt a twist-boat conformation. This makes the β-addition pathway endergonic and reversible, while the α-addition is nearly thermoneutral and thus favored thermodynamically.

The four protected Tn antigen mimics **25-28** were next engaged in SPPS (figure **4.11**) to obtain the target α-*O*-pseudoglycohexapeptides **33-36** following the same protocol as previously described for pseudoglycohexapeptides **29-32**.

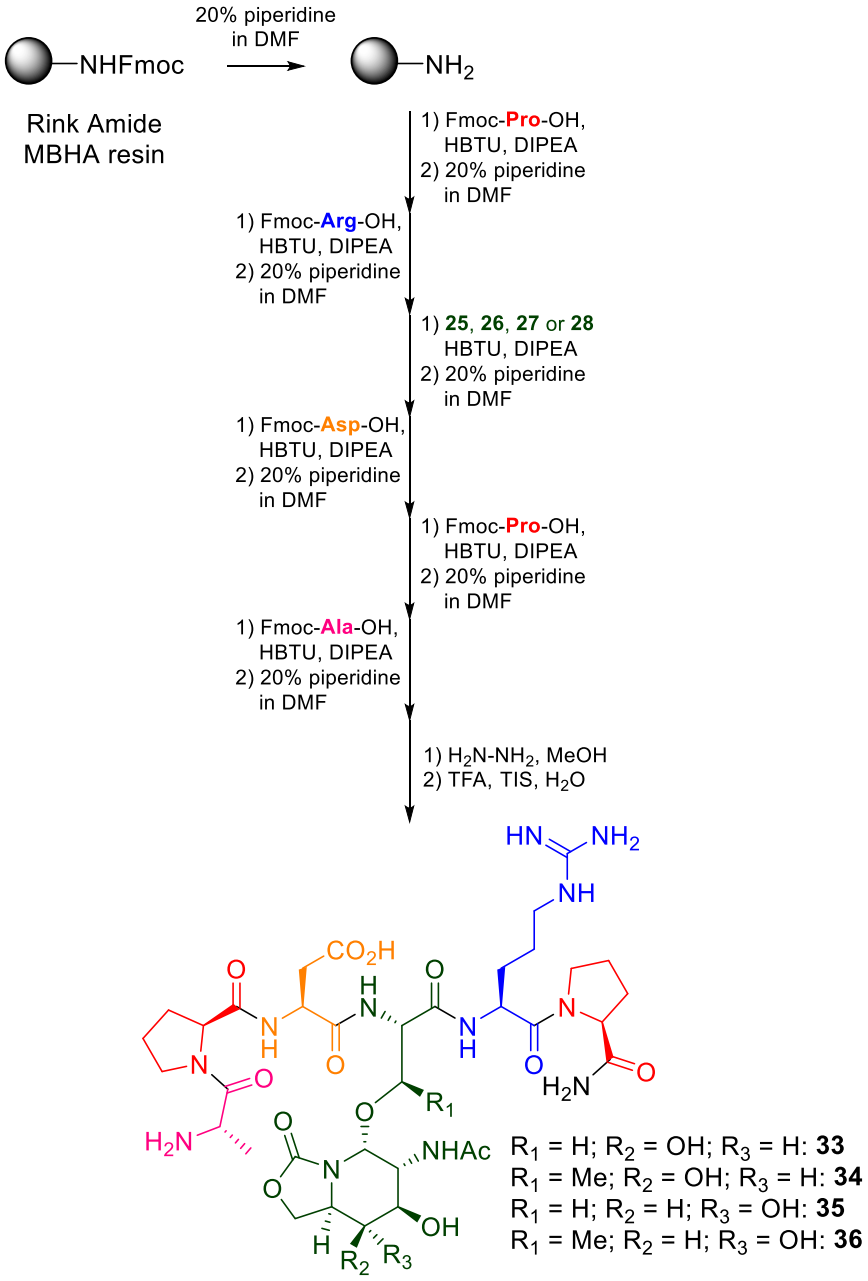

Figure 4.11. Synthetic strategy for obtaining glycopeptides **33-36** by SPPS.

Taking into account the interactions found for the natural MUC1 glycopeptide epitope **43** in complex with the anti-MUC1 monoclonal SM3 antibody,[25] which involved a hydrogen bond between the hydroxymethyl group and a tyrosine residue of the antibody, as well as a hydrophobic contact between the *N*-acetyl group and a tryptophan residue, we envisioned that these pseudoglycopeptides may represent suitable candidates for the development of new anticancer vaccines, if they are able to adopt the right peptidic conformation (figure **4.12**). The presence of unnatural carbohydrate moieties may besides enhance the stability towards chemical or enzymatic degradation and, therefore, improving recognition.

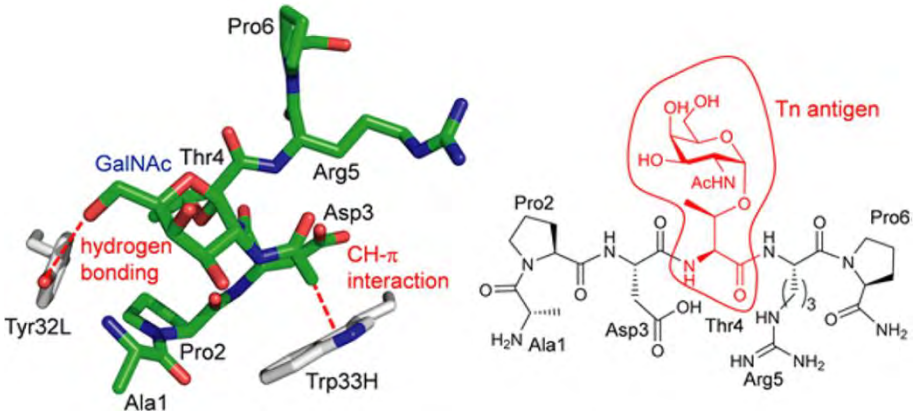

Figure 4.12. Key binding interactions of natural glycopeptide **43** with scFv-SM3 antibody, as observed in the X-ray crystal structure (PDB: 5a2k).[25]

In this sense, the binding affinities of sp^2-iminosugar pseudoglycopeptides **29-36** towards scFv-SM3 antibody were evaluated through Bio-Layer Interferometry (BLI) experiments.[26] This optical technique is based on measuring the interference pattern of white light reflected from both, a

layer of immobilized antibody on the tip of the biosensor and an internal reference layer. Changes in the nature of the antibodies (binding and dissociation of antigens) lead to a shift in the pattern (wavelength, Δλ) that can be measured and related to the dissociation constant (K_D), to the binding specificity or the concentration with high precision and accuracy (figure **4.13**).

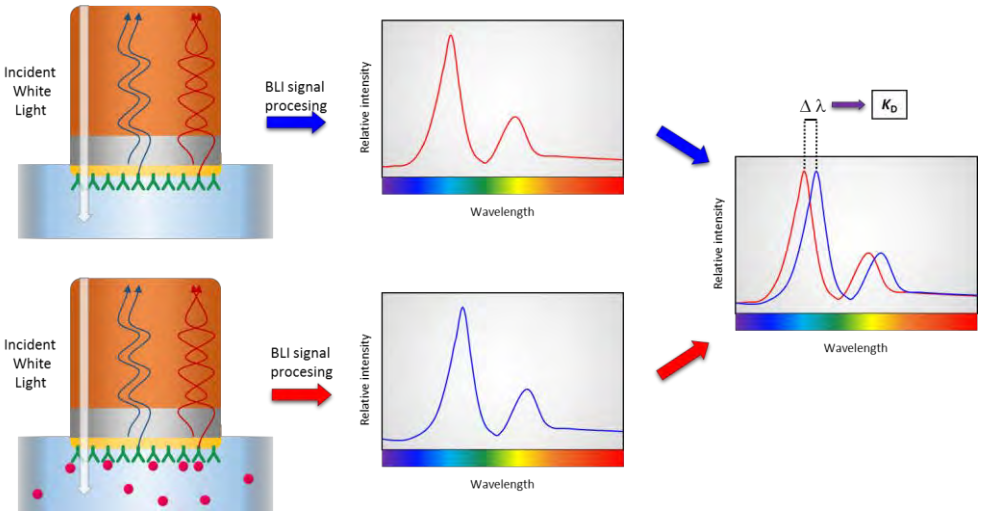

Figure 4.13. Bio-Layer Interferometry (BLI).

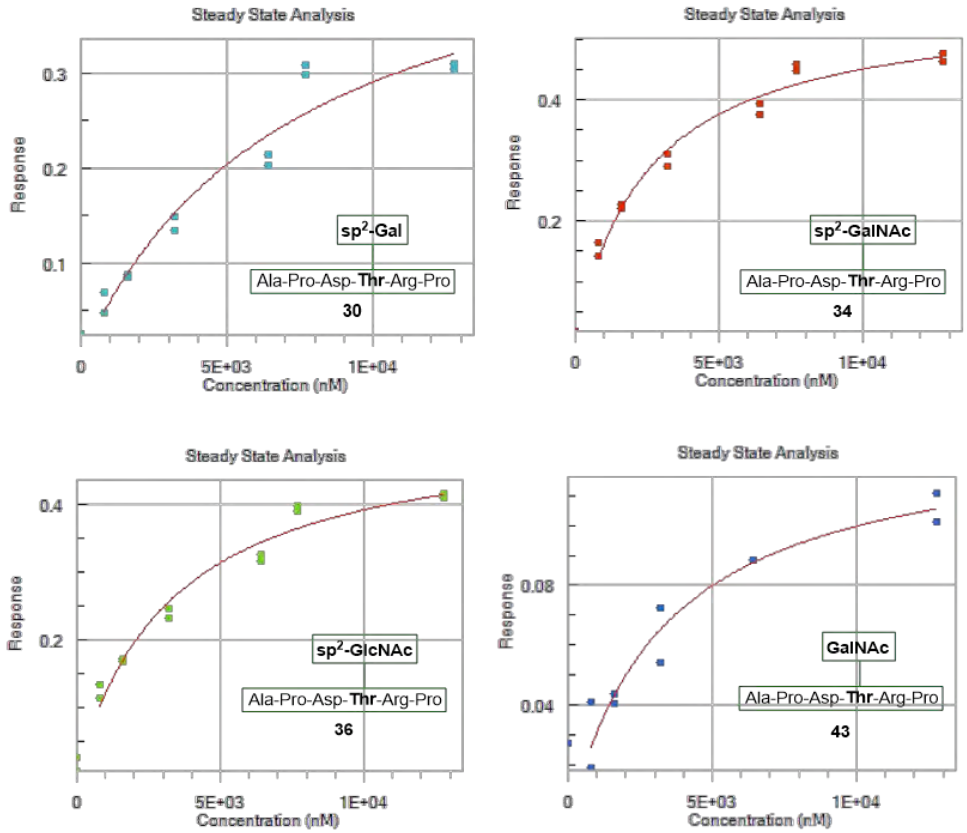

Figure 4.14. Curves obtained from the bio-layer interferometry (BLI) assays for glycopeptides **30**, **34**, **36**, and **43**.

In this sense and in collaboration with Gonçalo Bernardes' group (University of Cambridge, UK), the K_D constant for glycopeptides **29-36** and **43** with scFv-SM3 were measured. As can be inferred from the data (table **4.4**), monoclonal antibody scFv-SM3 exhibited high affinity towards the natural glycopeptide **43** used as positive control.[13] Thr-linked derivatives (**30**, **32**, **34**, **36**) showed higher affinities than Ser-linked derivatives (**29**, **31**, **33**, **35**) at the same concentration, which agrees with previous observations.[25] Compound *sp*^{2}-GalNAc **34**, which incorporates a "true" Tn antigen mimic moiety, showed the higher affinity, this being 2-fold higher

than the natural glycopeptide **43**. These results confirmed that the presence of a hydroxymethyl group (C6) in the sugar moiety is not strictly necessary for binding to SM3 mAb, and demonstrated the potential of *sp²*-iminosugar for the development and design of new carbohydrate-based cancer vaccines.

Table 4.4. Determination of K_D values of MUC1-*sp²*-iminosugars with scFv-SM3 mAb by BLI assays.

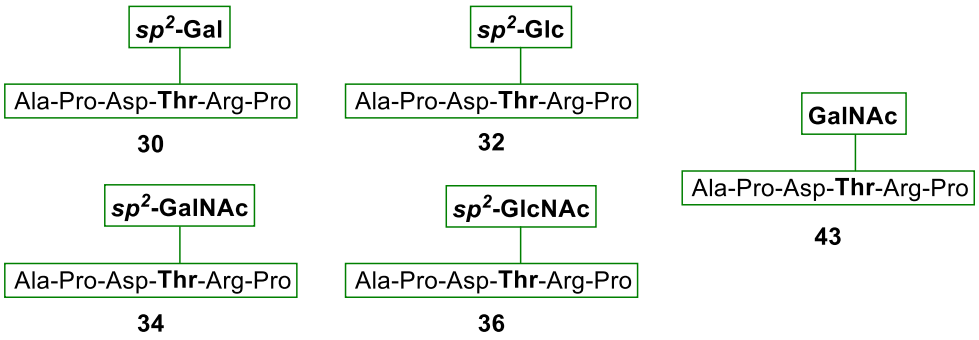

Glycopeptide	30	32	34	36	43
K_D (μM)	4.10 ± 1.10	---	1.60 ± 0.16	2.00 ± 0.30	3.30 ± 0.84

Conformational analysis

To develop a synthetic cancer vaccine based on a structural design, it is mandatory to anticipate the structure of the epitope recognized by the corresponding antibody. Fortunately, high quality crystals of the SM3:**34** complex were obtained in collaboration with Ramón Hurtado-Guerrero's group (University of Zaragoza). The corresponding crystallographic analysis revealed that the surface groove of the recombinant SM3 antibody nicely fits all of the peptide residues. This fact was previously observed for the complex with natural glycopeptide **43** and for the naked peptide APDTRP[25] (figure **4.15A**). Despite the presence of the non-natural *sp²*-iminosugar moiety, the overall conformation of the peptide fragment, as well as the glyco-

sidic linkage, is almost identical to those found for natural glycopeptide **43** and for the naked peptide APDTRP (figure **4.14B**). In fact, the interactions displayed between the antibody and the non-natural antigen are quite similar, involving several hydrogen bonds, some of them water-mediated, as well as stacking interactions. Thus, Pro2 stacks with Tyr32L, Trp91L and Trp96L, whereas Asp3 and Arg5 interact hydrophobically with Trp33H and Tyr32L, respectively. Besides, the NH group of Ala1 is engaged in hydrogen bond with Tyr32L and the CO group of Thr4 with Gln97H. Due to the presence of the oxazolidinone ring in which the hydroxymethyl group of the carbohydrate moiety is involved, there is no interaction between it and the side chain of Tyr32L, which is indeed found in glycopeptide **43** (figure **4.14C**). Additionally, the water-mediated hydrogen bond network within glycopeptide **34** showed a quite similar profile to the found for the natural glycopeptide **43** (figure **4.14D**).

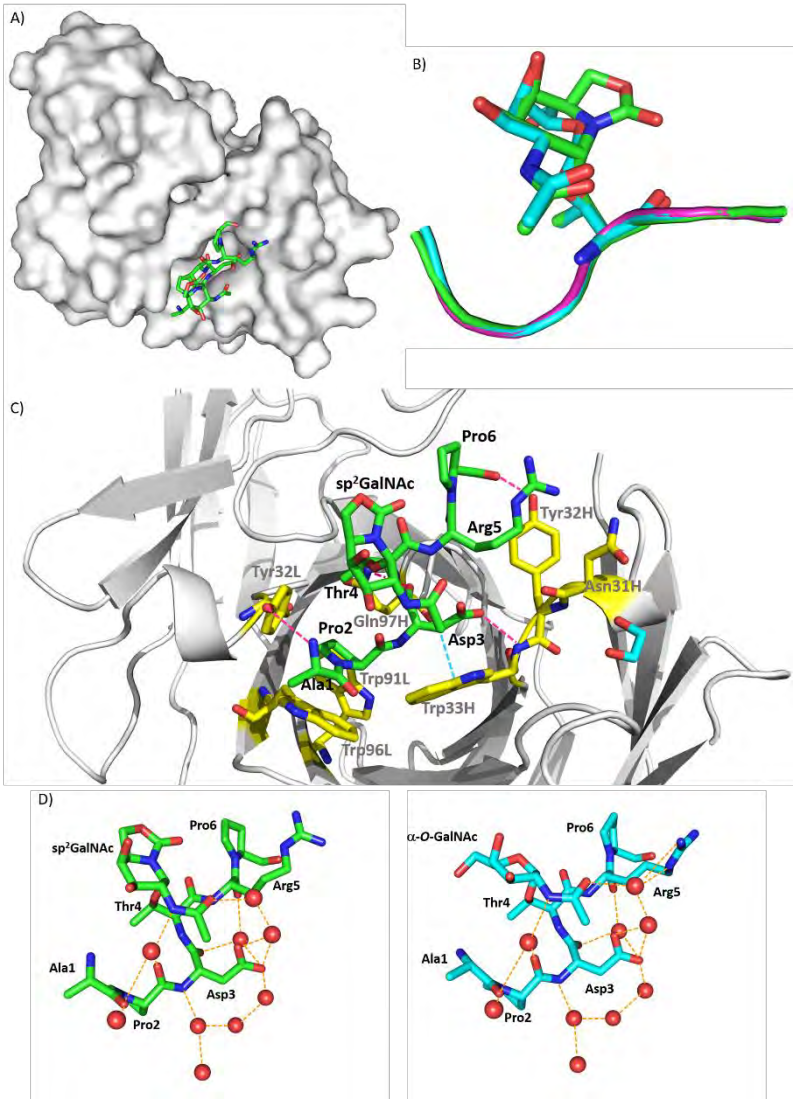

Figure 4.15. A) Surface representation of SM3 in complex with glycopeptide **34**. The antigen is shown as a stick model with carbon atoms in green. B) Superposition of the peptide backbone of compounds **34** (green), **43** (blue) and naked **APDTRP**[25] (pink) in complex with SM3. C) Key binding interactions of glycopeptide **34** in complex with SM3, as observed in the X-ray crystal structures. Glycopeptide carbon atoms are shown in green. Carbon atoms of key residues of SM3 are colored yellow. Blue dashed lines indicate interactions between *sp²*GalNAc and SM3 surface, and pink dashed lines indicate hydrogen bonds between peptide backbones and SM3 antibody. D) Water contacts for glycopeptides **34** (green) and **43** (cyan) in complex with scFv-SM3 antibody obtained from the X-ray structures. Red spheres represent water molecules and orange dashed lines indicate water contacts.

Once the molecular recognition of unnatural glycopeptide by the antibody was described at atomic level, the next task to perform is its conformational analysis in unbound state in aqueous solution in order to investigate the rigidity or flexibility of the molecule, and to which extent the bioactive conformation is shown. This feature would justify a possible entropic contribution to the binding, especially taking into account that the interaction of the hydroxymethyl group of the sugar with the antibody is lost in the unnatural glycopeptide (enthalpic penalty), and that there are no interactions different from those observed in the natural glycopeptide.

In a first step, full assignment of the hydrogen atoms in compound **34** was carried out using COSY and HSQC experiments. Then, 2D NOESY experiments in H_2O/D_2O (9:1) were carried out. In addition, $^3J_{(H\alpha,H\beta)}$ and $^3J_{(NH,H\alpha)}$ coupling constants were measured. The observation of key sequential strong Hα–NH (*i*,*i* + 1) connectivities such as $H\alpha_{Pro}$–NH_{Asp}, $H\alpha_{Thr}$–NH_{Arg} or $H\alpha_{Asp}$–NH_{Thr} along with weak or absent NH–NH (*i*,*i*+ 1) NOE interactions suggests a conformational preference for extended conformations (figure **4.16**).[27]

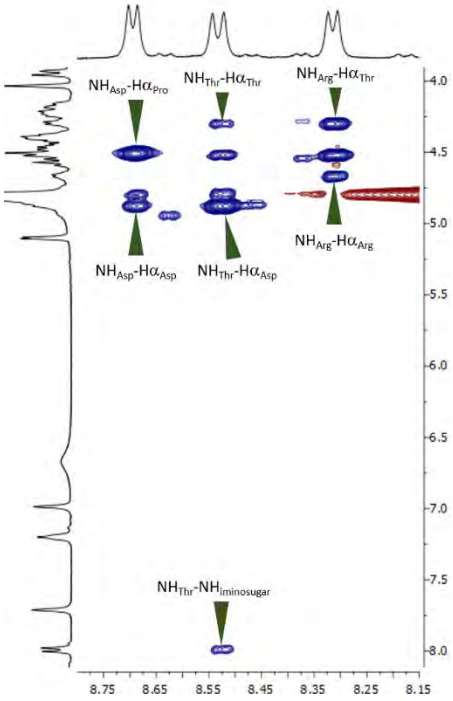

Figure 4.16. Section of the 500 ms 2D NOESY spectrum (400 MHz) in H_2O/D_2O (9:1) at 25 °C for compound **34**, showing the amide region. Diagonal peaks and exchange cross-peaks connecting NH protons and water are negative (red). NOE contacts are represented as positive cross-peaks (blue).

The next step in the conformational analysis of the glycopeptide was to get a conformational ensemble that could reproduce the experimental NMR spectroscopic data. It is important to note that the unrestricted molecular dynamics (MD-free) simulations carried out on small systems typically fail to reproduce the conformational behavior of small peptides backbone due to their high flexibility, and to the force fields tendency to overestimate some stable conformations of bigger systems, such as helix-like arrangements. On the other hand, the direct interpretation of NOE data in small and flexible molecules may lead to the generation of high-energy virtual conformations in terms of a single conformer, since the NOE peaks can corre-

spond to the average of several conformations that co-exist in solution.[28] Therefore, and following our reported protocol,[29] the NMR spectroscopic data were combined with time-averaged restrained molecular dynamics (MD-tar) simulations, aiming to obtain a distribution of low-energy conformers able to quantitatively reproduce the NMR spectroscopic data. This procedure overcomes the limitations inherent in both techniques, NMR analysis and unrestricted MD simulations, and provides a robust method to consider the flexibility of the molecule in the interpretation of the NMR spectroscopic data. Therefore, MD-free and MD-tar[21] simulations were performed for glycopeptide **34** in the free state in water for comparison purposes. The rigidity of this glycopeptide was corroborated, as can be inferred from table **4.5**, since MD-free and MD-tar averaged distances for the peptidic backbone of glycopeptide **34** are quite similar. Both agree with the experimental distances, semi-quantitatively determined by integrating the volume of the corresponding cross-peaks in the NOE spectra.

Table 4.5. Comparison of the experimental, MD-tar and MD-free derived average distances for glycopeptide **34**. All distances are given in Å. Red values mean significant deviation.

Distance	Experimental	MD-tar	MD-free
NH_{Asp}-$H\alpha_{Asp}$	2.8	2.9	2.8
NH_{Asp}-$H\alpha_{Pro}$	2.0	2.2	2.3
NH_{Thr}-$H\alpha_{Thr}$	2.8	2.9	2.9
NH_{Thr}-$H\alpha_{Asp}$	2.1	2.2	2.2
NH_{Arg}-$H\alpha_{Arg}$	2.8	2.9	3.1
NH_{Arg}-$H\alpha_{Thr}$	2.2	2.4	2.9
NH_{Thr}-$NH_{iminosugar}$	3.0	2.9	3.0

These simulations suggest that glycopeptide **34** adopts conformations in water solution that are very similar to that found in the crystal structure in complex with SM3 antibody. For instance, in the SM3:**34** complex, the glycosidic bond adopts an exo-anomeric/syn conformation with ϕ and ψ values around 73.8º and 66.4º, respectively. This conformation is similar to those exhibited for natural glycopeptide **43** bound to SM3[25] and to a model lectin (Soybean agglutinin),[23] and is compatible with the unbound-state conformation. It is important to note that the eclipsed conformation of ψ glycosidic torsional angle takes values around 120°, characteristic of an eclipsed conformation.[21] This geometry is supported by a key NOE cross-peak between the NH group of the threonine residue and the NH of GalNAc (Table **4.5** and Figure **4.16**). The conformations of the glycosylated threonine side chain, as well as the peptide backbone conformations determined by MD-tar simulations match to those found in the crystal structure. Only Thr4 residue presents a considerably deviated ϕ value (4.1º for the X-ray structure, 140-170º from the MD-tar simulation). These results indicate that the bioactive conformation of glycopeptide **34** is predetermined and maintained when interacting with the antibody, even though it contains a non-natural sp^2-iminosugar, which validates the potential of sp^2-iminosugars for the development and design of new carbohydrate-based cancer vaccines (figure **4.17**).

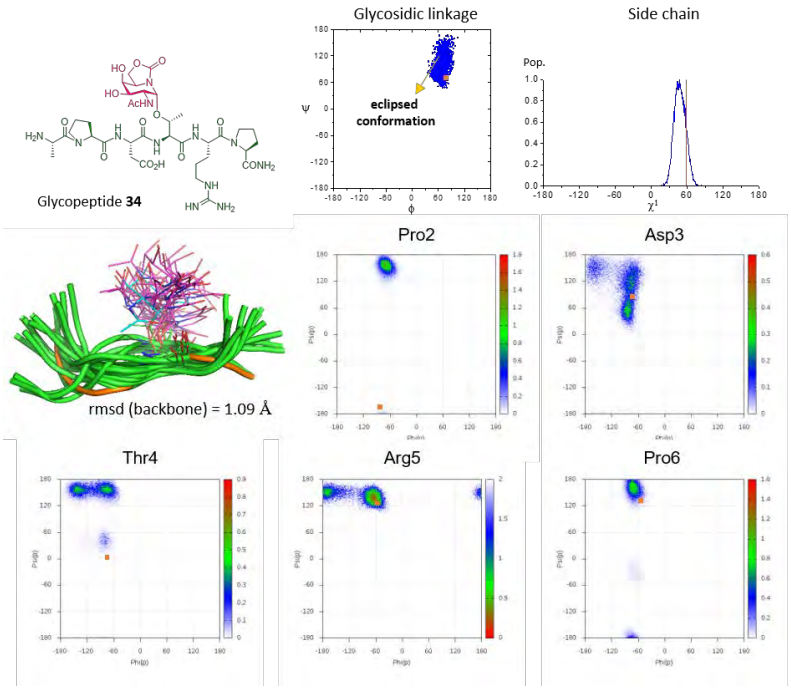

Figure 4.17. Ensembles obtained from 20 ns MD-tar simulations in explicit water performed on glycopeptide **34**, together with the χ^1 distribution for Thr4 and ϕ/ψ distributions for the peptide backbone and the glycosidic linkages. The peptide backbone is shown as a green ribbon (orange for the crystal structure) and the sugar moiety is shown in pink (cyan for the crystal structure). The ϕ/ψ values displayed for the glycopeptide **34** in the complex with SM3 are shown as orange dots.

4.5. Synthesis of a *sp*^{2}-iminosugar containing vaccine

Cancer immunotherapy is not a modern concept. The first reported example dates back to 1893 when William Coley observed a tumor-eliminated immune response by injecting live or inactivated *Streptococcus pyrogenes* and *Serratia marcescens* into tumor tissue.[30] However, the application of TACAs to cancer vaccines is more recent. Although the carbohydrate epitopes were initially extracted from the tumor tissue,[31] being time-consuming and hard to isolate them, the recent developments in carbohy-

drate chemistry[32–34] have enabled obtaining highly pure carbohydrate antigens. The poor immunogenicity of TACAs, probably due to induced immunotolerance is a considerable drawback. Modified TACAs could therefore be considered exogenous by the immune system and trigger a stronger or longer response.

In this context, and encouraged by the promising results obtained for the sp^2-imino-sugar containing peptides and their corresponding binding to SM3 antibody, we decided to incorporate the sp^2GalNAc-Thr amino acid **26** into a carbohydrate-based vaccine. The target glycopeptide **51** (figure **4.17**) is based on the 20 residues tandem-repeated sequence of MUC1 (HGVTSAPDTRPAPGSTAPPA), where the sp^2-iminosugar moiety is attached to the Thr residue at the PDTR epitope. Due to the low molecular weight of these kind of oligopeptides, they usually have no immunogenicity. To solve this problem, they have to be conjugated to high molecular weight proteins such as keyhole limpet hemocyanin (KLH) or bovine serum albumin (BSA). A Cys residue allowing this conjugation is hence coupled at the *N*-terminal position of the peptide. Natural glycosylated and non-glycosylated peptides **52** and **53**, respectively, were also synthesized for comparison purposes.

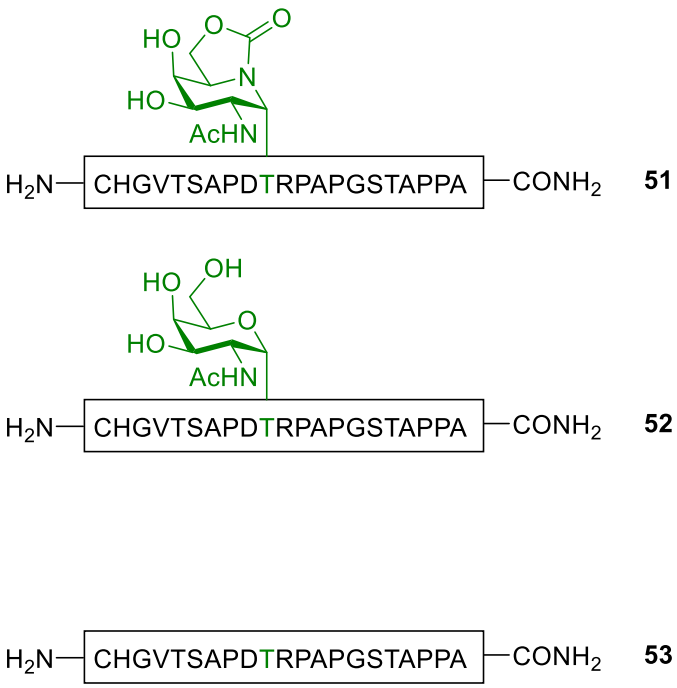

Figure 4.17. Structure of peptides **51**, **52**, and **53**.

The syntheses of MUC1-based peptides **51-53** were carried out in collaboration with Iris Bermejo, a group colleague granted by the Spanish Association Against Cancer (AECC, from the Spanish: Asociación Española Contra el Cáncer), using microwave-assisted solid phase peptide synthesis (MW-SPPS). Rink Amide MBHA resin, Fmoc-protected amino acids and were used and glycosylated building blocks **26** and **Fmoc-Thr(GalNAc)-OH**[19] were coupled manually (scheme **4.3**).

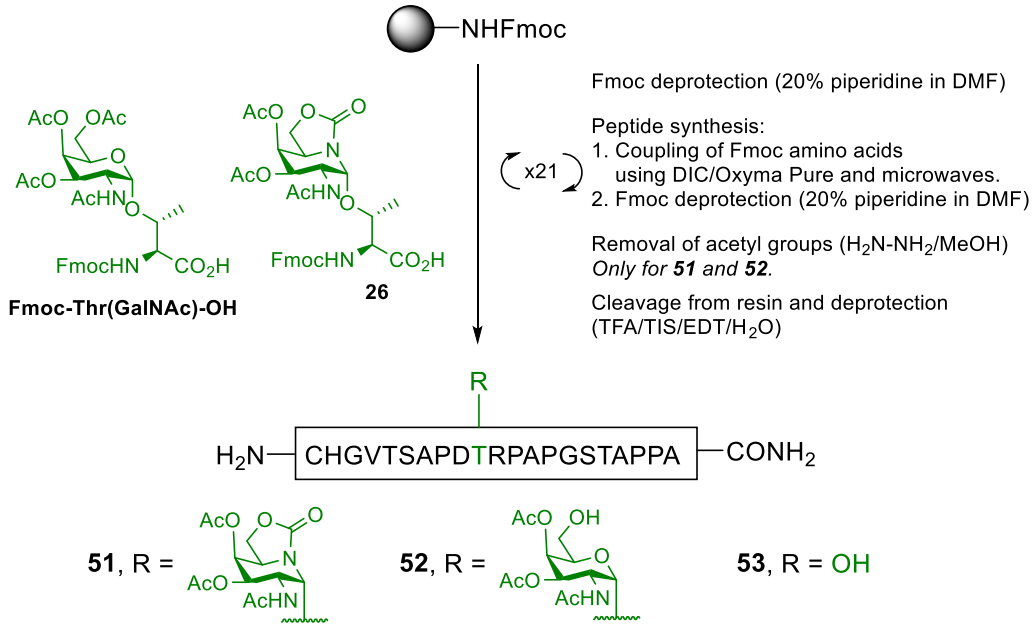

Scheme 4.3. Synthesis of MUC1-based peptides **51-53**.

Unfortunately, there are still no results for the immunogenicity of these vaccine candidates, since the corresponding assays and analyses are currently being performed.

4.6. Conclusions

An efficient methodology for synthesizing glycomimetic sp^2-iminosugar amino acids, as well as their incorporation into MUC1-based peptides, has been developed. Strong anomeric effects in the axially substituted adducts combined with the reduced torsional strain developed at the α-glycosylation TS dictate the consistently observed complete stereoselectivity towards the α-*O*-linkage. These novel conformationally locked compounds behave as glycosidase inhibitors, with selectivity patterns that depend on both the glycon and the aglycon moieties. They are also able to

emulate the binding mode of the natural Tn antigen to lectins and anti-MUC1 antibodies, despite the lack of the *N*-acetyl group at C2 or the axial disposition of the hydroxyl group at C4. The superior performance of Thr- over Ser-containing derivatives reinforces the key role of the underlying amino acid in the molecular recognition of glycopeptides. These unnatural glycopeptides will presumably be more stable to chemical or enzymatic degradation and may not suffer from immune suppression. These properties, together with the extra rigidity imposed by the fused rings of the sp^2-imino sugar, will hopefully lead to stronger and longer-lasting antigenic responses.

Part of this work has been published as an article entitled "Tn Antigen Mimics Based on sp^2-iminosugars with Affinity for an anti-MUC1 Antibody" in the journal *Organic Letters*, **2016**, *18*, 3890-3893.

On the other hand, three vaccine candidates, two natural peptides and one containing a sp^2-iminosugar moiety, have been synthesized and are currently being evaluated.

4.7. References

(1) Wrodnigg, T. M.; Steiner, A. J.; Ueberbacher, B. J. *Anticancer. Agents Med. Chem.* **2008**, *8*, 77–85.
(2) Compain, P.; Martin, O. R. *Iminosugars : From Synthesis to Therapeutic Applications*; Wiley-VCH, 2007.
(3) Allan, G.; Ouadid-Ahidouch, H.; Sanchez-Fernandez, E. M.; Risquez-Cuadro, R.; Garcia Fernandez, J. M.; Ortiz-Mellet, C.; Ahidouch, A. *PLoS One* **2013**, *8*, e76411.
(4) Stütz, A. E. *Iminosugars as Glycosidase Inhibitors : Nojirimycin and Beyond*; Wiley-VCH, 1999.
(5) Boisson, J.; Thomasset, A.; Racine, E.; Cividino, P.; Sainte-Luce, T. B.; Poisson, J.-F. O.; Behr, J.-B.; Py, S. *Org. Lett.* **2015**, *17*, 3662–3665.
(6) Doddi, V. R.; Kokatla, H. P.; Pal, A. P. J.; Basak, R. K.; Vankar, Y. D. *Eur. J.*

Org. Chem. **2008**, 5731–5739.
(7) Jiménez-Blanco, J. L.; Díaz-Pérez, V. M.; Ortiz Mellet, C.; Fuentes, J.; García-Fernandez, J. M.; Díaz-Arribas, J. C.; Cañada, F. J. *Chem. Commun.* **1997**, *45*, 1969–1970.
(8) Sánchez-Fernández, E. M.; Álvarez, E.; Ortiz Mellet, C.; García Fernández, J. M. *J. Org. Chem.* **2014**, *79*, 11722–11728.
(9) Sánchez-Fernández, E. M.; Rísquez-Cuadro, R.; Chasseraud, M.; Ahidouch, A.; Ortiz Mellet, C.; Ouadid-Ahidouch, H.; García Fernández, J. M. *Chem. Commun.* **2010**, *46*, 5328-5330.
(10) Sánchez-Fernández, E. M.; Rísquez-Cuadro, R.; Ortiz Mellet, C.; García Fernández, J. M.; Nieto, P. M.; Angulo, J. *Chem. Eur. J.* **2012**, *18*, 8527–8539.
(11) Sánchez-Fernández, E. M.; Rísquez-Cuadro, R.; Aguilar-Moncayo, M.; García-Moreno, M. I.; Ortiz Mellet, C.; García Fernández, J. M. *Org. Lett.* **2009**, *11*, 3306–3309.
(12) Rísquez-Cuadro, R.; García Fernández, J. M.; Nierengarten, J. F.; Ortiz Mellet, C. *Chem. Eur. J.* **2013**, *19*, 16791–16803.
(13) Karsten, U.; Serttas, N.; Paulsen, H.; Danielczyk, A.; Goletz, S. *Glycobiology* **2004**, *14*, 681–692.
(14) Pérez, P. D.; García-Moreno, M. I.; Ortiz Mellet, C.; García Fernández, J. M. *Eur. J. Org. Chem.* **2005**, 2903–2913.
(15) Shoda, S. I.; Kulkarni, S. S.; Gervay-Hague, J. In *Handbook of Chemical Glycosylation: Advances in Stereoselectivity and Therapeutic Relevance*; Wiley-VCH: Weinheim, Germany, 2008; pp 29–93.
(16) Paulsen, H.; Adermann, K. *Liebigs Ann. der Chemie* **1989**, 771–780.
(17) Wang, H.; Houk, K. N. *Chem. Sci.* **2014**, *5*, 462–470.
(18) Carballeira, L.; Pérez-Juste, I. *J. Phys. Chem. A* **2000**, *104*, 9362–9369.
(19) Madariaga, D.; Martínez-Sáez, N.; Somovilla, V. J.; García-García, L.; Berbis, M. Á.; Valero-Gónzalez, J.; Martín-Santamaría, S.; Hurtado-Guerrero, R.; Asensio, J. L.; Jiménez-Barbero, J.; Avenoza, A.; Busto, J. H.; Corzana, F.; Peregrina, J. M. *Chem. Eur. J.* **2014**, *20*, 12616–12627.
(20) Corzana, F.; Busto, J. H.; Jiménez-Osés, G.; Asensio, J. L.; Jiménez-Barbero, J.; Peregrina, J. M.; Avenoza, A. *J. Am. Chem. Soc.* **2006**, *128*, 14640–14648.
(21) Corzana, F.; Busto, J. H.; Jiménez-Osés, G.; García De Luis, M.; Asensio, J. L.; Jiménez-Barbero, J.; Peregrina, J. M.; Avenoza, A. *J. Am. Chem. Soc.* **2007**, *129*, 9458–9467.
(22) Aydillo, C.; Navo, C. D.; Busto, J. H.; Corzana, F.; Zurbano, M. M.; Avenoza, A.; Peregrina, J. M. *J. Org. Chem.* **2013**, *78*, 10968–10977.
(23) Madariaga, D.; Martinez-Sáez, N.; Somovilla, V. J.; Coelho, H.; Valero-González, J.; Castro-Lopez, J.; Asensio, J. L.; Jiménez-Barbero, J.; Busto, J. H.; Avenoza, A.; Marcelo, F.; Hurtado-Guerrero, R.; Corzana, F.; Peregrina, J. M. *ACS Chem. Biol.* **2015**, *10*, 747–756.
(24) Juers, D. H.; Heightman, T. D.; Vasella, A.; McCarter, J. D.; Mackenzie, L.; Withers, S. G.; Matthews, B. W. *Biochemistry* **2001**, *40*, 14781–14794.
(25) Martínez-Sáez, N.; Castro-López, J.; Valero-González, J.; Madariaga, D.;

Compañón, I.; Somovilla, V. J.; Salvadó, M.; Asensio, J. L.; Jiménez-Barbero, J.; Avenoza, A.; Busto, J. H.; Bernardes, G. J. L.; Peregrina, J. M.; Hurtado-Guerrero, R.; Corzana, F. *Angew. Chem. Int. Ed.* **2015**, *54*, 9830–9834.
(26) Concepcion, J.; Witte, K.; Wartchow, C.; Choo, S.; Yao, D.; Persson, H.; Wei, J.; Li, P.; Heidecker, B.; Ma, W.; Varma, R.; Zhao, L.-S.; Perillat, D.; Carricato, G.; Recknor, M.; Du, K.; Ho, H.; Ellis, T.; Gamez, J.; Howes, M.; Phi-Wilson, J.; Lockard, S.; Zuk, R.; Tan, H. *Comb. Chem. High Throughput Screen.* **2009**, *12*, 791–800.
(27) Dyson, H. J.; Wright, P. E. *Annu. Rev. Phys. Chem.* **1996**, *47*, 369–395.
(28) Cumming, D. A.; Carver, J. P. *Biochemistry* **1987**, *26*, 6664–6676.
(29) Corzana, F.; Busto, J. H.; Engelsen, S. B.; Jiménez-Barberó, J.; Asensio, J. L.; Peregrina, J. M.; Avenoza, A. *Chem. Eur. J.* **2006**, *12*, 7864–7871.
(30) Coley, W. B. *Am. J. Med. Sci.* **1893**, *105*, 487–511.
(31) Helling, F.; Shang, A.; Calves, M.; Zhang, S.; Ren, S.; Yu, R. K.; Oettgen, H. F.; Livingston, P. O. *Cancer Res.* **1994**, *54*, 197–203.
(32) Plante, O. J.; Palmacci, E. R.; Seeberger, P. H. *Science* **2001**, *291*, 1523–1527.
(33) Zhang, Z.; Ollmann, I. R.; Ye, X. S.; Wischnat, R.; Baasov, T.; Wong, C. H. *J. Am. Chem. Soc.* **1999**, *121*, 734–753.
(34) Huang, X.; Huang, L.; Wang, H.; Ye, X. S. *Angew. Chem. Int. Ed.* **2004**, *43*, 5221–5224.

Chapter 5. International short-term research stays

5.1. Synthesis of Glycocin F and an unnatural analog

Glycocin F (GccF) is a unique diglycosylated bacteriocin peptide, which presents a (β-*O*-GlcNAc)Ser residue and a unusual (β-*S*-GlcNAc)Cys residue important for antibacterial activity. GccF is a ribosomally synthesized and post-translationally modified peptide (RiPP) isolated from *Lactobacillus plantarum* KW30, which is comprised of 43 amino acids forming two α-helices connected by a short loop and tethered to each other by two nested disulfide bonds (figure **5.1**).[1,2]

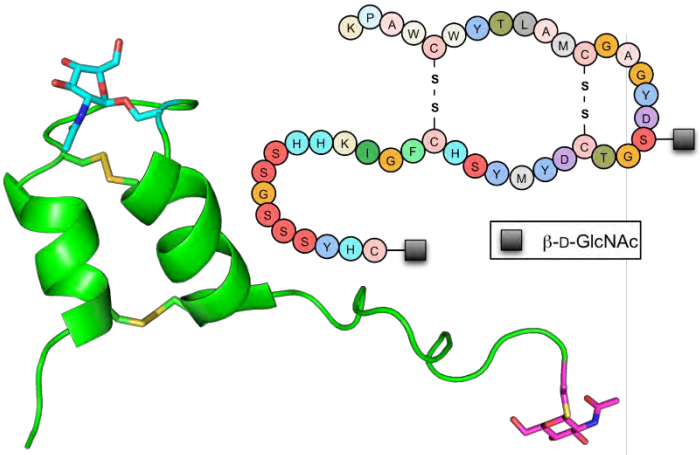

Figure 5.1. Sequence and three-dimensional structure of GccF elucidated from NMR experiments.[2]

Brimble and co-workers[3] described the first total synthesis of GccF using a native chemical ligation (NCL) strategy. However, due to the use of a Rink amide linker, the *C*-terminus of the synthesized peptide presented an amide, instead of a carboxylic acid as in the natural GccF, which resulted in lower antimicrobial activities.

With this background in mind, we proposed as the main goal for the short-stay at Brimble's lab (University of Auckland, New Zealand) to synthesize the natural GccF and an analog in which the Ser residue bearing the GlcNAc moiety was mutated to the quaternary amino acid α-methylserine (MeSer, figure **5.2**).[4] This unnatural amino acid is known to favor helix-like structures,[5] which would lead to a change in the structure and, since the interhelical loop region is essential for GccF activity,[6] in the biological activity.

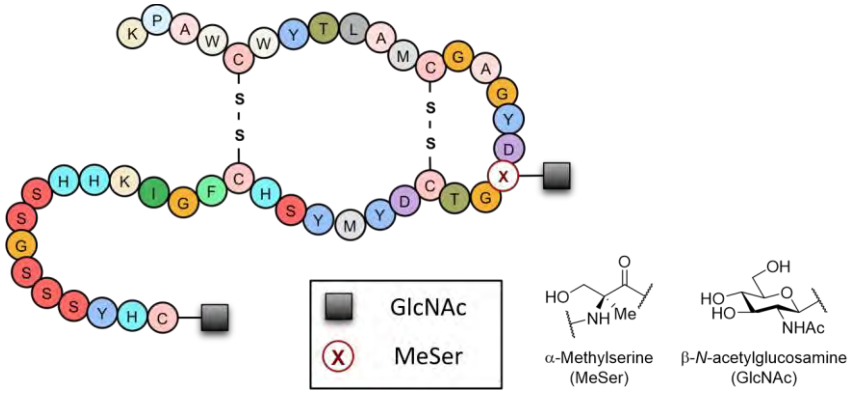

Figure 5.2. Structure of the GccF analog containing a glycosylated MeSer residue.

The synthesis of both the natural and the unnatural GccF peptides was accomplished utilizing a NCL[7] strategy, taking advantage of the position of the Cys residues and the reactivity of His and Met thioesters.[8] Two key ligation sites were identified, envisioning GccF to be assembled from three fragments (figure **5.3**). In this sense, **fragment 3**, which incorporates the (GlcNAc)Cys residue, was synthesized by SPPS using a 2-chlorotrityl chloride resin to afford the corresponding carboxylic acid at the *C*-terminus. **Fragment 2** was similarly synthesized, incorporating either the (GlcNAc)Ser or the (GlcNAc)MeSer residues, which were previously synthesized and **fragment 1** was synthesized following the described protocol.

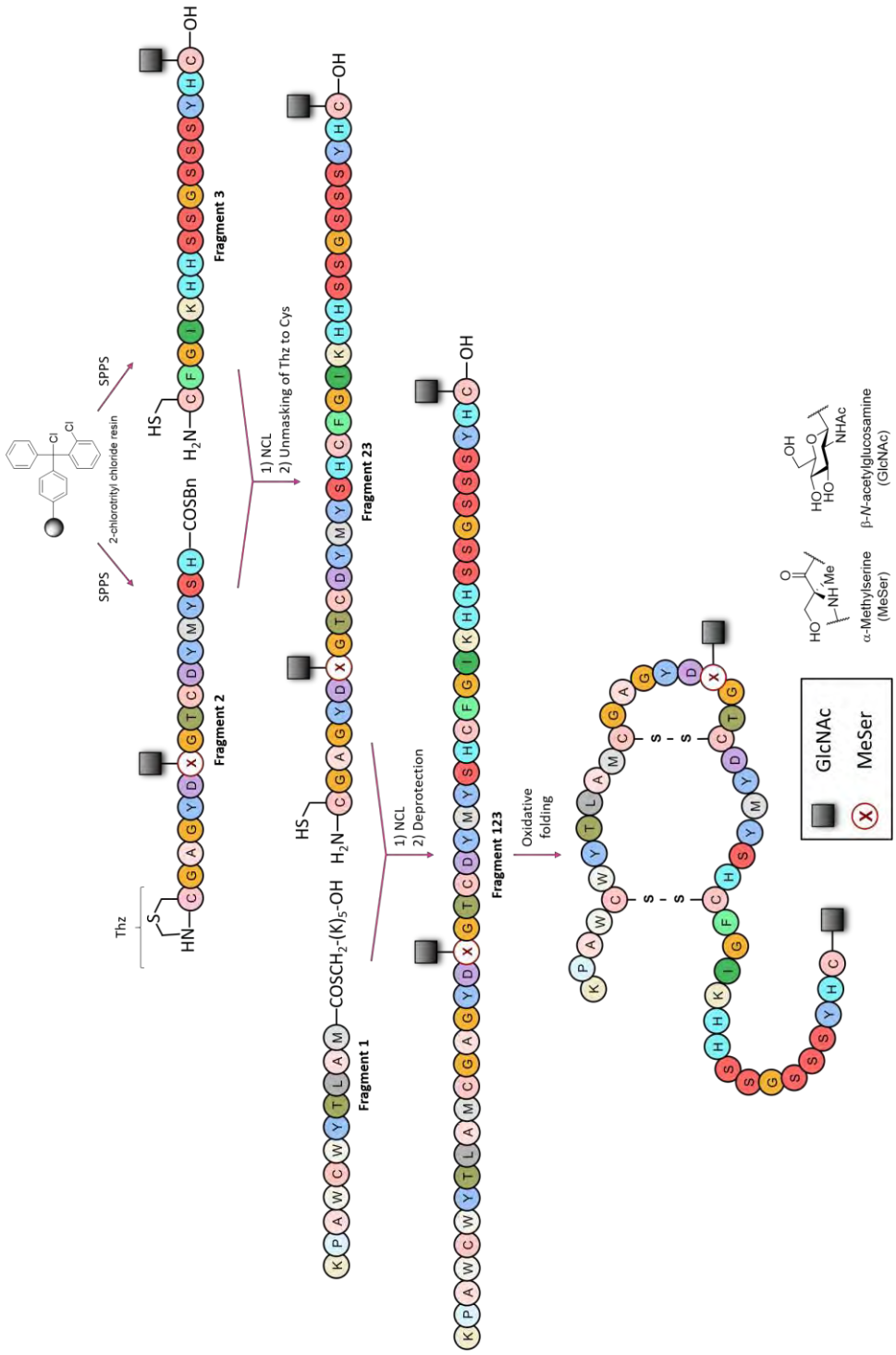

Figure 5.3. Synthetic route of GccF analog incorporating MeSer.

Fragments 2 and **3** were then coupled under NCL conditions followed by unmasking of the *N*-terminal thiazoline to Cys, to afford fragment **23**. This fragment was then coupled under NCL conditions to **fragment 1** and the protecting groups of Trp residues and *O*-acetyl groups of the carbohydrate moiety were deprotected to afford the unfolded GccF or the unfolded analog. Final oxidative folding using cysteine, cystine and EDTA at 4 ºC afforded the final folded glycopeptides.

The results corresponding to the natural GccF have been already published as an article entitled "Total chemical synthesis of glycocin F and analogs: *S*-glycosylation confers improved antimicrobial activity" in the journal *Chemical Science*, **2018**, *9*, 1686-1691.

The biological consequences in the antimicrobial activity of the synthesized analog of GccF are currently being investigated.

5.2. Theoretical study of macrocycles formation in lantipeptides

Lantipeptides[9] are a family of RiPPs characterized by the presence of thioether cross-links, forming rings that are crucial for antimicrobial activity and stability. These rings are formed by a Michel-type addition of the thiol of a Cys residue, to a pre-formed dehydroamino acid, namely dehydroalanine (Dha) or dehydrobutyrine (Dhb), affording in this way lanthionine (Lan) and methyllanthionine (MeLan) (figure **5.4**).

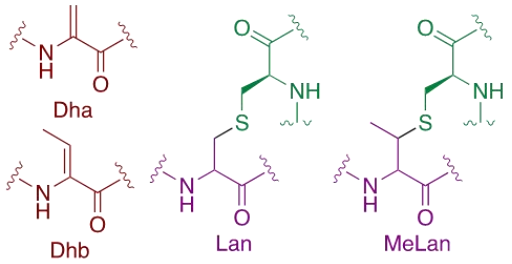

Figure 5.4. Chemical structure of dehydroalanine (Dha), dehydrobutyrine (Dhb), lanthionine (Lan) and methyllanthionine (MeLan).

Duramycin is a lantipeptide investigated as antibiotic, inhibitor of viral entry,[10] therapeutic of cystic fibrosis,[11] and tumor and vasculature imaging agent,[12] which contains a β-hydroxyaspartic acid residue (Hya), two MeLan rings, one Lan ring, and an essential lysinoalanine (Lal) crosslink.[13]

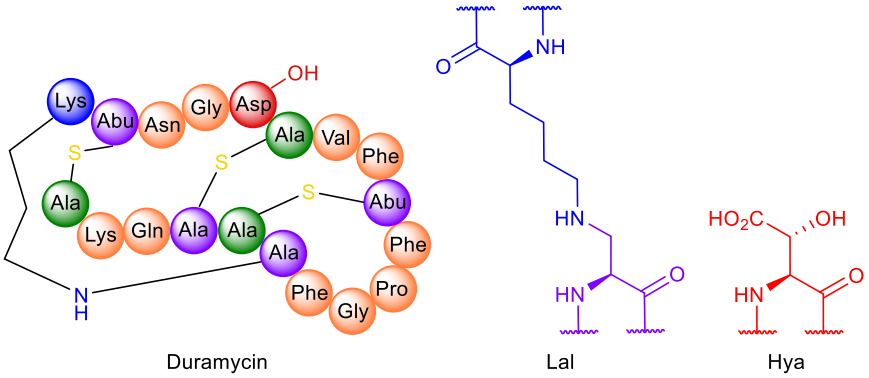

Figure 5.5. Structure of Duramycin, lysinoalanine (Lal) and β-hydroxyaspartic acid (Hya). Abu = 2-aminobutyric acid.

The enzyme DurN catalyzes the unprecedented formation of the Lal ring, crosslinking a Lys and a preformed Dha through an aza-Michael reaction. However, the exact mechanism is unknown. The main goal for the short-stay at van der Donk's lab (University of Illinois at Urbana-Champaign, USA) was therefore to provide insight into de reaction mecha-

nism and the role of critical amino acids through multiscale computational modeling.

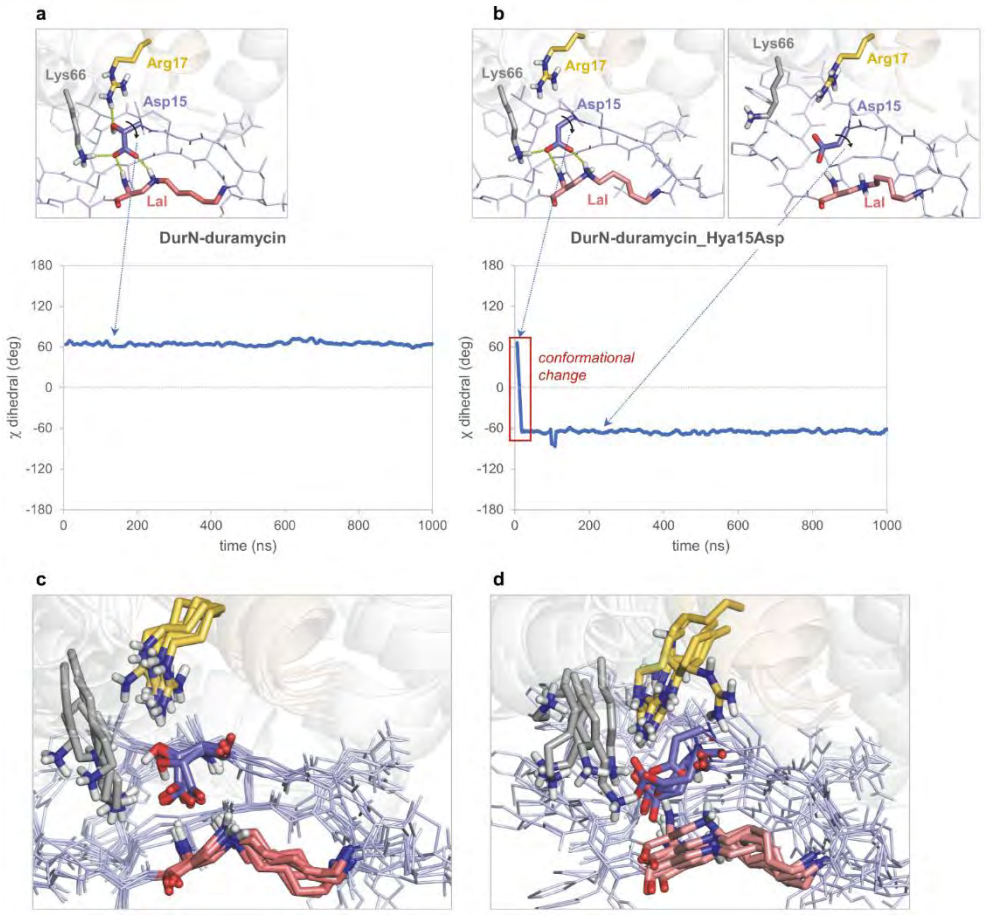

Figure 5.6. Conformational changes of the catalytic base in Hya residue upon mutation to Asp. The complex between DurN and duramycin was investigated through 1.0 μs MD simulations. Duramycin backbone and side chains are shown as dark and light blue lines, respectively. Lal, Hya/Asp15, Arg17 and Lys66 are shown as red, blue, yellow and grey sticks, respectively. a) χ dihedral angle values of Hya residue side chain throughout the whole simulation. b) χ dihedral angle values of mutated Hya15Asp residue side chain throughout the whole simulation. c) 5 superimposed representative snapshots derived from the trajectories for native duramycin and d) for the Hya14Asp mutant.

MD simulations performed on the complex between DurN and native duramycin suggested that the unnatural amino acid Hya plays a key role in the Lal formation mechanism, acting as catalytic base. According to the crystallographic structure of the complex, the hydroxyl group of Hya is engaged in a hydrogen bond with Arg17, while the carboxylate group interacts with Lys66 and Ala6. This hydrogen bond network is maintained throughout the whole simulation, as reflected by the conserved χ dihedral angle of *ca.* +60 º (figure **5.6a**). However, the hydrogen bond network is disrupted in the Hya15Asp mutant, compromising the integrity of the active site. The carboxylic acid of Asp15 quickly undergoes a 120º conformational twist to interact electrostatically with Arg17 and Lys66. The catalytic base is therefore trapped in a non-catalytic conformation as revealed by it χ dihedral angle (figure **5.6b**). Additionally, the simulation revealed a more rigid active site when native duramycin is bound to DurN (figure **5.6c**), unlike the more flexible arrangement with the Hya15Asp mutant (figure **5.6d**).

All these computational observations allowed to rationalize the lack of catalytic activity observed for the Hya15Asp mutant and to provide a rationale for the Lal formation mechanism. This work has just been published as an article entitled "Substrate-assisted enzymatic formation of lysinoalanine in duramycin" in the journal *Nature Chemical Biology*.

5.3. References

(1) Stepper, J.; Shastri, S.; Loo, T. S.; Preston, J. C.; Novak, P.; Man, P.; Moore, C. H.; Havlíček, V.; Patchett, M. L.; Norris, G. E. *FEBS Lett.* **2011**, *585*, 645–650.

(2) Venugopal, H.; Edwards, P. J. B.; Schwalbe, M.; Claridge, J. K.; Libich, D. S.; Stepper, J.; Loo, T.; Patchett, M. L.; Norris, G. E.; Pascal, S. M. *Biochemistry* **2011**, *50*, 2748–2755.

(3) Brimble, M. A.; Edwards, P. J.; Harris, P. W. R.; Norris, G. E.; Patchett, M. L.; Wright, T. H.; Yang, S. H.; Carley, S. E. *Chem. Eur. J.* **2015**, *21*, 3556–3561.
(4) Corzana, F.; Busto, J. H.; Marcelo, F.; García de Luis, M.; Asensio, J. L.; Martín-Santamaría, S.; Sáenz, Y.; Torres, C.; Jiménez-Barbero, J.; Avenoza, A.; Peregrina, J. M. *Chem. Commun.* **2011**, *47*, 5319.
(5) Corzana, F.; Busto, J. H.; Marcelo, F.; García de Luis, M.; Asensio, J. L.; Martín-Santamaría, S.; Jiménez-Barbero, J.; Avenoza, A.; Peregrina, J. M. *Chem. Eur. J.* **2011**, *17*, 3105–3110.
(6) Bisset, S. W.; Yang, S.-H.; Amso, Z.; Harris, P. W. R.; Patchett, M. L.; Brimble, M. A.; Norris, G. E. *ACS Chem. Biol.* **2018**, *13*, 1270–1278.
(7) Dawson, P. E.; Muir, T. W.; Clark-Lewis, I.; Kent, S. B. *Science* **1994**, *266*, 776–779.
(8) Hackeng, T. M.; Griffin, J. H.; Dawson, P. E. *Proc. Natl. Acad. Sci.* **1999**, *96*, 10068–10073.
(9) Knerr, P. J.; van der Donk, W. A. *Annu. Rev. Biochem.* **2012**, *81*, 479–505.
(10) Richard, A. S.; Zhang, A.; Park, S.-J.; Farzan, M.; Zong, M.; Choe, H. *Proc. Natl. Acad. Sci.* **2015**, *112*, 14682–14687.
(11) Oliynyk, I.; Varelogianni, G.; Roomans, G. M.; Johannesson, M. *APMIS* **2010**, *118*, 982–990.
(12) Zhao, M.; Li, Z.; Bugenhagen, S. *J. Nucl. Med.* **2008**, *49*, 1345–1352.
(13) Huo, L.; Ökesli, A.; Zhao, M.; van der Donk, W. A. *Appl. Environ. Microbiol.* **2017**, *83*.

Chapter 6.
Conclusions/conclusiones

6.1. Conclusions

The following conclusions can be drawn from the results obtained throughout this Thesis:

1. Completely diastereoselective double asymmetric *C*-Michael additions of serine equivalent *C*-nucleophiles to 2-nitroglycals have been developed to afford fully protected α-(α-*C*-GalNAc)serine or α-(β-*C*-GlcNAc)serine derivatives. Galactose derivatives can be transformed in different families of *C*-glyco-amino-acids, which present conformational restrictions. The *C*-glycosidic bond is a chemical restriction itself, which, in addition to the formation of bicyclic carbohydrate moieties, encompass the restrictions. Despite having conformational constraints, these unnatural derivatives are recognized by different lectins (SBA, VVA), and can therefore be regarded as Tn antigen mimics, although they are not structurally close analogs of the Tn antigen.

2. We have contrived an efficient methodology for the synthesis of conformationally locked *C*-glycosides that enables the incorporation of mono and multibranched aglycone moieties. Derivatives bearing long hydrophobic substituents behaved as micromolar competitive inhibitors of mammalian glycosidases and, most interestingly, as selective inhibitors of human lysosomal β-glucosidase (GCase) at neutral pH, with a remarkable decrease in the inhibitory activity at pH 5. This fact makes them good candidates as pharmacological chaperones for Gaucher disease, being in fact one of the candidates able to increase the activity of N370S and F213I GCase mutants in fibroblasts of Gaucher patients

with an efficiency similar to that of the reference compound Ambroxol®.

3. We have synthesized the first examples of amino acid (Ser/Thr)-glycomimetic conjugates featuring an α-*O*-linked pseudoanomeric linkage with sp^2-iminosugars. The stereoselectivity towards the α-derivatives is dictated mainly by the strong anomeric effect in the subsequent axially-substituted product. Mucin-related glycopeptides that incorporate these motifs are recognized by Tn specific lectins, as well as by complementary glycosidases, with activities conditioned by the hydroxylation pattern (Glc, Gal, GlcNAc, GalNAc) and the underlying amino acid (Ser or Thr). These conjugates are able to bind to an anti-MUC1 antibody despite the bicyclic structure, which, combined with the presumable immune suppression and stability towards enzymatic or chemical degradation owed to the rigidity imposed by the fused ring, will hopefully lead to stronger and longer-lasting antigenic responses.

4. By means of an international short-term research stay at Brimble's group (University of Auckland, New Zealand), the bacteriocin peptide glycocin F and an analog containing the quaternary amino acid α-methylserine were synthesized combining solid phase peptide synthesis (Fmoc and Boc chemistry) with native chemical ligation. The biological and conformational consequences of incorporating the non-natural amino acid are currently being evaluated.

5. In a second short-term research stay, this time at van der Donk's group (University of Illinois at Urbana-Champaign, USA), we have provided a mechanistic rationale for the DurN catalyzed formation of lysino-

alanine crosslink in duramycin. The computational results suggest that the presence of the unnatural β-hydroxyaspartic acid in duramycin is crucial for catalysis.

6. The aforementioned outcomes were deduced by a multidisciplinary approach that involves the use of different techniques such as, NMR, X-ray diffraction, ELLA, BLI, and QM and MD simulation techniques.

6.2. Conclusiones

Del trabajo desarrollado en esta Tesis Doctoral se pueden extraer las siguientes conclusiones:

1. Se ha desarrollado una nueva metodología para obtener derivados de α-(α-*C*-GalNAc)serina y α-(β-*C*-GlcNAc)serina convenientemente protegidos mediante una reacción de tipo *C*-Michael asimétrica doble completamente diastereoselectiva entre un equivalente bicíclico de serina quiral y 2-nitroglicales. Los derivados de galactosa pueden ser transformados en varias familias de *C*-glico-aminoácidos conformacionalmente restringidos. El enlace *C*-glicosídico es una restricción química en sí mismo, que junto a la formación de estructuras bicíclicas en torno al carbohidrato conforman las limitaciones conformacionales. A pesar de estas restricciones, estos derivados no naturales son reconocidos por distintas lectinas (SBA, VVA) y, por tanto, pueden ser considerados miméticos del antígeno Tn, aunque no sean estructuralmente similares.

2. Hemos diseñado una metodología eficaz para sintetizar *C*-glicósidos conformacionalmente restringidos que permiten incorporar una o más

subestructuras agliconas. Se ha demostrado que los compuestos que presentan sustituyentes hidrofóbicos largos se comportan como inhibidores competitivos de glicosidasas de mamíferos y, lo que es más interesante, como inhibidores selectivos de la enzima lisosomal β-glucocerebrosidasa (GCasa) a pH neutro, con un descenso significativo de la actividad a pH 5. Esto los convierte en buenos candidatos para actuar como chaperonas farmacológicas para la enfermedad de Gaucher. De hecho, uno de los candidatos es capaz de aumentar la actividad de la enzima en pacientes de Gaucher que presentan fibroblastos con mutaciones N370S y F213I, con eficacias similares a las que presenta el compuesto de referencia Ambroxol®.

3. Se han sintetizado los primeros ejemplos de aminoácidos (Ser y Thr) que está unidos mediante un enlace de tipo α-*O*-glicosídico al carbono pseudoanomérico de iminoazúcares de tipo sp^2. La estereoselectividad mostrada en la reacción de glicosilación en favor de los α-derivados es debida principalmente al fuerte efecto anomérico de los correspondientes productos con sustituyentes en posición axial. Estas estructuras se han incorporado en glicopéptidos de tipo mucina, los cuales son reconocidos por lectinas específicas del antígeno Tn, así como por diversas glicosidasas, cuyas actividades varían en función de los patrones de hidroxilación (Gal, Glc, GalNAc, GlcNAc) y del aminoácido subyacente (Ser o Thr). Estos compuestos también son capaces de unirse a anticuerpos anti-MUC1 a pesar de su estructura bicíclica, lo que, combinado con la presumible supresión inmune y mayor estabilidad química y enzimática debida a la rigidez estructural, conllevará a respuestas antigénicas más fuertes y duraderas.

4. A través de una estancia breve de investigación en el grupo de la Profesora Margaret Brimble (Universidad de Auckland, Nueva Zelanda), se ha sintetizado el péptido bactericida glicocina F, así como un análogo que incorpora el aminoácido no natural α-metilserina. La síntesis se llevó a cabo combinando síntesis de péptidos en fase sólida utilizando química Boc y Fmoc, con ligación química nativa. Las consecuencias conformacionales y biológicas debidas a la presencia del aminoácido no natural están siendo evaluadas en estos momentos.

5. En una segunda estancia breve de investigación, esta vez en el grupo del Profesor Wilfred A. van der Donk (Universidad de Illinois en Urbana-Champaign, EEUU), se propuso un mecanismo plausible para la formación de lisinoalanina catalizada por la enzima DurN en el péptido duramicina. El estudio computacional corrobora la teoría de que la presencia del grupo hidroxilo en el aminoácido no natural β-hidroxiaspártico es crucial para la catálisis.

6. Todas estas conclusiones han sido deducidas mediante una aproximación multidisciplinar utilizando diferentes técnicas tanto experimentales como teóricas, como pueden ser los experimentos de Resonancia Magnética Nuclear, ELLAs, BLIs, simulaciones de dinámicas moleculares, estudios mecanocuánticos, difracción de rayos-X…

6.3. Scientific publications derived from this Thesis

- *A double diastereoselective Michael-type addition as an entry to conformationally restricted Tn antigen mimics.*
  C. Aydillo, C. D. Navo, J. H. Busto, F. Corzana, M. M. Zurbano, A. Avenoza, J. M. Peregrina.
  The Journal of Organic Chemistry **2013**, *78*, 10968-10977.

- *Conformationally-locked C-glycosides: tuning aglycone interactions for optimal chaperone behaviour in Gaucher fibroblasts.*
  C. D. Navo, F. Corzana, E. M. Sánchez-Fernández, J. H. Busto, A. Avenoza, M. M. Zurbano, E. Nanba, K. Higaki, C. Ortíz-Mellet, J. M. García-Fernández, J. M. Peregrina.
  Organic & Biomolecular Chemistry **2016**, *14*, 1473-1484.

- *Tn antigen mimics based on sp^2-iminosugars with affinity for an anti-MUC1 Antibody.*
  E. M. Sánchez-Fernández, C. D. Navo, N. Martínez-Sáez, R. Gonçalves-Pereira, V. J. Somovilla, A. Avenoza, J. H. Busto, G. J. L. Bernardes, G. Jiménez-Osés, F. Corzana, J. M. García-Fernández, C. Ortíz-Mellet, J. M. Peregrina.
  Organic Letters **2016**, *18*, 3890-3893.

- *Total chemical synthesis of glycocin F and analogues: S-glycosylation confers improved antimicrobial activity.*
  Z. Amso, S. W. Bisset, S. H. Yang, P. W. R. Harris, T. H. Wright, C. D. Navo, M. L. Pratchett, G. E. Norris, M. A. Brimble.
  Chemical Science **2018**, *9*, 1686-1691.

- *Substrate-assisted enzymatic formation of lysinoalanine in duramycin.*
  L. An, D. P. Cogan, C. D. Navo, G. Jiménez-Osés, S. K. Nair, W. A. van der Donk
  Nature Chemical Biology **2018**, *accepted manuscript.*

6.4. Other scientific publications

- *Synthesis of mixed α/β^{2,2}-peptides by site-selective ring-opening of cyclic quaternary sulfamidates.*
  N. Mazo, I. García-González, C. D. Navo, F. Corzana, G. Jiménez-Osés, A. Avenoza, J. H. Busto, J. M. Peregrina
  Organic Letters **2015**, *17*, 5804-5807.

- *Bifunctional chiral dehydroalanines for peptide coupling and stereoselective S-Michael addition.*
  M. I. Gutiérrez-Jiménez, C. Aydillo, C. D. Navo, A. Avenoza, F. Corzana, G. Jiménez-Osés, M. M. Zurbano, J. H. Busto, J. M. Peregrina
  Organic Letters **2016**, *18*, 2796-2799.

- *Substituent effects on the reactivity of cyclic tertiary sulfamidates.*
  C. D. Navo, N. Mazo, A. Avenoza, J. H. Busto, J. M. Peregrina, G. Jiménez-Osés
  The Journal of Organic Chemistry **2017**, *82*, 13250-13255.

- *Cell-penetrating peptides containing fluorescent D-cysteines.*
  C. D. Navo, A. Asín, E. Gómez-Orte, M. I. Gutiérrez-Jiménez, I. Compañón, B. Ezcurra,A. Avenoza, J. H. Busto, F. Corzana, M. M. Zurbano, G. Jiménez-Osés, J. Cabello, J. M. Peregrina
  Chemistry – A European Journal **2018**, *24*, 7991-8000.

6.5. Contribution to congresses

- **Keynote lecture**: *Unusual reactivity patterns in unnatural amino acids derivatives explained by quantum mechanics*. C. D. Navo, A. Avenoza, J. M. Peregrina, G. Jiménez-Osés. *XXXVI Biennial Meeting of the RSEQ*. Sitges (Spain). June 25-29 of 2017.

- **Oral communication**: *Bicyclic C-glycosidase inhibitors: A new pharmacological chaperone for Gaucher's disease*. C. D. Navo, F. Corzana, K. Higaki, J. H. Busto, M. M. Zurbano, A. Avenoza, C. Ortíz-Mellet, J. M. García-Fernández, J. M. Peregrina. *11th International Meeting of the Portuguese Carbohydrate Group (GLUPOR11)*. Viseu (Portugal). September 06-10 of 2015.

- **Oral communication**: *Patrones de reactividad inusuales en aminoácidos no naturales explicados por mecánica cuántica*. C. D. Navo, A. Avenoza, J. M. Peregrina, G. Jiménez-Osés. *VIII Jornada de Química CISQ*. Logroño (Spain). June 16 of 2017.

- **Poster**: *Síntesis estereoselectiva de miméticos restringidos del antígeno Tn.* C. D. Navo, C. Aydillo, F. Corzana, J. H. Busto, M. M. Zurbano, A. Avenoza, J. M. Peregrina. *XXXIV Biennial Meeting of the RSEQ*. Santander (Spain). September 15-18 of 2013.

- **Poster**: *Stereoselective synthesis of bicyclic analogs of glycosidase inhibitors.* C. D. Navo, C. Aydillo, F. Corzana, J. H. Busto, M. M. Zurbano, A. Avenoza, C. Ortíz-Mellet, J. M. García-Fernández, J. M. Peregrina. *II Meeting of the RSEQ Chemical Biological Group*. Bilbao (Spain). February 04-06 of 2014.
- **Poster**: *A double diastereoselective Michael-type addition as an entry to Tn antigen mimics and analogs of Thiamet-G.* C. D. Navo, C. Aydillo, F. Corzana, J. H. Busto, M. M. Zurbano, A. Avenoza, C. Ortíz-Mellet, J. M. García-Fernández, J. M. Peregrina. *XI Carbohydrate Symposium*. Logroño (Spain). May 28-30 of 2014.

- **Poster**: *Synthesis of a C-glycoside analog of Tn antigen.* C. D. Navo, C. Aydillo, F. Corzana, J. H. Busto, M. M. Zurbano, A. Avenoza, J. M. Peregrina. *XI Young Researcher Symposium*. Bilbao (Spain). November 04-07 of 2014.

- **Poster**: *Bicyclic C-glycosidase inhibitors: A new pharmacological chaperone for Gaucher's disease.* C. D. Navo, F. Corzana, K. Higaki, J. H. Busto, M. M. Zurbano, A. Avenoza, C. Ortíz-Mellet, J. M. García-Fernández, J. M. Peregrina. *XXXV Biennial Meeting of the RSEQ*. A Coruña (Spain). July 19-23 of 2015.

- **Poster**: *Tuning the reactivity of cyclic quaternary sulfamidates: a computational approach.* C. D. Navo, N. Mazo, J. H. Busto, A. Avenoza, J. M. Peregrina, G. Jiménez-Osés. *XIII Young Researcher Symposium*. Logroño (Spain). November 08-11 of 2016.

- **Poster**: *Sequence control in regioselective lantipeptide biosynthesis.* C. D. Navo, G. Jiménez-Osés, W. A. van der Donk. *16th Iberian Peptide Meeting (16EPI) / 4th Chemical Biology Group Meeting (4GEQB)*. Barcelona (Spain). February 05-07 of 2018.

Chapter 7.
Experimental section

7.1. Reagents and general procedures

Commercially available reagents were used without further purification. All the solvents were purified using standard procedures. Thin-layer chromatography (TLC) was performed on silicagel plates (Polychrom SI F_{254}), using UV-light, phosphomolybdic acid, potassium permanganate or ninhydrin as stains. Column chromatography was performed using silica gel (0.04-0.06 mm, 230-240 mesh). Melting points were determined on a Buchi B-545. Mass spectrometry analyses were performed on a HP 5989B, using electron impact ionization (EI). Electrospray-mass spectrometry (ESI-MS) were performed on the same equipment with HP 59987A interface and were registered in positive ion mode. A Bruker Microtof-Q spectrometer was also used. Sodium formate was used as external reference for high-resolution mass spectroscopy (HRMS). Optical rotation angles were measured on a Perkin-Elmer 341 polarimeter, using a sodium lamp (λ = 589 nm) at 25 ºC in 1.0 dm long cells (0.35 or 1.0 mL).

7.2. NMR experiments

^{1}H (^{13}C) NMR experiments were performed at 300 (75.5), 400 (100.6) and 500 (125.7) MHz. ^{19}F NMR experiments were performed at 376 MHz. 2-D COSY and HSQC experiments were carried out to assist on signal assignment. NOESY experiments were recorded at 298 K and pH = 6.0-6.5 in H_2O/D_2O (9:1) using phase-sensitive ge-2D NOESY with WATERGATE for H_2O/D_2O (9:1). NOEs intensities were normalized with respect to the diagonal peak at zero mixing time. Distances with structural information were semi-quantitatively determined by integrating the volume of the corresponding cross-peaks. Chemical shifts are given in ppm (δ) and

coupling constants (*J*) in hertz (Hz). Chloroform, with TMS as internal reference, methanol and water were used as deuterated solvents. The results of these experiments were processed with MestReNova software.

7.3. Unrestrained molecular dynamics (MD) simulations

Molecular dynamics simulations were carried out at the Finis-Terrae cluster of the *Centro de Supercomputación de Galicia* (CESGA) and at an in-house GPU cluster. The starting geometries for the complexes were generated from the available data deposited in the Protein Data Bank (PDB codes: 1SBF, 4D69 – SBA lectin; 5LVX – human β-glucocerebrosidase; 1JYN – β-galactosidase) and modified accordingly. Each model complex was immersed in a 10 Å-sided cube with pre-equilibrated TIP3P water molecules. The system was equilibrated as follows. First, only the water molecules were minimized. The water box, together with Na^+, was the minimized, and this was followed by a short MD simulation at 300 K. At this point, the systems was minimized in the four following steps with positional restraints imposed on the solute, decreasing the force constant step by step from 20 to 5 kcal mol^{-1}. Finally, an unrestrained minimization was performed. The production dynamics simulations were accomplished at a constant temperature of 300 K (by applying the Berendsen coupling algorithm for the temperature scaling) and constant pressure (1 atm). The particle-mesh Ewald method and periodic boundary conditions were also used. The SHAKE algorithm for hydrogen atoms, which allows the use of a 2 fs time stem, was also employed. Finally, a 9 Å cutoff was applied for the Lennard-Jones interactions. MD simulations were performed with Sander module of AMBER 11, AMBER 12 or AMBER 16 (parm99 force field),[1] which was

implemented with GAFF parameters[2] to accurately simulate the corresponding mimics.

7.4. MD simulations with time-averaged restraints (MD-tar)

MD-tar simulations were performed with the pmemd.cuda module of AMBER 12 and AMBER 16 (parm99 force field), which was implemented with GAFF parameters. Distances derived from the NOE interactions were included as time-averaged distance restraints. A $\langle r^{-6} \rangle^{1/6}$ average was used for the distances. Final trajectories were run using an exponential decay constant of 8000 ps with a dielectric constant $\varepsilon = 80$ or in explicit TIP3P water molecules.

7.5. Competition-tailored enzyme-linked lectin assay (ELLA)

An ELISA plate (Pierce Amine-binding, Maleic anhydride 96 well-plate) was coated with 100 μL/well of a solution of 70 nmol of glycopeptide APDT*R (* = α-*O*-GalNAc) in carbonate/bicarbonate buffer (0.2 M, pH 9.4) and incubated overnight at 25 ºC. The unbound sites were the blocked by adding 200 μL/well of blocking buffer (Thermo Scientific SuperBlock Blocking Buffer, product no. 37515). After 1 h at 25 ºC, the blocking buffer was removed, and the plate wells were washed (3 x 200 μL/well) with PBST [phosphate-buffered saline (0.1 M sodium phosphate, 0.15 M sodium chloride, pH 7.2) containing 0.05% Tween-20 detergent, product no-28320]. As the next step, the wells were incubated with biotin-conjugated soybean lectin or V. villosa-B-4 agglutinin from EY laboratories (100 μL/well, diluted 1/150 in PBST buffer) and increasing amounts of the different Tn mimics for 2 h. The wells were then washed with PBST (3 x 200

μL/well, 2 min/well) and treated with horseradish peroxidase (HRP)-conjugated streptavidin from Rockland (100 μL, diluted 1/4000 in PBST buffer) for 1 h at 25 ºC. The wells were again washed first with PBST (3 x 200 μl/well, 2 min/well) and then with 350 μL of water. 3,3,5,5-tetramethylbenzidine (TMB) was added (90 μL/well), and after incubation for 10 min, the reaction was terminated by the addition of 50 μL/well of stop solution (1 M H_2SO_4). Absorbance detection of the wells was immediately performed at 450 nm using an ELISA plate reader (Bio-rad, iMark plate reader). The average absorbance intensities of three replica were plotted against the Tn mimic concentration.

7.6. Enzyme-linked lectin assay (ELLA)

An ELISA plate (Pierce Amine-binding, Maleic anhydride 96 well-plate) was coated with 100 μL/well of a solution of the corresponding glycopeptide varying from 0 to 350 nmol/well in carbonate/bicarbonate buffer (0.2 M, pH 9.4) and incubated overnight at 25 ºC. As the next step, the wells were incubated with biotin-conjugated SBA lectin (100 μL/well, diluted 1/150 in PBST buffer) for 2 h. The wells were then washed with PBST (3 x 200 μL/well, 2 min/well) and treated with horseradish peroxidase (HRP)-conjugated streptavidin from Rockland (100 μL, diluted 1/3000 in PBST buffer) for 1 h at 25 ºC. The wells were again washed first with PBST (3 x 200 μl/well, 2 min/well) and then with 350 μL of water. TMB was added (90 μL/well), and after incubation for 10 min, the reaction was terminated by the addition of 50 μL/well of stop solution (1 M H_2SO_4). Absorbance detection of the wells was immediately performed at 450 nm using an ELI-

SA plate reader. The average absorbance intensities of three replica were plotted against the Tn mimic concentration.

7.7. Inhibition studies with commercial enzymes

Inhibition constant (K_i) values were determined by spectrophotometrically measuring the residual hydrolytic activities of the glycosidases against the respective *p*-nitrophenyl α- or β-D-glycopyranoside, or α- or β-D-galactopyranoside (for β-galactosidases), in the presence of the inhibitors. Each assay was performed in PBS buffer at the optimal pH of each enzyme. The reactions were initiated by addition of enzyme to a solution of the substrate in the absence or presence of various concentrations of inhibitor. The mixture was incubated for 10-30 min at 37 ºC, and the reaction was quenched by addition of 1 M Na_2CO_3. Reaction times were appropriate to obtain 10-20% conversion of the substrate in order to achieve linear rates. The absorbance of the resulting mixture was determined at 405 nm. Approximate values of K_i were determined using a fixed concentration of substrate (around the K_m value for the different glycosidases) and various concentrations of inhibitor. Full K_i determinations and enzyme inhibition mode were determined from the slope of Lineweaver-Burk plots and double reciprocal analysis.

7.8. Lysosomal enzyme activity assay

Lysosomal enzyme activities in cell lysates were determined as described previously.[3–5] Briefly, cells were scraped in ice-cold 0.1% Triton X-100 in water. After centrifugation (6000 rpm for 15 min at 4 ºC) to remove insoluble materials, protein concentrations were determined using Protein

Assay Rapid Kit (Wako, Tokyo, Japan). The lysates were incubated at 37 ºC with the corresponding 4-methylumbelliferyl β-D-glycopyranoside solution in 0.1 M citrate buffer (pH 4.5). The liberated 4-methylumbelliferone was measured with a fluorescence plate reader (excitation 340 nm; emission 460 nm; Infinite F500, TECAN Japan, Kawasaki, Japan). For enzyme inhibition assay, cell lysates from normal skin fibroblasts were mixed with the 4-methylumbelliferyl β-D-glycopyranoside substrates in the absence or presence of increasing concentrations of the tested derivatives.

7.9. Measurement of purified human GCase inhibition activities *in vitro*

Purified human GCase, obtained from Genzyme (Genzyme Japan, Tokyo, Japan) was mixed with the indicated concentrations of each chaperone. The incubation and the measurement of 4-methylumbelliferyl β-D-glycopyranoside substrates in the mixture was performed at pH 7 as described. In a parallel series of experiments, the inhibition activities were determined at pH 5 (citrate buffer).

7.10. Cell culture and GCase activity enhancement assay

Human skin fibroblasts from a healthy and three Gaucher disease patients (with N370S, F213I and L444P mutations) were maintained in our laboratory with DMEM (Dulbecco's Modified Eagle Medium) supplemented with 10% FBS (Fetal Bovine Serum) as the culture medium. For enzyme activity enhancement assay, cells were cultured in the presence of different concentrations of the candidates or DMSO alone (as a control) for 5 days and harvested by scraping.[3–5] Cytotoxicity of the compounds was monitored

by measuring the lactate dehydrogenase activities in the cultured supernatants (LDH assay kit, Wako, Tokyo, Japan).

7.11. Bio-layer interferometry

Binding assays were performed on an Octet Red Instrument (fortéBIO). Ligand immobilization, binding reactions, regeneration and washes were conducted in wells of black polypropylene 96-well microplates. Pseudoglycopeptides (10 mg/mL) were immobilized on amine-reactive biosensors (AR2G biosensors) in 10 mM sodium acetate pH 5.5 buffer, using EDCI (1-ethyl-3-(3-dimethylaminopropyl)-carbodiimide) and HOSu (*N*-hydroxysuccinimide) for 10 min at 1000 rpm at 25 ºC. All biosensors were subsequently modified by a solution of ethanolamine hydrochloride (1 M, pH 8.5), followed by regeneration and wash. Binding analysis were carried out at 25 ºC, 1000 rpm in 10 mM sodium phosphate buffer (pH 7.4) containing 150 mM NaCl, with a 120 s of association followed by a 180 s of dissociation. The surface was thoroughly washed with the running bugger without regeneration solution. Data were analyzed using Data Analysis (fortéBIO), with Savitzky-Golay filtering. Binding was fitted to a 2:1 heterogeneous ligand model. Steady state analyses were performed to obtain the binding kinetics constants (K_D).

7.12. Quantum Mechanical (QM) calculations

QM calculations were performed at Memento cluster (BiFi, University of Zaragoza) and Beronia cluster (University of La Rioja). Full geometry optimizations were carried out with the meta-hybrid M06-2X[6] functional and def2-TZVPP basis set[7] using the Gaussian 09 package.[8] Thermal

and entropic corrections to energy were calculated from vibrational frequencies. The nature of the stationary points was determined according to the appropriate number of negative eigenvalues of the Hessian matrix from the frequency calculations. Scaled frequencies were not considered.

Mass-weighted intrinsic reaction coordinate (IRC) calculations were carried out using the Gonzalez and Schlegel scheme[9,10] in order to ensure that the TSs indeed connect the appropriate reactants and products.

Bulk solvent effects were considered implicitly during optimization through the IEF-PCM polarizable continuum model[11] as implemented in Gaussian 09 and using the internally stored parameters for water. Electronic energies, entropies, enthalpies, Gibbs free energies and lowest frequencies of the different conformations of all structures are available in the *Supplementary Information* (SI.2) section.

Hyperconjugative interactions were estimated by calculating the second order perturbation energies between occupied (donor) and empty (acceptor) Natural Bond Orbitals, as implemented in NBO 6.[12]

7.13. Solid-phase peptide synthesis (SPPS)

Rink Amide MBHA resin (178 mg, 0.1 mmol of NH_2) was put into a vessel reactor. Convenient protected amino acids were put into cartridges (1 mmol). Automatic synthesis started with a piperidine washing during 7 min. Then, the starting cartridge is expelled and the first amino acid was dissolved in DMF (2 g) containing DIPEA (3 mL of 2 M solution in NMP), HBTU (0.9 mmol of 0.45 M) and added to the reactor for 10 min. Consecu-

tive washes for Fmoc deprotection with piperidine and DMF were also made during 30 min. The process followed expelling the cartridge and starting the process again with the next cartridge. These steps were repeated as many times as amino acids were needed to be coupled. When a glycosylated building block was coupled, the synthesis was carried out manually, obtaining better yields and reducing the equivalents to 2. HBTU (1.1 equiv.), DIPEA (0.5 mL of 2M solution in NMP) and DMF (2 mL) were added to the glycosylated amino acid. The reaction was stirred until the coupling was completed as deduced by Kaiser test.[13] The resin was the placed again in the synthesizer to obtain the complete sequence of the desired glycopeptide. As a next step, the resin was taken out from the synthesizer and acetate groups of the carbohydrate were deprotected with 10 mL of hydrazine/MeOH (7:3) solution 3 times of 45 min each one. Several washes with DMF and DCM were needed. After filtration, TFA (1.90 mL), TIS (50 μL) and H_2O (50 μL) were added for the cleavage reaction and removal of the side chain protecting groups. The mixture was stirred for 2 h. At this point, Et_2O (10 mL) was added producing a precipitate that was filtered and redissolved in water. The final glycopeptide was purified by RP-HPLC.

Final vaccine (glyco)peptide candidates **51-53** were synthesized by a stepwise MW-SPPS on a Liberty Blue synthesizer using the Fmoc strategy on Rink Amide MBHA resin (0.1 mmol). The natural Fmoc-protected amino acids were automatically coupled using DIC/Oxyma Pure as coupling agents and a 20% solution of piperidine in DMF for Fmoc deprotection Glycosylated amino acid building blocks (2 equiv.) coupling, acetate groups deprotection, cleavage and purification were performed as previously addressed.

7.14. Crystallization, structure determination and refinement

Expression and purification of scFv-SM3 was performed as previously described.[14] Crystals were grown by sitting drop diffusion at 18 ºC. The drops were prepared by mixing 0.5 μL of protein solution containing 15 mg/mL scFv-SM3 and 10 mM of the peptide with 0.5 μL mother liquor. Crystals of scFv-SM3 with the glycopeptide were grown in 20% PEG 3350, 0.2 M disodium hydrogen phosphate. The crystals were cryoprotected in mother liquor solutions containing 20% ethylenglycol and frozen in a nitrogen gas stream cooled to 100 K.

The data was processed and scaled using the XDS package[15] and CCP4 software,[16,17] relevant statistics are given in Annex II. The crystal structures were solved by molecular replacement with Phaser[18] and using the PDB entry 1SM3 as the template. Initial phases were further improved by cycles of manual model building in Coot63 and refinement with REFMAC5.[19] The final models were validated with PROCHECK.[20]

7.15. Synthesis

Methyl (3*S*,7*R*,7a*S*)-7-methoxy-7,7a-dimethyl-5-oxotetrahydro-5*H*-oxazolo[4,3-*b*]oxazole-3-carboxylate (1a).

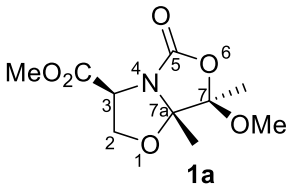

1a

A round-bottom flask was charged with (*S*)-*N*-Boc-serine methyl ester (11.2 g, 45.8 mmol), TMB (16.3 g, 91.2 mmol), toluene (300 mL), and TsOH·H_2O (860 mg, 4.6 mmol). The solution was stirred under reflux for 3 h. The reaction mixture was cooled down to room temperature, diluted with diethyl ether (100 mL), and quenched with an

aqueous saturated $NaHCO_3$ solution (100 mL). The aqueous phase was extracted with diethyl ether (2 × 80 mL) and the organic layers were combined, washed with brine, and dried over anhydrous Na_2SO_4. The solvent was evaporated, and the crude product was purified by column chromatography (hexane/EtOAc, 9:1) to give methyl ester bicyclic compound **1a** as a yellow oil (9.4 g, 31.9 mmol, 75%). The physical properties coincide with those described in the bibliography.[21]

Benzyl (3*S*,7*R*,7a*S*)-7-methoxy-7,7a-dimethyl-5-oxotetrahydro-5*H*-oxazolo[4,3-*b*]oxazole-3-carboxylate (1b).

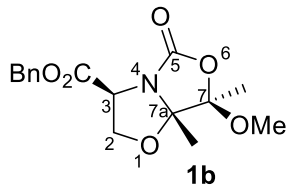

1b

A round-bottom flask was charged with (*S*)-*N*-Boc-serine benzyl ester (2.10 g, 7.12 mmol), TMB (2.54 g, 14.24 mmol), toluene (50 mL), and $TsOH \cdot H_2O$ (203 mg, 1.07 mmol). The solution was stirred under reflux for 16 h. The reaction mixture was cooled down to room temperature, diluted with diethyl ether (50 mL), and quenched with aqueous saturated $NaHCO_3$ solution (50 mL). The aqueous phase was extracted with diethyl ether (2 × 25 mL) and the organic layers were combined, washed with brine, and dried over anhydrous Na_2SO_4. The solvent was evaporated, and the crude product was purified by column chromatography (hexane/EtOAc, 8:2) to give benzyl ester bicyclic compound **1b** as a yellow oil (1.53 g, 4.77 mmol, 67%). $[\alpha]_D^{25} = -85.2$ (c 1.02, $CHCl_3$). HRMS ESI+ (m/z): 344.1119 [$M+Na^+$]; calcd for $C_{16}H_{19}NO_6Na^+$, 344.1105. ^1H NMR (400 MHz, $CDCl_3$) δ (ppm) 1.29 (s, 3H, CH_3), 1.55 (s, 3H, CH_3), 3.44 (s, 3H, OCH_3), 4.10 (dd, J = 8.9, 5.8 Hz, 1H, H^2), 4.27 (t, J = 9.0 Hz, 1H, H^2), 4.79 (dd, J = 8.9, 5.9 Hz, 1H, H^3), 5.19-5.25 (m, 2H, CH_2Ph), 7.30-7.40 (m, 5H, Ph). ^{13}C NMR (100 MHz, $CDCl_3$) δ (ppm) 15.5

(CH_3), 16.3 (CH_3), 51.0 (OCH_3), 60.1 (C^3), 66.7 (C^2), 67.7 (CO_2CH_2Bn), 101.5 (C^{7a}), 107.2 (C^7), 128.5 (Ph), 128.7 (Ph), 128.7 (Ph), 135.0 (Ph), 160.6 (C^5), 169.9 (CO_2Bn).

***tert*-Butyl (3*S*,7*R*,7a*S*)-7-methoxy-7,7a-dimethyl-5-oxotetrahydro-5*H*-oxazolo[4,3-*b*]oxazole-3-carboxylate (1c).**

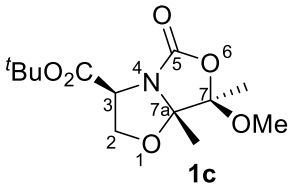

1c

Methyl ester bicyclic compound **1a** (4.0 g, 16.31 mmol) was dissolved in THF (25 mL), and the solution was stirred at 0 ºC. $LiOH \cdot H_2O$ (3.42 g, 91.57 mmol) was then added as a solution in water (25 mL), and the mixture was stirred for 5 min. Next, the reaction was quenched with an aqueous 4 M HCl solution (20 mL) to reach pH 1. EtOAc (25 mL) was added, and the aqueous layer was extracted with more EtOAc (4 x 25 mL). The combined organic layers were dried over anhydrous Na_2SO_4, and the solvent was evaporated to give the corresponding acid as a white crystalline solid (3.50 g, 15.17 mmol, 93%) that could be used without further purification. This compound was dissolved in ^{t}BuOH (25 mL), and Boc_2O (6.62 g, 30.34 mmol) and DMAP (556 mg, 4.55 mmol) were added. The solution was stirred at room temperature until completion of the reaction (3 h) as monitored by TLC. The solvent was removed, and the crude material was purified by column chromatography (hexane/EtOAc, 1:1) to give the bicyclic *tert*-butyl compound **1c** (3.97 g, 13.80 mmol, 91%) as a white solid. Mp: 35-37 ºC. $[\alpha]_D^{25}$ = −112.1 (c 1.07, $CHCl_3$). HRMS ESI+ (m/z): 310.1276 [M+Na^+]; calcd for $C_{13}H_{21}NO_6Na^+$, 310.1261. ^{1}H NMR (400 MHz, $CDCl_3$) δ (ppm) 1.34 (s, 3H, CH_3), 1.48 (s, 9H, $C(CH_3)_3$), 1.55 (s, 3H, CH_3), 3.45 (s, 3H, OCH_3), 4.05 (dd, J = 8.8, 5.8 Hz, 1H, H^2), 4.23 (t, J = 9.0 Hz, 1H, H^2), 4.64 (dd, J = 9.0, 5.8 Hz, 1H, H^3). ^{13}C NMR (100 MHz,

$CDCl_3$) δ (ppm) 16.6 (CH_3), 16.4 (CH_3), 27.9 ($C(CH_3)_3$), 51.0 (OCH_3), 60.7 (C^3), 66.9 (C^2), 82.8 ($C(CH_3)_3$), 101.5 (C^{7a}), 107.0 (C^7), 160.7 (C^5), 169.0 ($CO_2{}^t$Bu).

Methyl (3*R*,7*R*,7a*S*)-3-((2′*S*,3′*S*,4′*R*,5′*R*,6′*R*)-4′,5′-bis(benzyloxy)-6′-(benzyloxymethyl)-3′-nitrotetrahydro-2*H*-pyran-2′-yl)-7-methoxy-7,7a-dimethyl-5-oxotetrahydro-2*H*-oxazolo[3,2-*c*]oxazole-3-carboxylate (3a).

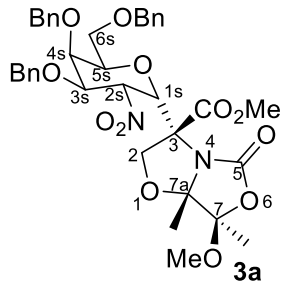

3a

Tri-*O*-benzyl-D-galactal (**2-Gal**)[22] (848 mg, 1.84 mmol) was added to a dry THF solution (48 mL) of compound **1a** (450 mg, 1.84 mmol) under an Ar atmosphere at -78 ºC. A 1 M THF solution of LHMDS (4.8 mL, 4.8 mmol) was added dropwise under vigorous stirring. After 1 h of reaction, a saturated aqueous NH_4Cl solution (50 mL) was added, and the mixture was warmed up to room temperature. The crude mixture was diluted with Et_2O, and the aqueous phase was extracted with more Et_2O. The organic phases were collected, washed with brine, and dried with anhydrous Na_2SO_4. Concentration and purification by silica gel column chromatography (hexane/EtOAc, 9:1) afforded compound **3a** (686 mg, 0.97 mmol, 53%) as a white solid. Mp: 106-108 ºC. $[\alpha]_D^{25}$ = −5.1 (c 1.03, $CHCl_3$). HRMS ESI+ (m/z): 729.2630 [M+Na^+]; calcd for $C_{37}H_{42}N_2O_{12}Na^+$, 729.2630. ^{1}H NMR (400 MHz, $CDCl_3$) δ (ppm) 1.37 (s, 3H, CH_3), 1.43 (s, 3H, CH_3), 3.35 (s, 3H, OCH_3), 3.70-3.74 (m, 1H, H^{6s}), 3.78-3.82 (m, 1H, H^{6s}), 3.88 (s, 3H, CO_2Me), 4.18-4.23 (m, 1H, H^{4s}), 4.23-4.31 (m, 2H, H^{5s}, H^2), 4.39-4.45 (m, 2H, PhC*H*^{a}H^{b}O, H^{3s}), 4.51 (d, *J* = 11.6 Hz, 1H, PhCH^a*H*^{b}O), 4.55-4.62 (m, 3H, H^2, $PhCH_2O$), 4.66 (d, *J* = 12.0 Hz, 1H, PhC*H*^{c}H^{d}O), 4.79 (d, *J* = 11.5 Hz, 1H, PhCH^c*H*^{d}O), 5.08 (t, *J* = 6.0 Hz, 1H, H^{2s}), 6.13 (d, *J* = 4.8 Hz, 1H, H^{1s}), 7.19-7.40 (m, 15H, Ph). ^{13}C NMR (100 MHz, $CDCl_3$) δ (ppm) 17.4

(CH_3), 19.2 (CH_3), 51.9 (OCH_3), 53.7 (CO_2CH_3), 66.0 (C^{6s}), 67.4 (C^3), 71.3 (C^2), 71.7 (C^{4s}), 71.9 (C^{1s}), 72.8 (Ph*C*H^{a}H^{b}O), 73.3 (Ph*C*H^{c}H^{d}O), 73.4 (C^{3s}), 73.9 (Ph*C*H$_2$O), 77.3 (C^{2s}), 77.4 (C^{5s}), 101.9 (C^{7a}), 109.6 (C^7), 127.7, 128.1, 128.3, 128.3, 128.4, 128.5, 128.7, 136.9, 137.9, 138.5 (Arom.), 152.5 (C^5), 168.5 (*C*O$_2$Me).

Benzyl (3*R*,7*R*,7a*S*)-3-((2′*S*,3′*S*,4′*R*,5′*R*,6′*R*)-4′,5′-bis(benzyloxy)-6′-(benzyloxymethyl)-3′-nitrotetrahydro-2*H*-pyran-2′-yl)-7-methoxy-7,7a-dimethyl-5-oxotetrahydro-2*H*-oxazolo[3,2-*c*]oxazole-3-carboxylate (3b).

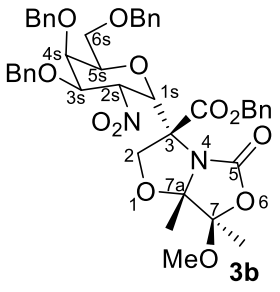

Tri-*O*-benzyl-D-galactal (**2-Gal**)[22] (600 mg, 1.3 mmol) was added to a dry THF solution (35 mL) of compound **1b** (418 mg, 1.3 mmol) under an Ar atmosphere at -78 ºC. A 1 M THF solution of LHMDS (3.5 mL, 3.5 mmol) was added dropwise under vigorous stirring. After 1 h of reaction, a saturated aqueous NH_4Cl solution (40 mL) was added, and the mixture was warmed up to room temperature. The crude mixture was diluted with Et_2O, and the aqueous phase was extracted with more Et_2O. The organic phases were collected, washed with brine, and dried with anhydrous Na_2SO_4. Concentration and purification by silica gel column chromatography (hexane/EtOAc, 9:1) afforded compound **3b** (410 mg, 0.52 mmol, 40%) as a colorless oil. $[\alpha]_D^{25} = -18.6$ (c 1.00, $CHCl_3$). HRMS ESI+ (m/z): 783.3138 [M+H$^+$]; calcd for $C_{43}H_{47}N_2O_{12}^+$, 783.3124. ^{1}H NMR (400 MHz, $CDCl_3$) δ (ppm) 1.36 (s, 3H, CH_3), 1.47 (s, 3H, CH_3), 3.34 (s, 3H, OCH_3), 3.73-3.85 (m, 2H, H^{6s}), 4.21-4.23 (m, 1H, H^{4s}), 4.25-4.31 (m, 2H, H^{5s}, H^2), 4.35-4.41 (m, 1H, H^{3s}), 4.42-4.45 (m, 1H, PhC*H*^{a}H^{b}O), 4.46 (s, 2H, PhCH$_2$O), 4.59-4.62 (m, 3H, H^2, PhCH^a*H*^{b}O, PhC*H*^{c}H^{d}O), 4.69-4.74 (m, 1H, PhCH^c*H*^{d}O), 5.01 (t, *J* = 5.2 Hz, 1H, H^{2s}), 5.28 (d, *J* = 12.3 Hz, 1H, CO$_2$C*H*^{e}H^{f}Ph), 5.38

(d, J = 12.3 Hz, 1H, $CO_2CH^eH^fPh$), 6.19 (d, J = 3.0 Hz, 1H, H^{1s}), 7.20-7.39 (m, 20H, Ph). ^{13}C NMR (100 MHz, $CDCl_3$) δ (ppm) 17.4 (CH_3), 19.2 (CH_3), 52.0 (OCH_3), 66.8 (C^{6s}), 67.5 ($CO_2CH^eH^fPh$), 68.3 (C^3), 71.3 (C^2), 71.9 (C^{1s}), 72.0 (C^{4s}), 72.6 ($PhCH_2O$), 73.3 ($PhCH^aH^bO$), 73.4 (C^{3s}), 73.7 ($PhCH^cH^dO$), 77.2 (C^{2s}), 77.4 (C^{5s}), 101.8 (C^{7a}), 109.7 (C^7), 127.5, 127.9, 128.3, 128.3, 128.6, 128.7, 128.8, 134.7, 137.0, 137.9, 138.6 (Arom.), 152.3 (C^5), 167.7 (CO_2Bn).

***tert*-Butyl (3*R*,7*R*,7a*S*)-3-((2′*S*,3′*S*,4′*R*,5′*R*,6′*R*)-4′,5′-bis(benzyloxy)-6′-(benzyloxymethyl)-3′-nitrotetrahydro-2*H*-pyran-2′-yl)-7-methoxy-7,7a-dimethyl-5-oxotetrahydro-2*H*-oxazolo[3,2-*c*]oxazole-3-carboxylate (3a).**

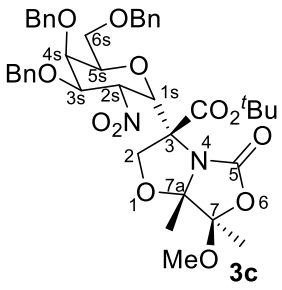

3c

Tri-*O*-benzyl-D-galactal (**2-Gal**)[22] (77 mg, 0.27 mmol) was added to a dry THF solution (7 mL) of compound **1c** (90 mg, 0.20 mmol) under an Ar atmosphere at -78 ºC. A 1 M THF solution of LHMDS (0.7 mL, 0.7 mmol) was added dropwise under vigorous stirring. After 1 h of reaction, a saturated aqueous NH_4Cl solution (10 mL) was added, and the mixture was warmed up to room temperature. The crude mixture was diluted with Et_2O, and the aqueous phase was extracted with more Et_2O. The organic phases were collected, washed with brine, and dried with anhydrous Na_2SO_4. Concentration and purification by silica gel column chromatography (hexane/EtOAc, 9:1) afforded compound **3c** (66 mg, 0.088 mmol, 44%) as a colorless oil. $[\alpha]_D^{25}$ = −13.7 (c 1.00, $CHCl_3$). HRMS ESI+ (m/z): 749.3264 [M+H$^+$]; calcd for $C_{40}H_{49}N_2O_{12}^+$, 749.3280. ^1H NMR (400 MHz, $CDCl_3$) δ (ppm) 1.36 (s, 3H, CH_3), 1.43 (s, 3H, CH_3), 1.59 (s, 9H, ^{t}Bu), 3.35 (s, 3H, OCH_3), 3.75-3.79 (m, 2H, H^{6s}), 4.21-4.28 (m, 3H, H^{4s}, H^{5s}, H^2), 4.41-4.44 (m, 2H, $PhCH^aH^bO$, H^{3s}), 4.51-4.66 (m, 5H, $PhCH_2O$, H^2, $PhCH^aH^bO$,

PhC*H*^{c}H^{d}O), 4.77 (d, *J* = 6.0 Hz, 1H, PhCH^{c}*H*^{d}O), 5.10 (t, *J* = 3.0 Hz, 1H, H^{2s}), 6.08 (d, *J* = 3.0 Hz, 1H, H^{1s}), 7.26-7.34 (m, 15H, Ph). ^{13}C NMR (100 MHz, $CDCl_3$) δ (ppm) 17.2 (CH_3), 19.2 (CH_3), 27.6 (C(*C*H_3)$_3$), 51.8 (OCH_3), 66.8 (C^{6s}), 68.1 (C^{3}), 70.9 (C^{2}), 72.0 (C^{4s}), 72.3 (C^{1s}), 72.7 (Ph*C*H^{a}H^{b}O), 73.1 (Ph*C*H_2O), 73.3 (C^{3s}), 73.8 (Ph*C*H^{c}H^{d}O), 77.1 (C^{2s}), 77.4 (C^{5s}), 83.8 (*C*(CH_3)$_3$), 101.4 (C^{7a}), 109.5 (C^{7}), 127.4, 127.9, 128.2, 128.4, 128.6, 136.9, 137.9, 138.5 (Arom.), 152.0 (C^{5}), 166.4 (*C*O_2^{t}Bu).

Methyl (3*R*,7*R*,7a*S*)-3-((2′*S*,3′*S*,4′*R*,5′*S*,6′*R*)-4′,5′-bis(benzyloxy)-6′-(benzyloxymethyl)-3′-nitrotetrahydro-2*H*-pyran-2′-yl)-7-methoxy-7,7a-dimethyl-5-oxotetrahydro-2*H*-oxazolo[3,2-*c*]oxazole-3-carboxylate (4α). Methyl (3*R*,7*R*,7a*S*)-3-((2′*R*,3′*S*,4′*R*,5′*S*,6′*R*)-4′,5′-bis(benzyloxy)-6′-(benzyloxymethyl)-3′-nitrotetrahydro-2*H*-pyran-2′-yl)-7-methoxy-7,7a-dimethyl-5-oxotetrahydro-2*H*-oxazolo[3,2-*c*]oxazole-3-carboxylate (4β)

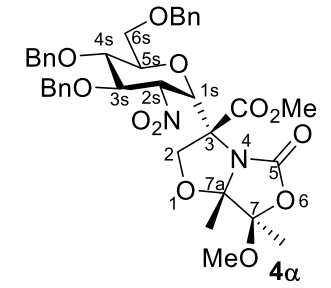

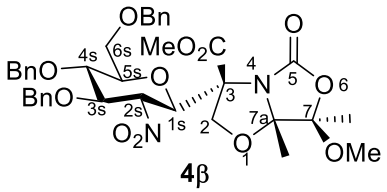

Tri-*O*-benzyl-D-glucal (**2-Glc**)[23] (240 mg, 0.52 mmol) and HMPA (180 μL, 1.04 mmol) were added to a dry THF solution (5 mL) of compound **1a** (64 mg, 0.26 mmol) under an Ar atmosphere at -78 ºC. A 1 M THF solution of LHMDS (390 μL, 0.39 mmol) was added dropwise under vigorous stirring. After 1 h of reaction, a saturated aqueous NH_4Cl solution (5 mL) was added, and the mixture was warmed up to room temperature. The crude mixture was diluted with Et_2O, and the aqueous phase was extracted with more Et_2O. The organic phases were collected, washed with brine, and dried with anhydrous Na_2SO_4. Concentration and purification by silica gel column chromatography (hexane/EtOAc, 9:1) afforded a 1:9 mixture of compounds **4α** and **4β** (64 mg, 0.091 mmol, 53%) as a colorless sticky oil. HRMS ESI+ (m/z): 707.2811 [$M+H^+$]; calcd for $C_{37}H_{43}N_2O_{12}^+$, 707.2811.

4α

^{1}H NMR (400 MHz, $CDCl_3$) δ (ppm) 1.40 (s, 3H, CH_3), 1.41 (s, 3H, CH_3), 3.37 (s, 3H, OCH_3), 3.70-3.84 (m, 2H, H^{6s}) 3.86 (s, 3H, CO_2Me), 3.93-3.97 (m, 1H, H^{4s}), 4.11-4.21 (m, 2H, H^{5s}, H^{3s}), 4.34-4.60 (m, 8H, 3x$PhCH_2O$,

H^2), 4.80-4.84 (m, 1H, H^{2s}), 5.83 (d, J = 4.3 Hz, 1H, H^{1s}), 7.14-7.36 (m, 15H, Ph). ^{13}C NMR (100 MHz, $CDCl_3$): could not be determined due to low intensities.

4β

^1H NMR (400 MHz, $CDCl_3$) δ (ppm) 1.34 (s, 3H, CH_3), 1.47 (s, 3H, CH_3), 3.41 (s, 3H, OCH_3), 3.70-3.76 (m, 4H, H^{6s}, CO_2Me), 3.82 (dd, J = 16.3, 6.5 Hz, 1H, H^{6s}), 3.89 (dd, J = 6.1, 3.2 Hz, 1H, H^{4s}), 4.11-4.21 (m, 2H, H^{5s}, H^{3s}), 4.34-4.60 (m, 8H, 3x$PhCH_2O$, H^2), 4.79 (dd, J = 9.2, 5.1 Hz, 1H, H^{2s}), 5.77 (d, J = 9.1 Hz, 1H, H^{1s}), 7.14-7.36 (m, 15H, Ph). ^{13}C NMR (100 MHz, $CDCl_3$) δ (ppm) 17.4 (CH_3), 18.7 (CH_3), 51.8 (OCH_3), 53.5 (CO_2CH_3), 65.2 (C^{1s}), 67.8 (C^{6s}), 69.5 (C^3), 72.2 (C^2), 72.4 (C^{4s}), 72.8 ($PhCH_2O$), 73.3 ($PhCH_2O$), 73.7 ($PhCH_2O$), 75.9 (C^{3s}), 76.2 (C^{5s}), 82.1 (C^{2s}), 102.8 (C^{7a}), 108.8 (C^7), 127.6, 128.1, 128.1, 128.1, 128.3, 128.3, 128.4, 128.7, 136.3, 137.6, 138.5 (Arom.), 153.2 (C^5), 170.5 (CO_2Me).

(3*R*,3a*S*,5*R*,6*R*,7*R*,7a*S*,7′*R*,7′a*S*)-6,7-Dibenzyloxy-5-(benzyloxymethyl)-7′-methoxy-7′,7′a-dimethylspiro[1,3a,5,6,7,7a-hexahydropyran[3,2-*b*]pyrrol-3,3′-2*H*-oxazolo[4,3-*b*]oxazol]- 2,5′-dione (5)

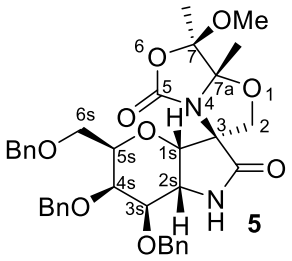

5

RANEY® Ni (2.00 g) was suspended in H_2O (12 mL), and hexachloroplatinic acid (50 mg) and sodium hydroxide 20% (400 μL) were added under stirring. The mixture was stirred at 50 °C for 2.5 h and sodium hydroxide 40% (6 mL) was added, keeping the stirring and the heating. After 1.5 h stirring, a white cloud on top of the flask appeared, which was removed by decantation; the resulting solution was then washed with warm water (3 × 15 mL) and ethanol (3 × 15 mL). The catalyst obtained was suspended in ethanol (10 mL) and prehy-

drogenated for 10 min. An ethanol/ethyl acetate solution (5:2, 7 mL) of Michael adduct **3a** (200 mg, 0.28 mmol) was added, and the mixture was stirred under molecular hydrogen at room temperature and atmospheric pressure for 5 h. The crude product was filtered, and the liquid phase was concentrated and purified by silica gel column chromatography (EtOAc/hexane, 7:3), to afford compound **5** (105 mg, 0.16 mmol, 57%) as a colorless oil. $[\alpha]_D^{25}$ = +4.2 (c 1.00, $CHCl_3$). HRMS ESI+ (m/z): 645.2812 [M+H$^+$]; calcd for $C_{36}H_{41}N_2O_9^+$, 645.2807. ^{1}H NMR (400 MHz, $CDCl_3$) δ (ppm) 1.59 (s, 3H, CH_3), 1.62 (s, 3H, CH_3), 3.49 (s, 3H, OCH_3), 3.57 (d, *J* = 5.7 Hz, 1H, H^{3s}) 3.72-3.76 (m, 2H, H^{6s}), 4.12-4.19 (m, 2H, H^{4s}, H^{5s}), 4.37 (d, *J* = 9.5 Hz, 1H, PhC*H*^{a}H^{b}O), 4.52-4.59 (m, 2H, H^2), 4.61-4.73 (m, 5H, H^{2s}, $PhCH_2O$, PhCH^a*H*^{b}O, PhC*H*^{c}H^{d}O), 4.92-4.97 (m, 2H, PhCH^c*H*^{d}O, H^{1s}), 7.29-7.40 (m, 15H, Ph). ^{13}C NMR (100 MHz, $CDCl_3$) δ (ppm) 16.9 (CH_3), 18.0 (CH_3), 51.6 (OCH_3), 57.8 (C^{2s}), 67.5 (C^{6s}), 68.7 (C^3), 69.1 (Ph*C*H_2O), 71.0 (C^{1s}), 71.9 (Ph*C*H^{a}H^{b}O), 72.3 (C^{5s}), 73.5 (C^2), 73.9 (Ph*C*H^{c}H^{d}O), 76.8 (C^{4s}), 80.6 (C^{3s}), 103.0 (C^{7a}), 108.1 (C^7), 127.7, 127.8, 127.8, 128.1, 128.4, 128.5, 128.7, 137.7, 138.1, 138.2 (Arom.), 154.8 (C^5), 173.6 (NH*C*O).

(3*R*,3a*S*,5*R*,6*R*,7*R*,7a*S*)-3-Acetamide-3-acetoxymethyl-6,7-dibenzyloxy-5-(benzyloxymethyl)-2-oxo-1,3a,5,6,7,7a-hexahydropyran[3,2-*b*]pyrrole (6).

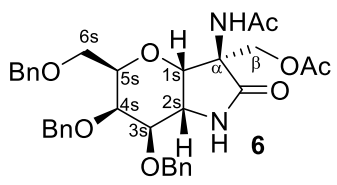

6

An aqueous 4 M HCl solution (2.5 mL) was added to a THF solution of compound **5** (150 mg, 0.23 mmol), and the mixture was stirred at 40 °C. After 12 h, the reaction mixture was concentrated and the resulting crude was dissolved in a mixture of pyridine and acetic anhydride (2:1, 6 mL). The mixture was stirred for 3 h, then concen-

trated, and the crude product was purified by silica gel column chromatography (DCM/MeOH, 15:1), affording compound **6** (122 mg, 0.20 mmol, 87%) as a colorless oil. $[\alpha]_D^{25}$ = +56.2 (c 1.00, $CHCl_3$). HRMS ESI+ (m/z): 603.2701 [M+H$^+$]; calcd for $C_{34}H_{39}N_2O_8^+$, 603.2701. ^{1}H NMR (400 MHz, $CDCl_3$) δ (ppm) 1.96 (s, 3H, OCO*C*H$_3$), 1.98 (s, 3H, NHCO*C*H$_3$), 3.55 (d, *J* = 7.6 Hz, 1H, H^{3s}), 3.61-3.65 (m, 2H, H^{6s}), 4.05-4.09 (m, 1H, H^{5s}), 4.13 (d, *J* = 4.4 Hz, 1H, H^{4s}), 4.27 (d, *J* = 11.6 Hz, 1H, PhC*H*^{a}H^{b}O), 4.31 (t, *J* = 7.6 Hz, 1H, H^{2s}), 4.46 (d, *J* = 11.7 Hz, 1H, PhC*H*^{c}H^{d}O), 4.51 (s, 2H, H$^{\beta}$), 4.52 (d, *J* = 11.6 Hz, 1H, PhCH^a*H*^{b}O), 4.58 (d, *J* = 11.7 Hz, 1H, PhCH^c*H*^{d}O), 4.66-4.72 (m, 2H, H^{1s}, PhC*H*^{e}H^{f}O), 4.88 (d, *J* = 11.6 Hz, 1H, PhCH^e*H*^{f}O), 6.18 (s, 1H, CONH), 6.42 (s, 1H, CONH), 7.25-7.40 (m, 15H, Ph). ^{13}C NMR (100 MHz, $CDCl_3$) δ (ppm) 20.9 (OCO*C*H$_3$), 23.2 (NHCO*C*H$_3$), 56.0 (C^{2s}), 63.2 (C^{5s}), 63.3 (C$^{\alpha}$), 67.8 (C^{6s}), 71.5 (C$^{\beta}$), 71.7 (Ph*C*H^{c}H^{d}O), 73.5 (Ph*C*H^{a}H^{b}O), 74.4 (Ph*C*H^{e}H^{f}O), 75.7 (C^{1s}), 76.5 (C^{4s}), 81.2 (C^{3s}), 127.8, 127.8, 127.9, 128.0, 128.3, 128.5, 128.6, 128.8, 137.6, 138.1, 138.3 (Arom.), 170.1 (O*C*OCH$_3$), 170.7 (NH*C*OCH$_3$), 172.4 (NH*C*O).

(3*R*,3a*S*,5*R*,6*R*,7*R*,7a*S*)-3-Acetamido-6,7-dibenzyloxy-5-(benzyloxymethyl)-3-(hydroxymethyl)-2-oxo-1,3a,5,6,7,7a-hexahydropyrane[3,2-*b*]pyrrole (7).

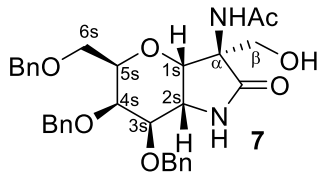

A MeOH solution of NaOMe (2 mL, 0.5 M) was added to a MeOH solution (4 mL) of compound **6** (122 mg, 0.20 mmol). The mixture was stirred for 1.5 h, and Dowex sulfonic acid resin was then added. The liquid phase was filtered and concentrated, and the residue was purified by silica column chromatography (DCM/MeOH, 15:1) to afford compound **7** (107 mg, 0.19 mmol, 95%) as a colorless oil. $[\alpha]_D^{25}$ = +89.8 (c

1.00, $CHCl_3$). HRMS ESI+ (m/z): 561.2595 [M+H^+]; calcd for $C_{32}H_{36}N_2O_7^+$, 561.2603. ^{1}H NMR (400 MHz, $CDCl_3$) δ (ppm) 2.03 (s, 3H, NHCO*C*H$_3$), 3.50-3.54 (m, 1H, H^{6s}), 3.62 (d, *J* = 8.0 Hz, H^{3s}), 3.72-3.81 (m, 2H, H^{6s}, PhC*H*^{a}H^{b}O), 4.03 (d, *J* = 12.0 Hz, 1H, PhCH^a*H*^{b}O), 4.13 (d, *J* = 4.5 Hz, 1H, H^{4s}), 4.15-4.24 (m, 1H, H^{5s}), 4.39 (t, *J* = 7.2 Hz, 1H, H^{2s}), 4.53 (d, *J* = 11.6 Hz, 1H, PhC*H*^{e}H^{d}O), 4.54 (s, 2H, H$^\beta$), 4.60 (d, *J* = 11.9 Hz, 1H, PhC*H*^{e}H^{f}O), 4.68 (d, *J* = 6.3 Hz, H^{1s}), 4.72 (d, *J* = 11.6 Hz, 1H, PhCH^c*H*^{d}O), 4.90 (d, *J* = 11.9 Hz, 1H, PhCH^e*H*^{f}O), 6.60 (s, 1H, CONH), 6.86 (s, 1H, CONH), 7.19-7.52 (m, 15H, Ph). ^{13}C NMR (100 MHz, $CDCl_3$) δ (ppm) 22.8 (NHCO*C*H$_3$), 56.4 (C^{2s}), 63.9 (Ph*C*H^{a}H^{b}O, C$^\alpha$), 67.4 (C^{6s}), 71.6 (C^{4s}), 71.7 (Ph*C*H^{c}H^{d}O), 73.5 (C$^\beta$), 74.3 (Ph*C*H^{e}H^{f}O), 76.6 (C^{1s}), 76.7 (C^{5s}), 81.3 (C^{3s}), 127.7, 127.9, 127.9, 128.0, 128.2, 128.5, 128.6, 128.8, 137.6, 137.8, 138.0 (Arom.), 170.6 (NH*C*OCH$_3$), 174.1 (NH*C*O).

(3*S*,3a*S*,5*R*,6*R*,7*R*,7a*S*)-3-Acetamido-6,7-dibenzyloxy-5-(benzyloxymethyl)-2-oxo-1,3a,5,6,7,7a-hexahydropyrane[3,2-*b*]pyrrole (8a).
(3*R*,3a*S*,5*R*,6*R*,7*R*,7a*S*)-3-Acetamido-6,7-dibenzyloxy-5-(benzyloxymethyl)-2-oxo-1,3a,5,6,7,7a-hexahydropyrane[3,2-*b*]pyrrole (8b).

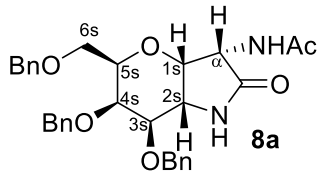

8a

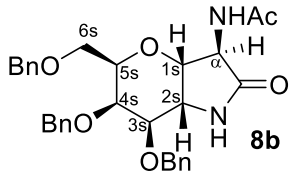

8b

A DCM solution of Dess−Martin periodinane (2 mL) was added to a DCM solution (2 mL) of compound **7** (100 mg, 0.18 mmol). The mixture was stirred at room temperature for 1 h. Saturated aqueous NaS_2O_3 (5 mL) and $NaHCO_3$ (5 mL) solutions were added, and the resulting mixture was diluted with DCM (10 mL). The phases were separated, and the aqueous one was washed with DCM (3 × 10 mL). The combined organic phases were washed with brine, dried with Na_2SO_4, and

concentrated. Meanwhile, $AgNO_3$ (365 mg, 2.1 mmol) was dissolved in the minimum volume of water, and an aqueous 10% NaOH solution was added dropwise. A dark-brown precipitate appeared, and NH_4OH was then added dropwise until it was totally dissolved. This solution was added to a DCM solution (5 mL) of the previously obtained crude product, and the mixture was stirred at 50 °C for 2 h. A black precipitate (Ag^0) was observed as it reacted. The pH was adjusted to 7 using an aqueous 2 M HNO_3 solution, and then aqueous 2 M HCl and saturated NH_4Cl solutions were added in order to precipitate AgCl, which was filtered off. The filtrate was concentrated and extracted with EtOAc and H_2O. The combined organic phases were dried (Na_2SO_4), concentrated, and purified by silica gel column chromatography ($CHCl_3$/MeOH, 95:5) to afford compounds **8a** (20 mg, 0.038 mmol, 21%) and **8b** (40 mg, 0.076 mmol, 42%) as yellow oils.

8a

$[\alpha]_D^{25}$ = +31.6 (c 1.00, $CHCl_3$). HRMS ESI+ (m/z): 531.2471 [M+H^+]; calcd for $C_{31}H_{35}N_2O_6^+$, 531.2490. ^{1}H NMR (400 MHz, $CDCl_3$) δ (ppm) 2.06 (s, 3H, NHCO*C*H_3), 3.55 (d, *J* = 5.0 Hz, 1H, H^{3s}), 3.70-3.79 (m, 2H, H^{6s}), 3.84-3.91 (m, 1H, H^{2s}), 4.16 (s, 1H, H^{4s}), 4.16-4.19 (m, 1H, H^{5s}), 4.52 (d, *J* = 12.0 Hz, 1H, PhC*H*^{a}H^{b}O), 4.56 (s, 2H, PhCH_2O), 4.62-4.69 (m, 2H, H^{1s}, PhC*H*^{c}H^{d}O), 4.77 (d, *J* = 12.0 Hz, 1H, PhCH^a*H*^{b}O), 4.81-4.90 (m, 2H, H^α, PhCH^c*H*^{d}O), 5.86 (s, 1H, CONH), 6.03 (d, *J* = 8.0 Hz, 1H, CONH), 7.26-7.47 (m, 15H, Ph). ^{13}C NMR (100 MHz, $CDCl_3$) δ (ppm) 22.8 (NHCOCH_3), 52.7 (C^α), 56.8 (C^{2s}), 67.3 (C^{6s}), 69.1 (C^{1s}), 72.0 (Ph*C*H^{a}H^{b}O), 72.8 (C^{4s}), 73.7 (Ph*C*H_2O), 74.4 (Ph*C*H^{c}H^{d}O), 76.5 (C^{5s}), 80.6 (C^{3s}), 127.8, 127.8, 127.9, 128.0, 128.0, 128.5, 128.6, 128.9, 137.5, 137.6, 138.1 (Arom.), 170.7 (NH*C*OCH$_3$), 173.6 (NH*C*O).

8b

$[\alpha]_D^{25}$ = +76.7 (c 1.00, $CHCl_3$). HRMS ESI+ (m/z): 531.2471 [M+H$^+$]; calcd for $C_{31}H_{35}N_2O_6^+$, 531.2490. ^{1}H NMR (400 MHz, $CDCl_3$) δ (ppm) 2.08 (s, 3H, NHCO*C*H$_3$), 3.56 (d, *J* = 8.2 Hz, 1H, H^{3s}), 3.65-3.69 (m, 2H, H^{6s}), 3.92 (t, *J* = 8.2 Hz, 1H, H^{2s}), 4.07 (t, *J* = 6.4 Hz, 1H, H^{5s}), 4.12 (s, 1H, H^{4s}), 4.20-4.53 (m, 3H, H^{1s}, PhC*H*^{a}H^{b}O, PhC*H*^{c}H^{d}O), 4.57 (d, *J* = 11.7, 1H, PhCH^c*H*^{d}O), 4.64 (d, *J* = 11.5, 1H, PhC*H*^{e}H^{f}O), 4.73 (d, *J* = 11.4 Hz, 1H, PhCH^a*H*^{b}O), 4.77-4.83 (m, 1H, H$^\alpha$), 4.86 (d, *J* = 11.5, 1H, PhCH^e*H*^{f}O), 6.13 (d, *J* = 7.5 Hz, 1H, CONH), 6.31 (s, 1H, CONH), 7.26-7.45 (m, 15H, Ph). ^{13}C NMR (100 MHz, $CDCl_3$) δ (ppm) 23.2 (NHCO*C*H$_3$), 50.4 (C$^\alpha$), 51.7 (C^{2s}), 68.3 (C^{6s}), 70.8 (C^{4s}), 71.6 (Ph*C*H^{a}H^{b}O), 72.4 (C^{5s}), 73.6 (Ph*C*H^{c}H^{d}O), 74.7 (Ph*C*H^{e}H^{f}O), 78.0 (C^{1s}), 82.0 (C^{3s}), 127.9, 128.0, 128.2, 128.4, 128.5, 128.6, 128.8, 137.4, 137.9, 138.3 (Arom.), 171.2 (NH*C*OCH$_3$), 171.9 (NH*C*O).

(3*R*,3a*S*,5*R*,6*R*,7*R*,7a*S*)-3-Acetamido-6,7-dihydroxy-3,5-bis-(hydroxymethyl)-2-oxo-1,3a,5,6,7,7a-hexahydropyrano[3,2-*b*]pyrrole (9).

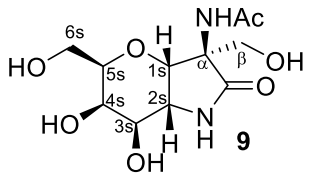

Hydrogenolysis of a MeOH/DCM solution (3:1, 8 mL) of compound **7** (72 mg, 0.13 mmol) was performed at atmospheric pressure and room temperature using Pd−C (46 mg) as catalyst. The reaction mixture was stirred for 12 h and the catalyst was then filtered over diatomaceous earth. The filtrate was concentrated and purified by extractions with water and EtOAc to afford compound **9** (20 mg, 0.069 mmol, 54%) in the aqueous phase as a colorless oil. $[\alpha]_D^{25}$ = +64.3 (c 0.75, H_2O). HRMS ESI+ (m/z): 291.1180 [M+H$^+$]; calcd for $C_{11}H_{19}N_2O_7^+$, 291.1187. ^{1}H NMR (400 MHz, CD_3OD) δ (ppm) 2.02 (s, 3H, NHCO*C*H$_3$), 3.71-3.75 (m, 1H,

H^{6s}), 3.78-3.83 (m, 2H, H^{6s}, H^{β}), 3.92-3.95 (m, 3H, H^{β}, H^{2s}, H^{4s}), 4.00-4.04 (m, 1H, H^{3s}), 4.05-4.10 (m, 1H, H^{5s}), 4.99 (d, J = 7.8 Hz, 1H, H^{1s}). ^{13}C NMR (100 MHz, CD_3OD) δ (ppm) 21.8 ($NHCOCH_3$), 53.7 (C^{2s}), 60.3 (C^{β}), 61.1 (C^{6s}), 64.9 (C^{α}), 67.9 (C^{3s}), 71.8 (C^{4s}), 75.2 (C^{1s}), 76.9 (C^{5s}), 173.5 ($NHCOCH_3$), 174.9 (NH*C*O).

(3*R*,3a*S*,5*R*,6*R*,7*R*,7a*S*)-3-Acetamido-6,7-dihydroxy-5-hydroxymethyl-2-oxo-1,3a,5,6,7,7a-hexahydropyrano[3,2-*b*]pyrrole (10).

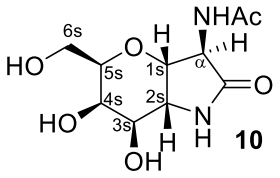

10

Hydrogenolysis of a MeOH/DCM solution (4:1, 8 mL) of compound **8b** (40 mg, 0.075 mmol) was performed at atmospheric pressure and room temperature using Pd−C (30 mg) and 3 drops of concentrated HCl as the catalyst. The reaction mixture was stirred for 36 h and the catalyst was then filtered over diatomaceous earth. The filtrate was concentrated and purified by extractions with water and EtOAc to afford compound **10** (18 mg, 0.069 mmol, 93%) in the aqueous phase as a yellowish oil. $[\alpha]_D^{25}$ = +80.2 (c 0.74, H_2O). HRMS ESI+ (m/z): 283.0899 [M+Na^+]; calcd for $C_{10}H_{16}N_2NaO_6^+$, 283.0901. ^{1}H NMR (400 MHz, D_2O) δ (ppm) 2.08 (s, 3H, $NHCOCH_3$), 3.66-3.75 (m, 3H, H^{6s}, H^{2s}), 3.79 (dd, J = 9.3, 2.6 Hz, 1H, H^{3s}), 3.89 (t, J = 5.9 Hz, 1H, H^{5s}), 3.93 (d, J = 2.6 Hz, 1H, H^{4s}), 4.70 (dd, J = 10.3, 7.9 Hz, 1H, H^{1s}), 4.87 (d, J = 10.4 Hz, 1H, H^{α}). ^{13}C NMR (100 MHz, D_2O) δ (ppm) 21.7 ($NHCOCH_3$), 49.9 (C^{α}), 51.8 (C^{2s}), 61.2 (C^{6s}), 67.1 (C^{4s}), 72.7 (C^{3s}), 73.4 (C^{5s}), 76.4 (C^{1s}), 173.5 ($NHCOCH_3$), 174.8 (NH*C*O).

(3*S*,3a*S*,5*R*,6*R*,7*R*,7a*S*)-3-Acetamido-6,7-dihydroxy-5-hydroxymethyl-2-oxo-1,3a,5,6,7,7a-hexahydropyrano[3,2-*b*]pyrrole (epi-10).

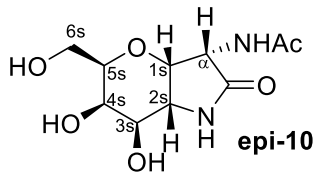

Hydrogenolysis of a MeOH/DCM solution (4:1, 5 mL) of compound **8a** (30 mg, 0.056 mmol) was performed at atmospheric pressure and room temperature using Pd−C (20 mg) and 3 drops of concentrated HCl as the catalyst. The reaction mixture was stirred for 36 h and the catalyst was then filtered over diatomaceous earth. The filtrate was concentrated and purified by extractions with water and EtOAc to afford compound **10** (14 mg, 0.053 mmol, 95%) in the aqueous phase as a colorless oil. $[\alpha]_D^{25}$ = +41.4 (c 0.72, H_2O). HRMS ESI+ (m/z): 283.0914 [M+Na^+]; calcd for $C_{10}H_{16}N_2NaO_6^+$, 283.0901. ^{1}H NMR (400 MHz, D_2O) δ (ppm) 2.11 (s, 3H, NHCO*C*H$_3$), 3.71 (d, *J* = 3.0 Hz, 1H, H^{6s}), 3.86 (d, *J* = 4.0 Hz, 1H, H^{2s}), 3.89 (d, *J* = 2.6 Hz, 1H, H^{3s}), 3.95 (m, 1H, H^{6s}), 4.00-4.04 (m, 1H, H^{5s}), 4.16 (dd, *J* = 4.7, 2.8 Hz, 1H, H^{4s}), 4.65 (m, 1H, H^{1s}), 4.92 (d, *J* = 5.4 Hz, 1H, H$^{\alpha}$). ^{13}C NMR (100 MHz, D_2O) δ (ppm) 21.7 (NHCOCH$_3$), 53.4 (C$^{\alpha}$), 57.2 (C^{2s}), 58.7 (C^{6s}), 67.3 (C^{4s}), 67.7 (C^{1s}), 70.1 (C^{3s}), 77.0 (C^{5s}), 174.8 (NH*C*OCH$_3$), 175.5 (NH*C*O).

Benzyl (2*R*,3*R*,4*R*,4a*S*,8*S*,10a*R*,10b*S*)-8-acetyl-3,4-bis(benzyloxy)-2-(benzyloxymethyl)-8-methyl-6-oxohexahydro-2*H*,8*H*-oxazolo[3,4-*c*]pyrano[2,3-*e*]pyrimidine-10a(10*H*)-carboxylate

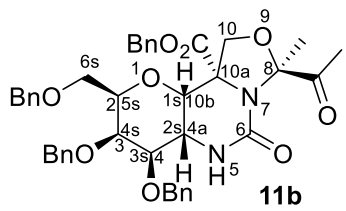

Compound **3b** (165 mg, 0.21 mmol) was dissolved in a mixture of THF (12 mL), concentrated HCl (0.5 mL), acetic acid (2.7 mL) and water (5 mL) and cooled to 0 ºC. Zn dust (334 mg, 5.11 mmol) was added portionwise. After 1 h stirring at 0 ºC, the residue was filtered, and the reaction mixture was diluted with DCM (30 mL), washed with water (15 mL), a saturated aqueous $NaHCO_3$ solution(15 mL), and brine (15 mL), and dried over anhydrous

Na_2SO_4. Purification by silica gel column chromatography (EtOAc/hexane, 2:8) afforded compound **11b** (83 mg, 0.12 mmol, 56%) as a yellowish oil. $[\alpha]_D^{25}$ = +9.1 (c 1.02, $CHCl_3$). HRMS ESI+ (m/z): 721.3111 [M+H$^+$]; calcd for $C_{42}H_{45}N_2O_9^+$, 721.3120. ^{1}H NMR (400 MHz, $CDCl_3$) δ (ppm) 1.75 (s, 3H, CH_3), 2.21 (s, 3H, $COCH_3$), 3.48-3.53 (m, 2H, H^{6s}), 3.56 (dd, *J* = 10.0, 2.2 Hz, 1H, H^{3s}), 3.73 (d, *J* = 8.8 Hz, 1H, H^{10}), 3.79-3.84 (m, 2H, H^{4s}, H^{5s}), 4.13 (ddd, *J* = 10.4, 7.3, 3.3 Hz, 1H, H^{2s}), 4.27 (d, *J* = 11.5 Hz, 1H, PhC*H*^{a}H^{b}O), 4.37-4.54 (m, 4H, PhCH^a*H*^{b}O PhCH$_2$O, PhC*H*^{c}H^{d}O), 4.60 (d, *J* = 7.5 Hz, 1H, H^{1s}), 4.75 (d, *J* = 11.3 Hz, 1H, PhCH^c*H*^{d}O), 4.87 (d, *J* = 8.8 Hz, 1H, H^{10}), 5.06 (d, *J* = 3.5 Hz, 1H, NH), 5.10-5.23 (m, 2H, PhCH$_2$OCO), 7.21-7.40 (m, 20H, Ph). ^{13}C NMR (75 MHz, $CDCl_3$) δ (ppm) 22.2 (CH_3), 25.3 ($COCH_3$), 50.2 (C^{2s}), 67.4 (C^{10a}), 68.3 (C^{6s}, Ph*C*H$_2$OCO), 71.7 (Ph*C*H^{a}H^{b}O), 72.0 (C^{5s}), 72.9 (C^{1s}), 73.5 (PhCH$_2$O), 74.0 (Ph*C*H^{c}H^{d}O), 74.4 (C^{4s}), 75.8 (C^{10}), 78.1 (C^{3s}), 95.8 (C^8), 127.7, 127.8, 127.8, 127.9, 127.9, 128.0, 128.0, 128.1, 128.5, 128.5, 128.6, 128.7, 128.9, 128.9, 134.5, 137.6, 138.0, 138.2 (Arom.), 153.1 (NCONH), 171.8 (*C*O$_2$Bn), 201.9 (CH$_3$*C*O).

tert-Butyl (2*R*,3*R*,4*R*,4a*S*,8*S*,10a*R*,10b*S*)-8-acetyl-3,4-bis(benzyloxy)-2-(benzyloxymethyl)-8-methyl-6-oxohexahydro-2*H*,8*H*-oxazolo[3,4-*c*]pyrano[2,3-*e*]pyrimidine-10a(10*H*)-carboxylate

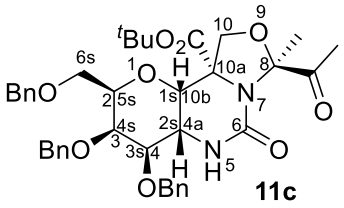

11c

Compound **3c** (112 mg, 0.15 mmol) was dissolved in a mixture of THF (7 mL), concentrated HCl (0.3 mL), acetic acid (1.6 mL) and water (3 mL) and cooled to 0 ºC. Zn dust (195 mg, 3.00 mmol) was added portionwise. After 1 h stirring at 0 ºC, the residue was filtered, and the reaction mixture was diluted with DCM (20 mL), washed with water (10 mL), saturated aqueous $NaHCO_3$ (10 mL), and brine (10 mL), and dried over anhydrous Na_2SO_4. Puri-

fication by silica gel column chromatography (EtOAc/hexane, 2:8) afforded compound **11c** (48 mg, 0.07 mmol, 46%) as a yellowish oil. $[\alpha]_D^{25}$ = +14.8 (c 0.91, $CHCl_3$). HRMS ESI+ (m/z): 687.3278 [M+H$^+$]; calcd for $C_{39}H_{47}N_2O_9^+$, 687.3276. ^{1}H NMR (400 MHz, $CDCl_3$) δ (ppm) 1.46 (s, 9H, $C(CH_3)_3$), 1.82 (s, 3H, CH_3), 2.22 (s, 3H, $COCH_3$), 3.48-3.64 (m, 2H, H^{6s}), 3.69 (d, *J* = 8.7 Hz, 1H, H^{10}), 3.82 (dd, *J* = 9.8, 2.4 Hz, 1H, H^{3s}), 3.94 (t, *J* = 2.3 Hz, 1H, H^{4s}), 3.82 (dd, *J* = 9.8, 2.4 Hz, 1H, H^{3s}), 4.02-4.07 (m, 1H, H^{5s}), 4.14 (ddd, *J* = 10.4, 7.2, 3.2 Hz, 1H, H^{2s}), 4.42-4.48 (m, 2H, $PhCH_2O$), 4.49-4.61 (m, 3H, H^{1s}, PhC*H*^{a}H^{b}O, PhC*H*^{c}H^{d}O), 4.72 (d, *J* = 11.4 Hz, 1H, PhCH^a*H*^{b}O), 4.76-4.81 (m, 2H, PhCH^c*H*^{d}O, H^{10}), 5.03 (d, *J* = 3.3 Hz, 1H, NH), 7.22-7.39 (m, 15H, Ph). ^{13}C NMR (75 MHz, $CDCl_3$) δ (ppm) 21.1 (CH_3), 25.3 ($COCH_3$), 27.8 ($C(CH_3)_3$), 50.4 (C^{2s}), 67.9 (C^{10a}), 68.4 (C^{6s}), 71.9 (C^{4s}), 72.3 (Ph*C*H^{a}H^{b}O), 73.0 (C^{1s}), 73.5 ($PhCH_2O$), 74.0 (C^{5s}), 74.4 (Ph*C*H^{c}H^{d}O), 76.2 (C^{10}), 78.5 (C^{3s}), 83.8 ($C(CH_3)_3$), 95.6 (C^8), 127.9, 127.9, 128.0, 128.1, 128.2, 128.5, 128.5, 128.7, 137.7, 138.1, 138.3 (Arom.), 153.1 (NCONH), 170.9 ($CO_2{}^t$Bu), 202.0 (CH_3CO).

(4*R*,4a*S*,6*R*,7*R*,8*R*,8a*R*)-7,8-dihydroxy-4,6-bis(hydroxymethyl)-2-oxooctahydro-1*H*-pyrano[3,2-*d*]pyrimidine-4-carboxylic acid

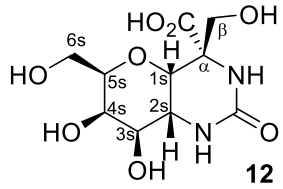

12

Via A: Compound **11b** (72 mg, 0.10 mmol) was suspended in 6 M HCl (15 mL) and stirred under reflux for 24 h. The solvent was then removed under vacuum and the resulting crude was dissolved in water and washed (5 mL) with EtOAc (5 mL). Purification by RP-HPLC (isocratic H_2O+0.1%TFA/MeCN, 95:5, Rt: 6.9 min) and lyophilization afforded compound **12** (11 mg, 0.04 mmol, 40%) as a white solid. Via B: Compound **11c** (35 mg, 0.05 mmol) was suspended in 6 M HCl (15 mL)

and stirred under reflux for 24 h. The solvent was then removed under vacuum and the resulting crude was dissolved in water and washed (5 mL) with EtOAc (5 mL). Purification by RP-HPLC (isocratic H_2O+0.1%TFA/MeCN, 95:5, Rt: 6.9 min) and lyophilization afforded compound **12** (6 mg, 0.02 mmol, 40%) as a white solid. HRMS ESI+ (m/z): 293.0984 [M+H^+]; calcd for $C_{10}H_{17}N_2O_8^+$, 293.0979. ^{1}H NMR (400 MHz, D_2O) δ (ppm) 3.66-3.71 (m, 2H, H^{2s}, H^{β}), 3.78 (dd, *J* = 13.0, 2.6 Hz, 1H, H^{6s}), 3.86 (d, *J* = 11.4 Hz, 1H, H^{β}), 4.00-4.08 (m, 2H, H^{3s}, H^{5s}), 4.16-4.26 (m, 2H, H^{4s}, H^{6s}), 4.44 (d, *J* = 2.4 Hz, 1H, H^{1s}). ^{13}C NMR (75 MHz, D_2O) δ (ppm) 52.6 (C^{2s}), 57.1 (C^{6s}), 60.6 (C^{1s}), 63.6 (C^{α}), 64.3 (C^{4s}), 65.5 (C^{β}), 68.0 (C^{3s}), 77.4 (C^{5s}), 163.7 (NHCONH), 172.7 (CO_2).

Methyl (3*R*,7*R*,7a*S*)-3-((2'*S*,3'*S*,4'*R*,5'*R*,6'*R*)-3-acetamido-4,5-bis-(benzyloxy)-6-(benzyloxymethyl)tetrahydro-2*H*-pyran-2-yl)-7-methoxy-7,7a-dimethyl-5-oxotetrahydro-5*H*-oxazolo[4,3-*b*]oxazole-3-carboxylate (13a).

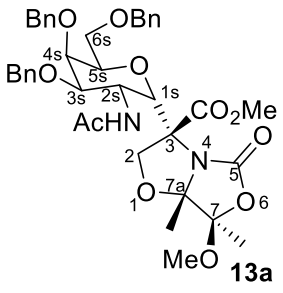

13a

Compound **3a** (354 mg, 0.50 mmol) was dissolved in a mixture of THF (6.3 mL), acetic acid (2.1 mL) and acetic anhydride (4.2 mL) and cooled to 0 ºC. Zn dust (350 mg) and a saturated aqueous $CuSO_4$ solution (500 uL) were added. After 4 h stirring at 0 ºC, the residue was filtered, and the solvent was removed. Purification by column chromatography (EtOAc/hexane, 1:1) afforded compound **13a** (165 mg, 0.23 mmol, 46%) as a colorless oil. $[\alpha]_D^{25}$ = -70.1 (c 1.00, $CHCl_3$). HRMS ESI+ (m/z): 719.3171 [M+H^+]; calcd for $C_{39}H_{47}N_2O_{11}^+$, 719.3174. ^{1}H NMR (400 MHz, $CDCl_3$) δ (ppm) 1.37 (s, 3H, CH_3), 1.40 (s, 3H, CH_3), 1.86 (s, 3H, $NHCOCH_3$), 3.38 (s, 3H, OMe), 3.68 (dd, *J* = 10.4, 4.3 Hz, 1H, H^{6s}), 3.80 (s, 3H, CO_2Me), 3.90-4.04 (m, 3H, H^{6s},

H^{3s}, H^{4s}), 4.30-4.37 (m, 1H, H^{5s}), 4.40-4.85 (m, 9H, 3 x $PhCH_2O$, H^2, H^{2s}), 5.44 (d, *J* = 10.6 Hz, 1H, NHAc), 5.97 (d, *J* = 4.5 Hz, 1H, H^{1s}), 7.22-8.03 (m, 15H, Ph). ^{13}C NMR (obtained from HSQC) δ (ppm) 17.0 (CH_3), 19.2 (CH_3), 23.1 ($NHCOCH_3$), 49.0 (C^{2s}), 51.8 (OMe), 53.7 (CO_2Me), 66.9 (C^{6s}), 71.5 (C^{3s}), 71.7 ($PhCH_2O$), 72.0 (C^2), 72.3 (C^{4s}), 73.1 ($PhCH_2O$), 73.2 ($PhCH_2O$), 76.9 (C^{5s}), 127.6, 127.8, 127.9, 128.2, 128.3, 128.7, 130.0, 133.6 (Arom.).

Benzyl (3*R*,7*R*,7a*S*)-3-((2'*S*,3'*S*,4'*R*,5'*R*,6'*R*)-3-acetamido-4,5-bis-(benzyloxy)-6-(benzyloxymethyl)tetrahydro-2*H*-pyran-2-yl)-7-methoxy-7,7a-dimethyl-5-oxotetrahydro-5*H*-oxazolo[4,3-*b*]oxazole-3-carboxylate (13b).

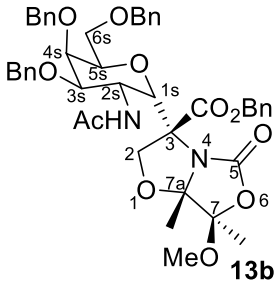

13b

Compound **3b** (350 mg, 0.45 mmol) was dissolved in a mixture of THF (9.0 mL), acetic acid (3.0 mL) and acetic anhydride (6.0 mL) and cooled to 0 ºC. Zn dust (325 mg) and a saturated aqueous $CuSO_4$ solution (600 uL) were added. After 4 h stirring at 0 ºC, the residue was filtered, and the solvent was removed. Purification by column chromatography (EtOAc/hexane, 1:1) afforded compound **13b** (199 mg, 0.25 mmol, 56%) as a colorless oil. $[\alpha]_D^{25}$ = -61.2 (c 1.00, $CHCl_3$). HRMS ESI+ (m/z): 795.3499 [$M+H^+$]; calcd for $C_{45}H_{51}N_2O_{11}^+$, 795.3487. ^1H NMR (400 MHz, $CDCl_3$) δ (ppm) 1.22 (s, 3H, CH_3), 1.35 (s, 3H, CH_3), 1.88 (s, 3H, $NHCOCH_3$), 3.34 (s, 3H, OMe), 3.58 (s, 1H, H^{3s}), 3.62-3.68 (m, 1H, H^{4s}), 3.76 (dd, *J* = 11.4, 2.1 Hz, 1H, H^{6s}), 4.15 (dd, *J* = 11.5, 9.8 Hz, 1H, H^{6s}), 4.29-4.53 (m, 7H, H^2, H^{2s}, H^{5s}, $PhCH_2O$, $PhCH^aH^bO$), 4.55-4.78 (m, 3H, $PhCH_2O$, $PhCH^aH^bO$), 5.16-5.36 (m, 3H, AcN*H*, $PhCH_2OCO$), 5.85 (s, 1H, H^{1s}), 7.12-7.48 (m, 20H, Ph). ^{13}C NMR (100 MHz, $CDCl_3$) δ (ppm) 17.1 (CH_3), 19.3 (CH_3), 23.5

(NHCOCH$_3$), 47.9 (C^{2s}), 51.9 (OMe), 66.2 (C^{6s}), 68.2 (Ph*C*H$_2$OCO), 68.6 (C^3), 71.0 (Ph*C*H$_2$O), 71.7 (C^2, C^{4s}), 71.9 (Ph*C*H$_2$O), 73.1 (Ph*C*H^{a}H^{b}O), 74.8 (C^{3s}), 77.4 (C^{5s}), 101.2 (C^{7a}), 109.3 (C^7), 127.4, 127.6, 127.7, 127.9, 128.1, 128.4, 128.5, 128.5, 128.7, 128.7, 135.0, 137.7 138.0, 139.2 (Arom.), 151.8 (C^5), 168.8 (NHCO), 169.3 (CO_2Bn).

***tert*-Butyl (3*R*,7*R*,7a*S*)-3-((2'*S*,3'*S*,4'*R*,5'*R*,6'*R*)-3-acetamido-4,5-bis-(benzyloxy)-6-(benzyloxymethyl)tetrahydro-2*H*-pyran-2-yl)-7-methoxy-7,7a-dimethyl-5-oxotetrahydro-5*H*-oxazolo[4,3-*b*]oxazole-3-carboxylate (13c).**

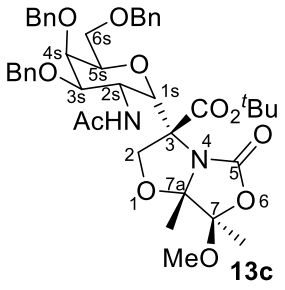

Compound **3c** (300 mg, 0.40 mmol) was dissolved in a mixture of THF (7.5 mL), acetic acid (2.5 mL) and acetic anhydride (5.0 mL) and cooled to 0 ºC. Zn dust (300 mg) and a saturated aqueous $CuSO_4$ solution (600 uL) were added. After 4 h stirring at 0 ºC, the residue was filtered, and the solvent was removed. Purification by column chromatography (EtOAc/hexane, 1:1) afforded compound **13c** (137 mg, 0.18 mmol, 45%) as a colorless oil. $[\alpha]_D^{25}$ = -66.5 (c 1.00, $CHCl_3$). HRMS ESI+ (m/z): 761.3672 [M+H$^+$]; calcd for $C_{42}H_{53}N_2O_{11}^+$, 761.3644. ^{1}H NMR (400 MHz, $CDCl_3$) δ (ppm) 1.32 (s, 3H, CH_3), 1.34 (s, 3H, CH_3), 1.48 (s, 9H, (C(CH_3)$_3$),1.91 (s, 3H, NHCOCH_3), 3.35 (s, 3H, OMe), 3.66 (dd, *J* = 6.8, 2.7 Hz, 1H, H^{4s}), 3.71 (t, *J* = 3.4 Hz, 1H, H^{3s}), 3.80 (d, *J* = 11.2 Hz, 1H, H^{6s}), 4.22 (dd, *J* = 11.2, 8.8 Hz, 1H, H^{6s}), 4.33-4.49 (m, 5H, H^{2s}, H^{5s}, PhCH_2O, PhC*H*^{a}H^{b}O), 4.55-4.74 (m, 4H, H^2, PhCH^a*H*^{b}O, PhC*H*^{c}H^{d}O), 4.80 (d, *J* = 12.3 Hz, 1H, PhCH^c*H*^{d}O), 5.41-5.52 (m, 1H, AcN*H*), 5.81 (s, 1H, H^{1s}), 7.16-7.54 (m, 15H, Ph). ^{13}C NMR (100 MHz, $CDCl_3$) δ (ppm) 17.0 (CH_3), 19.3 (CH_3), 23.4 (NHCOCH_3), 27.8

($C(CH_3)_3$), 47.9 (C^{2s}), 51.9 (OMe), 66.1 (C^{6s}), 69.2 (C^3), 70.8 (PhCH_2O), 71.4 (C^2), 72.1 (C^{4s}), 72.2 (PhCH^cH^dO), 73.0 (PhCH^aH^bO), 74.4 (C^{3s}), 77.4 (C^{5s}), 83.7 ($C(CH_3)_3$), 100.7 (C^{7a}), 109.2 (C^7), 127.3, 127.6, 127.6, 127.7, 127.9, 128.0, 128.4, 128.5, 128.8, 137.7, 138.0, 139.2 (Arom.), 151.3 (C^5), 167.8 (NHCO), 169.1 ($CO_2{}^t$Bu).

(4*R*,4a*S*,6*R*,7*R*,8*R*,8a*R*)-7,8-dihydroxy-4,6-bis(hydroxymethyl)-2-oxooctahydro-1*H*-pyrano[3,2-*d*]pyrimidine-4-carboxylic acid

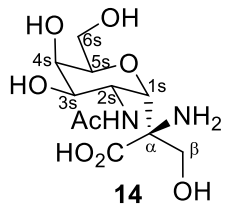

Compound **13b** (79 mg, 0.10 mmol) was dissolved in THF (2.4 mL) and 4 M HCl (1 mL) was then added. The mixture was stirred at 40 ºC for 24 h and the solvent was then removed under vacuum. The resulting crude was dissolved in water and washed (5 mL) with EtOAc (5 mL). Hydrogenolysis of a MeOH solution (2 mL) of the resulting crude was performed at atmospheric pressure and room temperature using Pd−C (25 mg) as catalyst. The reaction mixture was stirred for 12 h and the catalyst was then filtered over diatomaceous earth. The filtrate was concentrated, purified by RP-HPLC (isocratic H_2O+0.1%TFA/MeCN, 95:5, Rt: 6.9 min) and lyophilized to afford compound **14** (12 mg, 0.04 mmol, 40%) as a white solid. HRMS ESI+ (m/z): 309.1296 [$M+H^+$]; calcd for $C_{11}H_{21}N_2O_8^+$, 309.1292. ^{1}H NMR (400 MHz, D_2O) δ (ppm) 2.04 (s, 3H, NHCOCH_3), 3.78 (dd, J = 12.7, 2.3 Hz, 1H, H^{6s}), 3.86 (t, J = 3.6 Hz, 1H, H^{3s}), 3.90 (d, J = 12.0 Hz, 1H, H^β), 4.10-4.18 (m, 3H, H^{4s}, H^{6s}, H^β), 4.19-4.25 (m, 2H, H^{2s}, H^{5s}), 4.60 (d, J = 2.0 Hz, 1H, H^{1s}). ^{13}C NMR (75 MHz, D_2O) δ (ppm) 22.0 (Me), 50.1 (C^{2s}), 56.8 (C^{6s}), 60.8 (C^β), 64.5 (C^{4s}), 65.6 (C^{1s}), 66.4 (C^α), 69.0 (C^{3s}), 78.3 (C^{5s}), 170.2 (CO_2), 174.6 (NHCO).

(3*R*,3a*S*,5*R*,6*R*,7*R*,7a*S*)-3-Amino-6,7-bis(benzyloxy)-5-(benzyloxymethyl)-3-(hydroxymethyl)-2-oxo-1,3a,5,6,7,7a-hexahydropyrano[3,2-*b*]pyrrol (15).

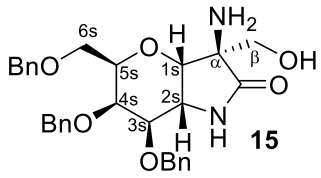

Compound **5** (105 mg, 0.163 mmol) was dissolved in THF (10 ml). An aqueous 4 M HCl solution (3.6 ml) was then added and the mixture was stirred at 40 ºC for 12 h. The crude obtained after concentration was dissolved in absolute EtOH (5 ml). Propylene oxide (5 ml) was added and the mixture was stirred under reflux for 2 h. Concentration and purification of the crude product by silica column chromatography (DCM/MeOH, 15:1) afforded compound **15** (60 mg, 0.116 mmol, 71%) as a colorless oil. $[\alpha]_D^{25}$ = +64.8 (c 0.99, $CHCl_3$). HRMS ESI+ (m/z): 519.2495 [M+H$^+$]; calcd for $C_{30}H_{35}N_2O_6^+$, 519.2490. ^{1}H NMR (400 MHz, $CDCl_3$) δ (ppm) 3.52-3.61 (m, 2H, H^{3s}, H^{6s}), 3.67 (d, *J* = 12.0 Hz, 1H, H$^{\beta}$), 3.71-3.83 (m, 2H, H$^{\beta}$, H^{6s}), 4.03-4.15 (m, 3H, H^{5s}, H^{4s}, H^{2s}), 4.24 (d, *J* = 4.8 Hz, 1H, H^{1s}), 4.48-4.59 (m, 4H, PhC*H*$_2$O, PhC*H*^{a}H^{b}O, PhC*H*^{c}H^{d}O), 4.68 (d, *J* = 11.6 Hz, 1H, PhCH^a*H*^{b}O) 4.84 (d, *J* = 11.6 Hz, 1H, PhCH^c*H*^{d}O), 6.84 (s, 1H, NH), 7.20-7.40 (m, 15H, Ph). ^{13}C NMR (100 MHz, $CDCl_3$) δ (ppm) 56.2 (C^{2s}), 62.3 (C$^{\alpha}$), 65.1 (C$^{\beta}$), 67.2 (C^{6s}), 71.9 (Ph*C*H^{a}H^{b}O), 72.5 (C^{4s}), 73.6 (Ph*C*H$_2$O), 74.5 (Ph*C*H^{c}H^{d}O), 76.2 (C^{5s}), 76.7 (C^{1s}), 81.3 (C^{3s}), 127.8, 127.9, 128.0, 128.3, 128.5, 128.6, 128.8, 137.6, 137.9, 138.1 (Arom), 177.8 (CO).

[(3*R*,3a*S*,5*R*,6*R*,7*R*,7a*S*)-6,7-Bis(benzyloxy)-5-(benzyloxymethyl)-2-oxo-3-palmitamido-1,3a,5,6,7,7a-hexahydropyrano[3,2-*b*]pyrrol-3-yl]methyl palmitate (16).

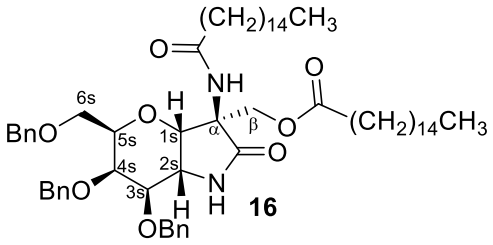

Compound **15** (45 mg, 0.086 mmol) was dissolved in DCM (2 ml) and palmitoyl chloride (80 µl, 0.26 mmol) was added. Et_3N (50 µl, 0.36 mmol) was then added and the mixture was stirred at room temperature for 12 h. An aqueous 0.5 M HCl solution (2 ml) was added. The organic layer was separated and the aqueous one was washed with DCM (3 x 2 ml). The organic phases were collected and dried with anhydrous Na_2SO_4. Concentration and purification of the crude product by silica column chromatography (EtOAc/hexane, 7:13) afforded compound **16** (60 mg, 0.06 mmol, 70%) as a colorless oil. $[\alpha]_D^{25}$ = +34.5 (c 1.00, $CHCl_3$). HRMS ESI+ (m/z): 995.7071 [M+H$^+$]; calcd for $C_{62}H_{95}N_2O_8^+$, 995.7083. ^{1}H NMR (400 MHz, $CDCl_3$) δ (ppm) 0.88 (t, *J* = 6.5 Hz, 6H, CH_3), 1.19-1.35 (m, 48H, $(CH_2)_{12}CH_3$), 1.51-1.64 (m, 4H, $CH_2(CH_2)_{12}CH_3$), 2.18 (t, *J* = 7.6 Hz, 2H, NHCOCH_2), 2.24 (t, *J* = 7.6 Hz, 2H, OCOCH_2), 3.52-3.60 (m, 2H, H^{3s}, H^{6s}), 3.63-3.70 (m, 1H, H^{6s}), 4.03-4.10 (m, 1H, H^{5s}), 4.11-4.15 (m, 1H, H^{4s}), 4.29-4.36 (m, 2H, H^{2s}, H$^{\beta}$), 4.42-4.54 (m, 4H, H$^{\beta}$, PhCH_2O, PhCH^aH^{b}O), 4.58 (d, *J* = 11.6 Hz, 1H, PhCH^cH^{d}O), 4.66-4.72 (m, 2H, H^{3a}, PhCH^aH^bO), 4.88 (d, *J* = 11.6 Hz, 1H, PhCH^cH^dO), 6.06 (s, 1H, NH), 6.32 (s, 1H, NH), 7.22-7.40 (m, 15H, Ph). ^{13}C NMR (100 MHz, $CDCl_3$) δ (ppm) 14.2 (CH_3), 22.8, 24.9, 25.3, 29.3, 29.5, 29.6, 29.7, 29.8, 32.1 (($CH_2)_{13}CH_3$), 34.2 (OCOCH_2), 36.2 (NHCOCH_2), 56.0 (C^{2s}), 60.5 (C$^{\alpha}$), 63.1 (C$^{\beta}$), 67.8 (C^{6s}), 71.5 (PhCH^aH^{b}O), 71.7 (C^{4s}), 73.6 (PhCH_2O), 74.4 (PhCH^cH^{d}O), 75.9 (C^{1s}), 76.5 (C^{5s}), 81.4

(C^{3s}), 127.7, 127.8, 127.9, 128.2, 128.4, 128.6, 128.8, 137.6, 138.1, 138.4 (Arom.), 172.4 (OCO), 173.2 (NHCO), 173.7 (NHCO).

[(3*R*,3a*S*,5*R*,6*R*,7*R*,7a*R*)-6,7-Dihydroxy-5-(hydroxymethyl)-2-oxo-3-palmitamido-1,3a,5,6,7,7a-hexahydropyrano[3,2-*b*]pyrrol-3-yl]methyl palmitate (APP-1).

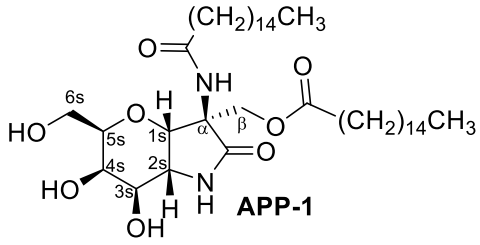

A hydrogenolysis of a methanol solution (5 ml) of the compound **16** (37 mg, 0.037 mmol) was held under ambient pressure and temperature, using Pd-C (35 mg) and HCl conc. (3 drops) as catalyst. The reaction was performed for 12 h and the catalyst was filtered over diatomaceous earth. The liquid phase was concentrated affording **APP-1** (25 mg, 0,034 mmol, 93%) as a yellow oil. $[\alpha]_D^{25}$ = +20.6 (c 0.99, MeOH). HRMS ESI+ (m/z): 725.5669 [M+H^+]; calcd for $C_{41}H_{77}N_2O_8^+$, 725.5674. ^{1}H NMR (400 MHz, CD_3OD) δ (ppm) 0.89 (t, *J* = 6.5 Hz, 6H, CH_3), 1.24-1.35 (m, 48H, (CH_2)$_{12}CH_3$), 1.54-1.67 (m, 4H, $CH_2(CH_2)_{12}CH_3$), 2.23 (t, *J* = 6.7 Hz, 2H, NHCOCH_2), 2.36 (t, *J* = 7.3 Hz, 2H, OCOCH_2), 3.70-3.78 (m, 3H, H^{6s}, H^{3s}), 3.79-3.85 (m,1H, H^{5s}), 3.91-4.02 (m, 2H, H^{4s}, H^{2s}), 4.31 (d, *J* = 10.7 Hz, 1H, H^{β}), 4.45-4.52 (m, 1H, H^{β}), 4.83 (m, 1H, H^{1s}). ^{13}C NMR (100 MHz, CD_3OD) δ (ppm) 14.4 (CH_3), 23.7, 25.8, 26.8, 30.2, 30.4, 30.5, 30.6, 30.7, 30.8, 33.0 ((CH_2)$_{13}CH_3$), 34.9 (OCOCH_2), 36.7 (NHCOCH_2), 56.9 (C^{2s}), 61.6 (C^{6s}), 62.6 (C^{β}), 63.1 (C^{α}), 69.4 (C^{4s}), 73.3 (C^{3s}), 76.0 (C^{1s}), 78.8 (C^{5s}), 174.7 (OCO), 175.7 (NHCO), 176.0 (NHCO).

_N_-[(3_R_,3a_S_,5_R_,6_R_,7_R_,7a_S_)-6,7-Bis(benzyloxy)-5-(benzyloxymethyl)-3-hydroxymethyl-2-oxo-1,3a,5,6,7,7a-hexahydropyrano[3,2-_b_]pyrrol-3-yl]palmitamide (17).

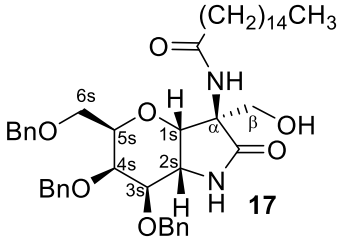

A methanol solution of NaOMe 0.5 M (2 ml) was added to a methanol solution (4 ml) of the compound **16** (76 mg, 0.076 mmol). The mixture was stirred for 1 h and sulfonic acid resine Dowex® was then added. The liquid phase was filtered, concentrated and the residue was purified by silica column chromatography (EtOAc/hexane, 17:3) to afford compound **17** (40 mg, 0.053, 70%) as a colorless oil. $[\alpha]_D^{25}$ = +66.0 (c 1.00, $CHCl_3$). HRMS ESI+ (m/z): 757.4788 [M+H$^+$]; calcd for $C_{46}H_{65}N_2O_7^+$, 757.4786. ^{1}H NMR (400 MHz, $CDCl_3$) δ (ppm) 0.88 (t, *J* = 6.7 Hz, 3H, CH_3), 1.22-1.33 (m, 24H, $(CH_2)_{12}CH_3$), 1.55-1.65 (m, 2H, $CH_2(CH_2)_{12}CH_3$), 2.20 (t, *J* = 7.6 Hz, 2H, $NHCOCH_2$), 3.48 (dd, *J* = 10.3, 4.7 Hz, 1H, H^{6s}), 3.56 (d, *J* = 8.1 Hz, 1H, H^{3s}) , 3.67-3.75 (m, 2H, H^{6s}, H^{β}), 3.98 (d, *J* = 12.0 Hz, 1H, H^{β}), 4.09 (d, *J* = 4.9 Hz, 1H, H^{4s}), 4.11-4.18 (m, 1H, H^{5s}), 4.38 (t, *J* = 7.2 Hz, 1H, H^{2s}), 4.47 (d, *J* =11.9 Hz, 1H, $PhCH^aH^bO$), 4.49 (s, 2H, $PhCH_2O$), 4.55 (d, *J* = 11.8 Hz, 1H, $PhCH^cH^dO$), 4.61 (d, *J* = 6.3, 1H, H^{1s}) 4.68 (d, *J* = 11.8 Hz, 1H, $PhCH^aH^bO$), 4.87 (d, *J* = 11.8 Hz, 1H, $PhCH^cH^dO$), 6.22 (s,1H, NH), 6.56 (s, 1H, NH), 7.20-7.39 (m, 15H, Ph). ^{13}C NMR (100 MHz, $CDCl_3$) δ (ppm) 14.1 (CH_3), 22.7, 25.3, 29.2, 29.4, 29.5, 29.7, 32.0 ($(CH_2)_{13}CH_3$), 35.8 ($NHCOCH_2$), 56.3 (C^{2s}), 63.5 (C^{α}), 64.0 (C^{β}), 67.4 (C^{6s}), 71.5 (C^{4s}), 71.6 ($PhCH^aH^bO$), 73.5 ($PhCH_2O$), 74.2 ($PhCH^cH^dO$), 76.7 (C^{5s}, C^{1s}), 81.4 (C^{3s}), 127.6, 127.8, 127.9, 128.2, 128.4, 128.5, 128.7, 137.5, 137.8, 138.0 (Arom.), 173.5 (NHCO), 173.9 (NHCO).

***N*-[(3*R*,3a*S*,5*R*,6*R*,7*R*,7a*R*)-6,7-Dihydroxy-3,5-bis(hydroxymethyl)-2-oxo -1,3a,5,6,7,7a-hexahydropyrano[3,2-*b*]pyrrol-3-yl]palmitamide (APP-2).**

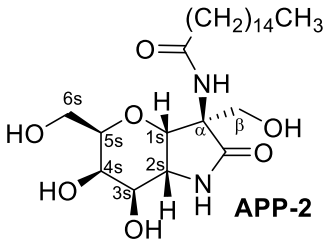

A hydrogenolysis of a methanol solution (5 ml) of the compound **17** (35 mg, 0.046 mmol) was held under ambient pressure and temperature, using Pd-C (35 mg) and HCl conc. (3 drops) as catalyst. The reaction was performed for 12 h and the catalyst was filtered over diatomaceous earth. The liquid phase was concentrated affording **APP-2** (22 mg, 0,045 mmol, 98%) as a yellow oil. $[\alpha]_D^{25}$ = +15.1 (c 1.00, MeOH). HRMS ESI+ (m/z): 487.3386 [M+H$^+$]; calcd for $C_{25}H_{47}N_2O_7^+$, 487.3378. ^{1}H NMR (400 MHz, CD_3OD) δ (ppm) 0.83 (t, *J* = 5.8 Hz, 3H, CH_3), 1.13-1.36 (m, 24H, $(CH_2)_{12}CH_3$), 1.49-1.62 (m, 2H, $CH_2(CH_2)_{12}CH_3$), 2.38 (t, *J* = 6.7 Hz, 2H, $NHCOCH_2$), 3.65-4.02 (m, 6H, H^{6s}, H^{5s}, H^{4s}, H^{3s}, H^{2s}), 4.39 (d, *J* = 11.3 Hz, 1H, H^{β}), 4.48 (d, *J* = 11.7 Hz, 1H, H^{β}), 4.74 (d, *J* = 5.3 Hz, 1H, H^{1s}). ^{13}C NMR (100 MHz, CD_3OD) δ (ppm) 14.3 (CH_3), 23.5, 25.5, 30.0, 30.3, 30.4, 30.5, 30.6, 32.9 ($(CH_2)_{13}CH_3$), 34.4 ($NHCOCH_2$), 55.8 (C^{2s}), 61.6 (C^{β}), 61.9 (C^{6s}), 63.0 (C^{α}), 69.2 (C^{4s}), 73.3 (C^{3s}), 74.6 (C^{1s}), 79.0 (C^{5s}), 174.1 (2 NHCO).

[(3*R*,3a*S*,5*R*,6*R*,7*R*,7a*S*)-3-Amino-6,7-bis(benzyloxy)-5-(benzyloxy-methyl)-2-oxo-1,3a,5,6,7,7a-hexahydropyrano[3,2-*b*]pyrrol-3-yl]methyl palmitate (18).

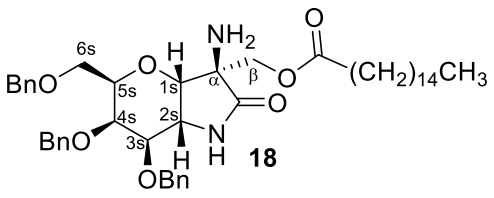

Compound **5** (82 mg, 0.127 mmol) was dissolved in THF (8 ml). An aqueous 4 M HCl solution (2.8 ml) was then added and the mixture was stirred at 40 ºC for 12. The crude obtained after concentration was dissolved

in TFA (4 ml) and palmitoyl chloride was added (385 µl, 1.27 mmol). The mixture was stirred at room temperature for 15 min and absolute EtOH (10 ml) was added to quench the reaction. After concentration, the crude was dissolved in absolute EtOH (5 ml). Propylene oxide (5 ml) was added and the mixture was stirred under reflux for 2 h. Concentration and purification of the crude product by silica column chromatography (EtOAc/hexane, 7:13) afforded compound **18** (64 mg, 0.085 mmol, 67%) as a colorless oil. $[\alpha]_D^{25}$ = +52.9 (c 1.00, $CHCl_3$). HRMS ESI+ (m/z): 757.4788 [$M+H^+$]; calcd for $C_{46}H_{65}N_2O_7^+$, 757.4786. ^{1}H NMR (400 MHz, $CDCl_3$) δ (ppm) 0.88 (t, *J* = 6.7 Hz, 3H, CH_3), 1.20-1.36 (m, 24H, $(CH_2)_{12}CH_3$), 1.54-1.64 (m, 2H, $CH_2(CH_2)_{12}CH_3$), 2.27 (t, *J* = 7.8 Hz, 2H, $OCOCH_2$), 3.55 (d, *J* = 5.3 Hz, 1H, H^{3s}), 3.67-3.74 (m, 2H, H^{6s}) , 4.05-4.12 (m, 2H, H^{1s}, H^{5s}), 4.14-4.20 (m, 2H, H^{2s}, H^{4s}), 4.39-4.47 (m, 2H, H^{β}), 4.49-4.61 (m, 4H, $PhCH^aH^bO$, $PhCH^cH^dO$, $PhCH_2O$), 4.69 (d, *J* = 11.8 Hz, 1H, $PhCH^aH^bO$), 4.81 (d, *J* = 11.5 Hz, 1H, $PhCH^cH^dO$), 6.57 (s, 1H, NH), 7.24-7.38 (m, 15H, Ph). ^{13}C NMR (100 MHz, $CDCl_3$) δ (ppm) 14.2 (CH_3), 22.8, 26.1, 29.3, 29.5, 29.6, 29.7, 29.8, 32.0 ($(CH_2)_{13}CH_3$), 28.2 ($OCOCH_2$), 57.3 (C^{2s}), 67.2 (C^{6s}), 68.3 (C^{β}), 72.0 ($PhCH^aH^bO$), 73.0 (C^{1s}), 73.5 ($PhCH_2O$), 74.2 ($PhCH^cH^dO$), 74.6 (C^{4s}), 76.2 (C^{5s}), 78.7 (C^{α}), 80.1 (C^{3s}), 127.8, 127.9, 128.2, 128.5, 128.6, 128.7, 137.7, 138.1, 138.2 (Arom.), 170.9 (OCO), 175.5 (NHCO).

[(3*R*,3a*S*,5*R*,6*R*,7*R*,7a*R*)-3-Amino-6,7-bis(hydroxy)-5-(hydroxymethyl)-2-oxo-1,3a,5,6,7,7a-hexahydropyrano[3,2-*b*]pyrrol-3-yl]methyl palmitate (18).

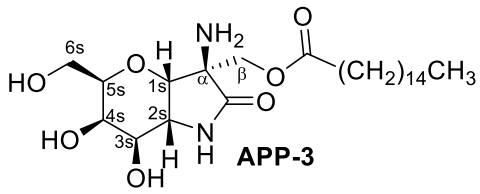

APP-3

A hydrogenolysis of a methanol solution (5 ml) of the compound **18** (50 mg, 0.065 mmol) was held under ambient pressure and temperature, using Pd-C (50 mg) and HCl conc. (3 drops) as catalyst. The reaction was performed for 12 h and the catalyst was filtered over diatomaceous earth. The liquid phase was concentrated affording **APP-3** (30 mg, 0,062 mmol, 94%) as a yellow oil. $[\alpha]_D^{25}$ = -3.9 (c 1.00, MeOH). HRMS ESI+ (m/z): 487.3388 [M+H$^+$]; calcd for $C_{25}H_{47}N_2O_7^+$, 487.3378. ^{1}H NMR (400 MHz, CD_3OD) δ (ppm) 0.89 (t, *J* = 6.4 Hz, 3H, CH_3), 1.22-1.39 (m, 24H, $(CH_2)_{12}CH_3$), 1.58-1.67 (m, 2H, $CH_2(CH_2)_{12}CH_3$), 2.43 (t, *J* = 7.4 Hz, 2H, $OCOCH_2$), 3.70-3.78 (m, 3H, H^{6s}, H^{3s}), 3.79-3.85 (m, 1H, H^{5s}), 3.93 (t, *J* = 7.6 Hz, 1H, H^{2s}), 3.99 (s, 1H, H^{4s}), 4.44 (d, *J* = 12.1 Hz, 1H, H^{β}), 4.53 (d, *J* = 11.9 Hz, 1H, H^{β}), 4.77 (d, *J* = 7.2 Hz, 1H, H^{1s}). ^{13}C NMR (100 MHz, CD_3OD) δ (ppm) 14.4 (CH_3), 23.7, 25.7, 30.1, 30.4, 30.6, 30.7, 30.8, 33.0 ($(CH_2)_{13}CH_3$), 34.5 ($OCOCH_2$), 55.9 (C^{2s}), 61.7 (C^{β}), 62.0 (C^{6s}), 63.1 (C^{α}), 69.3 (C^{4s}), 73.5 (C^{3s}), 74.8 (C^{1s}), 79.2 (C^{5s}), 170.3 (OCO), 174.1 (NHCO).

[(3*R*,3a*S*,5*R*,6*R*,7*R*,7a*S*)-3-Acetamido-6,7-bis(benzyloxy)-5-(benzyloxymethyl)-2-oxo-1,3a,5,6,7,7a-hexahydropyrano[3,2-*b*]pyrrol-3-yl]methyl palmitate (19).

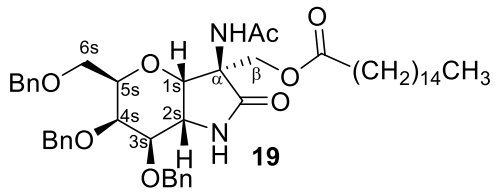

Compound **7** (60 mg, 0.107 mmol) was dissolved in DCM (2 ml) and palmitoyl chloride (70 µl, 0.23 mmol) was added. Et_3N (44 µl, 0.32 mmol) was then added and the mixture was stirred at room temperature for 12 h. An aqueous 0.5 M HCl solution (2 ml) was added. The organic phase was separated and the aqueous one was washed with DCM (3 x 2 ml). The organic phases were collected and dried with anhydrous Na_2SO_4. Concentration and purification of the crude product by silica column chromatography (EtOAc/hexane, 13:7) afforded the compound **19** (63 mg, 0.079 mmol, 74%) as a colorless oil. $[\alpha]_D^{25}$ = +41.0 (c 1.00, $CHCl_3$). HRMS ESI+ (m/z): 799.4853 [M+H$^+$]; calcd for $C_{48}H_{67}N_2O_8^+$, 799.4853. ^{1}H NMR (400 MHz, $CDCl_3$) δ (ppm) 0.88 (t, *J* = 6.7 Hz, 3H, CH_3), 1.21-1.30 (m, 24H, $(CH_2)_{12}CH_3$), 1.51-1.58 (m, 2H, $CH_2(CH_2)_{12}CH_3$), 1.98 (s, 3H, NHAc), 2.23 (t, *J* = 7.5 Hz, 2H, $OCOCH_2$), 3.53-3.59 (m, 2H, H^{6s}, H^{3s}), 3.66 (dd, *J* = 9.5, 6.9 Hz, 1H, H^{6s}), 4.07 (dd, *J* = 11.1, 6.3 Hz, 1H, H^{5s}), 4.13 (d, *J* = 4.2 Hz, 1H, H^{4s}), 4.27-4.34 (m, 2H, H^{2s}, H^{β}), 4.42-4.52 (m, 4H, H^{β}, $PhCH_2O$, $PhCH^aH^bO$), 4.58 (d, *J* = 11.6, 1H, $PhCH^cH^dO$), 4.66-4.72 (m, 2H, $PhCH^aH^bO$, H^{1s}), 4.87 (d, *J* = 11.6 Hz, 1H, $PhCH^eH^dO$), 6.07-6.18 (m, 1H, NHAc), 6.38 (s, 1H, NHCO), 7.22-7.40 (m, 15H, Ph). ^{13}C NMR (100 MHz, $CDCl_3$) δ (ppm) 14.1 (CH_3), 23.1 ($NHCOCH_3$), 22.7, 24.8, 29.2, 29.3, 29.4, 29.5, 29.7, 31.9, 34.1 ($CO(CH_2)_{14}CH_3$), 55.9 (C^{2s}), 63.0 (C^{β}), 63.2 (C^{α}) 67.7 (C^{6s}), 71.4 ($PhCH^aH^bO$), 71.6 (C^{4s}), 73.5 ($PhCH_2O$), 74.3 ($PhCH^cH^dO$), 75.7 (C^{1s}), 76.4 (C^{5s}), 81.2 (C^{3s}), 127.7, 127.8, 127.9, 128.2, 128.3, 128.5, 128.7,

137.5, 138.0, 138.2 (Arom.), 170.0 (O*C*O), 172.3 (NH*C*OCH$_3$), 173.6 (NH*C*O).

[(3*R*,3a*S*,5*R*,6*R*,7*R*,7a*R*)-3-Acetamido-6,7-bis(hydroxy)-5-(hydroxy-methyl)-2-oxo-1,3a,5,6,7,7a-hexahydropyrano[3,2-*b*]pyrrol-3-yl]methyl palmitate (APP-4).

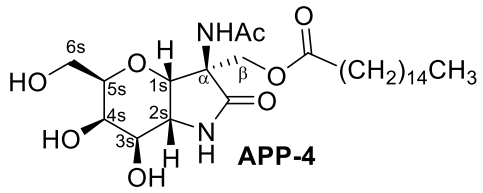

APP-4

A hydrogenolysis of a methanol solution (5 ml) of the compound **19** (63 mg, 0.079 mmol) was held under ambient pressure and temperature, using Pd-C (60 mg) and HCl conc. (3 drops) as catalyst. The reaction was performed for 12 h and the catalyst was filtered over diatomaceous earth. The liquid phase was concentrated affording the **APP-4** (35 mg, 0,066 mmol, 84 %) as a yellow oil. $[\alpha]_D^{25}$ = +22.7 (c 1.00, H_2O). HRMS ESI+ (m/z): 529.3493 [M+H$^+$]; calcd for $C_{27}H_{49}N_2O_8^+$, 529.3483. ^{1}H NMR (400 MHz, CD_3OD) δ (ppm) 0.88 (t, *J* = 6.4 Hz, 3H, CH_3), 1.19-1.37 (m, 24H, (C*H*$_2$)$_{12}$CH$_3$), 1.53-1.66 (m, 2H, C*H*$_2$(CH$_2$)$_{12}$CH$_3$), 2.26-2.39 (m, 2H, OCOC*H*$_2$), 3.68-4.03 (m, 6H, H^{6s}, H^{5s}, H^{4s}, H^{3s}, H^{2s}), 4.25-4.35 (m, 1H, H$^{\beta}$), 4.46-4.54 (m, 1H, H$^{\beta}$), 4.83 (m, 1H, H^{1s}). ^{13}C NMR (100 MHz, CD_3OD) δ (ppm) 14.3 (CH_3), 23.6, 25.8, 25.9, 30.1, 30.2, 30.3, 30.4, 30.5, 30.6, 30.7, 32.9 ((*C*H$_2$)$_{13}$CH$_3$), 34.7 (OCO*C*H$_2$), 56.9 (C^{2s}), 61.6 (C^{6s}), 62.2 (C$^{\beta}$), 64.9 (C$^{\alpha}$), 69.3 (C^{4s}), 73.1 (C^{3s}), 75.9 (C^{1s}), 78.7 (C^{5s}), 171.4 (OCO), 174.6 (NHCO), 176.0 (NHCO).

[(3*R*,3a*S*,5*R*,6*R*,7*R*,7a*S*)-3-Amino-6,7-bis(benzyloxy)-5-(benzyloxymethyl)-2-oxo-1,3a,5,6,7,7a-hexahydropyrano[3,2-*b*]pyrrol-3-yl]methyl acetate (20).

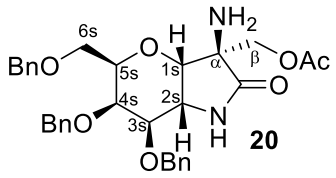

Compound **5** (73 mg, 0.113 mmol) was dissolved in THF (7 ml). An aqueous 4 M HCl solution (2.5 ml) was then added and the mixture was stirred at 40 ºC for 12 h. The crude obtained after concentration was dissolved in TFA (4 ml) and palmitoyl chloride was added (80 µl, 1.13 mmol). The mixture was stirred at room temperature for 15 min and absolute EtOH (10 ml) was added to quench the reaction. After concentration, the crude was dissolved in absolute EtOH (5 ml). Propylene oxide (5 ml) was added and the mixture was refluxed for 2 h. Concentration and purification of the crude product by silica column chromatography using EtOAc as eluent afforded compound **9** (27 mg, 0.048 mmol, 42 %) as a colorless oil. $[\alpha]_D^{25}$ = +76.7 (c 1.00, $CHCl_3$). HRMS ESI+ (m/z): 561.2590 [M+H$^+$]; calcd for $C_{32}H_{37}N_2O_7^+$, 561.2595. ^{1}H NMR (400 MHz, $CDCl_3$) δ (ppm) 1.99 (s, 3H, CH_3), 3.54 (s, 1H, H^{3s}), 3.67-3.73 (m, 2H, H^{6s}), 4.06-4.12 (m, 2H, H^{1s}, H^{5s}), 4.15-4.20 (m, 2H, H^{5s}, H^{2s}), 4.41-4.49 (m, 2H, H^{β}), 4.49-4.61 (m, 4H, PhC*H*^{a}H^{b}O, PhC*H*^{c}H^{d}O, PhCH_2O), 4.70 (d, *J* = 11.8 Hz, 1H, PhCH^a*H*^{b}O), 4.82 (d, *J* = 11.4 Hz, 1H, PhCH^c*H*^{d}O), 6.51 (s, 1H, NH), 7.24-7.39 (m, 15H, Ph). ^{13}C NMR (100 MHz, $CDCl_3$) δ (ppm) 14.0 (CH_3), 57.4 (C^{2s}), 67.2 (C^{6s}), 68.6 (C^{β}), 71.9 (Ph*C*H^{a}H^{b}O), 72.9 (C^{1s}), 73.5 (Ph*C*H_2O), 74.3 (Ph*C*H^{c}H^{d}O), 74.6 (C^{4s}), 76.2 (C^{5s}), 78.8 (C^{α}), 80.2 (C^{3s}), 127.8, 127.9, 128.3, 128.5, 128.6, 128.8, 137.7, 138.1, 138.2 (Arom.), 167.8 (O*C*OCH_3), 175.5 (NHCO).

[(3*R*,3a*S*,5*R*,6*R*,7*R*,7a*R*)-3-Amino-6,7-bis(hydroxy)-5-(hydroxymethyl)-2-oxo-1,3a,5,6,7,7a-hexahydropyrano[3,2-*b*]pyrrol-3-yl]methyl acetate (APP-6).

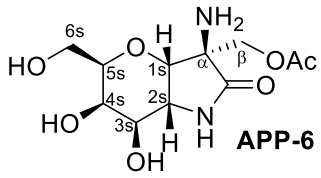

APP-6

A hydrogenolysis of a methanol solution (5 ml) of compound **20** (27 mg, 0.048 mmol) was held under atmospheric pressure and temperature, using Pd-C (25 mg) and HCl conc. (3 drops) as catalyst. The reaction was performed for 12 h, the catalyst was then filtered over diatomaceous earth and the liquid phase was concentrated. The residue was dissolved in H_2O (5 ml) and washed with EtOAc (2 x 5 ml). The combined aqueous phases were concentrated and the residue was dissolved in H_2O (2 ml) and eluted through a reverse-phase Sep-pak C18 cartridge affording **APP-6** (13 mg, 0,044 mmol, 94 %) as a yellow oil. $[\alpha]_D^{25}$ = +42.3 (c 1.00, H_2O). HRMS ESI+ (m/z): 291.1188 [M+H$^+$]; calcd for $C_{11}H_{19}N_2O_7^+$, 291.1187. ^{1}H NMR (400 MHz, D_2O) δ (ppm) 2.17 (s, 3H, CH_3), 3.69-3.84 (m, 2H, H^{6s}), 3.84-4.08 (m, 4H, H^{5s}, H^{4s}, H^{3s}, H^{2s}), 4.51 (d, *J* = 12.3 Hz, 1H, H^{β}), 4.66 (d, *J* = 12.3 Hz, 1H, H^{β}), 4.96 (d, *J* = 8.1 Hz, 1H, H^{1s}). ^{13}C NMR (100 MHz, D_2O) δ (ppm) 20.1 (CH_3), 53.1 (C^{2s}), 61.1 (C^{β}), 61.4 (C^{6s}), 61.8 (C^{α}), 67.4 (C^{4s}), 71.8 (C^{3s}), 74.3 (C^{1s}), 77.4 (C^{5s}), 169.7 (O*C*OCH$_3$), 172.6 (NH*C*O).

(3*R*,3a*S*,5*R*,6*R*,7*R*,7a*R*)-3-Amino-6,7-dihydroxy-3,5-bis(hydroxymethyl)-1,3a,5,6,7,7a-hexahydropyrano[3,2-*b*]pyrrol-2-one (APP-7).

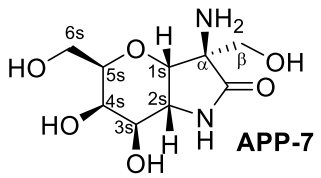

APP-7

A hydrogenolysis of a methanol solution (5 ml) of the compound **15** (35 mg, 0.067 mmol) was held under atmospheric pressure and temperature, using Pd-C (35 mg) and HCl conc. (3 drops) as

catalyst. The reaction was performed for 12 h. The catalyst was then filtered over diatomaceous earth and the liquid phase was concentrated. The residue was dissolved in H_2O (5 ml) and washed with EtOAc (2 x 5 ml). The combined aqueous phases were concentrated affording **APP-7** (16 mg, 0.064 mmol, 96 %) as a yellow oil. $[\alpha]_D^{25}$ = +32.6 (c 1.00, H_2O). HRMS ESI+ (m/z): 249.1087 [M+H^+]; calcd for $C_9H_{17}N_2O_6^+$, 249.1081. ^{1}H NMR (400 MHz, D_2O) δ (ppm) 3.71-3.84 (m, 2H, H^{6s}), 3.90-4.16 (m, 6H, H^{5s}, H^{4s}, H^{3s}, H^{2s}, H^{β}), 4.96 (d, *J* = 5.6 Hz, 1H, H^{1s}). ^{13}C NMR (100 MHz, D_2O) δ (ppm) 53.0 (C^{2s}), 59.0 (C^{β}), 61.4 (C^{6s}), 63.6 (C^{α}), 67.4 (C^{4s}), 71.8 (C^{3s}), 73.8 (C^{1s}), 77.3 (C^{5s}), 170.7 (NH*C*O).

General procedure for the preparation of pseudoglycoside iminosugar derivatives (21-24). $BF_3.OEt_2$ (20 μL, 0.15 mmol, 0.5 equiv.) was added to a stirred solution of the previously synthesized corresponding fluoroderivative **38-Gal** or **38-Glc**[24] (0.30 mmol) and **Fmoc-Ser-O^{t}Bu** or **Fmoc-Thr-O^{t}Bu** (0.30 mmol) in anhydrous DCM (4 mL) at 0 ºC under nitrogen atmosphere. The mixture was stirred for 60 min (TLC monitoring). The solvent was removed under reduced pressure and the resulting residue subjected to column chromatography to afford the corresponding α-*O*-glycosyl derivatives with *galacto* configuration (**21**, **22**) and *gluco* configuration (**23**, **24**).

1-*O*-(Fmoc-L-Ser)-(1*R*)-2,3,4-tri-*O*-acetyl-5*N*,6*ᵅ*-(oxomethylidene) galactonojirimycin (21).

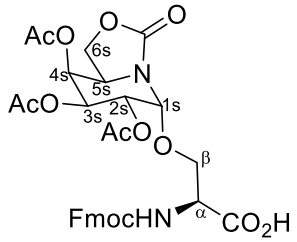

21

Purification by column chromatography (5:1 EtOAc/MeOH) afforded compound **21** (42 mg, 0.062 mmol, 73%). $[\alpha]_D^{25}$ = +61.8 (c 1.10, MeOH). HRMS ESI+ (m/z): 679.3 [M+K$^+$]; calcd for $C_{31}H_{32}KN_2O_{13}^+$, 679.1536. Elem. Anal.: C 57.85, H 5.11, N 4.10. Calcd for $C_{31}H_{32}N_2O_{13}$: C 58.12, H 5.04, N 4.37. ^{1}H NMR (500 MHz, CD_3OD) δ (ppm) 1.97 (s, 3H, CH_3CO), 2.04 (s, 3H, CH_3CO), 2.12 (s, 3H, CH_3CO), 3.83 (dd, *J* = 5.1 Hz, 1H, H^{β}), 3.94 (dd, *J* = 10.5, 3.3 Hz, 1H, H^{β}), 4.02-4.15 (m, 1 H, H^{6s}), 4.23 (t, *J* = 6.8 Hz, 1H, CH^{Fmoc}), 4.29-4.40 (m, 5H, H^{5s}, H^{6s}, H^{α}, CH_2^{Fmoc}), 4.99 (dd, *J* = 4.1 Hz, 1H H^{2s}), 5.36 (b, *J* = 10.7 Hz, 1H, H^{3s}), 5.40-5.50 (m, 2H, H^{1s}, H^{4s}), 7.25-7.85 (m, 8H, Fmoc). ^{13}C NMR (125.7 MHz, CD_3OD) δ (ppm) 20.5 (CH_3CO), 20.6 (CH_3CO), 20.6 (CH_3CO), 48.4 (CH_{Fmoc}), 52.1 (C^{5s}), 65.0 (C^{6s}), 68.2 (CH_2^{Fmoc}), 68.9 (C^{2s}), 69.6 (C^{3s}), 70.0 (C^{4s}), 70.2 (C^{β}), 81.4 (C^{1s}), 120.9-145.4 (Arom.^{Fmoc}), 158.3 (CO), 158.5 (CO), 171.5-172.0 (CH_3CO), 173.4 (CO_2H).

1-*O*-(Fmoc-L-Thr)-(1*R*)-2,3,4-tri-*O*-acetyl-5*N*,6*ᵅ*-(oxomethylidene) galactonojirimycin (22).

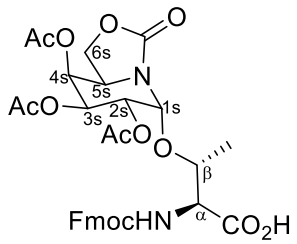

22

Purification by column chromatography (9:1 → 5:1 EtOAc/MeOH) afforded compound **22** (220 mg, 0.336 mmol, 91%). $[\alpha]_D^{25}$ = +50.5 (c 1.30, MeOH). HRMS ESI+ (m/z): 693.3 [M+K$^+$]; calcd for $C_{32}H_{34}KN_2O_{13}^+$, 693.7228. Elem. Anal.: C 58.37, H 5.41, N 4.16. Calcd for $C_{32}H_{34}N_2O_{13}$: C 58.71, H

5.24, N 4.28. ^{1}H NMR (500 MHz, CD_3OD) δ (ppm) 1.23 (d, *J* = 6.5 Hz, 3H, CH_3^{Thr}), 2.01 (s, 3H, CH_3CO), 2.11 (s, 3H, CH_3CO), 2.18 (s, 3H, CH_3CO), 4.07-4.17 (m, 1H, H^{6s}), 4.26-4.30 (m, 2H, H^{α}, CH^{Fmoc}), 4.33-4.50 (m, 5H, H^{6s}, H^{5s}, CH_2^{Fmoc}, H^{β}), 5.00 (dd, *J* = 4.0 Hz, 1H, H^{2s}), 5.37 (dd, *J* = 10.5, 2.5 Hz, 1H, H^{3s}), 5.46-5.51 (m, 2H, H^{1s}, H^{4s}), 7.25-7.83 (m, 8H, Fmoc). ^{13}C NMR (125.7 MHz, CD_3OD) δ (ppm) 18.7 (CH_3^{Thr}), 20.4 (*C*H_3CO), 20.6 (*C*H_3CO), 20.9 (*C*H_3CO), 47.0 (CH^{Fmoc}), 52.2 (C^{5s}), 59.9 (C^{α}), 64.9 (C^{6s}), 68.0 (C^{β}), 68.6 (C^{2s}), 69.4 (C^{3s}), 70.0 (C^{4s}), 77.1 (CH_2^{Fmoc}), 81.5 (C^{1s}), 120.9-145.3 (Arom.^{Fmoc}), 157.7 (CO), 159.0 (CO), 171.6-171.9 (CH_3CO), 173.1 (CO_2H).

1-*O*-(Fmoc-L-Ser)-(1*R*)-2,3,4-tri-*O*-acetyl-5*N*,6*O*-(oxomethylidene)noji-rimycin (23).

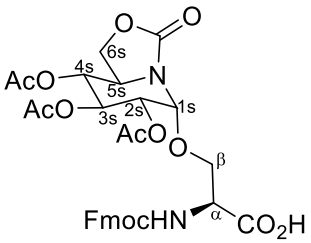

23

Purification by column chromatography (2:1 EtOAc/cyclohexane → 5:1 EtOAc/MeOH) afforded compound **23** (142 mg, 0.222 mmol, 72%). $[\alpha]_D^{25}$ = +36.7 (c 1.40, MeOH). HRMS ESI+ (m/z): 639.3 [M-H]; calcd for $C_{31}H_{33}N_2O_{13}^-$, 639.5905. Elem. Anal.: C 58.42, H 5.04, N 4.21. Calcd for $C_{31}H_{32}N_2O_{13}$: C 58.12, H 5.04, N 4.37. ^{1}H NMR (500 MHz, CD_3OD) δ (ppm) 2.01 (s, 3H, CH_3CO), 2.03 (s, 3H, CH_3CO), 2.04 (s, 3H, CH_3CO), 3.86 (dd, *J* = 5.6 Hz, 1H, H^{β}), 3.97 (dd, *J* = 10.0, 3.2 Hz, 1H, H^{β}), 4.05-4.15 (m, 1H, H^{5s}), 4.18-4.28 (m, 2H, H^{6s}, CH^{Fmoc}), 4.31-4.38 (m, 3H, CH_2^{Fmoc}, H^{α}), 4.42 (t, *J* = 8.5 Hz, 1H, H^{6s}), 4.90 (dd, *J* = 4.0 Hz, 1H, H^{2s}), 5.08 (t, *J* = 9.5 Hz, 1H, H^{4s}), 5.43 (d, *J* = 4.0 Hz, 1H, H^{1s}), 5.50 (t, *J* = 9.5 Hz, 1H, H^{3s}), 7.25-7.85 (m, 8H, Fmoc). ^{13}C NMR (125.7 MHz, CD_3OD) δ (ppm) 20.4 (C*H*$_3$CO), 20.5 (C*H*$_3$CO), 20.6 (C*H*$_3$CO), 48.3 (CH^{Fmoc}), 52.9

(C^{5s}), 56.7 (C^{α}), 68.1 (C^{6s}, CH_2^{Fmoc}), 70.6 (C^{3s}, C^{β}), 71.7 (C^{2s}), 73.5 (C^{4s}), 80.8 (C^{1s}), 120.9-145.3 (Fmoc), 157.9 (CO), 158.4 (CO), 171.4-171.8 (CH_3CO), 174.9 (CO_2H).

1-*O*-(Fmoc-L-Thr)-(1*R*)-2,3,4-tri-*O*-acetyl-5*N*,6*ᵅ*-(oxomethylidene)nojirimycin (22).

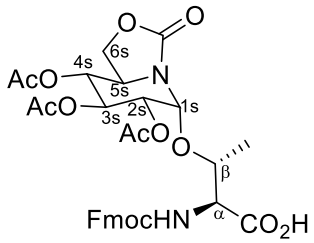

24

Purification by column chromatography (2:1 EtOAc/cyclohexane → 5:1 EtOAc/MeOH) afforded compound **24** (180 mg, 0.275 mmol, 71%). $[\alpha]_D^{25}$ = +45.0 (c 1.00, MeOH). HRMS ESI+ (m/z): 653.3 [M-H]; calcd for $C_{32}H_{34}N_2O_{13}^-$, 653.1988. Elem. Anal.: C 58.40, H 5.53, N 4.08. Calcd for $C_{32}H_{34}N_2O_{13}$: C 58.71, H 5.24, N 4.28. ^{1}H NMR (400 MHz, CD_3OD) δ (ppm) 1.22 (d, *J* = 6.5 Hz, 3H Me^{Thr}), 2.07 (s, 3H, CH_3CO), 2.08 (s, 3H, CH_3CO), 2.10 (s, 3H, CH_3CO), 4.05-4.15 (m, 1H, H^{5s}), 4.24-4.35 (m, 3H, H^{6s}, CH^{Fmoc}, H^{α}), 4.46-4.36 (m, 3H, CH_2^{Fmoc}, H^{β}), 4.54 (t, *J* = 8.0 Hz, 1H, H^{6s}), 4.85-4.91 (m, 1H, H^{2s}), 5.10 (t, *J* = 9.6 Hz, 1H, H^{4s}), 5.47 (d, *J* = 3.6 Hz, 1H, H^{1s}), 5.50 (t, *J* = 9.6 Hz, 1H, H^{3s}), 7.30-7.90 (m, 8H, Fmoc). ^{13}C NMR (100 MHz, CD_3OD) δ (ppm) 19.0 (Me^{Thr}), 20.5 (CH_3CO), 20.6 (CH_3CO), 20.7 (CH_3CO), 48.4 (CH^{Fmoc}), 53.2 (C^{5s}), 59.9 (C^{α}), 68.1 (C^{β}), 68.3 (C^{6s}), 70.5 (C^{3s}), 71.6 (C^{2s}), 73.6 (C^{4s}), 77.3 (CH_2^{Fmoc}), 81.1 (C^{1s}), 120.9-145.3 (Fmoc), 157.6 (CO), 159.1 (CO), 171.6-171.8 (Me*CO*), 173.1 (CO_2H).

General prodedure for the reduction-acetylation reaction. To a stirred solution of the corresponding glycoaminoacids (**46-50**, 50 mg, 0.08 mmol) in THF/AcOH/Ac_2O (1.8 mL, 3:2:1), cooled at 0 ºC, Zn (68 mg, 1.04 mmol) and saturated aq $CuSO_4$ (125 μL) were added. The reaction mixture was stirred for 2.5 h (TLC monitoring), filtered through Celite using EtOAc as eluent and concentrated. The resulting residue was purified by column chromatography to afford the corresponding 2-acetamido derivatives **25-28.**

1-*O*-(Fmoc-L-Ser)-(1*R*)-3,4-di-*O*-acetyl-2-acetamido-2-deoxy-5*N*,6*O*-(oxomethylidene)galactonojirimycin (25).

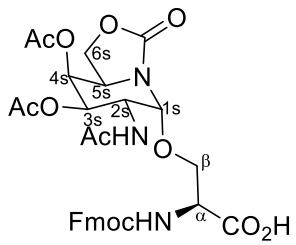

25

Purification by column chromatography (5:1 → 3:1 EtOAc/MeOH) afforded compound **25** (100 mg, 0.16 mmol, 88%). $[\alpha]_D^{25}$ = +60.3 (c 1.40, MeOH). HRMS ESI+ (m/z): 638.1 [M-H]; calcd for $C_{31}H_{32}N_3O_{12}^-$, 638.1991. Elem. Anal.: C 58.35, H 5.29, N 6.28. Calcd for $C_{31}H_{33}N_3O_{12}$: C 58.21, H 5.20, N 6.57. ^{1}H NMR (300 MHz, CD_3OD) δ (ppm) 1.96 (s, 3H, CH_3CO), 2.00 (s, 3H, CH_3CO), 2.15 (s, 3H, CH_3CONH), 3.82-3.95 (m, 2H, H^{β}), 4.01-4.12 (m, 1H, H^{6s}), 4.20 (t, *J* = 6.4 Hz, 1H, CH^{Fmoc}), 4.24-4.50 (m, 6H, H^{2s}, H^{5s}, H^{6s}, CH_2^{Fmoc}, H^{α}), 5.15 (d, *J* = 11.4 Hz, 1H, H^{3s}), 5.21 (d, *J* = 3.3 Hz, 1H, H^{1s}), 5.44 (t, *J* = 2.1 Hz, 1H, H^{4s}), 7.23-7.85 (m, 8H, Fmoc). ^{13}C NMR (75 MHz, CD_3OD) δ (ppm) 20.5 (CH_3CO), 20.6 (CH_3CO), 22.7 (CH_3CONH), 48.3 (CH^{Fmoc}), 52.3 (C^{5s}), 56.4 (C^{α}), 64.9 (C^{6s}), 68.0 (CH_2^{Fmoc}), 69.3 (C^{4s}), 70.1 (C^{3s}), 70.2 (C^{β}), 82.6 (C^{1s}), 121.0-145.3 (Fmoc), 158.3 (NCO), 158.2 (NCO), 171.9 (CH_3CO), 172.0 (CH_3CO), 172.0 (CH_3CONH), 173.6 (CH_3CONH), 174.7 (COOH).

1-*O*-(Fmoc-L-Thr)-(1*R*)-3,4-di-*O*-acetyl-2-acetamido-2-deoxy-5*N*,6*O*-(oxomethylidene)galactonojirimycin (26).

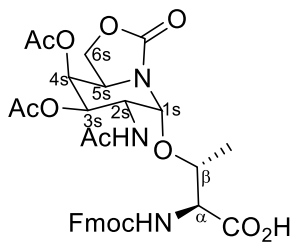

26

Purification by column chromatography (5:1 → 3:1 → 1:1 EtOAc/MeOH) afforded compound **26** (77 mg, 0.18 mmol, 74%). $[\alpha]_D^{25}$ = +41.6 (c 1.00, MeOH). HRMS ESI+ (m/z): 652.1 [M-H]; calcd for $C_{32}H_{34}N_3O_{12}^-$, 652.2148. Elem. Anal.: C 58.91, H 5.32, N 6.19. Calcd for $C_{32}H_{35}N_3O_{12}$: C 58.80, H 5.40, N 6.43. ^{1}H NMR (300 MHz, CD_3OD) δ (ppm) 1.17 (d, *J* = 6.0 Hz, 1H, Me^{Thr}), 1.96 (s, 3H, CH_3CO), 2.00 (s, 3H, CH_3CO), 2.16 (s, 3H, CH_3CONH), 4.07-4.16 (m, 2H, H^{α}, CH_2^{Fmoc}), 4.23 (t, *J* = 6.4 Hz, 1H, CH^{Fmoc}), 4.30-4.60 (m, 6H, H^{2s}, H^{5s}, H^{6s}, H^{β}, CH_2^{Fmoc}), 5.13 (d, *J* = 11.0 Hz, 1H, H^{3s}), 5.34 (d, *J* = 3.8 Hz, 1H, H^{1s}), 5.45 (t, *J* = 2.5 Hz, 1H, H^{4s}), 7.24-7.86 (m, 8H, Fmoc). ^{13}C NMR (75 MHz, CD_3OD) δ (ppm) 18.9 (CH_3^{Thr}), 20.7 (CH_3CO), 20.8 (CH_3CO), 23.1 (CH_3CONH), 48.5 (C^{2s}, CH^{Fmoc}), 52.6 (C^{5s}), 60.9 (C^{α}), 65.0 (CH_2^{Fmoc}), 67.7 (C^{6s}), 69.4 (C^{4s}), 70.3 (C^{3s}), 77.3 (C^{β}), 82.6 (C^{1s}), 120.9-145.4 ($Arom.^{Fmoc}$), 158.1 (NCO), 158.9 (NCO), 171.8 (CH_3CO), 171.9 (CH_3CO), 171.9 (CH_3CONH), 174.1 (COOH).

1-*O*-(Fmoc-L-Ser)-(1*R*)-3,4-di-*O*-acetyl-2-acetamido-2-deoxy-5*N*,6*O*-(oxomethylidene)nojirimycin (27).

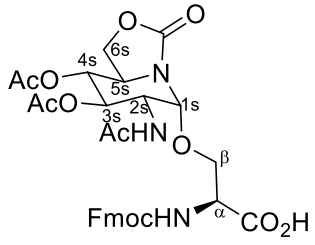

27

Purification by column chromatography (5:1 EtOAc/MeOH) afforded compound **27** (38 mg, 0.06 mmol, 73%). $[\alpha]_D^{25}$ = +33.9 (c 1.00, MeOH). HRMS ESI+ (m/z): 638.2 [M-H]; calcd for $C_{31}H_{32}N_3O_{12}^-$, 638.1991. Elem. Anal.: C 57.87, H 4.83, N 6.21. Calcd for $C_{31}H_{33}N_3O_{12}$: C 58.21, H

5.20, N 6.57. ^{1}H NMR (300 MHz, CD_3OD) δ (ppm) 1.96 (s, 3H, CH_3CO), 2.00 (s, 3H, CH_3CO), 2.03 (s, 3H, CH_3CONH), 3.89-3.94 (m, 2H, H^{β}), 4.08 (bq, J = 8.4 Hz, 1H, H^{5s}), 4.30-4.34 (m, 1H, H^{2s}), 4.21-4.52 (m, 6H, H^{6s}, CH_2^{Fmoc}, H^{α}, CH^{Fmoc}), 5.06 (t, J = 9.5 Hz, 1H, H^{4s}), 5.14 (d, J = 3.6 Hz, 1H, H^{1s}), 5.28 (t, J = 9.5 Hz, 1H, H^{3s}), 7.28-7.83 (m, 8H, Fmoc). ^{13}C NMR (75 MHz, CD_3OD) δ (ppm) 20.5 (CH_3CO), 20.5 (CH_3CO), 22.6 (CH_3CONH), 48.3 (CH^{Fmoc}), 52.4 (C^{2s}), 53.1 (C^{5s}), 55.1 (C^{α}), 68.1 (C^{6s}, CH_2^{Fmoc}), 70.1 (C^{β}), 71.6 (C^{3s}), 73.8 (C^{4s}), 82.4 (C^{1s}), 120.9-145.2 (Arom.^{Fmoc}), 157.9 (NCO), 158.4 (NCO), 171.7 (CH_3CO), 171.8 (CH_3CO), 171.8 (CH_3CONH), 173.4 (COOH).

1-*O*-(Fmoc-L-Thr)-(1*R*)-3,4-di-*O*-acetyl-2-acetamido-2-deoxy-5*N*,6*O*-(oxomethylidene)nojirimycin (28).

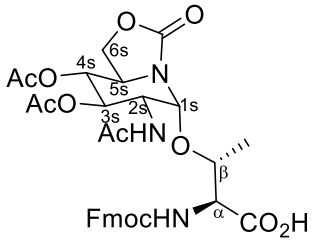

28

Purification by column chromatography (5:1 EtOAc/MeOH) afforded compound **28** (138 mg, 0.21 mmol, 93%). $[\alpha]_D^{25}$ = +38.9 (c 1.00, MeOH). HRMS ESI+ (m/z): 652.2 [M-H]; calcd for $C_{32}H_{34}N_3O_{12}^-$, 652.2148. Elem. Anal.: C 58.73, H 5.50, N 6.34. Calcd for $C_{32}H_{35}N_3O_{12}$: C 58.80, H 5.40, N 6.43. ^{1}H NMR (300 MHz, CD_3OD) δ (ppm) 1.17 (d, J = 6.0 Hz, 1H, Me^{Thr}), 2.00 (s, 3H, CH_3CO), 2.00 (s, 3H, CH_3CO), 2.06 (s, 3H, CH_3CONH), 4.02-4.12 (m, 1H, H^{5s}), 4.16-4.59 (m, 8H, H^{6s}, H^{2s}, CH_2^{Fmoc}, CH^{Fmoc}, H^{β}, H^{α}), 5.08 (t, J = 10.0 Hz, 1H, H^{4s}), 5.22-5.32 (m, 2H, H^{1s}, H^{3s}), 7.24-7.90 (m, 8H, Fmoc). ^{13}C NMR (75 MHz, CD_3OD) δ (ppm) 18.8 (CH_3^{Thr}), 20.5 (CH_3CO), 20.6 (CH_3CO), 22.9 (CH_3CONH), 49.8 (CH^{Fmoc}), 52.4 (C^{2s}), 53.3 (C^{5s}), 60.4 (C^{α}), 67.7 (CH_2^{Fmoc}), 68.2 (C^{6s}), 71.8 (C^{3s}), 73.7 (C^{4s}), 77.6 (C^{β}), 82.3 (C^{1s}), 120.9-145.4 (Arom.^{Fmoc}), 157.6 (NCO), 158.8

(NCO), 171.7 (CH_3CO), 171.9 (CH_3CO), 171.9 (CH_3CONH), 173.6 (COOH).

H_2N-Ala-Pro-Asp-(sp^2Gal)Ser-Arg-Pro-NH_2 (29):

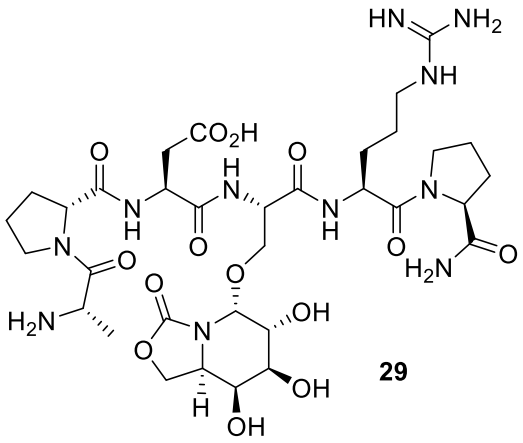

29

The glycosylated amino acid building block **21** (84 mg, 0.13 mmol) was coupled manually, while the other Fmoc-amino acids were coupled in the automated mode. After elimination of acetate groups and cleavage, glycopeptide **29** was obtained and then purified by reversed-phase HPLC and lyophilized.

Table 6.1. Semi-preparative HPLC gradient (t_R 27.4 min).

Time (min)	Flow (mL/min)	MeCN (%)	H_2O + 0.1% TFA (%)
0	10	2	98
30	10	10	90
35	10	20	80
40	10	2	98

HRMS (ESI) (m/z) 414.6964 $[M+H]^{2+}$, calcd for $C_{33}H_{55}N_{11}O_{14}^{2+}$: 414.6959. ^1H NMR (400 MHz, D_2O) δ (ppm) 1.56 (d, J = 7.0 Hz, 3H, CH_3 $_{Ala}$), 1.64-1.81 (m, 3H, 2Hγ $_{Arg}$, Hβ $_{Arg}$), 1.85-2.12 (m, 7H, Hβ $_{Arg}$, 2Hβ $_{Pro}$, 4Hγ $_{Pro}$), 2.29-2.40 (m, 2H, 2Hβ $_{Pro}$), 2.80-2.97 (m, 2H, 2Hβ $_{Asp}$), 3.24 (t, J = 6.9 Hz, 2H, Hδ $_{Arg}$), 3.62-3.69 (m, 2H, 2Hδ $_{Pro}$), 3.71-3.76 (m, 1H, Hδ $_{Pro}$), 3.78-3.93 (m, 5H, Hδ $_{Pro}$, 2Hβ $_{Ser}$, H^{2s}, H^{3s}), 3.99 (s, 1H, H^{4s}), 4.14 (t, J = 7.8 Hz, 1H,

H^{5s}), 4.35-4.57 (m, 5H, 2Hα $_{Pro}$, Hα $_{Ala}$, 2H^{6s}), 4.60-4.72 (m, 3H, Hα $_{Ser}$, Hα $_{Asp}$, Hα $_{Arg}$), 5.19 (d, J = 4.1 Hz, 1H, H^{1s}). ^{1}H NMR (400 MHz, D_2O/H_2O 1:9, amide region) δ (ppm) 7.00 (s, 1H, $NH_{2\ term.}$), 7.13-7.22 (m, 1H, NH $_{Arg}$), 7.71 (s, 1H, $NH_{2\ term.}$), 8.38 (d, J = 7.3 Hz, 1H, NH $_{Ser}$), 8.43 (d, J = 7.2 Hz, 1H, NH $_{Arg}$), 8.63 (d, J = 6.9 Hz, 1H, NH $_{Asp}$). ^{13}C NMR (100 MHz, D_2O) δ (ppm) 15.1 ($CH_{3\ Ala}$), 24.1 (Cγ $_{Arg}$), 24.7 (2Cγ $_{Pro}$), 27.5 (Cβ $_{Arg}$), 29.5 (2Cβ $_{Pro}$), 35.7 (Cβ $_{Asp}$), 40.5 (Cδ $_{Arg}$), 47.6 (Cδ $_{Pro}$), 47.9 (Cδ $_{Pro}$), 48.1 (Cα $_{Ala}$), 50.2 (Cα $_{Arg}$), 51.3 (Cα $_{Asp}$), 52.7 (C^{5s}), 53.1 (Cα $_{Ser}$), 60.3 (Cα $_{Pro}$), 60.4 (Cα $_{Pro}$), 64.5 (C^{6s}), 67.0 (Cβ $_{Ser}$), 67.5 (C^{2s}), 69.0 (C^{4s}), 69.3 (C^{3s}), 82.0 (C^{1s}), 156.7 (C=N $_{Arg}$), 169.3, 170.8, 172.2, 173.5, 174.4, 174.7, 176.8 (CO).

H_2N-Ala-Pro-Asp-(*sp*^{2}Gal)Thr-Arg-Pro-NH_2 (30):

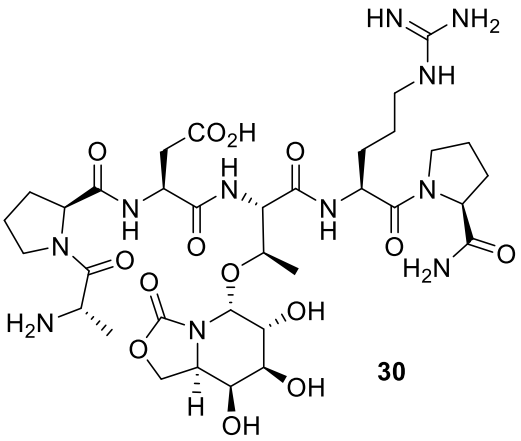

30

The glycosylated amino acid building block **22** (81 mg, 0.13 mmol) was coupled manually, while the other Fmoc-amino acids were coupled in the automated mode. After elimination of acetate groups and cleavage, glycopeptide **30** was obtained and then purified by reversed-phase HPLC and lyophilized.

Table 6.2. Semi-preparative HPLC gradient (t_R 34.0 min).

Time (min)	Flow (mL/min)	MeCN (%)	H_2O + 0.1% TFA (%)
0	10	2	98
30	10	10	90
35	10	20	80
40	10	2	98

HRMS (ESI) (m/z) 421.7047 $[M+2H]^+$, calcd for $C_{34}H_{57}N_{11}O_{14}^{2+}$: 421.7038. ^{1}H NMR (400 MHz, D_2O) δ (ppm) 1.17 (d, *J* = 6.4 Hz, 3H, $CH_{3\ Thr}$)**,** 1.56 (d, *J* = 6.9 Hz, 3H, $CH_{3\ Ala}$), 1.67-1.84 (m, 3H, 2Hγ $_{Arg}$, Hβ $_{Arg}$), 1.86-2.13 (m, 7H, Hβ $_{Arg}$, 2Hβ $_{Pro}$, 4Hγ $_{Pro}$), 2.28-2.40 (m, 2H, 2Hβ $_{Pro}$), 2.84-3.04 (m, 2H, 2Hβ $_{Asp}$), 3.25 (t, *J* = 7.1 Hz, 2H, 2Hδ $_{Arg}$), 3.61-3.76 (m, 3H, 3Hδ $_{Pro}$), 3.78-3.89 (m, 2H, Hδ $_{Pro}$, H^{2s}), 3.94 (dd, *J* = 10.2, 2.6 Hz, 1H, H^{3s}), 4.02 (s, 1H, H^{4s}), 4.21-4.31 (m, 2H, H^{5s}, Hβ $_{Thr}$), 4.35-4.46 (m, 3H, Hα $_{Pro}$, Hα $_{Ala}$, H^{6s}), 4.50 (t, *J* = 7.4 Hz, 1H, Hα $_{Pro}$), 4.53-4.59 (m, 2H, Hα $_{Thr}$, H^{6s}), 4.67-4.72 (m, 1H, Hα $_{Arg}$), 4.79 (m, 1H, Hα $_{Asp}$), 5.28 (d, *J* = 4.5 Hz, 1H, H^{1s}). ^{1}H NMR (400 MHz, D_2O/H_2O 1:9, amide region) δ (ppm) 6.69 (s, 1H, $NH_{2\ term.}$), 7.14-7.20 (m, 1H, NH $_{Arg}$), 7.69 (s, 1H, $NH_{2\ term.}$), 8.23 (d, *J* = 7.2 Hz, 1H, NH $_{Arg}$), 8.52 (d, *J* = 8.3 Hz, 1H, NH $_{Thr}$), 8.69 (d, *J* = 7.1 Hz, 1H, NH $_{Asp}$). ^{13}C NMR (75 MHz, D_2O) δ (ppm) 15.0 ($CH_{3\ Ala}$), 17.2 ($CH_{3\ Thr}$), 24.1 (Cγ $_{Arg}$), 24.6 (2Cγ $_{Pro}$), 27.5 (Cβ $_{Arg}$), 29.4 (Cβ $_{Pro}$), 29.6(Cβ $_{Pro}$), 35.5 (Cβ $_{Asp}$), 40.5 (Cδ $_{Arg}$), 47.7 (Cδ $_{Pro}$), 47.9 (Cδ $_{Pro}$), 48.0 (Cα $_{Ala}$), 50.1 (Cα $_{Asp}$), 51.4 (Cα $_{Arg}$), 52.9 (C^{5s}), 56.9 (Cα $_{Thr}$), 60.3 (2Cα $_{Pro}$), 64.5 (C^{6s}), 67.5 (C^{2s}), 69.1 (C^{4s}), 69.3 (C^{3s}), 73.9 (Cβ $_{Thr}$), 82.0 (C^{1s}), 156.7 (C=N $_{Arg}$), 158.3 ($NCO_{2\ Gal}$), 169.2, 170.6, 171.4, 172.6, 173.4, 174.3, 176.8 (CO).

H_2N-Ala-Pro-Asp-(sp^2Glc)Ser-Arg-Pro-NH_2 (31):

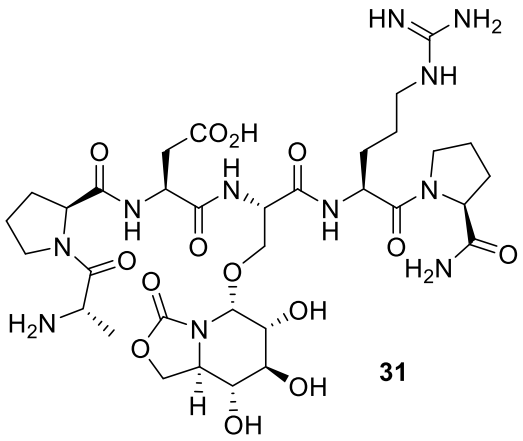

31

The glycosylated amino acid building block **23** (82 mg, 0.13 mmol) was coupled manually, while the other Fmoc-amino acids were coupled in the automated mode. After elimination of acetate groups and cleavage, glycopeptide **31** was obtained and then purified by reversed-phase HPLC and lyophilized.

Table 6.3. Semi-preparative HPLC gradient (t_R 25.0 min).

Time (min)	Flow (mL/min)	MeCN (%)	H_2O + 0.1% TFA (%)
0	10	2	98
30	10	15	85
40	10	2	98

HRMS (ESI) (m/z) 828.3838 $[M+H]^+$, calcd for $C_{33}H_{54}N_{11}O_{14}^+$: 828.3846. ^{1}H NMR (400 MHz, D_2O) δ (ppm) 1.58 (d, J = 7.0 Hz, 3H, CH_3 $_{Ala}$), 1.66-1.83 (m, 3H, 2Hγ $_{Arg}$, Hβ $_{Arg}$), 1.86-2.16 (m, 7H, Hβ $_{Arg}$, 2Hβ $_{Pro}$, 4Hγ $_{Pro}$), 2.29-2.42 (m, 2H, 2Hβ $_{Pro}$), 2.71-2.90 (m, 2H, 2Hβ $_{Asp}$), 3.26 (t, J = 7.0 Hz, 2H, 2Hδ $_{Arg}$), 3.55 (t, J = 9.3 Hz, 1H, H^{4s}), 3.61-3.73 (m, 4H, 2Hδ $_{Pro}$, H^{2s}, H^{3s}), 3.77-3.92 (m, 5H, 2Hδ $_{Pro}$, 2Hβ $_{Ser}$, H^{5s}), 4.36-4.48 (m, 3H, Hα $_{Ala}$, Hα $_{Pro}$, H^{6s}), 4.50-4.54 (m, 1H, Hα $_{Pro}$), 4.63-4.74 (m, 4H, H^{6s}, Hα $_{Asp}$, Hα $_{Arg}$, Hα $_{Ser}$), 5.16 (d, J = 4.0 Hz, 1H, H^{1s}). ^{1}H NMR (400 MHz, D_2O/H_2O 1:9, amide region) δ (ppm) 6.57-6.77 (br s, 2H, NH_2 $_{Arg}$), 7.00 (s, 1H, NH_2 $_{term.}$), 7.27 (t, J = 5.8 Hz, 1H, NH $_{Arg}$), 7.70 (s, 1H, NH_2 $_{term.}$), 8.36 (d, J = 7.4 Hz,

1H, NH $_{Ser}$), 8.47 (d, J = 7.3 Hz, 1H, NH $_{Arg}$), 8.55 (d, J = 6.7 Hz, 1H, NH $_{Asp}$). ^{13}C NMR (100 MHz, D_2O) δ (ppm) 15.1 ($CH_{3\ Ala}$), 24.0 (Cγ $_{Arg}$), 24.7 (2Cγ $_{Pro}$), 27.6 (Cβ $_{Arg}$), 29.3 (Cβ $_{Pro}$), 29.6 (Cβ $_{Pro}$), 37.2 (Cβ $_{Asp}$), 40.6 (Cδ $_{Arg}$), 47.7 (Cδ $_{Pro}$), 47.9 (Cδ $_{Pro}$), 48.1 (Cα $_{Ala}$), 50.9 (Cα $_{Asp}$), 51.2 (Cα $_{Arg}$), 53.0 (Cα $_{Ser}$), 53.2 (C^{5s}), 60.3 (Cα $_{Pro}$), 60.5 (Cα $_{Pro}$), 66.9 (Cα $_{Ser}$), 67.7 (C^{6s}), 70.9 (C^{2s}), 72.4 (C^{3s}), 73.5 (C^{4s}), 81.8 (C^{1s}), 156.8 (C=N $_{Arg}$), 158.2 ($NCO_{2\ Glc}$), 169.4, 170.9, 171.3, 172.8, 173.5, 174.3, 176.9 (CO).

H_2N-Ala-Pro-Asp-(*sp*^{2}Glc)Thr-Arg-Pro-NH_2 (32):

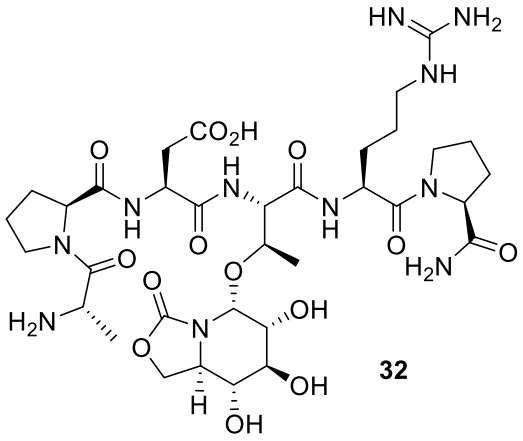

32

The glycosylated amino acid building block **24** (82 mg, 0.13 mmol) was coupled manually, while the other Fmoc-amino acids were coupled in the automated mode. After elimination of acetate groups and cleavage, glycopeptide **32** was obtained and then purified by reversed-phase HPLC and lyophilized.

Table 6.4. Semi-preparative HPLC gradient (t_R 34.9 min).

Time (min)	Flow (mL/min)	MeCN (%)	H_2O + 0.1% TFA (%)
0	10	2	98
30	10	10	90
35	10	20	80
40	10	2	98

HRMS (ESI) (m/z) 842.3992 $[M+H]^+$, calcd for $C_{34}H_{56}N_{11}O_{14}^+$: 842.4003. ^{1}H NMR (400 MHz, D_2O) δ (ppm) 1.19 (d, *J* = 6.4 Hz, 3H, $CH_{3\ Thr}$), 1.56 (d, *J* = 7.0 Hz, 3H, $CH_{3\ Ala}$), 1.69-2.10 (m, 10H, 2Hγ $_{Arg}$, 2Hβ $_{Arg}$, 2Hβ $_{Pro}$, 4Hγ $_{Pro}$), 2.26-2.38 (m, 2H, 2Hβ $_{Pro}$), 2.68-2.90 (m, 2H, 2Hβ $_{Asp}$), 3.19-3.29 (m, 2H, 2Hδ $_{Arg}$), 3.50-3.58 (m, 2H, H^{2s}, H^{4s}), 3.62-6.79 (m, 4H, H^{3s}, 3Hδ $_{Pro}$), 3.83-3.95 (m, 2H, Hδ $_{Pro}$, H^{5s}), 4.30-4.45 (m, 4H, Hβ $_{Thr}$, H^{6s}, Hα $_{Ala}$, Hα $_{Pro}$), 4.50 (dd, *J* = 7.6, 6.8 Hz, 1H, Hα $_{Pro}$), 4.55 (d, *J* = 2.6 Hz, 1H, Hα $_{Thr}$), 4.63-4.74 (m, 3H, H^{6s}, Hβ $_{Asp}$, Hα $_{Arg}$), 5.23 (d, *J* = 4.0 Hz, 1H, H^{1s}). ^{1}H NMR (400 MHz, D_2O/H_2O 1:9, amide region) δ (ppm) 6.99 (s, 1H, $NH_{2\ term.}$), 7.35 (t, *J* = 5.2 Hz, 1H, NH $_{Arg}$), 7.69 (s, 1H, $NH_{2\ term.}$), 8.29 (d, *J* = 6.8 Hz, 1H, NH $_{Arg}$), 8.53 (d, *J* = 8.4 Hz, 1H, NH $_{Thr}$), 8.61 (d, *J* = 6.9 Hz, 1H, NH $_{Asp}$). ^{13}C NMR (100 MHz, D_2O) δ (ppm) 15.1 ($CH_{3\ Ala}$), 17.4 ($CH_{3\ Thr}$), 24.0 (Cγ $_{Arg}$), 24.7 (2Cγ $_{Pro}$), 27.3 (Cβ $_{Arg}$), 29.4 (Cβ $_{Pro}$), 29.6 (Cβ $_{Pro}$), 37.8 (Cβ $_{Asp}$), 40.6 (Cδ $_{Arg}$), 47.7 (Cδ $_{Pro}$), 47.9 (Cδ $_{Pro}$), 48.1 (Cα $_{Ala}$), 51.0 (Cα $_{Arg}$), 51.7 (Cα $_{Asp}$), 53.5 (C^{5s}), 57.1 (Cα $_{Thr}$), 60.3 (2Cα $_{Pro}$), 67.5 (C^{6s}), 71.1 (C^{2s}), 72.4 (C^{3s}), 73.4 (C^{4s}), 74.2 (Cβ $_{Thr}$), 82.0 (C^{1s}), 156.8 (C=N $_{Arg}$), 157.9 ($NCO_{2\ Glc}$), 163.2, 169.2, 170.9, 171.6, 173.4, 173.5, 176.9 (CO).

H_2N-Ala-Pro-Asp-(sp^2GalNAc)Ser-Arg-Pro-NH_2 (33):

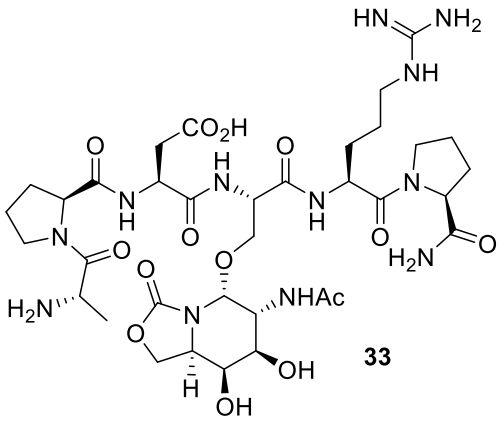

33

The glycosylated amino acid building block **25** (82 mg, 0.13 mmol) was coupled manually, while the other Fmoc-amino acids were coupled in the automated mode. After elimination of acetate groups and cleavage, glycopeptide **33** was obtained and then purified by reversed-phase HPLC and lyophilized.

Table 6.5. Semi-preparative HPLC gradient (t_R 29.1 min).

Time (min)	Flow (mL/min)	MeCN (%)	H_2O + 0.1% TFA (%)
0	10	2	98
30	10	10	90
35	10	20	80
40	10	2	98

HRMS (ESI) (m/z) 869.4109 $[M+H]^+$, calcd for $C_{35}H_{57}N_{12}O_{14}^+$: 869.4112. ^{1}H NMR (400 MHz, D_2O) δ (ppm) 1.52 (d, *J* = 7.0 Hz, 3H, $CH_{3\ Ala}$), 1.63-1.79 (m, 3H, $2H_{\gamma\ Arg}$, $H_{\beta\ Arg}$), 1.83-2.11 (m, 10H, $H_{\beta\ Arg}$, $2H_{\beta\ Pro}$, $4H_{\gamma\ Pro}$, NHCOC*H*$_3$), 2.25-2.38 (m, 2H, $2H_{\beta\ Pro}$), 2.83-3.00 (m, 2H, $2H_{\beta\ Asp}$), 3.21 (t, *J* = 6.7 Hz, 2H, $2H_{\delta\ Arg}$), 3.58-3.86 (m, 6H, $4H_{\delta\ Pro}$, $2H_{\beta\ Ser}$) 3.89 (dd, *J* = 11.0, 2.1 Hz, 1H, H^{3s}), 3.98 (s, 1H, H^{4s}), 4.09-4.15 (m, 1H, H^{5s}), 4.21 (dd, *J* = 10.8, 4.2 Hz, 1H, H^{2s}), 4.32-4.39 (m, 2H, $H_{\alpha\ Pro}$, $H_{\alpha\ Ala}$), 4.40-4.56 (m, 3H, $H_{\alpha\ Pro}$, $2H^{6s}$), 4.59 (t, *J* = 5.6 Hz, 1H, $H_{\alpha\ Ser}$) 4.63-4.72 (m, 2H, $H_{\alpha\ Arg}$, $H_{\alpha\ Asp}$), 5.10 (d, *J* = 4.2 Hz, 1H, H^{1s}) ^{1}H NMR (400 MHz, D_2O/H_2O 1:9, amide region) δ (ppm) 7.02 (s, 1H, $NH_{2\ term.}$), 7.25-7.32 (m, 1H, NH_{Arg}), 7.72 (s, 1H, $NH_{2\ term.}$), 8.08 (d, *J* = 9.3 Hz, 1H, N<u>H</u>Ac), 8.41 (d, *J* = 7.2 Hz, 1H, NH_{Ser}), 8.48 (d, 1H, *J* = 6.9 Hz, NH_{Arg}), 8.54 (d, *J* = 6.7 Hz, 1H, NH_{Asp}). ^{13}C

NMR (100 MHz, D_2O) δ (ppm) 15.1 ($CH_{3\ Ala}$), 22.1 ($NHCO\underline{C}H_3$), 24.1 ($C_{\gamma\ Arg}$), 24.7 ($2C_{\gamma\ Pro}$), 27.6 ($C_{\beta\ Arg}$), 29.4 ($C_{\beta\ Pro}$), 29.6 ($C_{\beta\ Pro}$), 35.2 ($C_{\beta\ Asp}$), 40.5 ($C_{\delta\ Arg}$), 47.7 ($C_{\delta\ Pro}$), 47.9 ($C_{\delta\ Pro}$), 48.1 ($C_{\alpha\ Ala}$), 48.7 (C^{2s}), 50.1 ($C_{\alpha\ Asp}$), 51.2 ($C_{\alpha\ Arg}$), 52.7 (C^{5s}), 53.1 ($C_{\alpha\ Ser}$), 60.3 ($C_{\alpha\ Pro}$), 60.4 ($C_{\alpha\ Pro}$), 64.6 (C^{6s}), 67.0 ($C_{\beta\ Ser}$), 67.8 (C^{3s}), 68.3 (C^{4s}), 80.7 (C^{1s}), 156.8 ($C{=}NH_{\ Arg}$), 158.4 (NCO_2), 169.3, 170.6, 171.2, 172.1, 173.6, 173.8, 174.5, 176.8 (CO).

H_2N-Ala-Pro-Asp-(*sp*^{2}GalNAc)Thr-Arg-Pro-NH_2 (34):

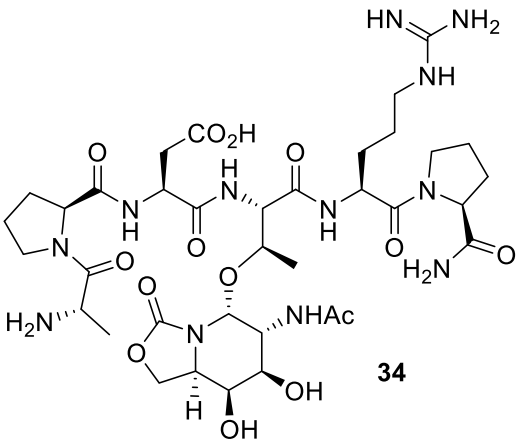

34

The glycosylated amino acid building block **26** (82 mg, 0.13 mmol) was coupled manually, while the other Fmoc-amino acids were coupled in the automated mode. After elimination of acetate groups and cleavage, glycopeptide **34** was obtained and then purified by reversed-phase HPLC and lyophilized.

Table 6.6. Semi-preparative HPLC gradient (t_R 34.6 min).

Time (min)	Flow (mL/min)	MeCN (%)	H_2O + 0.1% TFA (%)
0	10	2	98
30	10	10	90
35	10	20	80
40	10	2	98

HRMS (ESI) (m/z) 442.2161 $[M+2H]^{2+}$, calcd for $C_{36}H_{60}N_{12}O_{14}^{2+}$: 442.2170. ^1H NMR (400 MHz, D_2O) δ (ppm) 1.18 (d, 3H, J = 6.4 Hz, $CH_{3\ Thr}$) 1.54 (d, J = 7.0 Hz, 3H, $CH_{3\ Ala}$), 1.61-1.78 (m, 3H, $2H_{\gamma\ Arg}$, $H_{\beta\ Arg}$),

1.83-2.12 (m, 10H, $H\beta_{\ Arg}$, $2H\beta_{\ Pro}$, $4H\gamma_{\ Pro}$, NHCOC$\underline{H}_3$), 2.25-2.40 (m, 2H, $2H\beta_{\ Pro}$), 2.84-3.05 (m, 2H, $2H\beta_{\ Asp}$), 3.22 (t, J = 6.4 Hz, 2H, $2H\delta_{\ Arg}$), 3.59-3.77 (m, 4H, $4H\delta_{\ Pro}$), 3.93 (d, J = 10.9 Hz, 1H, H^{3s}), 4.02 (s, 1H, H^{4s}), 4.14-4.25 (m, 2H, H^{2s}, H^{5s}), 4.26-4.32 (m, 1H, $H\beta_{\ Thr}$), 4.34-4.59 (m, 6H, $H\alpha_{\ Ala}$, $2H\alpha_{\ Pro}$, $H\alpha_{\ Thr}$, $2H^{6s}$), 4.64-4.70 (m, 1H, $H\alpha_{\ Arg}$), 4.86-4.90 (m, 1H, $H\alpha_{\ Asp}$), 5.10 (d, J = 4.1 Hz, 1H, H^{1s}) ^{1}H NMR (400 MHz, D_2O/H_2O 1:9, amide region) δ (ppm) 6.99 (s, 1H, $NH_{2\ term.}$), 7.16-7.24 (m, 1H, $NH_{\ Arg}$), 7.71 (s, 1H, $NH_{2\ term.}$), 7.99 (d, J = 9.8 Hz, 1H, N$\underline{H}$Ac), 8.31 (d, J = 7.2 Hz, 1H, $NH_{\ Arg}$), 8.53 (d, J = 8.7 Hz, 1H, $NH_{\ Thr}$), 8.69 (d, J = 7.0 Hz, 1H, $NH_{\ Asp}$). ^{13}C NMR (100 MHz, D_2O) δ (ppm) 15.1 ($CH_{3\ Ala}$), 18.1 ($CH_{3\ Thr}$), 22.3 (NHCO$\underline{C}H_3$), 24.2 ($C\gamma_{\ Arg}$), 24.7 ($2C\gamma_{\ Pro}$), 27.8 ($C\beta_{\ Arg}$), 29.5 ($C\beta_{\ Pro}$), 29.6 ($C\beta_{\ Pro}$), 35.2 ($C\beta_{\ Asp}$), 40.6 ($C\delta_{\ Arg}$), 47.7 ($C\delta_{\ Pro}$), 47.9 ($C\delta_{\ Pro}$), 48.1 ($C\alpha_{\ Ala}$), 48.7 (C^{2s}), 49.9 ($C\alpha_{\ Asp}$), 51.2 ($C\alpha_{\ Arg}$), 53.0 (C^{5s}), 57.2 ($C\alpha_{\ Thr}$), 60.2 ($C\alpha_{\ Pro}$), 60.3 ($C\alpha_{\ Pro}$), 64.5 (C^{6s}), 68.2 (C^{3s}), 68.5 (C^{4s}), 74.5 ($C\beta_{\ Thr}$), 81.2 (C^{1s}), 156.8 ($C{=}NH_{\ Arg}$), 158.1 (NCO_2), 169.3, 170.8, 171.0, 172.7, 173.5, 173.9, 174.0, 176.8 (CO).

H_2N-Ala-Pro-Asp-(*sp*^{2}GlcNAc)Ser-Arg-Pro-NH_2 (35):

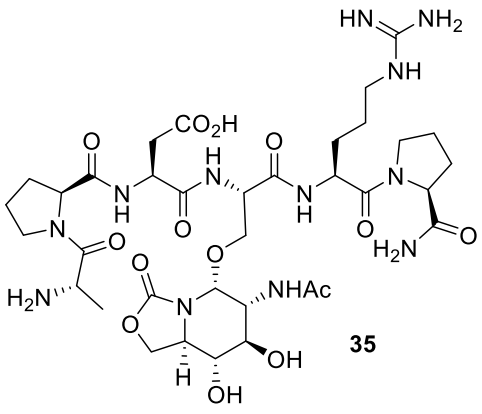

35

The glycosylated amino acid building block **27** (82 mg, 0.13 mmol) was coupled manually, while the other Fmoc-amino acids were coupled in the automated mode. After elimination of acetate groups and cleavage, glycopeptide **35** was obtained and then purified by reversed-phase HPLC and lyophilized.

Table 6.7. Semi-preparative HPLC gradient (t_R 29.0 min).

Time (min)	Flow (mL/min)	MeCN (%)	H_2O + 0.1% TFA (%)
0	10	2	98
30	10	10	90
35	10	20	80
40	10	2	98

HRMS (ESI) (m/z) 869.4109 $[M+H]^+$, calcd for $C_{35}H_{57}N_{12}O_{14}^+$: 869.4112. ^{1}H NMR (400 MHz, D_2O) δ (ppm) 1.55 (d, J = 7.0 Hz, 3H, $CH_{3\ Ala}$), 1.65-1.81 (m, 3H, $2H_{\gamma\ Arg}$, $H_{\beta\ Arg}$), 1.86-2.13 (m, 10H, $H_{\beta\ Arg}$, $2H_{\beta\ Pro}$, $4H_{\gamma\ Pro}$, NHCOC$\underline{H}_3$), 2.27-2.40 (m, 2H, $2H_{\beta\ Pro}$), 2.83-3.00 (m, 2H, $2H_{\beta\ Asp}$), 3.24 (t, J = 6.7 Hz, 2H, $2H_{\delta\ Arg}$), 3.58-3.87 (m, 9H, $4H_{\delta\ Pro}$, $2H_{\beta\ Ser}$, H^{3s}, H^{4s}, H^{5s}), 4.01 (dd, J = 10.1, 3.8 Hz, 1H, H^{2s}), 4.34-4.53 (m, 2H, $2H_{\alpha\ Pro}$, $H_{\alpha\ Ala}$, H^{6s}), 4.60-4.67 (m, 3H, $H_{\alpha\ Ser}$, H^{6s}), 4.68-4.72 (m, 2H, $H_{\alpha\ Arg}$, $H_{\alpha\ Asp}$), 5.10 (d, J = 3.8 Hz, 1H, H^{1s}). ^{1}H NMR (400 MHz, D_2O/H_2O 1:9, amide region) δ (ppm) 7.00 (s, 1H, $NH_{2\ term.}$), 7.14-7.20 (m, 1H, $NH_{\ Arg}$), 7.69 (s, 1H, $NH_{2\ term.}$), 8.11 (d, J = 9.3 Hz, 1H, N$\underline{H}$Ac) 8.31 (d, J = 7.3 Hz, 1H, $NH_{\ Ser}$), 8.48 (d, J = 7.4 Hz, 1H, $NH_{\ Arg}$), 8.61 (d, J = 6.9 Hz, 1H, $NH_{\ Asp}$). ^{13}C NMR (100 MHz, D_2O) δ (ppm) 15.1 ($CH_{3\ Ala}$), 22.0 (NHCO$\underline{C}H_3$), 24.1 ($C_{\gamma\ Arg}$), 24.7 ($2C_{\gamma\ Pro}$), 27.7 ($C_{\beta\ Arg}$), 29.3 ($C_{\beta\ Pro}$), 29.6 ($C_{\beta\ Pro}$), 35.4 ($C_{\beta\ Asp}$), 40.5 ($C_{\delta\ Arg}$), 47.7 ($C_{\delta\ Pro}$), 47.9 ($C_{\delta\ Pro}$), 48.0 ($C_{\alpha\ Ala}$), 50.1 ($C_{\alpha\ Asp}$), 51.1 ($C_{\alpha\ Arg}$), 52.8 (C^{2s}), 52.9 ($C_{\alpha\ Ser}$), 53.2 (C^{5s}), 60.3 ($C_{\alpha\ Pro}$), 60.4 ($C_{\alpha\ Pro}$), 66.7 ($C_{\beta\ Ser}$), 67.7 (C^{6s}), 70.7 (C^{3s}), 73.8 (C^{4s}), 80.5 (C^{1s}), 156.8 ($C{=}NH_{\ Arg}$), 158.0 (NCO_2), 169.3, 170.6, 171.2, 172.1, 173.6, 174.1, 174.3, 176.8 (CO).

H_2N-Ala-Pro-Asp-(sp^2GlcNAc)Thr-Arg-Pro-NH_2 (36):

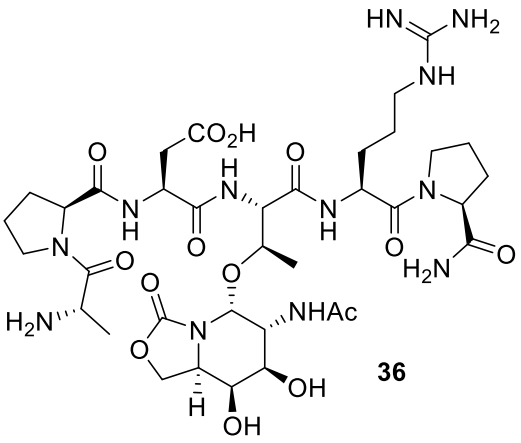

36

The glycosylated amino acid building block **28** (82 mg, 0.13 mmol) was coupled manually, while the other Fmoc-amino acids were coupled in the automated mode. After elimination of acetate groups and cleavage, glycopeptide **36** was obtained and then purified by reversed-phase HPLC and lyophilized.

Table 6.8. Semi-preparative HPLC gradient (t_R 34.6 min).

Time (min)	Flow (mL/min)	MeCN (%)	H_2O + 0.1% TFA (%)
0	10	2	98
30	10	10	90
35	10	20	80
40	10	2	98

HRMS (ESI) (m/z) 442.2170 $[M+2H]^{2+}$, calcd for $C_{36}H_{60}N_{12}O_{14}^{2+}$: 442.2170. ^{1}H NMR (400 MHz, D_2O) δ (ppm) 1.19 (d, *J* = 6.4 Hz, 3H, $CH_{3\ Thr}$) 1.56 (d, *J* = 7.0 Hz, 3H, $CH_{3\ Ala}$), 1.64-1.79 (m, 3H, $2H_{\gamma\ Arg}$, $H_{\beta\ Arg}$), 1.85-2.12 (m, 10H, $H_{\beta\ Arg}$, $2H_{\beta\ Pro}$, $4H_{\gamma\ Pro}$, $NHCOC\underline{H}_3$), 2.26-2.40 (m, 2H, $2H_{\beta\ Pro}$), 2.84-3.04 (m, 2H, $2H_{\beta\ Asp}$), 3.23 (t, *J* = 6.6 Hz, 2H, $2H_{\delta\ Arg}$), 3.59-3.79 (m, 6H, $4H_{\delta\ Pro}$, H^{3s}, H^{4s}), 3.87-3.97 (m, 2H, H^{2s}, H^{5s}), 4.28-4.34 (m, 1H, $H_{\beta\ Thr}$), 4.36-4.43 (m, 3H, $H_{\alpha\ Ala}$, $H_{\alpha\ Pro}$, H^{6s}), 4.48-4.56 (m, 2H, $H_{\alpha\ Pro}$, $H_{\alpha\ Thr}$), 4.63-4.70 (m, 2H, $H_{\alpha\ Arg}$, H^{6s}), 4.87 (t, *J* = 7.0 Hz, 1H, $H_{\alpha\ Asp}$) 5.10 (d, *J* = 4.0 Hz, 1H, H^{1s}) ^{1}H NMR (400 MHz, D_2O/H_2O 1:9, amide region) δ

(ppm) 6.98 (s, 1H, $NH_{2\ term.}$), 7.19 (t, 1H, NH_{Arg}), 7.69 (s, 1H, $NH_{2\ term.}$), 8.01 (d, J = 9.5 Hz, 1H, NHAc), 8.33 (d, J = 7.3 Hz, 1H, NH_{Arg}), 8.50 (d, J = 8.8 Hz, 1H, NH_{Thr}), 8.70 (d, J = 7.1 Hz, 1H, NH_{Asp}). ^{13}C NMR (100 MHz, D_2O) δ (ppm) 15.1 ($CH_{3\ Ala}$), 18.1 ($CH_{3\ Thr}$), 22.2 ($NHCOCH_3$), 24.2 ($C_{\gamma\ Arg}$), 24.7 ($2C_{\gamma\ Pro}$), 27.7 ($C_{\beta\ Arg}$), 29.5 ($C_{\beta\ Pro}$), 29.6 ($C_{\beta\ Pro}$), 35.5 ($C_{\beta\ Asp}$), 40.5 ($C_{\delta\ Arg}$), 47.7 ($C_{\delta\ Pro}$), 47.8 ($C_{\delta\ Pro}$), 48.0 ($C_{\alpha\ Ala}$), 50.0 ($C_{\alpha\ Asp}$), 51.2 ($C_{\alpha\ Arg}$), 52.9 (C^{2s}), 53.4 (C^{5s}), 57.1 ($C_{\alpha\ Thr}$), 60.2 ($C_{\alpha\ Pro}$), 60.3 ($C_{\alpha\ Pro}$), 67.5 (C^{6s}), 71.0 (C^{3s}), 73.4 (C^{4s}), 74.9 ($C_{\beta\ Thr}$), 81.1 (C^{1s}), 156.8 ($C{=}NH_{Arg}$), 157.6 (NCO_2), 169.2, 170.8, 171.0, 172.8, 173.4, 173.8, 174.3, 176.8 (CO).

General procedure for the total deprotection reaction (39-42). 20% Piperidine-MeOH (180 μL) was added over a stirred solution of the corresponding precursors **21-24** (0.19 mmol) in DCM (3 mL) and the reaction mixture was stirred at room temperature for 5 h (TLC monitoring). The solvent was removed under reduced pressure and the resulting crude filtrated through a pad of SiO_2 using 2:1→1:2 EtOAc/MeOH as eluent. After conventional de-*O*-acetylation using Zemplén procedure, which involved the addition of NaOMe (0.1 equiv./Ac mol) in MeOH at room termperature, followed by neutralization with solid CO_2, and evaporation of the solvent, the desired fully deprotected compounds (**39-42**) were obtained.

1-*O*-L-Ser-(1*R*)-5*N*,6*O*-(oxomethylidene)galactonojirimycin (39).

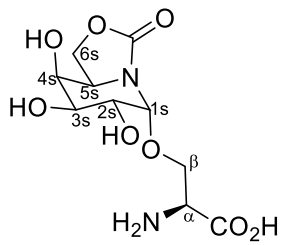

39

Yield: 9 mg, 0.031 mmol, 49% in two steps. $[\alpha]_D^{25}$ = +20.1 (c 1.00, MeOH). HRMS ESI+ (m/z): 290.8 [M-H]; calcd for $C_{10}H_{15}N_2O_8^-$, 291.2365. Elem. Anal.: C 40.89, H 5.34, N 9.28. Calcd for $C_{10}H_{16}N_2O_{13}$: C 41.10, H 5.52, N 9.59. ^{1}H NMR (400 MHz, CD_3OD) δ (ppm) 3.39-3.43 (m, 1H, H^{α}), 3.48 (t, *J* = 7.8 Hz, 1H, H^{β}), 3.80 (dd, *J* = 10.0 Hz, 1H, H^{2s}), 3.79-3.84 (m, 2H, H^{3s}, H^{β}), 3.85 (t, *J* = 2.0 Hz, 1H, H^{4s}), 4.09 (ddd, *J* = 8.0, 6.0, 2.0 Hz, 1H, H^{5s}), 4.41-4.51 (m, 2H, H^{6s}), 5.07 (d, *J* = 4.0 Hz, 1H, H^{1s}). ^{13}C NMR (100 MHz, CD_3OD) δ (ppm) 52.7 (C^{5s}), 55.5 (C^{α}), 64.5 (C^{6s}), 67.6 (C^{2s}), 69.1 (C^{3s}), 69.3 (C^{4s}), 69.7 (C^{β}), 81.8 (C^{1s}), 158.7 (CO), 178.6 (CO_2H).

1-*O*-L-Thr-(1*R*)-5*N*,6*O*-(oxomethylidene)galactonojirimycin (40).

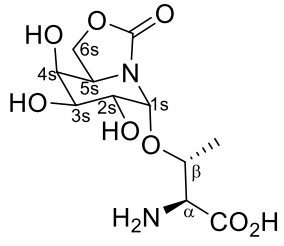

40

Yield: 21 mg, 0.069 mmol, 67% in two steps. $[\alpha]_D^{25}$ = +28.9 (c 1.00, H_2O). HRMS ESI+ (m/z): 304.9 [M-H]; calcd for $C_{11}H_{18}N_2O_8^-$, 305.0990. Elem. Anal.: C 42.87, H 5.88, N 9.10. Calcd for $C_{11}H_{18}N_2O_8$: C 43.14, H 5.92, N 9.15. ^{1}H NMR (300 MHz, D_2O) δ (ppm) 1.35 (d, *J* = 6.5 Hz, 3H, Me^{Thr}), 3.73 (d, *J* = 3.9 Hz, 1H, H^{α}), 3.75-3.81 (m, 1H, H^{2s}), 3.88 (dd, *J* = 10.0 Hz, 1H, H^{3s}), 4.00 (t, *J* = 2.4 Hz, 1H, H^{4s}), 4.20-4.26 (m, 1H, H^{5s}), 4.39-4.30 (m, 1H, H^{β}), 4.41 (d, *J* = 5.7 Hz, 1H, H^{6s}), 4.55 (t, *J* = 9.0 Hz, 1H, H^{6s}), 5.30 (d, *J* = 4.2 Hz, 1H, H^{1s}). ^{13}C NMR (75 MHz, D_2O) δ (ppm) 18.1 (Me^{Thr}), 52.9 (C^{5s}), 59.1 (C^{α}), 64.5 (C^{6s}), 67.7 (C^{2s}), 69.0 (C^{4s}), 69.2 (C^{3s}), 74.0 (C^{β}), 82.6 (C^{1s}), 158.1 (CO), 171.8 (CO_2H).

1-*O*-L-Ser-(1*R*)-5*N*,6*O*-(oxomethylidene)nojirimycin (41).

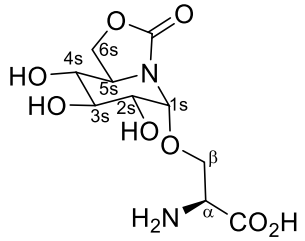

41

Yield: 35 mg, 0.120 mmol, 64% in two steps. $[\alpha]_D^{25}$ = +52.2 (c 1.00, H_2O). HRMS ESI+ (m/z): 290.9 [M-H]; calcd for $C_{10}H_{15}N_2O_8^-$, 291.2365. Elem. Anal.: C 40.82, H 5.60, N 9.42. Calcd for $C_{10}H_{16}N_2O_{13}$: C 41.10, H 5.52, N 9.59. ^{1}H NMR (500 MHz, D_2O) δ (ppm) 3.59-5.67 (m, 1H, H^{4s}), 3.69-3.75 (m, 1H, H^{2s}), 3.81 (t, *J* = 10.0 Hz, 1H, H^{3s}), 3.86-3.94 (m, 1H, H^{β}), 3.96-4.04 (m, 1H, H^{5s}), 4.04-4.08 (m, 1H, H^{α}), 4.15 (dd, *J* = 10.5, 3.0 Hz, H^{β}), 4.42-4.46 (m, 1H, H^{6s}), 4.74 (t, *J* = 9.0 Hz, 1H, H^{6s}), 5.24 (d, *J* = 4.0 Hz, 1H, H^{1s}). ^{13}C NMR (125.7 MHz, D_2O) δ (ppm) 53.1 (C^{5s}), 54.7 (H^{α}), 66.5 (H^{β}), 67.7 (C^{6s}), 71.0 (C^{2s}), 72.4 (C^{3s}), 73.5 (C^{4s}), 81.9 (C^{1s}), 158.2 (CO), 171.7 (CO_2H).

1-*O*-L-Thr-(1*R*)-5*N*,6*O*-(oxomethylidene)nojirimycin (42).

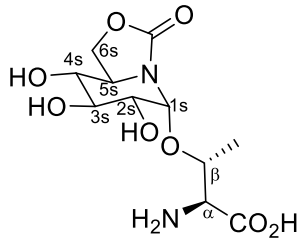

42

Yield: 10 mg, 0.033 mmol, 50% in two steps. $[\alpha]_D^{25}$ = +37.4 (c 0.90, H_2O). HRMS ESI+ (m/z): 329.1 [M+Na^+]; calcd for $C_{11}H_{18}NaN_2O_8^+$, 329.2602. Elem. Anal.: C 42.79, H 5.94, N 9.06. Calcd for $C_{11}H_{18}N_2O_8$: C 43.14, H 5.92, N 9.15. ^{1}H NMR (500 MHz, D_2O) δ (ppm) 1.37 (d, *J* = 6.5 Hz, 3H, Me^{Thr}), 3.53-3.59 (m, 1H, H^{4s}), 3.58-3.63 (m, 1H, H^{2s}), 3.72 (t, *J* = 9.5 Hz, 1H, H^{3s}), 3.76 (d, *J* = 3.5 Hz, 1H, H^{α}), 3.94 (dt, *J* = 9.0, 6.0 Hz, H^{5s}), 4.44-4.35 (m, 2H, H^{6s}, H^{β}), 4.68 (t, *J* = 9.0 Hz, 1H, H^{6s}), 5.26 (d, *J* = 4.5 Hz, 1H, H^{1s}). ^{13}C NMR (125.7 MHz, D_2O) δ (ppm) 18.2 (Me^{Thr}), 53.3 (C^{5s}),

59.2 (C^{α}), 67.5 (C^{6s}), 71.1 (C^{2s}), 72.3 (C^{3s}), 73.4 (C^{4s}), 74.2 (C^{β}), 82.4 (C^{1s}), 157.7 (CO), 171.8 (CO_2H).

(7*R*,8*S*,8a*R*)-3-oxo-1,7,8,8a-tetrahydro-3*H*-oxazolo[3,4-*a*]pyridine-7,8-diyl diacetate (44-Gal).

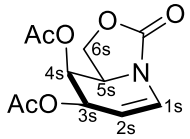

44-Gal

To a solution of **37-Gal**[25] (1.16 g, 3.11 mmol) in anhydrous DCM (5 mL), HBr/AcOH (33%, 2.0 mL) were dropwise added at 0 ºC and the reaction mixture was stirred for 15 min, diluted with DCM (50 mL) and washed with saturated aqueous $NaHCO_3$ (10 mL). The organic layer was dried ($MgSO_4$) and concentrated under reduced pressure to yield the corresponding 1-bromo derivative as a white solid. This product was used without further purification in the next step. A mixture of Cp_2TiCl_2 (774 mg, 3.11 mmol) and Mn dust (445 mg, 8.1 mmol) in deoxygenated THF (10 mL) was stirred at room temperature until the red solution turned green. Then, the glycosylbromo derivative (1.22 g, 3.11 mmol) in deoxygenated THF (20 mL) was added and the reaction mixture was stirred for 40 min. The solvent was removed under reduced pressure, diluted with EtOAc (60 mL), quenched with 1 M HCl (2 x 10 mL), washed with brine, and dried ($MgSO_4$). The resulting crude was purified by column chromatography (1:2 → 1:1 EtOAc/cyclohexane) to yield **44-Gal** (484 mg, 1.895 mmol, 61%). $[\alpha]_D^{25}$ = +57.6 (c 1.00, DCM). HRMS ESI+ (m/z): 277.9 [M+Na^+]; calcd for $C_{11}H_{13}NNaO_6^+$, 278.0635. Elem. Anal.: C 51.85, H 5.28, N 5.35. Calcd for $C_{11}H_{13}NO_6$: C 51.77, H 5.13, N 5.49. ^{1}H NMR (300 MHz, $CDCl_3$) δ (ppm) 2.06 (s, 3H, CH_3CO), 2.17 (s, 3H, CH_3CO), 4.04 (t, *J* = 8.0 Hz, 1H, H^{6s}), 4.46-4.37 (m, 1H, H^{5s}), 4.48 (t, *J* = 8.0 Hz, 1H, H^{6s}), 4.84-4.90 (m, 1H, H^{2s}), 5.46 (dt, *J* = 4.0, 1.7 Hz, 1H, H^{4s}), 5.67-5.62 (m, 1H, H^{3s}), 6.73 (dd, *J* = 8.2,

2.2 Hz, 1H, H^{1s}). ^{13}C NMR (75.5 MHz, $CDCl_3$) δ (ppm) 20.6 (*C*H_3CO), 20.7 (*C*H_3CO), 53.5 (C^{5s}), 61.4 (C^{4s}), 63.3 (C^{6s}), 66.6 (C^{3s}), 104.8 (C^{2s}), 123.9 (C^{1s}), 153.6 (NCO), 170.2 (CH_3*C*O), 170.5 (CH_3*C*O).

(7*R*,8*R*,8a*R*)-3-oxo-1,7,8,8a-tetrahydro-3*H*-oxazolo[3,4-*a*]pyridine-7,8-diyl diacetate (44-Glc).

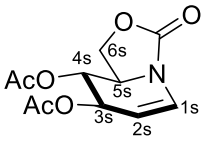

44-Glc

To a solution of **37-Glc**[26] (1.16 g, 3.11 mmol) in anhydrous DCM (5 mL), HBr/AcOH (33%, 2.0 mL) were dropwise added at 0 ºC and the reaction mixture was stirred for 15 min, diluted with DCM (50 mL) and washed with saturated aqueous $NaHCO_3$ (10 mL). The organic layer was dried ($MgSO_4$) and concentrated under reduced pressure to yield the corresponding 1-bromo derivative as a white solid. This product was used without further purification in the next step. A mixture of Cp_2TiCl_2 (774 mg, 3.11 mmol) and Mn dust (445 mg, 8.1 mmol) in deoxygenated THF (10 mL) was stirred at room temperature until the red solution turned green. Then, the glycosylbromo derivative (1.22 g, 3.11 mmol) in deoxygenated THF (20 mL) was added and the reaction mixture was stirred for 40 min. The solvent was removed under reduced pressure, diluted with EtOAc (60 mL), quenched with 1 M HCl (2 x 10 mL), washed with brine, and dried ($MgSO_4$). The resulting crude was purified by column chromatography (1:3 → 1:1 EtOAc/cyclohexane) to yield **44-Glc** (682 mg, 2.67 mmol, 86%). $[\alpha]_D^{25}$ = -31.8 (c 1.00, DCM). HRMS ESI+ (m/z): 278.1 [$M+Na^+$]; calcd for $C_{11}H_{13}NNaO_6^+$, 278.0635. Elem. Anal.: C 51.89, H 5.33, N 5.40. Calcd for $C_{11}H_{13}NO_6$: C 51.77, H 5.13, N 5.49. ^1H NMR (300 MHz, $CDCl_3$) δ (ppm) 2.06 (s, 3H, CH_3CO), 2.09 (s, 3H, CH_3CO), 4.15-4.19 (m, 1H, H^{5s}), 4.25 (t, *J* = 9.0 Hz, 1H, H^{6s}), 4.49 (t, *J* = 8.0 Hz, 1H, H^{6s}), 4.91-4.95 (m, 1H, H^{2s}),

5.16 (dd, *J* =10.5 Hz, 1H, H^{4s}), 5.63 (dt, *J* = 7.5, 2.5 Hz, 1H, H^{3s}), 6.67 (dd, *J* = 8.0, 2.0 Hz, 1H, H^{1s}). ^{13}C NMR (75 MHz, $CDCl_3$) δ (ppm) 20.6 (*C*H_3CO), 20.8 (*C*H_3CO), 53.9 (C^{5s}), 67.0 (C^{6s}), 70.1 (C^{3s}), 71.0 (C^{4s}), 105.8 (C^{2s}), 123.4 (C^{1s}), 153.0 (NCO), 170.1 (CH_3*C*O), 170.5 (CH_3*C*O).

(5*R*,6*R*,7*R*,8*S*,8a*R*)-6-azido-5-hydroxy-3-oxohexahydro-3*H*-oxazolo[3,4-*a*]pyridine-7,8-diyl diacetate (45-Gal)

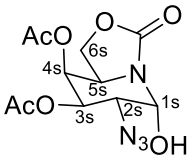

45-Gal

A solution of **44-Gal** (378 mg, 1.48 mmol) in MeCN (10 mL) was added, under Ar atmosphere at -20 ºC, to a mixture of NaN_3 (144 mg, 2.22 mmol) and ceric ammonium nitrate (CAN) (2.43 g, 4.44 mmol). The reaction mixture was stirred at -20 ºC for 5 h. Then, cold Et_2O (30 mL) and H_2O (10 mL) were added. The organic layer was separated and washed with cold H_2O (2 x 10 mL), dried ($MgSO_4$), filtered and concentrated. Purification by column chromatography (1:1 EtOAc/cyclohexane) yielded **45-Gal** (300 mg, 0.95 mmol, 64%). $[\alpha]_D^{25}$ = +62.2 (c 1.00, DCM). HRMS ESI+ (m/z): 337.0 [M+Na^+]; calcd for $C_{11}H_{14}N_4NaO_7^+$, 337.0755. Elem. Anal.: C 42.04, H 4.49, N 17.83. Calcd for $C_{11}H_{14}N_4O_7$: C 41.04, H 4.49, N 17.83. ^{1}H NMR (300 MHz, $CDCl_3$) δ (ppm) 2.10 (s, 3H, *C*H_3CO), 2.20 (s, 3H, *C*H_3CO), 3.78 (d, *J* = 3.9 Hz, 1H, H^{2s}), 4.00 (dd, = 13.4, 10.5 Hz, 1H, H^{6s}), 4.22 (bd, 1H, OH), 4.32-4.45 (m, 2H, H^{5s}, H^{6s}), 5.36 (d, *J* = 10.7 Hz, 1H, H^{3s}), 5.46 (t, *J* = 2.6 Hz, 1H, H^{4s}), 5.65 (bt, *J* = 3.0 Hz, 1H, H^{1s}). ^{13}C NMR (75 MHz, $CDCl_3$) δ (ppm) 20.6 (*C*H_3CO), 20.6 (*C*H_3CO), 50.8 (C^{5s}), 58.0 (C^{2s}), 63.3 (C^{6s}), 67.7 (C^{4s}), 69.2 (C^{3s}), 74.6 (C^{1s}), 155.6 (NCO), 169.9 (CH_3*C*O), 170.2 (CH_3*C*O).

(5*R*,6*R*,7*R*,8*R*,8a*R*)-6-azido-5-hydroxy-3-oxohexahydro-3*H*-oxazolo[3,4-*a*]pyridine-7,8-diyl diacetate (45-Glc)

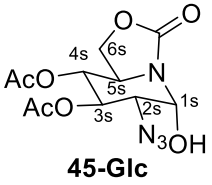

45-Glc

A solution of **44-Glc** (378 mg, 1.48 mmol) in MeCN (10 mL) was added, under Ar atmosphere at -20 ºC, to a mixture of NaN_3 (144 mg, 2.22 mmol) and ceric ammonium nitrate (CAN) (2.43 g, 4.44 mmol). The reaction mixture was stirred at -20 ºC for 5 h. Then, cold Et_2O (30 mL) and H_2O (10 mL) were added. The organic layer was separated and washed with cold H_2O (2 x 10 mL), dried ($MgSO_4$), filtered and concentrated. Purification by column chromatography (1:3 → 1:2 EtOAc/cyclohexane) yielded **45-Gal** (162 mg, 0.516 mmol, 35%). $[\alpha]_D^{25}$ = +38.5 (c 1.00, DCM). HRMS ESI+ (m/z): 337.0 [M+Na^+]; calcd for $C_{11}H_{14}N_4NaO_7^+$, 337.0755. Elem. Anal.: C 42.04, H 4.49, N 17.83. Calcd for $C_{11}H_{14}N_4O_7$: C 41.85, H 4.30, N 17.74. ^{1}H NMR (300 MHz, $CDCl_3$) δ (ppm) 2.07 (s, 3H, *C*H_3CO), 2.12 (s, 3H, *C*H_3CO), 3.49-3.54 (m, 1H, H^{2s}), 4.08-4.27 (m, 2H, H^{5s}, H^{6s}), 4.43 (dd, *J* = 9.0, 7.8 Hz, 1H, H^{6s}), 4.93 (t, *J* = 9.5 Hz, 1H, H^{4s}), 5.57 (t, *J* = 10.5, 9.5 Hz, 1H, H^{3s}), 5.62 (d, *J* = 3.3 Hz, 1H, H^{1s}). ^{13}C NMR (75 MHz, $CDCl_3$) δ (ppm) 20.5 (*C*H_3CO), 20.6 (*C*H_3CO), 51.8 (C^{5s}), 61.9 (C^{2s}), 66.8 (C^{6s}), 69.9 (C^{3s}), 72.6 (C^{4s}), 74.4 (C^{1s}), 155.4 (CO), 169.7 (CH_3*C*O), 170.2 (CH_3*C*O).

(5*R*,6*R*,7*R*,8*S*,8a*R*)-6-azido-5-fluoro-3-oxohexahydro-3*H*-oxazolo[3,4-*a*]pyridine-7,8-diyl diacetate (46-Gal)

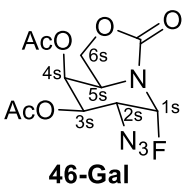

46-Gal

Compound **45-Gal** (157 mg, 0.5 mmol) was acetylated following the conventional procedure (Ac_2O/Pyridine, 1:2), obtaining a peracetylated intermediate. This intermediate was placed in a polyethylene vessel, cooled at -40 ºC, and treated with poly(hydrogen fluoride)pyridinium complex (70% HF, 0.4 mL).

The reaction mixture was stirred at this temperature for 90 min (TLC monitoring), diluted with Et_2O (20 mL), washed with saturated aq KF (10 mL) and extracted with Et_2O (3 x 20 mL). The organic layer was washed with saturated aq $NaHCO_3$ (10 mL), dried ($MgSO_4$), concentrated, and purified by column chromatography (2:3 EtOAc/cyclohexane) to afford **46-Gal** (110 mg, 0.35 mmol, 70% two steps). $[\alpha]_D^{25}$ = +63.7 (c 1.00, DCM). HRMS ESI+ (m/z): 339.2 [M+Na^+]; calcd for $C_{11}H_{13}FN_4NaO_6^+$, 339.0711. Elem. Anal.: C 41.94, H 4.22, N 17.56. Calcd for $C_{11}H_{13}FN_4O_6$: C 41.78, H 4.14, F 6.01, N 17.56. ^{1}H NMR (300 MHz, $CDCl_3$) δ (ppm) 2.11 (s, 3H, CH_3CO), 2.21 (s, 3H, CH_3CO), 3.80-3.90 (m, 1H, H^{2s}), 4.00-4.05 (m, 1H, H^{6s}), 4.33-4.41 (m, 1H, H^{5s}), 4.46 (t, *J* = 8.8 Hz, 1H, H^{6s}), 5.31 (d, *J* = 11.0 Hz, 1H, H^{3s}), 5.52 (t, *J* = 2.2 Hz, 1H, H^{4s}), 6.13 (dd, $J_{1,F}$ = 50.0 Hz, $J_{1,2}$ = 3.3 Hz, H^{1s}). ^{13}C NMR (75 MHz, $CDCl_3$) δ (ppm) 20.5 (CH_3CO), 20.5 (CH_3CO), 51.0 (C^{5s}), 57.1 (d, $J_{C2,F}$ = 24.6 Hz, C^{2s}), 63.2 (C^{6s}), 66.8 (C^{4s}), 69.0 (C^{3s}), 89.9 (d, $J_{C1,F}$ = 208.3 Hz, C^{1s}), 154.4 (NCO), 169.6 (CH_3CO), 169.9 (CH_3CO). ^{19}F NMR (376 MHz, $CDCl_3$) δ (ppm) −164.1 (dd, *J* = 50.4, 24.3 Hz, F).

(5*R*,6*R*,7*R*,8*R*,8a*R*)-6-azido-5-fluoro-3-oxohexahydro-3*H*-oxazolo[3,4-*a*]pyridine-7,8-diyl diacetate (46-Glc)

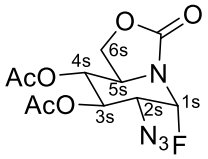

46-Glc

Compound **45-Glc** (157 mg, 0.5 mmol) was acetylated following the conventional procedure (Ac_2O/Pyridine, 1:2), obtaining a peracetylated intermediate. This intermediate was placed in a polyethylene vessel, cooled at -40 ºC, and treated with poly(hydrogen fluoride)pyridinium complex (70% HF, 0.4 mL). The reaction mixture was stirred at this temperature for 90 min (TLC monitoring), diluted with Et_2O (20 mL), washed with saturated aq KF

(10 mL) and extracted with Et_2O (3 x 20 mL). The organic layer was washed with saturated aq $NaHCO_3$ (10 mL), dried ($MgSO_4$), concentrated, and purified by column chromatography (2:3 EtOAc/cyclohexane) to afford **46-Glc** (123 mg, 0.39 mmol, 77% two steps). $[\alpha]_D^{25}$ = +47.7 (c 1.00, DCM). HRMS ESI+ (m/z): 339.0 [M+Na^+]; calcd for $C_{11}H_{13}FN_4NaO_6^+$, 339.0711. Elem. Anal.: C 41.99, H 4.31, N 17.44. Calcd for $C_{11}H_{13}FN_4O_6$: C 41.78, H 4.14, F 6.01, N 17.56. ^{1}H NMR (300 MHz, $CDCl_3$) δ (ppm) 2.08 (s, 3H, *C*H_3CO), 2.13 (s, 3H, *C*H_3CO), 3.50-3.60 (m, 1H, H^{2s}), 4.04-4.16 (m, 1H, H^{5s}), 4.25-4.28 (m, 1H, H^{6s}), 4.49 (dd, *J* = 9.0, 8.0 Hz, 1H, H^{6s}), 4.96 (t, *J* = 9.6, 1H, H^{4s}), 5.52 (dd, *J* = 10.5, 9.6 Hz, 1H, H^{3s}), 6.10 (dd, $J_{1,F}$ = 51.0 Hz, $J_{1,2}$ = 3.3 Hz, 1H, H^{1s}). ^{13}C NMR (75 MHz, $CDCl_3$) δ (ppm) 20.4 (*C*H_3CO), 20.5 (*C*H_3CO), 52.0 (C^{5s}), 60.9 (d, $J_{C2,F}$ = 24.9 Hz, C^{2s}), 67.1 (C^{6s}), 69.3 (C^{3s}), 72.1 (C^{4s}), 89.5 (d, $J_{C1,F}$ = 211.4 Hz, C^{1s}), 154.0 (NCO), 169.4 (CH_3*C*O), 170.0 (CH_3*C*O). ^{19}F NMR (376 MHz, CD_3OD) δ (ppm) −164.0 (dd, $^2J_{F,H}$ = 51.2 Hz, $^3J_{F,H}$ = 24.5 Hz, F).

General procedure for the preparation of pseudoglycoside iminosugar derivatives (47-50). $BF_3.OEt_2$ (0.5 equiv.) was added to a stirred solution of the corresponding fluoroderivative **46-Gal** or **46-Glc** (1.0 equiv.) and **Fmoc-Ser-O^{t}Bu** or **Fmoc-Thr-O^{t}Bu** (1.0 equiv.) in anhydrous DCM (12.5 mL/mmol) at 0 ºC under nitrogen atmosphere. The mixture was stirred for 2 h (TLC monitoring). The solvent was removed under reduced pressure and the resulting residue subjected to column chromatography to afford the corresponding 2-azido-α-*O*-glycosyl derivatives with *galacto* configuration (**47**, **48**) and *gluco* configuration (**49**, **50**).

1-*O*-(Fmoc-L-Ser)-(1*R*)-3,4-di-*O*-acetyl-2-azido-2-deoxy-5*N*,6*ᵅ*-(oxomethylidene)galactonojirimycin (47).

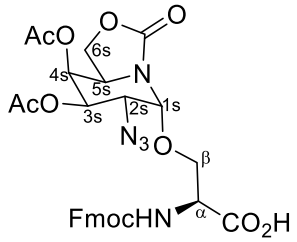

47

Purification by column chromatography (1:1 EtOAc/cyclohexane → EtOAc → 8:1 EtOAc/ MeOH) afforded compound **47** (130 mg, 0.21 mmol, 87%). $[\alpha]_D^{25}$ = +52.7 (c 1.30, MeOH). HRMS ESI+ (m/z): 622.0 [M-H]; calcd for $C_{29}H_{28}N_5O_{11}^-$, 622.1791. Elem. Anal.: C 55.71, H 4.76, N 10.99. Calcd for $C_{29}H_{29}N_5O_{11}$: C 55.86, H 4.69, N 11.23. ^{1}H NMR (300 MHz, $(CD_3)_2CO$) δ (ppm) 2.10 (s, 3H, CH_3CO), 2.15 (s, 3H, CH_3CO), 3.82-3.86 (m, 1H, H^{2s}), 4.01-4.14 (m, 3H, H^{6s}, H^{β}), 4.20-4.49 (m, 4H, H^{6s}, CH_2^{Fmoc}, CH^{Fmoc}), 4.53-4.65 (m, 2H, H^{5s}, H^{α}), 5.30-5.40 (m, 2H, H^{3s}, H^{1s}), 5.47 (t, *J* = 2.4 Hz, 1H, H^{4s}), 7.25-7.90 (m, 8H, Fmoc). ^{13}C NMR (75 MHz, $(CD_3)_2CO$) δ (ppm) 20.6 (CH_3CO), 20.6 (CH_3CO), 47.9 (CH^{Fmoc}), 51.5 (C^{5s}), 55.1 (C^{α}), 57.9 (C^{2s}), 64.1 (C^{6s}), 67.5 (CH_2^{Fmoc}), 68.9 (C^{4s}), 69.6 (C^{3s}), 69.5 (C^{β}), 82.7 (C^{1s}), 120.8-145.1 (Arom.^{Fmoc}), 156.6 (NCO), 156.7 (NCO), 170.2 (CH_3CO), 170.8 (CH_3CO), 171.7 (COOH).

1-*O*-(Fmoc-L-Thr)-(1*R*)-3,4-di-*O*-acetyl-2-azido-2-deoxy-5*N*,6*O*-(oxomethylidene)galactonojirimycin (48).

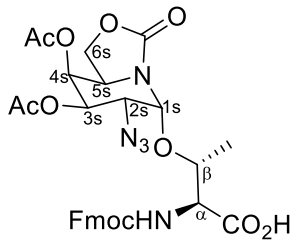

48

Purification by column chromatography (1:1 EtOAc/cyclohexane → EtOAc → 8:1 EtOAc/ MeOH) afforded compound **48** (120 mg, 0.19 mmol, 72%). $[\alpha]_D^{25}$ = +51.8 (c 1.30, MeOH). HRMS ESI+ (m/z): 636.1 [M-H]; calcd for $C_{30}H_{31}N_5O_{11}^-$, 636.1947. Elem. Anal.: C 56.16, H 4.70, N 10.60. Calcd for $C_{30}H_{32}N_5O_{11}$: C 56.51, H 4.90, N 10.98. ^{1}H NMR

(300 MHz, CD_3OD) δ (ppm) 1.25 (d, *J* = 6.3 Hz, 3H, Me^{Thr}), 2.03 (s, 3H, CH_3CO), 2.15 (s, 3H, CH_3CO), 3.82-3.86 (m, 1H, H^{2s}), 4.11-4.14 (m, 1H, H^{6s}), 4.20-4.30 (m, 2H, CH^{Fmoc}, H^{α}), 4.34-4.43 (m, 4H, H^{5s}, H^{β}, CH_2^{Fmoc}), 4.46 (t, *J* = 8.6 Hz, 1 H, H-6a), 5.32 (d, *J* = 11.0 Hz, 1 H, H^{3s}), 5.45 (d, *J* = 4.0 Hz, 1H, H^{1s}), 5.48 (t, *J* = 2.2 Hz, 1H, H^{4s}), 7.25-7.85 (m, 8H, Fmoc). ^{13}C NMR (75 MHz, CD_3OD) δ (ppm) 18.9 (Me^{Thr}), 20.5 (CH_3CO), 20.6 (CH_3CO), 48.4 (CH^{Fmoc}), 52.4 (C^{5s}), 59.1 (C^{2s}), 60.3 (C^{α}), 64.9 (C^{6s}), 68.3 (C^{β}),69.5 (C^{4s}), 70.6 (C^{3s}), 77.4 (CH_2^{Fmoc}), 82.9 (C^{1s}), 120.9-145.3 ($Arom.^{Fmoc}$), 157.8 (NCO), 158.9 (NCO), 171.3 (CH_3CO), 171.8 (CH_3CO), 174.1 (COOH).

1-*O*-(Fmoc-L-Ser)-(1*R*)-3,4-di-*O*-acetyl-2-azido-2-deoxy-5*N*,6*O*-(oxo-methylidene)nojirimycin (49).

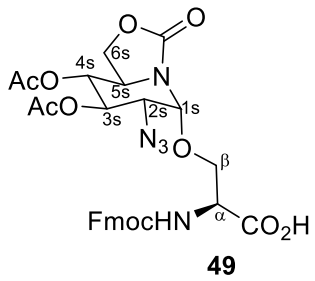

49

Purification by column chromatography (1:1 EtOAc/cyclohexane → EtOAc → 8:1 EtOAc/ MeOH) afforded compound **49** (75 mg, 0.12 mmol, 75%). $[\alpha]_D^{25}$ = +50.8 (c 0.90, MeOH). HRMS ESI+ (m/z): 646.3 [M+Na^+]; calcd for $C_{29}H_{29}NaN_5O_{11}^+$, 646.1756. Elem. Anal.: C 55.57, H 4.38, N 10.86. Calcd for $C_{29}H_{29}N_5O_{11}$: C 55.86, H 4.69, N 11.23. ^1H NMR (300 MHz, CD_3OD) δ (ppm) 1.99 (s, 3H, CH_3CO), 2.04 (s, 3H, CH_3CO), 3.50-3.53 (m, 1H, H^{2s}), 3.91 (d, *J* = 7.0 Hz, 1H, H^{β}), 4.03 (dd, *J* = 10.0, 3.6 Hz, 1H, H^{β}), 4.07-4.16 (m, 1H, H^{5s}), 4.16-4.46 (m, 6H, H^{6s}, CH_2^{Fmoc}, CH_{Fmoc}, H^{α}), 5.04 (t, *J* = 9.5 Hz, 1H, H^{4s}), 5.33 (d, *J* = 3.6 Hz, 1H, H^{1s}), 5.48 (dd, *J* = 10.5, 9.5 Hz, 1H, H^{3s}), 7.20-7.82 (m, 8H, Fmoc). ^{13}C NMR (75 MHz, CD_3OD) δ (ppm) 20.5 (CH_3CO), 20.6 (CH_3CO), 48.3 (CH^{Fmoc}), 53.1 (C^{5s}), 57.6 (C^{α}), 62.0 (C^{2s}), 68.1 (C^{6s}, CH_2^{Fmoc}), 70.8 (C^{β}),

71.2 (C^{3s}), 73.7 (C^{4s}), 82.9 (C^{1s}), 120.9-145.3 (Arom.^{Fmoc}), 157.7 (NCO), 158.4 (NCO), 171.3 (CH_3CO), 171.7 (CH_3CO), 176.1 (COOH).

1-*O*-(Fmoc-L-Thr)-(1*R*)-3,4-di-*O*-acetyl-2-azido-2-deoxy-5*N*,6*O*-(oxo-methylidene)nojirimycin (50).

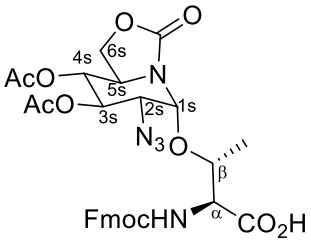

50

Purification by column chromatography (1:1 EtOAc/cyclohexane → EtOAc → 8:1 EtOAc/ MeOH) afforded compound **48** (120 mg, 0.25 mmol, 80%). $[\alpha]_D^{25}$ = +48.4 (c 1.00, MeOH). HRMS ESI+ (m/z): 660.5 [M+Na^+]; calcd for $C_{30}H_{32}NaN_5O_{11}^+$, 660.1912. Elem. Anal.: C 56.39, H 4.87, N 10.76. Calcd for $C_{30}H_{32}N_5O_{11}$: C 56.51, H 4.90, N 10.98. ^{1}H NMR (300 MHz, CD_3OD) δ (ppm) 1.24 (d, *J* = 6.2 Hz, 3H, Me^{Thr}), 2.04 (s, 3H, CH_3CO), 2.04 (s, 3H, CH_3CO), 3.65 (dd, *J* = 10.0, 3.0 Hz, 1H, H^{2s}), 4.03-4.14 (m, 1H, H^{5s}), 4.18-4.47 (m, 6H, H^{6s}, CH_2^{Fmoc}, CH^{Fmoc}, H^{β}, H^{α}), 4.53 (t, *J* = 8.6 Hz, 1H, H^{6s}), 5.08 (t, *J* = 9.5 Hz, 1H, H^{4s}), 5.40-5.50 (m, 2H, H^{1s}, H^{3s}), 7.20-7.90 (m, 8H, Fmoc). ^{13}C NMR (75 MHz, CD_3OD) δ (ppm) 19.3 (Me^{Thr}), 20.5 (CH_3CO), 20.6 (CH_3CO), 48.3 (CH^{Fmoc}), 53.2 (C^{5s}), 60.5 (C^{α}), 62.5 (C^{2s}), 68.1 (C^{6s}), 68.2 (CH_2^{Fmoc}), 71.2 (C^{3s}), 73.7 (C^{4s}), 77.2 (H^{β}), 82.3 (C^{1s}), 120.9-145.2 (Fmoc), 157.5 (NCO), 158.8 (NCO), 171.4 (CH_3CO), 171.4 (CH_3CO), 174.1 (COOH).

Cys-His-Gly-Val-Thr-Ser-Ala-Pro-Asp-Thr(*sp*^{2}GalNAc)-Arg-Pro-Ala-Pro-Gly-Ser-Thr-Ala-Pro-Pro-Ala (51):

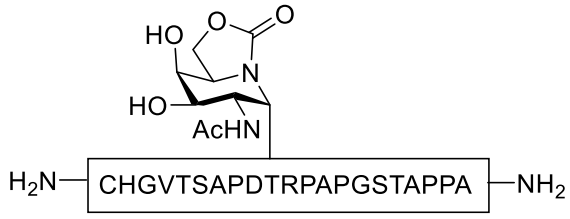

51

The glycosylated amino acid building block **26** (91 mg, 0.14 mmol) was coupled manually, while the other Fmoc-amino acids were coupled in the automated mode using microwave assistance. After elimination of acetate groups and cleavage, glycopeptide **51** was obtained and then purified by reversed-phase HPLC and lyophilized.

Table 6.9. Semi-preparative HPLC gradient (t_R 8.5 min).

Time (min)	Flow (mL/min)	MeCN (%)	H_2O + 0.1% TFA (%)
0	10	10	90
17	10	17	83
19	10	10	90

MS (MALDI) (m/z) 2216.86 $[M+H]^+$, calcd for $C_{92}H_{145}N_{29}O_{33}S^+$: 2216.03.

Cys-His-Gly-Val-Thr-Ser-Ala-Pro-Asp-Thr(GalNAc)-Arg-Pro-Ala-Pro-Gly-Ser-Thr-Ala-Pro-Pro-Ala (52):

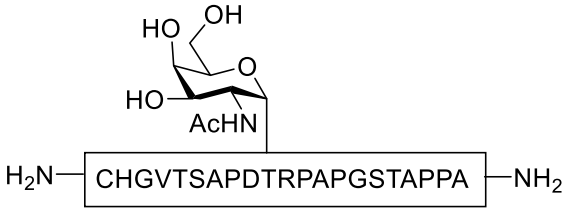

52

The glycosylated amino acid building block **Fmoc-Thr(GalNAc)-OH**[27] (100 mg, 0.15 mmol) was coupled manually, while the other Fmoc-amino acids were coupled in the automated mode using microwave assistance. After elimination of acetate groups and cleavage, glycopeptide **52** was obtained and then purified by reversed-phase HPLC and lyophilized.

Table 6.10. Semi-preparative HPLC gradient (t_R 15.6 min).

Time (min)	Flow (mL/min)	MeCN (%)	H_2O + 0.1% TFA (%)
0	10	10	90
20	10	17	83
22	10	10	90

MS (MALDI) (m/z) 2191.50 $[M+H]^+$, calcd for $C_{91}H_{146}N_{28}O_{33}S^+$: 2191.03.

Cys-His-Gly-Val-Thr-Ser-Ala-Pro-Asp-Thr-Arg-Pro-Ala-Pro-Gly-Ser-Thr-Ala-Pro-Pro-Ala (53):

53

Fmoc-amino acids were coupled in the automated mode using microwave assistance. After cleavage, glycopeptide **53** was obtained and then purified by reversed-phase HPLC and lyophilized.

Table 6.11. Semi-preparative HPLC gradient (t_R 15.4 min).

Time (min)	Flow (mL/min)	MeCN (%)	H_2O + 0.1% TFA (%)
0	10	10	90
17	10	17	83
19	10	10	90

MS (MALDI) (m/z) 1988.99 $[M+H]^+$, calcd for $C_{83}H_{133}N_{27}O_{28}S^+$: 1987.95.

7.16. References

(1) Wang, J.; Cieplak, P.; Kollman, P. A. *J. Comput. Chem.* **2000**, *21*, 1049–1074.
(2) Wang, J.; Wolf, R. M.; Caldwell, J. W.; Kollman, P. A.; Case, D. A. *J. Comput. Chem.* **2004**, *25*, 1157–1174.
(3) Lin, H.; Sugimoto, Y.; Ohsaki, Y.; Ninomiya, H.; Oka, A.; Taniguchi, M.; Ida, H.; Eto, Y.; Ogawa, S.; Matsuzaki, Y.; Sawa, M.; Inoue, T.; Higaki, K.; Nanba, E.; Ohno, K.; Suzuki, Y. *Biochim. Biophys. Acta* **2004**, *1689*, 219–228.
(4) Iwasaki, H.; Watanabe, H.; Iida, M.; Ogawa, S.; Tabe, M.; Higaki, K.; Nanba, E.; Suzuki, Y. *Brain Dev.* **2006**, *28*, 482–486.
(5) Suzuki, H.; Ohto, U.; Higaki, K.; Mena-Barragán, T.; Aguilar-Moncayo, M.; Ortiz Mellet, C.; Nanba, E.; Garcia Fernandez, J. M.; Suzuki, Y.; Shimizu, T. *J. Biol. Chem.* **2014**, *289*, 14560–14568.
(6) Zhao, Y.; Truhlar, D. G. *Theor. Chem. Acc.* **2008**, *120*, 215–241.
(7) Weigend, F.; Ahlrichs, R. *Phys. Chem. Chem. Phys.* **2005**, *7*, 3297.
(8) Frisch, M. J.; Trucks, G. W.; Schlegel, H. B.; Scuseria, G. E.; Robb, M. A.; Cheeseman, J. R.; Scalmani, G.; Barone, V.; Mennucci, B.; Petersson, G. A.; Nakatsuji, H.; Caricato, M.; Li, X.; Hratchian, H. P.; Izmaylov, A. F.; Bloino, J.; Zheng, G.; Sonnenberg, J. L.; Hada, M.; Ehara, M.; Toyota, K.; Fukuda, R.; Hasegawa, J.; Ishida, M.; Nakajima, T.; Honda, Y.; Kitao, O.; Nakai, H.; Vreven, T.; Montgomery Jr., J. A.; Peralta, J. E.; Ogliaro, F.; Bearpark, M.; Heyd, J. J.; Brothers, E.; Kudin, K. N.; Staroverov, V. N.; Kobayashi, R.; Normand, J.; Raghavachari, K.; Rendell, A.; Burant, J. C.; Iyengar, S. S.; Tomasi, J.; Cossi, M.; Rega, N.; Millam, J. M.; Klene, M.; Knox, J. E.; Cross, J. B.; Bakken, V.; Adamo, C.; Jaramillo, J.; Gomperts, R.; Stratmann, R. E.; Yazyev, O.; Austin, A. J.; Cammi, R.; Pomelli, C.; Ochterski, J. W.; Martin, R. L.; Morokuma, K.; Zakrzewski, V. G.; Voth, G. A.; Salvador, P.; Dannenberg, J. J.; Dapprich, S.; Daniels, A. D.; Farkas, Ö.; Foresman, J. B.; Ortiz, J. V; Cioslowski, J.; Fox, D. J. *Gaussian 09*; Wallingford, CT, 2009.
(9) Gonzalez, C.; Bernhard Schlegel, H. *J. Chem. Phys.* **1989**, *90*, 2154–2161.
(10) Gonzalez, C.; Schlegel, H. B. *J. Phys. Chem.* **1990**, *94*, 5523–5527.
(11) Scalmani, G.; Frisch, M. J. *J. Chem. Phys.* **2010**, *132*, 114110.
(12) Glendening, E. D.; Badenhoop, J. K.; Reed, A. E.; Carpenter, J. E.; Bohmann, J. A.; Morales, C. M.; Landis, C. R.; Wein-hold, F. Theoretical Chemistry Institute, University of Wisconsin, Madison, WI, 2013.
(13) Kaiser, E.; Colescott, R. L.; Bossinger, C. D.; Cook, P. I. *Anal. Biochem.* **1970**, *34*, 595–598.
(14) Martínez-Sáez, N.; Castro-López, J.; Valero-González, J.; Madariaga, D.; Compañón, I.; Somovilla, V. J.; Salvadó, M.; Asensio, J. L.; Jiménez-Barbero, J.; Avenoza, A.; Busto, J. H.; Bernardes, G. J. L.; Peregrina, J. M.; Hurtado-Guerrero, R.; Corzana, F. *Angew. Chem. Int. Ed.* **2015**, *54*, 9830–9834.
(15) Kabsch, W. *Acta Crystallogr. Sect. D Biol. Crystallogr.* **2010**, *66*, 133–144.
(16) Winn, M. D.; Ballard, C. C.; Cowtan, K. D.; Dodson, E. J.; Emsley, P.; Evans,

P. R.; Keegan, R. M.; Krissinel, E. B.; Leslie, A. G. W.; McCoy, A.; McNicholas, S. J.; Murshudov, G. N.; Pannu, N. S.; Potterton, E. A.; Powell, H. R.; Read, R. J.; Vagin, A.; Wilson, K. S. *Acta Crystallogr. Sect. D Biol. Crystallogr.* **2011**, *67*, 235–242.
(17) Collaborative Computational Project, N. 4. *Acta Crystallogr. Sect. D Biol. Crystallogr.* **1994**, *50*, 760–763.
(18) Emsley, P.; Cowtan, K. *Acta Crystallogr. Sect. D Biol. Crystallogr.* **2004**, *60*, 2126–2132.
(19) Murshudov, G. N.; Skubák, P.; Lebedev, A. A.; Pannu, N. S.; Steiner, R. A.; Nicholls, R. A.; Winn, M. D.; Long, F.; Vagin, A. A. *Acta Crystallogr. Sect. D Biol. Crystallogr.* **2011**, *67*, 355–367.
(20) Laskowski, R. A.; MacArthur, M. W.; Moss, D. S.; Thornton, J. M. *J. Appl. Crystallogr.* **1993**, *26*, 283–291.
(21) Aydillo, C.; Jiménez-Osés, G.; Busto, J. H.; Peregrina, J. M.; Zurbano, M. M.; Avenoza, A. *Chem. Eur. J.* **2007**, *13*, 4840–4848.
(22) Winterfeld, G. A.; Ito, Y.; Ogawa, T.; Schmidt, R. R. *Eur. J. Org. Chem.* **1999**, 1167–1171.
(23) Winterfeld, G. A.; Schmidt, R. R. *Angew. Chem. Int. Ed.* **2001**, *40*, 2654–2657.
(24) Sánchez-Fernández, E. M.; Gonçalves-Pereira, R.; Rísquez-Cuadro, R.; Plata, G. B.; Padrón, J. M.; García Fernández, J. M.; Ortiz Mellet, C. *Carbohydr. Res.* **2016**, *429*, 113–122.
(25) Pérez, P. D.; García-Moreno, M. I.; Ortiz Mellet, C.; García Fernández, J. M. *Eur. J. Org. Chem.* **2005**, 2903–2913.
(26) Díaz Pérez, V. M.; García Moreno, M. I.; Ortíz-Mellet, C.; Fuentes, J.; Díaz Arribas, J. C.; Cañada, F. J.; García Fernández, J. M. *J. Org. Chem.* **2000**, *65*, 136–143.
(27) Madariaga, D.; Martínez-Sáez, N.; Somovilla, V. J.; García-García, L.; Berbis, M. Á.; Valero-Gónzalez, J.; Martín-Santamaría, S.; Hurtado-Guerrero, R.; Asensio, J. L.; Jiménez-Barbero, J.; Avenoza, A.; Busto, J. H.; Corzana, F.; Peregrina, J. M. *Chem. Eur. J.* **2014**, *20*, 12616–12627.

SI.1 NMR spectra

SI.2 Computational details

SI.1. NMR spectra

NMR spectra for the compounds described throughout *Chapter 7: Experimental section* are collected in the following pages. 2D COSY and HSQC experiments performed for describing the following compounds have been omitted in this section.

^{1}H NMR 400 MHz in $CDCl_3$

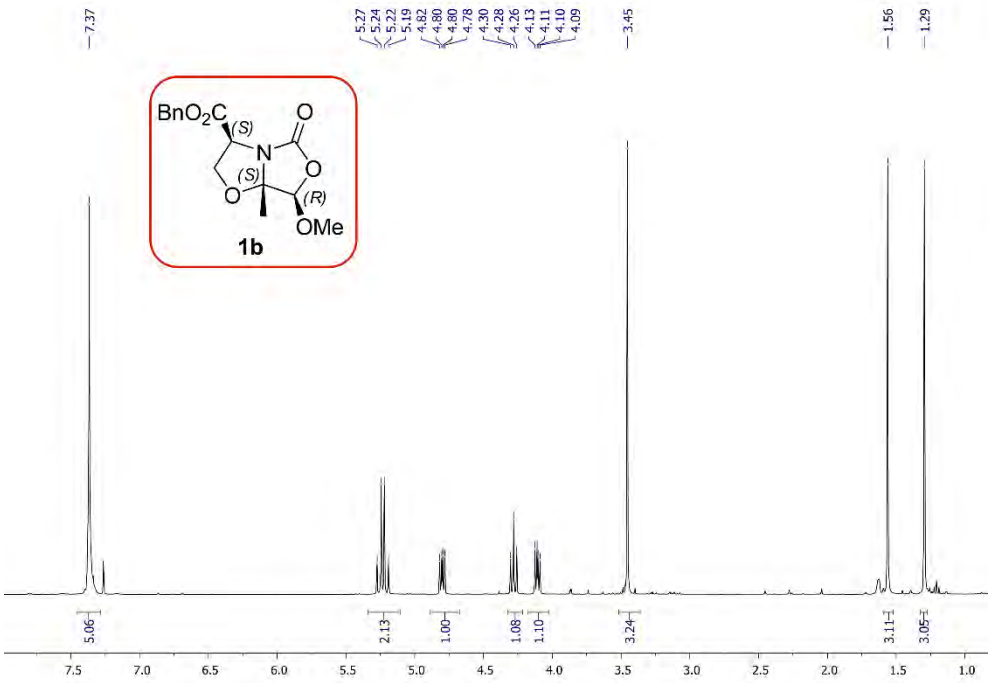

^{13}C NMR 100 MHz in $CDCl_3$

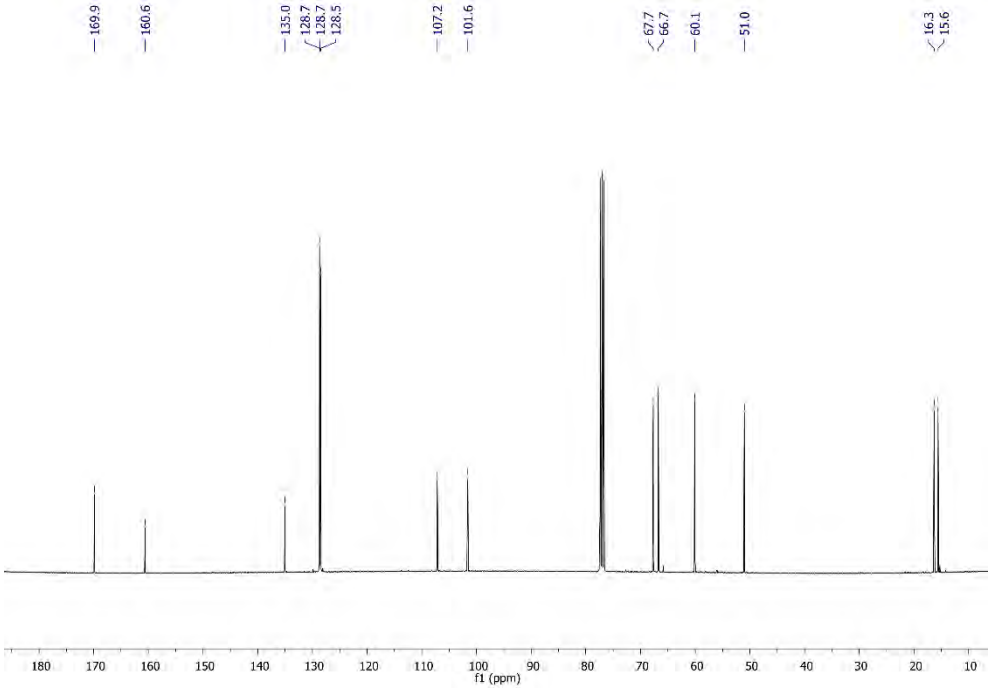

^{1}H NMR 400 MHz in $CDCl_3$

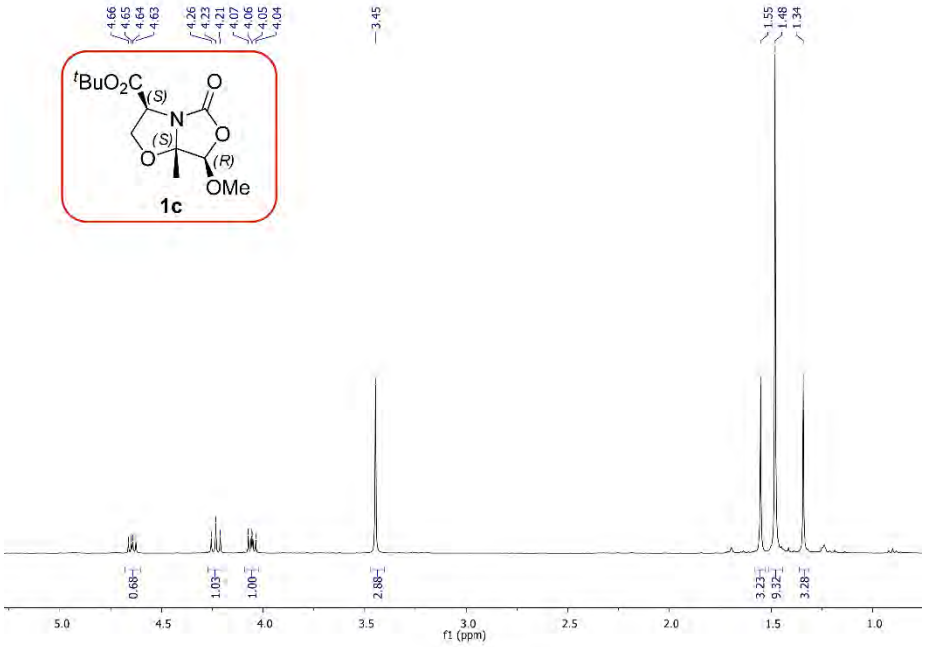

^{13}C NMR 100 MHz in $CDCl_3$

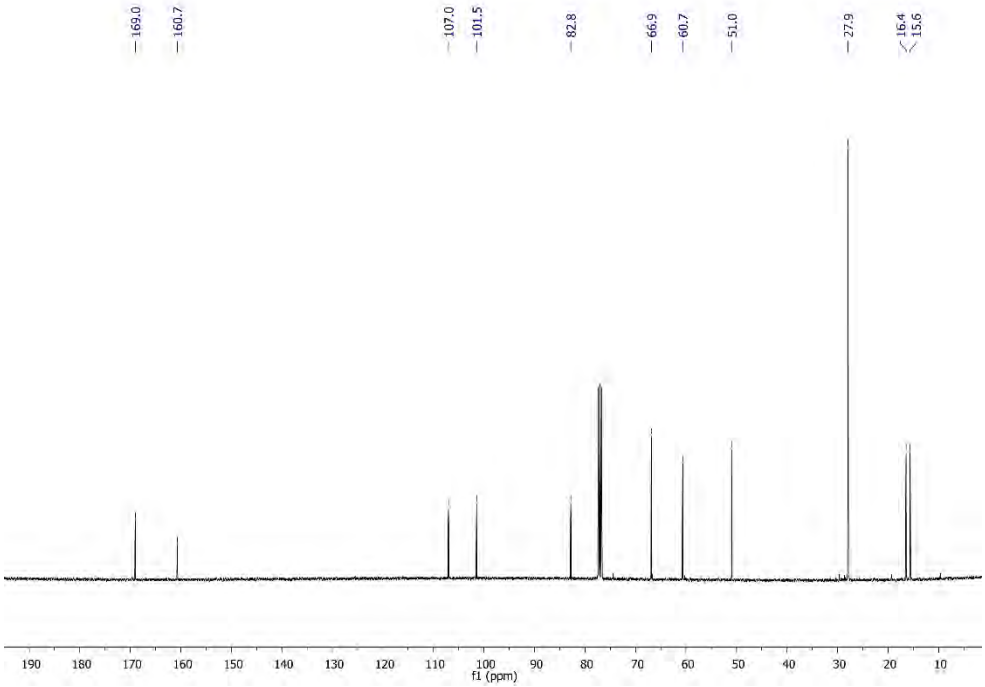

^{1}H NMR 400 MHz in $CDCl_3$

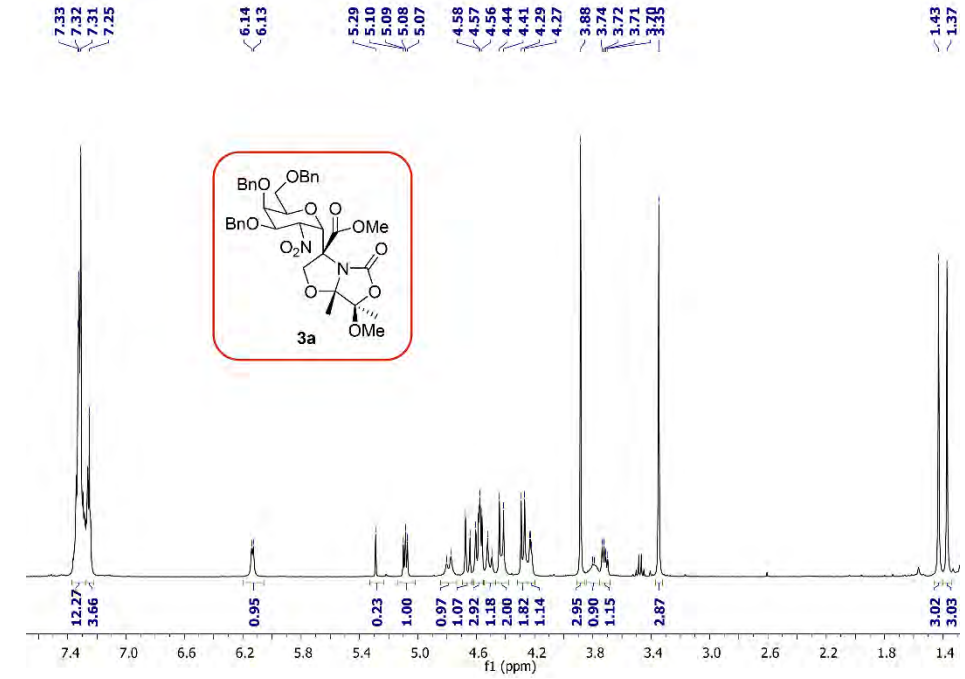

^{13}C NMR 100 MHz in $CDCl_3$

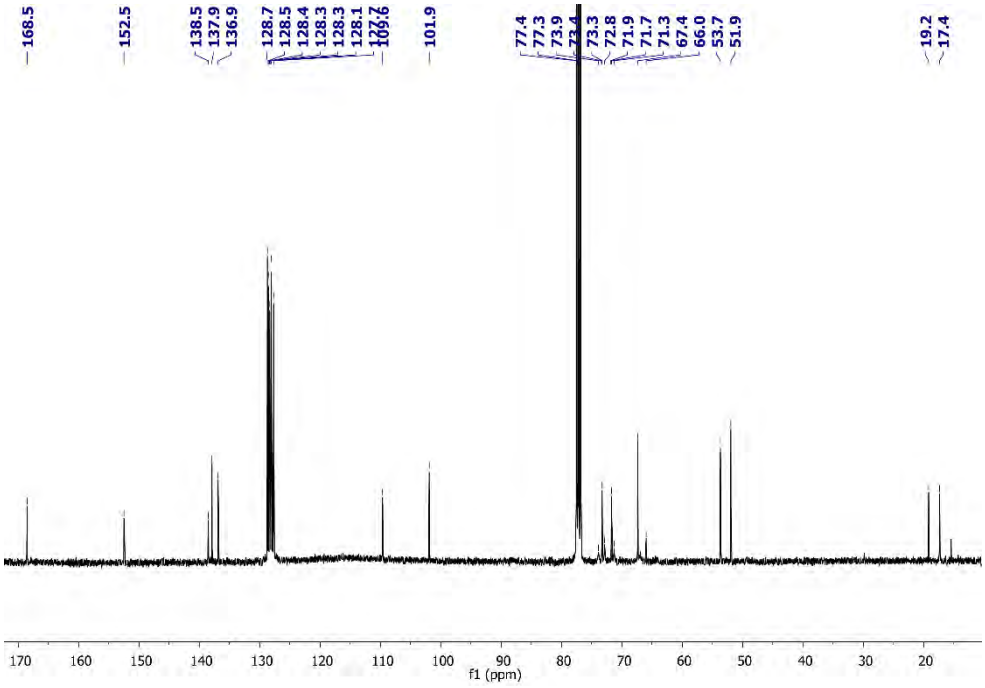

^{1}H NMR 400 MHz in $CDCl_3$

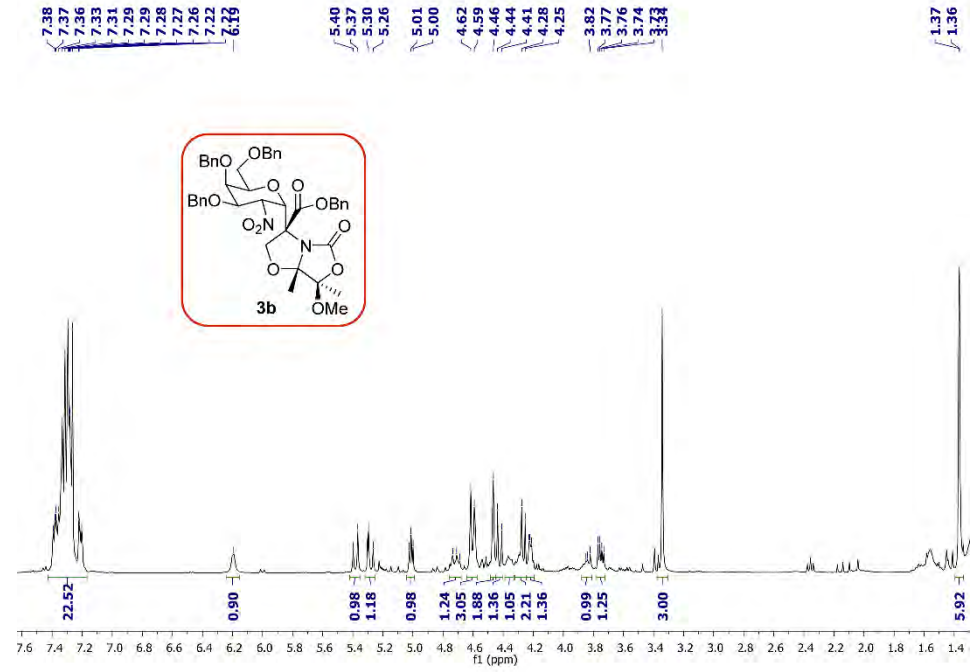

^{13}C NMR 100 MHz in $CDCl_3$

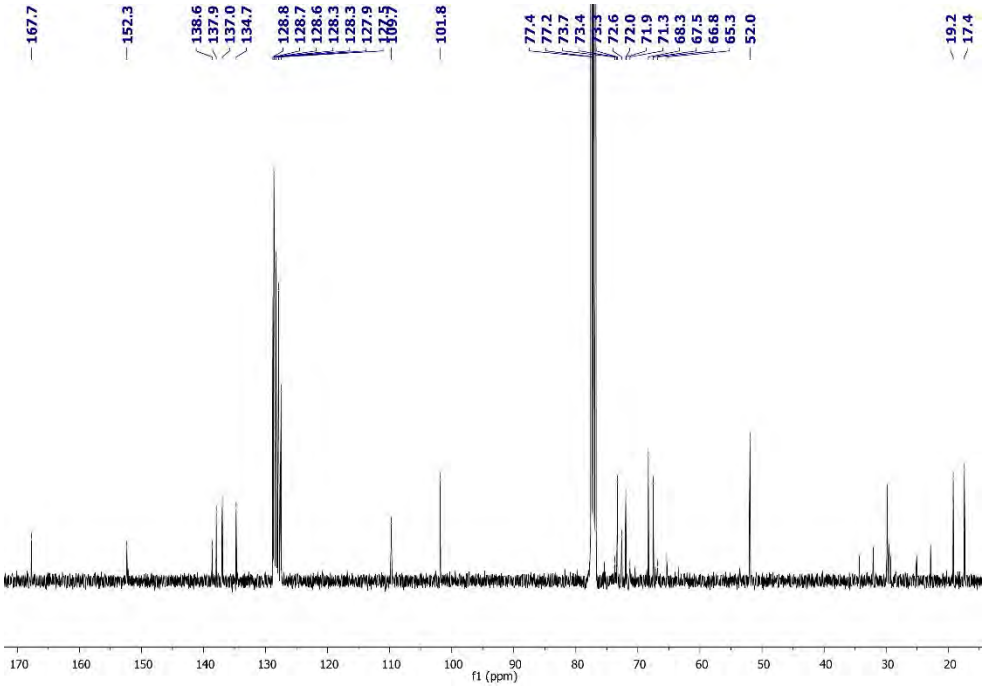

^{1}H NMR 400 MHz in $CDCl_3$

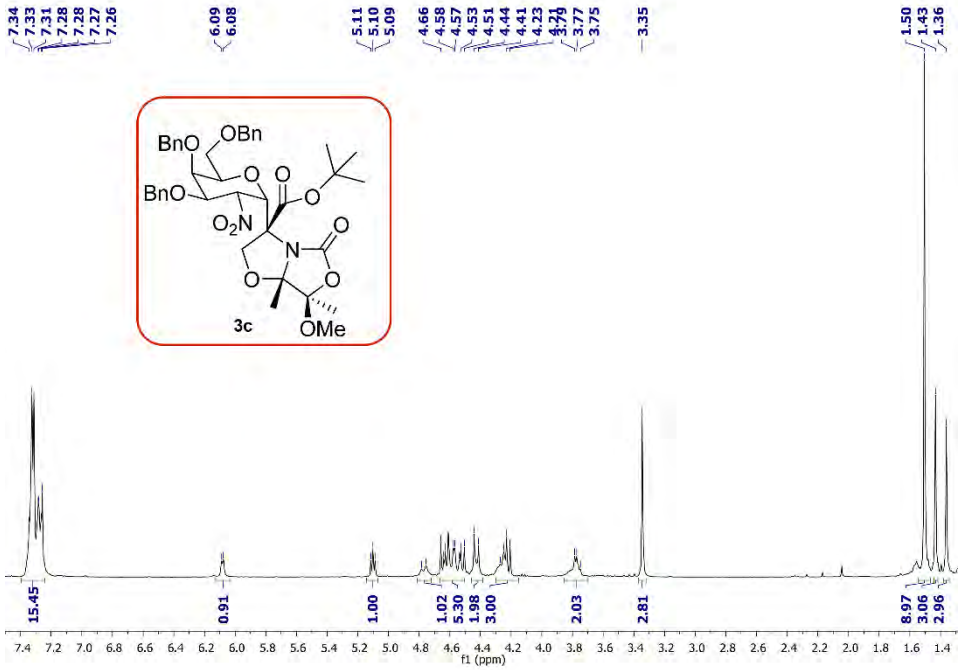

^{13}C NMR 100 MHz in $CDCl_3$

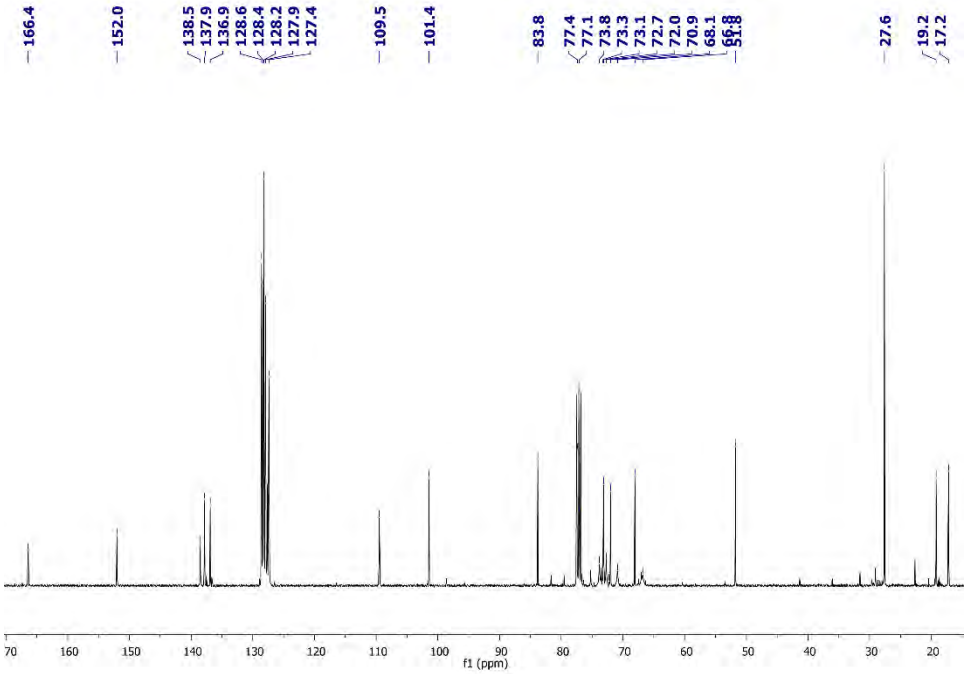

^{1}H NMR 400 MHz in $CDCl_3$

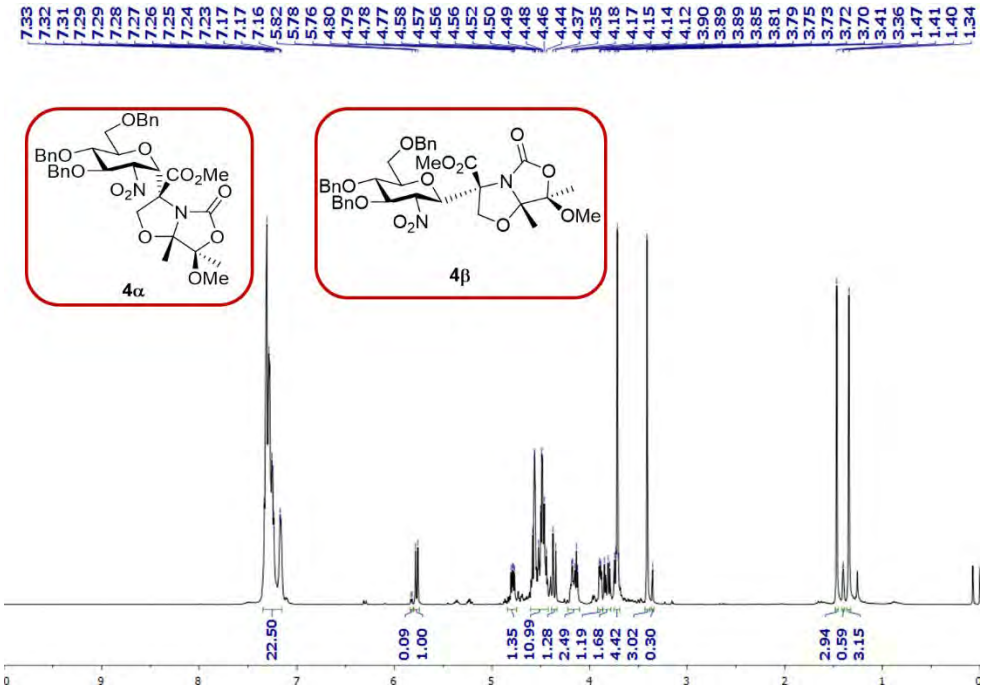

^{13}C NMR 100 MHz in $CDCl_3$

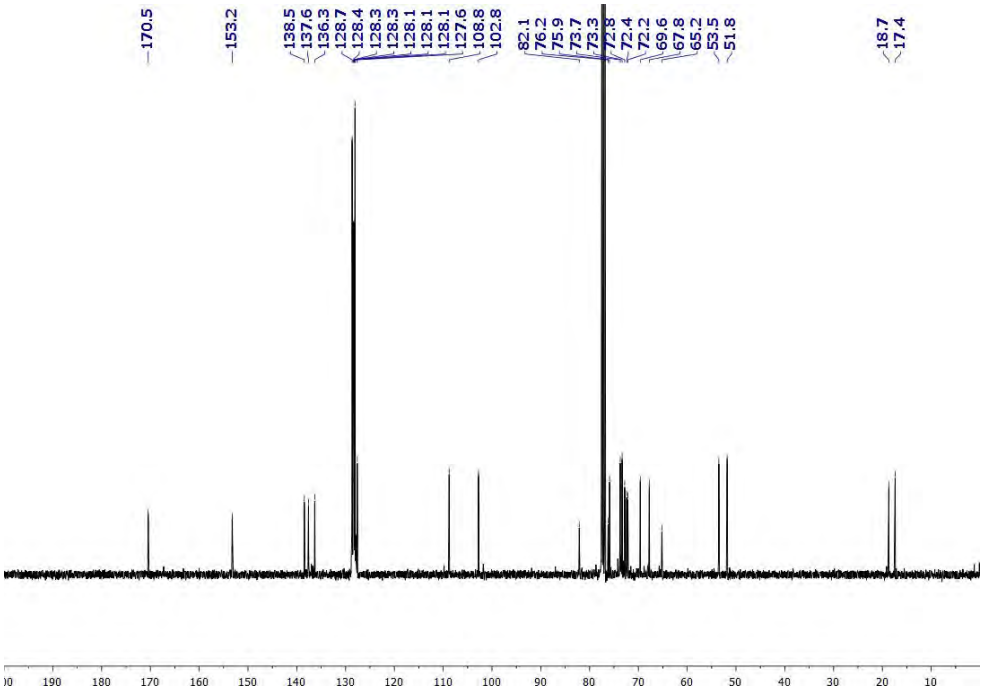

^{1}H NMR 400 MHz in $CDCl_3$

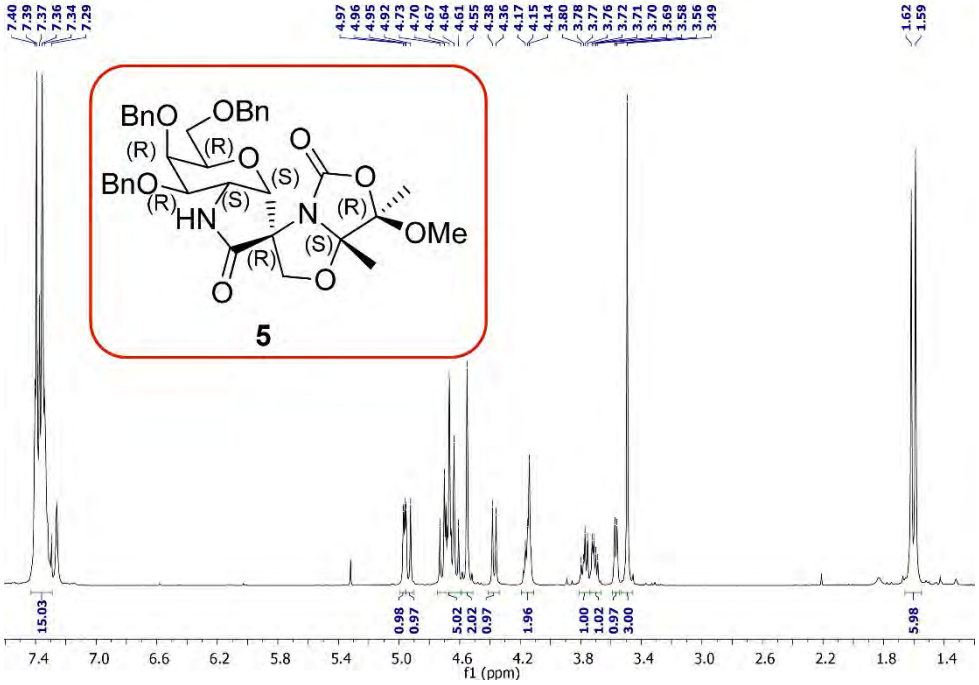

^{13}C NMR 100 MHz in $CDCl_3$

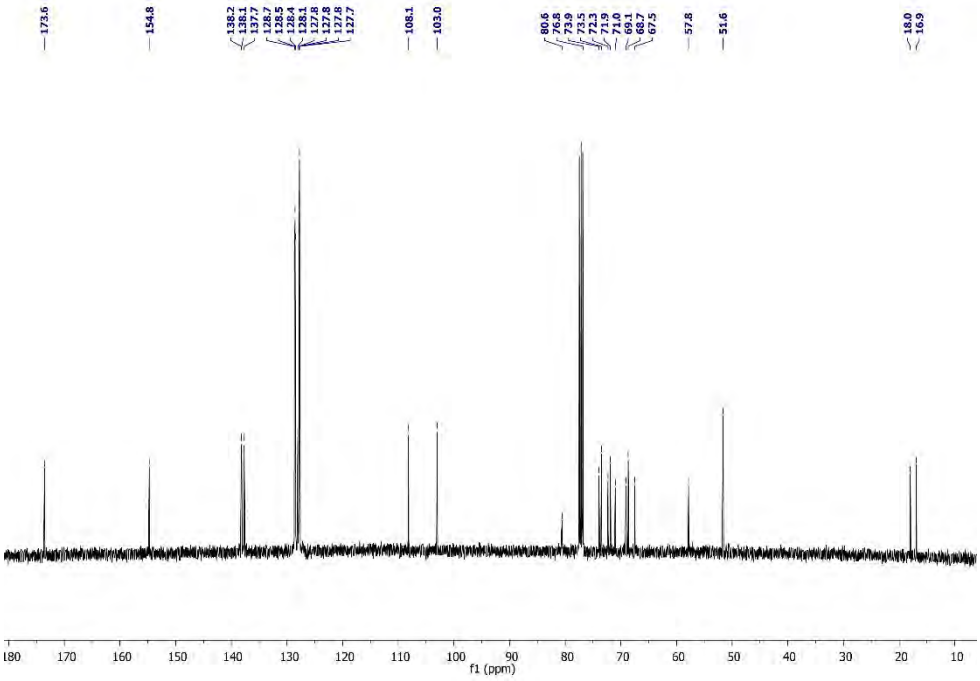

^{1}H NMR 400 MHz in $CDCl_3$

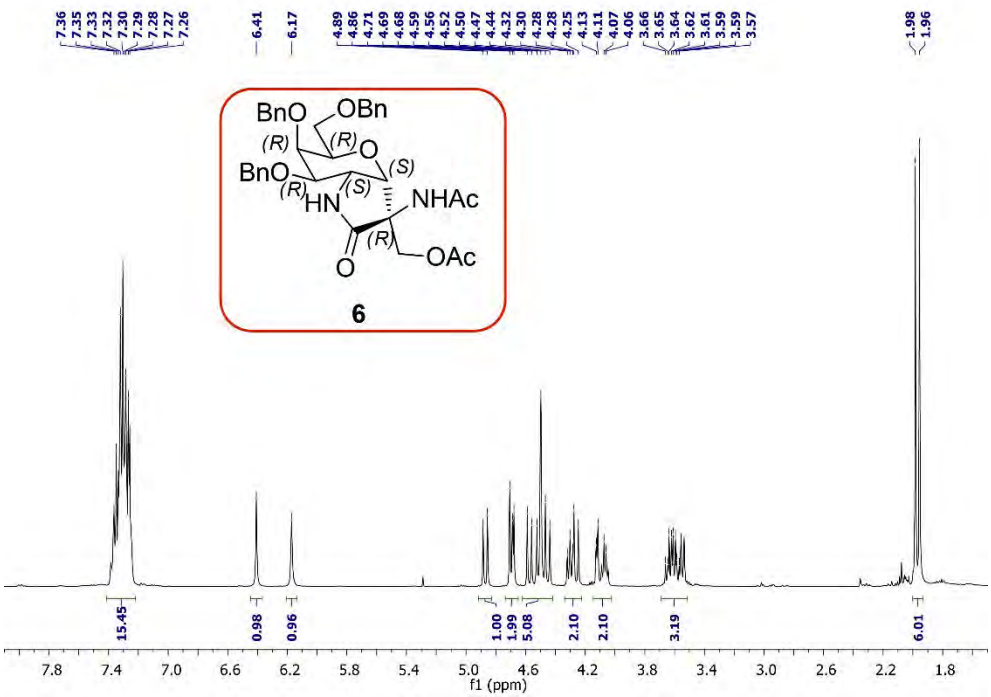

^{13}C NMR 100 MHz in $CDCl_3$

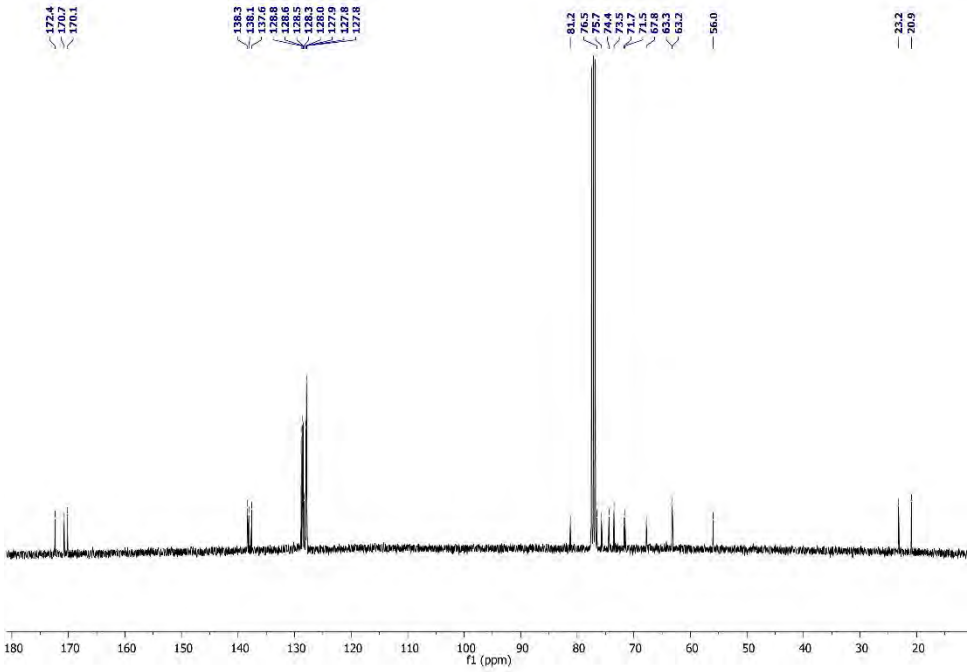

^{1}H NMR 400 MHz in $CDCl_3$

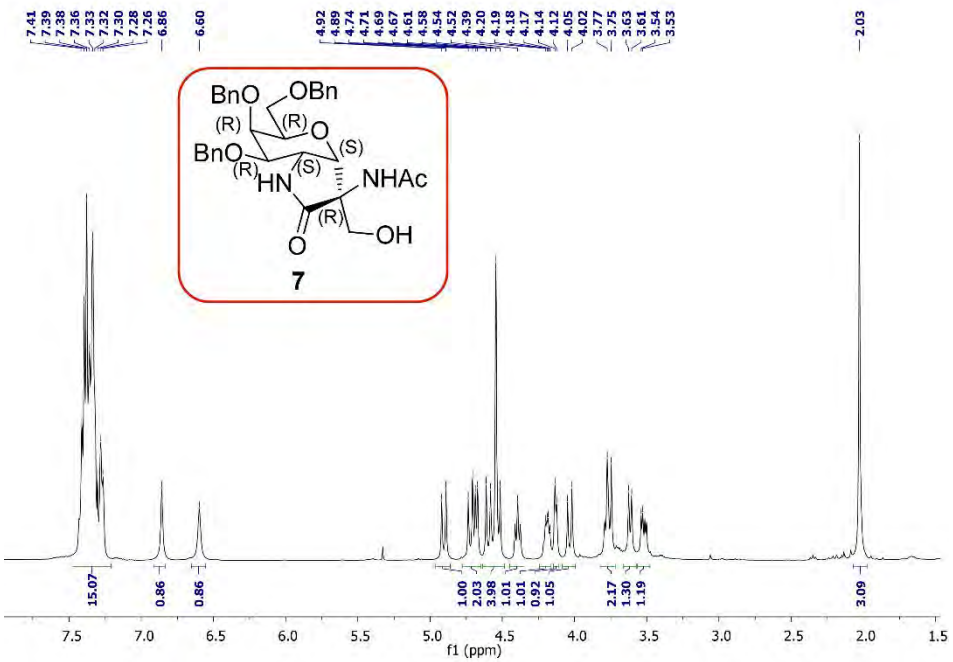

^{13}C NMR 100 MHz in $CDCl_3$

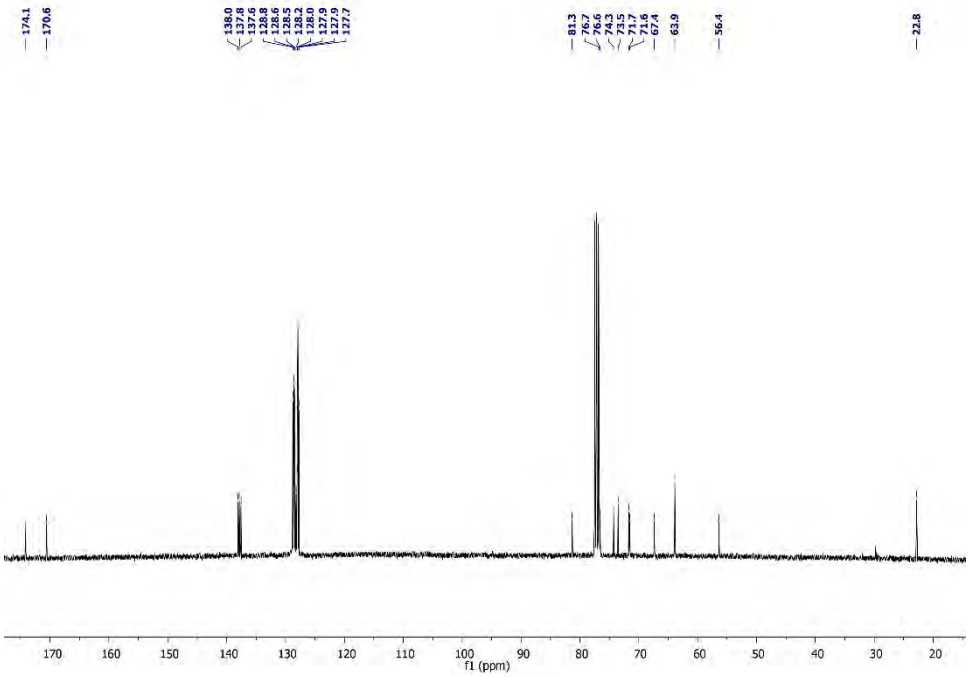

^{1}H NMR 400 MHz in $CDCl_3$

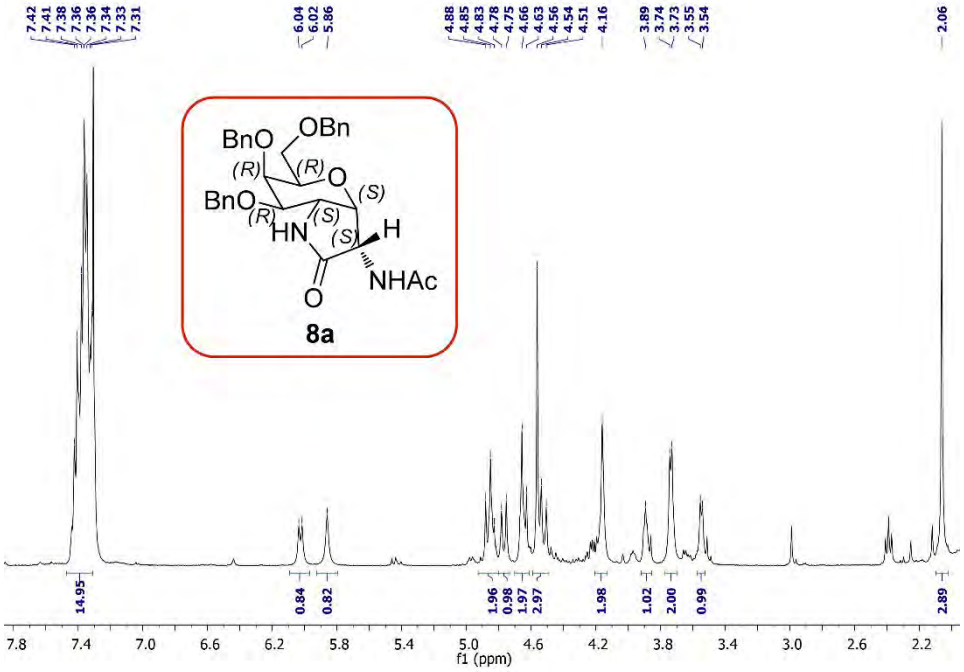

^{13}C NMR 100 MHz in $CDCl_3$

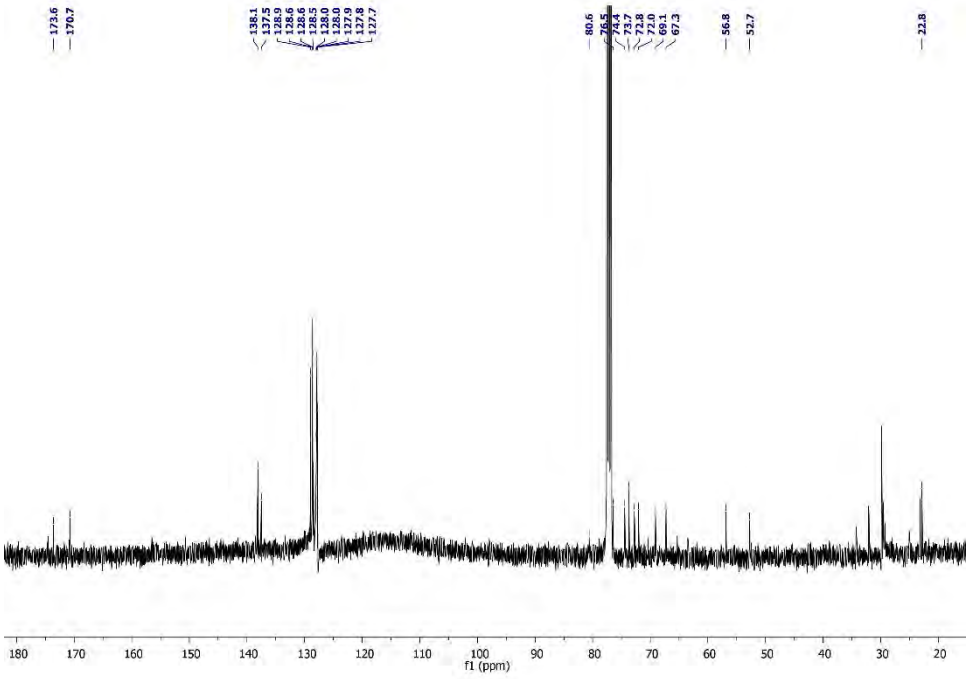

^{1}H NMR 400 MHz in $CDCl_3$

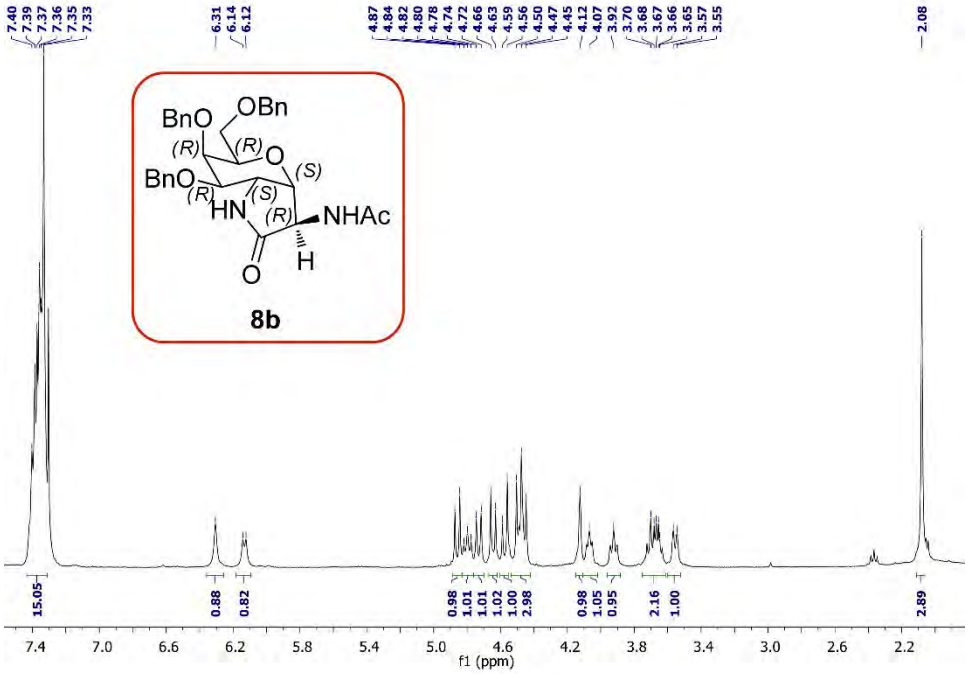

^{13}C NMR 100 MHz in $CDCl_3$

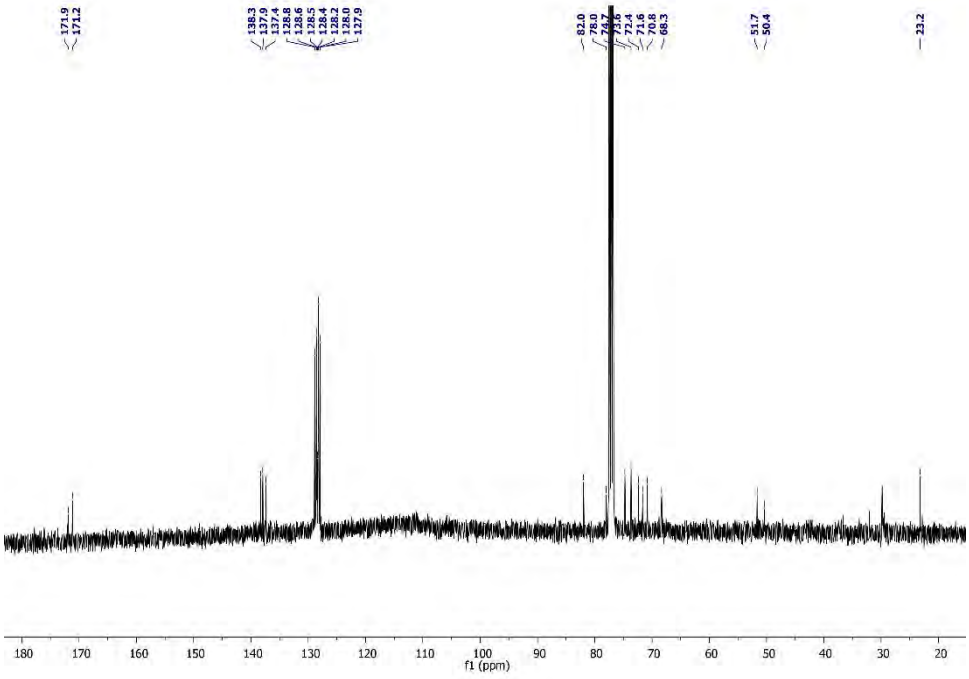

^{1}H NMR 400 MHz in CD_3OD

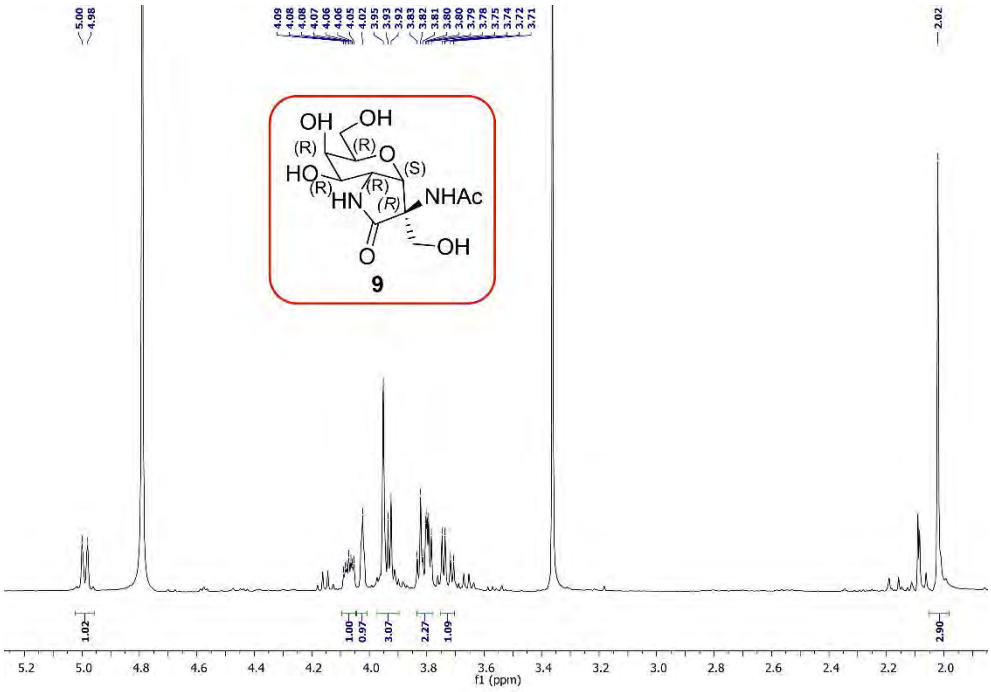

^{13}C NMR 100 MHz in CD_3OD

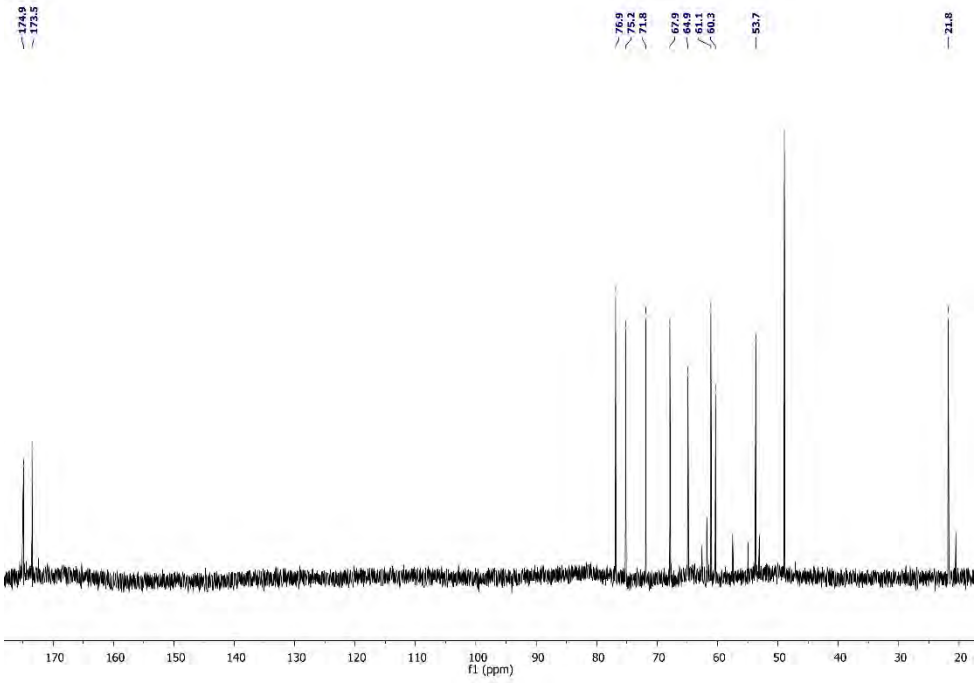

NOESY in H_2O/D_2O (9:1)

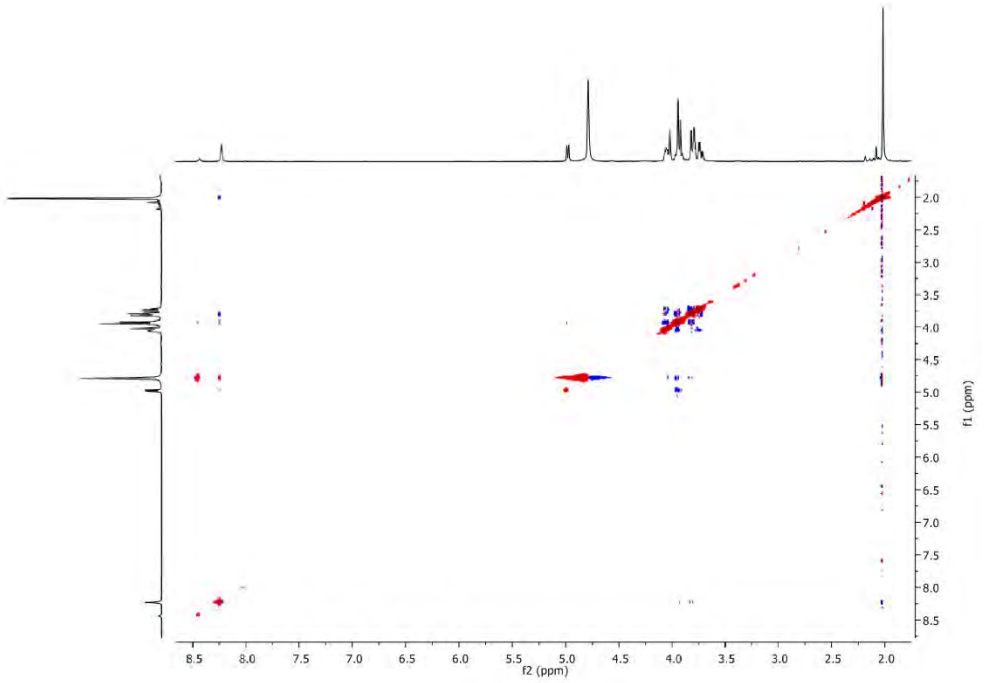

^{1}H NMR 400 MHz in D_2O

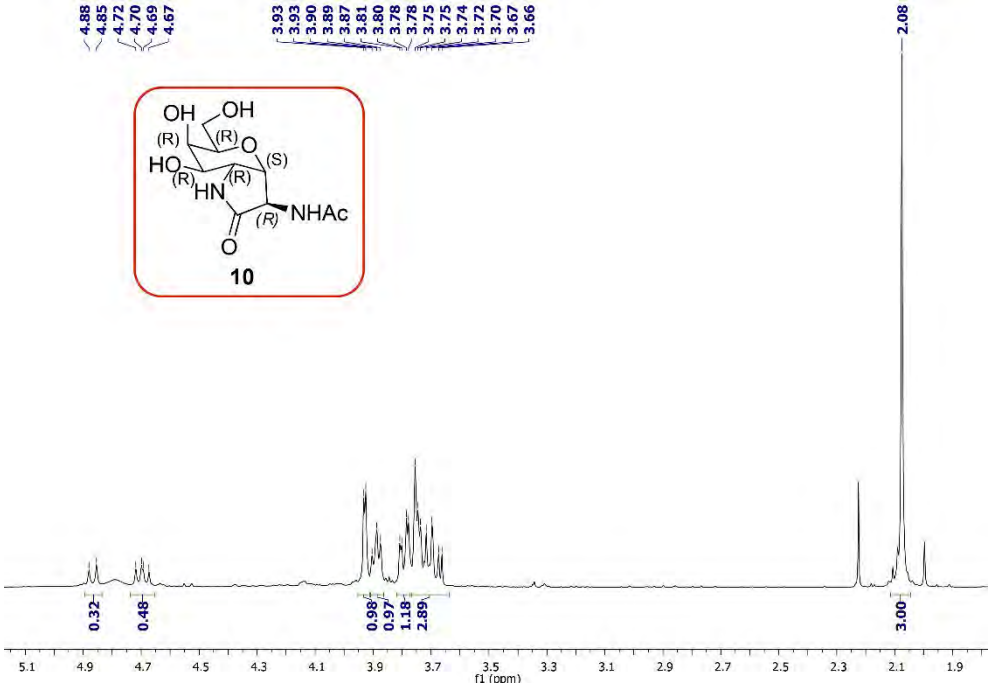

^{13}C NMR 100 MHz in D_2O

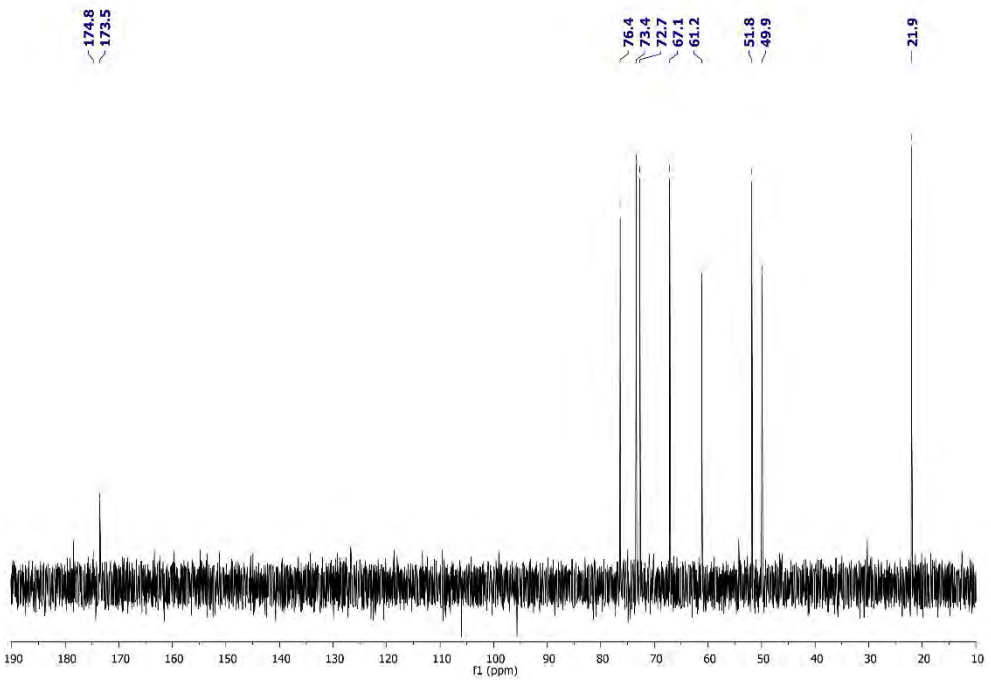

NOESY in H_2O/D_2O (9:1)

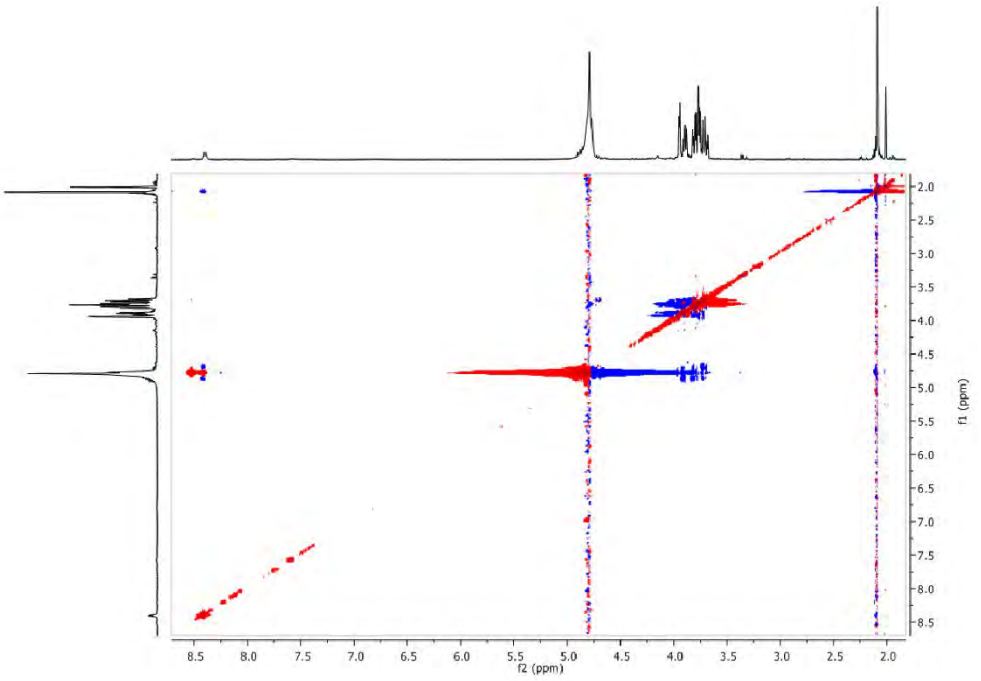

^{1}H NMR 400 MHz in D_2O

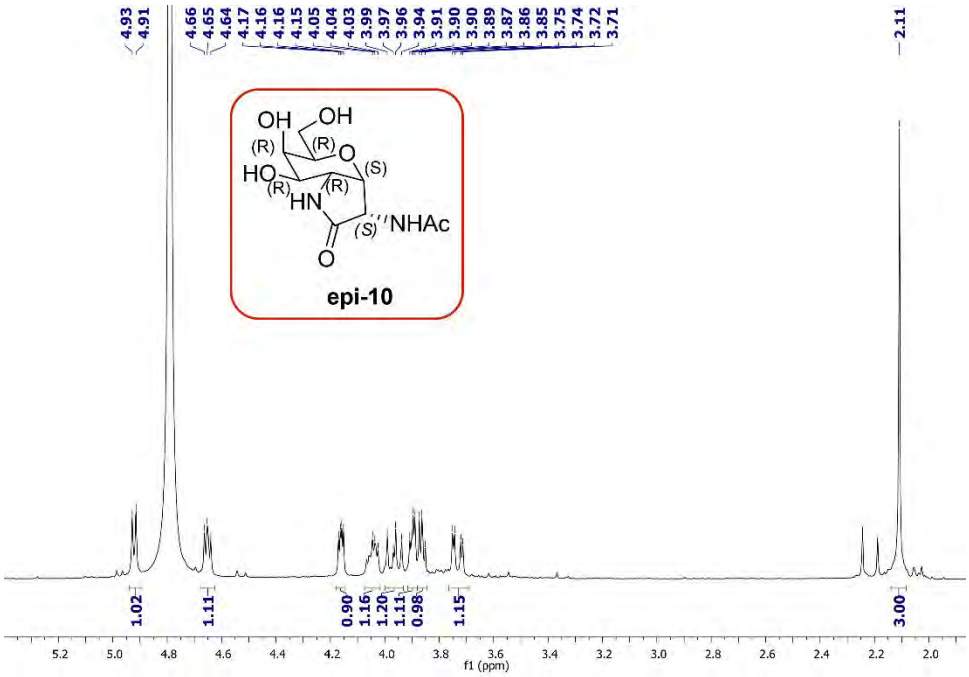

^{13}C NMR 100 MHz in D_2O

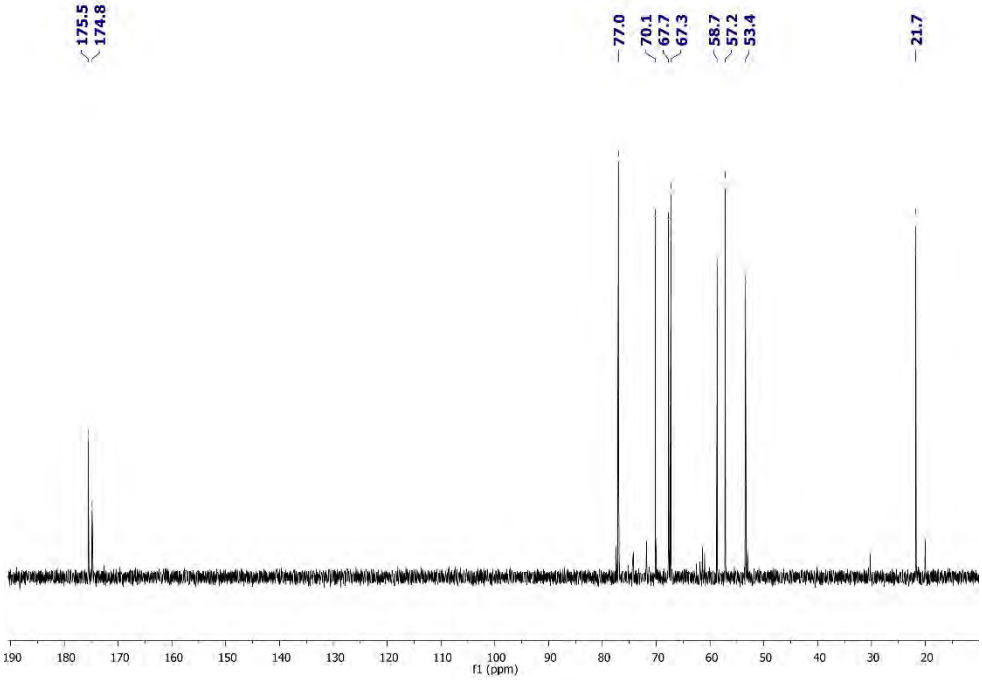

NOESY in H_2O/D_2O (9:1)

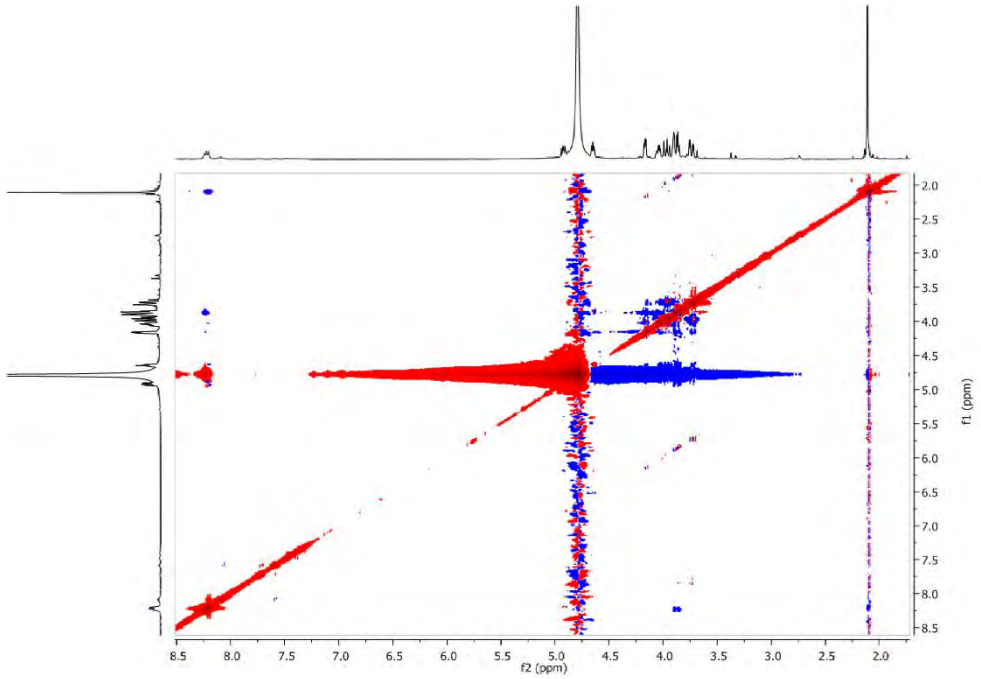

^{1}H NMR 400 MHz in $CDCl_3$

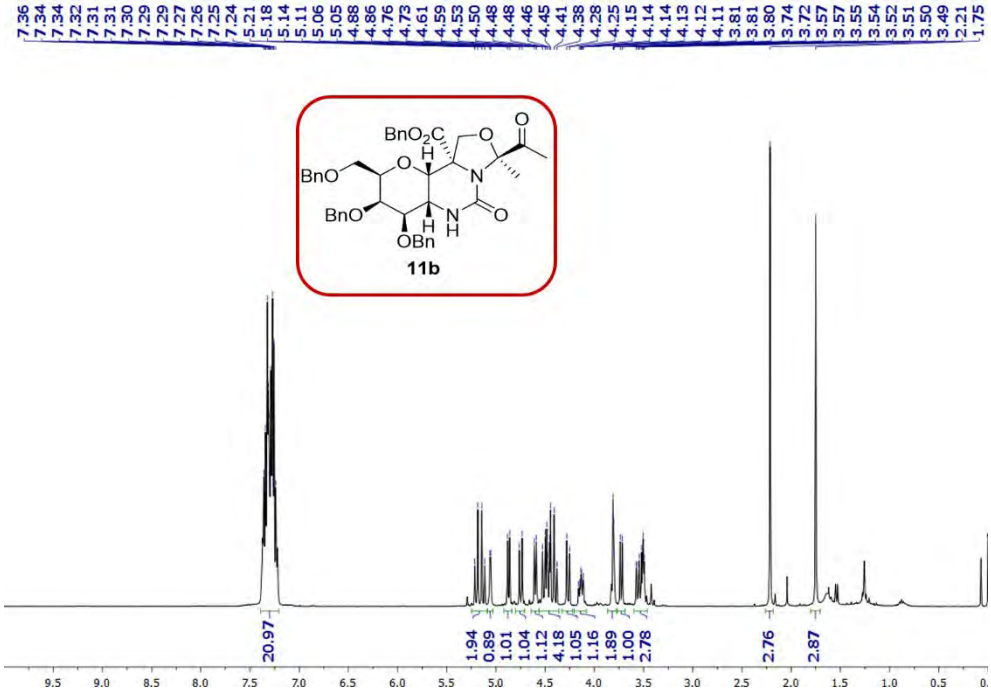

^{13}C NMR 100 MHz in $CDCl_3$

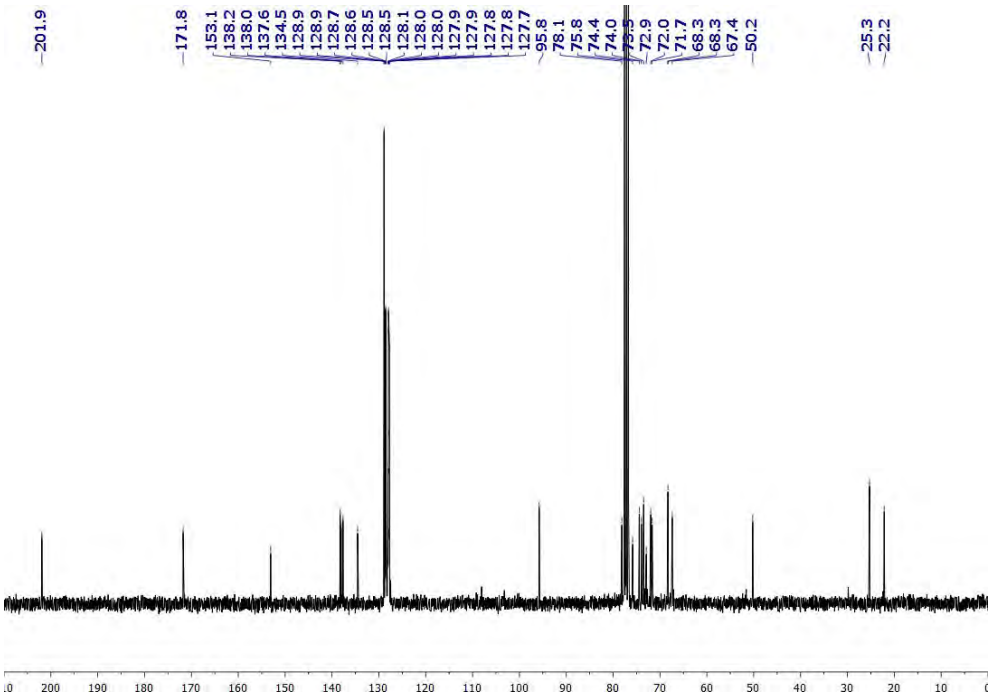

^{1}H NMR 400 MHz in $CDCl_3$

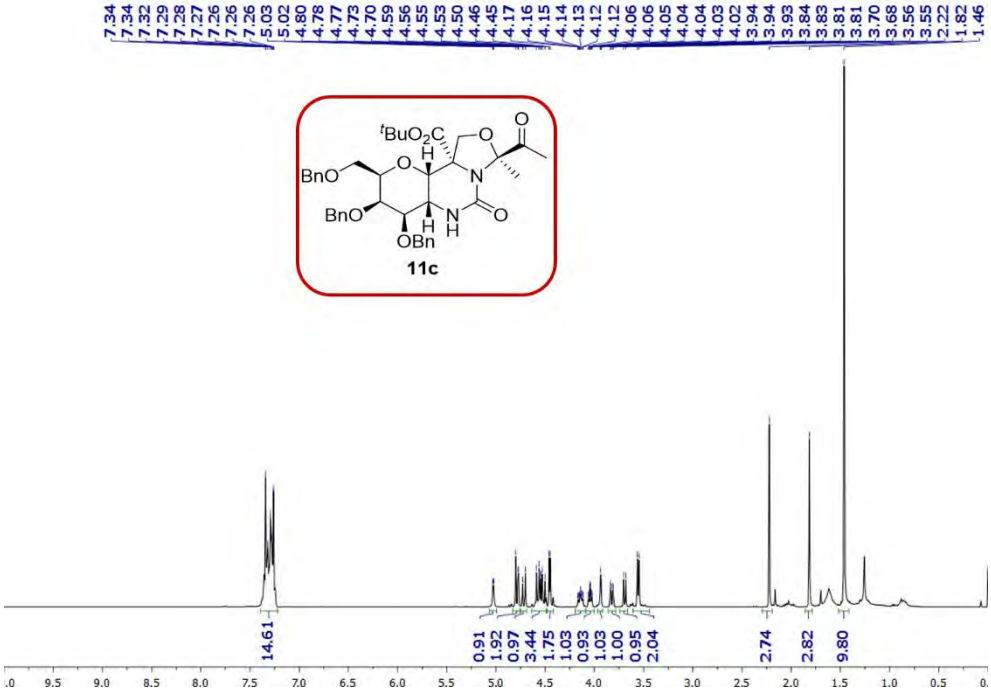

^{13}C NMR 100 MHz in $CDCl_3$

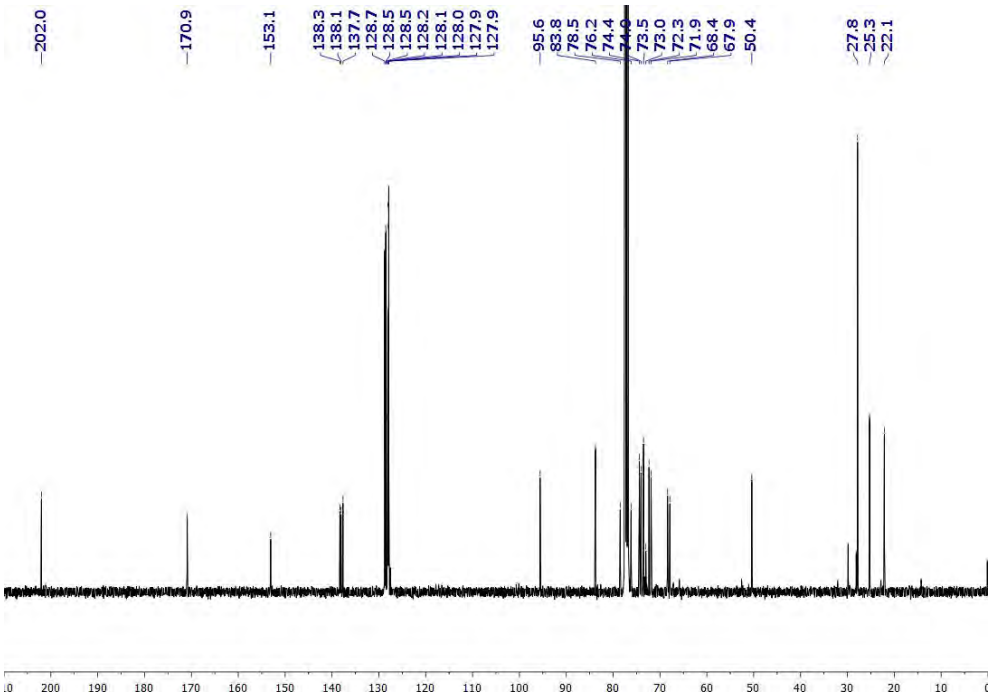

^{1}H NMR 400 MHz in D_2O

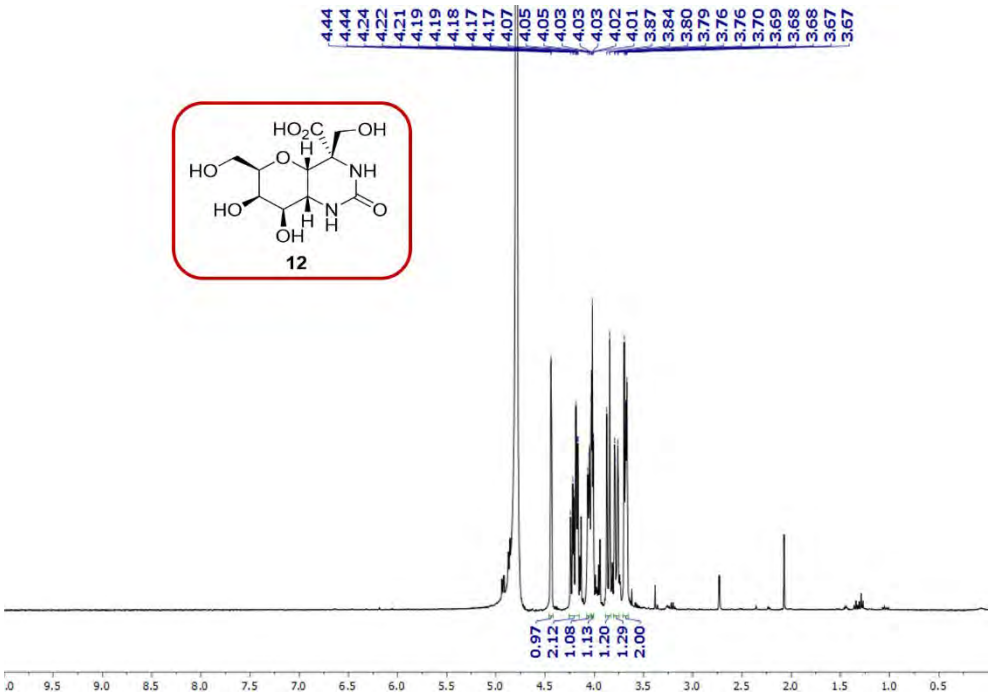

^{13}C NMR 100 MHz in D_2O

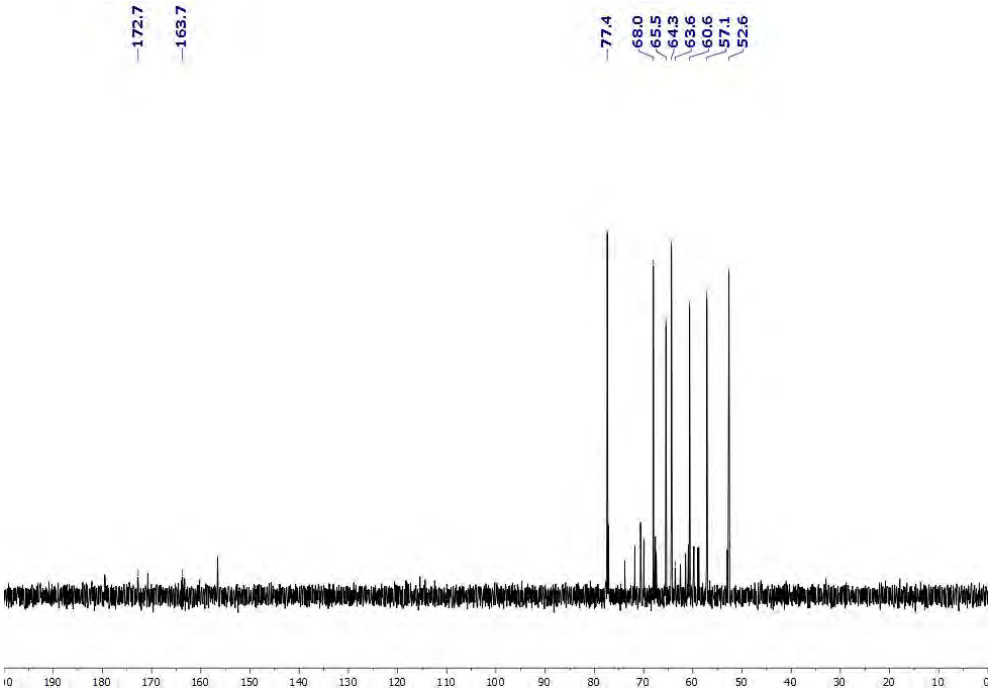

NOESY in H_2O/D_2O

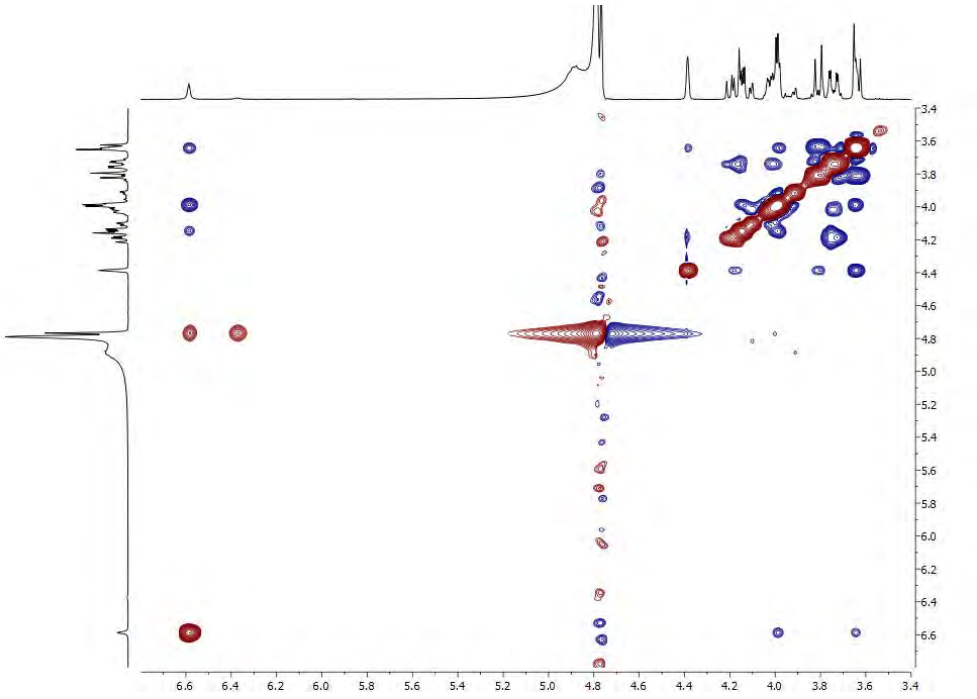

^{1}H NMR 400 MHz in $CDCl_3$

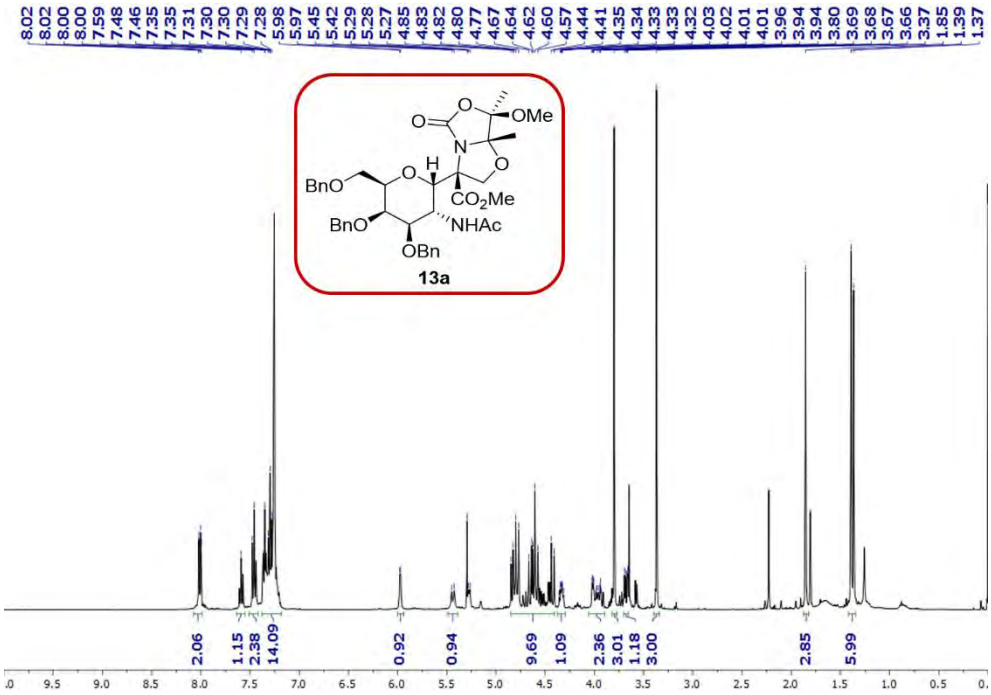

HSQC in $CDCl_3$

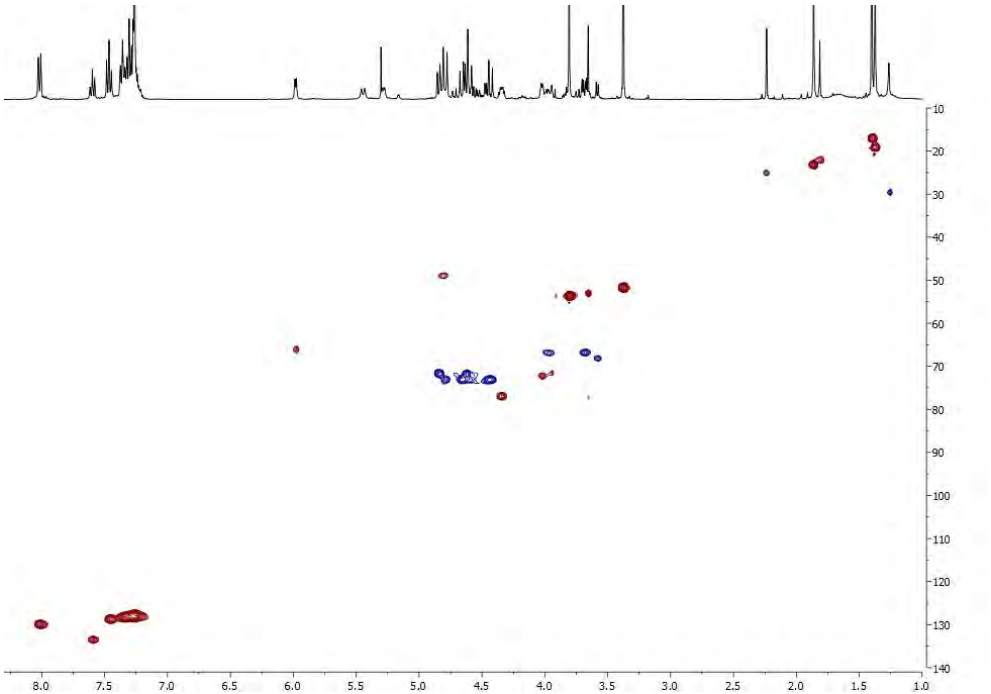

^{1}H NMR 400 MHz in $CDCl_3$

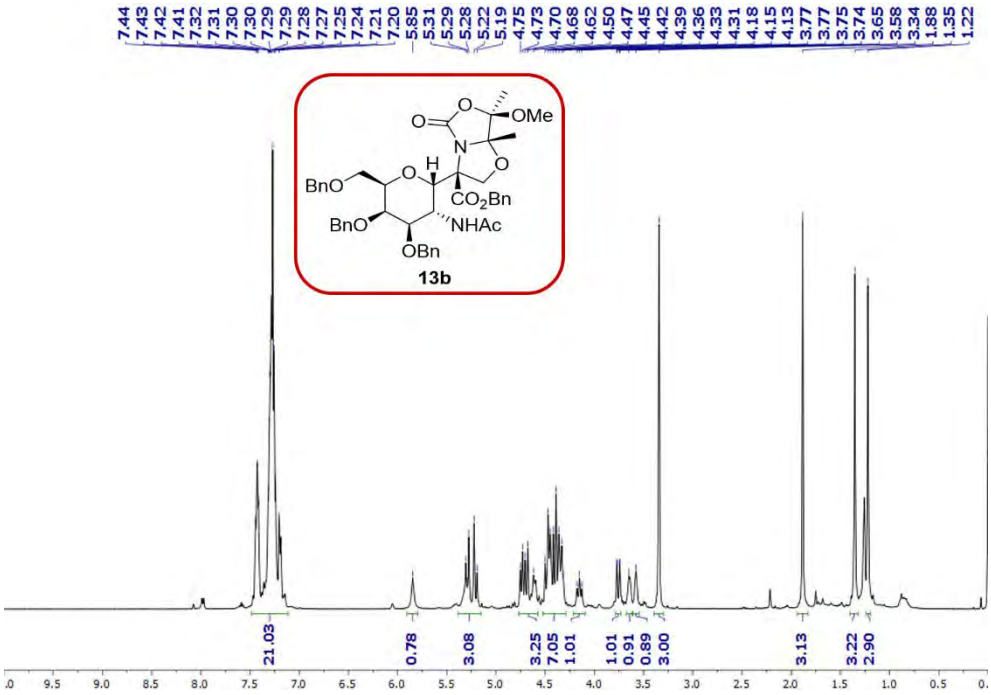

^{13}C NMR 100 MHz in $CDCl_3$

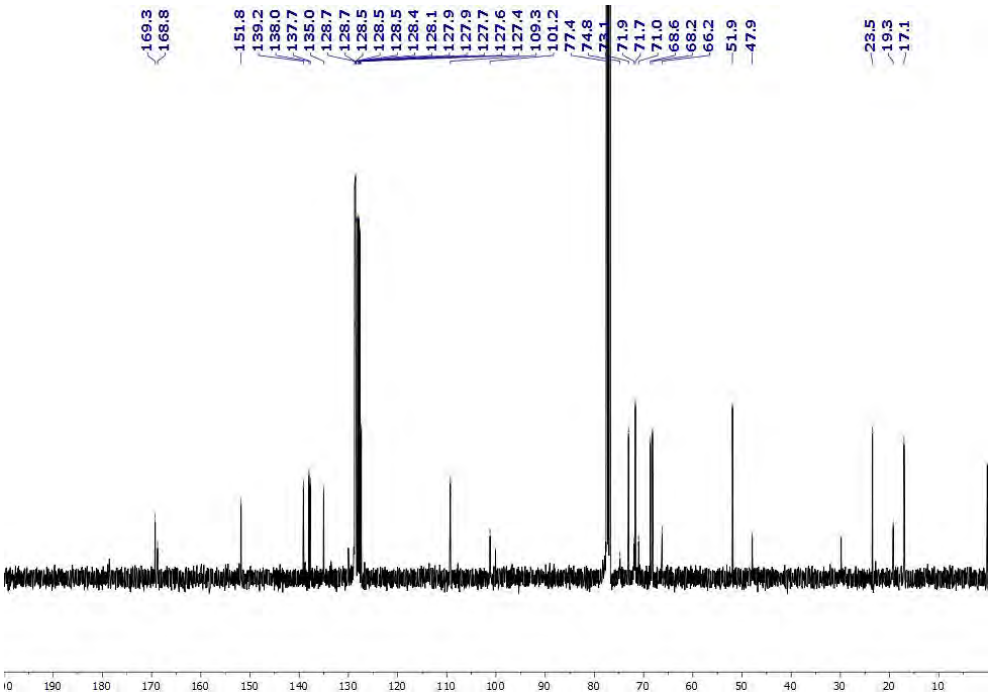

^{1}H NMR 400 MHz in $CDCl_3$

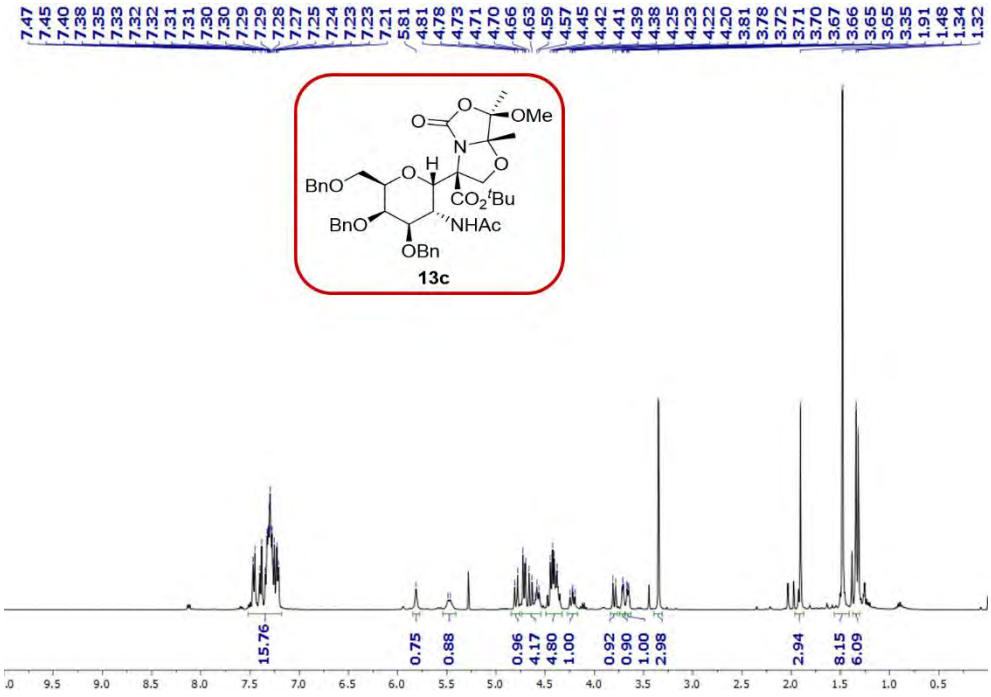

^{13}C NMR 100 MHz in $CDCl_3$

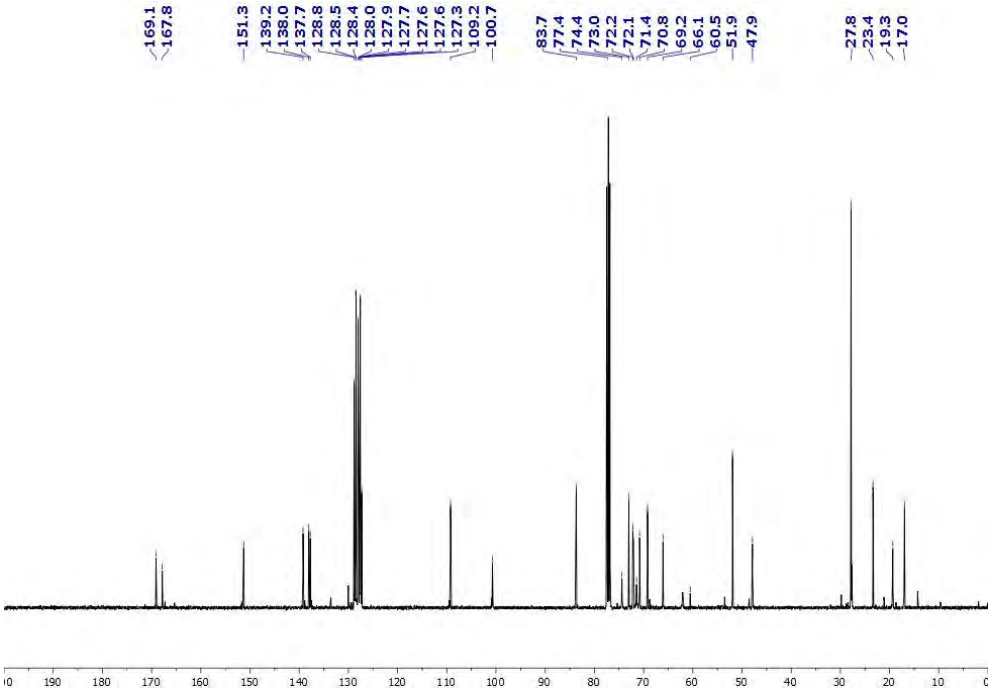

^{1}H NMR 400 MHz in D_2O

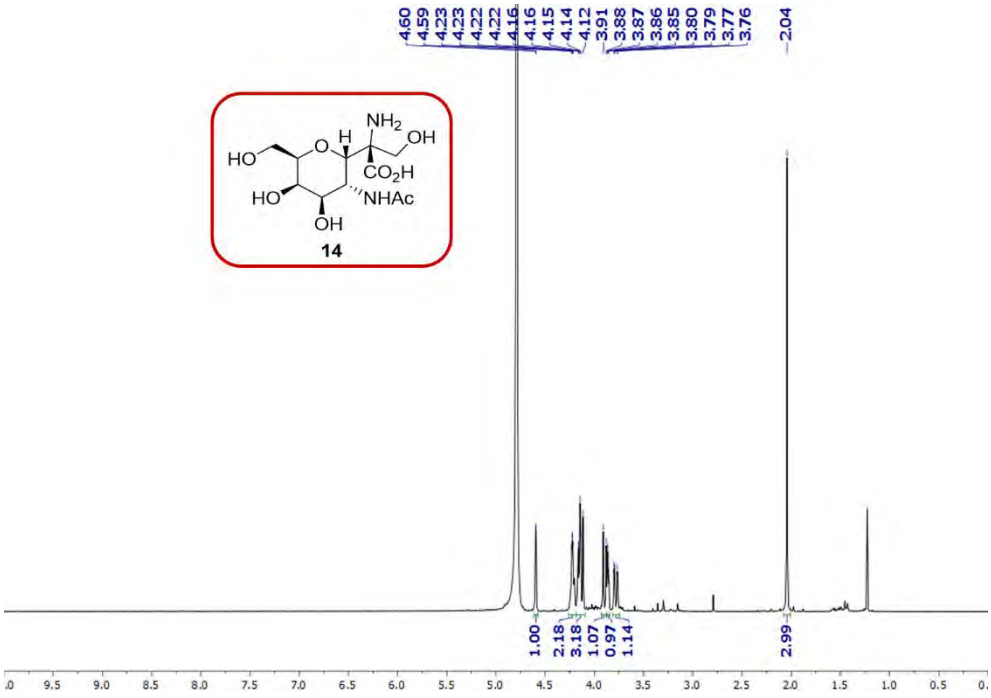

^{13}C NMR 100 MHz in D_2O

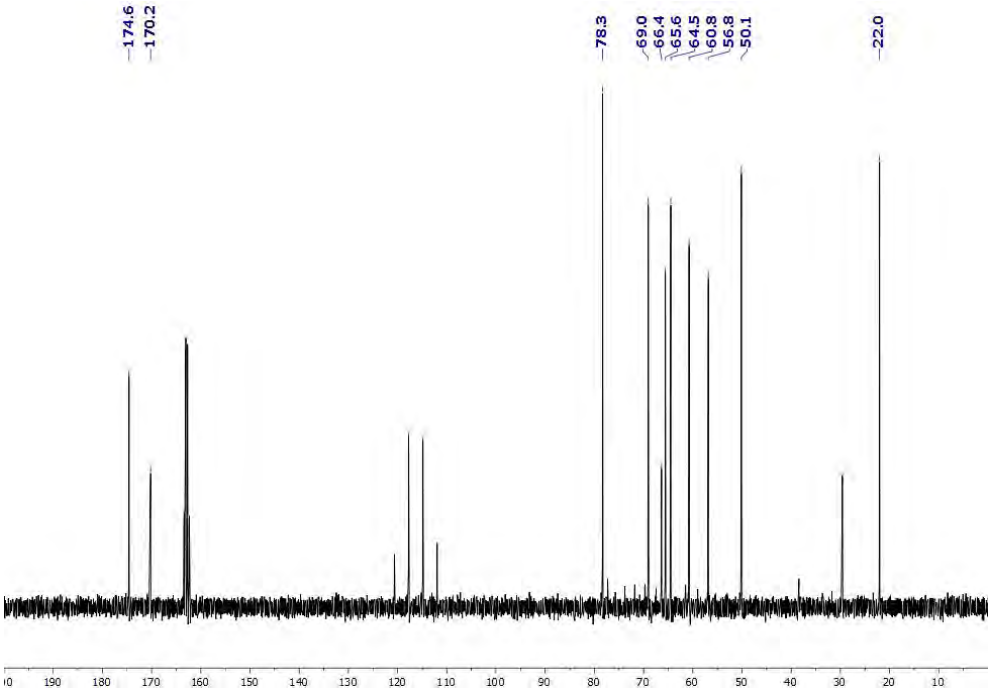

NOESY in H_2O/D_2O

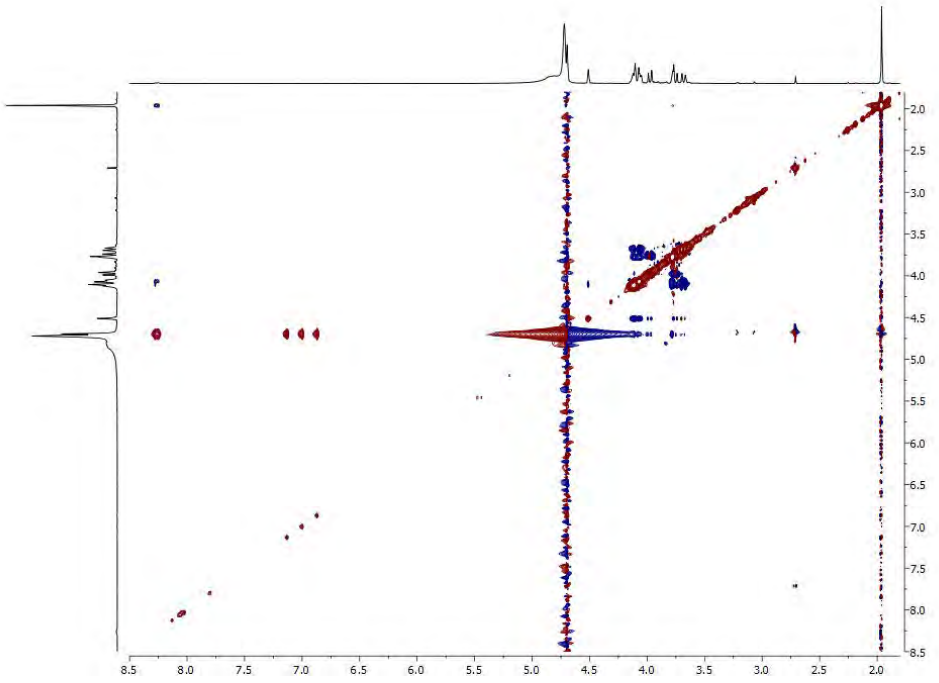

^{1}H NMR 400 MHz in $CDCl_3$

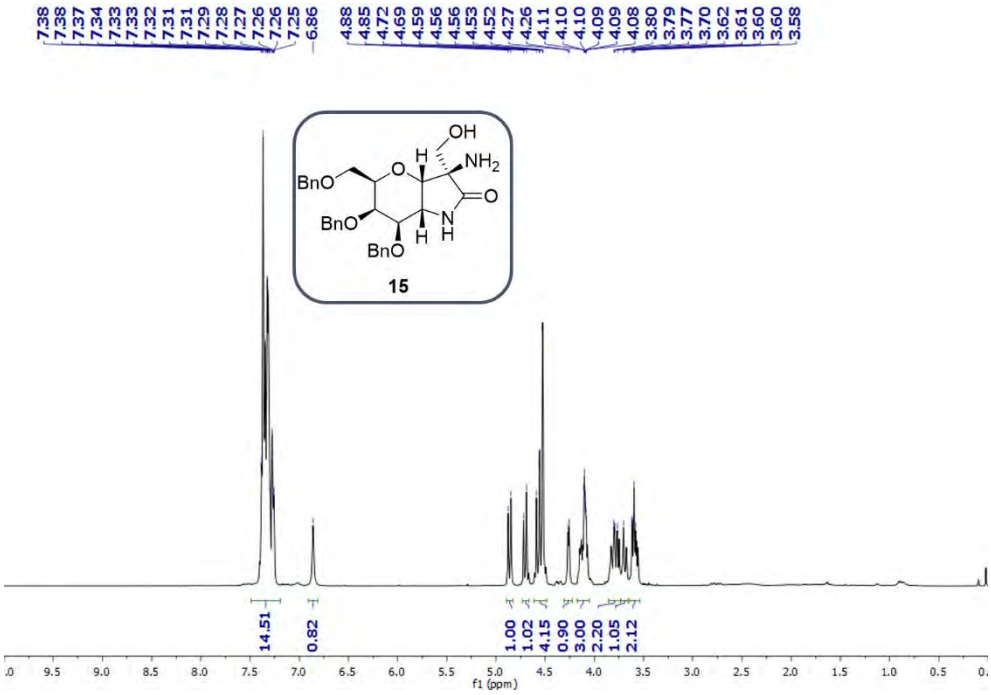

^{13}C NMR 100 MHz in $CDCl_3$

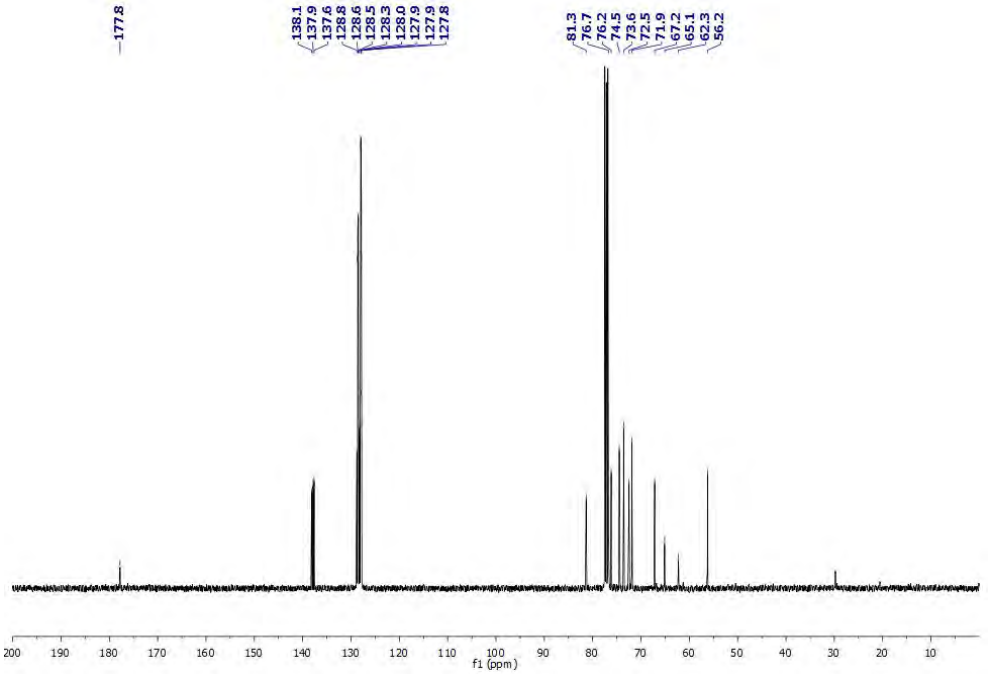

^{1}H NMR 400 MHz in $CDCl_3$

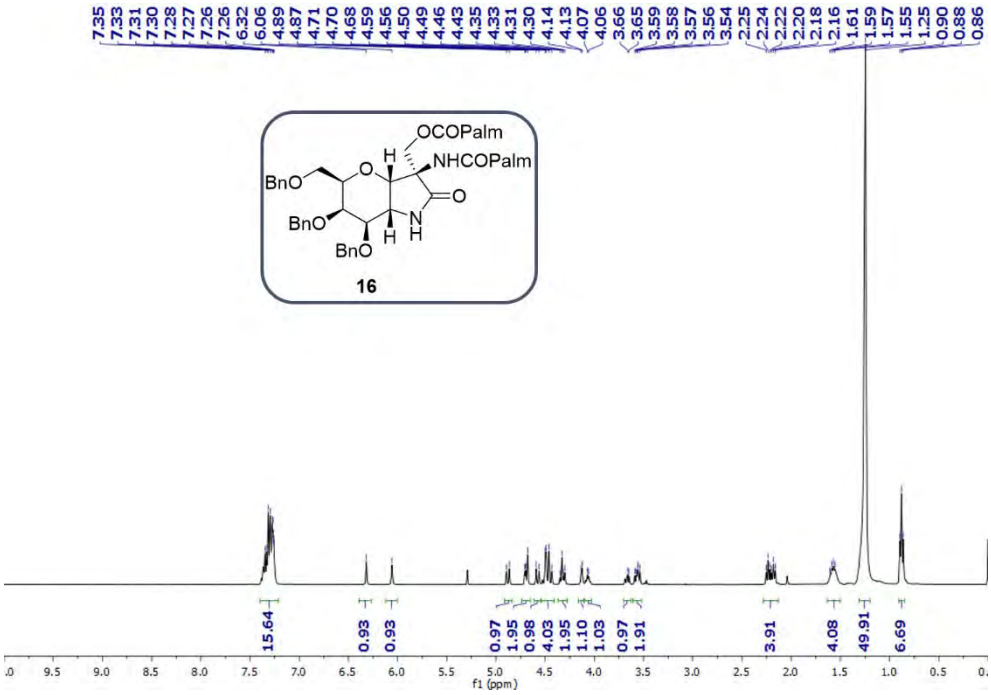

^{13}C NMR 100 MHz in $CDCl_3$

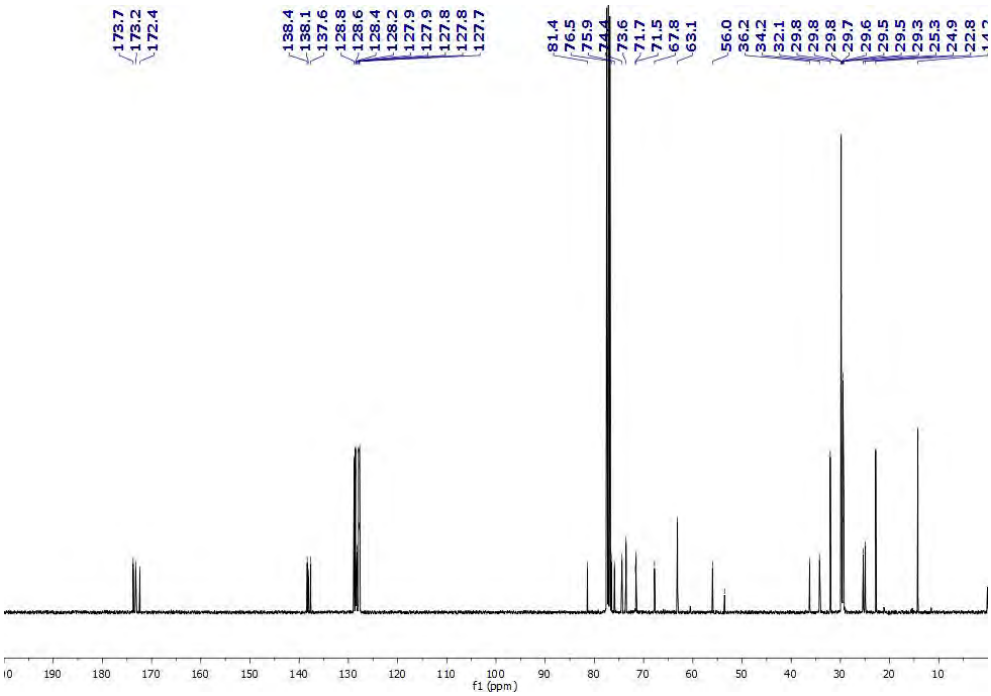

^{1}H NMR 400 MHz in CD_3OD

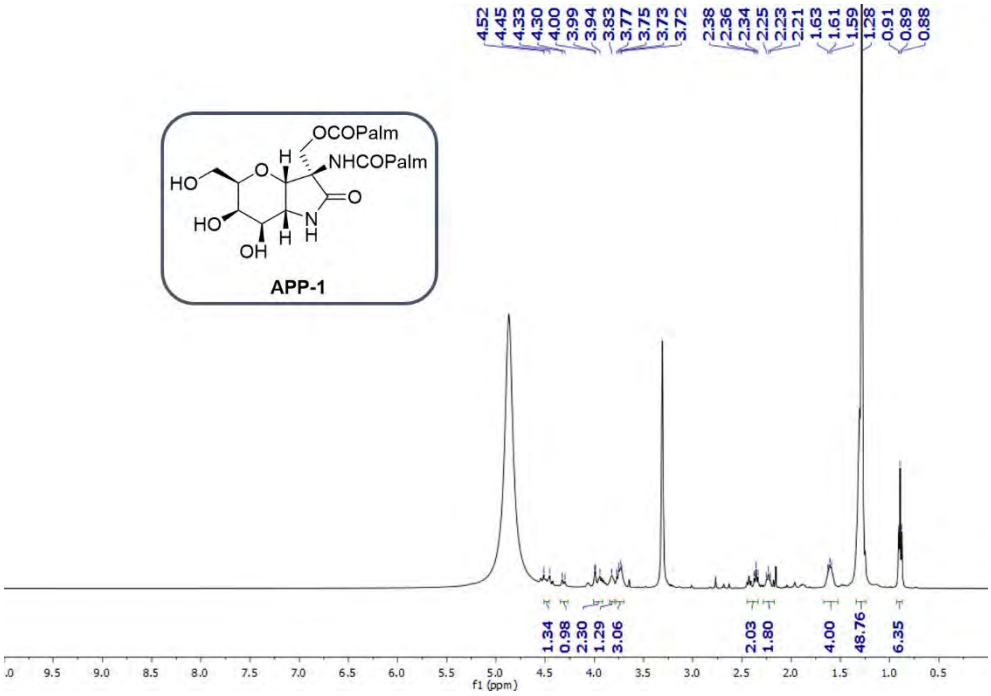

^{13}C NMR 100 MHz in CD_3OD

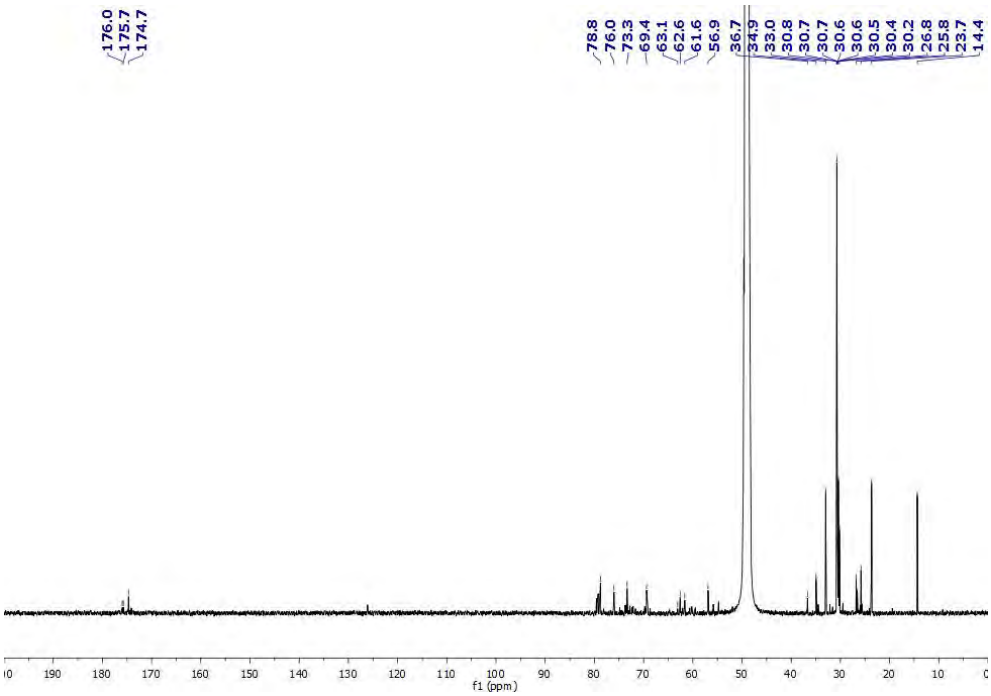

^{1}H NMR 400 MHz in $CDCl_3$

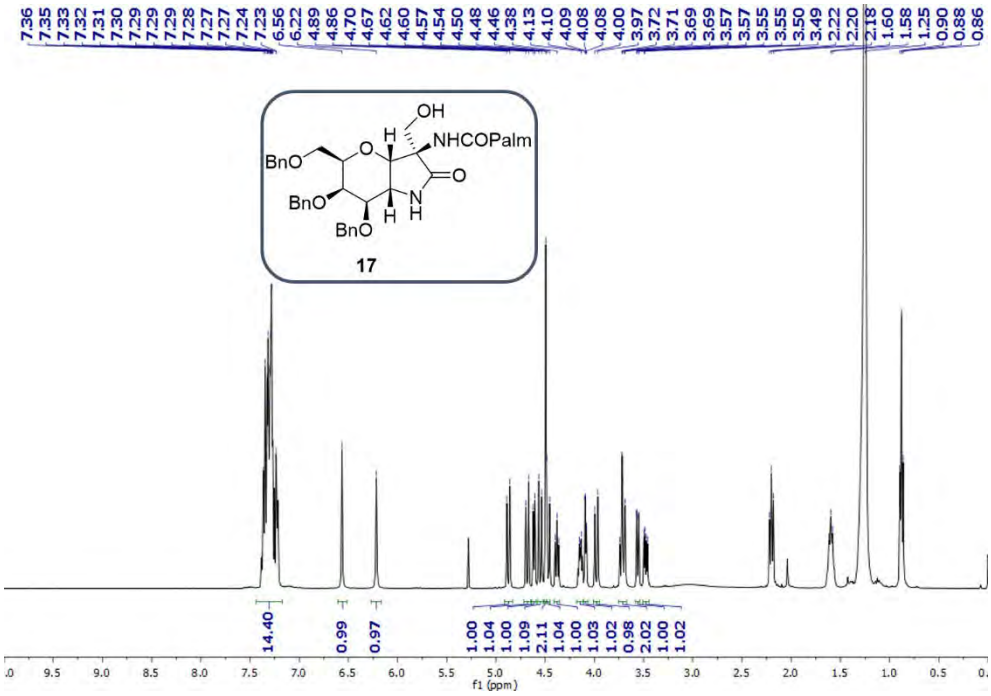

^{13}C NMR 100 MHz in $CDCl_3$

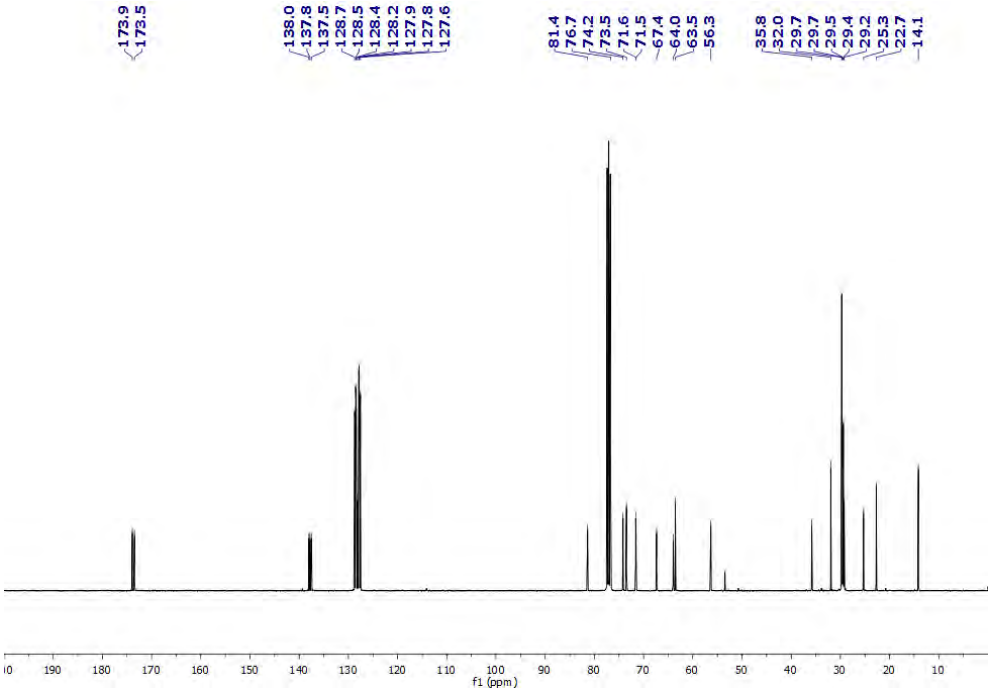

^{1}H NMR 400 MHz in CD_3OD

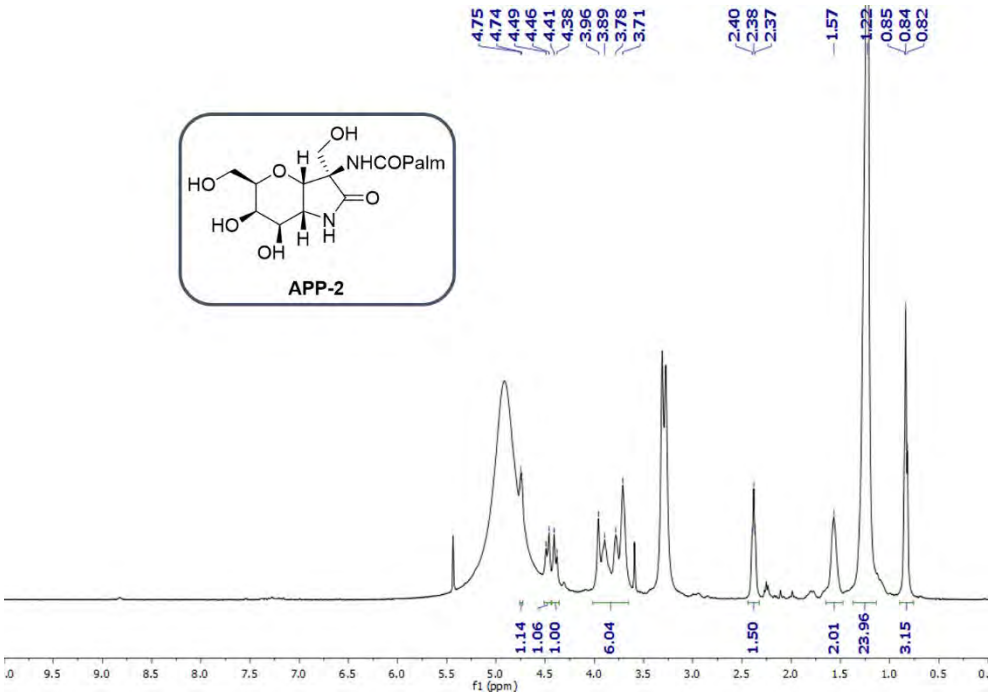

^{13}C NMR 100 MHz in CD_3OD

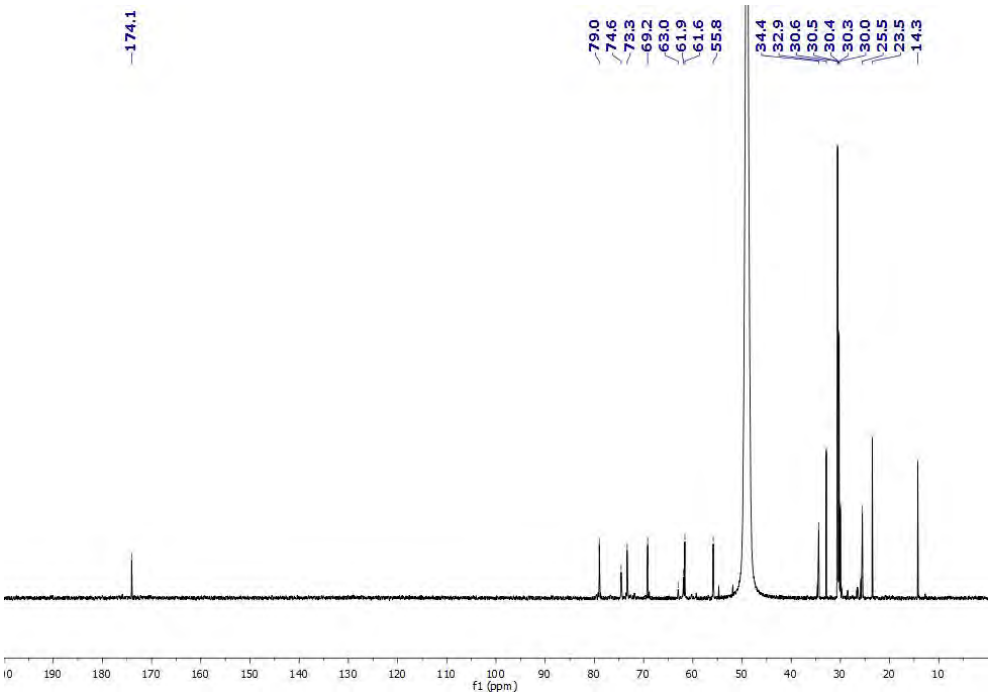

^{1}H NMR 400 MHz in $CDCl_3$

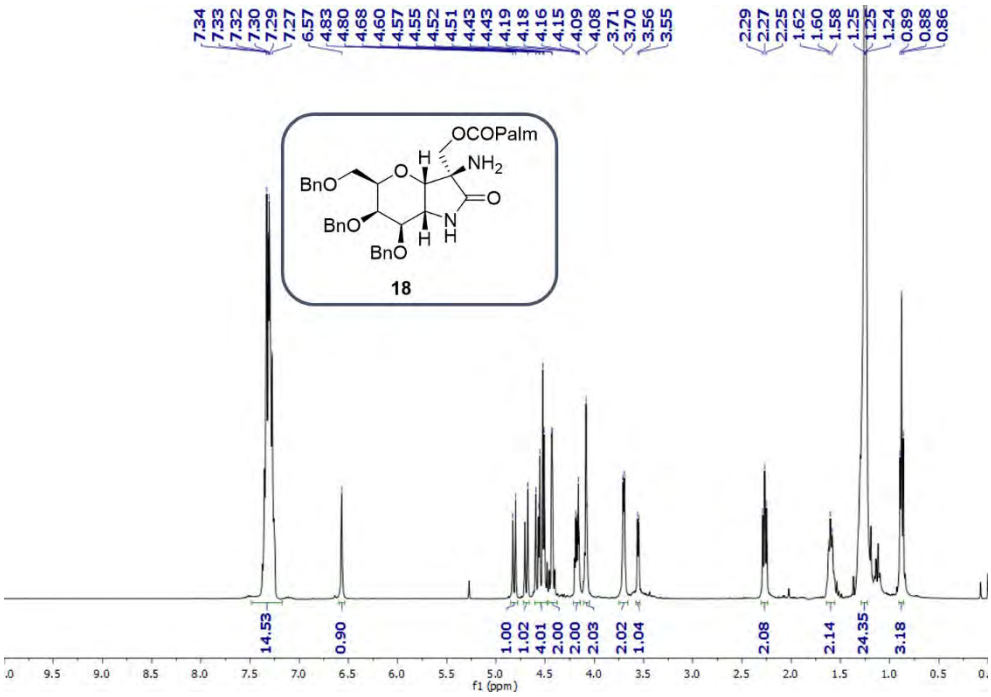

^{13}C NMR 100 MHz in $CDCl_3$

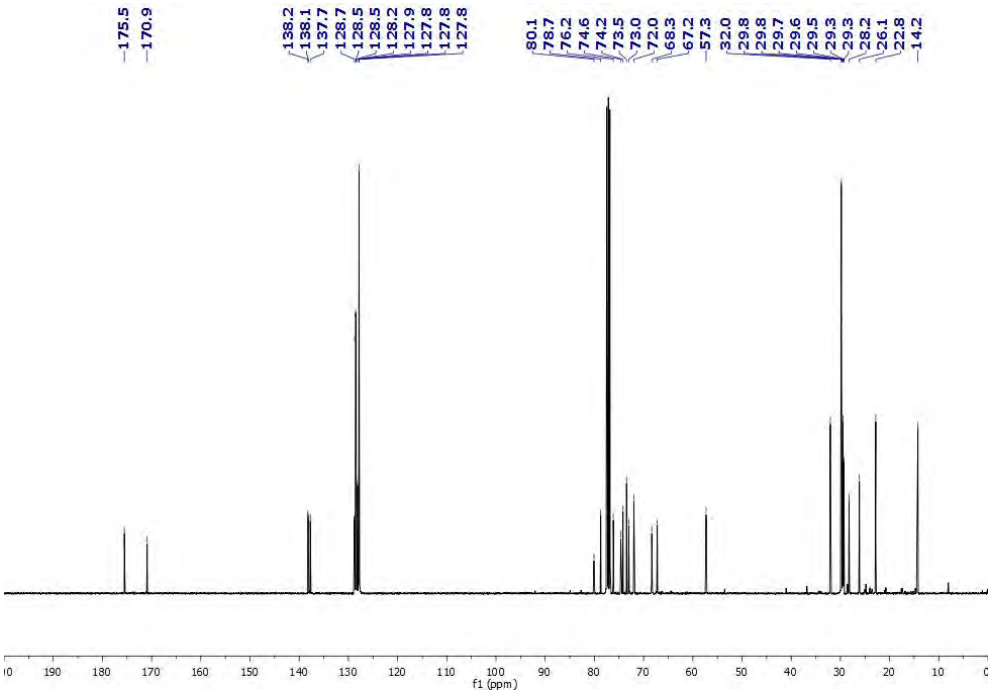

^{1}H NMR 400 MHz in CD_3OD

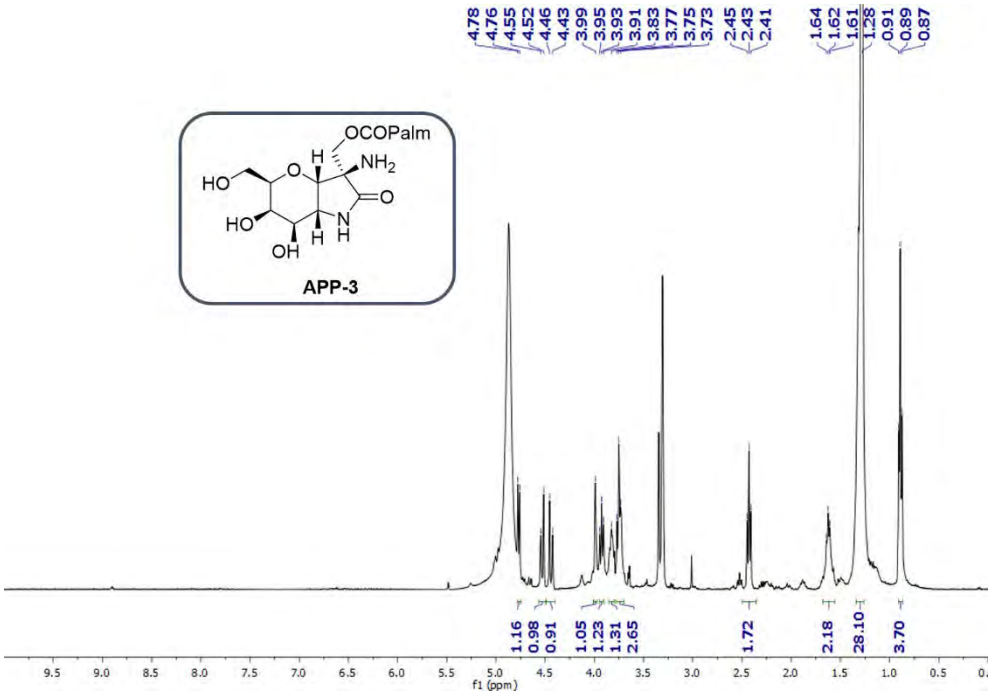

^{13}C NMR 100 MHz in CD_3OD

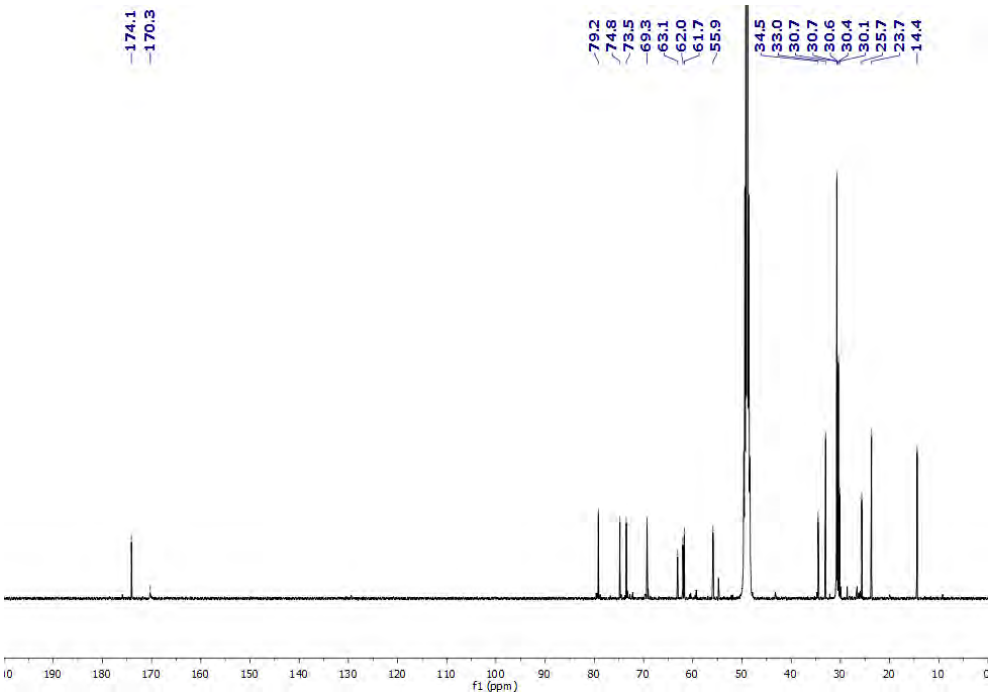

^{1}H NMR 400 MHz in $CDCl_3$

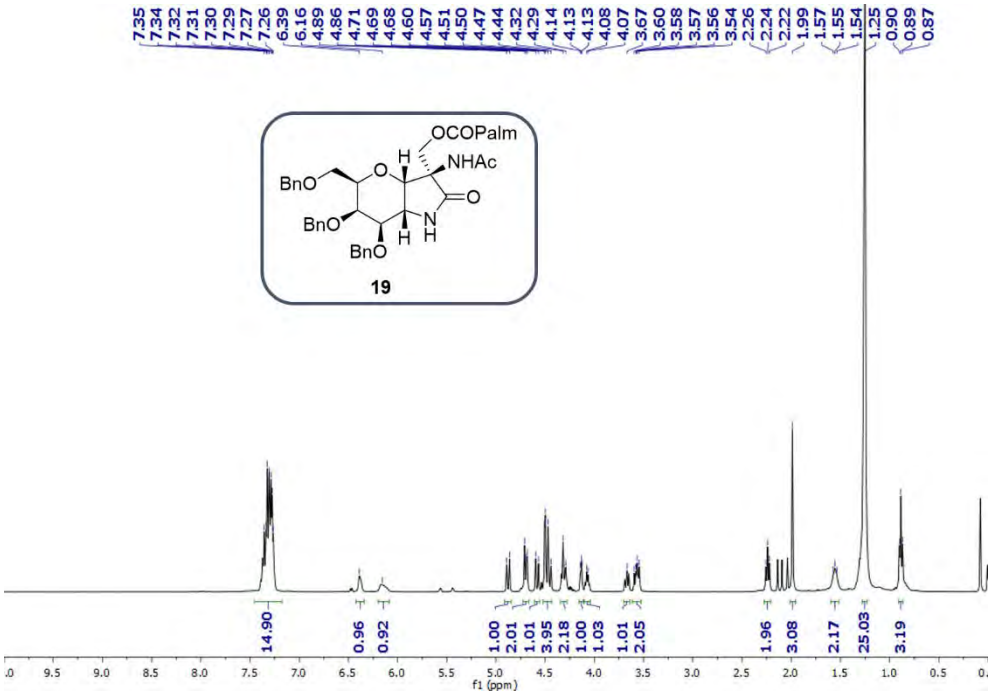

^{13}C NMR 100 MHz in $CDCl_3$

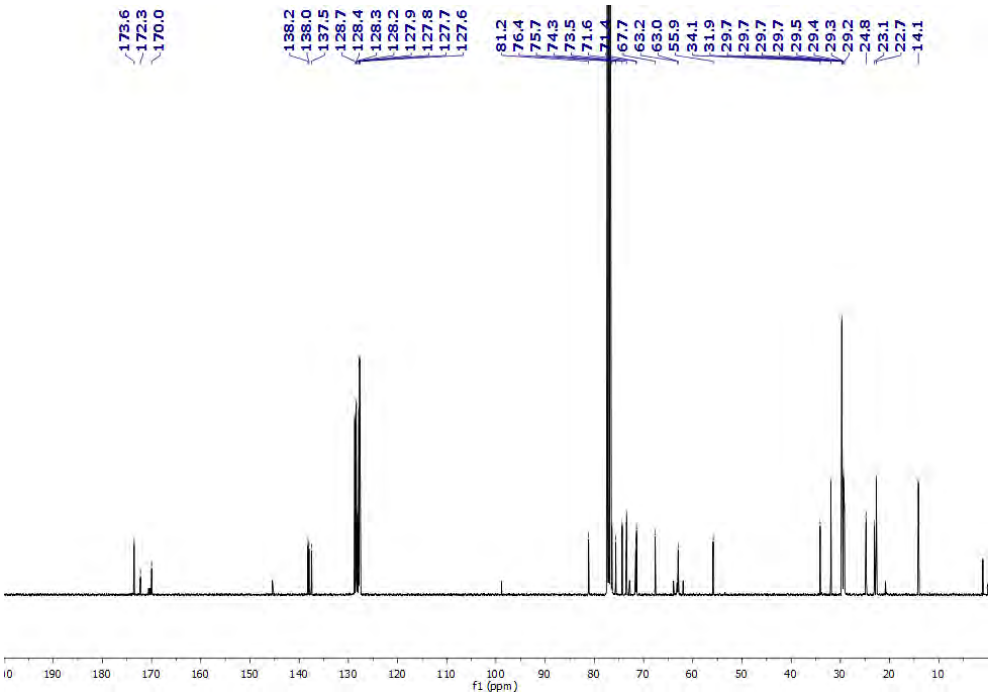

^{1}H NMR 400 MHz in CD_3OD

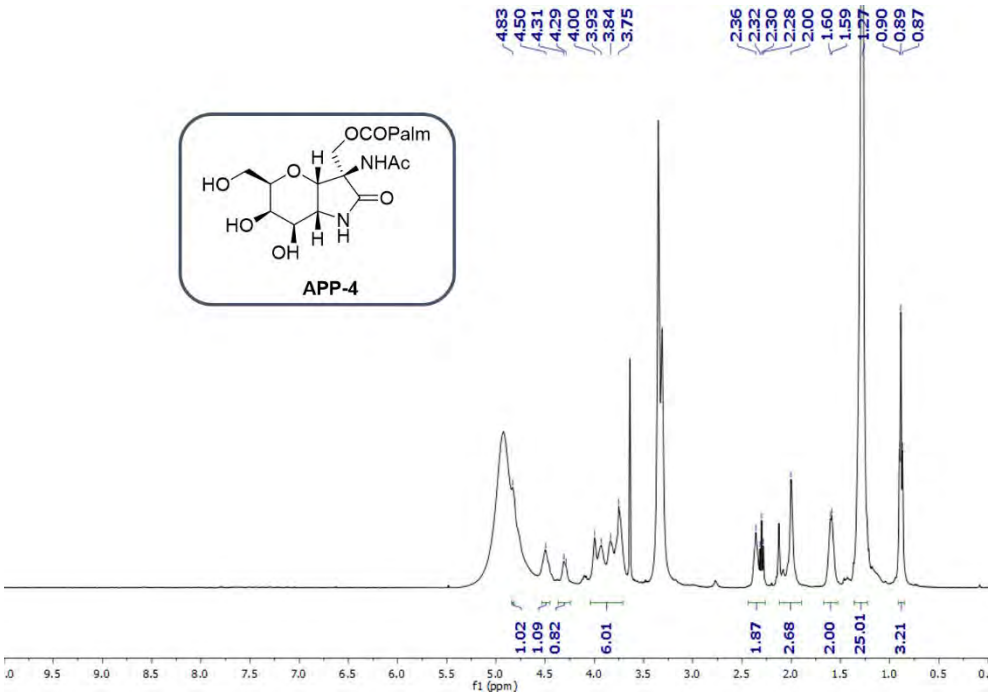

^{13}C NMR 100 MHz in CD_3OD

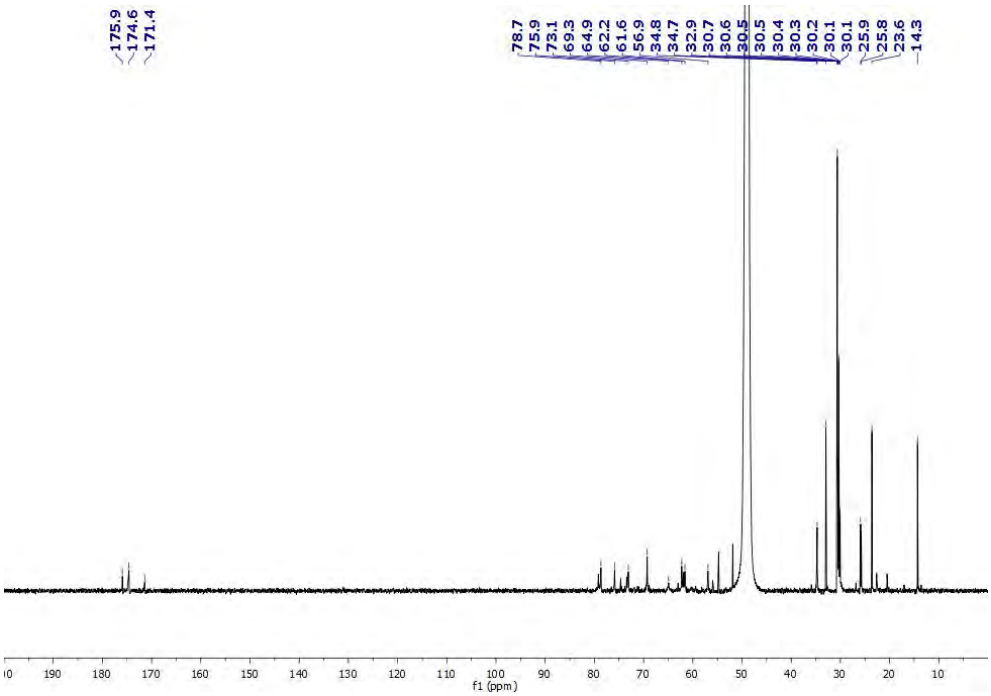

^{1}H NMR 400 MHz in $CDCl_3$

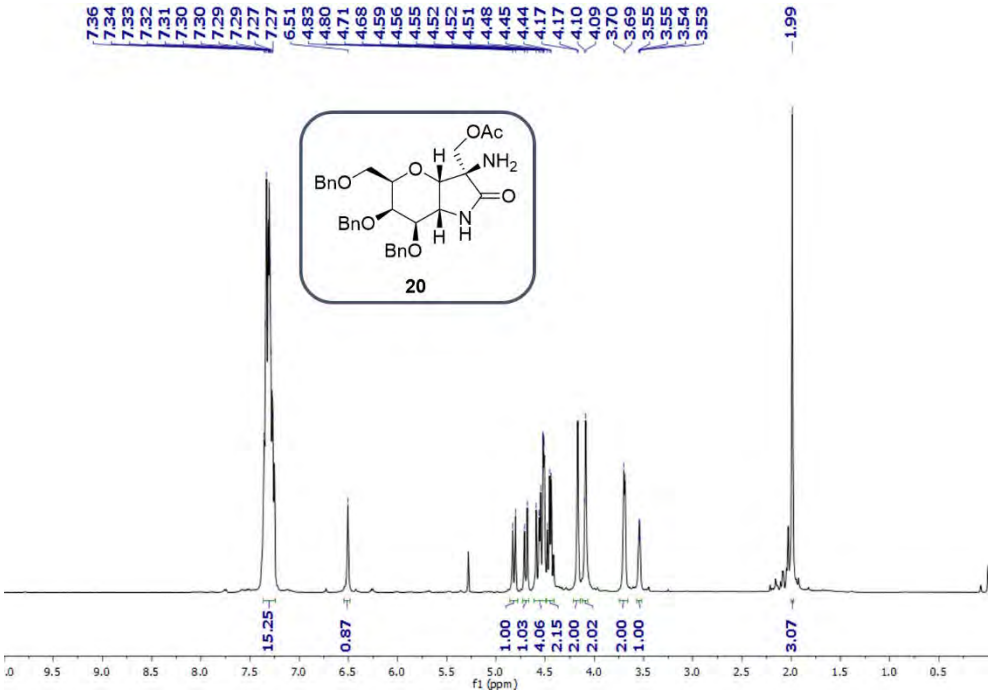

^{13}C NMR 100 MHz in $CDCl_3$

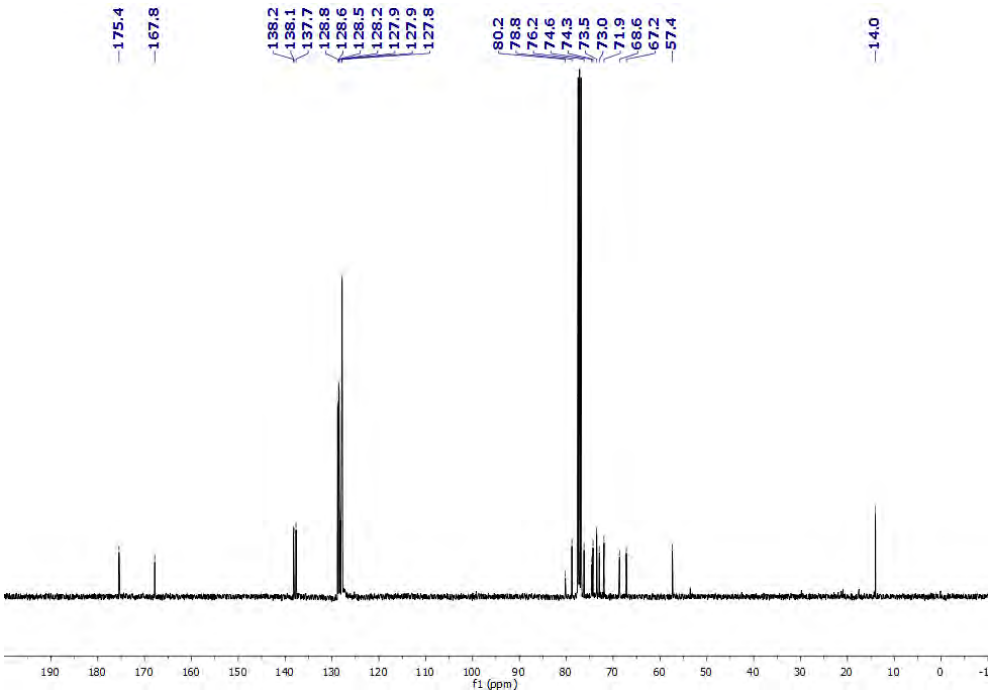

^{1}H NMR 400 MHz in D_2O

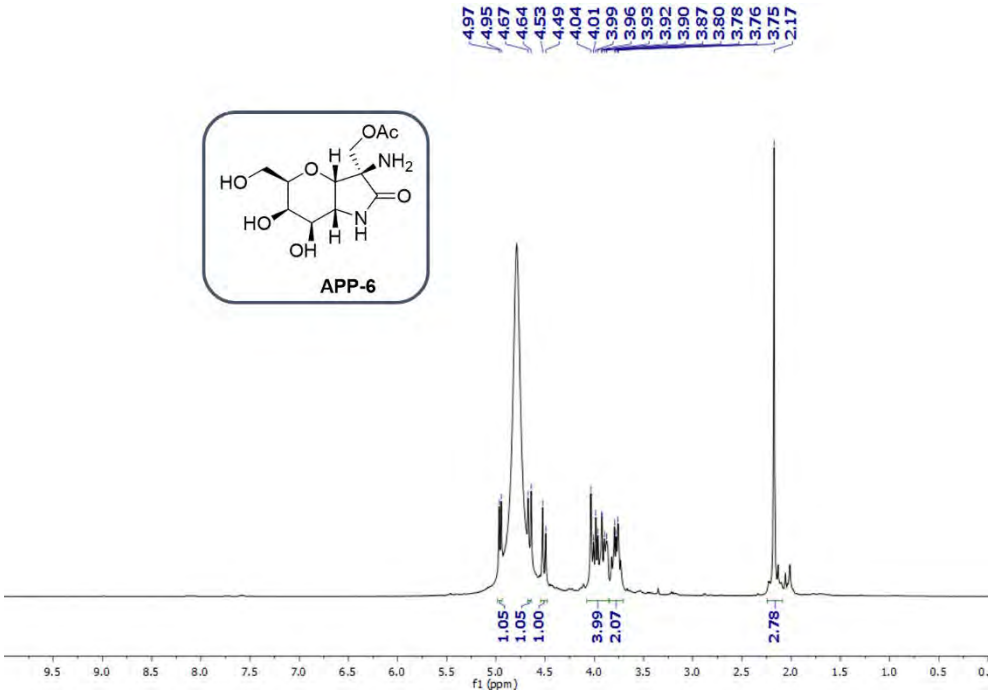

^{13}C NMR 100 MHz in D_2O

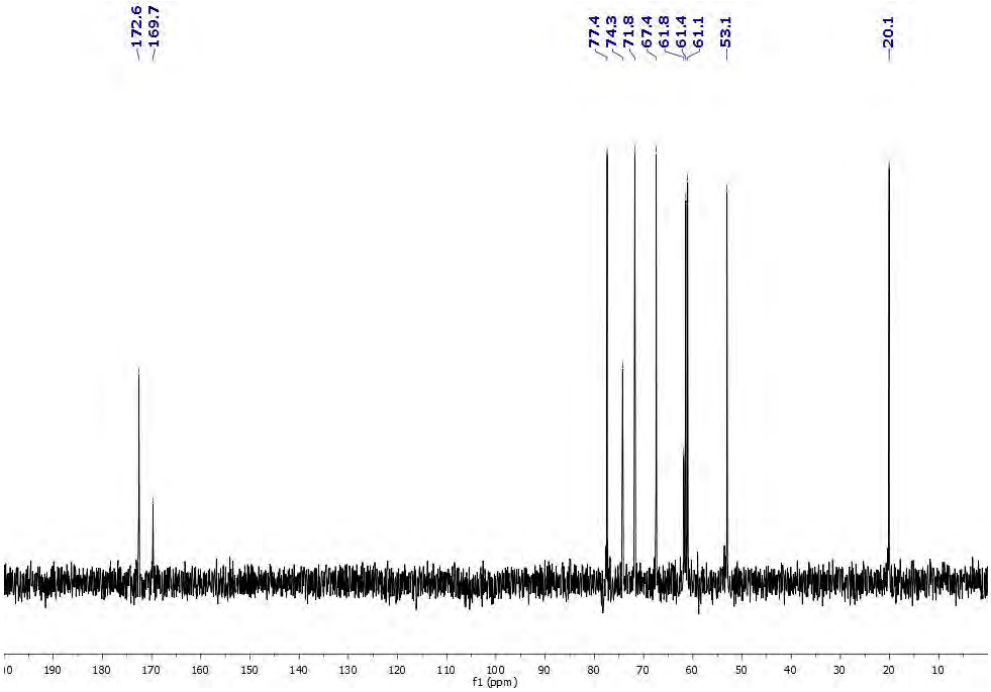

^{1}H NMR 400 MHz in D_2O

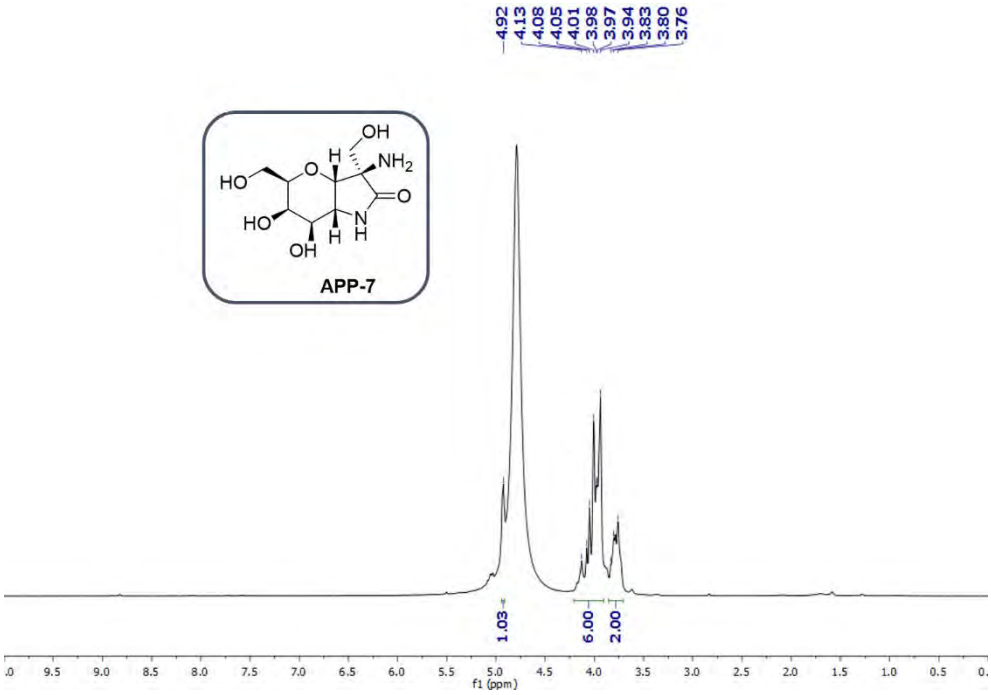

^{13}C NMR 100 MHz in D_2O

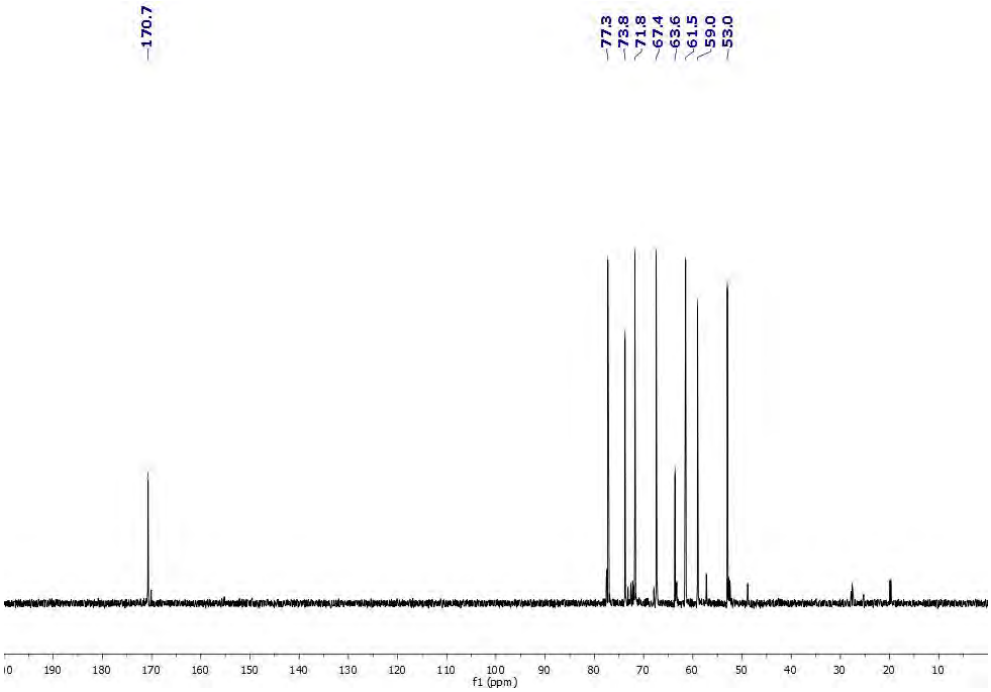

^{1}H NMR 500 MHz in CD_3OD

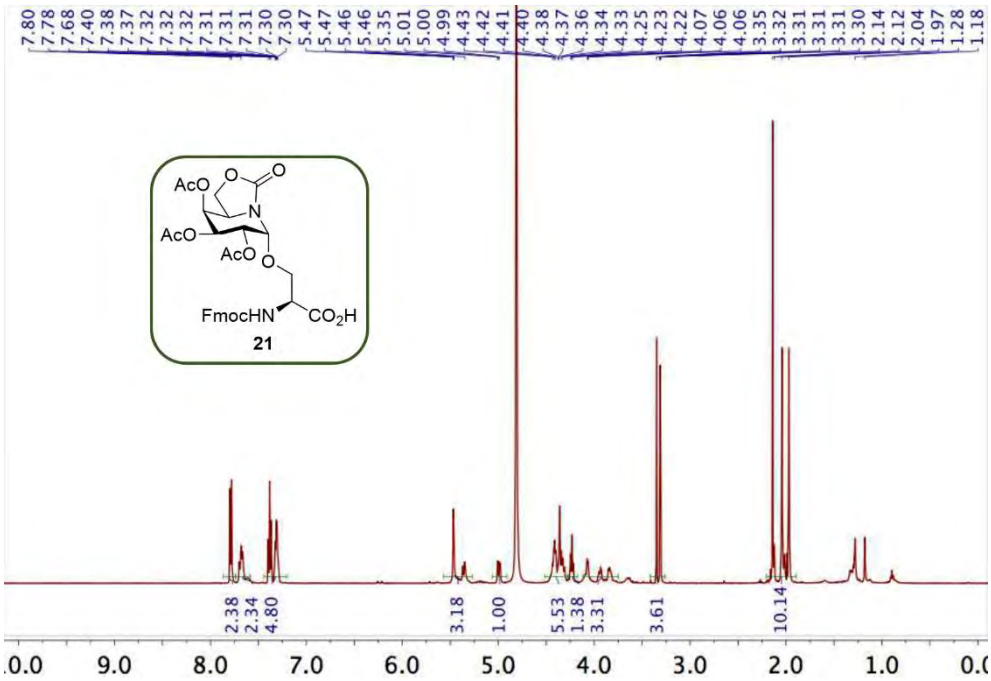

^{13}C NMR 125 MHz in CD_3OD

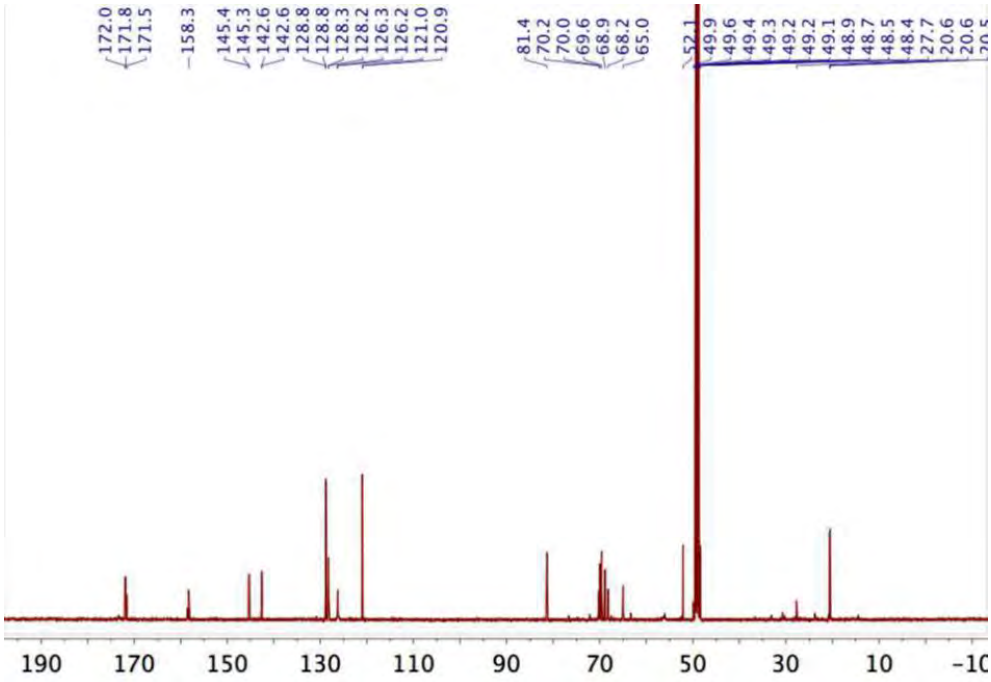

^{1}H NMR 500 MHz in CD_3OD

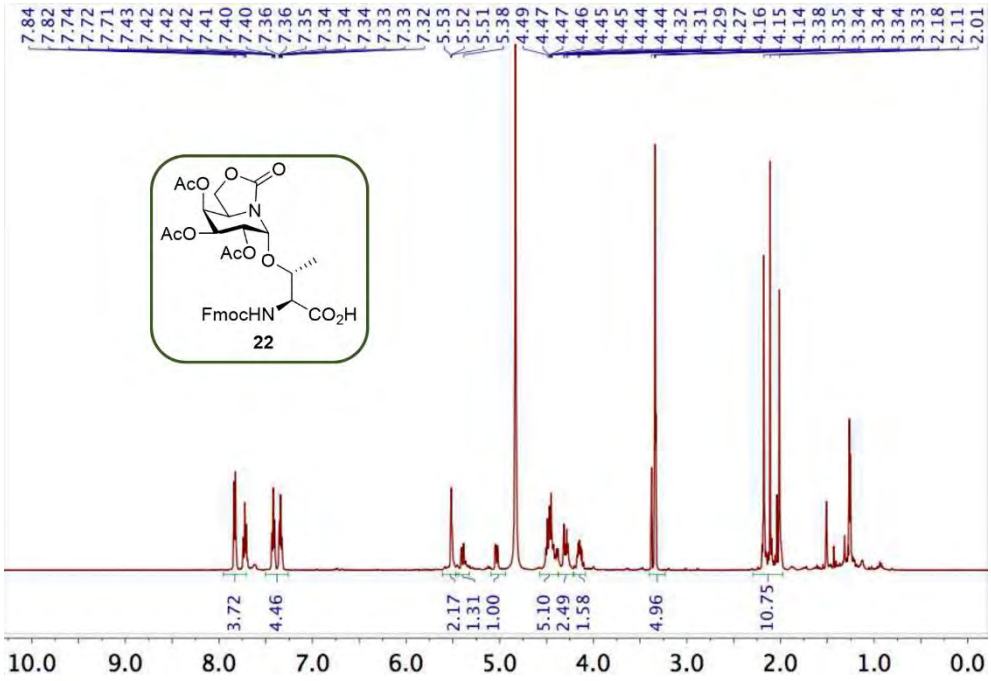

^{13}C NMR 125 MHz in CD_3OD

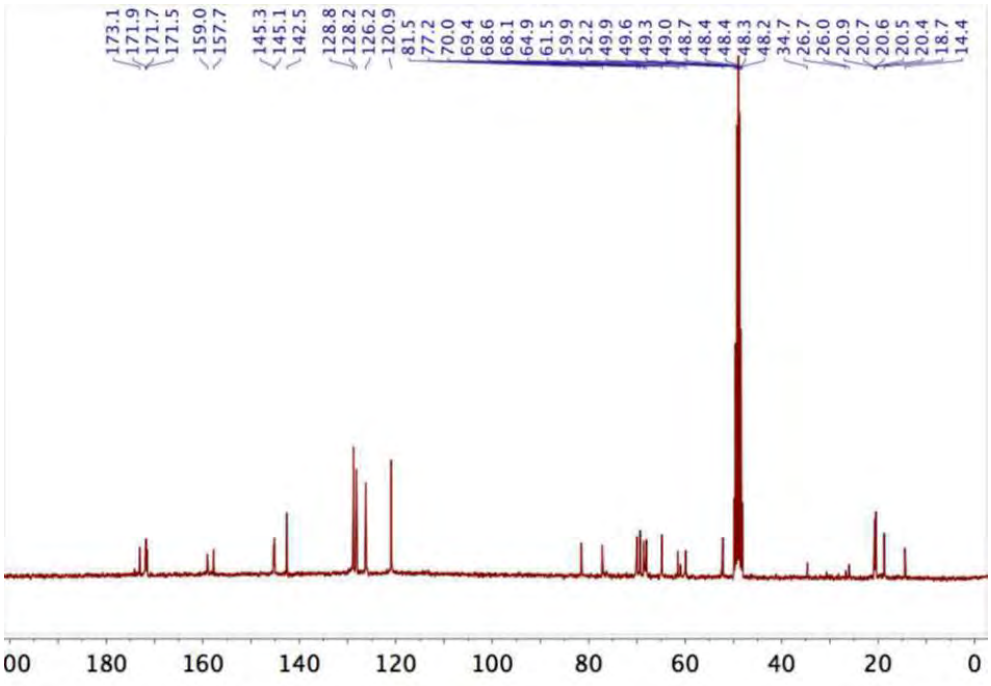

^{1}H NMR 500 MHz in CD_3OD

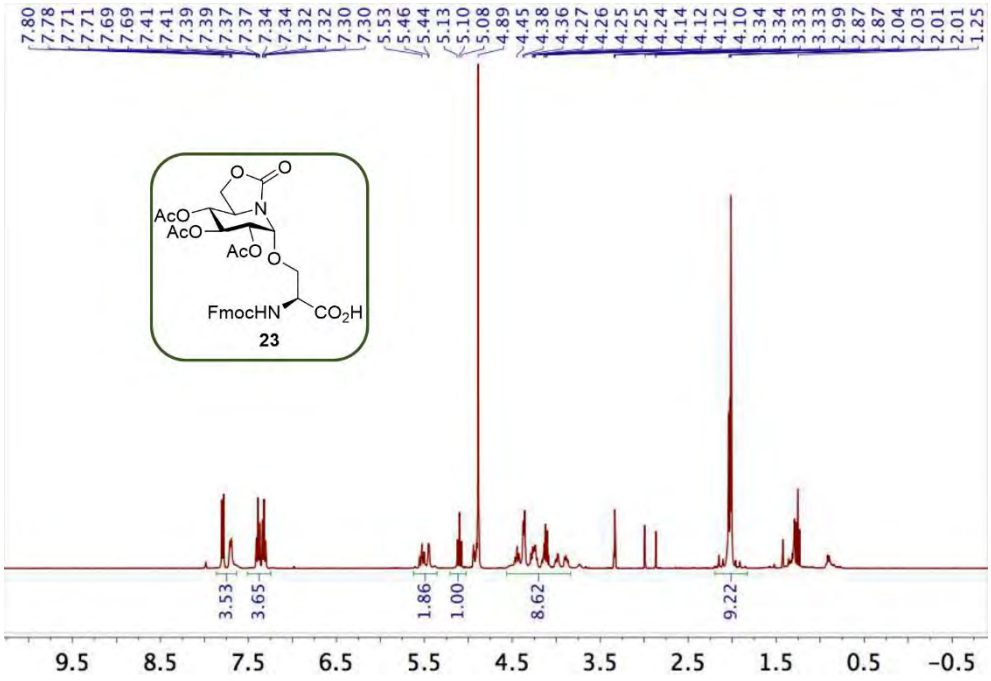

^{13}C NMR 125 MHz in CD_3OD

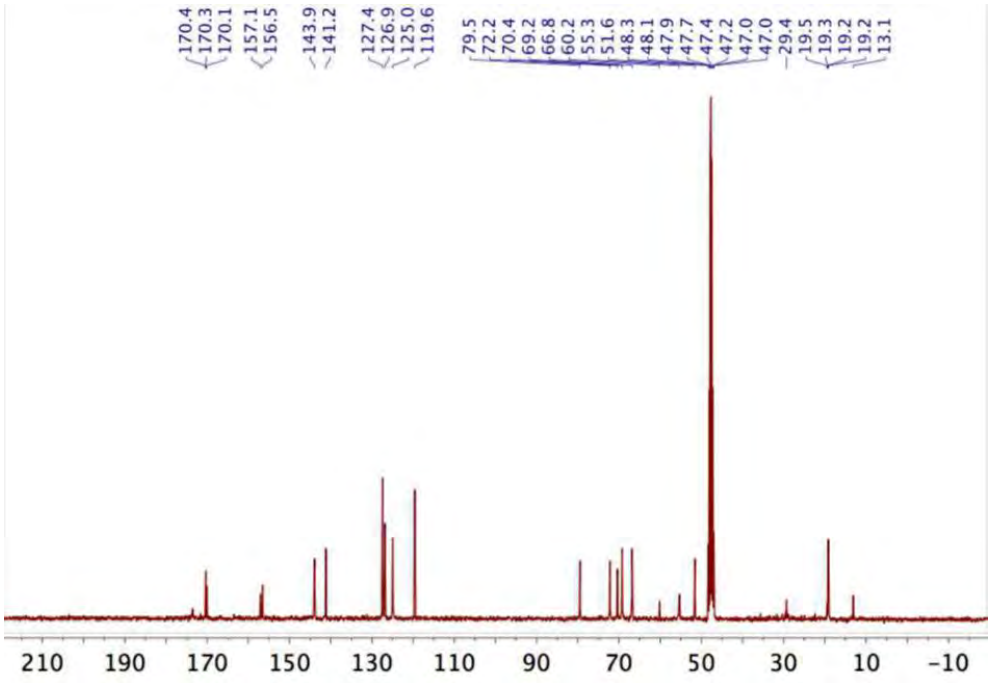

^{1}H NMR 400 MHz in CD_3OD

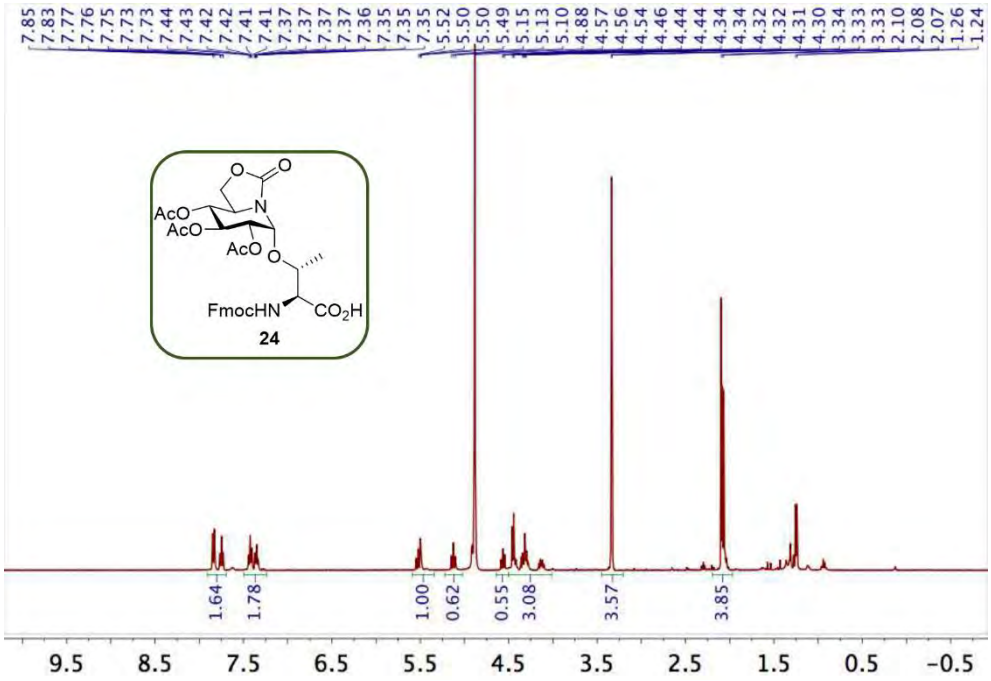

^{13}C NMR 100 MHz in CD_3OD

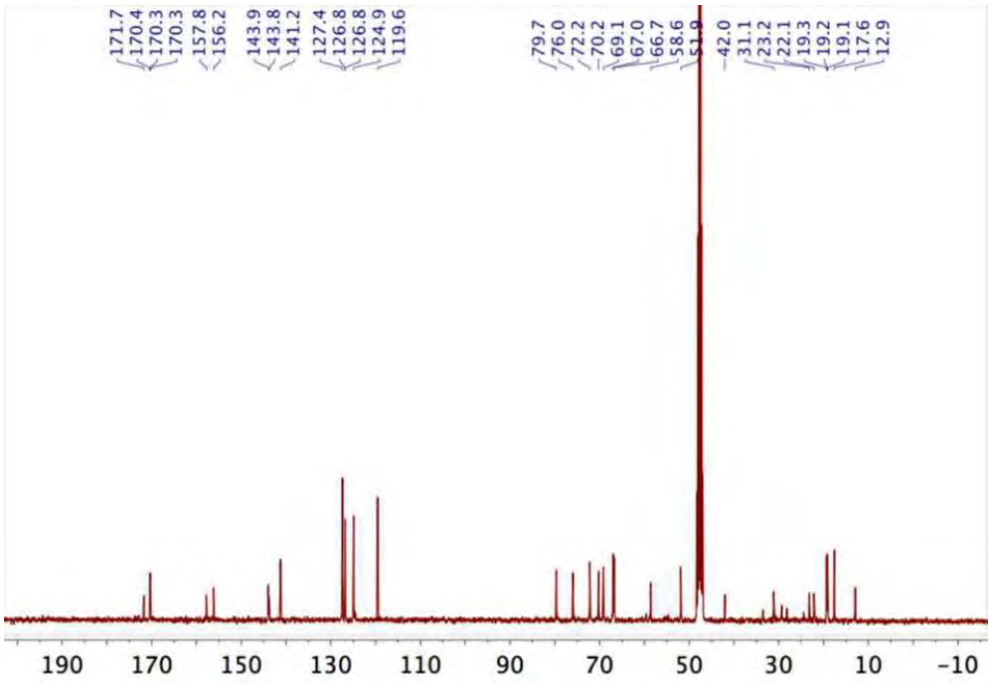

^{1}H NMR 300 MHz in CD_3OD

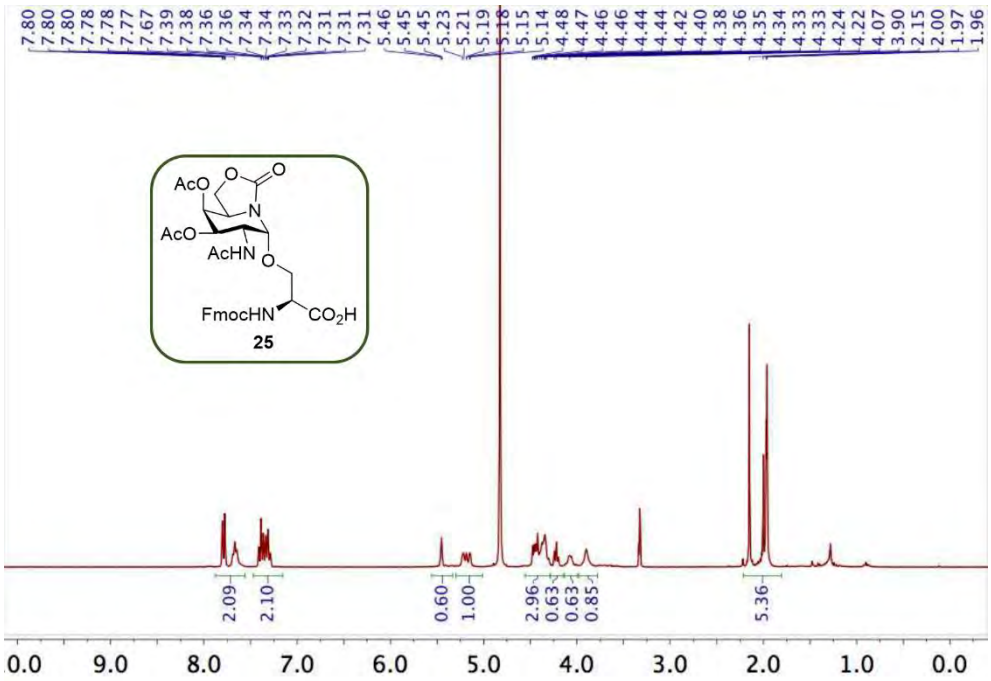

^{13}C NMR 75 MHz in CD_3OD

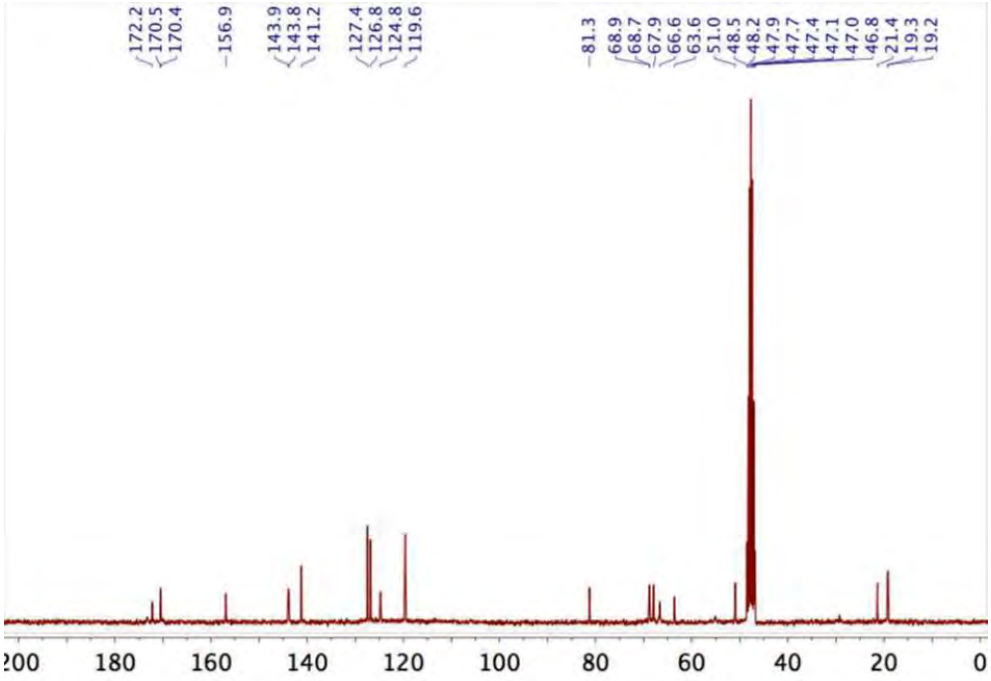

^{1}H NMR 300 MHz in CD_3OD

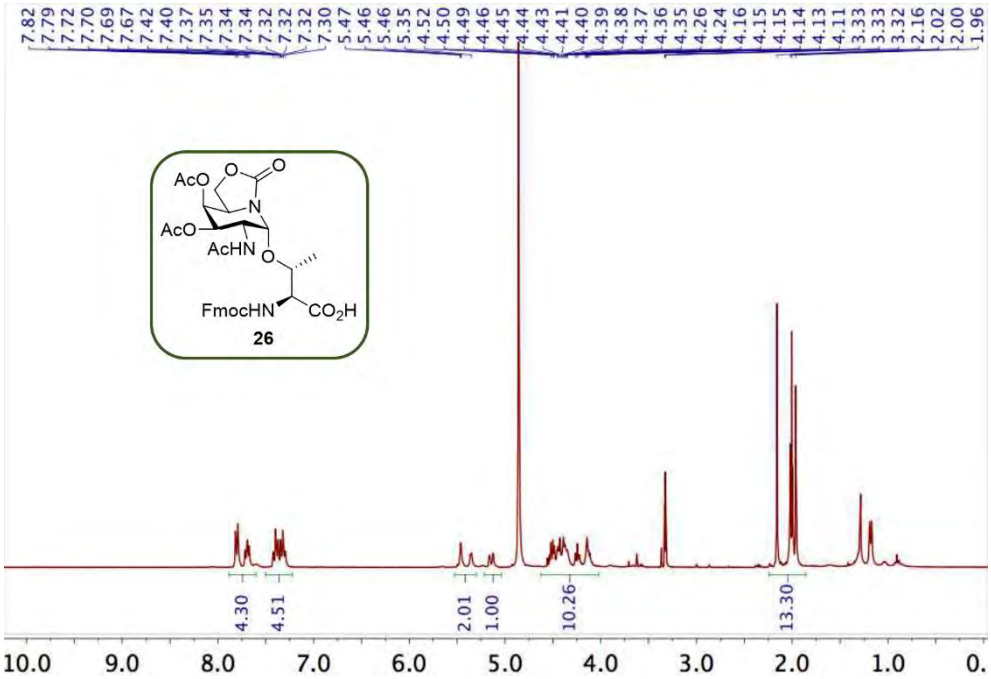

^{13}C NMR 75 MHz in CD_3OD

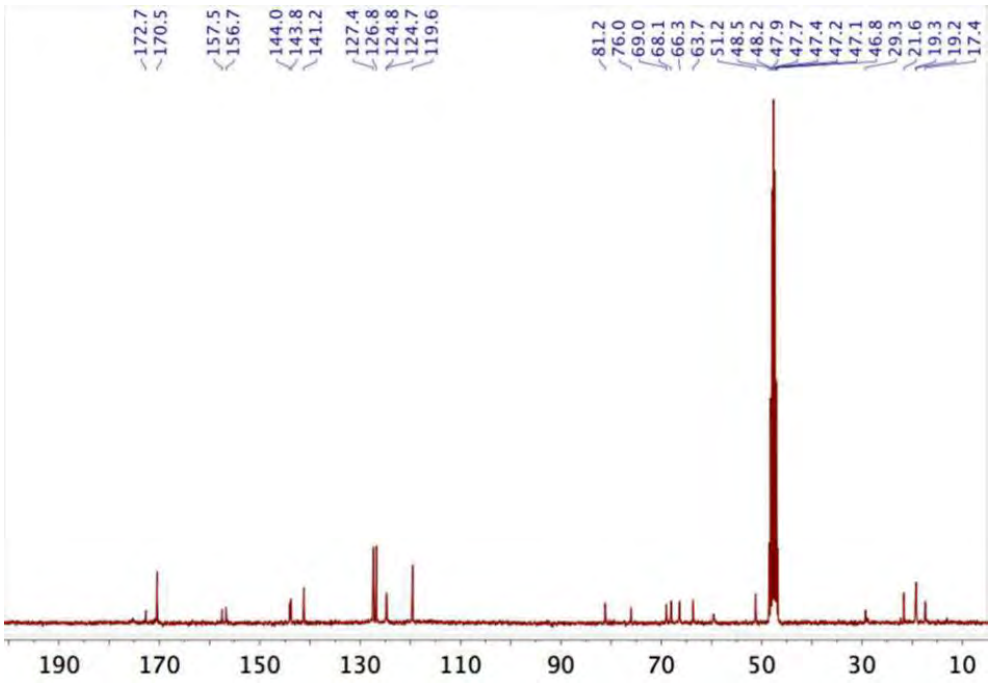

^{1}H NMR 300 MHz in CD_3OD

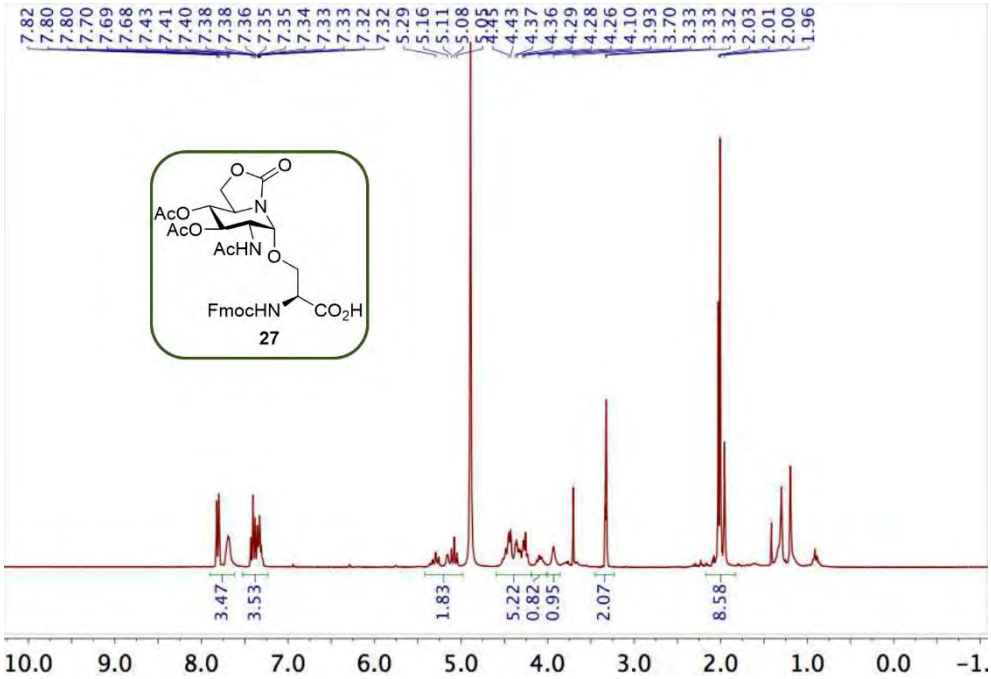

^{13}C NMR 75 MHz in CD_3OD

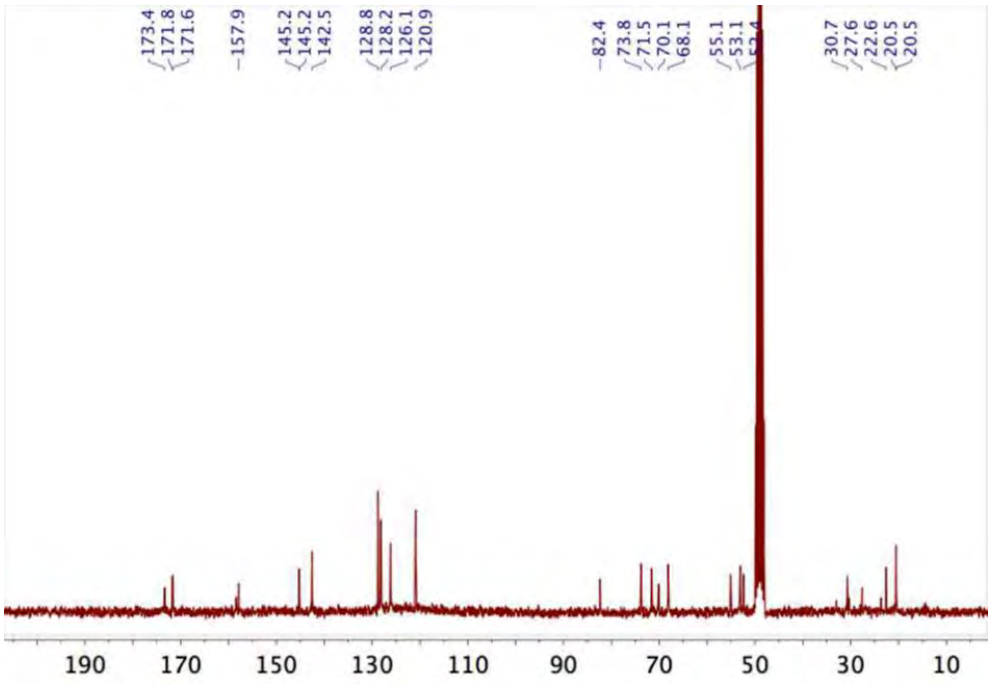

^{1}H NMR 300 MHz in CD_3OD

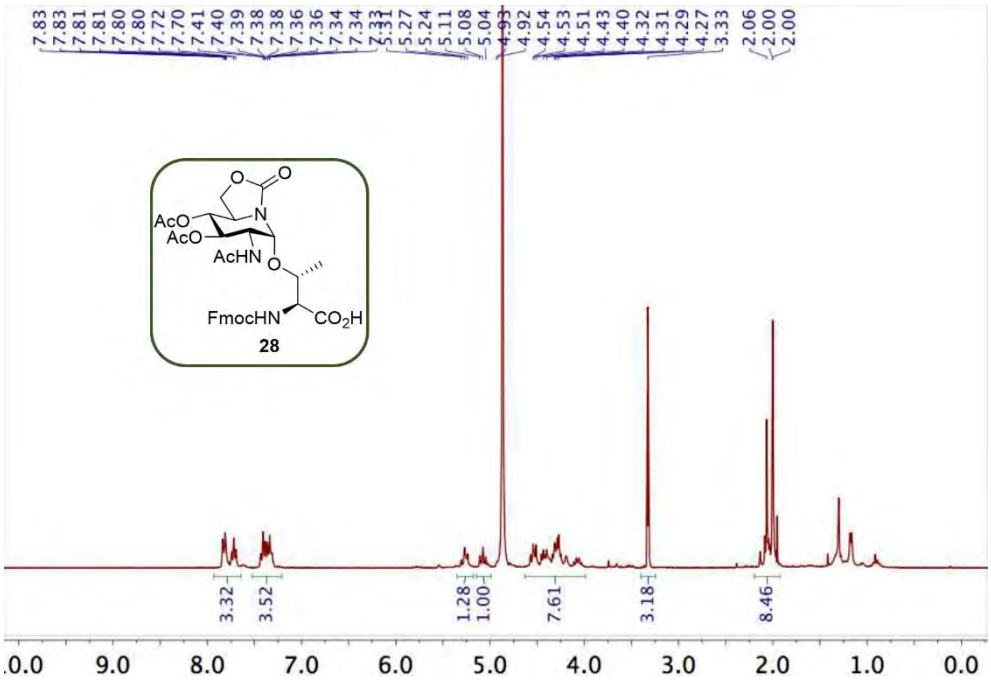

^{13}C NMR 75 MHz in CD_3OD

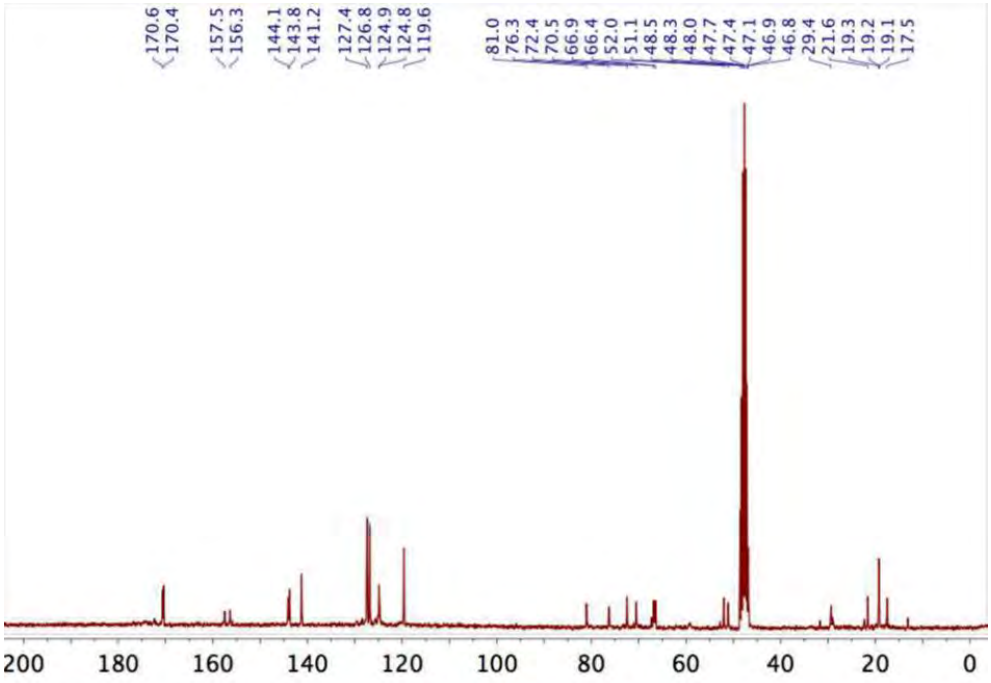

^{1}H NMR 400 MHz in D_2O

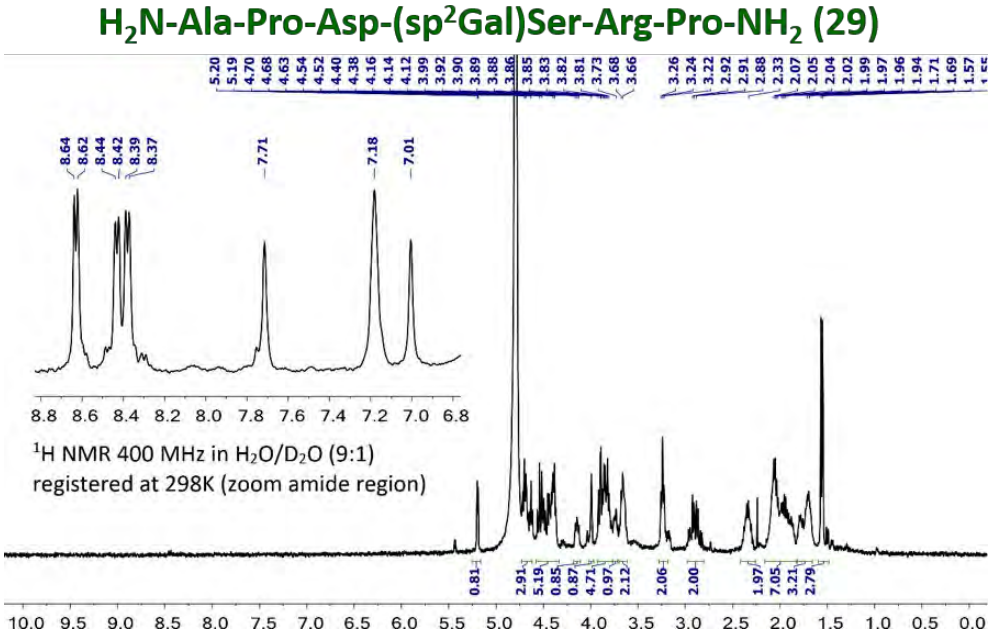

HSQC in D_2O

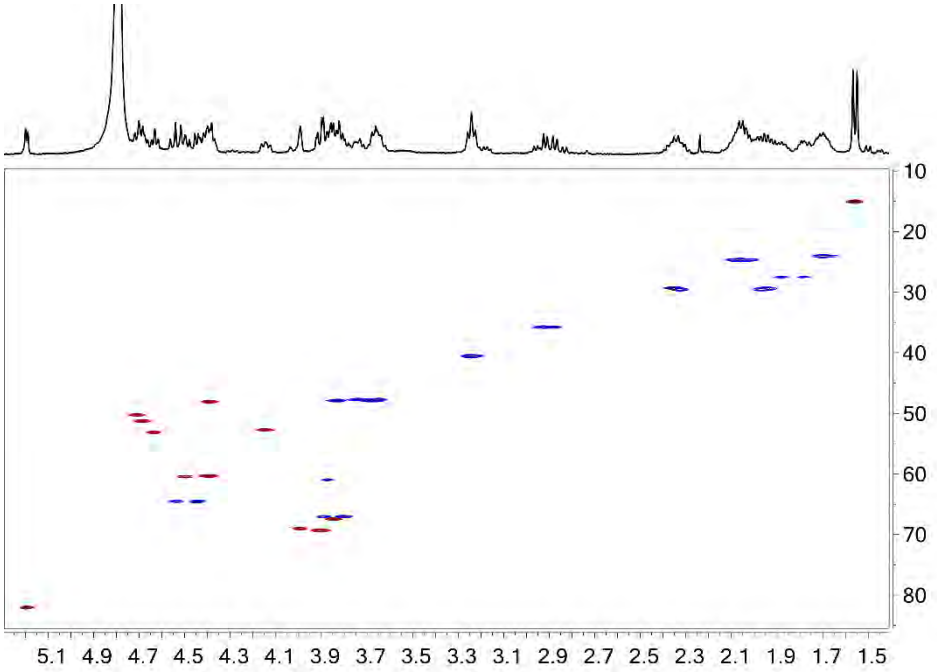

HMBC in D_2O

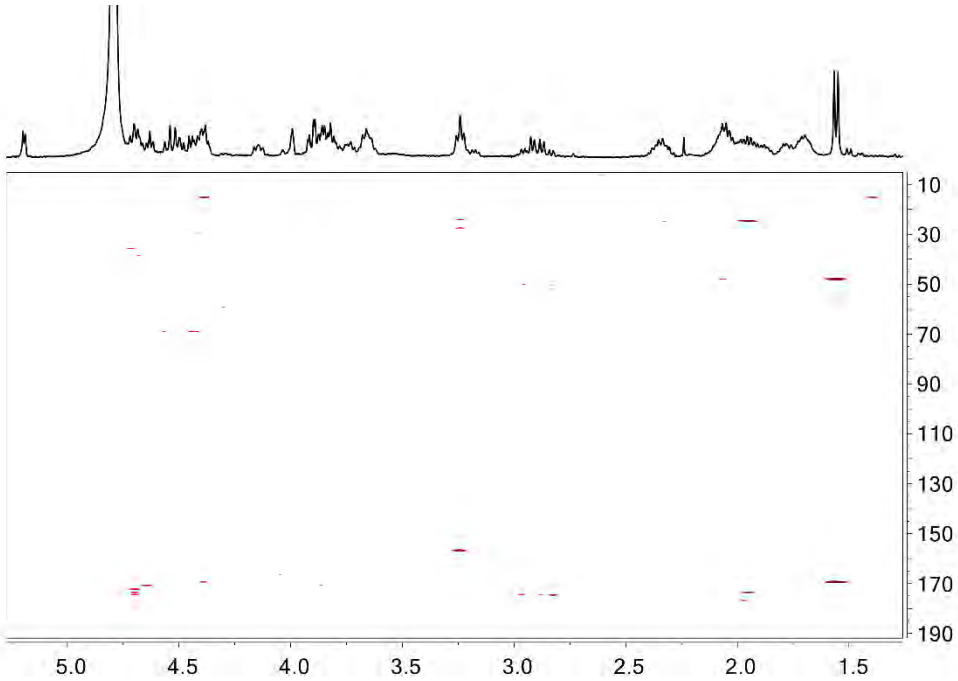

NOESY in H_2O/D_2O

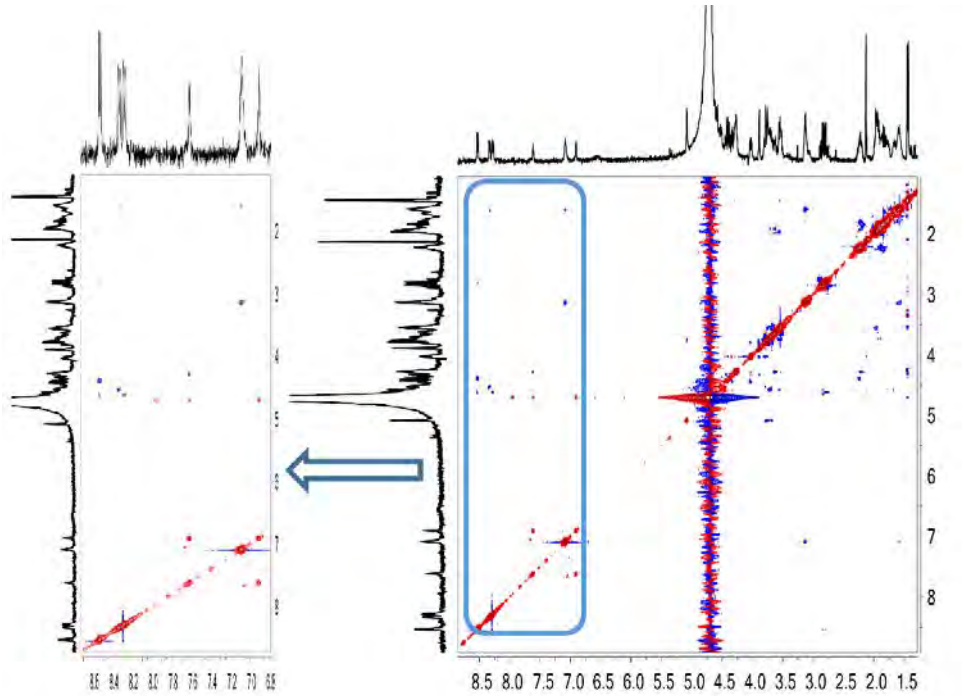

^{1}H NMR 400 MHz in D_2O

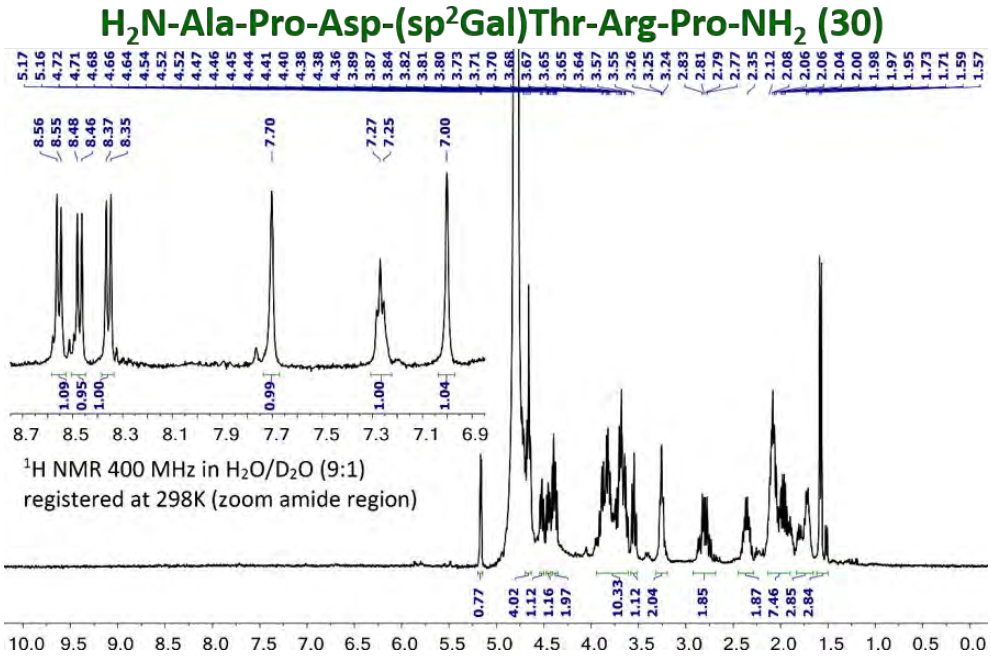

^{13}C NMR 100 MHz in D_2O

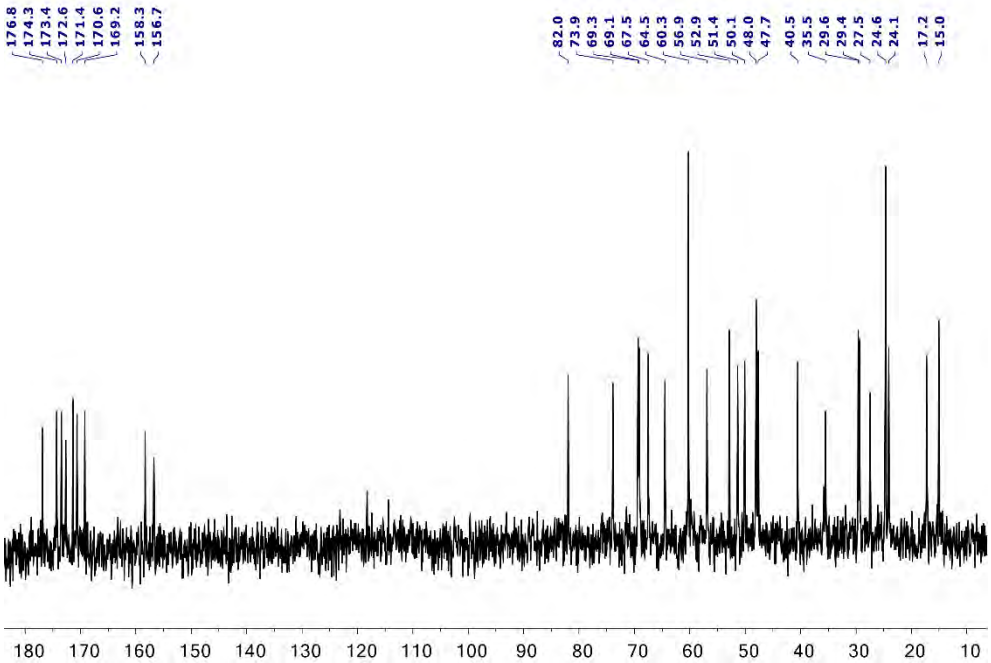

NOESY in H_2O/D_2O

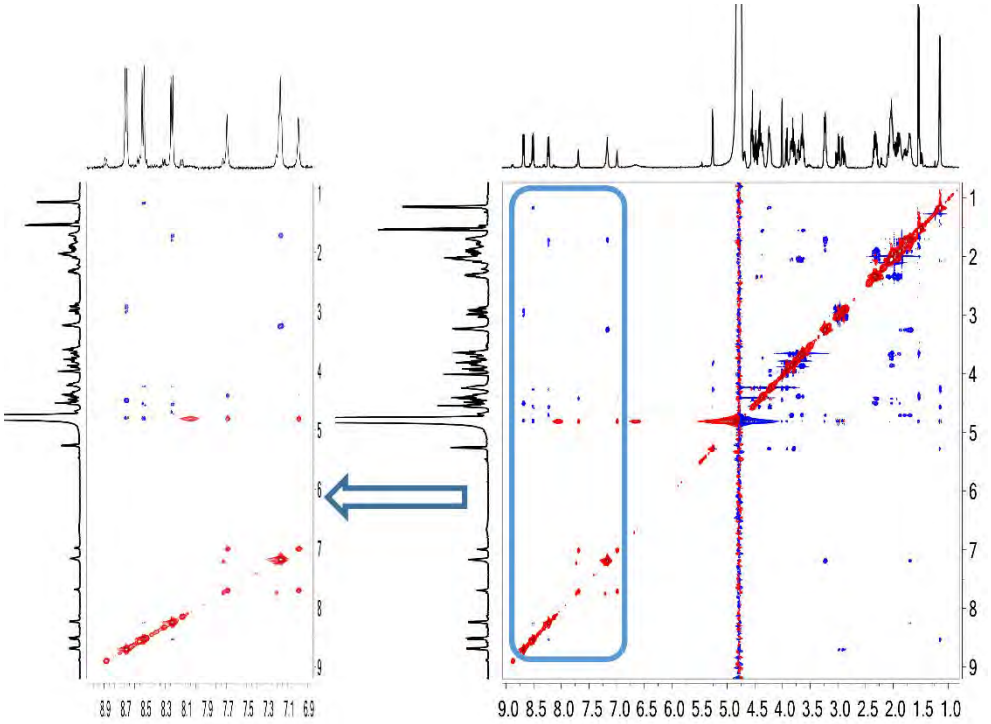

^{1}H NMR 400 MHz in D_2O

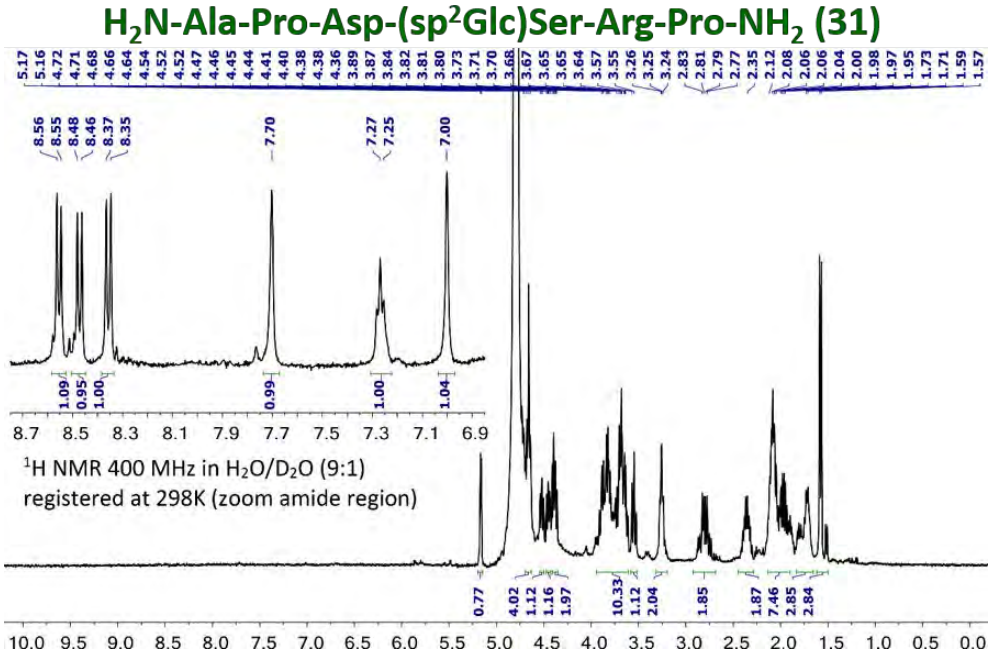

^{13}C NMR 100 MHz in D_2O

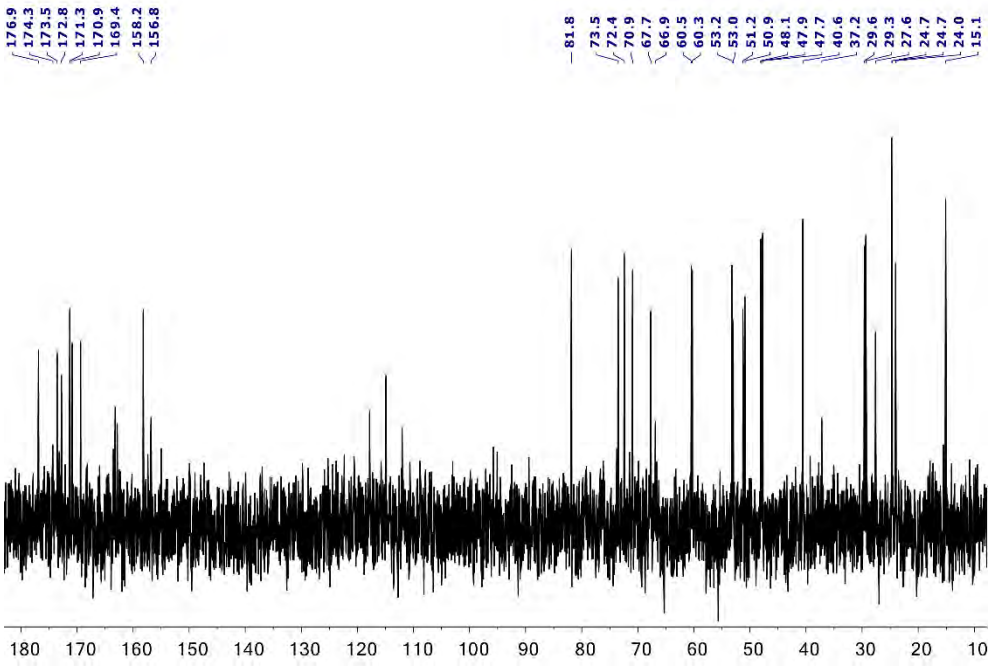

NOESY in H_2O/D_2O

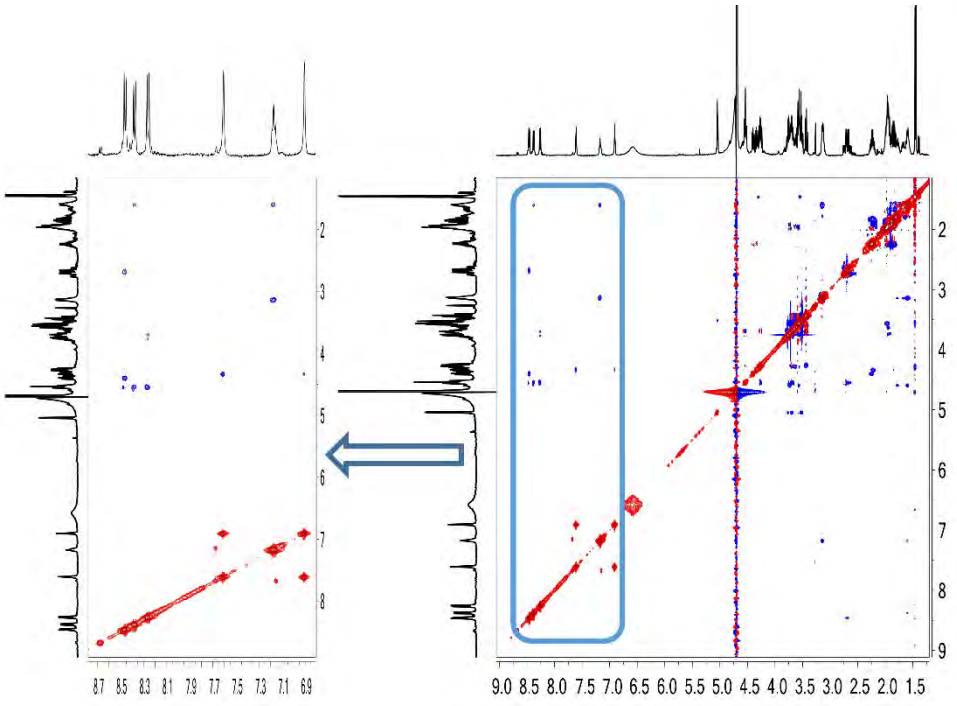

^{1}H NMR 400 MHz in D_2O

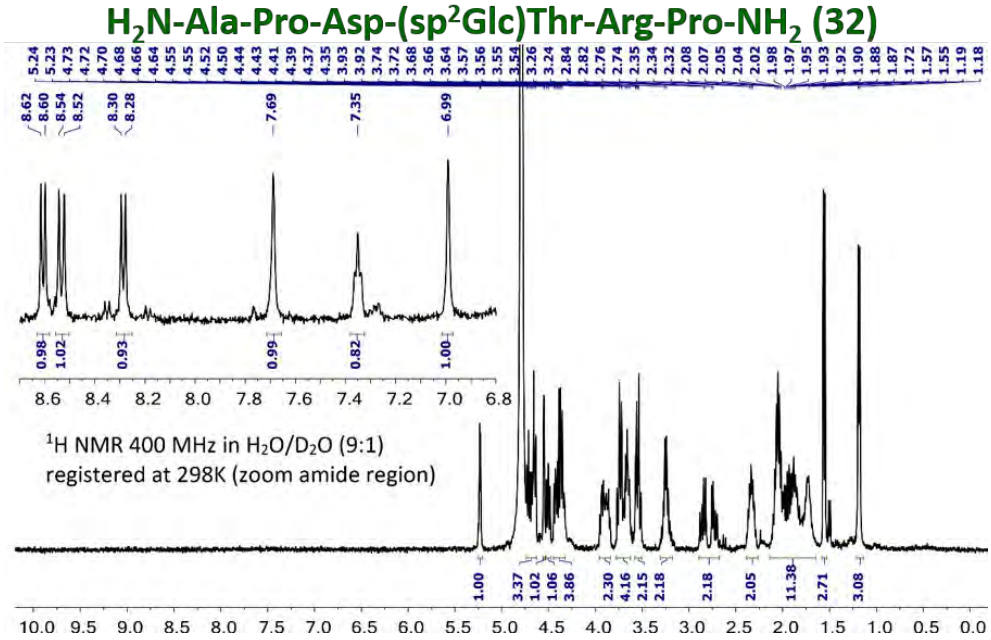

^{13}C NMR 100 MHz in D_2O

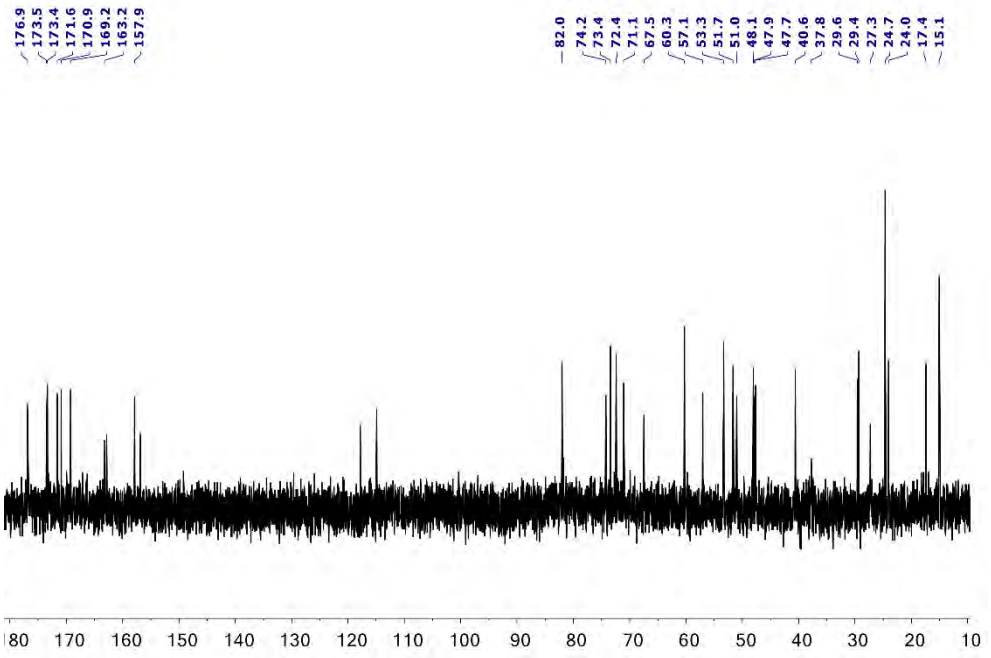

NOESY in H_2O/D_2O

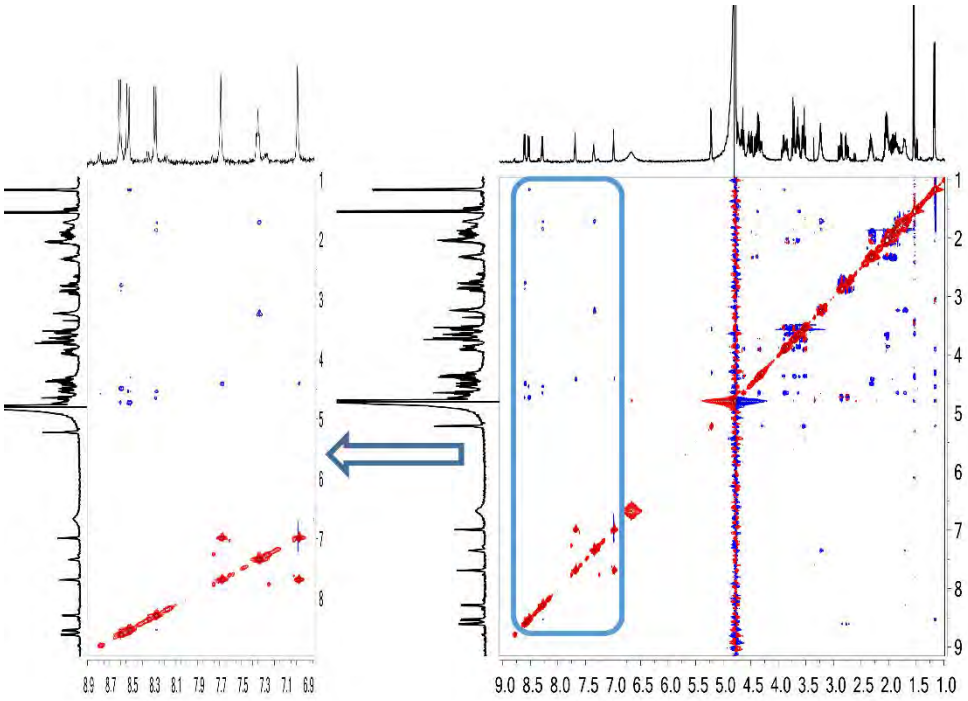

^{1}H NMR 400 MHz in D_2O

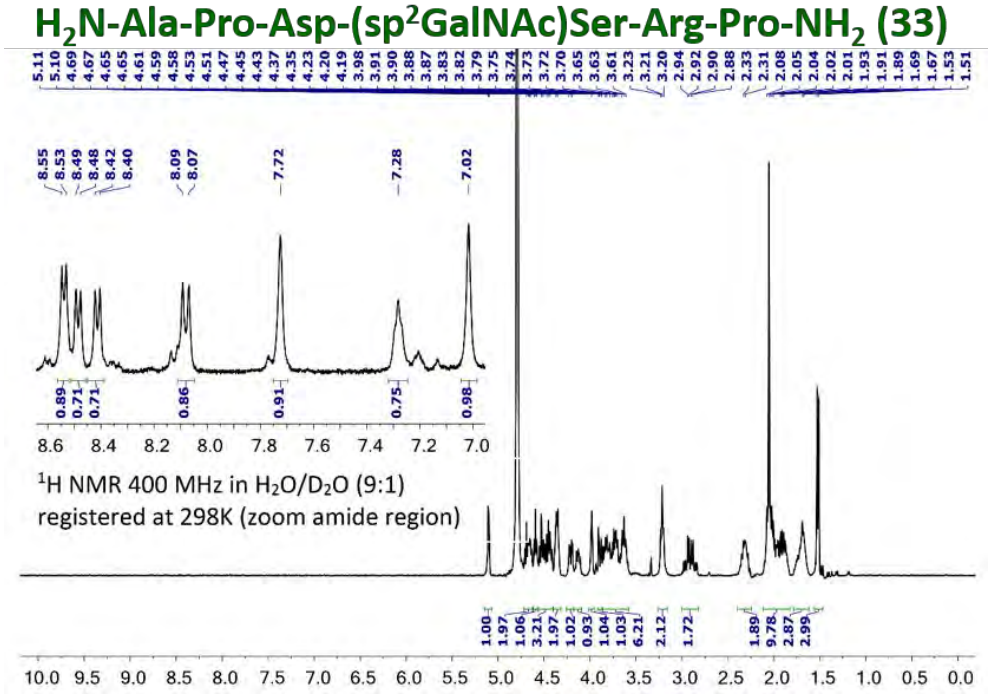

^{13}C NMR 100 MHz in D_2O

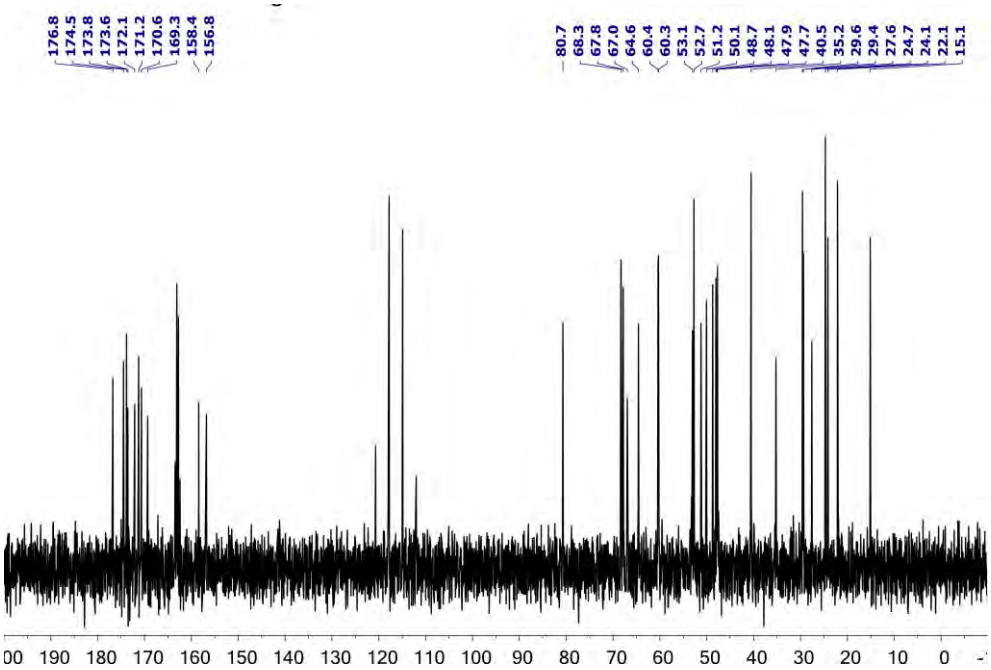

NOESY in H_2O/D_2O

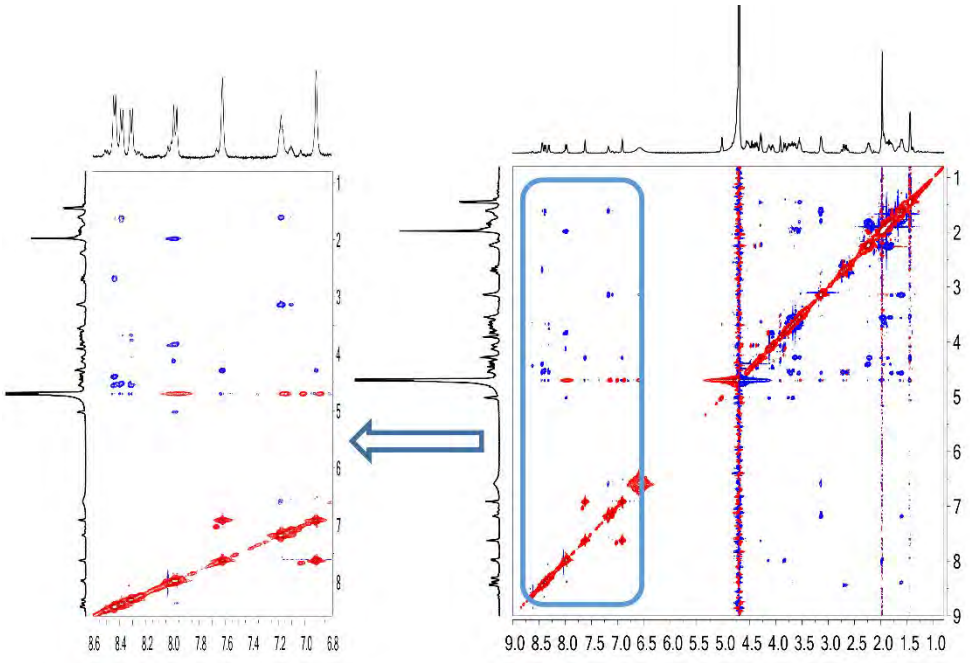

^{1}H NMR 400 MHz in D_2O

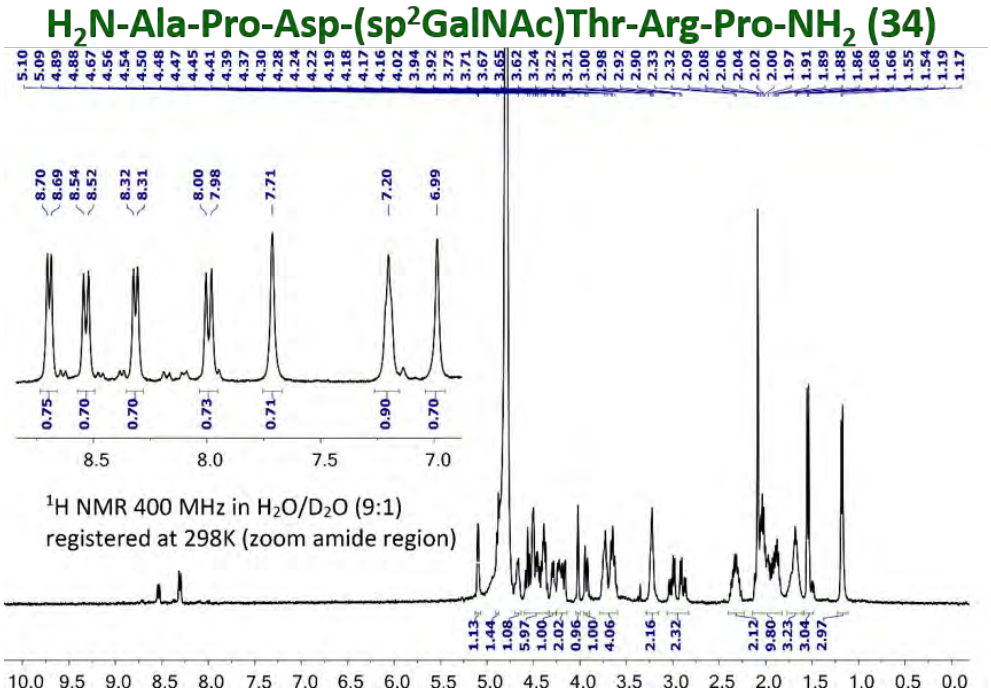

^{13}C NMR 100 MHz in D_2O

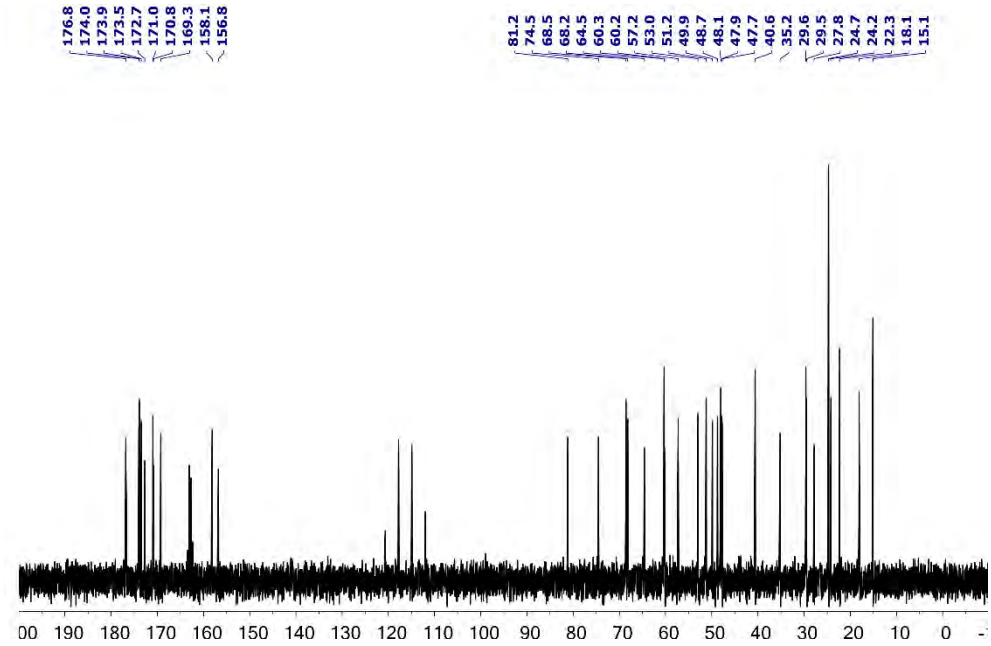

NOESY in H_2O/D_2O

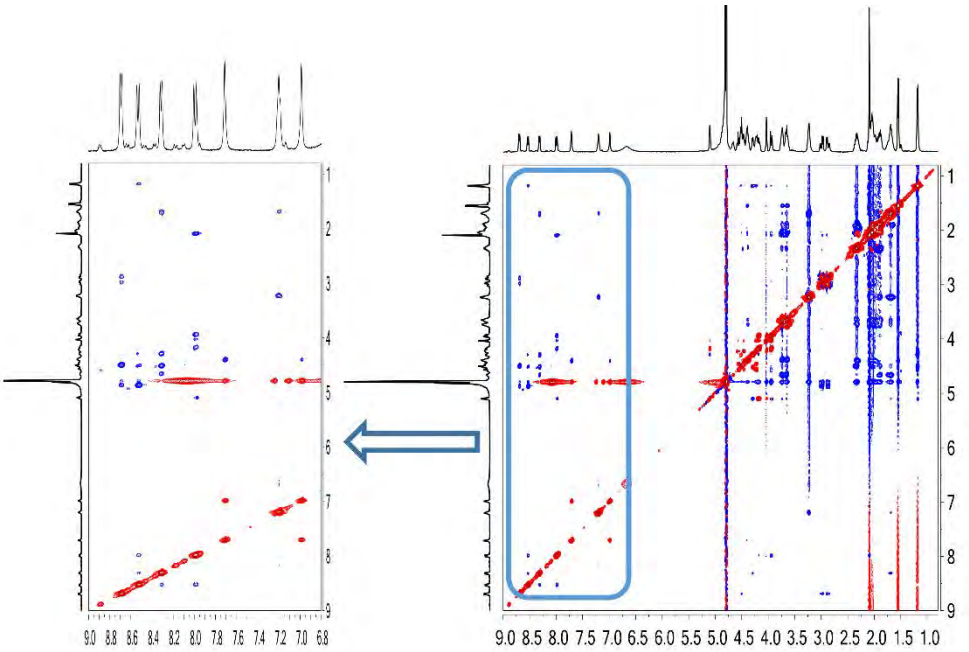

^{1}H NMR 400 MHz in D_2O

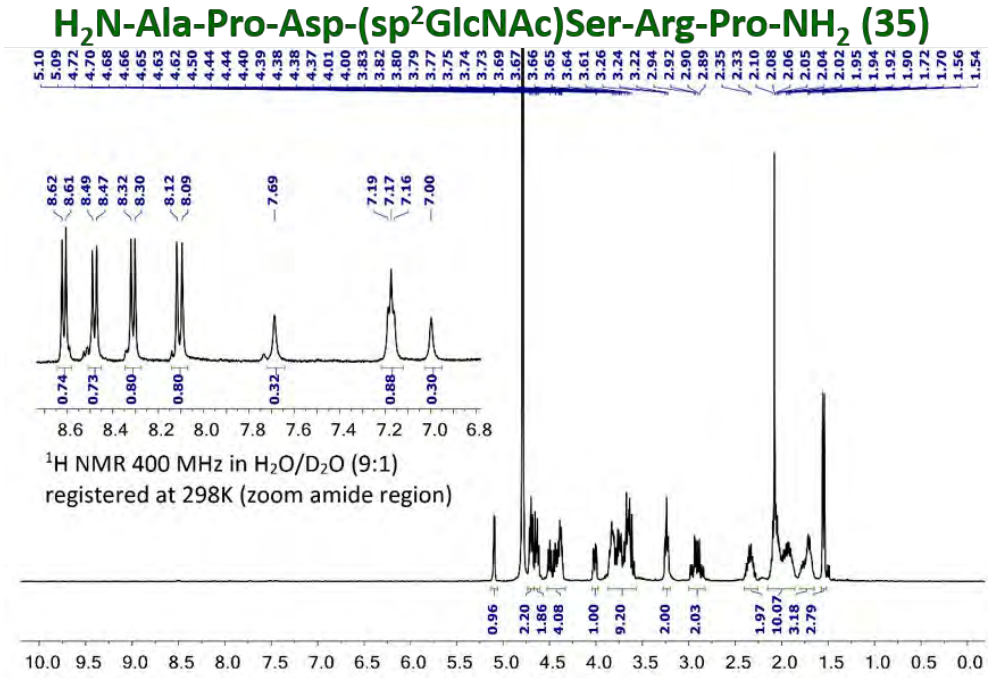

^{13}C NMR 100 MHz in D_2O

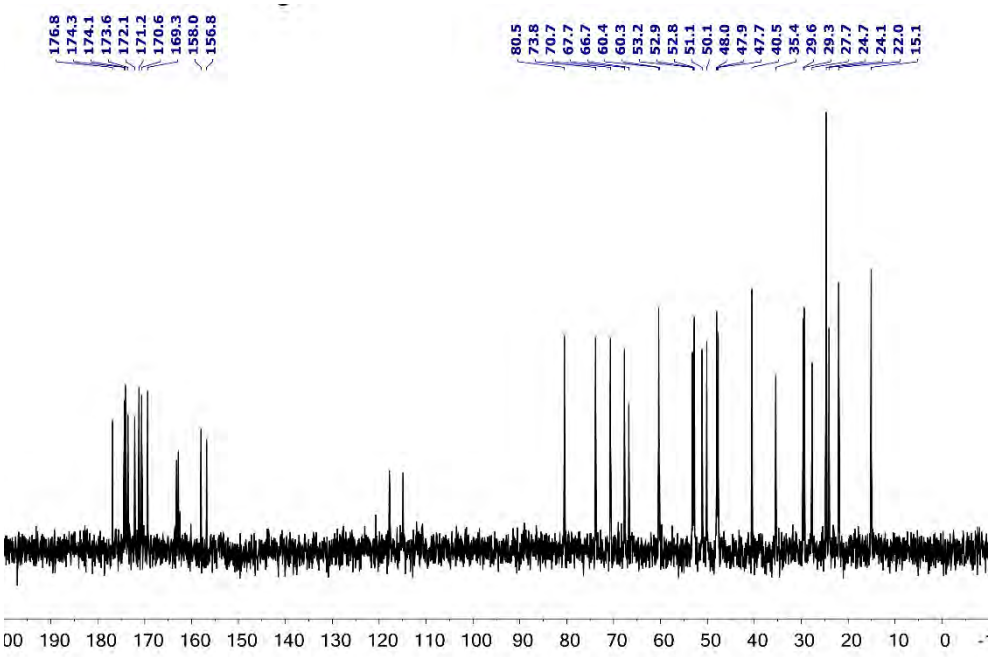

NOESY in H_2O/D_2O

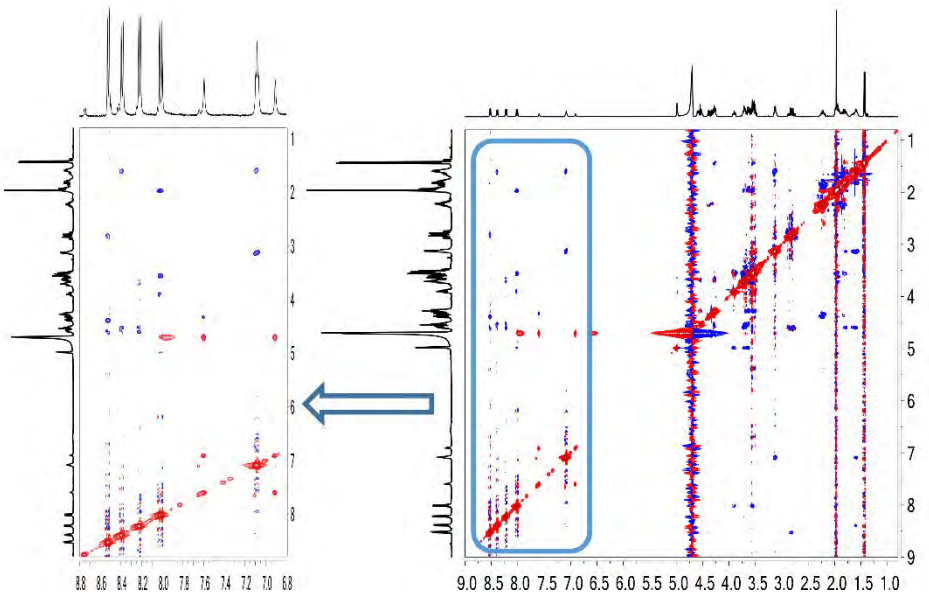

^{1}H NMR 400 MHz in D_2O

H_2N-Ala-Pro-Asp-(sp^{2}GlcNAc)Thr-Arg-Pro-NH_2 (36)

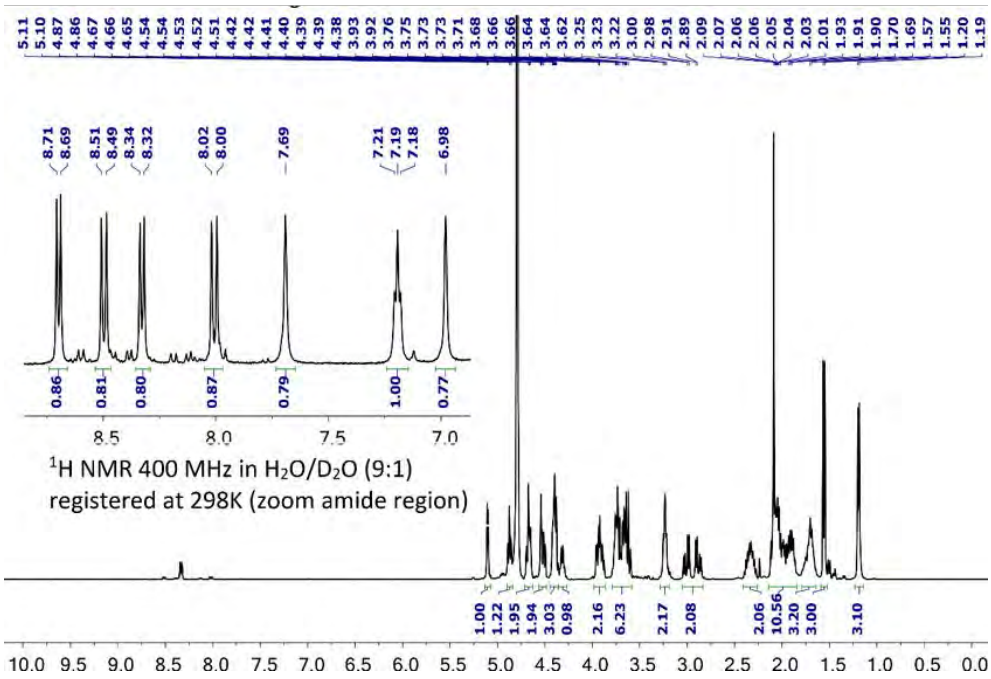

^{13}C NMR 100 MHz in D_2O

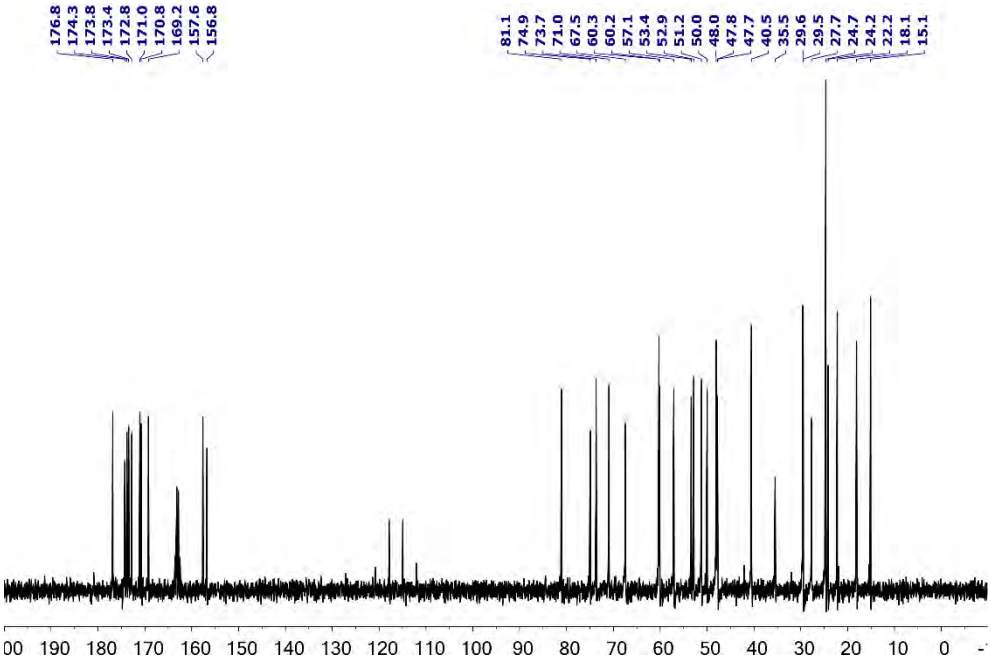

NOESY in H_2O/D_2O

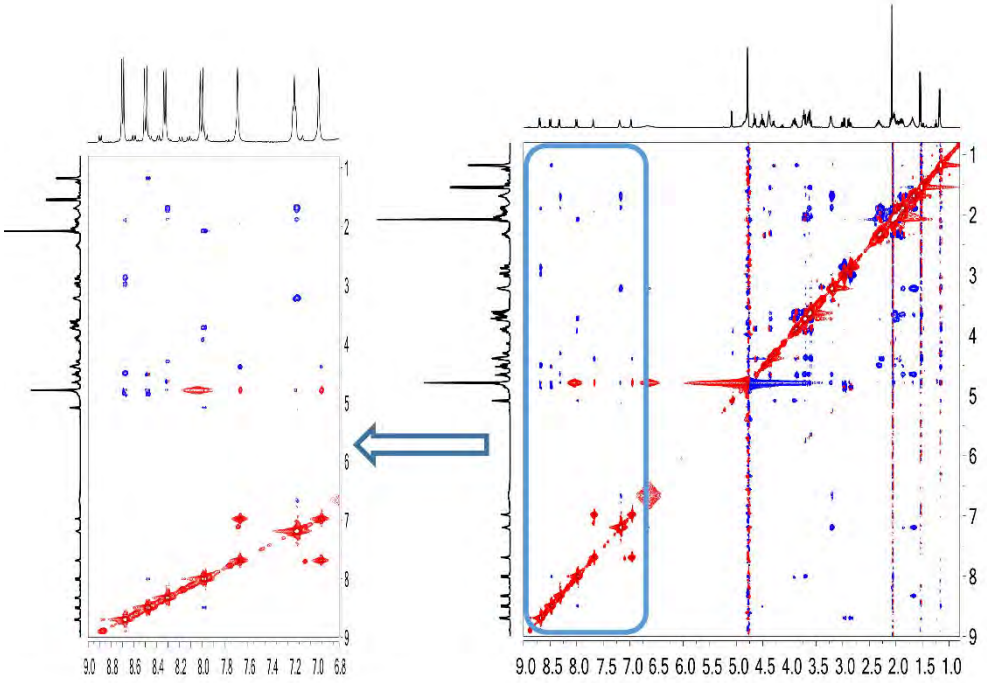

^{1}H NMR 400 MHz in CD_3OD

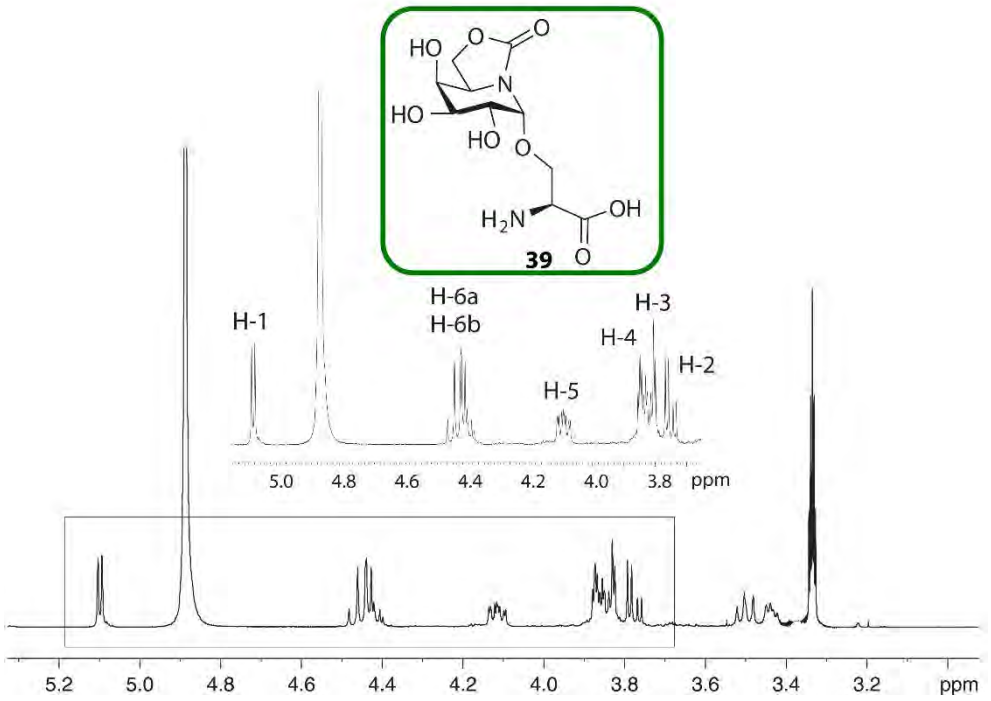

^{13}C NMR 100 MHz in CD_3OD

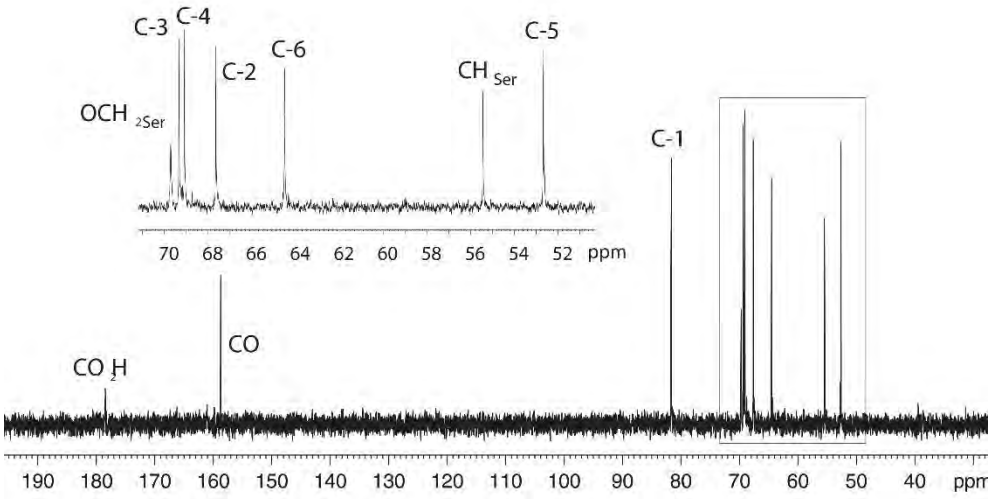

^{1}H NMR 300 MHz in D_2O

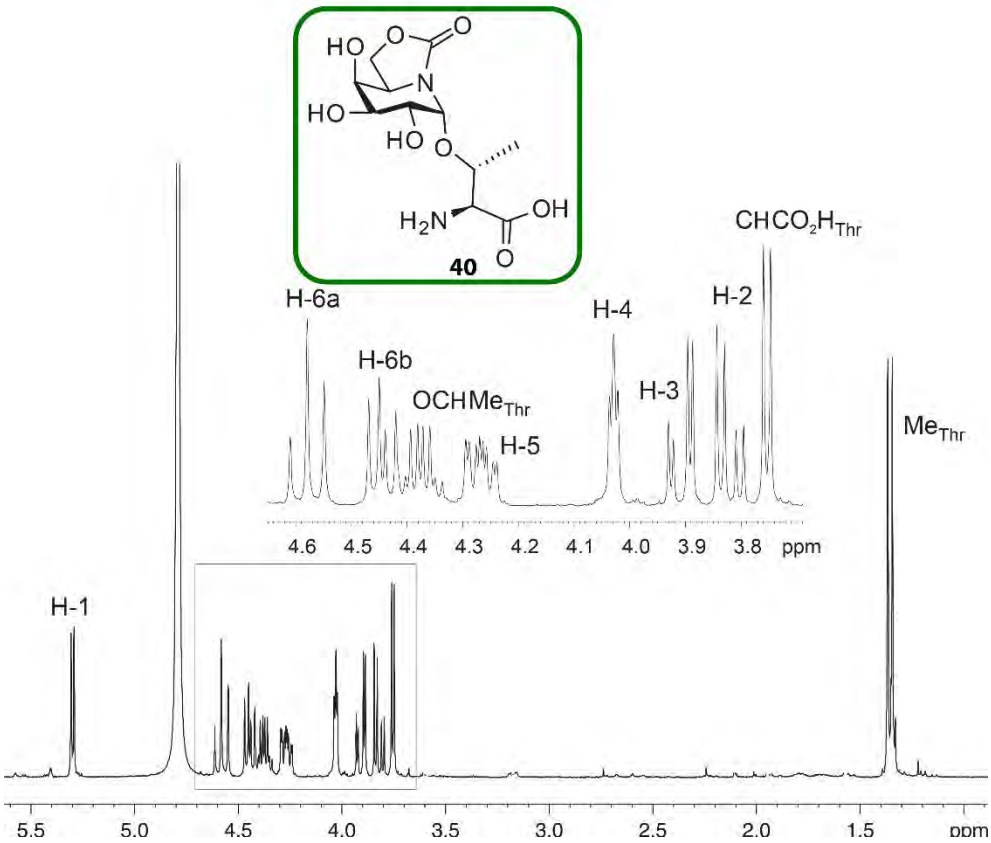

^{13}C NMR 75 MHz in D_2O

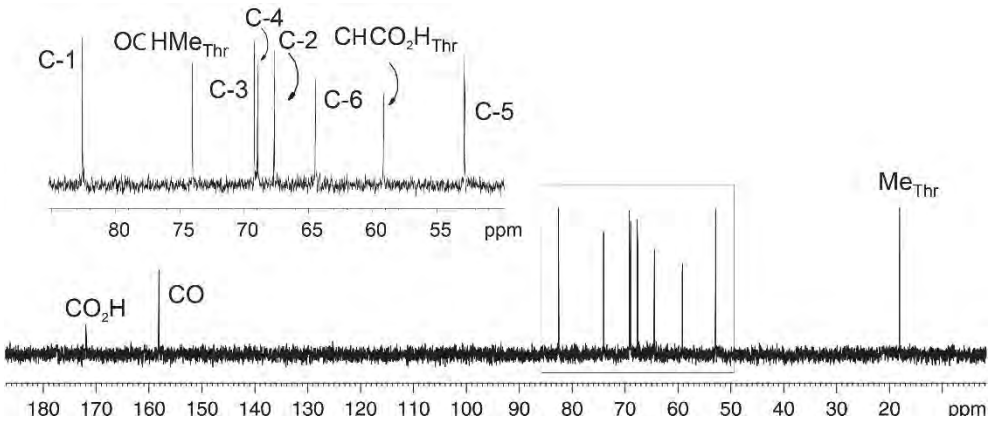

^{1}H NMR 500 MHz in D_2O

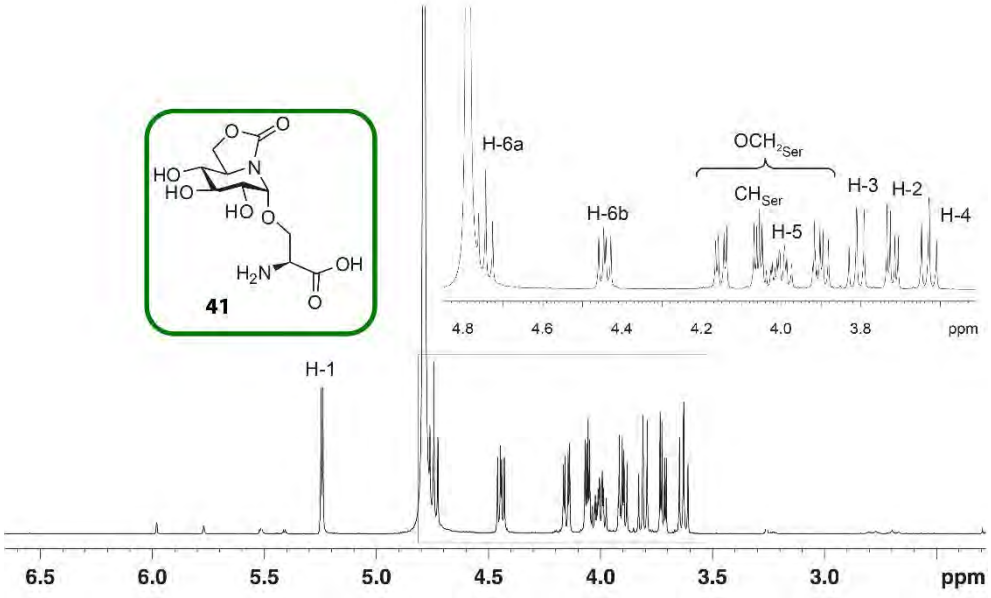

^{13}C NMR 125 MHz in D_2O

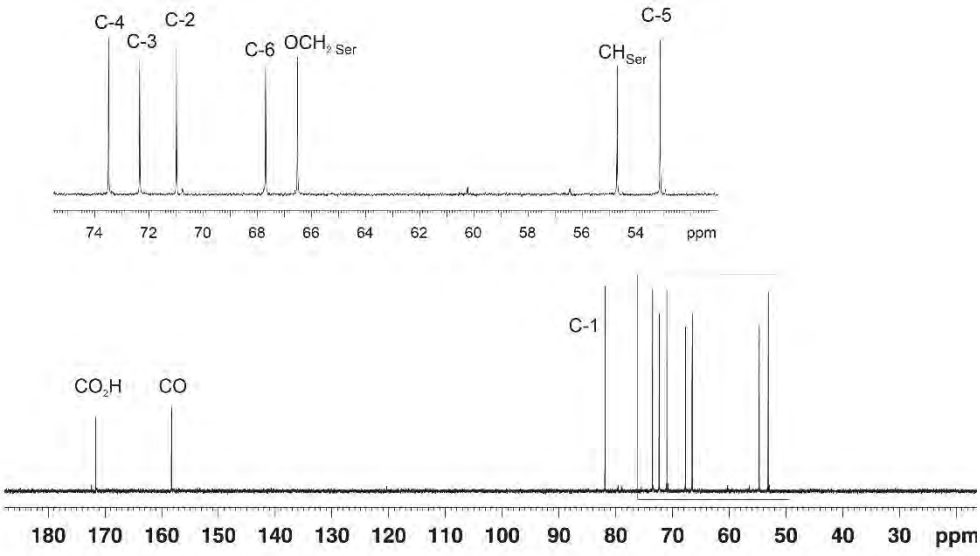

^{1}H NMR 500 MHz in D_2O

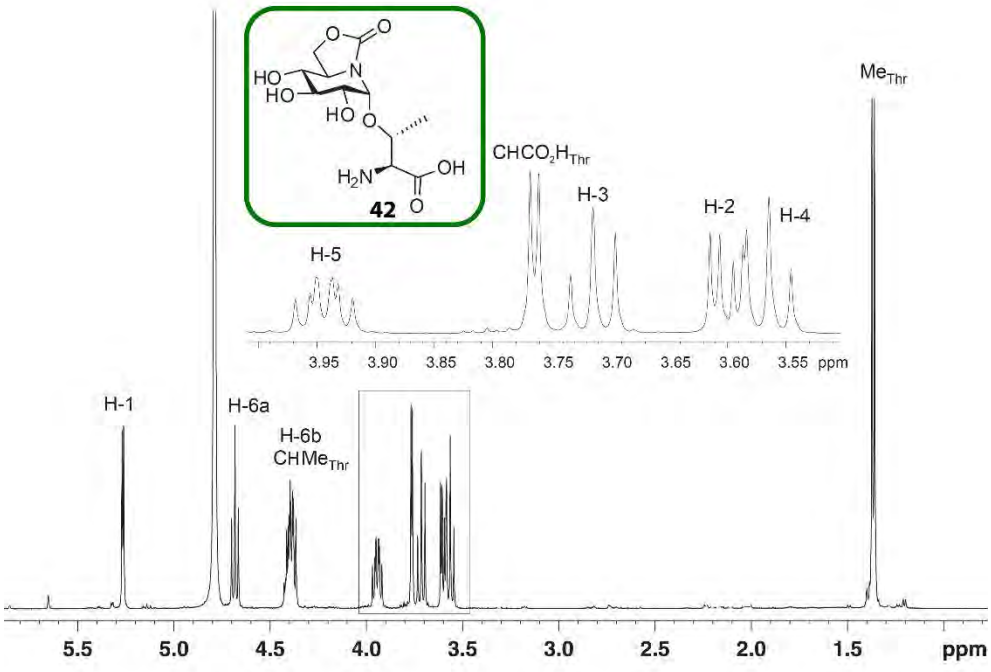

^{13}C NMR 125 MHz in D_2O

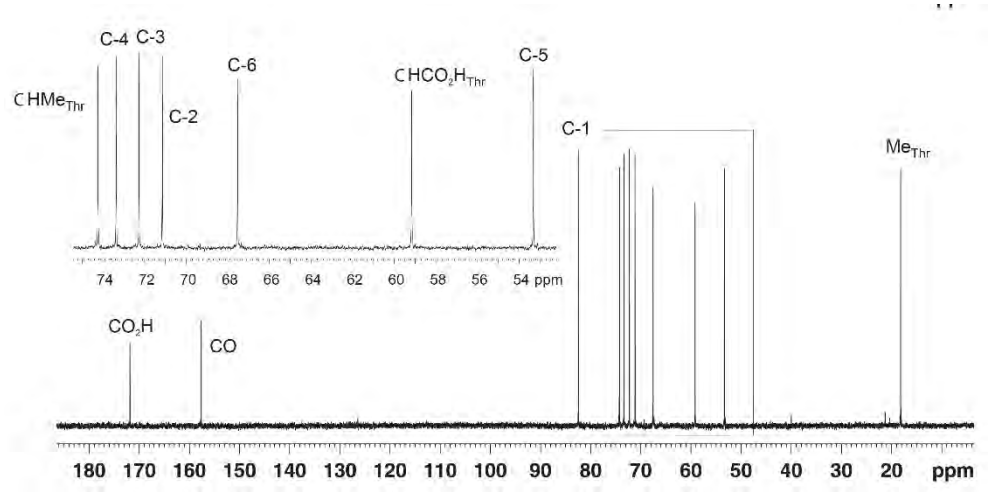

^{1}H NMR 300 MHz in $CDCl_3$

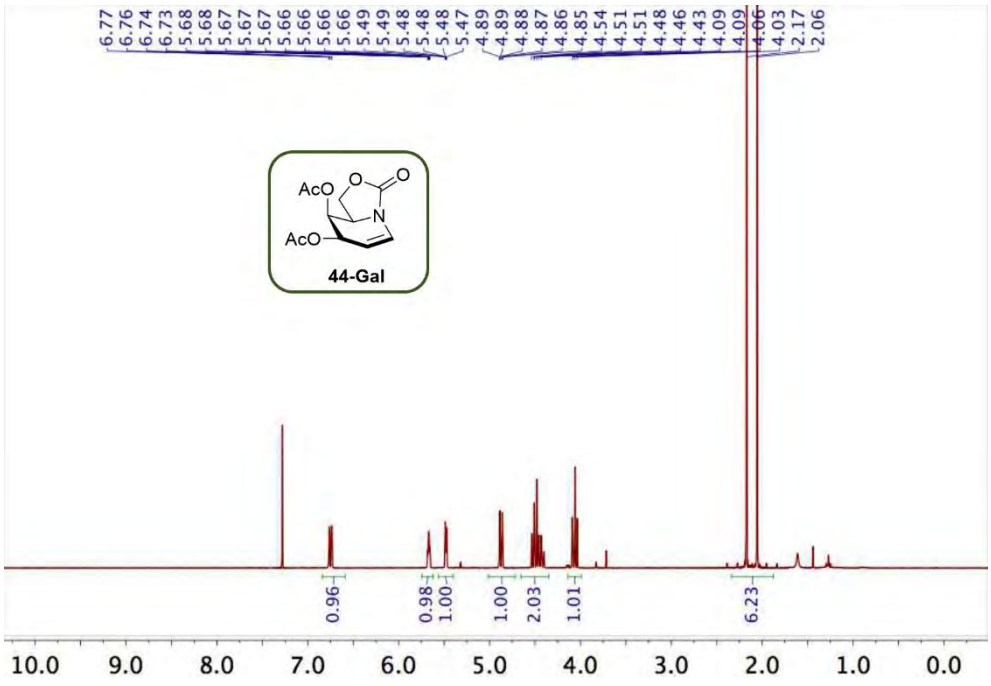

^{13}C NMR 75 MHz in $CDCl_3$

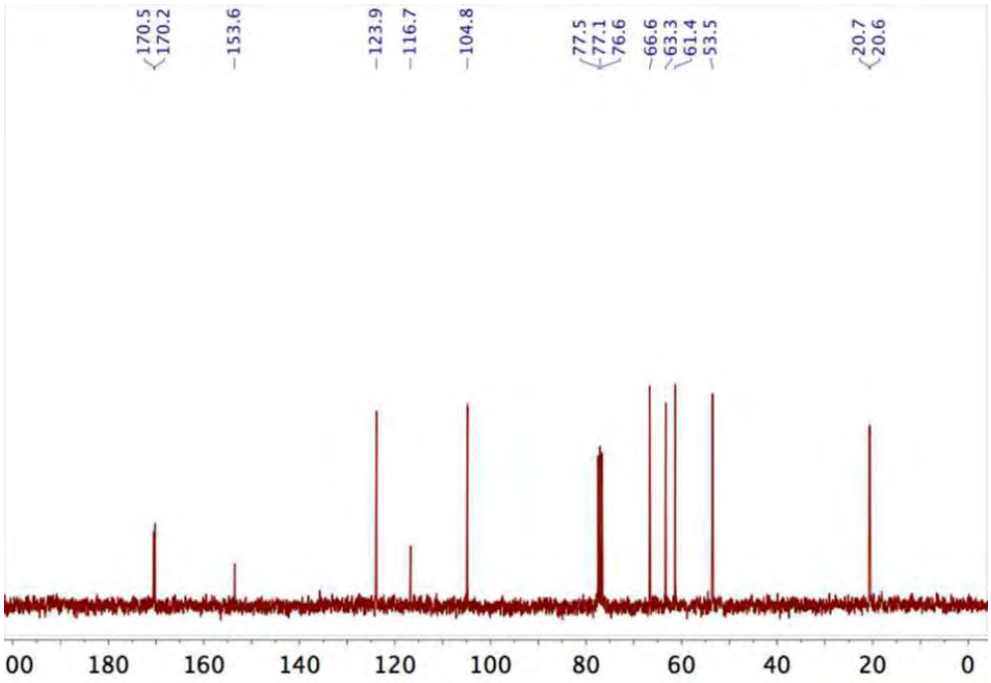

^{1}H NMR 300 MHz in $CDCl_3$

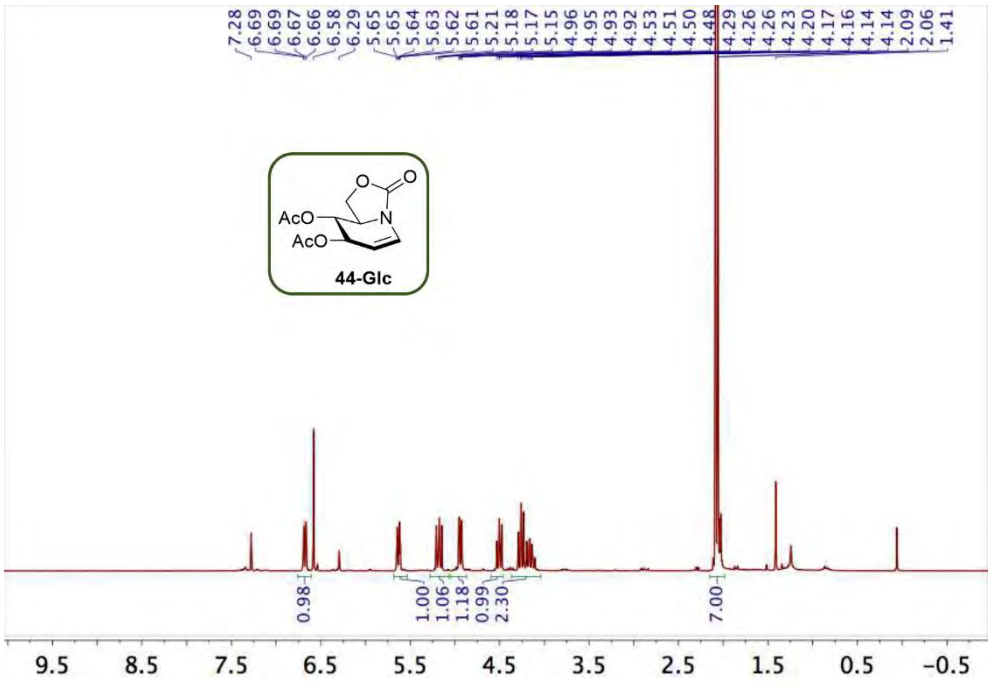

^{13}C NMR 75 MHz in $CDCl_3$

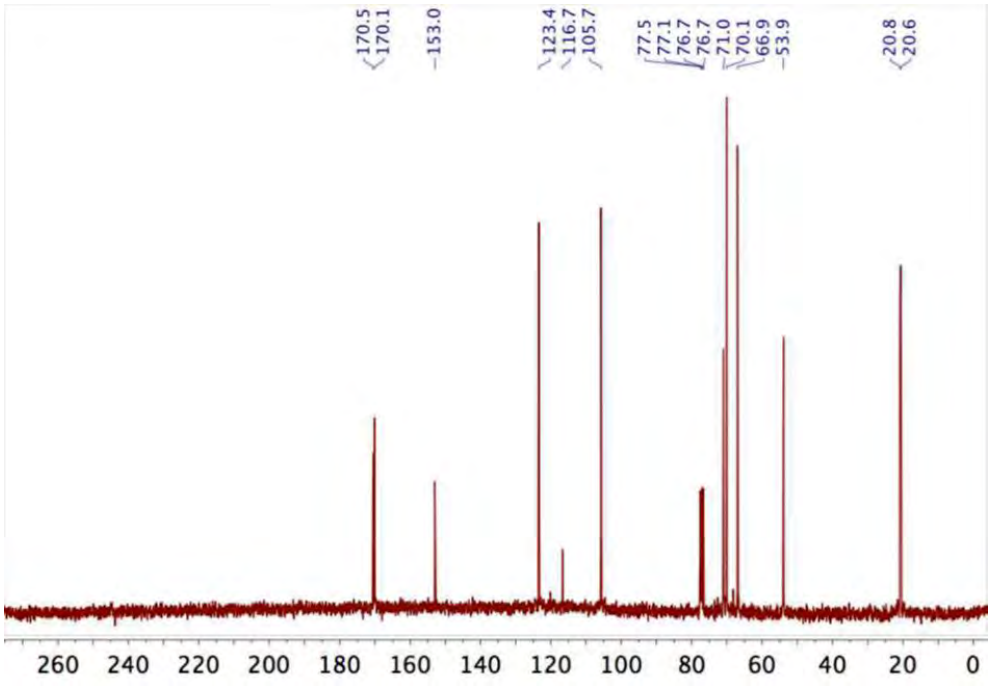

^{1}H NMR 300 MHz in $CDCl_3$

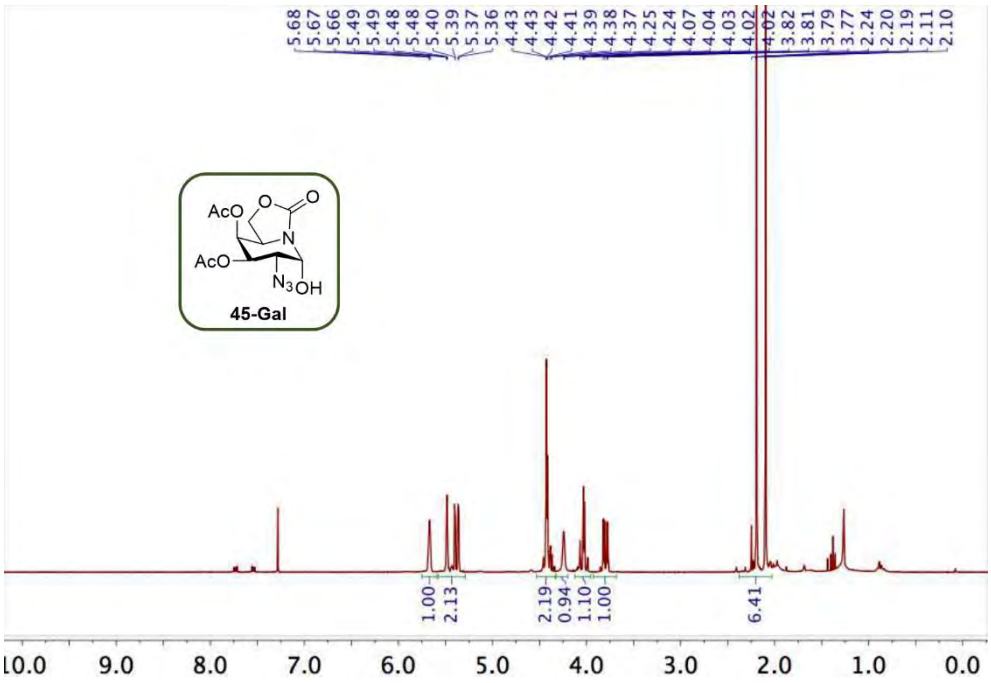

^{13}C NMR 75 MHz in $CDCl_3$

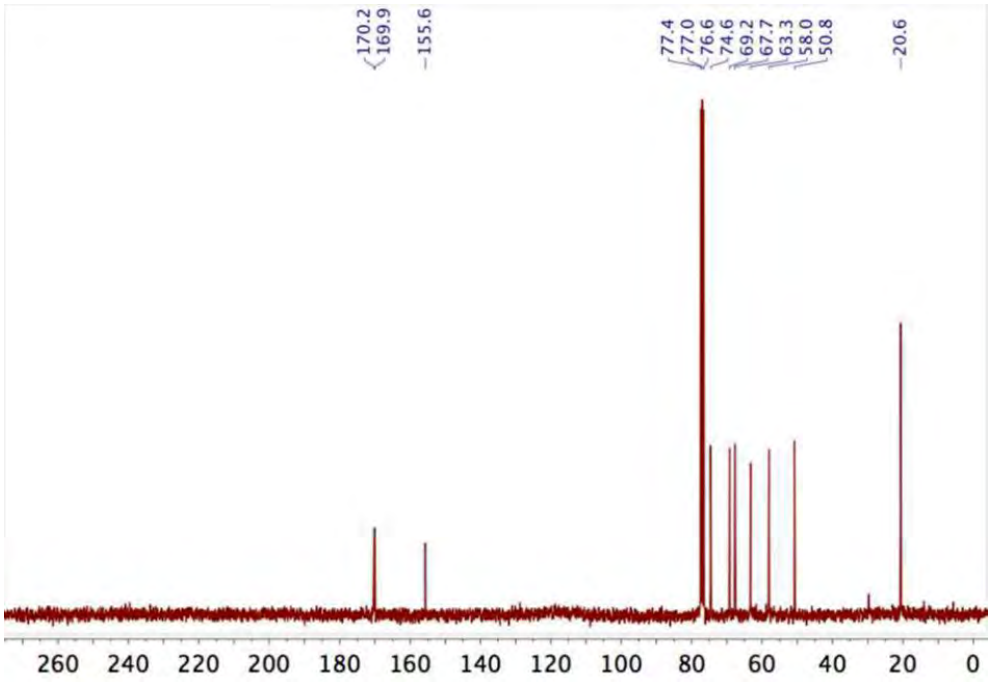

^{1}H NMR 300 MHz in $CDCl_3$

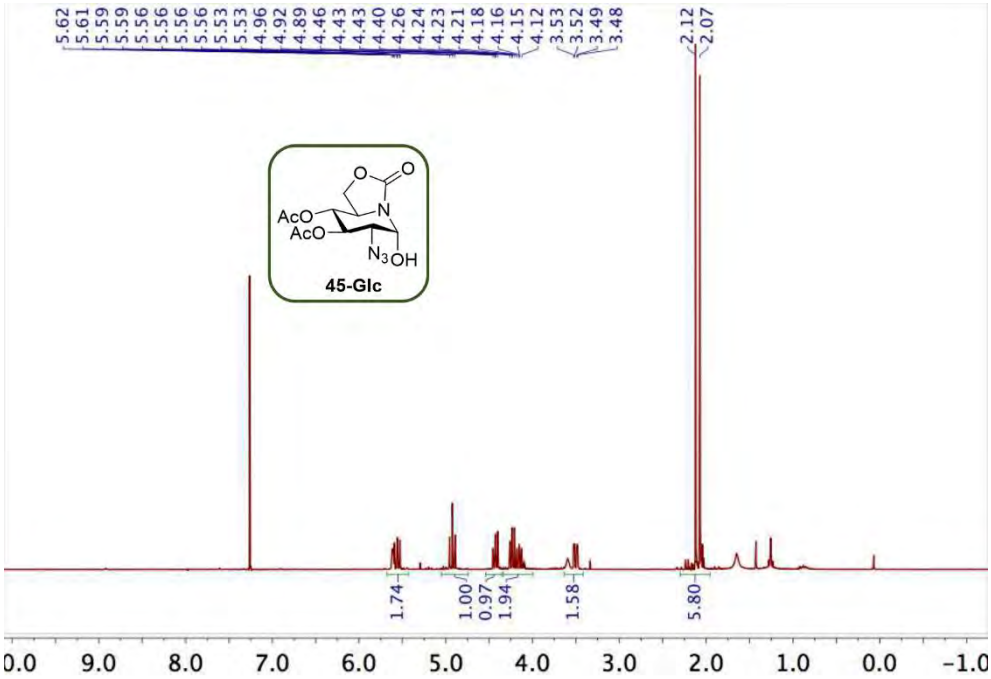

^{13}C NMR 75 MHz in $CDCl_3$

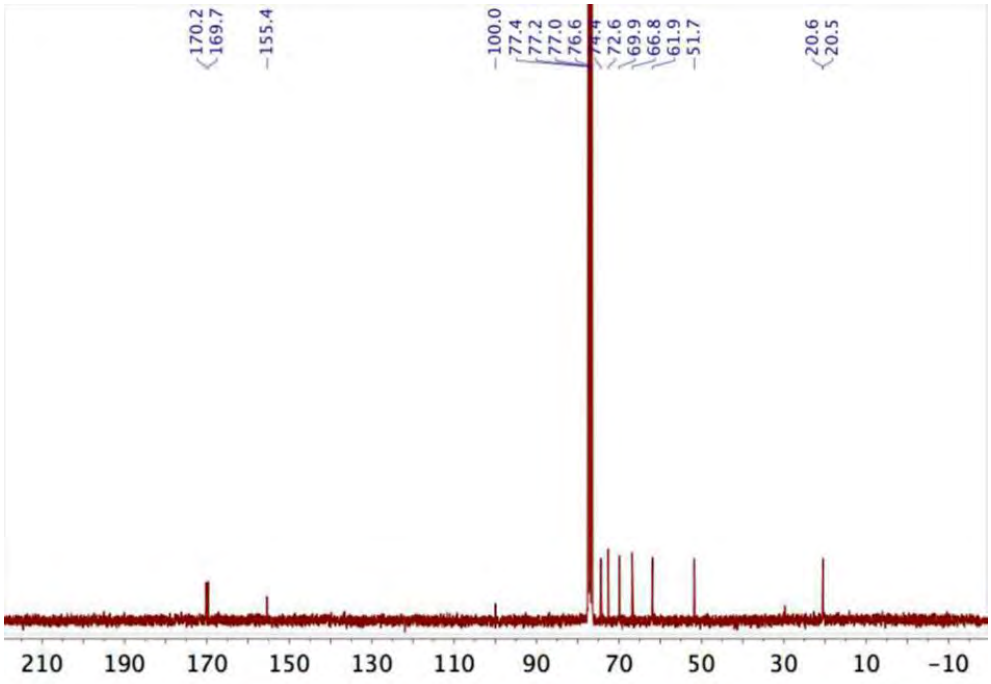

^{1}H NMR 300 MHz in $CDCl_3$

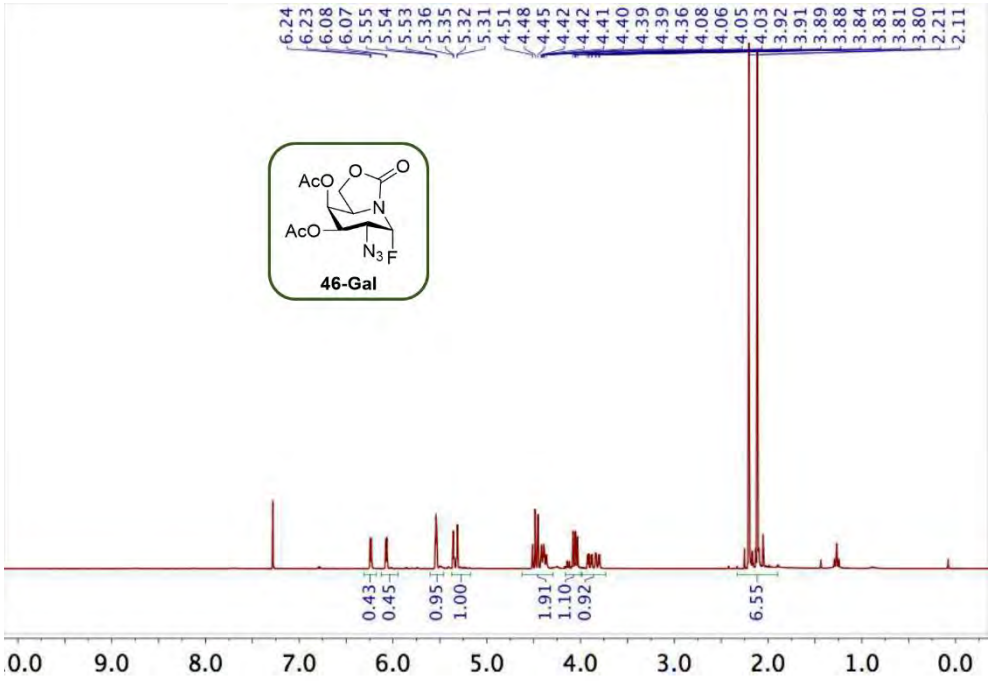

^{13}C NMR 75 MHz in $CDCl_3$

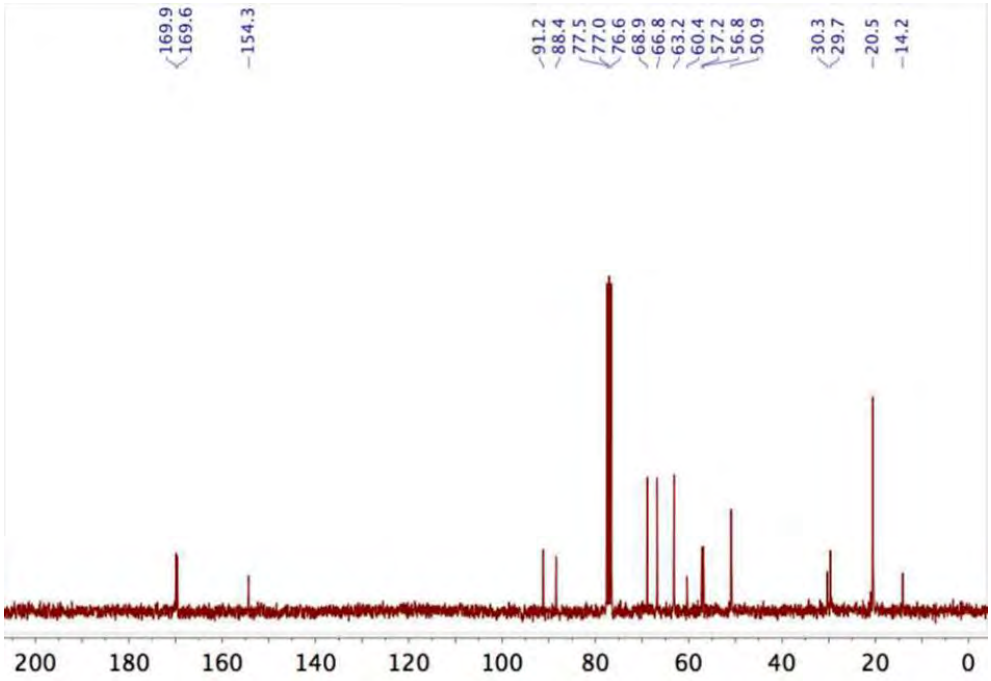

^{1}H NMR 300 MHz in $CDCl_3$

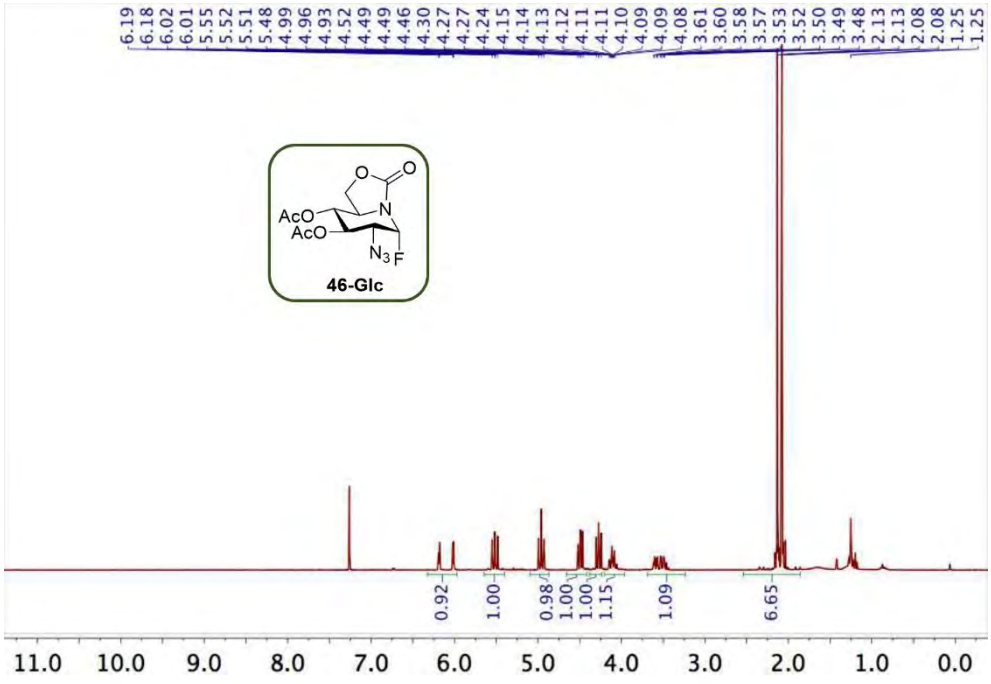

^{13}C NMR 75 MHz in $CDCl_3$

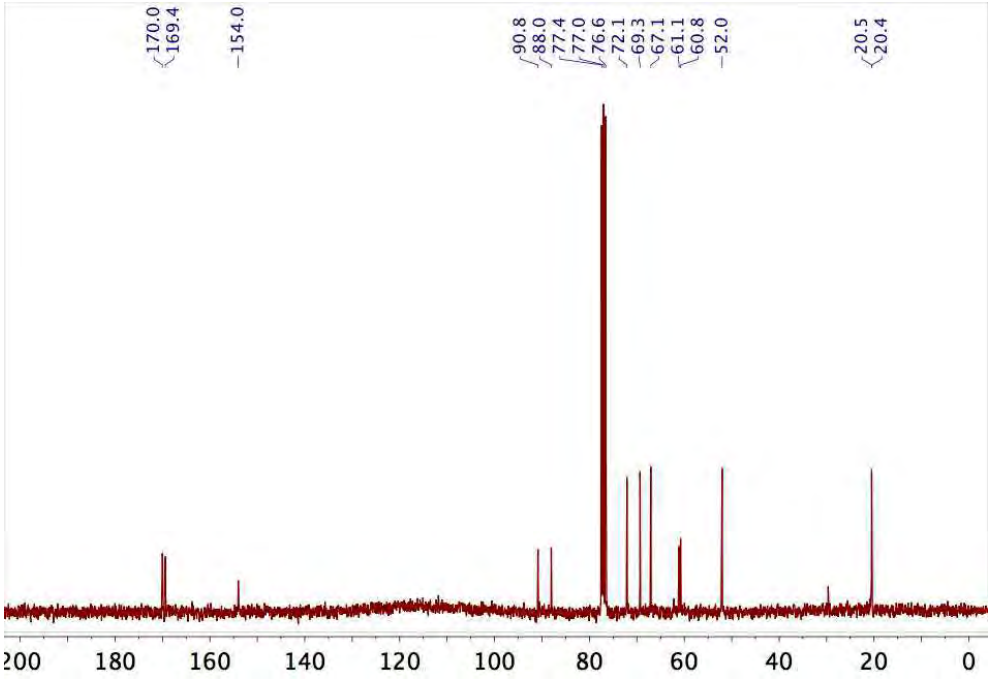

^{1}H NMR 300 MHz in $(CD_3)_2CO$

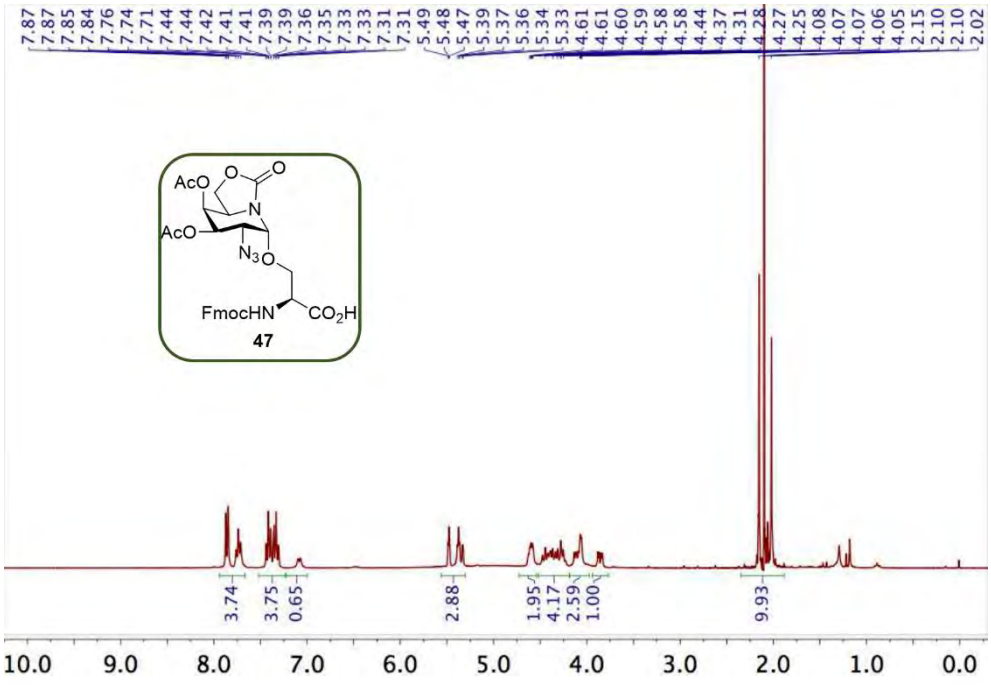

^{13}C NMR 75 MHz in $(CD_3)_2CO$

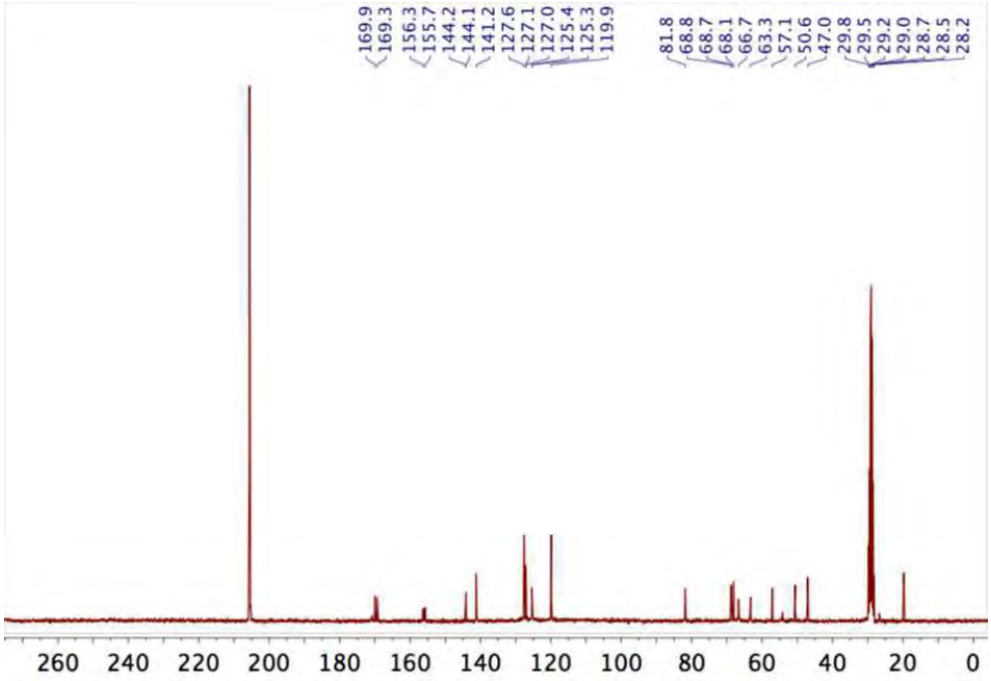

^{1}H NMR 300 MHz in CD_3OD

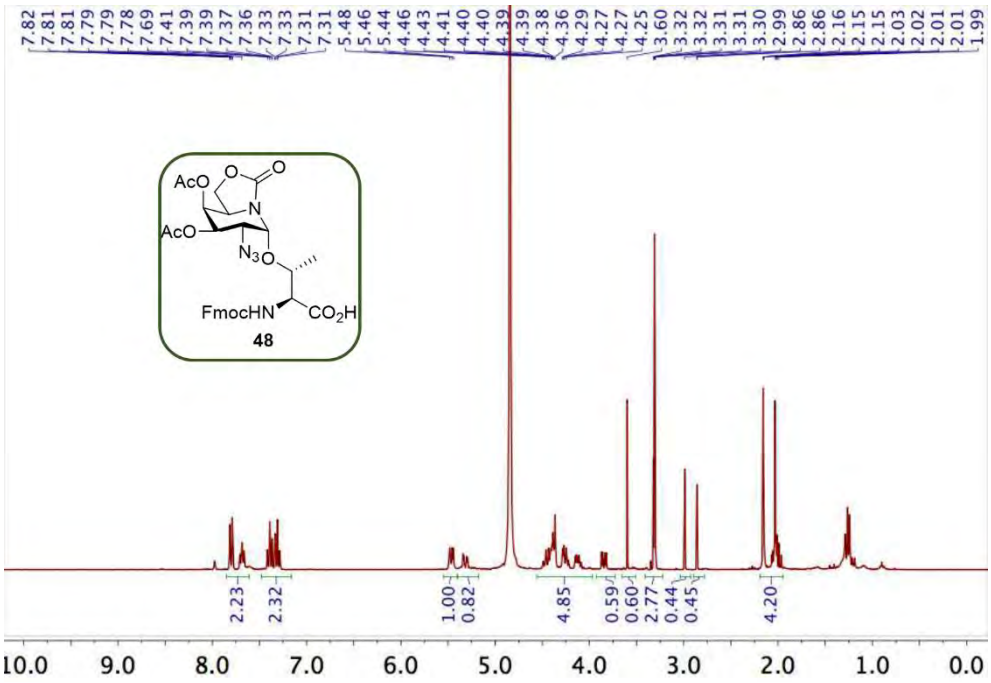

^{13}C NMR 75 MHz in CD_3OD

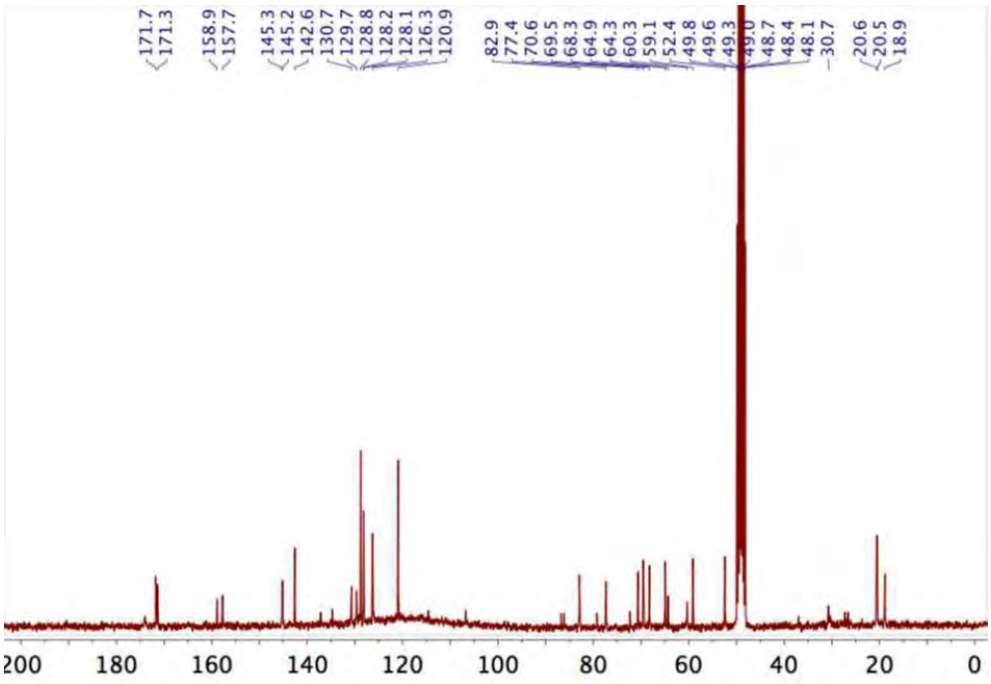

^{1}H NMR 300 MHz in CD_3OD

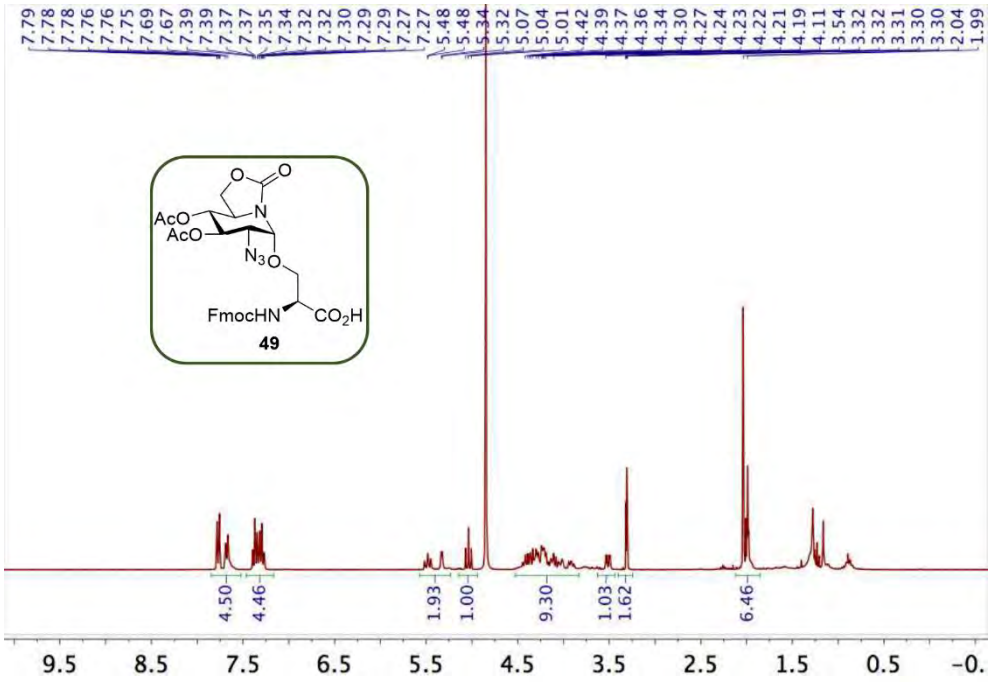

^{13}C NMR 75 MHz in CD_3OD

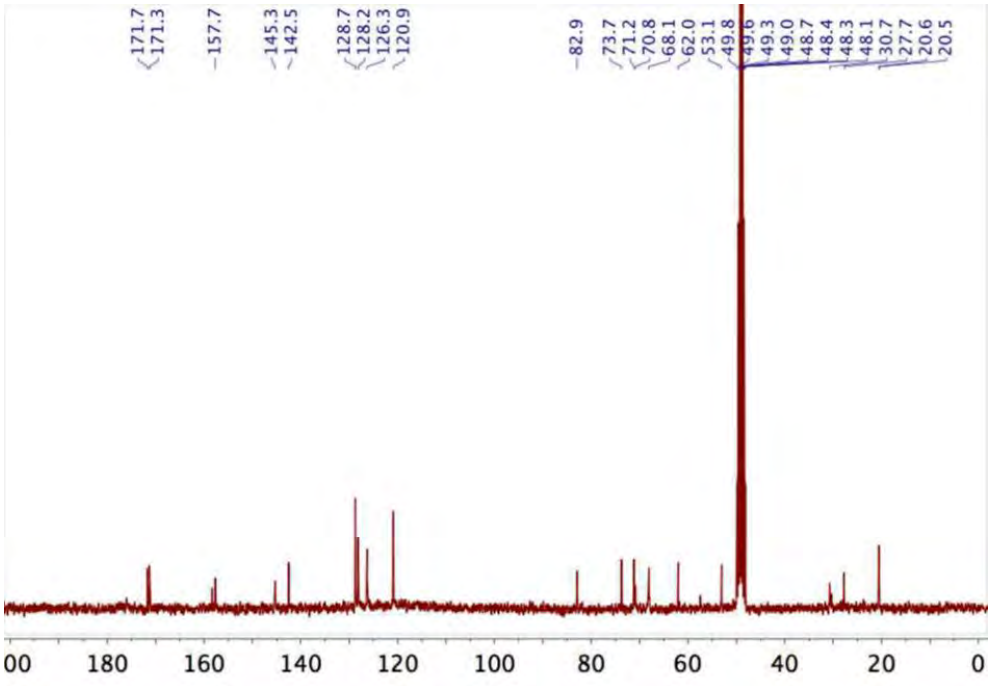

^{1}H NMR 300 MHz in CD_3OD

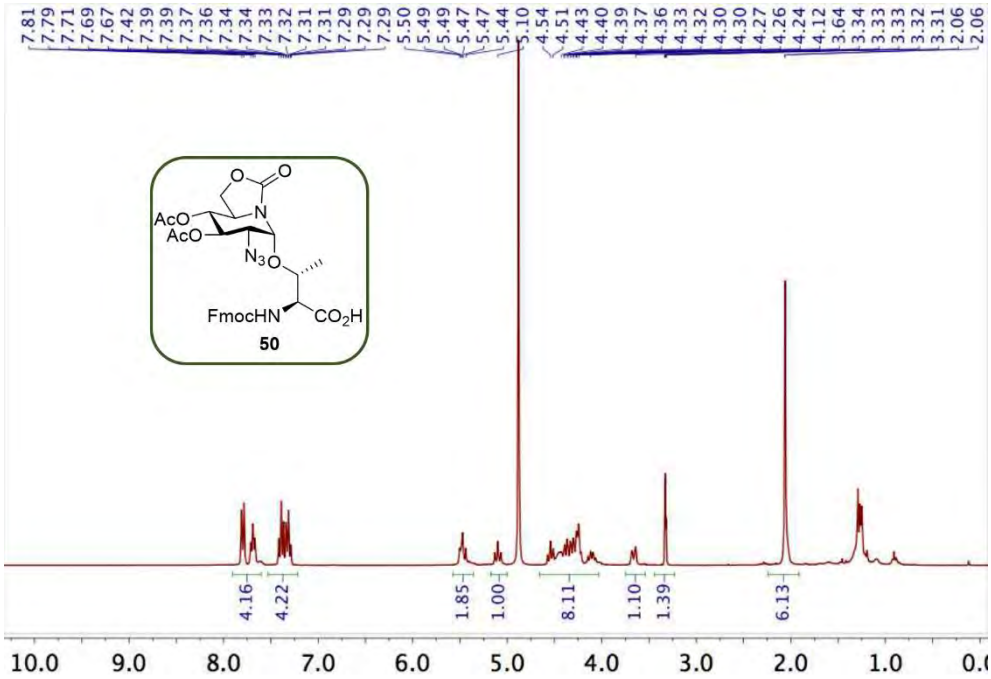

^{13}C NMR 75 MHz in CD_3OD

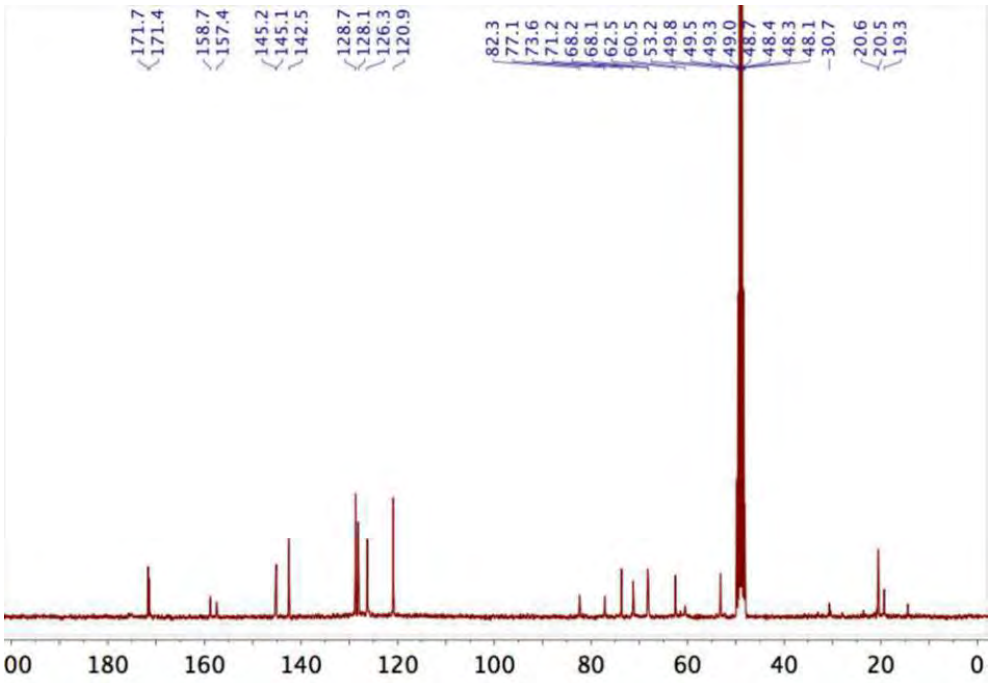

SI.2. Computational details

Table of energies, entropies, and lowest frequencies of calculated structures (PCM_{H2O}/M06-2X/def2-TZVPP) for glycosylation reaction of sp^2-iminosugars.

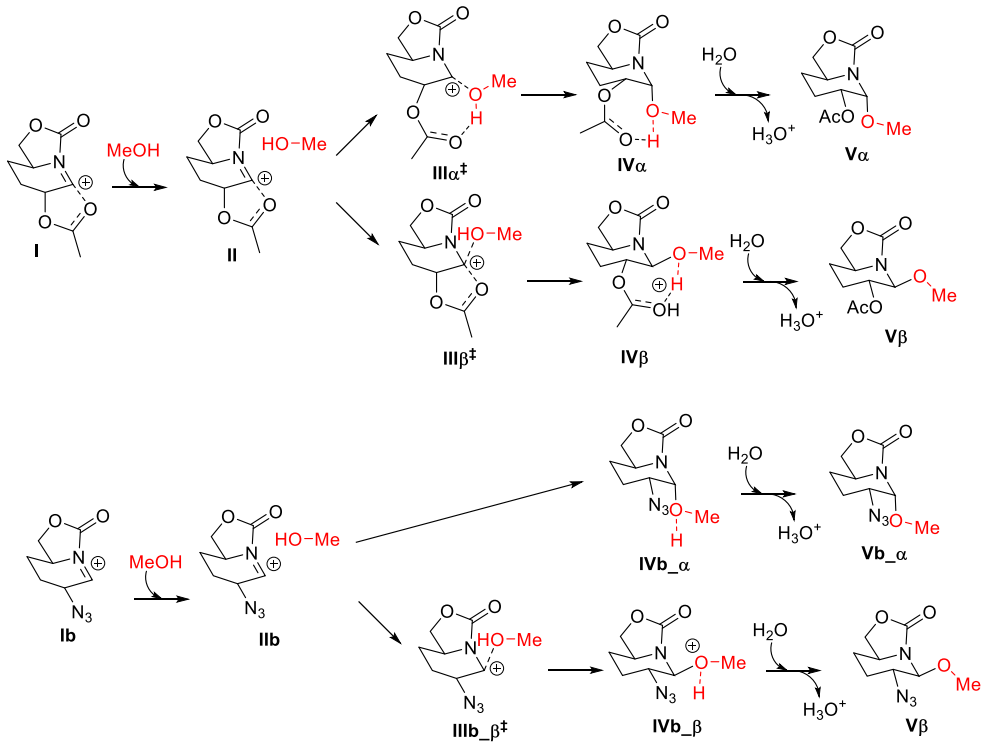

Structure	E_{elec} (Hartree)[a]	E_{elec} + ZPE (Hartree)[a]	H (Hartree)[a]	S (cal mol^{-1} K^{-1})[b]	G (Hartree)[a,b]	Lowest freq. (cm^{-1})	# of imag freq.
MeOH	-115.722108	-115.670409	-115666096	57.0	-115.693201	282.6	0
I *(conf 1)*	-705.666045	-705.452012	-705.438667	112.0	-705.491871	46.0	0
I *(conf 2)*	-705.679660	-705.463064	-705.450684	105.6	-705.500875	72.7	0
I *(conf 3)*	-705.665677	-705.451621	-705.438223	112.4	-705.491607	44.3	0
IIα	-821.406865	-821.138615	-821.120757	133.9	-821.184378	36.2	0
IIβ *(conf 1)*	-821.401356	-821.132812	-821.115103	133.2	-821.178385	39.5	0
IIβ *(conf 2)*	-821.411612	-821.141552	-821.124185	132.1	-821.186964	40.9	0
IIIα‡	-821.395373	-821.127157	-821.110291	129.9	-821.171997	-36.1	1
IIIβ‡	-821.397894	-821.128172	-821.111972	123.7	-821.170729	-176.5	1
IVα	-821.521647	-821.151478	-821.135502	123.0	-821.193963	55.9	0
IVβ	-821.413098	-821.142824	-821.126951	122.6	-821.185195	39.6	0
Vα	-821.020484	-820.762133	-820.745981	125.2	-820.805464	53.7	0
Vβ *(conf 1)*	-821.011267	-820.753145	-820.736986	125.3	-820.796512	41.8	0
Vβ *(conf 2)*	-821.013552	-820.755211	-820.739066	124.9	-820.798422	47.5	0

Ib ***(conf 1)***	-641.364134	-641.188963	-641.177489	103.4	-641.226635	27.7	0
Ib ***(conf 2)***	-641.364121	-641.188884	-641.177429	103.2	-641.226469	28.5	0
Ib ***(conf 3)***	–641.363233	–641.187920	–641.176472	103.5	–641.225629	24	0
IIb_α ***(conf 1)***	–757.097931	–756.869320	–756.853086	127.5	–756.913673	31.7	0
IIb_α ***(conf 2)***	–757.098567	–756.868807	–756.853092	123.2	–756.911619	30.9	0
IIb_β ***(conf 1)***	–757.098617	–756.869818	–756.853552	128	–756.914391	31.7	0
IIb_β ***(conf 2)***	–757.096999	–756.867937	–756.851786	126.6	–756.911959	27	0
IIIb_β‡ ***(conf 1)***	–757.092577	–756.862625	–756.847729	119.7	–756.904607	–147.6	1
IIIb_β‡ ***(conf 2)***	–757.092092	–756.862310	–756.847347	120.1	–756.904405	–147.2	1
IVb_α ***(conf 1)***	–757.111262	–756.879298	–756.864670	117.8	–756.920634	36.3	0
IVb_α ***(conf 2)***	–757.103185	–756.870633	–756.856026	116.8	–756.911502	37.3	0
IVb_β ***(conf 1)***	–757.095669	–756.863472	–756.848833	117	–756.904426	31.1	0
IVb_β ***(conf 2)***	–757.095201	–756.863416	–756.848637	117.4	–756.904407	39.3	0
IVb_β' ***(conf 1)***	–757.093952	–756.861142	–756.846687	116.5	–756.902023	30.6	0
IVb_β' ***(conf 2)***	–757.093775	–756.861246	–756.846741	116.4	–756.902027	39.1	0
IVb_β' ***(conf 3)***	–757.092297	–756.859043	–756.844798	114.3	–756.899120	50.1	0
Vb_α' ***(conf 1)***	–756.721206	–756.501569	–756.487428	114.6	–756.541892	62.1	0
Vb_α' ***(conf 2)***	–756.718815	–756.499534	–756.485278	116.2	–756.540492	35	0
Vb_α' ***(conf 3)***	–756.719044	–756.499577	–756.485376	115.7	–756.540371	34.5	0
Vb_β ***(conf 1)***	–756.711845	–756.492553	–756.478286	115.9	–756.533337	41.5	0
Vb_β ***(conf 2)***	–756.711346	–756.492089	–756.477791	116.7	–756.533257	28	0
Vb_β ***(conf 3)***	–756.709333	–756.490370	–756.475810	119.1	–756.532419	37	0
Vb_β ***(conf 4)***	–756.708775	–756.489654	–756.475145	118.9	–756.531619	30.1	0
Vb_β' ***(conf 1)***	–756.712079	–756.492932	–756.478721	115.3	–756.533502	42.7	0
Vb_β' ***(conf 2)***	–756.709889	–756.490863	–756.476543	117.6	–756.532418	20.6	0
Vb_β' ***(conf 3)***	–756.708698	–756.489407	–756.475206	115.8	–756.530223	34.9	0

Table of NBO second order perturbation energies (kcal mol^{-1}) of calculated structures (PCM_{H2O}/M06-2X/def2-TZVPP) for glycosylation reaction of *sp*^{2}-iminosugars.

Structure	Endo-anomeric effect $n_{Nendo} \rightarrow \sigma^*_{C1\text{-}Oexo}$	Exo-anomeric effect $N_{Oexo} \rightarrow \sigma^*_{C1\text{-}Nendo}$	TOTAL
IVα	20.5	3.8 + 5.7	30.0
IVβ	1.7	4.8 + 5.9	12.4
Vα	16.2	1.4 + 14.1	31.7
Vβ ***(conf 1)***	2.4	15.0	17.4
Vβ ***(conf 2)***	18.5	1.4 + 14.4	34.3
IVb_α ***(conf 1)***	39.9	1.5	41.4
IVb_β ***(conf 1)***	48.9	0.6	49.5
IVb_β' ***(conf 1)***	6.3	4.5	10.8
Vb_α ***(conf 1)***	17.0	1.3 + 14.1	32.4
Vb_β ***(conf 1)***	18.3	1.6 + 14.0	33.9
Vb_β' ***(conf 1)***	1.9	15.6	17.5

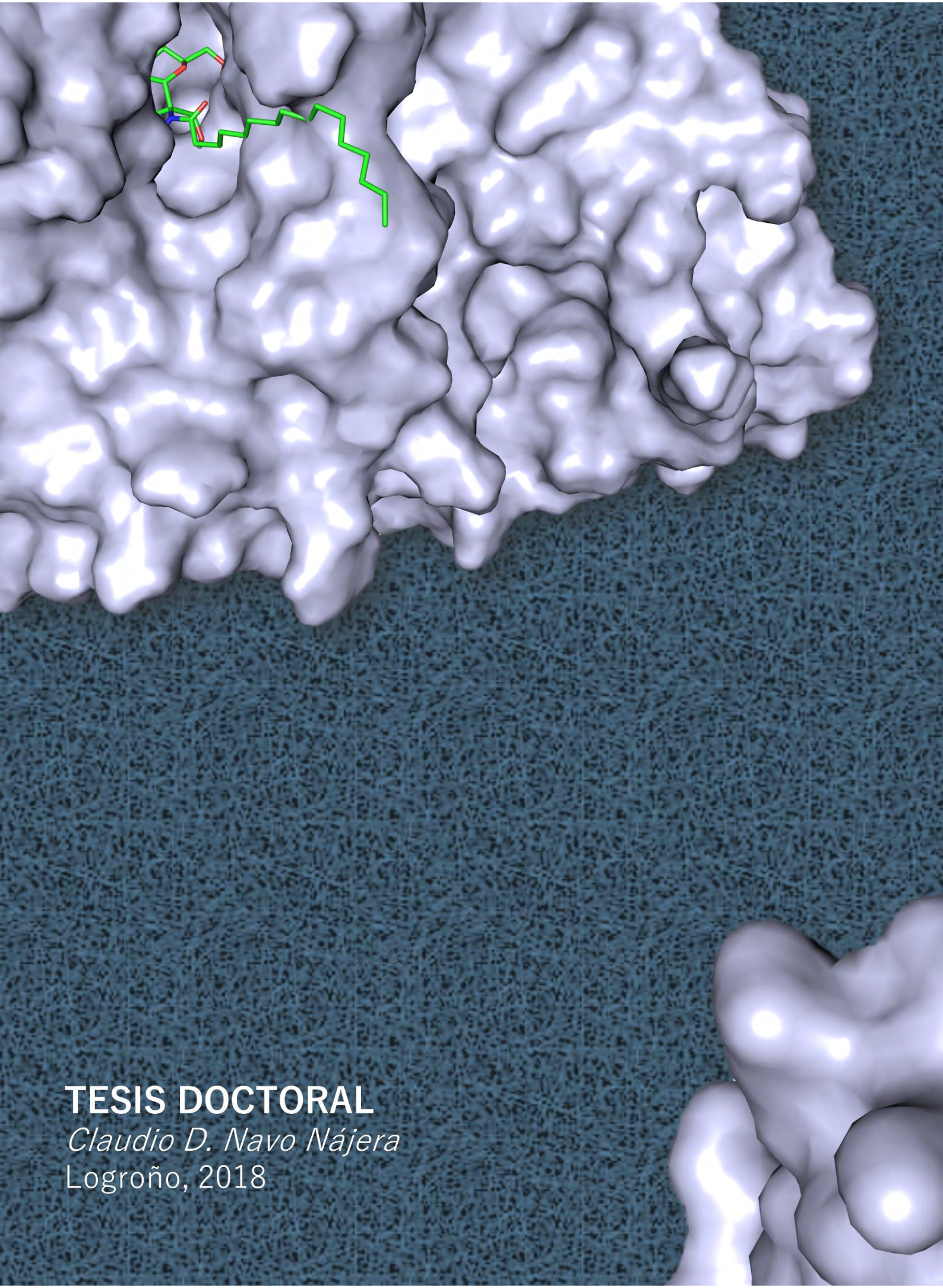

TESIS DOCTORAL

Claudio D. Navo Nájera

Logroño, 2018